

**Universidad CEU San Pablo**  
**CEINDO – CEU Escuela Internacional de Doctorado**

**PROGRAMA en MEDICINA TRASLACIONAL**



**CEU**

*Escuela Internacional  
de Doctorado*

# **BIOMARCADORES ASOCIADOS A ASMA GRAVE Y POLIPOSIS NASOSINUSAL**

TESIS DOCTORAL

Presentada por:  
María Isabel Delgado Dolset

Dirigida por:  
Dra. María Marta Escribese Alonso  
Dra. Cristina Gómez Casado

MADRID  
2022



# Agradecimientos



## Resumen

El asma es una enfermedad multifactorial muy compleja que puede afectar hasta a un 18% de la población mundial. Su manifestación clínica es muy heterogénea, con fenotipos clínicos distintos y mecanismos subyacentes diferentes. Por ejemplo, el fenotipo de asma alérgico se caracteriza por una inflamación tipo Th2, mientras que el asma no alérgico puede tener una inflamación tipo Th1, Th17, o mixta. Existen diversos fármacos disponibles para el tratamiento del asma, como los glucocorticoides, la inmunoterapia (en el caso de los fenotipos alérgicos) o medicamentos biológicos (como anti-IgE, anti-IL5 o anti-IL-4R $\alpha$ ). No obstante, existen algunos pacientes que no responden a ninguno de estos tratamientos, y que presentan un fenotipo grave, asociado a un mayor número de exacerbaciones y hospitalizaciones, así como a ciertas comorbilidades. Entre éstas, y en particular en el fenotipo de asma no alérgico, destacan la poliposis nasosinusal y la hipersensibilidad a AINES. El motivo por el que los tratamientos disponibles no son capaces de controlar los síntomas en estos pacientes es desconocido. La estratificación de los pacientes y la comprensión de los mecanismos subyacentes a los distintos fenotipos sería de utilidad en la elección del tratamiento del paciente, y revelaría posibles dianas terapéuticas aún hoy desconocidas. Para ello, las técnicas ómicas pueden resultar de gran utilidad, al permitir la evaluación de múltiples biomarcadores candidatos a la vez.

El objetivo de esta tesis es encontrar biomarcadores de estratificación en pacientes con asma alérgicos y no alérgicos, y con poliposis nasosinusal alérgicos y no alérgicos. Para ello, se plantearon una serie de objetivos secundarios que se abordaron en cada uno de los **BLOQUES**.

Para identificar biomarcadores de estratificación por gravedad en pacientes con asma, se reclutaron pacientes asmáticos con y sin alergia. En primer lugar, los pacientes con asma alérgico se estratificaron en función de su gravedad en cuatro grupos: leves controlados con corticosteroides (ICS), moderados controlados con inmunoterapia (IT), graves controlados con biológicos (BIO) y graves no controlados (UCA). De estos pacientes se obtuvieron muestras de suero y se analizaron por medio de metabolómica, utilizando cromatografía líquida acoplada a espectrometría de masas (LC-MS), y por proteómica, mediante la tecnología Olink. Además, utilizando las variables ómicas y clínicas se construyó un modelo de aprendizaje automático para clasificar a los pacientes. Los resultados demostraron que los pacientes no controlados mostraban un perfil de marcadores diferencial al de los pacientes controlados, particularmente en la comparación con el fenotipo más leve. En concreto, los pacientes UCA presentaban una activación de las rutas del ácido araquidónico y la fosfolipasa A2, así como de la respuesta de linfocitos Th2,

comparados con los pacientes ICS. Además, el modelo de aprendizaje automático creado con los datos clínicos y metabolómicos de los pacientes permitió una clasificación con un 80% de precisión.

A continuación, y para discernir la contribución del fenotipo alérgico en la patología asmática, los pacientes asmáticos alérgicos graves no controlados (UCA) se compararon con pacientes asmáticos no alérgicos graves no controlados (UCNA) utilizando LC-MS no dirigido. Este análisis reveló una activación de la ruta de la fosfolipasa A2 y una alteración en el perfil de esteroides, particularmente en los ácidos biliares, en los pacientes UCA con respecto a los pacientes UCNA.

Por último, para entender el papel de la alergia en la poliposis nasal, se reclutaron pacientes con poliposis con y sin alergia. Se realizó un análisis LC-MS no dirigido en muestras de plasma; además, aquellos metabolitos que se vieron significativamente alterados en plasma se analizaron de forma dirigida en el pólipo de un grupo de pacientes. Por último, se realizaron tinciones histológicas en biopsias de pólipo y mucosa nasal para analizar el remodelado y la infiltración en estos pacientes. Los resultados muestran que los pacientes alérgicos presentaban niveles disminuidos de lisofosfolípidos, incluyendo lisofosfatidilcolinas, bilirrubina y cortisol. Además, el análisis metabolómico en tejido de pólipo, una metodología novedosa puesta a punto en este estudio, reveló tendencias similares a nivel local, si bien las diferencias no fueron significativas. Por último, los pacientes alérgicos presentaban un mayor infiltrado de eosinófilos en sus pólipos que los pacientes no alérgicos.

En conjunto, el desarrollo de esta tesis ha permitido la identificación de biomarcadores para la estratificación de pacientes con asma y otras comorbilidades frecuentes, y supone un avance en el camino para lograr una medicina personalizada y de precisión.

# Abstract

Asthma is a multifactorial, complex disease that affects around 18% of global population. It can display multiple clinical phenotypes with diverse underlying mechanisms. For example, allergic asthma is characterized by a Th2 high response, while non-allergic asthma may have either a Th1, Th17 or mixed inflammation. There are several available medications for these patients, including corticosteroids, allergen immunotherapy (for the allergic phenotypes) or biologics (such as anti-IgE, anti-IL5 and anti-IL4R $\alpha$ ). However, there is a group of patients who do not respond to any of these treatments. These patients are characterized by a severe phenotype, associated to frequent exacerbations and hospitalizations, and often related to certain comorbidities. Among these, non-allergic patients frequently have associated nasal polyposis and non-steroidal anti-inflammatory drug hypersensitivity. The reason why these patients do not respond to treatment is unknown. Nonetheless, the stratification of patients could lead to a better understanding of the underlying endotypes and improve the management of the disease by improving the decision-making when electing the treatment and revealing novel therapeutical targets. In this, the use of omics sciences could be helpful, as it allows the testing of several potential biomarkers at once.

Here, we aim to find biomarkers that can be used in the stratification of allergic and non-allergic asthma, as well as in allergic and non-allergic nasal polyposis.

To find biomarkers for the stratification of patients with asthma, we recruited asthmatic patients with and without allergic sensitization. First, allergic asthmatic patients were classified in four groups according to their response to treatment: mild patients controlled with corticosteroids (ICS), moderate patients controlled with allergen immunotherapy (IT), severe patients controlled with biologics (BIO) and uncontrolled severe patients (UCA). We performed both an untargeted metabolomics analysis with liquid chromatography coupled to mass spectrometry (LC-MS) and a proteomics analysis with Olink using serum from these patients. Moreover, omics and clinical variables were used to build a machine learning classifier. Our results show that uncontrolled allergic asthmatic patients have a characteristic marker fingerprint that can differentiate them from controlled patients. In particular, UCA patients display an activation of the arachidonic and phospholipase A2 pathways, as well as an enhanced Th2 response, compared to ICS patients. Moreover, the machine learning model was able to correctly classify 80% of the patients.

Next, to uncover the role of allergy in asthma, severe uncontrolled allergic asthmatic patients (UCA) were compared with severe uncontrolled non-allergic asthmatic patients (UCNA) using untargeted LC-MS. We found that UCA patients present a higher activation of the phospholipase A2 pathway, as well as an alteration of steroids, specifically bile acids.

Finally, to understand the role of allergy in the pathogenesis of nasal polyps, we recruited patients with nasal polyps with and without allergy. Plasma from these patients was analysed using untargeted LC-MS; moreover, polyp biopsies were analysed in a targeted LC-MS approach, looking at those metabolites that were significantly different in the systemic analysis. Polyp and nasal mucosa biopsies were also obtained and stained to study the inflammatory infiltrate and local remodelling. We found that allergic patients had a systemic decrease in lysophospholipids, bilirubin and cortisol. Moreover, we were able to perform a metabolomic analysis in nasal polyps, a novel methodology, and found similar tendencies in the metabolites found in plasma. In addition, allergic patients had higher numbers of eosinophils in their nasal polyps than non-allergic patients.

Overall, this work has led to the identification of biomarkers that could be used in the stratification of patients with asthma and its frequent comorbidities and is a step forward in the road to a personalised and precision medicine.



# Índice

<b>AGRADECIMIENTOS.....</b>	<b>3</b>
<b>RESUMEN .....</b>	<b>5</b>
<b>ABSTRACT .....</b>	<b>7</b>
<b>ÍNDICE .....</b>	<b>9</b>
<b>ÍNDICE DE FIGURAS .....</b>	<b>13</b>
<b>ÍNDICE DE TABLAS .....</b>	<b>19</b>
<b>ABREVIATURAS Y ACRÓNIMOS.....</b>	<b>21</b>
<b>1. INTRODUCCIÓN .....</b>	<b>25</b>
1.1. ASMA.....	25
1.1.1. <i>Asma alérgico</i> .....	28
1.1.1.1. Enfermedad alérgica.....	28
1.1.1.2. Asma alérgico .....	29
1.1.1.2.1. Asma alérgico grave no controlado .....	31
1.1.2. <i>Asma no alérgico</i> .....	33
1.1.3. <i>Comorbilidades de asma</i> .....	35
1.1.3.1. Obesidad .....	35
1.1.3.2. Reflujo gastroesofágico .....	36
1.1.3.3. Rinitis alérgica, rinosinusitis crónica y pólipos nasales.....	36
1.1.3.4. Enfermedad respiratoria asociada a aspirina .....	36
1.2. BIOMARCADORES .....	37
1.3. CIENCIAS ÓMICAS: METABOLÓMICA .....	38
<b>2. HIPÓTESIS Y OBJETIVOS. ....</b>	<b>43</b>
<b>3. MATERIALES Y MÉTODOS .....</b>	<b>45</b>
3.1. BLOQUES I Y II. ESTUDIO DE FENOTIPOS ASMÁTICOS.....	45
3.1.1. <i>Reclutamiento, clasificación, y obtención de muestras</i> .....	45
3.1.1.1. Reclutamiento y clasificación de los pacientes.....	45
3.1.1.2. Análisis estadístico de las características clínicas de los pacientes .....	47
3.1.1.3. Obtención de suero .....	47
3.1.2. <i>Diseño experimental: metabolómica no dirigida</i> .....	47
3.1.2.1. Preparación de las muestras .....	47
3.1.2.2. Análisis instrumental .....	48
3.1.2.3. Procesamiento de datos, calidad de los datos e integración de lotes.....	49
3.1.2.1. Análisis estadístico .....	50
3.2. BLOQUE I. ESTUDIO DEL ASMA ALÉRGICO ESTRATIFICADO POR GRAVEDAD.....	52

3.2.1. <i>Análisis metabólico</i> .....	52
3.2.1.1. Anotación de metabolitos .....	52
3.2.2. <i>Análisis proteómico</i> .....	52
3.2.3. <i>Construcción de modelos de aprendizaje automático</i> .....	53
3.3. BLOQUE II. ESTUDIO DEL PAPEL DE LA ALERGIA EN PACIENTES ASMÁTICOS GRAVES NO CONTROLADOS.....	55
3.3.1. <i>Análisis metabólico</i> .....	55
3.3.1.1. Anotación de compuestos .....	55
3.4. BLOQUE III. ESTUDIO DEL PAPEL DE LA ALERGIA EN LA POLIPOSIS NASOSINUSAL .....	57
3.4.1. <i>Reclutamiento de pacientes</i> .....	57
3.4.2. <i>Obtención de muestras</i> .....	57
3.4.3. <i>Metabólica no dirigida en plasma</i> .....	58
3.4.3.1. Preparación de las muestras.....	58
3.4.3.2. Análisis instrumental .....	58
3.4.3.3. Procesamiento de los datos y análisis de calidad .....	59
3.4.3.4. Anotación de compuestos. ....	59
3.4.4. <i>Metabólica dirigida en tejido: pólipos</i> .....	59
3.4.4.1. Preparación de las muestras.....	59
3.4.4.2. Análisis instrumental .....	60
3.4.4.3. Adquisición y procesamiento de datos.....	60
3.4.5. <i>Tinciones histológicas</i> .....	61
3.4.5.1. Tinción de Masson .....	61
3.4.5.2. Tinción de ácido periódico de Schiff .....	61
3.4.5.3. Tinción de Luna.....	61
3.4.5.4. Inmunohistoquímica: tinción de elastasa (neutrófilos), CD3 (linfocitos T) y CD11c (presentadoras)62	
3.4.5.5. Análisis histológico .....	62
3.4.6. <i>Análisis estadístico</i> .....	62
3.4.6.1. Análisis metabólico no dirigido .....	62
3.4.6.2. Análisis metabólico dirigido.....	63
3.4.6.3. Análisis histológico .....	63
<b>4. RESULTADOS</b> .....	<b>65</b>
4.1. BLOQUES I Y II. ESTUDIO DE FENOTIPOS ASMÁTICOS .....	65
4.1.1. <i>Normalización de muestras medidas en distintos lotes</i> .....	65
4.1.2. <i>Pacientes incluidos en el estudio</i> .....	67
4.2. BLOQUE I. ESTUDIO DEL ASMA ALÉRGICO ESTRATIFICADO POR GRAVEDAD .....	68
4.2.1. <i>Descripción de la población de estudio</i> .....	68
4.2.2. <i>Análisis metabólico</i> .....	69
4.2.3. <i>Análisis proteómico</i> .....	86
4.2.4. <i>Construcción de modelos de predicción y aprendizaje automático</i> .....	90
4.3. BLOQUE II. ESTUDIO DEL PAPEL DE LA ALERGIA EN PACIENTES ASMÁTICOS GRAVES NO CONTROLADOS.....	92

4.3.1. Descripción de la población de estudio .....	92
4.3.2. Análisis metabólico .....	92
4.4. BLOQUE III. ESTUDIO DEL PAPEL DE LA ALERGIA EN LA POLIPOSIS NASOSINUSAL.....	100
4.4.1. Descripción de la población de estudio .....	100
4.4.2. Análisis metabólico sistémico en suero.....	100
4.4.3. Análisis metabólico local en pólipo .....	103
4.4.4. Análisis histológico en pólipo y mucosa nasal.....	104
<b>5. DISCUSIÓN.....</b>	<b>109</b>
<b>6. CONCLUSIONES.....</b>	<b>121</b>
<b>7. CONCLUSIONS .....</b>	<b>123</b>
<b>8. BIBLIOGRAFÍA.....</b>	<b>125</b>
<b>ANEXOS.....</b>	<b>143</b>
I. PUBLICACIONES CIENTÍFICAS DERIVADAS DE ESTA TESIS DOCTORAL .....	145
II. OTRAS PUBLICACIONES .....	205
A) Artículos de investigación original.....	205
B) Artículos de revisión bibliográfica.....	205



# Índice de Figuras

<b>Figura 1.</b> Representación esquemática de los cambios que se producen en la vía aérea entre una persona sana (izquierda) y una asmática (derecha). Cuando se desarrolla el asma, se produce un remodelado del tejido. Las glándulas submucosas y las células caliciformes aumentan en volumen, lo que deriva en un exceso en la producción de moco. También se produce una angiogénesis, aumentando la circulación y la infiltración de células inflamatorias, y un aumento en la fibrosis y en el volumen de las células de músculo liso.....	26
<b>Figura 2.</b> Características fenotípicas asociadas a endotipos del asma. <b>LTRA:</b> antileucotrieno. Fuente: (16). .....	28
<b>Figura 3.</b> Esquema de las actuales dianas terapéuticas de medicamentos biológicos aprobados para el tratamiento de asma alérgico. <b>APC:</b> Célula presentadora de antígenos, <b>Eos:</b> eosinófilo, <b>Linf B:</b> linfocito B, <b>Mast:</b> mastocito, <b>Th2:</b> linfocito T colaborador. ....	31
<b>Figura 4.</b> Tratamientos disponibles indicados para asma en función de la gravedad de los pacientes. <b>Leyenda:</b> <b>LABA:</b> agonista adrenérgico de larga duración, <b>LTRA:</b> antileucotrieno, <b>SABA:</b> agonista adrenérgico de corta duración. Fuente: (1). .....	32
<b>Figura 5.</b> Mapa de los niveles del alérgeno Der p 1 en España. Datos cedidos por ALK-Abelló.	33
<b>Figura 6.</b> Esquema de la inflamación asociada a los endotipos asmáticos. El asma alérgico eosinofílico (izquierda) se caracteriza por una respuesta inflamatoria tipo Th2, con infiltración de eosinófilos y producción de IgE. El asma neutrofílico (centro) se caracteriza por una inflamación tipo Th17, donde la actuación de neutrófilos y la señalización por IL-17 son clave. En el asma paucigranulocítico (derecha) la infiltración de células inflamatorias (sobre todo de eosinófilos y neutrófilos) está ausente, pero se caracteriza por un remodelado extensivo del tejido. <b>Leyenda:</b> <b>AC:</b> acetilcolina, <b>APC:</b> célula presentadora de antígenos, <b>EOS:</b> eosinófilo, <b>His:</b> histamina, <b>ILC:</b> célula linfoide innata, <b>Linf B:</b> linfocito B, <b>LT:</b> leucotrieno, <b>Mast:</b> mastocito, <b>MMP:</b> metaloproteasa, <b>NEUT:</b> neutrófilo, <b>PG:</b> prostaglandina, <b>Th:</b> linfocito T colaborador. Fuentes: (3,16,36,46,48).....	34
<b>Figura 7.</b> Comorbilidades del asma. Fuente: (50) .....	35
<b>Figura 8.</b> Matrices más utilizadas en enfermedades respiratorias, como el asma, ordenadas de más a menos invasivas. Fuentes: (70,71). .....	38
<b>Figura 9.</b> Cronología del proceso de descubrimiento de biomarcadores, desde su hallazgo en el laboratorio hasta su aplicación en la clínica. La demostración de la hipótesis de partida implica el diseño de un estudio piloto que incluya un número reducido de pacientes con el objetivo de encontrar un gran número de posibles biomarcadores. Posteriormente, utilizando grandes cohortes de pacientes, se llevan a cabo varias etapas de validación, y solamente aquellos biomarcadores que demuestren su eficacia serán utilizados en la práctica clínica. Fuentes: (72,73) .....	38

**Figura 10.** Diagrama resumen de las biomoléculas que pueden analizarse con cada técnica ómica. Se indica además el número de cada tipo de biomolécula que se estima que hay en el ser humano. Fuentes: (77–79). ..... 39

**Figura 11.** Diagrama del flujo de trabajo utilizado en un análisis de metabolómica no dirigida. .... 41

**Figura 12.** Esquema del modelo de aprendizaje automático. Para la construcción del algoritmo, se utiliza el set de entrenamiento, que está compuesto por el 60% de las muestras utilizadas en el análisis. Utilizando las variables clínicas y metabolómicas de estos pacientes se construye un modelo con los parámetros  $k$  obtenidos con el método del codo. El modelo se utiliza posteriormente para la predicción del set de evaluación, compuesto por el 40% de las muestras restantes, ocultando al programa el grupo al que pertenecen..... 54

**Figura 13.** Análisis PCA de las 165 muestras analizadas para ESI+ (izquierda) y ESI- (derecha) antes de la normalización y tras aplicar las distintas estrategias de normalización (normalización por el patrón interno (IS), normalización por TUS, normalización por QC-SVRC, y normalización combinada QC-SVRC + QC-norm), coloreadas en función del lote en el que se midieron. .... 66

**Figura 14.** Representación de la agrupación de las muestras medidas en más de un lote antes (arriba) y después (debajo) de la normalización con QC-SVRC + QC-norm, para ESI+ (izquierda) y ESI- (derecha). Los puntos están coloreados en función de la muestra y, para los PCA, la forma indica el lote en el que se midió..... 67

**Figura 15.** Análisis PCA de las 87 muestras del **BLOQUE I** para comprobar la calidad de los datos en ESI+ (**A**) y ESI- (**B**). La agrupación de las muestras QC (en negro) prueba que las diferencias entre las muestras (en gris) son debidas a las diferencias entre grupos, y no a las técnicas analíticas.... 69

**Figura 16.** Análisis multivariante de los grupos incluidos en el estudio. Se muestran los resultados para un análisis no supervisado PCA de los cuatro grupos utilizando las 833 señales que cumplieron con los estándares de calidad en polaridad positiva (ESI+) (**A**) y las 565 de la polaridad negativa (ESI-) (**B**). Dado que no se observó una agrupación clara, aunque sí una tendencia para los grupos más extremos, se realizó un nuevo análisis PCA incluyendo solo los grupos ICS y UCA en ESI+ (**C**) y ESI- (**D**). Además, se realizaron dos análisis supervisados: un PLS-DA en ESI+ (**E**) y ESI- (**F**) y un OPLS-DA, también en ambas polaridades ESI+ (**G**) y ESI- (**H**). ICS: azul; IT: amarillo; BIO: naranja; UCA: rojo.  $R^2$  hace referencia a la capacidad de clasificación del modelo; y  $Q^2$ , a la capacidad de predicción. ... 70

**Figura 17.** Análisis multivariante PCA de los grupos ICS y UCA para ESI+ (**A**) y ESI- (**B**), coloreados de acuerdo con el rango de edad. **Leyenda:** En azul, pacientes ICS, siendo azul claro: menores de 35 años; azul oscuro: 35-60 años. En rojo: pacientes UCA, siendo rojo-naranja: menores de 35 años; rojo: 35-60 años; y granate: mayores de 60 años. .... 71

**Figura 18.** *Heatmap* creado tras el análisis de agrupamiento jerárquico (HCA) de los pacientes de los cuatro grupos (en filas), utilizando los 280 metabolitos significativamente distintos entre los pacientes ICS y UCA (en columnas). El color de las celdas representa una expresión disminuida (azul) o aumentada (rojo). Los pacientes y los metabolitos se agruparon según su similitud (izquierda).72

**Figura 19.** Trayectorias de los metabolitos significativamente distintos entre ICS (en azul) y UCA (en rojo). La media se muestra como '+' dentro de las cajas. Se seleccionaron los  $m/z$  más abundantes para aquellos metabolitos en los que se detectó más de un  $m/z$ , o que se detectaron en varias polaridades. \*:  $P<.05$ ; \*\*:  $P<.01$ . *LPC*: lisofosfatidilcolina; *LPE*: lisofosfatidiletanolamina; *LPI*: lisofosfatidilinositol, *PC*: fosfatidilcolina..... 83

**Figura 20.** Cambios en la abundancia de metabolitos en la ruta  $PLA_2$  entre ICS y UCA. *LPC*: lisofosfatidilcolina; *PC*: fosfatidilcolina..... 85

**Figura 21.** Rutas metabólicas relacionadas con los lisofosfolípidos y ácidos grasos encontrados. Se muestra el nombre de cada ácido graso, así como su estructura. El color rojo indica que se encontró aumentado en UCA, mientras que el gris se utiliza para los que no se vieron alterados. *LPC*: lisofosfatidilcolina; *LPE*: lisofosfatidiletanolamina; *LPI*: lisofosfatidilinositol. .... 86

**Figura 22.** Análisis proteómico del suero de los pacientes ICS (azul) y UCA (rojo). **A.** Gráficos de volcán de las diferencias entre ambos grupos de pacientes. **B.** Análisis STRING de las proteínas significativas; en el que se muestran incrementos en los logFC mediante el aumento de la intensidad del color y del tamaño de los círculos. Además, el aumento o reducción en la expresión de una proteína en UCA se muestra en una escala rojo-azul; en la que el rojo indica un aumento y el azul una reducción. **C.** Trayectorias y valores individuales de expresión de proteína en los pacientes. \*:  $P<.05$ ; \*\* $P<.01$ . **NPX**: expresión de proteína normalizada..... 88

**Figura 23.** Representación gráfica del método del codo para los modelos que utilizaban solamente variables clínicas (**A**) o metabolómicas (**B**), y para el método que combina ambos tipos de variables (**C**). .... 90

**Figura 24.** Resultados de los dos modelos de aprendizaje automático ( $k = 2$  y  $k = 3$ , respectivamente) creados con el algoritmo  $k$ -NN. En la imagen se muestran sus valores de precisión, especificidad y sensibilidad, así como su valor predictivo positivo (PPV) y negativo (NPV)..... 91

**Figura 25.** Análisis PCA de las muestras para comprobar la calidad de los datos en las polaridades ESI+ (**A**) y ESI- (**B**). La agrupación de las muestras QC (en negro) prueba que las diferencias que puedan encontrarse en las muestras (en gris) son debidas a las diferencias entre grupos, y no a las técnicas analíticas. .... 93

**Figura 26.** Análisis multivariante para la comparación de los 23 pacientes UCA y UCNA. Se muestran los resultados para un análisis no supervisado PCA de los dos grupos utilizando las 833 señales que cumplieron con los estándares de calidad en polaridad positiva (ESI+) (**A**) y las 565 de

la polaridad negativa (ESI-) (B). Dado que no se observó una agrupación clara, aunque sí una tendencia para los grupos más extremos, se realizó un análisis PLS-DA en ESI+ (B) y ESI- (C) y un OPLS-DA, también en ambas polaridades ESI+ (E) y ESI- (F). Sin embargo, para la polaridad ESI+, no se encontraron modelos supervisados. UCA: rojo; UCNA: morado. R<sup>2</sup> hace referencia a la capacidad de clasificación del modelo; y Q<sup>2</sup>, a la capacidad de predicción. .... 93

**Figura 27.** *Heatmap* creado tras el análisis de agrupamiento jerárquico de los pacientes (en columnas), utilizando los 103 metabolitos significativamente distintos (en filas). El color de las celdas representa una expresión disminuida (azul) o aumentada (rojo). Los pacientes y los metabolitos se agruparon según su similitud (izquierda). .... 94

**Figura 28.** Trayectorias de los metabolitos significativamente distintos entre UCA (en rojo) y UCNA (en morado). La media se muestra como '+' dentro de las cajas. Se seleccionaron los *m/z* más abundantes para aquellos metabolitos en los que se detectó más de un *m/z*. Para aquellos metabolitos con una misma identidad, pero distintos tiempos de retención, se identificaron con su valor *m/z*@RT en lugar de con sus identificaciones. \*: *P*<.05; \*\*: *P*<.01; \*\*\*: *P*<.001. LPC: lisofosfatidilcolina. .... 95

**Figura 29.** Análisis de enriquecimiento para la comparación UCA vs UCNA. En este análisis se representan las categorías de metabolitos que sufren más cambios al comparar ambos grupos.. 97

**Figura 30.** Porcentaje de pacientes del total de alérgicos sensibilizados a cada uno de los aeroalérgenos estudiados..... 100

**Figura 31.** Análisis multivariante PCA de las muestras de plasma en ambas polaridades. El agrupamiento de las muestras QC (en verde) demuestra la calidad de los datos. Ambos grupos (poliposis con alergia, en rojo, y poliposis sin alergia, en azul) se agrupaban juntos, por lo que se intentaron construir modelos supervisados PLS-DA. Sin embargo, no se obtuvieron modelos. .. 101

**Figura 32.** *Heatmap* de los metabolitos obtenidos para la comparación de poliposis alérgica (rojo) y no alérgica (azul) en ESI+ (izquierda) y ESI- (derecha). El color de las celdas indica si los metabolitos (en filas) se encuentran aumentados (rojo) o disminuidos (azul) en cada muestra (en columnas). Las muestras se agrupan en función de su similitud. .... 102

**Figura 33.** *Heatmap* de las abundancias medias de cada metabolito en los grupos..... 103

**Figura 34.** Trayectorias de los metabolitos identificados en el análisis no dirigido en plasma (parte superior) y en el análisis dirigido en pólipo (parte inferior) para los pacientes con poliposis no alérgicos (en azul) y alérgicos (en rojo)..... 103

**Figura 35. A.** Imágenes representativas de tejido de mucosa nasal (parte superior) y pólipo (parte inferior) de pacientes con poliposis no alérgicos (izquierda) y alérgicos (derecha) para la tinción de Luna. Las flechas negras señalan la posición de los eosinófilos (teñidos en rojo), y las barras de escala



indican 50  $\mu\text{m}$ . **B.** Análisis estadístico del infiltrado de eosinófilos en las muestras de tejido anteriores. NA: no alérgico, en azul, A: alérgico, en rojo..... 104

**Figura 36. A.** Imágenes representativas de tejido de mucosa nasal (parte superior) y pólipo (parte inferior) de pacientes con poliposis no alérgicos (izquierda) y alérgicos (derecha) para la tinción con anti-elastasa de neutrófilos. Las flechas negras señalan la posición de los neutrófilos (teñidos en marrón), y las barras de escala indican 50  $\mu\text{m}$ . **B.** Análisis estadístico del infiltrado de neutrófilos en las muestras de tejido anteriores. NA: no alérgico, en azul, A: alérgico, en rojo... 105

**Figura 37. A.** Imágenes representativas de tejido de mucosa nasal (parte superior) y pólipo (parte inferior) de pacientes con poliposis no alérgicos (izquierda) y alérgicos (derecha) para la tinción con anti-CD3. Las flechas negras señalan la posición de las células CD3<sup>+</sup> (teñidas en marrón), y las barras de escala indican 50  $\mu\text{m}$ . **B.** Análisis estadístico del infiltrado de células CD3<sup>+</sup> en las muestras de tejido anteriores. NA: no alérgico, en azul, A: alérgico, en rojo. .... 105

**Figura 38. A.** Imágenes representativas de tejido de mucosa nasal (parte superior) y pólipo (parte inferior) de pacientes con poliposis no alérgicos (izquierda) y alérgicos (derecha) para la tinción con anti-CD11c. Las flechas negras señalan la posición de las células CD11c<sup>+</sup> (teñidas en marrón), y las barras de escala indican 50  $\mu\text{m}$ . **B.** Análisis estadístico del infiltrado de células CD11c<sup>+</sup> en las muestras de tejido anteriores. NA: no alérgico, en azul, A: alérgico, en rojo. .... 106

**Figura 39. A.** Imágenes representativas de tejido de mucosa nasal (parte superior) y pólipo (parte inferior) de pacientes con poliposis no alérgicos (izquierda) y alérgicos (derecha) para la tinción de Masson. Con ella, las fibras de colágeno se tiñen de color verde; los citoplasmas, de color rojo/marrón, y los eritrocitos, de color dorado. Las barras de escala indican 50  $\mu\text{m}$ . **B.** Análisis estadístico del área teñida en verde en las muestras de tejido anteriores. NA: no alérgico, en azul, A: alérgico, en rojo..... 107

**Figura 40. A.** Imágenes representativas de tejido de mucosa nasal (parte superior) y pólipo (parte inferior) de pacientes con poliposis no alérgicos (izquierda) y alérgicos (derecha) para la tinción PAS. Con ella, los polisacáridos, y particularmente las glándulas y células caliciformes del epitelio, se tiñen de rosa fucsia intenso, mientras que los citoplasmas se tiñen de morado/azul. Las barras de escala indican 50  $\mu\text{m}$ . **B.** Análisis estadístico del área teñida en rosa en el epitelio en las muestras de tejido anteriores. NA: no alérgico, en azul, A: alérgico, en rojo. .... 107

**Figura 41.** Perfil metabólico asociado a cPLA<sub>2</sub> en pacientes con asma alérgico grave no controlado. PLA<sub>2</sub> actúa sobre los fosfolípidos de la membrana plasmática liberando lisofosfolípidos y ácidos grasos libres. Los lisofosfolípidos, como las LPC, pueden actuar sobre células diana (eosinófilos) induciendo su activación y causando hiperreactividad bronquial. Entre los ácidos grasos, el ácido araquidónico puede servir como sustrato a distintas enzimas que producen mediadores inflamatorios y de resolución de la inflamación. En la figura, se muestran en rojo

aquellos metabolitos que se encontraron incrementados en los pacientes graves en este estudio.

**EOS:** eosinófilos, **COX:** ciclooxigenasa, **CYP450:** citocromo P450, **LOX:** lisil oxidasa, **LPC:** lisofosfolina, **HETEs:** ácidos hidroxieicosatetraenoicos. .... 112

# Índice de Tablas

<b>Tabla 1.</b> Criterios de clasificación para los pacientes de los <b>BLOQUES I y II</b> incluidos en el estudio. .....	45
<b>Tabla 2.</b> Composición del patrón interno (IS). Los compuestos aparecen ordenados por tiempo de retención.....	48
<b>Tabla 3.</b> Parámetros optimizados para el análisis de MS.....	60
<b>Tabla 4.</b> Información clínica de los pacientes. ....	68
<b>Tabla 5.</b> Resultados del análisis ANCOVA entre los grupos ICS y UCA considerando la edad como una covariable.....	74
<b>Tabla 6.</b> Características fisicoquímicas de las señales anotadas mediante LC-MS/MS significativamente distintas en la comparación UCA vs ICS. ....	76
<b>Tabla 7.</b> Comparaciones dos a dos que muestran el grado de significación y el porcentaje de cambio entre todos los grupos. Las diferencias significativas se marcan en negrita; y los porcentajes de cambio se marcan en color rojo para los metabolitos que aumentan y en azul para los metabolitos que disminuyen. ....	79
<b>Tabla 8.</b> Rutas metabólicas enriquecidas en los pacientes UCA comparados con ICS con un FDR<0.2.....	84
<b>Tabla 9.</b> Expresión diferencial de proteínas en suero entre ICS y UCA. Los valores de expresión de proteína normalizada (NPX) entre ICS y UCA fueron analizados mediante una prueba estadística de t-test .....	87
<b>Tabla 10.</b> Listado de los 25 procesos biológicos de GO más asociados a la expresión de las proteínas significativamente diferentes entre grupos.....	89
<b>Tabla 11.</b> Características clínicas de los pacientes del estudio .....	92
<b>Tabla 12.</b> Características fisicoquímicas y valores estadísticos de las señales anotadas mediante LC-MS/MS significativamente distintas en la comparación UCA vs UCNA.....	96
<b>Tabla 13.</b> Rutas metabólicas enriquecidas significativamente en los pacientes UCA ( $P<.05$ )....	98
<b>Tabla 14.</b> Compuestos encontrados en la comparación de pacientes de poliposis no alérgica y alérgica.....	102



## Abreviaturas y acrónimos

**ACN:** acetonitrilo

**ACT:** test de control del asma

**ADN:** ácido desoxirribonucleico

**AINES:** antiinflamatorios no esteroideos

**ANCOVA:** análisis de covarianza

**ANOVA:** análisis de varianza

**ARG-1:** arginasa 1

**ARN:** ácido ribonucleico

**BAL:** lavado bronco-alveolar

**BIO:** pacientes graves controlados con biológicos anti-IgE

**BRCA2:** gen *Breast Cancer 2*

**CASP-8:** caspasa 8

**CCL-13:** ligando 13 de la quimiocina con motivo C-C

**CCL-19:** ligando 19 de la quimiocina con motivo C-C

**CD:** complejo de diferenciación

**CE:** electroforesis capilar

**CLCA1:** *Chloride Channel Accessory 1*

**COVID-19:** enfermedad del SARS-CoV2

**COX:** ciclooxigenasa

**CRSwNP:** rinosinusitis crónica con pólipos nasales

**CV:** coeficiente de variaciones

**Da:** Dalton

**DALY:** años de vida ajustados por discapacidad

**ECP:** proteína catiónica de eosinófilos

**EPOC:** enfermedad pulmonar obstructiva crónica

**EREA:** enfermedad respiratoria exacerbada por aspirina

**ESI:** ionización por electrospray

**FA:** ácido fórmico

**Fbl:** algoritmo 'Encontrar por Ion'

**FC:** *Fold Change*

**FcεRI:** receptor de IgE de alta afinidad

**FcγR:** receptor de fagocitosis

**FDR:** tasa de falsos positivos

**FeNO:** concentración fraccional de óxido nítrico exhalado

**FEV1:** volumen espiratorio forzado en el primer segundo

**FVC:** capacidad vital forzada

**GATA-3:** proteína 3 de unión a GATA

**GBD:** carga global de la enfermedad (estudio de la revista '*The Lancet*')

**GC:** cromatografía de gases

**GINA:** Iniciativa Global para el Asma

**GO:** ontología genética

**HCA:** análisis de agrupamiento jerárquico

**HETES:** ácidos hidroxieicosatetraenoicos

**HPLC:** cromatografía líquida de alta eficacia

**ICS:** pacientes leves controlados con corticosteroides inhalados o tópicos

**IFNγ:** interferón γ

**Ig:** inmunoglobulina

**IL:** interleucina

**IL-4Rα:** subunidad α del receptor de interleucina 4

**IL-5Rα:** subunidad α del receptor de interleucina 5

**ILC:** células linfoides innatas

**IS:** patrón interno estándar

**IT:** pacientes moderados controlados con inmunoterapia

**k-NN:** algoritmo 'k- vecinos más cercanos'

**LABA:** agonistas adrenérgicos de larga duración

**LC:** cromatografía líquida

**LPA:** ácido lisofosfatídico

**LPC:** lisofosfatidilcolina

**LPE:** lisofosfatidiletanolamina

**LPI:** lisofosfatidilinositol

**LTB4:** leucotrieno B4

**m/z:** masa/carga

**MBP:** proteína básica principal

**MD-2:** factor de diferenciación mieloide 2

**MFE:** algoritmo 'Extracción de Características Moleculares'

**MHC:** complejo mayor de histocompatibilidad

**MS/MS:** espectrometría de masas en tándem

**MS:** espectrometría de masas

**NO:** óxido nítrico

**NPV:** valor predictivo negativo

**NPX:** valores de expresión de proteína normalizados

**OCT RF Vpp:** voltaje de radiofrecuencia del octopolo

**OPLS-DA:** análisis discriminante de las proyecciones ortogonales a las estructuras latentes

**ORMDL3:** proteína reguladora de biosíntesis de esfingolípidos ORMDL 3

**OSM:** oncoestatina M

**PAS:** ácido peródico de Schiff

**PBS:** tampón fosfato salino

**PCA:** análisis de componente principal

**PCR:** reacción en cadena de la polimerasa

**PEA:** análisis de extensión por proximidad

**PFA:** paraformaldehído

**PLA<sub>2</sub>:** fosfolipasa A<sub>2</sub>

**PLS-DA:** análisis discriminante de mínimos cuadrados parciales

**POSTN:** periostina

**PPV:** valor predictivo positivo

**Q:** cuadrupolo

**Q<sup>2</sup>:** capacidad de predicción

**QC:** muestra de control de calidad

**R<sup>2</sup>:** capacidad de clasificación

**RSD:** desviación estándar relativa

**RT:** tiempo de retención

**SABA:** agonistas adrenérgicos de corta duración

**sCD4:** CD4 soluble

**SERPIN B2:** *Serpin Family B Member 2*

**TFA:** ácido trifluoroacético

**Th:** linfocitos T colaboradores

**TNFRSF12:** miembro 12 de la superfamilia de receptores del factor de necrosis tumoral. También conocida como Fn14, TweakR o CD266.

**TOF:** analizador de tiempo de vuelo

**TSLP:** linfopoyetina estromal tímica

**TUS:** señal útil total

**TWSS:** suma total de cuadrados dentro de los grupos

**UCA:** pacientes no controlados alérgicos

**UCNA:** pacientes no controlados no alérgicos

**UV:** escalado de univarianza

**VCAM-1:** molécula de adhesión a células vasculares



# 1. Introducción

## 1.1. Asma

El asma se define como “una enfermedad heterogénea, normalmente caracterizada por la inflamación crónica de las vías aéreas, y que cursa con síntomas respiratorios, tales como sibilancias, dificultad para respirar, opresión en el pecho y tos, que pueden variar a lo largo del tiempo y en intensidad, junto a una limitación variable de la capacidad espiratoria” (1). Aunque el término asma, del griego “jadeo” o “respiración fuerte”, englobaba originalmente todas las enfermedades que dificultaban la respiración, hacia el siglo XIX y XX la definición se refina gracias a los esfuerzos del doctor Henry Hyde Salter, dando lugar a la que se utiliza hoy día (2). Sin embargo, aún hoy, el asma se considera una enfermedad muy heterogénea, y, a veces, el diagnóstico es complejo (3).

Hoy en día, se estima que el asma afecta a entre el 1 y el 18% de la población mundial, y su prevalencia varía según el país (1). El estudio de *Global Burden of Disease 2019* (GBD), publicado por la revista *The Lancet*, hace una estimación del coste que suponen distintas enfermedades a nivel mundial, utilizando como indicador los Años de Vida Ajustados por Discapacidad (*Disability Adjusted Life Year, DALY*), que indican aquellos años de salud perdidos por culpa de la enfermedad debido a la sintomatología, discapacidad, o muerte prematura que ésta puede provocar. El GBD estima que el asma fue responsable de 21.6 millones de DALYs en 2019, lo que supone alrededor de una quinta parte de los DALYs para enfermedades respiratorias. Además, pese a que la prevalencia es mayor en países con índices de desarrollo elevados, el coste de la enfermedad es superior en los países menos desarrollados (4).

El asma es más frecuente en mujeres que en hombres dentro de un mismo grupo de edad. No obstante, esta tendencia es opuesta en la infancia. Una posible explicación puede estar en las hormonas sexuales: mientras que las hormonas femeninas producen un incremento de la inflamación de las vías aéreas en asma, la testosterona tiene el efecto contrario. No obstante, los mecanismos por los que esto sucede no se conocen (5,6).

Debido a la heterogeneidad del asma, es fundamental el diagnóstico diferencial para poder distinguirla de otras enfermedades respiratorias similares, como la enfermedad pulmonar obstructiva crónica (EPOC). La guía de manejo de asma de la organización Iniciativa Global por el Asma (*Global Initiative for Asthma, GINA*) (1) recoge los criterios de práctica clínica para diagnosticar y tratar el asma. En el asma, los síntomas (sibilancias, dificultad para respirar, opresión en el pecho y tos) no suelen aparecer aislados, sino que los pacientes sufren, al menos, dos o más

## Introducción

de ellos simultáneamente. También es indicativa de asma una historia clínica con sintomatología respiratoria frecuente en la niñez (tanto por infecciones víricas frecuentes como por rinitis alérgica), así como eczemas u otros signos de atopia. No obstante, estos criterios no son específicos de asma ni encajan en todos los fenotipos clínicos.

La prueba diagnóstica más utilizada es el análisis del flujo espiratorio variable, que se encuentra limitado en estos pacientes. Los indicadores que se utilizan son el volumen espiratorio forzado en el primer segundo (*Forced expiratory volumen in 1 second, FEV1*), la capacidad vital forzada (*Forced Vital Capacity, FVC*) y el índice de Tiffenau, que relaciona ambos ( $FEV1/FVC$ ). Este último es el indicador más fiable de la limitación espiratoria, ya que el FEV1 puede estar alterado en varias enfermedades. Los volúmenes espiratorios pueden variar en un mismo paciente en distintos momentos, por ello, estas pruebas suelen realizarse en varias ocasiones, y complementarse con otras que permitan medir la respuesta de las vías aéreas como la concentración fraccional de óxido nítrico exhalado (*Fractional concentration of exhaled Nitric Oxid, FeNO*) (1).

A nivel de tejido, el asma lleva asociado un remodelado y una inflamación localizada en las vías áreas (**Figura 1**).

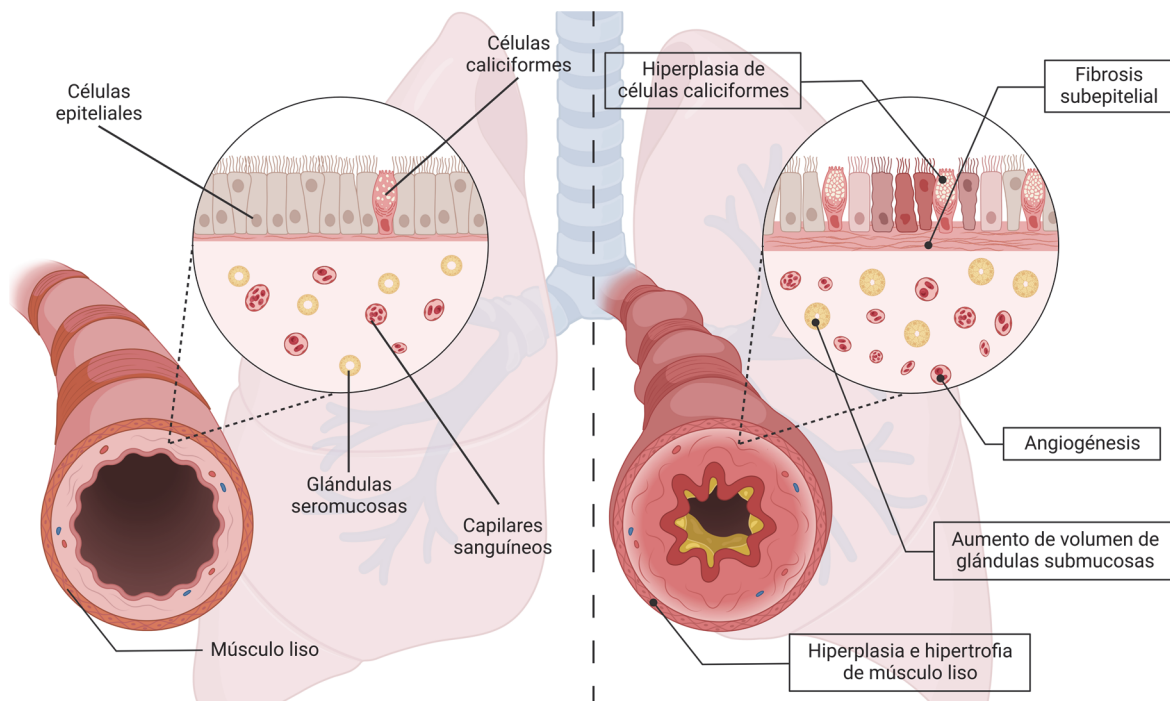


**Figura 1.** Representación esquemática de los cambios que se producen en la vía aérea entre una persona sana (izquierda) y una asmática (derecha). Cuando se desarrolla el asma, se produce un remodelado del tejido. Las glándulas submucosas y las células caliciformes aumentan en volumen, lo que deriva en un exceso en la producción de moco. También se produce una angiogénesis, aumentando la circulación y la infiltración de células inflamatorias, y un aumento en la fibrosis y en el volumen de las células de músculo liso.

El remodelado se caracteriza por el aumento en el volumen de las células del músculo liso, el engrosamiento de la membrana basal, la aparición fibrosis debida al aumento de deposición de

## Introducción

colágeno, la angiogénesis, la proliferación neuronal y la metaplasia del epitelio mucoso. En conjunto, estos cambios afectan a las vías respiratorias, produciendo un aumento de la hipersensibilidad aérea y de la producción de moco (7,8).

Este remodelado está altamente ligado a la inflamación (9). Tradicionalmente, el asma se ha asociado con una inflamación tipo Th2, caracterizada por una infiltración extensiva de eosinófilos, mastocitos y linfocitos T; así como citoquinas tales como las interleucinas (IL-)4, IL-5, IL-9 e IL-13 (10–12). De hecho, los niveles de eosinofilia pueden utilizarse como marcador para clasificar la enfermedad, ya que se encuentran aumentados en el líquido bronco-alveolar (*Bronchoalveolar Lavage*, BAL), el esputo e incluso en la sangre periférica de pacientes con asma; y, en ciertos casos, pueden ayudar a predecir la respuesta a tratamiento (13).

Sin embargo, no todos los pacientes se ajustan a estas características. Hace una década, Woodruff y colaboradores (14) describieron dos fenotipos diferenciales en asma: un fenotipo caracterizado por una inflamación tipo Th2, o 'Th2 *high*', que presentaba niveles altos de POSTN, CLCA1 y SERPINB2 (que, en estudios anteriores, habían descrito como marcadores subrogados de IL-4 e IL-13), y un fenotipo sin inflamación tipo Th2, o 'Th2 *low*', con niveles de estos mismos marcadores indistinguibles de los de la población no asmática. Este segundo grupo de pacientes asmáticos Th2 *low* no responde bien a los tratamientos utilizados para los pacientes con inflamación Th2, lo que apunta a que el mecanismo subyacente es diferente. Gracias a éste y otros experimentos se ha puesto de manifiesto la necesidad de diferenciar los distintos fenotipos del asma y, aún más importante, de entender los distintos endotipos (15).

El fenotipo de una enfermedad describe sus características clínicas observables, las cuales no necesariamente tienen por qué relacionarse con su patogenia. El endotipo, sin embargo, es un término más reciente que se utiliza para describir los subtipos de una enfermedad de forma inequívoca en función de sus características patogénicas (16,17). Conocer los mecanismos subyacentes que llevan al desarrollo del asma (es decir, el endotipo) es muy importante a la hora de entender cómo se desarrolla y, por tanto, cómo tratarla y/o prevenirla. Además, es fundamental relacionar los fenotipos clínicos observables con los endotipos que los causan.

Actualmente, se han descrito varios endotipos de asma (**Figura 2**) (16). Una de las primeras clasificaciones se basaba en dos categorías mayoritarias: el asma alérgico y el asma no alérgico.

## Introducción

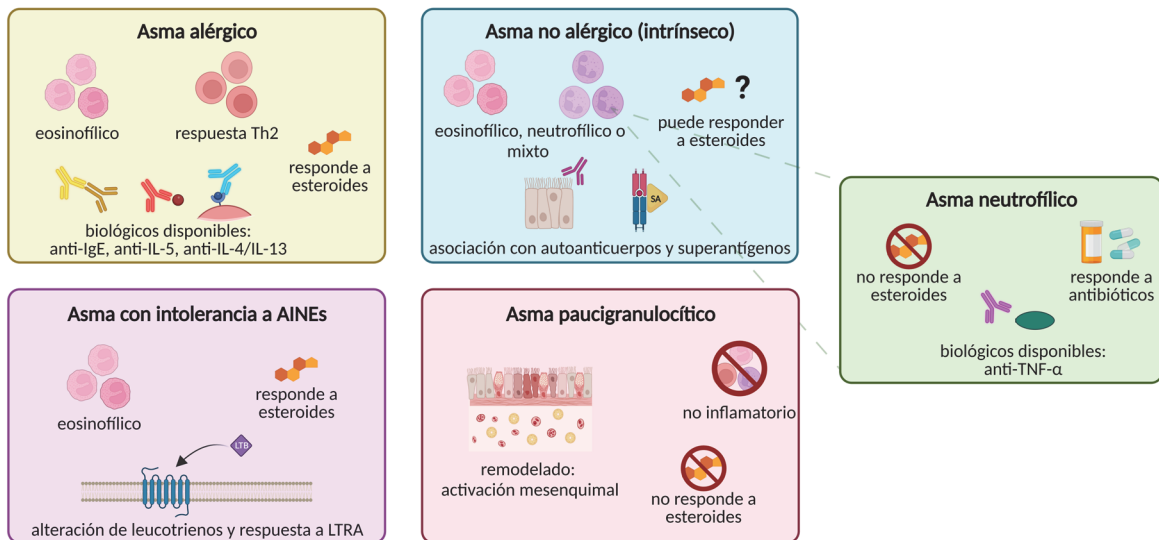


**Figura 2.** Características fenotípicas asociadas a endotipos del asma. **LTRA:** antileucotrieno. Fuente: (16).

### 1.1.1. Asma alérgico

#### 1.1.1.1. Enfermedad alérgica

La alergia es una reacción de hipersensibilidad mediada por IgE frente a una sustancia, denominada alérgeno, y asociada a una inflamación tipo Th2, con infiltración de células efectoras tales como eosinófilos, linfocitos, mastocitos, basófilos o linfocitos Th2 (10) y citoquinas entre las que destacan IL-4, IL-5, IL-9 e IL-13 (11). Esta enfermedad se produce en dos fases: una de sensibilización y otra de reacción.

La sensibilización alérgica se produce cuando el sistema inmune entra en contacto con el alérgeno en un ambiente que favorece el desarrollo de una respuesta inflamatoria tipo Th2 en lugar de una respuesta reguladora o tolerogénica. Esta respuesta es iniciada por citoquinas epiteliales tales como TSLP, IL-25 e IL-33, que son secretadas en un contexto de daño epitelial. Así, el alérgeno es reconocido por fagocitos y células presentadoras de antígenos, que lo presentan mediante el complejo principal de histocompatibilidad tipo 2 (*Major Histocompatibility Complex type 2*, MHC-II) a los linfocitos T *naïve* y, en el contexto de estas citoquinas epiteliales, se activa una diferenciación a linfocitos Th2, caracterizada por el factor de transcripción GATA-3 y la producción de IL-4, IL-5, IL-9 e IL-13. A su vez, los linfocitos Th2 favorecen la activación y diferenciación de linfocitos B, y el cambio de isotipo a IgE. Durante la fase de reacción, esta IgE específica del alérgeno (sIgE), unida al receptor Fc $\epsilon$ RI de mastocitos y basófilos, es capaz de reconocer el alérgeno cuando se produce un nuevo contacto, y produce reacciones inmediatas al inducir la desgranulación de mastocitos, basófilos y eosinófilos.

## Introducción

Las citoquinas epiteliales también activan la diferenciación de las células linfoides innatas (*innate lymphoid cells*, ILC) a ILC2, las cuales, al igual que los linfocitos Th2, producen IL-5, IL-9 e IL-13. Estas citoquinas favorecen la estimulación de las células caliciformes, así como la activación de eosinófilos y mastocitos (11).

En los últimos años, la incidencia de la patología alérgica ha ido en aumento (18). Existen dos hipótesis aceptadas por la comunidad científica que podrían explicar este hecho. Una de ellas es la hipótesis de la higiene, que sostiene que la mejora de las condiciones de vida gracias al acceso generalizado a aguas no contaminadas y al aumento en el uso de productos de higiene o cosméticos podría causar una pérdida de tolerancia. Esto iría acompañado de una disminución de enfermedades parasitarias en los países industrializados; lo que en conjunto favorecería que el sistema inmune reaccionara a otros estímulos inocuos, como los alérgenos (19).

Esta hipótesis se relaciona con la hipótesis del daño de la barrera protectora (20), según la cual existen diversos factores (como las infecciones víricas o bacterianas, algunos alérgenos con actividad proteasa, como los de los ácaros del polvo, los agentes tóxicos presentes en jabones y detergentes, o determinados contaminantes ambientales) que son capaces de dañar la barrera epitelial. Este daño permitiría el acceso de los alérgenos y otras sustancias al sistema inmune, además de inducir un ambiente proinflamatorio por la producción de citoquinas epiteliales en respuesta a esos agentes externos.

Ambas hipótesis pueden contribuir a explicar el aumento en el número de casos de alergia que está teniendo lugar en los últimos años, ya que la industrialización ha llevado consigo tanto el aumento en la higiene como en los niveles de contaminación (18).

La respuesta inflamatoria que tiene lugar en la patología alérgica (o en otras patologías) es una respuesta fisiológica de defensa ante un daño externo. Cuando este cesa, es necesario poner fin a la respuesta activa y reparar el tejido (21). Si este sistema de resolución de la inflamación falla, o si se producen exposiciones muy recurrentes que produzcan una activación continuada del sistema inmune, se produce la cronificación de la inflamación. Esto da lugar al desarrollo de fenotipos más graves, ya que la reparación incompleta del tejido produce remodelados. Un ejemplo puede ser el asma, particularmente en sus fenotipos más graves (22).

### *1.1.1.2. Asma alérgico*

El asma alérgico o extrínseco es aquel asociado a la rinitis alérgica en un individuo. Es, por tanto, un fenotipo asociado a una inflamación tipo Th2, con infiltrados de células efectoras tales como eosinófilos y mastocitos. Entre un 50 y un 80% de los pacientes asmáticos tienen un fenotipo de asma alérgico (23–25); y su prevalencia se encuentra en aumento, mientras que la del asma no

## Introducción

alérgico se mantiene estable (26). En concreto, la sensibilización a ácaros del polvo se asocia con el desarrollo del asma (27), con hasta un 85% de los pacientes asmáticos sensibilizados a estos alérgenos (28).

Los ácaros del polvo son arácnidos responsables de un gran número de las reacciones alérgicas (29). Se encuentran frecuentemente en ambientes de interior, particularmente en textiles como los colchones o la ropa (30). Son muy comunes en islas y zonas tropicales, ya que el clima de alta humedad y temperaturas cálidas estables favorece su crecimiento. En estas zonas la sensibilización alérgica es muy común, y la prevalencia de asma se encuentra aumentada (29,31–33). Además, algunos pacientes graves alérgicos a ácaros del polvo sufren reacciones anafilácticas tras el consumo de harinas contaminadas (34).

Los motivos por los que existe una relación entre alergia a ácaros y asma no están aún bien definidos, si bien algunas hipótesis apuntan a las características de los alérgenos de los ácaros del polvo. Algunos de estos alérgenos tienen actividad proteasa (Der p 1, Der f 1, Blo t 1, Der p 3, Der p 6, Der p 9, ...), siendo capaces de dañar el tejido y permitir que penetren otros alérgenos, facilitando su contacto con el sistema inmune; otros funcionan como activadores del sistema inmune de distintos tipos, tales como proteínas de unión a lípidos (Der p 5, Der p 7, Der p 21), análogos del factor 2 de diferenciación mielóide (*Myeloid Differentiation factor 2*, MD-2) (Der p 2, Eur m 2) o proteínas asociadas a quitina, que favorecen la respuesta Th2 (Der p 23) (29).

Uno de los factores que puede afectar a la evolución de la enfermedad es la edad de inicio. El asma alérgico que debuta en la niñez suele asociarse a la presencia de otras enfermedades alérgicas, como dermatitis atópica, y suele derivar a formas más agresivas de la enfermedad (3). Algo similar parece ocurrir en las infecciones por virus respiratorios en la niñez, relacionadas con el desarrollo de asma (7), que podrían impedir una correcta maduración del epitelio de las vías respiratorias.

Para el tratamiento del asma alérgico, caracterizado por una inflamación tipo Th2, se utilizan diversos fármacos, incluyendo glucocorticoides en distintas aplicaciones (tópicos, inhalados u orales), que suelen aplicarse de forma intermitente; broncodilatadores de acción corta o duradera, antileucotrienos y/o anticolinérgicos; siendo frecuente que se prescriba una combinación de ellos. Los corticoides orales se reservan para los casos más graves (1). Algunos pacientes se benefician de la inmunoterapia, tratamiento capaz de modificar la enfermedad alérgica y detenerla, mejorando sus síntomas respiratorios. Para los pacientes graves está indicado el uso de medicamentos biológicos, destinados a bloquear las rutas inflamatorias activadas en la enfermedad (**Figura 3**). Entre ellos se incluyen omalizumab (anti-IgE, el primero aprobado para su uso en asma),

mepolizumab y reslizumab (anti-IL5, que bloquean la proliferación de eosinófilos), benralizumab (anti-IL-5R $\alpha$ , que bloquea la señalización de IL5 de forma similar a los anteriores) y dupilumab (anti-IL-4R $\alpha$ , que permite bloquear la señalización por IL-4 e IL-13). Además, existen otros biológicos que se encuentran actualmente en desarrollo, como tezepelumab (anti-TSLP, citoquina proinflamatoria asociada a la barrera epitelial) (35,36). Estos tratamientos se han aprobado para asma grave de manera secuencial; y funcionan para asma asociada a alergia, eosinofilia, y respuesta Th2. Pese a ello, existe un porcentaje de pacientes que no responden a las medicaciones disponibles. Estos pacientes asmáticos graves no controlados se caracterizan por una falta de respuesta a los tratamientos disponibles, la presencia de comorbilidades, y una peor calidad de vida debido a que sufren exacerbaciones frecuentes y, a menudo, hospitalizaciones (1,37–39).

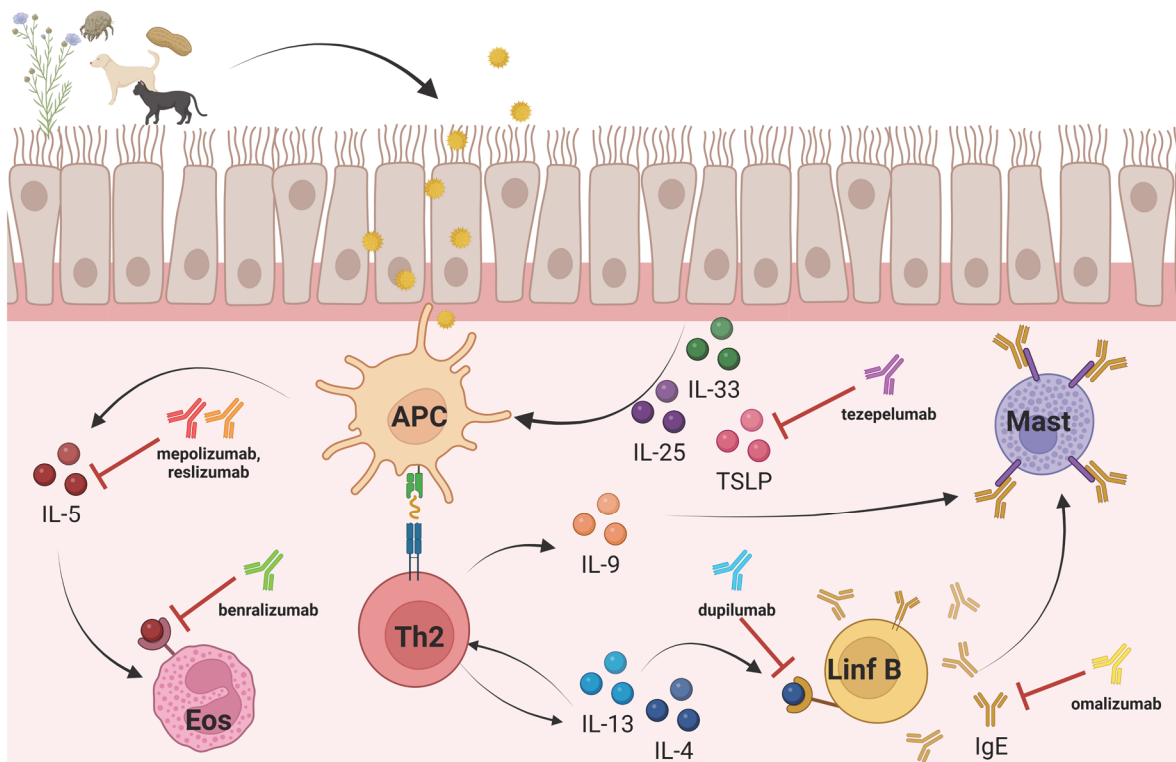


**Figura 3.** Esquema de las actuales dianas terapéuticas de medicamentos biológicos aprobados para el tratamiento de asma alérgico. **APC:** Célula presentadora de antígenos, **Eos:** eosinófilo, **Linf B:** linfocito B, **Mast:** mastocito, **Th2:** linfocito T colaborador.

#### 1.1.1.2.1. Asma alérgico grave no controlado

La clasificación de pacientes asmáticos puede hacerse de acuerdo al tratamiento que necesitan, según la guía GINA o sus homólogas en cada país (**Figura 4**) (1). Pese a todas las medicaciones disponibles, existe un porcentaje de pacientes (entre un 3% y un 10%) que no responde a ninguna de ellas, y cuyos síntomas permanecen sin controlar. Estos pacientes suelen tener más comorbilidades asociadas, además de una peor calidad de vida, dadas las exacerbaciones recurrentes, y una mortalidad aumentada (40,41). Particularmente, en zonas como las Islas Canarias o Reino Unido, donde

## Introducción

la exposición a ácaros es alta por sus condiciones climáticas, entre un 16% y un 18% de pacientes tienen asma no controlado (**Figura 5**) (42,43).

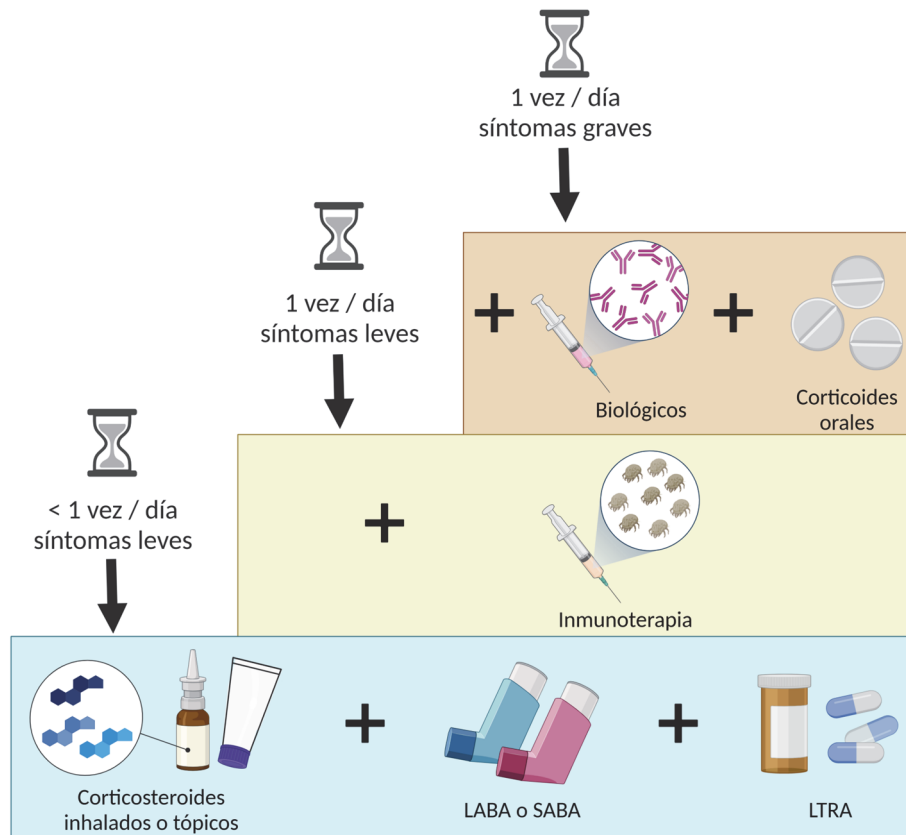


**Figura 4.** Tratamientos disponibles indicados para asma en función de la gravedad de los pacientes. **Leyenda:** LABA: agonista adrenérgico de larga duración, LTRA: antileucotrieno, SABA: agonista adrenérgico de corta duración. Fuente: (1).

Estos pacientes difíciles de tratar conllevan un gran gasto en los servicios de salud, al necesitar visitas frecuentes al hospital para el seguimiento de su enfermedad, tratamientos de rescate durante las frecuentes exacerbaciones y, en algunos casos, hospitalizaciones (44,45).

La estrategia de intervención actual se basa en una pauta de tratamiento seriada desde el tratamiento más leve al más agresivo, que se elige según la sintomatología del paciente. El problema de esta estrategia es que incluso aquellos pacientes que son capaces de responder a alguno de los tratamientos disponibles permanecen sin controlar durante un tiempo indeterminado, si el tratamiento prescrito no es suficiente para su control.

El uso de biomarcadores que permitan estratificar a los pacientes podría facilitar este proceso. Si es posible distinguir desde el inicio qué pacientes van a responder a qué medicación, el tiempo desde el diagnóstico hasta el control de la enfermedad se verá significativamente disminuido; y será posible detener la progresión de la enfermedad.



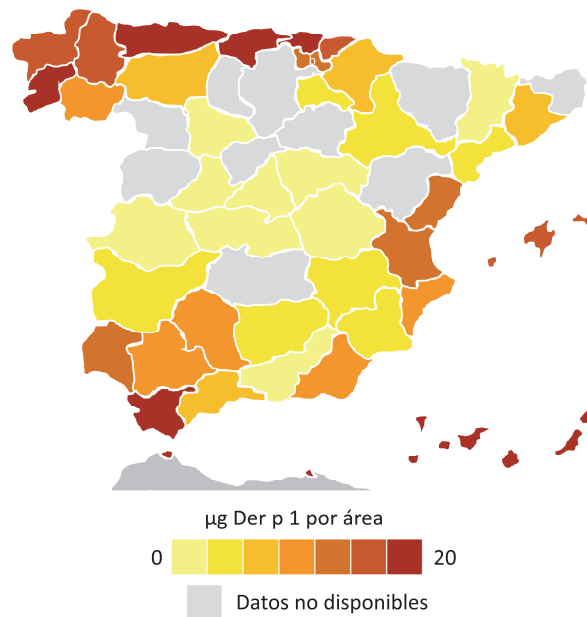


**Figura 5.** Mapa de los niveles del alérgeno Der p 1 en España. Datos cedidos por ALK-Abelló.

### 1.1.2. Asma no alérgico

El asma no alérgico o intrínseco es aquel que no se asocia con un diagnóstico de alergia en el paciente, por lo que no se producen exacerbaciones en presencia de un agente externo. Es más común que aparezca en mujeres adultas a partir de los 30 años; de hecho, se calcula que, a partir de los 40 años, la mayoría de nuevos casos diagnosticados de asma son en ausencia de sensibilización alérgica. En cambio, sólo entre un 20 y un 30% del asma diagnosticado en la infancia es no alérgico (23,24).

El perfil inflamatorio de estos pacientes es más heterogéneo que en los pacientes con asma alérgico (**Figura 6**). Algunos pacientes presentan una inflamación tipo Th2, al igual que los pacientes con asma alérgico, con eosinófilos, linfocitos Th2, y mastocitos activados, aunque, según se ha descrito, sin IL-4 (16). En otros pacientes, particularmente aquellos en los que el asma no alérgico debuta en la infancia, la inflamación se caracteriza por la neutrofilia, con una señalización mediada por IL-8, IL-17A y LTB4 (16). Además, algunos pacientes presentan una infiltración mixta de eosinófilos y neutrófilos, y otros tienen un perfil paucigranulocítico, sin eosinófilos ni neutrófilos (46). Los endotipos Th2-*low* han sido tradicionalmente menos estudiados, por lo que sus mecanismos subyacentes no son conocidos en tanto detalle como los del asma Th2-*high*.

El tratamiento en pacientes con asma no alérgico es complejo. En general, en los pacientes que no tienen una inflamación tipo Th2, la respuesta a los tratamientos clásicos, como corticosteroides, y a algunos más modernos, como los medicamentos biológicos aprobados para asma, es limitada. En estos pacientes pueden utilizarse macrólidos (antibióticos caracterizados por un anillo

## Introducción

macrocíclico de 14 a 16 carbonos, como la eritromicina), cuyo éxito ha sido probado en otras enfermedades de infiltración neutrofílica. Sin embargo, su uso extensivo puede representar un problema debido a los efectos secundarios que producen y, sobre todo, al posible desarrollo de resistencias microbianas. Otras terapias en desarrollo son, por ejemplo, el uso de antagonistas de muscarínicos de larga duración, aunque su efecto es limitado, o la termoplastia bronquial, aunque el mecanismo de acción de esta última no se conoce en profundidad (47).

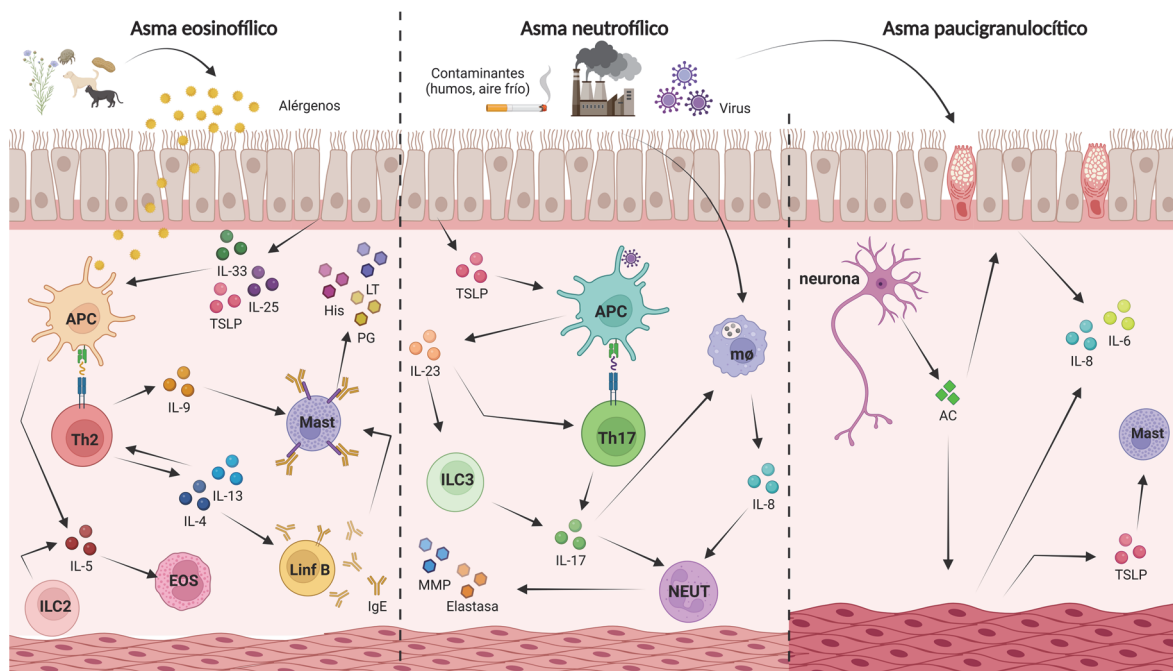


**Figura 6.** Esquema de la inflamación asociada a los endotipos asmáticos. El asma alérgico eosinofílico (izquierda) se caracteriza por una respuesta inflamatoria tipo Th2, con infiltración de eosinófilos y producción de IgE. El asma neutrofílico (centro) se caracteriza por una inflamación tipo Th17, donde la actuación de neutrófilos y la señalización por IL-17 son clave. En el asma paucigranulocítico (derecha) la infiltración de células inflamatorias (sobre todo de eosinófilos y neutrófilos) está ausente, pero se caracteriza por un remodelado extensivo del tejido. **Legenda:** AC: acetilcolina, APC: célula presentadora de antígenos, EOS: eosinófilo, His: histamina, ILC: célula linfocítica innata, Linf B: linfocito B, LT: leucotrieno, Mast: mastocito, MMP: metaloproteasa, NEUT: neutrófilo, PG: prostaglandina, Th: linfocito T colaborador. Fuentes: (3,16,36,46,48).

El asma no alérgico se asocia, además, a la enfermedad respiratoria exacerbada por la aspirina (EREA), caracterizada por la presencia de pólipos nasales y la hipersensibilidad a antiinflamatorios no esteroideos (AINES) (16).

El desencadenante en el asma no alérgico, a diferencia de en el asma alérgico, es desconocido; si bien las infecciones víricas también pueden jugar un papel. En este sentido, la aparición de la enfermedad producida por el coronavirus SARS-cov-2 (COVID-19) y otros virus que afecten a las vías respiratorias podrían inducir el desarrollo de asma en pacientes con predisposición genética (49). Por ello, desarrollar tratamientos más eficaces para pacientes, particularmente para aquellos

cuya activación de la ruta eosinofílica y Th2 es reducida, es urgente; y, para ello, encontrar biomarcadores que permitan una clasificación más específica es fundamental.

### 1.1.3. Comorbilidades de asma

El asma se ha asociado a diversas enfermedades, incluyendo obesidad, rinosinusitis (incluyendo rinosinusitis crónica, poliposis nasal y EREA), reflujo gastroesofágico, apnea del sueño, depresión y/o ansiedad (**Figura 7**) (50).

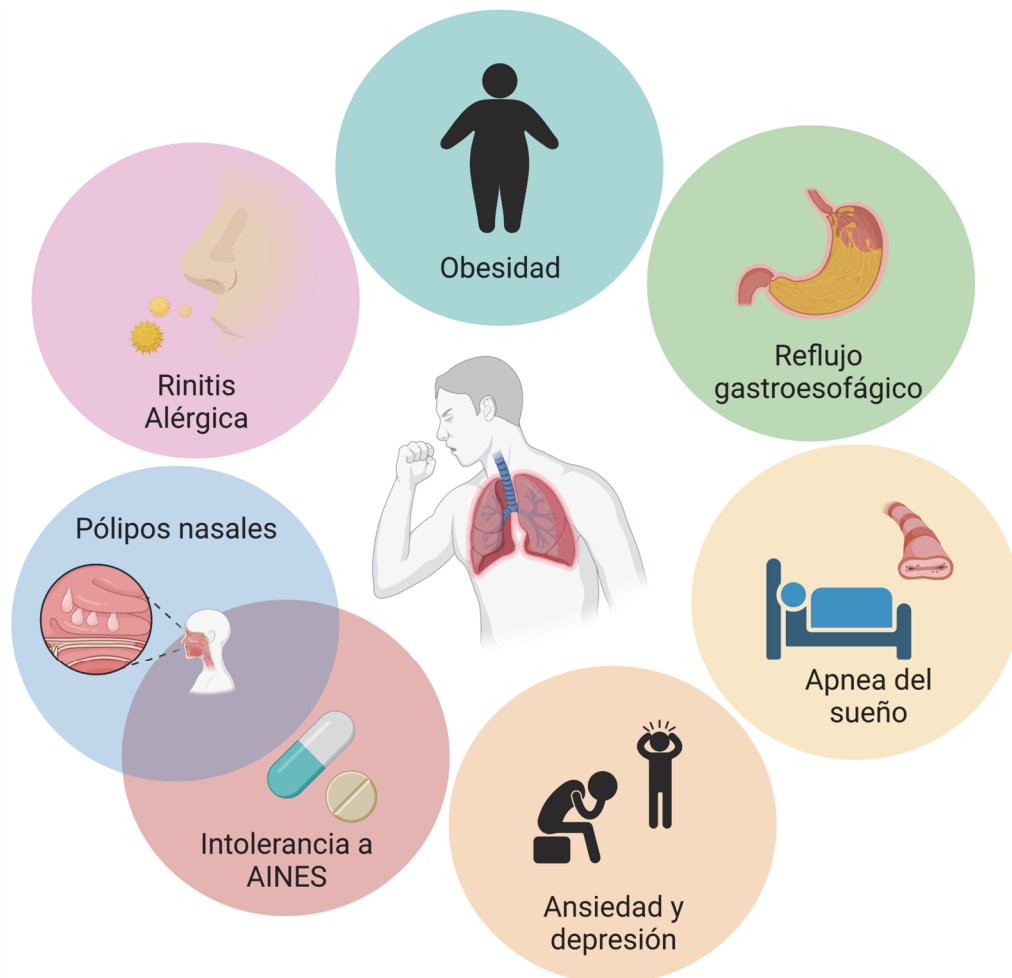


**Figura 7.** Comorbilidades del asma. Fuente: (50)

#### 1.1.3.1. Obesidad

Existe una fuerte correlación entre la obesidad y el asma. Un índice de masa corporal (IMC) igual o superior a 30 aumenta significativamente el riesgo de desarrollar asma en la edad adulta, particularmente cuando la acumulación de grasa se produce en la zona abdominal. Del mismo modo, el asma también puede predisponer a la obesidad. Además, parece que la obesidad se asocia a perfiles inflamatorios neutrofílicos, más que a los eosinofílicos (51). Por otra parte, existen estudios que describen un perfil inflamatorio más activo en pacientes asmáticos obesos que en

## Introducción

pacientes no obesos, lo que podría relacionar la obesidad con la gravedad del asma (52). Se ha descrito que asma, obesidad, reflujo gastroesofágico y apnea de sueño se relacionan entre sí, alimentándose en una especie de “cuadrado” vicioso (53).

### *1.1.3.2. Reflujo gastroesofágico*

La enfermedad de reflujo gastroesofágico se relaciona con asma y otras enfermedades respiratorias, posiblemente porque la aspiración de jugos gástricos es capaz de dañar las vías aéreas. Entre un 50-80% de los pacientes con asma presentan síntomas de reflujo gastroesofágico (50). Los pacientes con asma y reflujo sufren un descenso en su calidad de vida y un peor control de la enfermedad. En parte, esto se debe a que ciertas medicaciones utilizadas para el control del asma, como los broncodilatadores, favorecen la aparición de reflujo (54).

### *1.1.3.3. Rinitis alérgica, rinosinusitis crónica y pólipos nasales*

La rinitis alérgica y la rinosinusitis crónica tienen una prevalencia aumentada en la población asmática. En particular, la rinosinusitis crónica asociada a poliposis nasosinusal (*Chronic Rhinosinusitis with Nasal Polyps*, CRSwNP) se asocia al asma no alérgico (1,3).

La CRSwNP es una enfermedad inflamatoria crónica de los senos paranasales que conlleva la aparición de un pólipo nasal, con una prevalencia estimada de entre el 1% y el 4% de la población (55). Un pólipo es un crecimiento tumoral benigno del tejido, que se caracteriza por la aparición de edema y/o fibrosis (dando lugar a fenotipos diferenciados (56)), el engrosamiento de la membrana basal, y la infiltración de células inflamatorias (57,58). Los pacientes con pólipos nasales presentan mucosidad recurrente, tos, dificultad para respirar, pérdida parcial o total de olfato y, en los casos más graves, un bloqueo total del tracto respiratorio superior (59,60). Para el tratamiento se utilizan corticoides tópicos para los casos más leves, y biológicos (como omalizumab o mepolizumab), además de la intervención quirúrgica para la extirpación del pólipo, en los casos más graves (60,61). Sin embargo, los pólipos pueden reaparecer en hasta el 70% de los casos (62).

Su etiopatología es desconocida, si bien se cree que la aparición de pólipos está supeditada a la presencia de una inflamación crónica en el tejido que resulta en un remodelado debido al sistema de reparación (63–65). La asociación entre CRSwNP y alergia es controvertida, existiendo evidencias tanto a favor como en contra (66). No obstante, en el contexto del asma, la CRSwNP se asocia al asma no alérgico, tanto si aparece junto a hipersensibilidad a AINES (EREA) como si no.

### *1.1.3.4. Enfermedad respiratoria asociada a aspirina*

La EREA, también conocida como ASA triada, es una enfermedad causada no por una reacción alérgica, sino por una intolerancia a AINES relacionada con la acción de estos fármacos sobre COX-

1, enzima implicada en el metabolismo del ácido araquidónico (67). Aparece en entre un 5% y un 10% de pacientes asmáticos cuya enfermedad debutó en la adultez, siendo rara en niños, y más frecuente en mujeres que en hombres. Esta enfermedad conlleva una exacerbación del asma ante la toma de aspirinas y otros AINES, asociada a la presencia de CRSwNP (68,69).

Como ha quedado reflejado a lo largo de la introducción, el asma es una enfermedad compleja, en la que la elección del tratamiento es difícil. Además, no existen tratamientos efectivos para todos los pacientes, y se desconoce el porqué. Entender los mecanismos subyacentes en estos fenotipos permitiría diseñar tratamientos personalizados, frenando la progresión de la enfermedad y mejorando la calidad de vida de los pacientes. Para ello, la identificación de biomarcadores que permitan la estratificación de los pacientes de forma objetiva es fundamental.

## 1.2. Biomarcadores

Un biomarcador es una característica que puede ser medida de forma objetiva y evaluada como indicador de procesos biológicos normales, procesos patogénicos, o respuesta a intervenciones terapéuticas (70). Para este fin, pueden utilizarse como biomarcadores valores *in vivo* de pruebas diagnósticas (como las pruebas cutáneas o las de provocación, utilizadas para el diagnóstico de alergias), niveles de células o proteínas en un tejido, perfiles genéticos, etcétera.

En función de la utilidad del biomarcador, se distinguen varios tipos, tales como biomarcadores diagnósticos (que pretenden un diagnóstico sensible y afinado; por ejemplo, la medida de IgE nos permite determinar el alérgeno contra el que se está sensibilizado), biomarcadores pronósticos (que dan información sobre la evolución del paciente; como pueden ser los niveles de eosinofilia en pacientes con asma) y marcadores predictivos (que identifican la probabilidad de que un determinado individuo responda favorablemente a un tratamiento; en asma, no existen ejemplos de marcadores de este tipo, pero sí los hay en otras enfermedades, como es el caso de la mutación BRCA2 en cáncer).

Un biomarcador ideal debe ser sensible, específico, predictivo, rápido y económico de medir, estable en la muestra biológica, poco invasivo, y presentar relevancia preclínica. Para que cumpla todos estos requisitos, además de la selección del propio biomarcador, es importante la elección de la matriz en la que se va a medir (**Figura 8**).

## Introducción

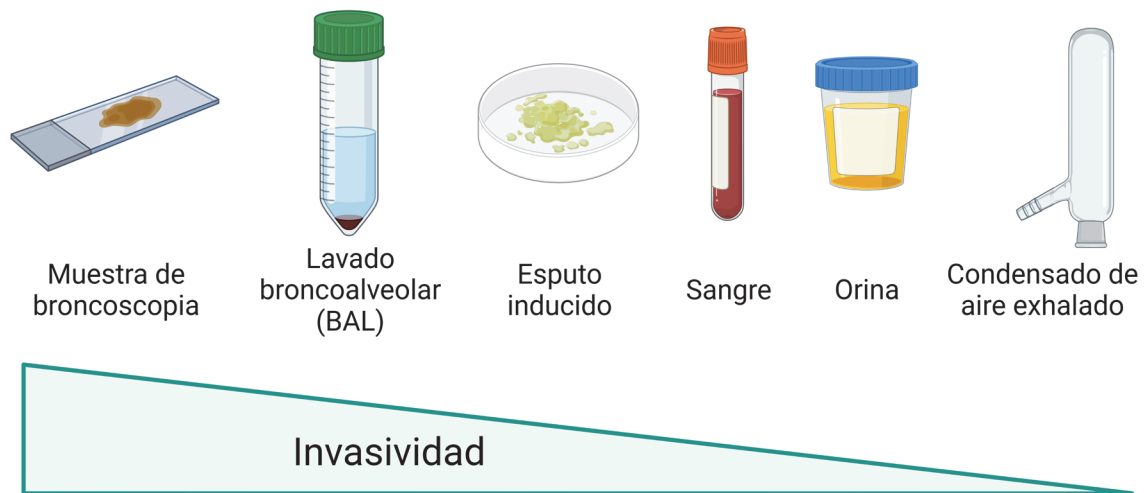


**Figura 8.** Matrices más utilizadas en enfermedades respiratorias, como el asma, ordenadas de más a menos invasivas. Fuentes: (70,71).

Por otra parte, la búsqueda de biomarcadores es un proceso largo y complicado, que requiere de una gran inversión (**Figura 9**). En ese sentido, el reciente desarrollo de las técnicas ómicas ha permitido que el descubrimiento de biomarcadores candidatos se agilice, al permitir el análisis simultáneo de un gran número de biomoléculas.

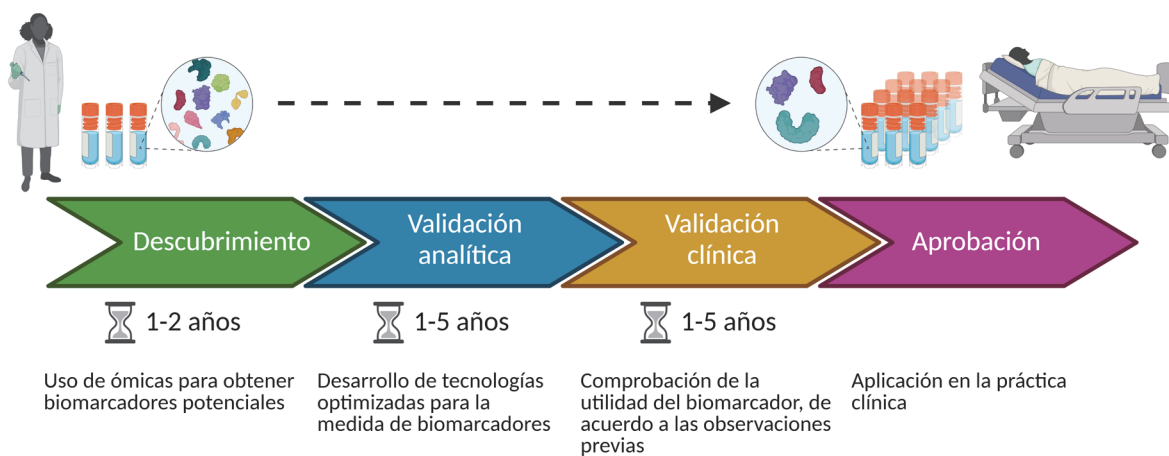


**Figura 9.** Cronología del proceso de descubrimiento de biomarcadores, desde su hallazgo en el laboratorio hasta su aplicación en la clínica. La demostración de la hipótesis de partida implica el diseño de un estudio piloto que incluya un número reducido de pacientes con el objetivo de encontrar un gran número de posibles biomarcadores. Posteriormente, utilizando grandes cohortes de pacientes, se llevan a cabo varias etapas de validación, y solamente aquellos biomarcadores que demuestren su eficacia serán utilizados en la práctica clínica. Fuentes: (72,73)

### 1.3. Ciencias ómicas: Metabolómica

Las ciencias ómicas son técnicas que utilizan aproximaciones de alto rendimiento para medir simultáneamente un gran número de biomoléculas. Existen varios tipos de ómicas en función de la información que proporcionan (**Figura 10**): la genómica permite el análisis de la totalidad del ADN;

## Introducción

la transcriptómica, el análisis de los transcritos de ARN; la proteómica, el análisis de conjunto de las proteínas de una muestra, y la metabolómica, el análisis del conjunto de metabolitos de un sistema. Además, existen algunos tipos particulares de cada una de ellas, como la epigenómica, que analiza las modificaciones epigenéticas del ADN; la lipidómica, que se centra sólo en los metabolitos lipídicos, o la microbiómica, que se encarga del análisis de las distintas especies microbianas de una muestra (normalmente mediante el estudio metagenómico) (74,75).

La elección de la técnica adecuada depende del problema o planteamiento que se quiera abordar, y la integración de varios tipos de ómicas resulta una de las estrategias más interesantes a la hora de entender el funcionamiento de un sistema, ya que permite analizar distintos conjuntos de datos procedentes del análisis de distintos tipos de moléculas y relacionarlos entre sí (76).

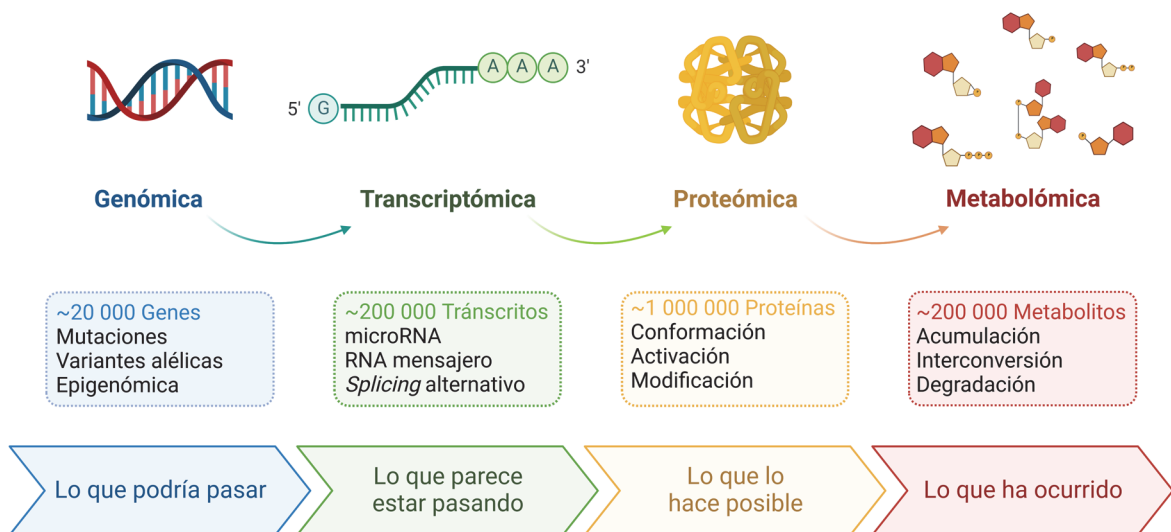


**Figura 10.** Diagrama resumen de las biomoléculas que pueden analizarse con cada técnica ómica. Se indica además el número de cada tipo de biomolécula que se estima que hay en el ser humano. Fuentes: (77–79).

La metabolómica se encarga del estudio del metaboloma, o conjunto de metabolitos, de una muestra. Los metabolitos son los compuestos finales o intermediarios del metabolismo, y presentan un bajo peso molecular (<1500Da). Esta técnica permite obtener información precisa sobre el estado del sistema en el momento de la medición, ya que la composición de metabolitos es altamente variable (80).

Existen dos aproximaciones distintas en metabolómica, que pretenden responder a diferentes preguntas. En la búsqueda de biomarcadores, donde el objetivo es encontrar un gran número de metabolitos diferencialmente expresados entre grupos, lo ideal es utilizar métodos no dirigidos, en los que se fragmentará y medirá el total de los compuestos que hayan sido extraídos en la muestra (si bien qué compuestos serán visibles dependerá de la técnica utilizada). Aunque esta aproximación genera una cantidad de datos mayor, las abundancias obtenidas son

## Introducción

semicuantitativas, por lo que no es posible medir la concentración exacta de una sustancia en la muestra. Por otra parte, también es posible seleccionar un número reducido de metabolitos y, mediante el uso de métodos dirigidos, cuantificar con exactitud sus concentraciones en una muestra, al comparar las abundancias de cada metabolito con las de una curva patrón preparada con un estándar de ese metabolito de concentración conocida. Esta técnica resulta útil a la hora de validar los biomarcadores.

La metabolómica no dirigida sigue, habitualmente, un esquema como el representado en la **Figura 11**. En la recolección de la muestra, es importante tener en cuenta que factores como el tiempo de ayuno o los ritmos circadianos en el momento de la recogida pueden influir en el metaboloma. Además, la conservación de la muestra a largo plazo requiere de bajas temperaturas (preferiblemente, por debajo de los  $-80\text{ }^{\circ}\text{C}$ ), siendo muy importante evitar los ciclos de congelación/descongelación para impedir la degradación de los metabolitos (81).

Por otra parte, es necesario aislar los metabolitos de forma eficiente (eliminando las proteínas y concentrando la muestra), además de conseguir un extracto compatible con la técnica a utilizar. La elección de la técnica depende de las características de los compuestos que se quieran analizar (como el tamaño, la polaridad o la volatilidad). Así, la cromatografía de líquidos (LC) separa los compuestos en función de su polaridad, permitiendo ver un amplio rango de metabolitos; la cromatografía de gases (GC) permite medir compuestos muy volátiles; y la electroforesis capilar (CE), compuestos de pequeño tamaño (82). El desarrollo de técnicas de mayor resolución ha permitido aumentar la sensibilidad de la técnica y obtener más metabolitos en una sola lectura (83).

El análisis instrumental, pese a su complejidad, es la parte más breve del proceso y, tras realizarlo, las señales adquiridas tienen que ser procesadas, para lo que se utilizan *softwares* comerciales. A lo largo de este procesamiento se realiza una corrección del ruido, y se comprueba que los picos detectados son correctos y están bien integrados de forma individual, así como la alineación de los cromatogramas en las muestras (84). Después, se realiza un análisis estadístico; y los compuestos significativamente distintos entre grupos se analizan para su identificación mediante plataformas *online* y bases de datos, como HMDB (*Human Metabolome Database*), METLIN, o CEU Mass Mediator (79,85,86). Por último, los compuestos obtenidos se asocian con sus posibles funciones biológicas y su participación en rutas metabólicas para obtener una interpretación biológica de lo que puede estar ocurriendo. Este proceso se realiza mediante búsquedas bibliográficas, así como con herramientas tales como Metaboanalyst o HMDB (84).

Una de las desventajas de la aproximación no dirigida es la necesidad de medir todas las muestras de una sola vez, dado que no se obtienen concentraciones absolutas sino valores relativos



## Introducción

que sólo se pueden comparar con otros medidos en las mismas condiciones, sin interrupción del método. Dependiendo de la técnica, el número de muestras que se pueden medir de una vez es limitado, debido a factores como la caída de señal asociada a la acumulación de suciedad en la fuente de ionización, o la duración de la medida de cada muestra. Recientemente se han desarrollado algunas estrategias, como la medida simultánea de varias muestras mediante inyección seriada en CE-MS (87) o la integración de muestras medidas en lotes diferentes (88). Esto permitiría abordar estudios con diseños más complejos, que tengan muchas muestras por grupo o una mayor cantidad de grupos.

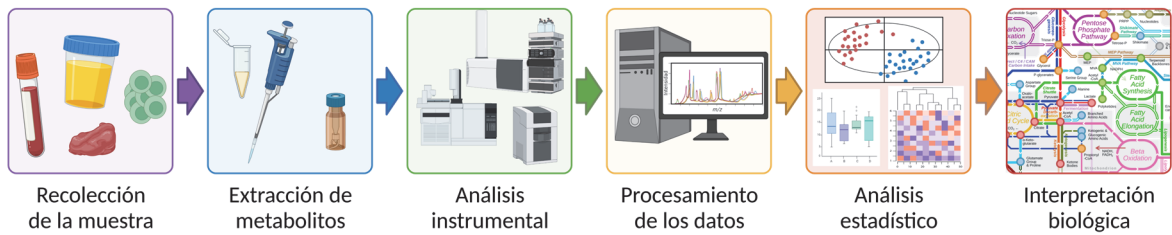


**Figura 11.** Diagrama del flujo de trabajo utilizado en un análisis de metabolómica no dirigida.



## 2. Hipótesis y objetivos

La hipótesis de este trabajo es que los diferentes fenotipos asmáticos, diferenciados por las características de la enfermedad (tales como la gravedad o la alergia), presentan marcadores distintos que podrían permitir la estratificación de los pacientes y servir como nuevas dianas terapéuticas para ofrecer a los pacientes un tratamiento personalizado.

Así, el objetivo principal de este trabajo es encontrar biomarcadores para la estratificación en pacientes con asma alérgico, asma no alérgico, y con comorbilidades como la poliposis nasosinusal. Para ello, se plantean los siguientes objetivos concretos, asociados a cada uno de los bloques de esta tesis:

1. Identificar los biomarcadores de estratificación por gravedad y las rutas biológicas asociados con el asma alérgico inducido por ácaros (**BLOQUE I**).
2. Identificar los biomarcadores y las rutas biológicas asociados con la contribución del fenotipo alérgico a la patología asmática (**BLOQUE II**).
3. Identificar los biomarcadores y las rutas biológicas asociados con la contribución del fenotipo alérgico a la poliposis nasal (**BLOQUE III**).



### 3. Materiales y métodos

A continuación, se va a proceder a la descripción de los métodos y el diseño experimental que se emplearon para cumplir con los objetivos planteados en esta tesis.

Dado que las muestras utilizadas en los análisis de los **BLOQUES I y II** provenían de la misma cohorte de pacientes, algunos de los métodos utilizados son comunes en ambos análisis. Éstos se detallan a continuación:

#### 3.1. BLOQUES I y II. Estudio de fenotipos asmáticos

##### 3.1.1. Reclutamiento, clasificación, y obtención de muestras

###### 3.1.1.1. Reclutamiento y clasificación de los pacientes

Para el estudio de asma se reclutaron 165 pacientes en el Hospital Universitario de Gran Canaria Doctor Negrín (Las Palmas, Gran Canaria) a lo largo de un año (entre el 1 de julio de 2016 y el 30 de junio de 2017). Los criterios de inclusión fueron: pacientes mayores de edad, diagnosticados con asma, que llevaran en seguimiento por parte del equipo médico un mínimo de cinco años antes del comienzo del estudio. Los pacientes se clasificaron en grupos utilizando dos criterios: (I) según su respuesta al tratamiento y (II) en función de su estado alérgico.

De acuerdo con esta clasificación, se obtuvieron ocho grupos iniciales; sin embargo, tres de ellos fueron excluidos del análisis, ya que sus características (falta de respuesta al tratamiento, pero sin cumplir criterios de gravedad, contraindicación del tratamiento biológico) no encajaban con los objetivos planteados inicialmente. Así, solamente 100 de los 165 pacientes fueron incluidos en alguno de los cinco grupos del análisis, cuyos criterios de clasificación se describen en la **Tabla 1**.

**Tabla 1.** Criterios de clasificación para los pacientes de los **BLOQUES I y II** incluidos en el estudio.

<b>CRITERIOS DE INCLUSIÓN EN CADA GRUPO</b>
<b>ICS<sup>a</sup></b>
<ul style="list-style-type: none"><li>• Prueba cutánea positiva frente a <i>Dermatophagoides pteronyssinus</i>, <i>Dermatophagoides farinae</i>, <i>Blomia tropicalis</i>, <i>Acarus siro</i>, <i>Lepidoglyphus destructor</i> y/o <i>Tyrophagus putrescentiae</i>.</li><li>• Controlados<sup>b</sup> con tratamiento farmacológico, excluyendo corticosteroides sistémicos (tratamiento de nivel 1-2 según la guía GINA (1))</li></ul>

<sup>a</sup> **ICS:** corticosteroides inhalados (*inhaled corticosteroids*).

<sup>b</sup> El control de la enfermedad se definió utilizando criterios objetivos, como el control de síntomas, la disminución de exacerbaciones con respecto al año previo, la reducción en el uso de medicación broncodilatadora, etcétera; además de la Prueba de Control de Asma (*Asthma Control test*, ACT).

---

**IT<sup>c</sup>**

---

- Prueba cutánea positiva frente a *Dermatophagoides pteronyssinus*, *Dermatophagoides farinae*, *Blomia tropicalis*, *Acarus siro*, *Lepidoglypus destructor* y/o *Tyrophagus putrescentiae*.
- Falta de control del asma alérgico con el tratamiento farmacológico por sí solo
- Conseguir el control de la enfermedad tras el tratamiento con inmunoterapia contra alérgenos de ácaro + tratamiento farmacológico, excluyendo corticosteroides sistémicos (tratamiento de nivel 2-3 según la guía GINA)
- Tratamiento con inmunoterapia de una duración mínima de 2 años antes de la inclusión

---

**BIO<sup>d</sup>**

---

- Prueba cutánea positiva frente a *Dermatophagoides pteronyssinus*, *Dermatophagoides farinae*, *Blomia tropicalis*, *Acarus siro*, *Lepidoglypus destructor* y/o *Tyrophagus putrescentiae*
- Falta de control del asma alérgico con el tratamiento farmacológico por sí solo
- Falta de respuesta a inmunoterapia
- Conseguir el control de la enfermedad tras el tratamiento con anti-IgE + tratamiento farmacológico, incluyendo corticosteroides sistémicos puntuales (tratamiento de nivel 4-5 según la guía GINA)
- Tratamiento con biológicos de una duración mínima de 1 año previo a su inclusión

---

**UCA<sup>e</sup>**

---

- Prueba cutánea positiva frente a *Dermatophagoides pteronyssinus*, *Dermatophagoides farinae*, *Blomia tropicalis*, *Acarus siro*, *Lepidoglypus destructor* y/o *Tyrophagus putrescentiae*
- Falta de control del asma alérgico con tratamiento farmacológico (incluyendo corticosteroides sistémicos a altas dosis), inmunoterapia o anti-IgE<sup>f</sup>
- Presentar un mínimo de 3 exacerbaciones al año<sup>g</sup>

---

**UCNA<sup>h</sup>**

---

- Prueba cutánea negativa frente a *Dermatophagoides pteronyssinus*, *Dermatophagoides farinae*, *Blomia tropicalis*, *Acarus siro*, *Lepidoglypus destructor* y/o *Tyrophagus putrescentiae*, o a cualquier otro alérgeno
- Falta de control del asma alérgico con tratamiento farmacológico (incluyendo corticosteroides sistémicos a altas dosis), inmunoterapia o anti-IgE
- Presentar un mínimo de 3 exacerbaciones al año

En el **BLOQUE I** se compararon pacientes alérgicos estratificados en función de su gravedad (grupos ICS, IT, BIO y UCA), mientras que en el **BLOQUE II** se compararon los grupos graves no controlados con y sin alergia (grupos UCA y UCNA).

---

<sup>c</sup> IT: inmunoterapia

<sup>d</sup> BIO: biológicos.

<sup>e</sup> UCA: alérgicos no controlados (*uncontrolled allergic*).

<sup>f</sup> Nótese que, al momento de inclusión de pacientes, el único medicamento biológico aprobado para el tratamiento del asma era omalizumab, un anti-IgE.

<sup>g</sup> De media, los pacientes graves no controlados presentaban 5 exacerbaciones anuales.

<sup>h</sup> UCNA: no alérgicos no controlados (*uncontrolled non-allergic*).

## Materiales y métodos

### 3.1.1.2. Análisis estadístico de las características clínicas de los pacientes

Para las variables continuas (edad, IMC, edad de aparición del asma e IgE total) se aplicó la prueba de Shapiro-Wilk para comprobar la normalidad de los datos, y se aplicó un análisis de varianza (ANOVA) con la prueba *post hoc* de Tukey, para aquellas variables que cumplieran con una distribución normal (edad, IMC); y Kruskal Wallis con la prueba *post hoc* de Dunn, para aquellas que no seguían una distribución normal (IgE total, edad de aparición de la enfermedad). Las variables categóricas (sexo, tabaquismo, medicación y sensibilización a un determinado ácido) se analizaron mediante la prueba de Chi cuadrado, utilizando el estadístico exacto de Fisher en aquellas con grupos con una  $n < 5$ . Los análisis se realizaron con GraphPad Prism v.8.0 (GraphPad Software, San Diego, California, USA) y IBM SPSS Statistics for Windows, v. 24.0 (IBM Corp, Armonk, Nueva York, USA).

### 3.1.1.3. Obtención de suero

Se obtuvieron muestras de sangre en tubos de coagulación Vacutainer SST II de cada paciente. Las muestras se mantuvieron a temperatura ambiente durante 30 min y se centrifugaron a 2000 x *g* durante 10 min a temperatura ambiente para obtener el suero, que fue conservado a -80 °C hasta su utilización.

## 3.1.2. Diseño experimental: metabolómica no dirigida

El análisis metabolómico se realizó para el total de muestras de los 165 pacientes reclutados inicialmente, con la finalidad de poder utilizar los datos en futuros estudios. El elevado número de muestras obligó a que su análisis metabolómico se realizara en lotes (*batches*) para evitar la caída de la señal analítica. Las muestras se dividieron en dos lotes (de 82 y 83 muestras, respectivamente), y fueron medidas en orden aleatorio dentro de cada lote. Además, para demostrar la calidad del análisis global y validar el funcionamiento de la normalización entre ambos lotes, un subgrupo de muestras fue medido de manera aleatoria en ambos lotes.

### 3.1.2.1. Preparación de las muestras

Para la precipitación de proteínas y extracción de metabolitos, las muestras de suero fueron descongeladas en hielo y, a cada 100 µl de muestra, se añadieron 300 µl de una mezcla fría de metanol-etanol 1:1 (-20 °C) y 20 µl de una mezcla de patrones internos marcados (*internal standards*, IS). La mezcla IS estaba formada por cinco metabolitos marcados (bien con deuterio, bien con <sup>13</sup>C y <sup>15</sup>N), y se incluyó como una prueba adicional del correcto funcionamiento de la técnica analítica (88). El IS se diseñó con el objetivo de cubrir un amplio rango de tiempos de retención (*retention time*, RT) y propiedades fisicoquímicas (polaridad y masa molecular). Los

componentes del IS están listados en la **Tabla 2**. Después, las muestras se mezclaron con un agitador vórtex, se dejaron reposar en hielo durante 5 min y se centrifugaron a 16000 x *g* durante 20 min a 4 °C. El sobrenadante fue medido mediante cromatografía de líquidos acoplada a espectrometría de masas (*liquid chromatography coupled to mass spectrometry*, LC-MS). Las muestras fueron preparadas en grupos secuencialmente en función del momento en el que serían analizadas, evitando que el tiempo entre la extracción de metabolitos y la medición en el equipo superara las 24 horas.

**Tabla 2.** Composición del patrón interno (IS). Los compuestos aparecen ordenados por tiempo de retención.

Compuesto	Fórmula	Masa Molecular (Da)	RT (min)	Concentración (mM)
Carnitina-D <sub>3</sub>	C <sub>7</sub> H <sub>12</sub> D <sub>3</sub> NO	144.1454	0.70	0.02
Isoleucina- <sup>13</sup> C, <sup>15</sup> N	<sup>13</sup> C <sub>6</sub> H <sub>13</sub> <sup>15</sup> NO <sub>2</sub>	138.1118	0.77	0.18
Esfingosina-D <sub>7</sub>	C <sub>18</sub> H <sub>30</sub> D <sub>7</sub> NO <sub>2</sub>	306.3264	14.38	0.02
LPC 18:1-D <sub>7</sub>	C <sub>26</sub> H <sub>45</sub> D <sub>7</sub> NO <sub>7</sub> P	528.3921	19.30; 20.00	0.01
Ácido esteárico-D <sub>5</sub>	C <sub>18</sub> H <sub>31</sub> D <sub>5</sub> O <sub>2</sub>	289.3029	34.54	0.17

RT: tiempo de retención; LPC: lisofosfatidilcolina (*lysophosphatidilcholine*). LPC 18:1 presenta dos picos en dos tiempos de retención distintos.

La preparación de blancos se realizó utilizando agua destilada en lugar de suero siguiendo el mismo procedimiento. La muestra de control de calidad (*quality control*, QC) consistió en una mezcla (*pool*) de muestras utilizadas en este análisis; y se preparó usando una misma cantidad de volumen de suero de una cuarta parte de los pacientes (elegidos al azar incluyendo muestras de todos los grupos). La muestra QC fue medida regularmente a lo largo del proceso de análisis de los lotes para asegurar la estabilidad del sistema, el rendimiento y la reproducibilidad del tratamiento.

### 3.1.2.2. Análisis instrumental

Las muestras se midieron en un sistema de cromatografía líquida de alta eficacia (*high-performance liquid chromatography*, HPLC) Agilent (serie 1200), equipado con un desgasificador, dos bombas binarias y un muestreador automático climatizado; acoplado a un analizador de masa tipo cuadrupolo-tiempo de vuelo (*quadrupole time-of-flight*, Q-ToF) MS 6520 (Agilent Technologies, Waldbronn, Alemania).

Se inyectaron 10 µl de cada muestra a un flujo constante de 0.6 mL/min de fase móvil en una columna Discovery HS C18 (2.1 × 150 mm, 3.0 µm; Supelco, Sigma Aldrich, Alemania), equipada con una precolumna Discovery® HS C18 (2.1 × 20 mm, 3 µm; Supelco), ambas mantenidas a una temperatura de 40 °C. Las fases móviles del gradiente de elución estaban compuestas por: (A) 0.1% v/v de ácido fórmico (*formic acid*, FA) en agua; y (B) 0.1% de FA en acetonitrilo (ACN). El gradiente



## Materiales y métodos

de elución se fijó con unas condiciones iniciales de un 25% de (B), que aumentaba linealmente a lo largo de 35 min hasta un 95% de (B), para volver por último a las condiciones iniciales en 1 min. La columna se reacondicionó manteniendo las condiciones iniciales durante 9 min después de medir cada muestra.

Los datos de fuente de ionización se adquirieron tanto en polaridad positiva (*positive electrospray ionization*, ESI+, con un voltaje del capilar de 3500 V) como en polaridad negativa (ESI-, voltaje de 4000 V). El flujo de gas de secado se estableció en 10.5 L/min, a 330 °C, con una presión de gas de nebulización de 52 psi de presión; el voltaje del fragmentador se fijó a 175 V, el voltaje del cono del *skimmer* a 65 V, y el voltaje de radiofrecuencia del octopolo (OCT RF Vpp) a 750 V. Los espectros de masa se recogieron en formato centroide, con una frecuencia de barrido de 1.2 Hz. Se realizó un escaneo completo con un rango de 100 a 1200  $m/z$  en ambos modos. Para poder recalibrar y corregir la masa de forma constante se inyectaron iones de referencia de forma continua. Estos iones fueron, para ESI+, purina ( $m/z = 121.0508$ ) y HP-0921 ( $m/z = 922.0097$ ); y para ESI-, TFA-NH4 ( $m/z = 119.0363$ ) y HP-0921 ( $m/z = 966.0007$ ).

### 3.1.2.3. Procesamiento de datos, calidad de los datos e integración de lotes

Las señales obtenidas se limpiaron de ruido por medio del *software* MassHunter Profinder B.09.00, SP3 (Agilent Technologies). Además, para reducir la complejidad de los datos, se aplicaron dos algoritmos: 'Extracción de Características Moleculares' (*Molecular Feature Extraction*, MFE) y 'Encontrar Por Ion' (*Find by Ion*, Fbi). En total, obtuvimos 1382 señales para ESI+ y 887 señales para ESI-.

Después, se realizó un filtrado, eliminando aquellas señales que cumplieran alguna de las siguientes condiciones: 1) que se encontraban en los blancos; 2) que no se hallaban en, al menos, el 50% de las muestras QC; y/o 3) que no se encontraban en, al menos, el 75% de las muestras, salvo si las muestras en las que no estaba pertenecían todas al mismo grupo.

Las señales químicas que presentaban valores faltantes para algunas de las muestras (los cuales se pudieron haber generado debido a la complejidad de los algoritmos MFE y Fbi) se estimaron mediante el algoritmo *k-nearest neighbours* ( $k$ -NN, o ' $k$ -vecinos más cercanos') (89). Esta estimación se hace comparando cada muestra con el resto de las muestras de su grupo, y el algoritmo utiliza aquellas más cercanas para estimar cuál debería ser la abundancia de la señal que no conocemos.

Para la normalización e integración de los lotes se probaron varias estrategias, a fin de poder comparar las muestras medidas en diferentes momentos entre sí. Así pues, se diseñaron distintas aproximaciones para la normalización dentro de los lotes (o *inratabatch*), incluyendo: (I)

## Materiales y métodos

normalización por el área bajo la curva de la mezcla IS; **(II)** normalización en función de la señal útil total (*total useful signal*, TUS) del perfil de cada muestra; y **(III)** normalización por el método conocido como QC-SVRC (90). Además, para realizar una normalización global entre lotes (o *interbatch*), se aplicó **(IV)** el método QC-norm (91), que ajusta la señal promedio de las muestras QC entre los lotes. Finalmente, en este trabajo, la combinación de las estrategias **(III)** y **(IV)** permitió una normalización combinada para eliminar las diferencias analíticas de las muestras dentro de un mismo lote y entre lotes. Por último, se excluyeron del análisis aquellas señales que tenían un coeficiente de variación (CV) en las muestras QC mayor del 30%. El coeficiente de variación equivale a la desviación estándar relativa (*relative standard deviation*, RSD), y se utiliza para garantizar la reproducibilidad de la técnica.

Para comprobar el éxito de cada estrategia de normalización, la calidad de los datos y el correcto agrupamiento de los lotes tras la normalización, se realizaron modelos de análisis de componente principal (*Principal Component Analysis*, PCA), y un análisis de agrupación jerárquica (*Hierarchical clustering analysis*, HCA) de las muestras medidas en ambos lotes.

### 3.1.2.4. Análisis estadístico

Primero se realizó un análisis multivariante utilizando el *software* SIMCA v.16.0 (Sartorius Stedim Data Analytics). Se construyeron modelos no supervisados mediante PCA, y modelos supervisados mediante análisis discriminante de mínimos cuadrados parciales (*Partial Least Square Discriminant Analysis*, PLS-DA) y análisis discriminante a las proyecciones ortogonales a las estructuras latentes (*Orthogonal Projections to Latent Structures Discriminant Analysis*, OPLS-DA). Los modelos PLS-DA y OPLS-DA fueron validados mediante la división de los datos en 7 subgrupos aleatorios, 6 de los cuales se utilizaron para construir el modelo, prediciendo luego el último subgrupo y repitiendo el proceso hasta que todos los subgrupos habían sido utilizados tanto para construir el modelo como para su predicción (92), obteniéndose así el valor de  $Q^2$ . En todos los modelos se utilizó un escalado de varianza unitaria (*unit variance*, UV). Para evaluar la calidad de los modelos se utilizaron los valores de  $R^2$  (que hace referencia a la capacidad de clasificación) y  $Q^2$  (que hace referencia a la capacidad de predicción).

Posteriormente, se compararon los grupos extremos (ICS o leve contra UCA o no controlado) mediante un análisis de dos colas de U de Mann-Whitney con corrección por tasa de falsos descubrimientos (*False Discovery Rate*, FDR) utilizando un código (*script*) programado en MatlabR2015a (Mathworks, Natick, Massachusetts, USA) desarrollado por el profesor Santiago Angulo. Aquellas señales significativamente diferentes se utilizaron para construir un modelo de

## Materiales y métodos

agrupación jerárquica, representado por medio de un *heatmap* con un HCA, utilizando RStudio 1.3.1075.

Además, puesto que la edad fue un factor significativo entre estos grupos, se realizó un análisis de covarianza (ANCOVA) para excluir aquellos compuestos en los que la edad fuera significativa como covariable. Este análisis se realizó mediante el *software* SPSS.

A partir de este punto, con objeto de anotar e identificar los metabolitos que eran significativamente distintos en las distintas comparaciones, se realizaron dos métodos analíticos distintos para el **BLOQUE I** y el **BLOQUE I**, que se detallan a continuación.

## 3.2. BLOQUE I. Estudio del asma alérgico estratificado por gravedad

### 3.2.1. Análisis metabolómico

#### 3.2.1.1. Anotación de metabolitos

La anotación de metabolitos se llevó a cabo en dos fases. En primer lugar, a las señales químicas (identificadas mediante la masa y el RT) que tenían abundancias significativamente diferentes entre grupos ( $P < .05$ ) se les asignó una identidad tentativa mediante la plataforma CEU Mass Mediator 3.0, que busca en distintas bases de datos tales como KEGG, METLIN, LipidMaps y HMDB (85,86,93,94).

Estas anotaciones fueron confirmadas mediante un experimento de masas en tándem (*Liquid Chromatography coupled to Tandem Mass Spectrometry*, LC-MS/MS). El análisis se realizó en el mismo equipo en el que se hizo el análisis no dirigido (Agilent QToF 6520), utilizando las mismas condiciones cromatográficas. Los iones de interés fueron fragmentados utilizando una ventana de  $m/z$  estrecha (1.3 Da) y una energía de colisión en el cuadrupolo de 20 eV, en primera estancia, y de 40 eV para aquellos compuestos que no se fragmentaron a 20 eV. Los espectros de fragmentación obtenidos fueron comparados con la estructura encontrada en las bases de datos o explicados mediante las reglas de fragmentación para confirmar las identidades (95–97).

Además, para aquellos metabolitos que tenían un patrón comercial disponible, se realizó una comprobación adicional comparando el RT y el espectro de fragmentación del patrón comercial con el obtenido de las muestras.

Por último, se realizó un análisis de rutas sobre los compuestos significativos e identificados utilizando la herramienta online IMPaLA (v12.0) (<http://impala.molgen.mpg.de/>)

### 3.2.2. Análisis proteómico

La concentración de proteínas del suero fue medida mediante un ensayo de extensión de proximidad (*Proximity Extension Assay*, PEA) (Olink®, Uppsala). Los ensayos PEA se basan en la utilización de oligonucleótidos acoplados a anticuerpos. Cuando dos anticuerpos se unen específicamente a una proteína, los oligonucleótidos se encuentran lo suficientemente cerca como para emparejarse, generando un fragmento que es amplificado mediante una reacción en cadena de la polimerasa (*Polymerase Chain Reaction*, PCR). Tras la PCR, se obtiene un archivo de Expresión de Proteína Normalizada (*Normalized Protein Expression*, NPX).

## Materiales y métodos

Para los pacientes ICS o leves ( $n = 15$ ) y UCA o graves no controlados ( $n = 11$ ), se analizó 1  $\mu\text{l}$  de suero mediante Olink utilizando el panel Target 96 Immuno-Oncology (ref 95311, Olink®, Uppsala), que consta de 92 proteínas relacionadas con la respuesta inflamatoria, quimiotaxis, remodelado tisular, apoptosis, y metabolismo y autofagia, entre otras funciones.

A cada una de las muestras se le añadieron tres controles de calidad diferentes relacionados con la integridad del anticuerpo y el proceso de reconocimiento de la proteína, la extensión del par hibridado de oligonucleótidos, y la amplificación y detección de los fragmentos generados. Se descartaron aquellas muestras (en este caso 2, una de cada grupo) con una desviación (en valor absoluto) en cualquiera de esos controles superior a 0.3 NPX de la media de la placa.

Para el análisis estadístico, los datos en formato NPX se procesaron utilizando el paquete OlinkR package (<https://github.com/ge11232002/OlinkR>) para el *software* RStudio. Los valores de *Fold-change*, *p*-valor y FDR se estimaron mediante la comparación de los valores de cada proteína con un modelo lineal (98).

Las proteínas estadísticamente significativas se analizaron con la herramienta *online* STRING para descubrir posibles interacciones entre ellas. Además, para relacionar estas proteínas con las posibles alteraciones funcionales, se realizó un análisis de ontología genética (*Gene Ontology*, GO).

### 3.2.3. Construcción de modelos de aprendizaje automático

Con el objetivo de descubrir cuáles de las variables con contribución a la enfermedad eran más relevantes a la hora de predecir la gravedad de los pacientes, se creó un modelo de aprendizaje automático utilizando las variables ómicas (metabolitos identificados y proteínas significativas) y clínicas. Para ello, se utilizó el *software* RStudio y los paquetes de análisis *caret*, *mlbench*, *sjmisc* y *class*, y se aplicó un algoritmo *k*-NN.

Las variables categóricas se codificaron en variables numéricas para poder ser analizadas junto a las variables cuantitativas. Además, se eliminaron aquellas variables: 1) en las que faltara algún valor para una de las muestras; 2) que tenían una correlación superior a 0.75 con otras en una matriz de correlación, para evitar información duplicada; 3) con un único valor o en los que uno de los valores estuviera en el 95% o más de los casos, pues la información que aportan al modelo es mínima; y 4) que correspondían a la medicación, al ser el tratamiento uno de los factores utilizados para la construcción de los grupos.

Tras el procesamiento, obtuvimos 50 variables clínicas y 86 metabólicas, que fueron utilizadas para construir el modelo. Todas las variables proteómicas fueron descartadas en algún punto del

## Materiales y métodos

procesamiento. Se construyeron tres modelos: uno incluyendo solamente las variables clínicas, uno incluyendo solamente las variables metabolómicas, y uno integrando todas las variables.

Para evitar que el modelo estuviera inclinado hacia el grupo más grande, se eliminaron algunas muestras (*downsampling*) del grupo ICS utilizando la función 'downSample' del paquete *caret*, manteniendo 10 muestras por grupo. Además, para evitar el sobreajuste (*overfitting*) y elegir el parámetro  $k$  óptimo, se realizó el método del codo, que consiste en realizar agrupamientos secuenciales con un valor de  $k$  de entre 1 y 10, permitiendo seleccionar el número de grupos (*clusters*) mediante la suma total de cuadrados dentro de los grupos (*Total Within-clusters Sum of Squares*, TWSS), ya que, al representarlo, aparecerá un codo o giro brusco en el número óptimo de agrupaciones (99–101).

Se crearon dos grupos aleatoriamente con una proporción de 60/40 para el entrenamiento (*training set*) y la evaluación (*testing set*) del modelo de  $k$ -NN utilizando el paquete *caret*. Además, se intentó minimizar el número de variables mediante filtros utilizando ANOVA, *random forest* y *cv repeat*. En la **Figura 12** se muestra un esquema del proceso de creación del algoritmo predictivo.

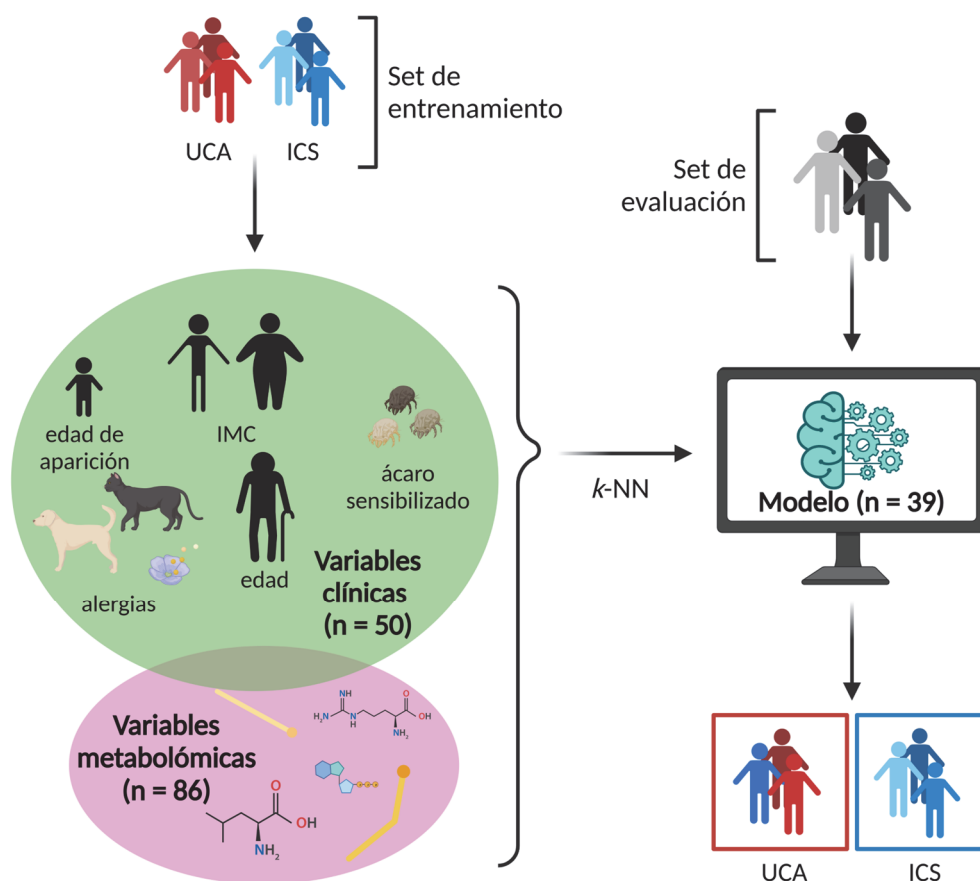


**Figura 12.** Esquema del modelo de aprendizaje automático. Para la construcción del algoritmo, se utiliza el set de entrenamiento, que está compuesto por el 60% de las muestras utilizadas en el análisis. Utilizando las variables clínicas y metabolómicas de estos pacientes se construye un modelo con los parámetros  $k$  obtenidos con el método del codo. El modelo se utiliza posteriormente para la predicción del set de evaluación, compuesto por el 40% de las muestras restantes, ocultando al programa el grupo al que pertenecen.

### 3.3. BLOQUE II. Estudio del papel de la alergia en pacientes asmáticos graves no controlados

#### 3.3.1. Análisis metabolómico

##### 3.3.1.1. Anotación de compuestos

Al igual que para el **BLOQUE I**, la anotación de metabolitos se llevó a cabo en dos fases. En primer lugar, a las señales químicas (identificadas mediante la masa y el RT) que tenían abundancias significativamente diferentes entre grupos ( $P < .05$ ) se les asignó una identidad tentativa mediante la plataforma CEU Mass Mediator 3.0 (85,86,93,94). Estas anotaciones fueron confirmadas mediante LC-MS/MS.

Debido a la falta del equipo en el que se analizaron las muestras inicialmente, este análisis se realizó en un equipo HPLC Agilent serie 1290 acoplado a un Q-ToF serie 6550, lo que obligó a adaptar el método cromatográfico. El método resultante fue más corto (15 min); por lo que, para encontrar los nuevos RT, se realizó primero un análisis de tipo *scan* de una selección de las muestras. Posteriormente, se asociaron los  $m/z$  a los nuevos RT; y estos  $m/z@RT$  se utilizaron para la identificación mediante LC-MS/MS.

En este nuevo método, se intentaron mantener las condiciones analíticas del método anterior en la medida de lo posible. Se utilizó una columna Zorbax C18-Extend USH BD06804 (2.1 × 150 mm, 5.0  $\mu$ m; Agilent Technologies). Se inyectaron 2  $\mu$ l de cada muestra en la columna, mantenida a una temperatura de 60 °C. Se estableció un flujo de 0.6 mL/min; y se utilizaron las mismas fases móviles que en el caso anterior. Se estableció un 5% de (B) para las condiciones iniciales. La concentración de (B) aumentaba de forma lineal hasta un 80% a lo largo de 7 min; y hasta un 100% a lo largo de 4.5 min más. Después, se volvía a las condiciones iniciales en 0.5 min; manteniéndolas durante 3 min para reacondicionar la columna entre inyecciones.

Para la medición en ESI+, se utilizó un voltaje de capilar de 3000 V, y para ESI-, de 4000 V. El flujo de gas secante se estableció en 12 L/min, a 250 °C; y las condiciones de nebulizador de gas (52 psi) y voltajes del fragmentador (175 V), *skimmer* (65 V) y OCT RF Vpp (750 V) fueron iguales a las del método anterior. Los espectros MS/MS se recogieron en formato centroide, y se utilizó una energía de colisión de 20 eV y 40 eV y una ventana de fragmentación estrecha (1.3 Da), al igual que en el caso anterior. Del mismo modo, los espectros de fragmentación obtenidos fueron comparados con la estructura encontrada en las bases de datos o explicados mediante las reglas de fragmentación para confirmar las identidades (95–97).

## Materiales y métodos

Por último, se realizó un análisis de rutas sobre los compuestos significativos e identificados utilizando la herramienta online IMPaLA (v12.0) (<http://impala.molgen.mpg.de/>); así como un análisis de enriquecimiento en Metaboanalyst 5.0 (<https://www.metaboanalyst.ca>), que indica los tipos de metabolitos que se encuentran más aumentados.



### 3.4. BLOQUE III. Estudio del papel de la alergia en la poliposis nasosinusal

#### 3.4.1. Reclutamiento de pacientes

Se reclutaron 22 pacientes diagnosticados con poliposis nasosinusal, con y sin sensibilización alérgica, en el Servicio de Otorrinolaringología del Hospital Madrid Montepíncipe. Los criterios de inclusión fueron:

- Pacientes mayores de edad.
- Pacientes con pólipos nasales que tuvieran que ser extraídos mediante cirugía según el criterio clínico.
- Ausencia de enfermedades concomitantes (enfermedades autoinmunes, cáncer, ...).
- En el caso de los pacientes alérgicos, tener niveles positivos de IgE en plasma contra uno o varios alérgenos que, en su conjunto, resultaran en una exposición perenne (esto es, que estuvieran sensibilizados a uno o varios alérgenos perennes y/o a un conjunto de alérgenos estacionales).

Antes del día de obtención de la muestra se mantuvo a los pacientes sin medicación durante dos semanas.

#### 3.4.2. Obtención de muestras

Se obtuvieron tres tipos de muestra. Antes de la operación, se obtuvieron 20 mL de sangre en tubos heparinizados, que se utilizaron para obtener plasma mediante centrifugación en gradiente de densidad con Ficoll-Paque (GE Healthcare™). El plasma se conservó a -80 °C para su análisis metabolómico, así como para su análisis del perfil de IgE. Éste se realizó utilizando un ImmunoCAP™ ISAC siguiendo las instrucciones del fabricante.

Durante la cirugía endoscópica para eliminar el pólipo, se obtuvieron biopsias de 5 mm tanto de pólipos nasales como de tejido epitelial sano, las cuales se fijaron en paraformaldehído (PFA) entre 24 y 48h. En los casos en los que fue posible, una biopsia adicional se conservó en RNAlater®. Las muestras fijadas en PFA se conservaron a 4 °C y se procesaron para poder realizar tinciones histoquímicas e inmunohistoquímicas, mientras que las conservadas en RNAlater® se conservaron a -80 °C hasta que fueron utilizadas para un análisis metabolómico dirigido.

### 3.4.3. Metabolómica no dirigida en plasma

La metabolómica en plasma se realizó de manera similar a la descrita anteriormente. Sin embargo, dado que el número de muestras en esta ocasión permitió realizar el análisis en un solo lote, existen ciertas diferencias en el procedimiento y el análisis.

#### 3.4.3.1. Preparación de las muestras

A 100  $\mu$ l de plasma descongelado en hielo se añadieron 300  $\mu$ l de metanol-etanol 1:1 frío (a -20 °C); después, las muestras se mezclaron con un vórtex, se mantuvieron en hielo durante 5 min y se centrifugaron a 16000 x *g* durante 20 min a 4 °C. El sobrenadante se recuperó y se midió por LC-MS. Para la preparación de blancos se sustituyó el plasma por agua destilada, siguiendo el mismo proceso. La muestra QC se preparó mezclando todos los plasmas medidos, y se midió regularmente a lo largo del análisis. El orden de extracción de metabolitos y medición de las muestras fue aleatorio.

#### 3.4.3.2. Análisis instrumental

El análisis se realizó en un sistema HPLC Agilent (serie 1200), equipado con un desgasificador, dos bombas binarias y un muestreador automático climatizado; acoplado a un analizador Q-ToF MS 6520 (Agilent Technologies, Waldbronn, Alemania).

De cada muestra, 10  $\mu$ l fueron inyectados a un flujo constante de 0.6 mL/min en la columna Discovery HS C18 column (2.1  $\times$  150 mm, 3.0  $\mu$ m; Supelco, Sigma Aldrich, Alemania), equipada con una guarda Discovery® HS C18 (2.1  $\times$  20 mm, 3  $\mu$ m; Supelco), mantenidas a una temperatura de 40 °C. Las fases móviles estaban compuestas por: (A) 0.1% v/v de FA en agua; y (B) 0.1% de FA en ACN. El gradiente de elución se fijó con unas condiciones iniciales de un 25% de (B), que aumentaba linealmente a lo largo de 35 min hasta un 95% de (B), para volver a las condiciones iniciales en 1 min. Las condiciones iniciales se mantuvieron durante 9 min después de medir cada muestra para reacondicionar la columna antes de una nueva muestra.

Cada muestra fue analizada dos veces, una en ESI+, con un voltaje del capilar de 3500 V, y otra en ESI-, con un voltaje de 4000 V. El flujo de gas de secado se estableció en 10.5 L/min, a 330 °C, con una presión de gas de nebulización a 52 psi; el voltaje del fragmentador se fijó a 175 V, el del cono del *skimmer* a 65 V, y el OCT RF Vpp a 750 V. Los espectros de masa se recogieron en formato centroide, con una ratio de escaneo de 1.2 Hz. Se realizó un escaneo completo con un rango de 100 a 1200 *m/z* en ambos modos. La calibración de del equipo se realizó por medio de la inyección continua de masas de referencia: para ESI+ se utilizaron purina (*m/z* = 121.0508) y HP-0921 (*m/z* =

## Materiales y métodos

922.0097); mientras que para ESI<sup>-</sup> se usaron TFA-NH<sub>4</sub> ( $m/z = 119.0363$ ) y HP-0921 ( $m/z = 966.0007$ ).

### 3.4.3.3. Procesamiento de los datos y análisis de calidad

Las señales obtenidas se limpiaron de ruido por medio del *software* MassHunter Profinder B.09.00, SP3 (Agilent Technologies). Además, para reducir la complejidad de los datos, se aplicaron los MFE y Fbl. En total, obtuvimos 698 señales para ESI<sup>-</sup> y 1654 señales para ESI<sup>+</sup>.

Después, se realizó un filtrado, eliminando aquellas señales: 1) que se encontraban en los blancos; 2) que no se hallaban en, al menos, el 50% de las muestras QC; y 3) que tenían un CV en las muestras QC superior al 30%. En total, se obtuvieron 535 señales en ESI<sup>+</sup> y 429 señales en ESI<sup>-</sup>.

### 3.4.3.4. Anotación de compuestos.

Como en los bloques anteriores, la identificación de compuestos se llevó a cabo en dos fases: una anotación tentativa mediante la plataforma CEU Mass Mediator 3.0, y un análisis de masas en tándem LC-MS/MS en el mismo equipo en el que se hizo el análisis LC-MS (HPLC Agilent serie 1200 acoplado a Agilent QToF 6520), utilizando las mismas condiciones cromatográficas. Los iones de interés fueron fragmentados utilizando una ventana de  $m/z$  estrecha (1.3 Da) y una energía de fragmentación en el cuadrupolo de 20 eV. Finalmente, los espectros fragmentados se compararon con los almacenados en bases de datos, o fueron explicados mediante las reglas de fragmentación para confirmar las identidades asignadas.

## 3.4.4. Metabolómica dirigida en tejido: pólipos

El análisis metabolómico en tejido de pólipo fue desarrollado desde cero para este proyecto, y se llevó a cabo en un total de seis muestras (tres de cada grupo). El procedimiento se describe en detalle a continuación:

### 3.4.4.1. Preparación de las muestras

Las muestras se lavaron tres veces con PBS 1X para eliminar los restos de RNAlater<sup>®</sup> y, posteriormente se congelaron en nitrógeno líquido durante 30 s. Una vez congeladas, se introdujeron en una bolsa CryoPREP<sup>™</sup>CP02 (Covaris, MA, United States) y se mantuvieron 30 s más en nitrógeno líquido. Las muestras criogenizadas se pulverizaron utilizando el pulverizador automático CryoPREP<sup>™</sup>CP02, con el que se aplicaron dos impactos consecutivos de fuerzas 2/6 y 4/6. El producto se recogió y pesó, y se añadieron 100  $\mu$ l de etanol:metanol 1:1 v/v frío (-20 °C) y 0.5  $\mu$ l de estándar interno (lisofosfatidilcolina (LPC) 18:1-d7; 0.01 mM) por cada 10 mg de tejido. Después, las muestras se mezclaron mediante agitador vórtex y se homogeneizaron en un

## Materiales y métodos

homogeneizador Tissue-Lyser LT (Qiagen, Alemania) durante 5 min a 50 Hz tres veces consecutivas. Por último, las muestras se centrifugaron (2000 x *g* durante 10 min a 4 °C), y 70 µl del sobrenadante se transfirieron a un vial de cromatografía con 490 µl de fase móvil en las condiciones iniciales (compuesta por un 5% de agua en un 95% de ACN, ambos con 7.5 mM de acetato de amonio y 0.1% de ácido acético). El orden de extracción y análisis instrumental de las muestras fue aleatorio.

### 3.4.4.2. Análisis instrumental

Las muestras se midieron en un sistema HPLC serie 1260 Infinity acoplado a un analizador de triple cuadrupolo-espectrómetro de masas (QQQ-MS) ESI(AJS)QQQ-MS 6470 (Agilent Technologies, Waldbronn, Alemania).

De cada muestra, 5 µl fueron inyectados a un flujo constante de 0.5 mL/min en una columna de sílice de cromatografía líquida de interacción hidrofílica (*hydrophilic interaction liquid chromatography*, HILIC) Kinetex (150 mm × 2.1 mm, tamaño de partícula 100 Å, Phenomenex, United States) mantenida a una temperatura constante de 25 °C. Las fases móviles estaban compuestas por: (A) 0.1% v/v de ácido acético y 7.5 mM de acetato de amonio en agua (pH = 4.0); y (B) 0.1% v/v de ácido acético y 7.5 mM de acetato de amonio en ACN. El gradiente de elución se fijó con unas condiciones iniciales de un 5% de (A) durante 2 min, que aumentaba a un 50% de (A) a lo largo de 10 min, y finalmente volvía a las condiciones iniciales en 10 min.

Las muestras fueron ionizadas en ESI+ con un voltaje capilar de 5500 V, un flujo de gas de nebulización de 11 L/min, una temperatura de la fuente de 250 °C, y una presión en la fuente de 60 psi. Las muestras se mantuvieron a 4 °C, y las condiciones de transición para cada uno de los metabolitos diana fue optimizada de acuerdo con **Tabla 3**.

**Tabla 3.** Parámetros optimizados para el análisis de MS.

Compuesto	Ion precursor (m/z)	Ion producto (m/z)	RT (min)	Fragmentador (V)	Energía de colisión (eV)	Polaridad
Bilirrubina	585.3	299.1	0.91	131	25	+
LPC 16:0	496.3	183.9	9.95	100	28	+
LPC 18:0	524.4	183.8	9.80	100	28	+
LPI 20:4	621.3	361.3	7.83	84	17	+

LPC: Lisofosfatidilcolina, LPI: lisofosfatidilinositol, RT: tiempo de retención, V: voltio, eV: electronvoltio.

### 3.4.4.3. Adquisición y procesamiento de datos

Las señales se guardaron mediante el *software* MassHunter Workstation B.05.00 (Agilent Technologies), y se reprocesaron utilizando MassHunter QQQ Quantitative Analysis B.08.00 (Agilent Technologies) para integrar el área bajo los picos. La concentración de cada uno de los

metabolitos medidos se calculó mediante curvas de calibración por el método de adición de patrones.

### 3.4.5. Tinciones histológicas

Las muestras fijadas en PFA fueron deshidratadas en una serie de alcoholes de concentraciones crecientes y embebidas en parafina utilizando el procesador de tejidos Leica TP 1020 (Leica Systems, casa comercial). De los bloques de parafina se obtuvieron cortes de 3  $\mu\text{m}$  de espesor, que fueron utilizados para realizar tinciones histoquímicas e inmunohistoquímicas:

#### 3.4.5.1. Tinción de Masson

Para cuantificar la fibrosis del tejido, se realizó la tinción tricrómica de Masson (Sigma-Aldrich, ref. HT15-1KT) siguiendo el procedimiento estándar indicado en el manual de uso. Brevemente, tras desparafinar y rehidratar los cortes, se añadió la solución de Bouin como mordiente, se lavaron los portaobjetos y se tiñó con Hematoxilina de Hierro de Weigert. Tras volver a lavar, se añadió una solución de fucsina de Briebrich-Scarlett. Finalmente, se tiñó con anilina, se trató con ácido acético al 1%, y se lavaron y montaron los portaobjetos.

#### 3.4.5.2. Tinción de ácido periódico de Schiff

Para la cuantificación de células caliciformes en el epitelio, se realizó una tinción de ácido periódico de Schiff (*Periodic Acid-Schiff*, PAS). Tras desparafinar los cortes, se mantuvieron las muestras en una solución de ácido periódico al 0.5%, que después fueron teñidas con el reactivo de Schiff (Merck, ref. 109033) y lavadas. Para teñir el núcleo se utilizó una dilución 1:4 de la Hematoxilina de Harris, que se diferenció en una dilución de alcohol ácido 1% (1% de ácido clorhídrico en etanol al 70%) y una solución de carbonato de litio (Sigma-Aldrich, ref. 62470) saturada. Para finalizar, las muestras fueron montadas con medio DPX.

#### 3.4.5.3. Tinción de Luna

Para cuantificar los eosinófilos, se realizó una tinción de Luna. Las muestras desparafinadas se tiñeron utilizando una solución compuesta por un 90% de Hematoxilina de Hierro de Weigert (preparada en el laboratorio) y un 10% de la solución comercial Briebrich-Scarlett (Sigma Aldrich, ref. HT151) durante 5 min. Posteriormente, las muestras se diferenciaron en alcohol ácido al 1% y carbonato de litio al 0.25%.

## Materiales y métodos

### 3.4.5.4. Inmunohistoquímica: tinción de elastasa (neutrófilos), CD3 (linfocitos T) y CD11c (presentadoras)

Las tinciones inmunohistoquímicas (con anticuerpos dirigidos contra grupos de células de interés) se realizaron con el kit '*Bond Polymer refine Detection*' en un sistema de tinción automatizado BOND-MAX (Leica Biosystems) de acuerdo con las indicaciones del fabricante. Los anticuerpos utilizados fueron anti-elastasa de neutrófilo (ref. ab68672, ABCAM), anti-CD3 (ref. MCA 1477, AbD Serotec) y anti-CD11c (ref. NCL-LCD11c-563, Novocastra). Para el control negativo, se utilizó la solución para diluir anticuerpos Bond™ (Leica Biosystems) en lugar del anticuerpo.

### 3.4.5.5. Análisis histológico

Una vez finalizadas las tinciones, los portaobjetos fueron escaneados utilizando un escáner Leica SCN400 (Leica Biosystems). De cada archivo escaneado se obtuvo una imagen completa mediante el *software* Leica Scan Viewer.

Para el análisis del infiltrado celular de eosinófilos y neutrófilos se realizó el conteo de todas las células positivas para la tinción en el área total escaneada mediante el *software* Aperio Image Scope (Leica Biosystems); mientras que para el análisis de las células CD3<sup>+</sup> y CD11c<sup>+</sup> se seleccionaron cinco áreas representativas de cada muestra en Image-Pro Plus v4.5.0.29 (Media Cybernetics), en las que se contó las células que había. El área de conteo se cuantificó mediante ImageJ v1.51j8. Cada muestra fue analizada por un mínimo de dos investigadores independientes; y los resultados se presentan como número de células por área (mm<sup>2</sup>).

Para el análisis de la hiperplasia de células caliciformes, se analizó el área teñida positivamente con la tinción de PAS (PAS<sup>+</sup>) en el epitelio; mientras que para el análisis de la deposición de fibras de colágeno se analizó el porcentaje de área teñida en verde (positivo) en la tinción de Masson en el área total, utilizando en ambos casos el *software* Image-Pro Plus v4.5.0.29, con el plugin *Color Deconvolution*, que permite separar los canales de color de las imágenes para distinguir las zonas teñidas positivamente de las negativas.

## 3.4.6. Análisis estadístico

### 3.4.6.1. Análisis metabolómico no dirigido

Primero se realizó un análisis multivariante utilizando la herramienta online Metaboanalyst v5.0. Se construyeron modelos no supervisados mediante PCA con transformación logarítmica y escalado central.

## Materiales y métodos

El análisis univariante entre los pacientes con poliposis con y sin alergia se realizó mediante un análisis de dos colas de U de Mann-Whitney con corrección FDR (para un valor de significancia del 95%) utilizando un *script* de MatlabR2015a diseñado en el laboratorio. Las señales significativas se utilizaron para construir modelos HCA con Metaboanalyst v5.0.

### *3.4.6.2. Análisis metabolómico dirigido*

El análisis estadístico se realizó utilizando Excel 2016, MatlabR2018b y GraphPad Prism v8.1.2.

### *3.4.6.3. Análisis histológico*

Para el análisis estadístico de las tinciones, se utilizó GraphPad Prism v8.1.2. Se analizó la distribución de las muestras y, como no cumplían con una distribución normal, se utilizó el análisis de dos colas de U de Mann-Whitney para determinar las diferencias significativas con un valor de significancia del 95% ( $P < .05$ ).





## 4. Resultados

### 4.1. BLOQUES I y II. Estudio de fenotipos asmáticos

#### 4.1.1. Normalización de muestras medidas en distintos lotes

Aunque originalmente se planificó que la medida de las muestras se realizara en dos lotes, un fallo del equipo en la inyección de la muestra produjo que el segundo lote medido en polaridad negativa se detuviera a la mitad; en consecuencia, se generaron 3 lotes diferentes.

Para comprobar el funcionamiento de las distintas estrategias de normalización se utilizaron gráficos PCA (**Figura 13**). Este gráfico muestra diferencias en la agrupación de la muestra QC antes y después de las distintas estrategias de normalización, particularmente en la estrategia combinada de QC-SVRC + QCnorm; por ello, esta última fue la elegida. La agrupación de los QC indica que las diferencias no se deben al análisis instrumental (ya sea por la separación en lotes o por la deriva de la señal analítica), sino a las diferencias biológicas entre los pacientes. Además, se analizó el agrupamiento de las muestras de pacientes medidas en dos lotes antes y después de la estrategia de normalización elegida mediante PCA y HCA (**Figura 14**). En ambos se aprecia que las muestras se agrupan mejor tras la normalización.

Así, puede concluirse que la normalización de las muestras mejora el agrupamiento de las muestras QC y permite realizar comparaciones fiables de muestras medidas en distintos lotes.

Resultados

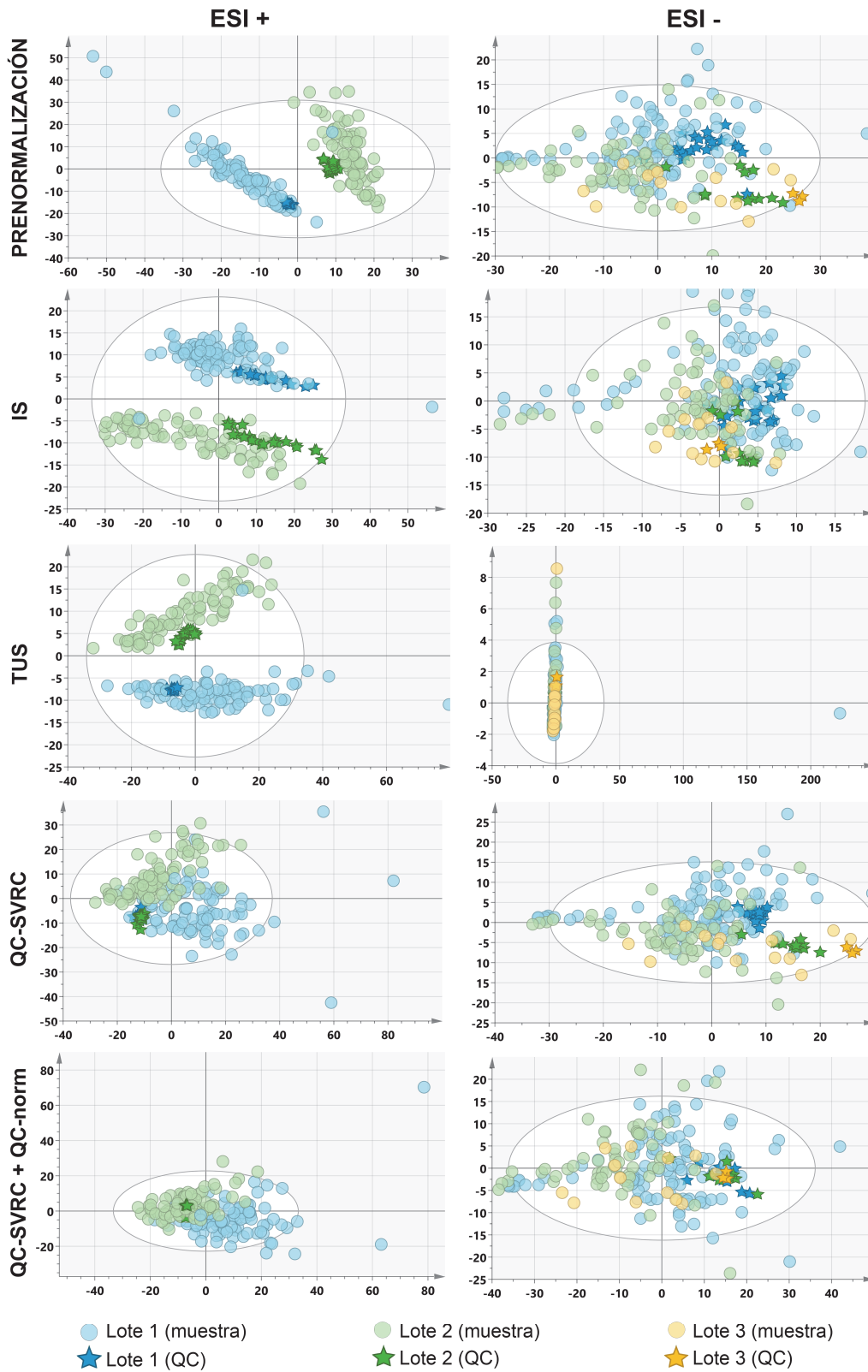


**Figura 13.** Análisis PCA de las 165 muestras analizadas para ESI+ (izquierda) y ESI- (derecha) antes de la normalización y tras aplicar las distintas estrategias de normalización (normalización por el patrón interno (IS), normalización por TUS, normalización por QC-SVRC, y normalización combinada QC-SVRC + QC-norm), coloreadas en función del lote en el que se midieron.

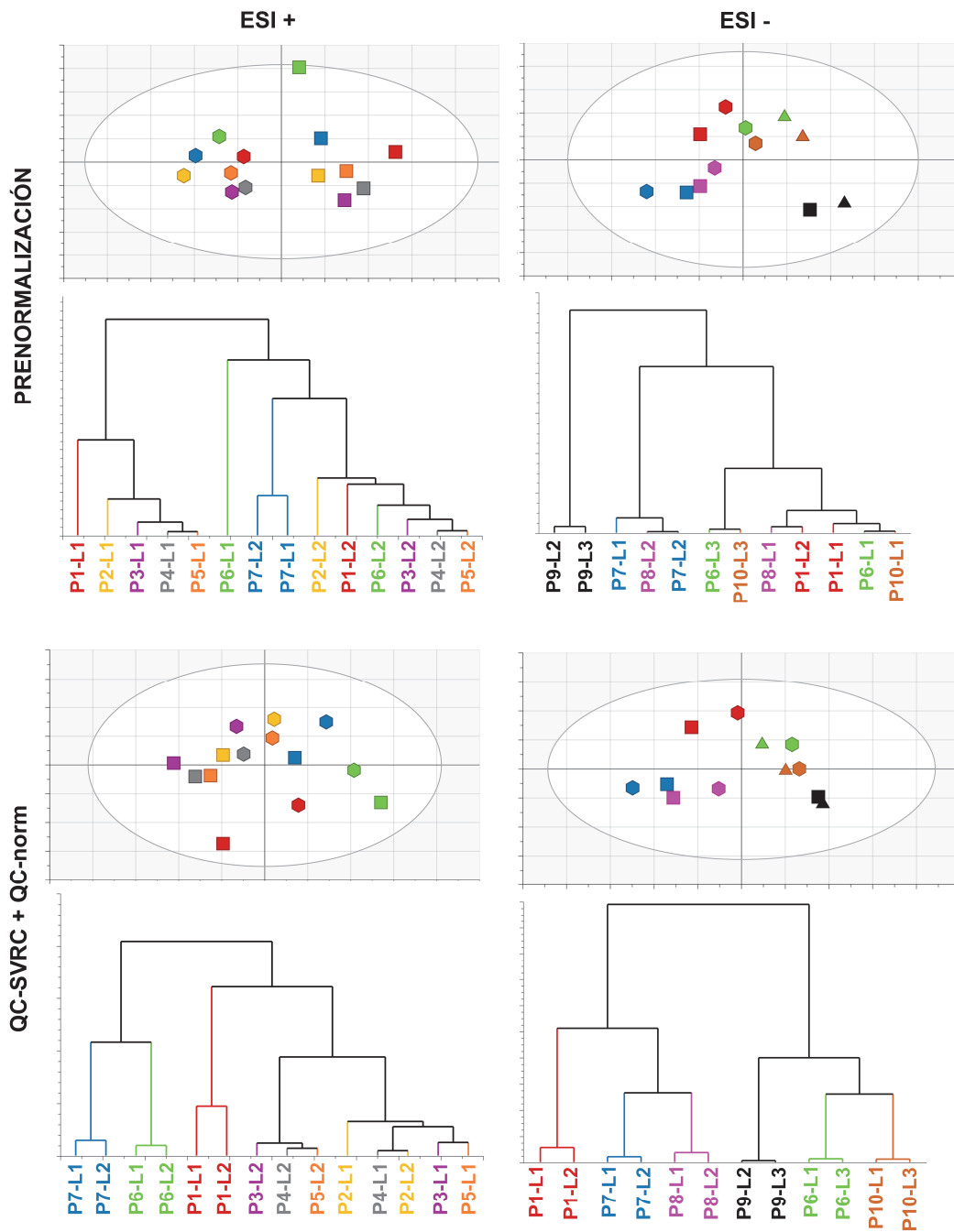


**Figura 14.** Representación de la agrupación de las muestras medidas en más de un lote antes (arriba) y después (debajo) de la normalización con QC-SVRC + QC-norm, para ESI+ (izquierda) y ESI- (derecha). Los puntos están coloreados en función de la muestra y, para los PCA, la forma indica el lote en el que se midió.

#### 4.1.2. Pacientes incluidos en el estudio

De las 165 muestras que se midieron originalmente, solamente 100 fueron incluidas finalmente en los **BLOQUES I y II** de esta tesis. Las otras 65 fueron descartadas por motivos clínicos (por ejemplo, aquellos pacientes con un asma no controlado leve o moderado, a los que no se les había prescrito un tratamiento con biológicos).

## 4.2. BLOQUE I. Estudio del asma alérgico estratificado por gravedad

### 4.2.1. Descripción de la población de estudio

De estos 100 pacientes, los 87 pacientes con una prueba cutánea positiva frente a ácaros fueron elegidos para el análisis del **BLOQUE I** y clasificados, según los criterios descritos en la **Tabla 1**, en cuatro grupos: controlados con corticosteroides inhalados y/o tópicos (ICS), controlados con inmunoterapia (IT), controlados con anti-IgE (BIO) y no controlados (UCA). El número de pacientes por grupo, el análisis estadístico y la descripción de la población se recogen en la **Tabla 4**.

**Tabla 4.** Información clínica de los pacientes.

	ICS	IT	BIO	UCA
N	15	44	16	12
Edad (años)	37.2 ± 2.3	37.3 ± 1.5†	43.3 ± 2.4	48.5 ± 3.6*
Edad de aparición (años)	15.8 ± 2.9	16.1 ± 1.7	12.1 ± 1.8	11.9 ± 2.7
Sexo (%F/%M)	66.7 / 33.3	77.3 / 22.7	87.5 / 12.5	58.3 / 41.7
IMC	26.7 ± 1.4	26.0 ± 0.6	26.8 ± 1.1	28.0 ± 1.2
Fumadores (%)	13.3	0	6.3	0
Exfumadores (%)	6.7	2.3	6.3	25
IgE total (U)	483.7 ± 164.7	396.2 ± 64.6	503.9 ± 161.5	536.3 ± 181.7
Anticolinérgicos (%)	0	0†	43.8*	50*
Antihistamínicos (%)	100	90.9†	37.5*	41.7*
Antileucotrienos (%)	13.3	11.4†	75*	75*
CS inhalados (%)	0	2.3	0	0
CS inhalados + LABA (%)	93.3	34.1*†	100	100
CS orales (%)	0	0	0	16.7
CS tópicos (%)	100	97.7†	68.8*	33.3*
SABA (%)	20	75*	93.8*	100*
Teofilina (%)	0	0	0	8.3
Hipersensibilidad AINES (%)	13.3	6.8	6.3	16.7
<i>D. pteronyssinus</i> (%)	93.3	97.7	93.8	91.7
<i>D. farinae</i> (%)	93.3	93.2	87.5	91.7
<i>L. destructor</i> (%)	66.7	50	43.8	58.3
<i>B. tropicalis</i> (%)	86.7	77.3	81.3	66.7
<i>A. siro</i> (%)	26.7	20.5	0	8.3
<i>T. putrescentiae</i> (%)	53.3	45.5	56.3	58.3

IMC: Índice de masa corporal, CS: corticosteroides, LABA: Agonistas adrenérgicos de larga duración (*Long-Acting Beta Agonists*), SABA: Agonistas adrenérgicos de corta duración (*Short-Acting Beta Agonists*). \*:  $P < .05$  en la comparación con ICS; †:  $P < .05$  en la comparación con UCA.

No se encontraron diferencias significativas en cuanto al sexo, etnia, IMC, número de fumadores y/o exfumadores, niveles de IgE total, número de pacientes con hipersensibilidad a AINES, o

## Resultados

número de pacientes sensibilizados frente a un ácaro concreto entre los grupos. Sin embargo, sí que fueron significativas las diferencias en edad (que aumentaba en función de la gravedad, siendo significativamente diferente entre los pacientes UCA y los ICS e IT). Una tendencia similar, aunque no significativa, se observó en la edad de aparición de la enfermedad, que fue menor en los pacientes más graves.

En cuanto a la medicación, los pacientes ICS o leves tomaban significativamente menos SABA que los pacientes del resto de grupos; además de tomar, al igual que los pacientes IT, significativamente menos anticolinérgicos y antileucotrienos y más antihistamínicos y corticosteroides tópicos que los grupos más graves (BIO y UCA). Por su parte, los pacientes IT o moderados fueron el grupo que menos corticosteroides inhalados tomaba. Los pacientes UCA no controlados, además, fueron los únicos que tomaban corticosteroides orales y/o teofilina.

### 4.2.2. Análisis metabólico

Tras la limpieza y filtrado de la matriz, se obtuvieron un total de 1398 señales (833 en ESI+ y 565 en ESI-) en el análisis por LC-MS. Se realizó un nuevo gráfico PCA incluyendo las muestras QC y las 87 muestras del **BLOQUE I** para demostrar que las muestras QC se agrupaban (**Figura 15**).

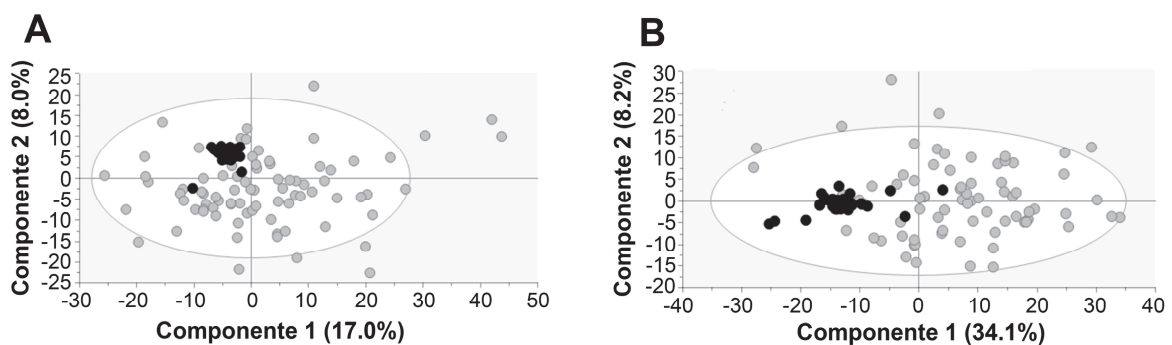


**Figura 15.** Análisis PCA de las 87 muestras del **BLOQUE I** para comprobar la calidad de los datos en ESI+ (**A**) y ESI- (**B**). La agrupación de las muestras QC (en negro) prueba que las diferencias entre las muestras (en gris) son debidas a las diferencias entre grupos, y no a las técnicas analíticas.

Para comprobar si existían diferencias evidentes entre los cuatro grupos, se realizó un PCA excluyendo las muestras QC. Este análisis no reveló un agrupamiento claro de las muestras por grupo (**Figura 16 A, B**); si bien los pacientes UCA parecían separarse de los pacientes ICS en ESI-. Por ello, se decidió realizar un análisis de PCA entre los grupos dos a dos. Se encontraron diferencias para la comparación entre los grupos ICS y UCA, los más extremos, en ambas polaridades (**Figura 16 C, D**); por lo que el resto del análisis multivariante se hizo solamente con estos dos grupos.

## Resultados

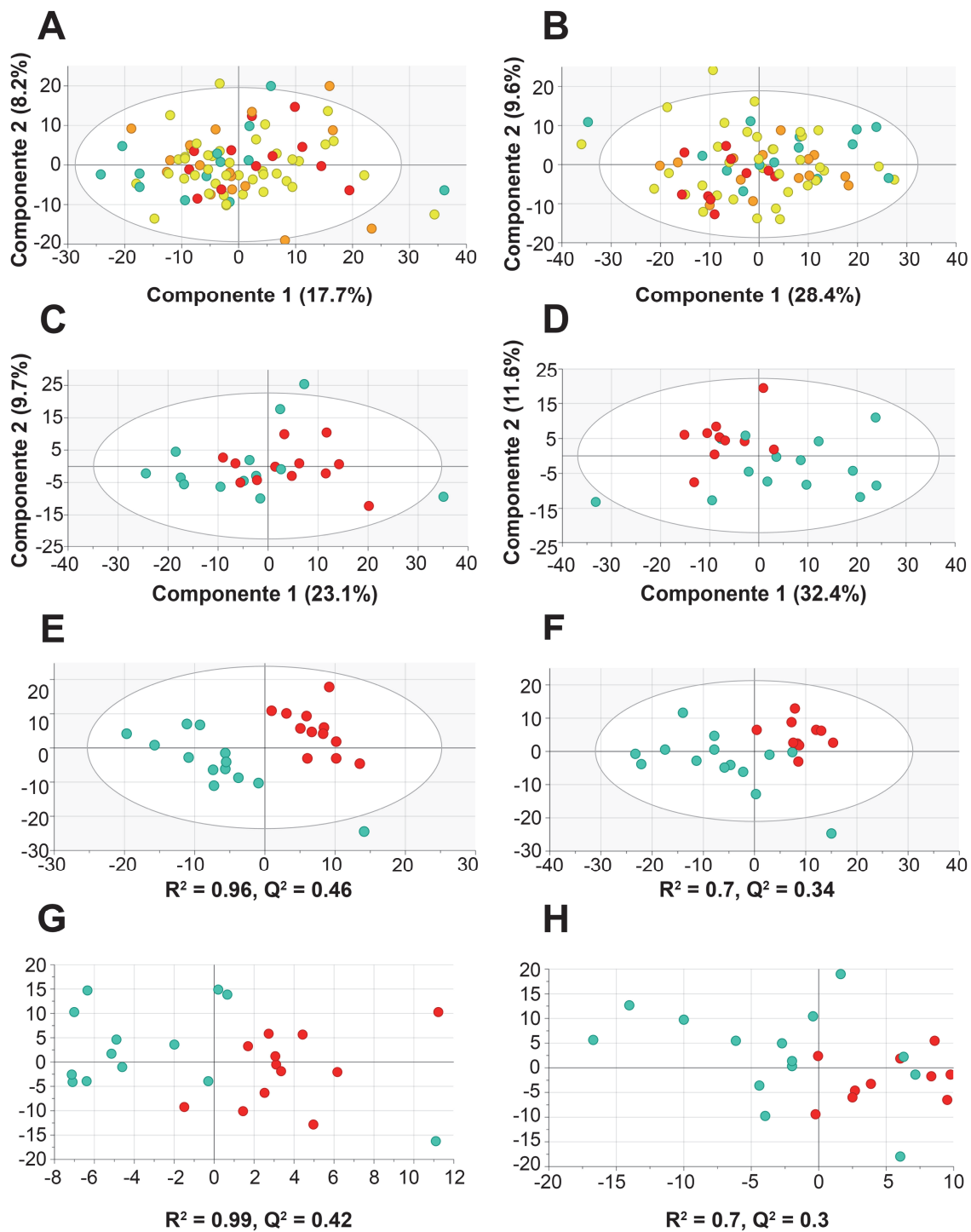


**Figura 16.** Análisis multivariante de los grupos incluidos en el estudio. Se muestran los resultados para un análisis no supervisado PCA de los cuatro grupos utilizando las 833 señales que cumplieron con los estándares de calidad en polaridad positiva (ESI+) (A) y las 565 de la polaridad negativa (ESI-) (B). Dado que no se observó una agrupación clara, aunque sí una tendencia para los grupos más extremos, se realizó un nuevo análisis PCA incluyendo solo los grupos ICS y UCA en ESI+ (C) y ESI- (D). Además, se realizaron dos análisis supervisados: un PLS-DA en ESI+ (E) y ESI- (F) y un OPLS-DA, también en ambas polaridades ESI+ (G) y ESI- (H). ICS: azul; IT: amarillo; BIO: naranja; UCA: rojo.  $R^2$  hace referencia a la capacidad de clasificación del modelo; y  $Q^2$ , a la capacidad de predicción.

Se realizó un análisis dirigido PLS-DA, que mostró una buena separación entre los grupos tanto en ESI+ como en ESI-, con valores de  $R^2$  de 0.96 y 0.7 y valores de  $Q^2$  de 0.34 y 0.46, respectivamente

## Resultados

(Figura 16 E, F). El modelo OPLS-DA obtuvo valores similares de  $R^2$  (0.99 y 0.7) y  $Q^2$  (0.42 y 0.3) (Figura 16 G, H), y la matriz de validación cruzada obtuvo una precisión del 84% para ESI+ y el 75% para ESI-. En conjunto, los modelos construidos con todas las variables muestran una buena capacidad para separar las muestras ICS y UCA, pero una capacidad predictiva limitada.

En los gráficos PLS-DA, además, se observa la presencia de valores atípicos para un punto del grupo ICS en ambas polaridades (Figura 16 E, F), que se localiza siempre en la esquina inferior derecha. Estos valores atípicos correspondían a dos pacientes distintos: en ESI+, el paciente presentaba unos valores muy bajos de FEV1 y FEVC con respecto al resto del grupo (69% y 64% frente a una media de 91% y 93% para FEV1 y FVC en ICS, respectivamente); mientras que en ESI-, se trataba de un paciente con sensibilidad a AINES. Sin embargo, se decidió mantener a ambos pacientes en el estudio al no considerarse ninguna de estas características un factor de exclusión.

Puesto que la edad fue un factor significativo entre estos grupos, se utilizó un modelo PCA para comprobar si los pacientes se agrupaban por la edad, observándose una cierta agrupación entre pacientes menores y mayores de 35 años sólo en ESI- (Figura 17).

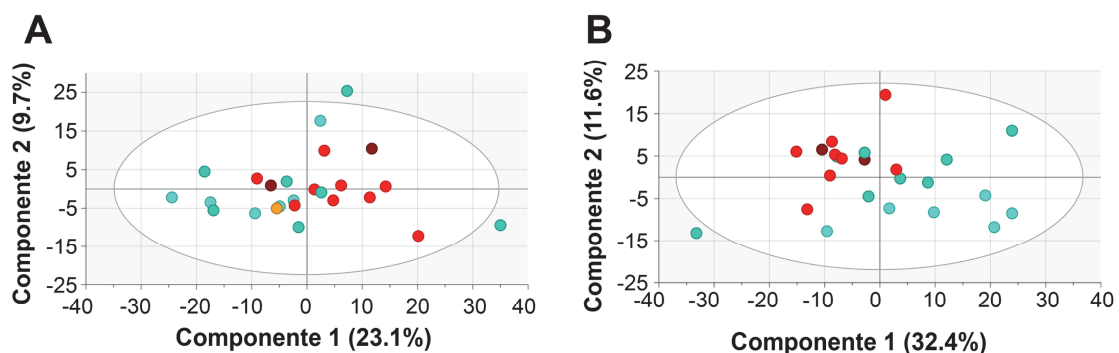


**Figura 17.** Análisis multivariante PCA de los grupos ICS y UCA para ESI+ (A) y ESI- (B), coloreados de acuerdo con el rango de edad. **Leyenda:** En azul, pacientes ICS, siendo azul claro: menores de 35 años; azul oscuro: 35-60 años. En rojo: pacientes UCA, siendo rojo-naranja: menores de 35 años; rojo: 35-60 años; y granate: mayores de 60 años.

Dado que las diferencias en el análisis multivariante se habían visto entre los grupos más extremos ICS y UCA, éstos se compararon mediante un análisis univariante, utilizando una U de Mann-Whitney. Se encontraron 280 metabolitos significativamente diferentes entre ambos grupos ( $P < .05$ ) teniendo en cuenta ambas polaridades. Estos metabolitos se utilizaron para construir un *heatmap* de las 87 muestras utilizando HCA (Figura 18), en el que las muestras ICS se agrupaban separadas de las muestras UCA, observándose un aumento en la abundancia de la mayoría de los metabolitos en los pacientes UCA. Las muestras IT y BIO, por su parte, no se agrupaban juntas, sino que se distribuían a lo largo del *heatmap*. No obstante, la mayoría de las muestras BIO (de mayor gravedad, aunque controladas) se agrupaban cerca de las muestras UCA.

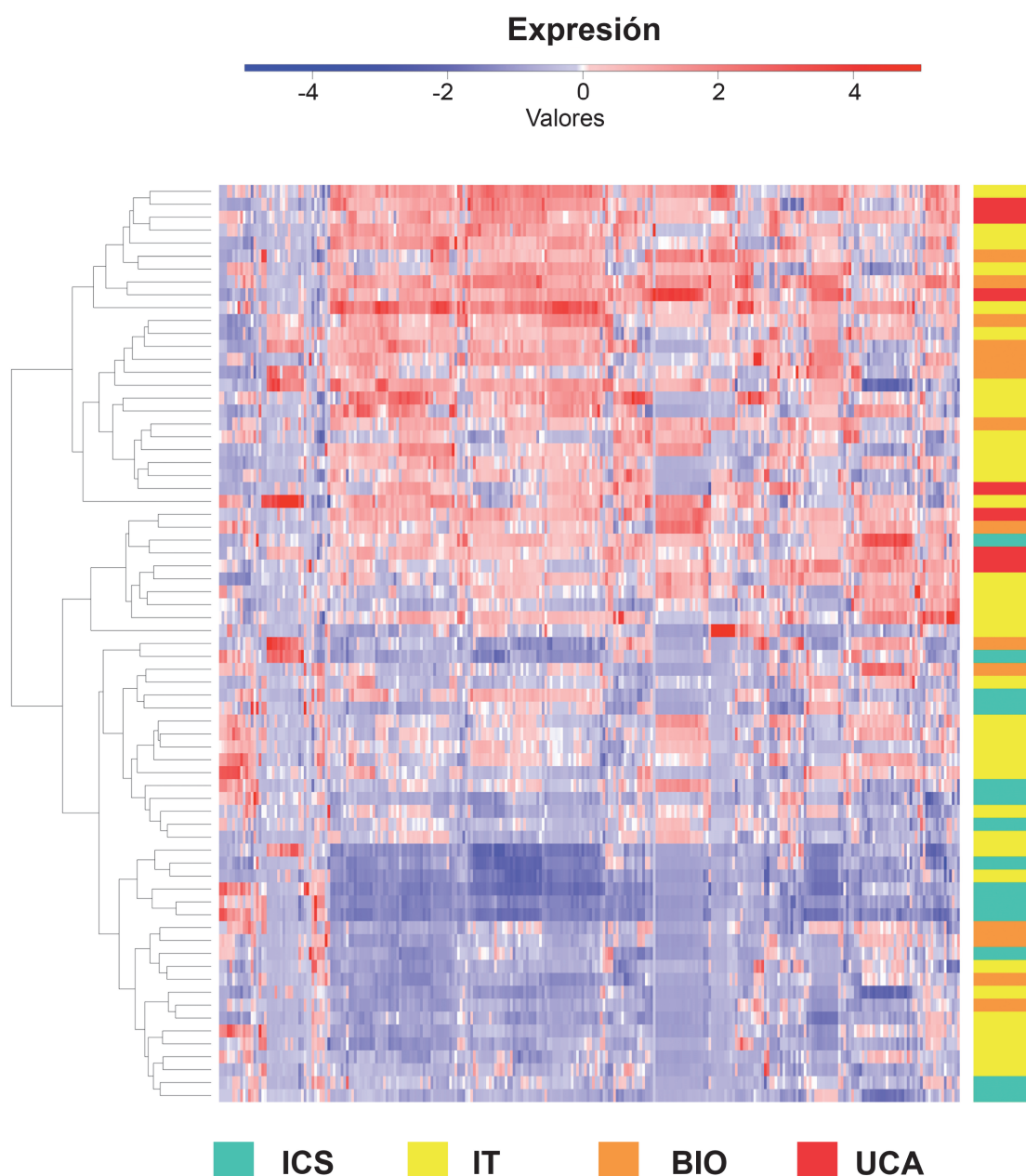


**Figura 18.** *Heatmap* creado tras el análisis de agrupamiento jerárquico (HCA) de los pacientes de los cuatro grupos (en filas), utilizando los 280 metabolitos significativamente distintos entre los pacientes ICS y UCA (en columnas). El color de las celdas representa una expresión disminuida (azul) o aumentada (rojo). Los pacientes y los metabolitos se agruparon según su similitud (izquierda).

A continuación, se procedió a la anotación tentativa de los 280 metabolitos significativamente distintos. Tras el cotejo con bases de datos y el análisis LC-MS/MS, se lograron identificar 89 metabolitos.

Ya que la edad había resultado un factor significativo entre ICS y UCA (**Tabla 4** y **Figura 17**), se realizó una prueba ANCOVA con la edad como covariable. De los 89 metabolitos, 86 seguían siendo estadísticamente significativos entre ICS y UCA tras eliminar el efecto de la edad. El listado de compuestos identificados, así como la información relativa al análisis estadístico y las características



## Resultados

fisicoquímicas y analíticas de estos compuestos se pueden encontrar en la **Tabla 5**, la **Tabla 6** y la **Tabla 7**. El número de la primera columna corresponde al mismo metabolito en todas las tablas.

De los 86 compuestos, se encontraron 33 identidades únicas; entre ellos, aminoácidos, ácidos biliares, ácidos grasos, fosfolípidos, esfingolípidos y vitaminas; siendo el grupo de los fosfolípidos el más abundante. Los cambios entre el grupo ICS y el grupo UCA se representan mediante diagramas de cajas y bigotes en la **Figura 19**. Todos estos compuestos se encontraban aumentados en los pacientes UCA, con la excepción de la bilirrubina, el ácido deoxicólico y la fosfatidilcolina 16:0/20:5, que se encontraban disminuidas en este grupo.

## Resultados

**Tabla 5.** Resultados del análisis ANCOVA entre los grupos ICS y UCA considerando la edad como una covariable.

Nº	Metabolito	Modelo corregido (p-valor)	Intercepto (p-valor)	Edad (p-valor)	Grupo (p-valor)
1	Ácido araquidónico	0.104	0.120	0.456	0.222
2	Ácido araquidónico	0.085	0.184	0.302	0.295
3	Bilirrubina	0.069	0.006	0.326	0.234
4	Glucurónido de ácido cólico O isómeros	0.138	0.125	0.674	0.176
5	Ácido deoxicólico O isómeros	0.050	0.053	0.351	0.171
6	Ácido deoxicólico O isómeros	0.049	0.053	0.373	0.157
7	Ácido hipúrico	0.020	0.330	0.883	0.180
8	LPC 16:0	0.156	0.001	0.076	0.169
9	LPC 16:0	0.161	0.007	0.856	0.149
10	LPC 16:0	0.178	0.002	0.960	0.140
11	LPC 16:0	0.137	0.001	0.979	0.103
12	LPC 16:0	0.234	0.006	0.827	0.213
13	LPC 16:0	0.166	0.001	0.795	0.168
14	LPC 16:0	0.158	0.005	0.805	0.158
15	LPC 16:0	0.241	0.002	0.895	0.199
16	LPC 16:1	0.016	0.014	0.594	0.038
17	LPC 16:1	0.009	0.045	0.385	0.040
18	LPC 16:1	0.008	0.047	0.346	0.043
19	LPC 16:1	0.008	0.047	0.376	0.040
20	LPC 16:1	0.009	0.044	0.391	0.041
21	LPC 16:1	0.008	0.045	0.386	0.037
22	LPC 16:1	0.008	0.050	0.332	0.045
23	LPC 16:1	0.009	0.041	0.404	0.039
24	LPC 17:0	0.082	0.004	0.448	0.034
25	LPC 17:1	0.005	0.004	0.739	0.004
26	LPC 18:0	0.072	0.001	0.558	0.034
27	LPC 18:0	0.080	0.001	0.379	0.030
28	LPC 18:0	0.072	0.001	0.341	0.027
29	LPC 18:0	0.111	0.002	0.521	0.049
30	LPC 18:0	0.096	0.001	0.582	0.046
31	LPC 18:0	0.069	0.001	0.545	0.032
32	LPC 18:1	0.015	0.071	0.253	0.101
33	LPC 18:1	0.007	0.074	0.181	0.082
34	LPC 18:1	0.022	0.030	0.304	0.109
35	LPC 18:1	0.013	0.112	0.204	0.114
36	LPC 18:1	0.012	0.110	0.201	0.110
37	LPC 18:1	0.022	0.091	0.257	0.129
38	LPC 18:1	0.022	0.087	0.259	0.128
39	LPC 18:1	0.015	0.107	0.214	0.122
40	LPC 18:1	0.019	0.074	0.238	0.129
41	LPC 18:1	0.023	0.053	0.213	0.165
42	LPC 18:1	0.057	0.058	0.309	0.215
43	LPC 18:3	0.107	0.022	0.687	0.057
44	LPC 18:3	0.016	0.092	0.990	0.018
45	LPC 20:2	0.191	0.013	0.483	0.080

## Resultados

46	LPC 20:3	0.029	0.022	0.923	0.026
47	LPC 20:3	0.047	0.042	0.940	0.048
48	LPC 20:3	0.023	0.031	0.910	0.028
49	LPC 20:3	0.001	0.623	0.131	0.014
50	LPC 20:3	0.045	0.034	0.990	0.041
51	LPC 20:4	0.017	0.044	0.685	0.033
52	LPC 20:4	0.015	0.128	0.389	0.062
53	LPC 20:4	0.005	0.099	0.302	0.037
54	LPC 20:4	0.007	0.123	0.264	0.054
55	LPC 20:4	0.005	0.044	0.336	0.030
56	LPC 20:4	0.056	0.004	0.751	0.075
57	LPC 20:4	0.012	0.131	0.355	0.059
58	LPC 20:4	0.014	0.110	0.311	0.075
59	LPC 20:4	0.016	0.125	0.305	0.087
60	LPC 20:5	0.005	0.854	0.172	0.071
61	LPC 20:5	0.003	0.711	0.163	0.045
62	LPC 20:5	0.005	0.679	0.203	0.053
63	LPC 22:4	0.023	0.070	0.740	0.037
64	LPC 22:5	0.032	0.168	0.471	0.087
65	LPC 22:5	0.259	0.081	0.905	0.165
66	LPC 22:5	0.061	0.301	0.503	0.132
67	LPC 22:5	0.063	0.100	0.839	0.071
68	LPC 22:6	0.098	0.376	0.294	0.335
69	LPC 22:6	0.208	0.546	0.303	0.558
70	LPC 22:6	0.220	0.505	0.325	0.545
71	LPC P-18:1	0.219	0.049	0.794	0.212
72	LPE 18:0	0.102	0.251	0.393	0.256
73	LPE 20:3	0.081	0.006	0.653	0.043
74	LPE 20:4	0.009	0.022	0.366	0.045
75	LPE 20:5	0.010	0.456	0.320	0.055
76	LPE 22:5	0.053	0.171	0.320	0.195
77	LPE 22:6	0.047	0.467	0.097	0.554
78	LPI 16:0	0.489	0.354	0.697	0.494
79	LPI 20:4	0.016	0.145	0.271	0.096
80	PC 16:0/20:5	0.150	0.016	0.174	0.719
81	Esfingosina-1-fosfato	0.078	0.001	0.890	0.078
82	L-Arginina	0.274	0.001	0.516	0.113
83	L-Leucina	0.051	0.006	0.125	0.315
84	LPE 20:4	0.047	0.010	0.219	0.169
85	LPE 20:4	0.023	0.008	0.200	0.100
86	Retinol	0.163	0.004	0.422	0.251
87	Ácido palmítico	0.001	0.346	0.007	0.369
88	Palmitoleil linoleato (18:2/16:1)	0.010	0.001	0.046	0.384
89	Phe-Ile O Phe-Leu	0.015	0.001	0.046	0.005

*Phe*: fenilalanina; *Ile*: isoleucina; *Leu*: Leucina; *LPC*: lisofosfatidilcolina; *LPE*: lisofosfatidiletanolamina; *LPI*: lisofosfatidilinositol; *PC*: fosfatidilcolina.

Tabla 6. Características fisicoquímicas de las señales anotadas mediante LC-MS/MS significativamente distintas en la comparación UCA vs ICS.

Nº	Técnica	Categoría biológica	Compuesto	m/z	Masa (Da)	RT (min)	Fórmula	Error (ppm)	Aducto	CV en QCs (%)
1	LC-MS-	Ácidos grasos	Ácido araquidónico †	371.2198	304.2402	27.79	C20H32O2	-0.1	M+HCOONa+H	17.2
2	LC-MS-	Ácidos grasos	Ácido araquidónico †	303.2328	304.2406	27.79	C20H32O2	1.3	M-H	9.1
3	LC-MS-	Otros	Bilirrubina †	583.255	584.2628	15.77	C33H36N4O6	-1.1	M-H	10.3
4	LC-MS-	Ácidos biliares	Glucurónido de ácido cólico	565.3008	584.3192	6.86	C30H48O11	-0.8	M-H-H2O	7.3
5	LC-MS-	Ácidos biliares	Ácido deoxicólico O isómeros †	437.2901	392.2924	14.73	C24H40O4	-0.5	M+FA-H	5.4
6	LC-MS-	Ácidos biliares	Ácido deoxicólico O isómeros †	391.2848	392.2926	14.73	C24H40O4	-0.1	M-H	6.7
7	LC-MS-	Otros	Ácido hipúrico †	178.0533	179.0611	1.04	C9H9NO3	16.1	M-H	5.9
8	LC-MS-	Fosfolípidos	LPC 16:0 †	584.3557	495.3318	18.37	C24H50NO7P	-1.3	M+C3H6O3+H	8.3
9	LC-MS-	Fosfolípidos	LPC 16:0 †	480.309	495.3325	19.16	C24H50NO7P	0	M-CH3-H	5.5
10	LC-MS-	Fosfolípidos	LPC 16:0 †	530.3025	495.3336	18.38	C24H50NO7P	2.3	M+Cl	6.3
11	LC-MS-	Fosfolípidos	LPC 16:0 †	540.3306	495.3329	18.38	C24H50NO7P	0.9	M+FA-H	7.4
12	LC-MS-	Fosfolípidos	LPC 16:0 †	608.317	495.3320	18.38	C24H50NO7P	-1.1	M+TFA-H	14.9
13	LC-MS-	Fosfolípidos	LPC 16:0 †	480.3089	495.3324	18.37	C24H50NO7P	-0.2	M-CH3-H	8.0
14	LC-MS-	Fosfolípidos	LPC 16:0 †	540.3306	495.3329	19.16	C24H50NO7P	0.9	M+FA-H	5.6
15	LC-MS-	Fosfolípidos	LPC 16:0 †	530.3032	495.3343	19.16	C24H50NO7P	3.8	M+Cl	5.5
16	LC-MS-	Fosfolípidos	LPC 16:1	538.3145	493.3168	16.27	C24H48NO7P	0	M+FA-H	8.5
17	LC-MS-	Fosfolípidos	LPC 16:1	538.3145	493.3168	16.27	C24H48NO7P	0	M+FA-H	8.9
18	LC-MS-	Fosfolípidos	LPC 16:1	538.3145	493.3168	16.27	C24H48NO7P	0	M+FA-H	8.6
19	LC-MS-	Fosfolípidos	LPC 16:1	538.3145	493.3168	16.27	C24H48NO7P	0	M+FA-H	8.6
20	LC-MS-	Fosfolípidos	LPC 16:1	538.3143	493.3166	15.58	C24H48NO7P	-0.4	M+FA-H	8.5
21	LC-MS-	Fosfolípidos	LPC 16:1	538.3143	493.3166	15.58	C24H48NO7P	-0.4	M+FA-H	8.7
22	LC-MS-	Fosfolípidos	LPC 16:1	538.3145	493.3168	16.27	C24H48NO7P	0	M+FA-H	8.5
23	LC-MS-	Fosfolípidos	LPC 16:1	528.2877	493.3188	16.27	C24H48NO7P	4.1	M-Cl	9.3
24	LC-MS-	Fosfolípidos	LPC 17:0 †	554.3458	509.3481	21.24	C25H52NO7P	0	M+FA-H	8.1
25	LC-MS-	Fosfolípidos	LPC 17:1	552.3292	507.3315	18.16	C25H50NO7P	-1.9	M+FA-H	15.5
26	LC-MS-	Fosfolípidos	LPC 18:0 †	508.3402	523.3637	23.40	C26H54NO7P	-0.2	M-CH3+H	7.3
27	LC-MS-	Fosfolípidos	LPC 18:0 †	568.3615	523.3638	22.58	C26H54NO7P	0.1	M+FA-H	8.6
28	LC-MS-	Fosfolípidos	LPC 18:0 †	560.3306	523.3461	23.41	C26H54NO7P	-33.8	M+Cl	5.1

Resultados

29	LC-MS-	Fosfolípidos	LPC 18:0 †	568.3619	523.3642	23.40	C26H54NO7P	0.9	M+FA-H	7.8
30	LC-MS-	Fosfolípidos	LPC 18:0 †	558.3314	523.3625	22.58	C26H54NO7P	-2.4	M+Cl	8.2
31	LC-MS-	Fosfolípidos	LPC 18:0 †	612.387	523.3631	23.40	C26H54NO7P	-1.3	M+C3H6O3-H	7.2
32	LC-MS-	Fosfolípidos	LPC 18:1 †	506.3246	521.3481	19.43	C26H52NO7P	-0.1	M-CH3-H	11.1
33	LC-MS-	Fosfolípidos	LPC 18:1 †	566.3458	521.3481	19.43	C26H52NO7P	0	M+FA-H	11.5
34	LC-MS-	Fosfolípidos	LPC 18:1 †	566.3458	521.3481	19.43	C26H52NO7P	0	M+FA-H	11.5
35	LC-MS-	Fosfolípidos	LPC 18:1 †	566.3463	521.3486	20.13	C26H52NO7P	1	M+FA-H	10.8
36	LC-MS-	Fosfolípidos	LPC 18:1 †	610.3711	521.3472	20.13	C26H52NO7P	-1.7	M+C3H6O3-H	10.4
37	LC-MS-	Fosfolípidos	LPC 18:1 †	506.3244	521.3479	20.13	C26H52NO7P	-0.5	M-CH3-H	12.7
38	LC-MS-	Fosfolípidos	LPC 18:1 †	566.3463	521.3486	20.13	C26H52NO7P	1	M+FA-H	10.6
39	LC-MS-	Fosfolípidos	LPC 18:1 †	566.3463	521.3486	20.13	C26H52NO7P	1	M+FA-H	10.5
40	LC-MS-	Fosfolípidos	LPC 18:1 †	556.3169	521.3480	20.13	C26H52NO7P	-0.2	M+Cl	11.1
41	LC-MS-	Fosfolípidos	LPC 18:1 †	634.3326	521.3476	20.13	C26H52NO7P	-1.1	M+TFA-H	18.0
42	LC-MS-	Fosfolípidos	LPC 18:1 †	634.3336	521.3486	19.43	C26H52NO7P	0.8	M+TFA-H	14.8
43	LC-MS-	Fosfolípidos	LPC 18:3	562.3139	517.3162	15.97	C26H48NO7P	-1.1	M+FA-H	12.6
44	LC-MS-	Fosfolípidos	LPC 18:3	562.3137	517.3160	15.63	C26H48NO7P	-1.5	M+FA-H	17.7
45	LC-MS-	Fosfolípidos	LPC 20:2	592.361	547.3633	21.19	C28H54NO7P	-0.8	M+FA-H	18.4
46	LC-MS-	Fosfolípidos	LPC 20:3	590.345	545.3473	20.03	C28H52NO7P	-1.5	M+FA-H	15.7
47	LC-MS-	Fosfolípidos	LPC 20:3	590.3453	545.3476	18.47	C28H52NO7P	-0.9	M+FA-H	19.9
48	LC-MS-	Fosfolípidos	LPC 20:3	590.3459	545.3482	19.06	C28H52NO7P	0.2	M+FA-H	18.3
49	LC-MS-	Fosfolípidos	LPC 20:3	590.3459	545.3482	19.06	C28H52NO7P	0.2	M+FA-H	19.1
50	LC-MS-	Fosfolípidos	LPC 20:4	588.3305	543.3328	17.70	C28H50NO7P	0.7	M+FA-H	14.4
51	LC-MS-	Fosfolípidos	LPC 20:4	588.3301	543.3324	17.13	C28H50NO7P	-0.1	M+FA-H	16.6
52	LC-MS-	Fosfolípidos	LPC 20:4	578.301	543.3321	17.13	C28H50NO7P	-0.6	M+Cl	15.5
53	LC-MS-	Fosfolípidos	LPC 20:4	588.3301	543.3324	17.13	C28H50NO7P	-0.1	M+FA-H	15.4
54	LC-MS-	Fosfolípidos	LPC 20:4	656.3182	543.3332	17.13	C28H50NO7P	1.2	M+TFA-H	27.1
55	LC-MS-	Fosfolípidos	LPC 20:4	528.3086	543.3321	17.71	C28H50NO7P	-0.8	M-CH3-H	13.6
56	LC-MS-	Fosfolípidos	LPC 20:4	656.3182	543.3332	17.13	C28H50NO7P	1.2	M+TFA-H	27.4
57	LC-MS-	Fosfolípidos	LPC 20:4	578.301	543.3321	17.71	C28H50NO7P	-0.6	M+Cl	10.7
58	LC-MS-	Fosfolípidos	LPC 20:4	580.3009	543.3164	17.70	C28H50NO7P	-29.6	M+Cl	11.2

Resultados

60	LC-MS-	Fosfolípidos	LPC 20:5	586.3143	541.3166	15.78	C28H48NO7P	-0.4	M+FA-H	14.5
61	LC-MS-	Fosfolípidos	LPC 20:5	586.3145	541.3168	15.23	C28H48NO7P	0	M+FA-H	10.8
62	LC-MS-	Fosfolípidos	LPC 20:5	586.3145	541.3168	15.23	C28H48NO7P	0	M+FA-H	11.7
63	LC-MS-	Fosfolípidos	LPC 22:4	616.3609	571.3632	20.62	C30H54NO7P	-0.9	M+FA-H	21.3
64	LC-MS-	Fosfolípidos	LPC 22:5	614.3462	569.3485	18.59	C30H52NO7P	0.7	M+FA-H	21.4
65	LC-MS-	Fosfolípidos	LPC 22:5	614.3483	569.3506	18.59	C30H52NO7P	4.4	M+FA-H	20.9
66	LC-MS-	Fosfolípidos	LPC 22:5	614.3435	569.3458	18.04	C30H52NO7P	-4	M+FA-H	18.7
67	LC-MS-	Fosfolípidos	LPC 22:5	614.347	569.3493	19.61	C30H52NO7P	2.1	M+FA-H	20.1
68	LC-MS-	Fosfolípidos	LPC 22:6	612.33	567.3323	17.63	C30H50NO7P	-0.3	M+FA-H	14.1
69	LC-MS-	Fosfolípidos	LPC 22:6	612.3297	567.3320	17.13	C30H50NO7P	-0.8	M+FA-H	16.6
70	LC-MS-	Fosfolípidos	LPC 22:6	612.3297	567.3320	17.13	C30H50NO7P	-0.8	M+FA-H	16.0
71	LC-MS-	Fosfolípidos	LPC P-18:1	550.3506	505.3529	21.20	C26H52NO6P	-0.5	M+FA-H	12.8
72	LC-MS-	Fosfolípidos	LPE 18:0 †	462.2984	481.3168	21.04	C23H48NO7P	-0.1	M-H-H2O	21.4
73	LC-MS-	Fosfolípidos	LPE 20:3	502.293	503.3008	18.93	C25H46NO7P	-0.7	M-H	10.2
74	LC-MS-	Fosfolípidos	LPE 20:4	500.2778	501.2856	17.54	C25H44NO7P	0.2	M-H	6.4
75	LC-MS-	Fosfolípidos	LPE 20:5	498.262	499.2698	15.65	C25H42NO7P	-0.1	M-H	6.1
76	LC-MS-	Fosfolípidos	LPE 22:5	526.2929	527.3007	18.46	C27H46NO7P	-0.9	M-H	12.0
77	LC-MS-	Fosfolípidos	LPE 22:6	524.2775	525.2853	17.49	C27H44NO7P	-0.4	M-H	5.9
78	LC-MS-	Fosfolípidos	LPI 16:0 †	571.2892	572.2970	22.67	C25H49O12P	1.5	M-H	21.3
79	LC-MS-	Fosfolípidos	LPI 20:4	619.288	620.2958	20.50	C29H49O12P	-0.6	M-H	17.9
80	LC-MS-	Fosfolípidos	PC 16:0/20:5	824.5453	779.5476	34.14	C44H78NO8P	1.5	M+FA-H	19.7
81	LC-MS-	Esfingolípidos	Esfingosina-1-fosfato †	378.2412	379.2490	14.85	C18H38NO5P	0.7	M-H	5.9
82	LC-MS+	Aminoácidos	L-Arginina †	175.1186	174.1108	0.75	C6H14N4O2	-5.2	M+H	16.9
83	LC-MS+	Aminoácidos	L-Leucina †	132.1006	131.0928	0.94	C6H13NO2	-14.1	M+H	9.8
84	LC-MS+	Fosfolípidos	LPE 20:4	502.2947	501.2869	17.58	C25H44NO7P	2.7	M+H	6.4
85	LC-MS+	Fosfolípidos	LPE 20:4	502.2947	501.2869	17.58	C25H44NO7P	2.7	M+H	6.8
86	LC-MS+	Vitaminas	Retinol	269.2266	286.2293	27.26	C20H30O	-1.1	M+H-H2O	6.4

LPC: lisofosfatidilcolina; LPE: lisofosfatidiletanolamina; LPI: lisofosfatidilinositol; PC: fosfatidilcolina. †: indica que la identidad se confirmó mediante un patrón comercial.

**Tabla 7.** Comparaciones dos a dos que muestran el grado de significación y el porcentaje de cambio entre todos los grupos. Las diferencias significativas se marcan en negrita; y los porcentajes de cambio se marcan en color rojo para los metabolitos que aumentan y en azul para los metabolitos que disminuyen.

Nº	Compuesto	Masa (Da)	RT (min)	ICS vs UCA			ICS vs IT			ICS vs BIO			IT vs UCA			BIO vs UCA					
				% cambio (UCA)	p-valor	FDR	% cambio (IT)	p-valor	FDR	% cambio (BIO)	p-valor	FDR	% cambio (UCA)	p-valor	FDR	% cambio (UCA)	p-valor	FDR			
1	Ácido araquidónico †	304.2402	27.79	<b>45.4</b>	<b>0.0281</b>	<b>0.1352</b>	<b>17.4</b>	0.1389	0.7152	<b>1.8</b>	0.4484	0.8998	<b>-13.3</b>	0.4303	0.9686	<b>23.9</b>	0.1131	0.4013	<b>42.9</b>	0.0177	0.4079
2	Ácido araquidónico †	304.2406	27.79	<b>46.7</b>	<b>0.0326</b>	<b>0.1415</b>	<b>18.6</b>	0.1277	0.7078	<b>0.4</b>	0.5351	0.9301	<b>-15.4</b>	0.3047	0.9686	<b>23.7</b>	0.1015	0.3785	<b>46.1</b>	0.0242	0.4079
3	Bilirrubina †	584.2628	15.77	<b>-37.6</b>	<b>0.0376</b>	<b>0.1491</b>	<b>19.1</b>	0.9397	0.9908	<b>-7.7</b>	0.4763	0.9180	<b>-22.5</b>	0.3363	0.9686	<b>-47.6</b>	0.0342	0.3084	<b>-32.4</b>	0.2787	0.5898
4	Glucurónido de ácido cólico	584.3192	6.86	<b>54.7</b>	<b>0.0177</b>	<b>0.1097</b>	<b>29.6</b>	0.0820	0.7078	<b>61.3</b>	0.0041	0.8682	<b>24.5</b>	0.0118	0.9686	<b>19.3</b>	0.0604	0.3288	<b>-4.1</b>	0.6187	0.8110
5	Ácido deoxicólico O isómeros †	392.2924	14.73	<b>-62.4</b>	<b>0.0128</b>	<b>0.0969</b>	<b>-1.3</b>	0.2947	0.7734	<b>-10.1</b>	0.1753	0.8682	<b>-8.9</b>	0.9054	0.9924	<b>-61.9</b>	0.1965	0.5143	<b>-58.1</b>	0.3055	0.6195
6	Ácido deoxicólico O isómeros †	392.2926	14.73	<b>-63.3</b>	<b>0.0128</b>	<b>0.0969</b>	<b>-10.3</b>	0.1075	0.7078	<b>-9.6</b>	0.1753	0.8682	<b>0.8</b>	0.8038	0.9810	<b>-59.1</b>	0.3052	0.6233	<b>-59.4</b>	0.3055	0.6195
7	Ácido hipúrico †	179.0611	1.04	<b>87.5</b>	<b>0.0077</b>	<b>0.0864</b>	<b>129.3</b>	0.0087	0.7078	<b>192.2</b>	0.0695	0.8682	<b>27.5</b>	0.5669	0.9686	<b>-18.2</b>	0.7192	0.8709	<b>-35.8</b>	0.7922	0.9040
8	LPC 16:0 †	495.3318	18.37	<b>28.4</b>	<b>0.0242</b>	<b>0.1256</b>	<b>4.2</b>	0.8543	0.9488	<b>7.3</b>	0.8005	0.9767	<b>3.0</b>	0.8883	0.9810	<b>23.2</b>	<b>0.0039</b>	<b>0.1871</b>	<b>19.6</b>	0.0207	0.4079
9	LPC 16:0 †	495.3325	19.16	<b>30.6</b>	<b>0.0242</b>	<b>0.1256</b>	<b>9.6</b>	0.3363	0.7736	<b>5.0</b>	0.5972	0.9394	<b>-4.3</b>	0.7377	0.9686	<b>19.1</b>	0.0503	0.3288	<b>24.4</b>	0.0242	0.4079
10	LPC 16:0 †	495.3336	18.38	<b>26.1</b>	<b>0.0376</b>	<b>0.1491</b>	<b>8.4</b>	0.4303	0.7976	<b>1.7</b>	1.0000	1.0000	<b>-6.1</b>	0.2848	0.9686	<b>16.3</b>	0.0569	0.3288	<b>23.9</b>	0.0065	0.4079
11	LPC 16:0 †	495.3329	18.38	<b>25.8</b>	<b>0.0177</b>	<b>0.1097</b>	<b>8.1</b>	0.2390	0.7734	<b>2.8</b>	0.7304	0.9596	<b>-4.9</b>	0.3363	0.9686	<b>16.4</b>	0.0262	0.3046	<b>22.4</b>	0.0177	0.4079
12	LPC 16:0 †	495.3320	18.38	<b>22.6</b>	<b>0.0376</b>	<b>0.1491</b>	<b>7.3</b>	0.4178	0.7895	<b>6.3</b>	0.6961	0.9510	<b>-1.0</b>	0.6578	0.9686	<b>14.3</b>	0.0390	0.3199	<b>15.4</b>	0.0434	0.4079
13	LPC 16:0 †	495.3324	18.37	<b>21.8</b>	<b>0.0151</b>	<b>0.1034</b>	<b>6.1</b>	0.2848	0.7734	<b>5.1</b>	0.6625	0.9497	<b>-0.9</b>	0.4692	0.9686	<b>14.8</b>	0.0366	0.3084	<b>15.9</b>	0.0376	0.4079
14	LPC 16:0 †	495.3329	19.16	<b>21.6</b>	<b>0.0207</b>	<b>0.1160</b>	<b>7.4</b>	0.2947	0.7734	<b>5.3</b>	0.5972	0.9394	<b>-2.0</b>	0.5669	0.9686	<b>13.2</b>	0.0320	0.3084	<b>15.5</b>	0.0434	0.4079
15	LPC 16:0 †	495.3343	19.16	<b>18.6</b>	<b>0.0281</b>	<b>0.1352</b>	<b>9.2</b>	0.1911	0.7466	<b>6.2</b>	0.7304	0.9596	<b>-2.7</b>	0.3815	0.9686	<b>8.6</b>	0.1787	0.4952	<b>11.7</b>	0.0570	0.4079
16	LPC 16:1	493.3168	16.27	<b>63.1</b>	<b>0.0038</b>	<b>0.0864</b>	<b>9.7</b>	0.5099	0.8493	<b>21.7</b>	0.2802	0.8682	<b>11.0</b>	0.6423	0.9686	<b>48.7</b>	<b>0.0021</b>	<b>0.1592</b>	<b>34.0</b>	0.0570	0.4079
17	LPC 16:1	493.3168	15.58	<b>61.0</b>	<b>0.0092</b>	<b>0.0875</b>	<b>6.7</b>	0.6894	0.9002	<b>21.4</b>	0.3462	0.8682	<b>13.7</b>	0.5817	0.9686	<b>50.9</b>	<b>0.0013</b>	<b>0.1592</b>	<b>32.7</b>	0.0651	0.4079
18	LPC 16:1	493.3168	16.27	<b>62.0</b>	<b>0.0038</b>	<b>0.0864</b>	<b>9.1</b>	0.5380	0.8556	<b>21.1</b>	0.3012	0.8682	<b>11.0</b>	0.6423	0.9686	<b>48.4</b>	<b>0.0023</b>	<b>0.1592</b>	<b>33.8</b>	0.0570	0.4079

Resultados

19	LPC 16:1	493.3168	16.27	<b>62.5</b>	<b>0.0054</b>	<b>0.0864</b>	8.3	0.5669	0.8658	22.6	0.2413	0.8682	13.2	0.5524	0.9686	<b>50.0</b>	<b>0.0018</b>	<b>0.1592</b>	32.6	0.0841	0.4079
20	LPC 16:1	493.3166	16.27	<b>61.6</b>	<b>0.0065</b>	<b>0.0864</b>	8.5	0.5817	0.8658	20.7	0.3462	0.8682	11.3	0.6116	0.9686	<b>48.9</b>	<b>0.0027</b>	<b>0.1592</b>	33.8	0.0841	0.4079
21	LPC 16:1	493.3166	15.58	<b>60.8</b>	<b>0.0065</b>	<b>0.0864</b>	6.8	0.6423	0.8816	21.0	0.3232	0.8682	13.3	0.5966	0.9686	<b>50.6</b>	<b>0.0012</b>	<b>0.1592</b>	32.9	0.0570	0.4079
22	LPC 16:1	493.3168	16.27	<b>60.2</b>	<b>0.0045</b>	<b>0.0864</b>	6.0	0.7215	0.9010	21.0	0.2603	0.8682	14.2	0.5239	0.9686	<b>51.1</b>	<b>0.0016</b>	<b>0.1592</b>	32.3	0.0651	0.4079
23	LPC 16:1	493.3188	16.27	<b>52.0</b>	<b>0.0065</b>	<b>0.0864</b>	7.6	0.7377	0.9039	15.6	0.4213	0.8821	7.4	0.6894	0.9686	<b>41.2</b>	<b>0.0035</b>	<b>0.1871</b>	31.5	0.0570	0.4079
24	LPC 17:0 †	509.3481	21.24	<b>47.9</b>	<b>0.0281</b>	<b>0.1352</b>	19.8	0.1224	0.7078	12.1	0.4213	0.8821	-6.4	0.4303	0.9686	23.5	0.1467	0.4423	32.0	0.0570	0.4079
25	LPC 17:1	507.3315	18.16	<b>73.9</b>	<b>0.0045</b>	<b>0.0864</b>	28.7	0.1634	0.7250	34.6	0.1753	0.8682	4.6	1.0000	1.0000	35.1	0.0148	0.2980	29.2	0.0841	0.4079
26	LPC 18:0 †	523.3637	23.40	<b>38.4</b>	<b>0.0281</b>	<b>0.1352</b>	18.2	0.0899	0.7078	17.3	0.3232	0.8682	-0.8	0.7377	0.9686	17.1	0.1324	0.4234	18.0	0.0952	0.4196
27	LPC 18:0 †	523.3638	22.58	<b>38.1</b>	<b>0.0281</b>	<b>0.1352</b>	17.6	0.1332	0.7152	16.3	0.2802	0.8682	-1.2	0.7705	0.9686	17.4	0.1324	0.4234	18.8	0.1354	0.4582
28	LPC 18:0 †	523.3461	23.41	<b>31.6</b>	<b>0.0376</b>	<b>0.1491</b>	16.7	0.1224	0.7078	13.4	0.2603	0.8682	-2.9	0.5817	0.9686	12.8	0.2577	0.5725	16.1	0.1073	0.4250
29	LPC 18:0 †	523.3642	23.40	<b>35.6</b>	<b>0.0326</b>	<b>0.1415</b>	16.6	0.1224	0.7078	16.1	0.3703	0.8682	-0.5	0.8543	0.9810	16.3	0.1542	0.4488	16.9	0.1207	0.4311
30	LPC 18:0 †	523.3625	22.58	<b>33.4</b>	<b>0.0326</b>	<b>0.1415</b>	23.4	0.0616	0.7078	24.8	0.0849	0.8682	1.1	0.9569	0.9981	8.1	0.4971	0.7456	6.9	0.5387	0.7703
31	LPC 18:0 †	523.3631	23.40	<b>33.9</b>	<b>0.0434</b>	<b>0.1629</b>	12.0	0.3256	0.7734	18.6	0.2413	0.8682	5.9	0.7871	0.9747	19.6	0.0473	0.3274	12.9	0.1207	0.4311
32	LPC 18:1 †	521.3481	19.43	<b>54.6</b>	<b>0.0077</b>	<b>0.0864</b>	22.9	0.0940	0.7078	9.3	0.3703	0.8682	-11.1	0.3150	0.9686	25.9	0.1015	0.3785	41.5	0.0498	0.4079
33	LPC 18:1 †	521.3481	19.43	<b>55.4</b>	<b>0.0065</b>	<b>0.0864</b>	29.2	0.0858	0.7078	12.8	0.4213	0.8821	-12.7	0.3150	0.9686	20.3	0.0535	0.3288	37.7	0.0376	0.4079
34	LPC 18:1 †	521.3481	19.43	<b>55.1</b>	<b>0.0077</b>	<b>0.0864</b>	28.4	0.1123	0.7078	13.2	0.3703	0.8682	-11.9	0.3473	0.9686	20.7	0.0444	0.3268	37.0	0.0651	0.4079
35	LPC 18:1 †	521.3486	20.13	<b>53.5</b>	<b>0.0038</b>	<b>0.0864</b>	29.3	0.0531	0.7078	14.3	0.3703	0.8682	-11.6	0.3585	0.9686	18.8	0.0960	0.3726	34.3	0.0498	0.4079
36	LPC 18:1 †	521.3472	20.13	<b>48.9</b>	<b>0.0177</b>	<b>0.1097</b>	22.7	0.1172	0.7078	15.5	0.2603	0.8682	-5.9	0.6735	0.9686	21.3	0.0416	0.3268	28.9	0.0570	0.4079
37	LPC 18:1 †	521.3479	20.13	<b>52.0</b>	<b>0.0065</b>	<b>0.0864</b>	28.6	0.1634	0.7250	11.9	0.4213	0.8821	-13.0	0.4178	0.9686	18.2	0.0366	0.3084	35.9	0.0741	0.4079
38	LPC 18:1 †	521.3486	20.13	<b>51.3</b>	<b>0.0054</b>	<b>0.0864</b>	27.2	0.0712	0.7078	13.3	0.3703	0.8682	-10.9	0.3815	0.9686	18.9	0.0811	0.3549	33.5	0.0651	0.4079
39	LPC 18:1 †	521.3486	20.13	<b>51.0</b>	<b>0.0054</b>	<b>0.0864</b>	27.1	0.0712	0.7078	13.2	0.3953	0.8682	-10.9	0.3363	0.9686	18.9	0.0960	0.3726	33.4	0.0570	0.4079
40	LPC 18:1 †	521.3480	20.13	<b>43.7</b>	<b>0.0109</b>	<b>0.0916</b>	27.1	0.0858	0.7078	15.2	0.3953	0.8682	-9.3	0.3150	0.9686	13.1	0.1394	0.4339	24.7	0.0651	0.4079
41	LPC 18:1 †	521.3476	20.13	<b>42.2</b>	<b>0.0128</b>	<b>0.0969</b>	20.4	0.1277	0.7078	11.5	0.3232	0.8682	-7.4	0.4178	0.9686	18.1	0.0858	0.3595	27.5	0.0570	0.4079



## Resultados

42	LPC 18:1 #	521.3486	19.43	<b>39.2</b>	<b>0.0376</b>	<b>0.1491</b>	17.6	0.3363	0.7736	4.8	0.7652	0.9703	-10.9	0.4303	0.9686	18.3	0.0681	0.3504	32.8	0.0376	0.4079
43	LPC 18:3	517.3162	15.97	<b>57.7</b>	<b>0.0207</b>	<b>0.1160</b>	6.4	0.5966	0.8658	14.9	0.3953	0.8682	8.0	0.4055	0.9686	48.3	0.0063	0.2306	37.3	0.0376	0.4079
44	LPC 18:3	517.3160	15.63	<b>124.5</b>	<b>0.0109</b>	<b>0.0916</b>	29.9	0.4055	0.7895	41.2	0.3012	0.8682	8.7	0.6735	0.9686	72.8	0.0074	0.2406	59.0	0.0498	0.4079
45	LPC 20:2	547.3633	21.19	<b>45.1</b>	<b>0.0498</b>	<b>0.1768</b>	27.7	0.1277	0.7078	5.2	0.6951	0.9510	-17.6	0.2752	0.9686	13.6	0.3445	0.6467	37.9	0.0952	0.4196
46	LPC 20:3	545.3473	20.03	<b>173.9</b>	<b>0.0009</b>	<b>0.0864</b>	73.2	0.0434	0.7078	73.1	0.0229	0.8682	0.0	0.4961	0.9686	58.2	0.0262	0.3046	58.2	0.0741	0.4079
47	LPC 20:3	545.3476	18.47	<b>67.1</b>	<b>0.0065</b>	<b>0.0864</b>	32.3	0.1701	0.7250	24.2	0.3012	0.8682	-6.1	0.8205	0.9810	26.4	0.0960	0.3726	34.6	0.0952	0.4196
48	LPC 20:3	545.3476	18.47	<b>67.6</b>	<b>0.0092</b>	<b>0.0875</b>	31.3	0.1701	0.7250	25.2	0.3012	0.8682	-4.6	0.9054	0.9924	27.7	0.0722	0.3504	33.8	0.0841	0.4079
49	LPC 20:3	545.3482	19.06	<b>69.3</b>	<b>0.0128</b>	<b>0.0969</b>	36.9	0.1277	0.7078	29.5	0.2802	0.8682	-5.4	0.7871	0.9747	23.7	0.1131	0.4013	30.7	0.1514	0.4923
50	LPC 20:3	545.3482	19.06	<b>71.2</b>	<b>0.0077</b>	<b>0.0864</b>	34.8	0.1447	0.7199	24.6	0.3462	0.8682	-7.6	0.6894	0.9686	27.0	0.0811	0.3549	37.4	0.0841	0.4079
51	LPC 20:4	543.3328	17.70	<b>74.2</b>	<b>0.0031</b>	<b>0.0864</b>	37.1	0.0456	0.7078	22.7	0.2064	0.8682	-10.5	0.4431	0.9686	27.1	0.0444	0.3268	42.0	0.0498	0.4079
52	LPC 20:4	543.3324	17.13	<b>73.4</b>	<b>0.0109</b>	<b>0.0916</b>	31.7	0.0820	0.7078	19.4	0.3232	0.8682	-9.4	0.5239	0.9686	31.6	0.0342	0.3084	45.2	0.0376	0.4079
53	LPC 20:4	543.3321	17.13	<b>69.9</b>	<b>0.0109</b>	<b>0.0916</b>	26.5	0.0983	0.7078	13.2	0.3703	0.8682	-10.6	0.3699	0.9686	34.3	0.0244	0.3046	50.1	0.0092	0.4079
54	LPC 20:4	543.3324	17.13	<b>72.6</b>	<b>0.0109</b>	<b>0.0916</b>	30.8	0.0858	0.7078	20.0	0.2802	0.8682	-8.3	0.6578	0.9686	32.0	0.0300	0.3084	43.8	0.0651	0.4079
55	LPC 20:4	543.3332	17.13	<b>64.2</b>	<b>0.0092</b>	<b>0.0875</b>	27.6	0.0899	0.7078	15.2	0.3232	0.8682	-9.7	0.4825	0.9686	28.7	0.0228	0.3046	42.6	0.0128	0.4079
56	LPC 20:4	543.3321	17.71	<b>70.6</b>	<b>0.0045</b>	<b>0.0864</b>	35.4	0.0371	0.7078	21.9	0.1904	0.8682	-9.9	0.4178	0.9686	26.0	0.0569	0.3288	39.9	0.0281	0.4079
57	LPC 20:4	543.3332	17.13	<b>63.6</b>	<b>0.0092</b>	<b>0.0875</b>	27.2	0.0820	0.7078	15.0	0.3232	0.8682	-9.6	0.5239	0.9686	28.5	0.0366	0.3084	42.2	0.0128	0.4079
58	LPC 20:4	543.3321	17.71	<b>65.1</b>	<b>0.0045</b>	<b>0.0864</b>	29.7	0.0333	0.7078	20.9	0.1478	0.8682	-6.8	0.5966	0.9686	27.3	0.0366	0.3084	36.6	0.0207	0.4079
59	LPC 20:4	543.3164	17.70	<b>36.4</b>	<b>0.0109</b>	<b>0.0916</b>	16.2	0.2222	0.7734	8.0	0.5657	0.9301	-7.1	0.4961	0.9686	17.4	0.0766	0.3549	26.3	0.0326	0.4079
60	LPC 20:5	541.3166	15.78	<b>168.4</b>	<b>0.0012</b>	<b>0.0864</b>	91.4	0.0940	0.7078	62.2	0.0935	0.8682	-15.3	0.9569	0.9981	40.2	0.0171	0.2980	65.5	0.0151	0.4079
61	LPC 20:5	541.3168	15.23	<b>155.2</b>	<b>0.0009</b>	<b>0.0864</b>	87.8	0.0531	0.7078	75.2	0.1129	0.8682	-6.7	0.9569	0.9981	35.9	0.0184	0.2980	45.7	0.0281	0.4079
62	LPC 20:5	541.3168	15.23	<b>154.0</b>	<b>0.0021</b>	<b>0.0864</b>	76.6	0.1332	0.7152	65.6	0.1611	0.8682	-6.3	0.8543	0.9810	43.8	0.0171	0.2980	53.4	0.0281	0.4079
63	LPC 22:4	571.3632	20.62	<b>79.4</b>	<b>0.0128</b>	<b>0.0969</b>	27.6	0.1769	0.7250	23.1	0.3232	0.8682	-3.5	0.9225	0.9943	40.6	0.0244	0.3046	45.7	0.0651	0.4079
64	LPC 22:5	569.3485	18.59	<b>85.3</b>	<b>0.0109</b>	<b>0.0916</b>	29.6	0.2062	0.7597	22.6	0.1753	0.8682	-5.4	0.9569	0.9981	43.0	0.0228	0.3046	51.1	0.1073	0.4250

Resultados

65	LPC 22:5	569.3506	18.59	<b>76.0</b>	<b>0.0151</b>	<b>0.1034</b>	28.7	0.2062	0.7597	17.3	0.3012	0.8682	-8.9	0.8543	0.9810	36.8	0.0159	0.2980	50.1	0.0741	0.4079
66	LPC 22:5	569.3458	18.04	<b>74.4</b>	<b>0.0077</b>	<b>0.0864</b>	28.0	0.1701	0.7250	20.8	0.1354	0.8682	-5.6	0.9397	0.9981	36.3	0.0148	0.2980	44.3	0.0741	0.4079
67	LPC 22:5	569.3493	19.61	<b>53.0</b>	<b>0.0281</b>	<b>0.1352</b>	41.0	0.0559	0.7078	35.1	0.2413	0.8682	-4.2	0.5239	0.9686	8.5	0.2467	0.5586	13.2	0.0651	0.4079
68	LPC 22:6	567.3323	17.63	<b>47.1</b>	<b>0.0151</b>	<b>0.1034</b>	22.4	0.0456	0.7078	3.0	0.3232	0.8682	-15.8	0.4055	0.9686	20.1	0.0722	0.3504	42.7	0.0741	0.4079
69	LPC 22:6	567.3320	17.13	<b>55.5</b>	<b>0.0151</b>	<b>0.1034</b>	30.0	0.0616	0.7078	11.8	0.3953	0.8682	-14.0	0.3473	0.9686	19.6	0.0908	0.3722	39.1	0.0841	0.4079
70	LPC 22:6	567.3320	17.13	<b>48.1</b>	<b>0.0128</b>	<b>0.0969</b>	23.5	0.0782	0.7078	3.6	0.4213	0.8821	-16.1	0.3815	0.9686	20.0	0.1015	0.3785	43.0	0.0841	0.4079
71	LPC P-18:1	505.3529	21.20	<b>38.3</b>	<b>0.0281</b>	<b>0.1352</b>	24.3	0.1570	0.7250	11.4	0.5657	0.9301	-10.4	0.5966	0.9686	11.3	0.2691	0.5887	24.2	0.2787	0.5898
72	LPE 18:0 †	481.3168	21.04	<b>55.4</b>	<b>0.0326</b>	<b>0.1415</b>	50.5	0.0480	0.7078	13.4	0.5657	0.9301	-24.7	0.3363	0.9686	3.2	0.4804	0.7299	37.1	0.2081	0.5479
73	LPE 20:3	503.3008	18.93	<b>47.1</b>	<b>0.0177</b>	<b>0.1097</b>	10.5	0.7871	0.9236	25.7	0.5053	0.9301	13.8	0.7705	0.9686	33.1	0.0148	0.2980	17.0	0.1207	0.4311
74	LPE 20:4	501.2856	17.54	<b>52.6</b>	<b>0.0065</b>	<b>0.0864</b>	19.7	0.1839	0.7433	15.1	0.3953	0.8682	-3.8	0.5966	0.9686	27.5	0.0087	0.2668	32.6	0.0177	0.4079
75	LPE 20:5	499.2698	15.65	<b>129.2</b>	<b>0.0038</b>	<b>0.0864</b>	56.7	0.3256	0.7734	55.2	0.1904	0.8682	-1.0	0.6269	0.9686	46.3	0.0102	0.2819	47.7	0.0570	0.4079
76	LPE 22:5	527.3007	18.46	<b>53.3</b>	<b>0.0498</b>	<b>0.1768</b>	-7.5	0.5817	0.8658	15.4	0.3953	0.8682	24.8	0.0456	0.9686	65.8	<b>0.0018</b>	<b>0.1592</b>	32.9	0.1073	0.4250
77	LPE 22:6	525.2853	17.49	<b>42.4</b>	<b>0.0242</b>	<b>0.1256</b>	12.3	0.2566	0.7734	8.8	0.4484	0.8998	-3.1	0.6894	0.9686	26.8	0.0858	0.3595	30.8	0.1073	0.4250
78	LPI 16:0 †	572.2970	22.67	<b>44.6</b>	<b>0.0151</b>	<b>0.1034</b>	24.4	0.0983	0.7078	11.9	0.2413	0.8682	-10.1	0.5966	0.9686	16.2	0.2156	0.5163	29.3	0.3055	0.6195
79	LPI 20:4	620.2958	20.50	<b>63.6</b>	<b>0.0065</b>	<b>0.0864</b>	24.1	0.2477	0.7734	16.9	0.4484	0.8998	-5.8	0.7053	0.9686	31.7	0.0262	0.3046	39.9	0.0326	0.4079
80	PC 16:0/20:5	779.5476	34.14	<b>-40.2</b>	<b>0.0326</b>	<b>0.1415</b>	-34.0	0.2305	0.7734	-26.6	0.5053	0.9301	11.2	0.6269	0.9686	-9.5	0.6222	0.8120	-18.6	0.5387	0.7703
81	Esfingosina-1-fosfato †	379.2490	14.85	<b>24.2</b>	<b>0.0242</b>	<b>0.1256</b>	7.6	0.3699	0.7857	0.9	0.8722	0.9847	-6.2	0.4178	0.9686	15.4	0.0444	0.3268	23.1	0.0242	0.4079
82	L-Arginina †	174.1108	0.75	19.0	0.0426	0.3035	19.9	0.0478	0.4563	28.3	0.1195	0.8001	7.1	0.9253	0.9986	-0.7	0.6062	0.9221	-7.3	0.7861	0.9711
83	L-Leucina †	131.0928	0.94	24.7	0.0426	0.3035	17.4	0.0572	0.4664	14.4	0.2278	0.8001	-2.6	0.6392	0.9986	6.2	0.3903	0.8716	9.1	0.2083	0.8588
84	LPE 20:4	501.2869	17.58	37.3	0.0370	0.3035	19.1	0.0913	0.4808	18.5	0.1958	0.8001	-0.5	0.8982	0.9986	15.3	0.0204	0.5008	15.8	0.0717	0.6872
85	LPE 20:4	501.2869	17.58	32.9	0.0426	0.3035	18.0	0.1115	0.4808	18.3	0.2114	0.8001	0.2	0.7916	0.9986	12.6	0.0588	0.5134	12.3	0.1323	0.7587
86	Retinol	286.2293	27.26	25.0	0.0426	0.3035	10.3	0.1870	0.5647	-0.6	0.6452	0.8754	-9.9	0.2569	0.9986	13.3	0.2051	0.7565	25.8	0.0318	0.6148

LPC: lisofosfatidilcolina; LPE: lisofosfatidiletanolamina; LPI: lisofosfatidilinositol; PC: fosfatidilcolina; FDR: tasa de falsos descubrimientos (False Discovery Rate), es el p-valor tras aplicar la corrección de Benjamini-Hochberg. †: indica que la identidad se confirmó mediante un patrón comercial.

## Resultados

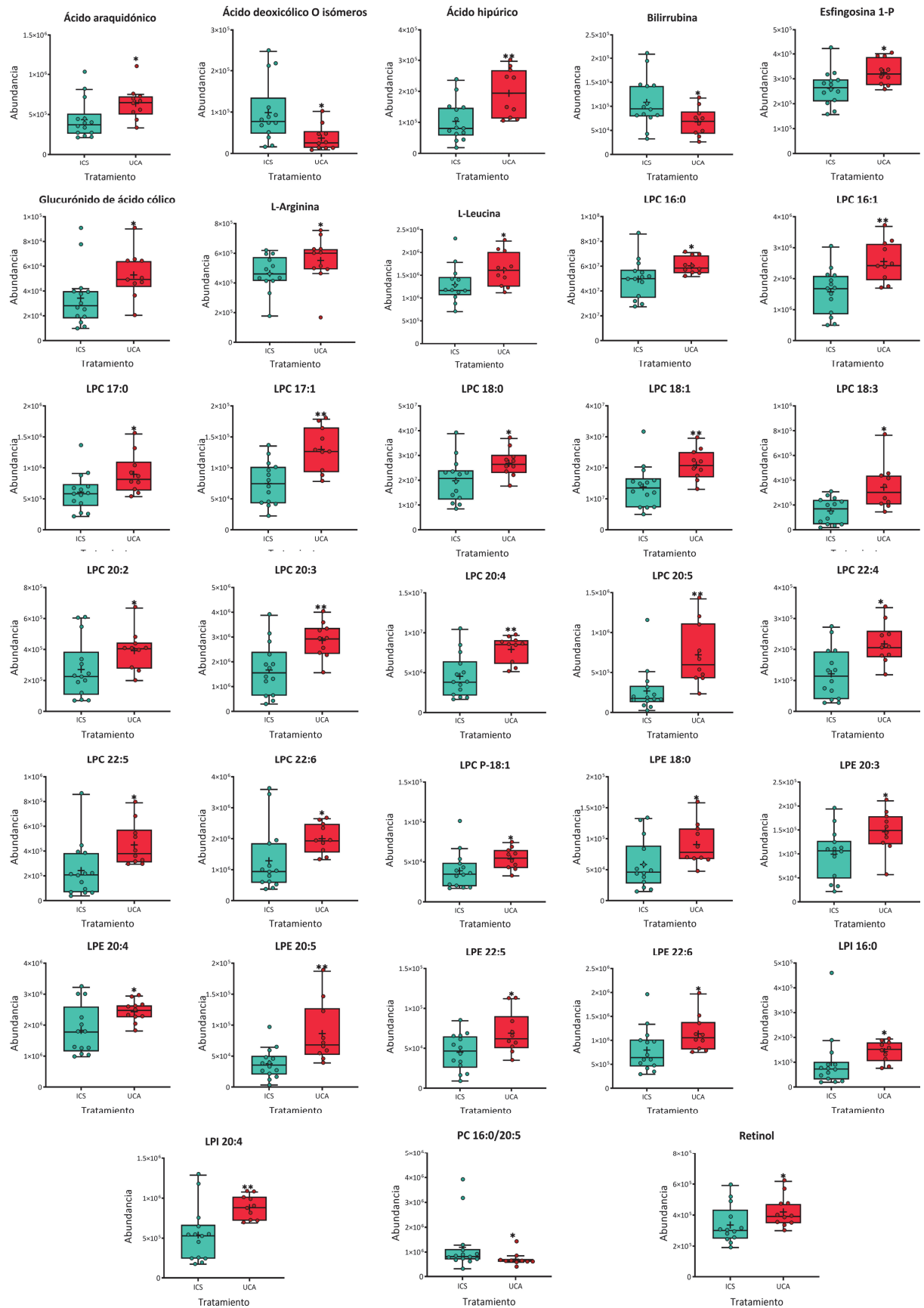


**Figura 19.** Trayectorias de los metabolitos significativamente distintos entre ICS (en azul) y UCA (en rojo). La media se muestra como '+' dentro de las cajas. Se seleccionaron los  $m/z$  más abundantes para aquellos metabolitos en los que se detectó más de un  $m/z$ , o que se detectaron en varias polaridades. \*:  $P < .05$ ; \*\*:  $P < .01$ . LPC: lisofosfatidilcolina; LPE: lisofosfatidiletanolamina; LPI: lisofosfatidilinositol, PC: fosfatidilcolina.

## Resultados

A continuación, con el fin de encontrar qué rutas se encontraban alteradas entre ambos grupos, se realizó un análisis de rutas metabólicas con los 33 metabolitos únicos identificados (**Tabla 8**).

**Tabla 8.** Rutas metabólicas enriquecidas en los pacientes UCA comparados con ICS con un FDR<0.2.

Ruta metabólica	<i>p</i> -valor	FDR	Metabolitos (%)	Fuente
Ruta de la fosfolipasa A <sub>2</sub> (PLA <sub>2</sub> )	1.43E-06	0.0061	100.00	Reactome
Eventos dependientes de calcio	6.67E-06	0.0142	91.67	Reactome
Eventos mediados por PLCβ	2.72E-05	0.0232	89.47	Reactome
Eventos mediados por proteína G	2.72E-05	0.0232	89.47	Reactome
Señalización por opioides	5.27E-05	0.0322	87.50	Reactome
Señalización <i>downstream</i> de GPCR	9.70E-05	0.0443	69.86	Reactome
Señalización por GPCR	1.04E-04	0.0443	69.48	Reactome
Biosíntesis de leucotrienos	1.43E-04	0.0553	96.67	HumanCyc
Remodelado de cardiolipina por cadenas acilo	2.01E-04	0.0661	50.00	Reactome
Remodelado de fosfatidilcolinas por cadenas acilo	2.01E-04	0.0661	46.15	Reactome
Fagocitosis mediada por FcγR en humanos ( <i>Homo sapiens</i> )	2.81E-04	0.0800	87.50	KEGG
Tráfico retrógrado de Golgi a RE independiente de COPI	2.81E-04	0.0800	87.50	Reactome
Transducción de señales	3.62E-04	0.0966	70.85	Reactome
Transporte retrógrado de Golgi a RE	4.80E-04	0.1060	90.00	Reactome
Eventos de señalización Gα (I)	5.48E-04	0.1060	70.44	Reactome
Remodelado HDL	5.99E-04	0.1060	58.82	Reactome
Remodelado de lipoproteínas plasmáticas	5.99E-04	0.1060	50.00	Reactome
Metabolismo de colina en cáncer ( <i>Homo sapiens</i> )	5.99E-04	0.1060	90.91	KEGG
Tráfico intra-Golgi y de Golgi a RE	7.30E-04	0.1060	91.67	Reactome
Ensamblaje, remodelado y limpieza de lipoproteína plasmática	0.001	0.1060	52.00	Reactome
Deficiencia en la biosíntesis del leucotrieno C4	0.0016	0.1060	91.55	SMPDB
Señalización retrógrada de endocannabinoides ( <i>Homo sapiens</i> )	0.0018	0.1100	89.47	KEGG
Metabolismo de ácido linoléico y α-linolénico	0.0018	0.1100	94.44	SMPDB
Ruta de acción de celecoxib	0.0019	0.1150	90.79	SMPDB
Metabolismo de ácido linoleico ( <i>Homo sapiens</i> )	0.0022	0.1340	67.86	KEGG
Tráfico de membrana	0.0025	0.1450	66.67	Reactome

## Resultados

Metabolismo del linoleato	0.0025	0.1450	83.33	EHMN
Transporte de pequeñas moléculas	0.0031	0.1670	78.32	Reactome
Metabolismo de ácido araquidónico	0.0032	0.1670	79.81	Reactome
Biosíntesis de fosfolípidos	0.0033	0.1670	95.83	SMPDB
Metabolismo de glicerofosfolípidos ( <i>Homo sapiens</i> )	0.0033	0.1670	44.23	KEGG

*FDR*: tasa de falsos descubrimientos (*False Discovery Rate*). Es el *p*-valor tras aplicar la corrección de Benjamini-Hochberg; *Metabolitos (%)*: Porcentaje de metabolitos que se han encontrado alterados con respecto a los de la ruta.

Se observó una alteración significativa en, entre otras, la ruta de la fosfolipasa A<sub>2</sub> (PLA<sub>2</sub>), en la que se identificaron el 100% de los metabolitos, y cuyos cambios entre grupos pueden apreciarse en detalle en la **Figura 20**; la síntesis de leucotrienos (96.67% de metabolitos presentes), el remodelado lipoproteico en plasma (50-52%), el metabolismo de los ácidos grasos linoleico y linolénico (94.44%), del linoleato (83.33%) y del ácido araquidónico (79.81%), además de la síntesis de fosfolípidos (95.83%). Todas estas rutas se encuentran activadas en UCA. La **Figura 21** muestra dos de ellas en las que se incluyen distintos metabolitos medidos.

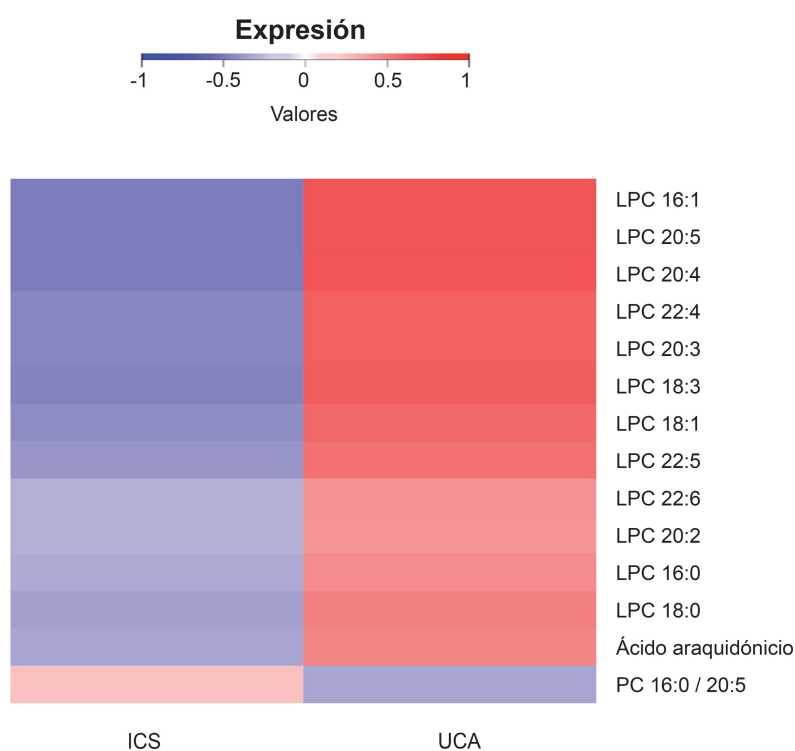


**Figura 20.** Cambios en la abundancia de metabolitos en la ruta PLA<sub>2</sub> entre ICS y UCA. *LPC*: lisofosfatidilcolina; *PC*: fosfatidilcolina

## Resultados

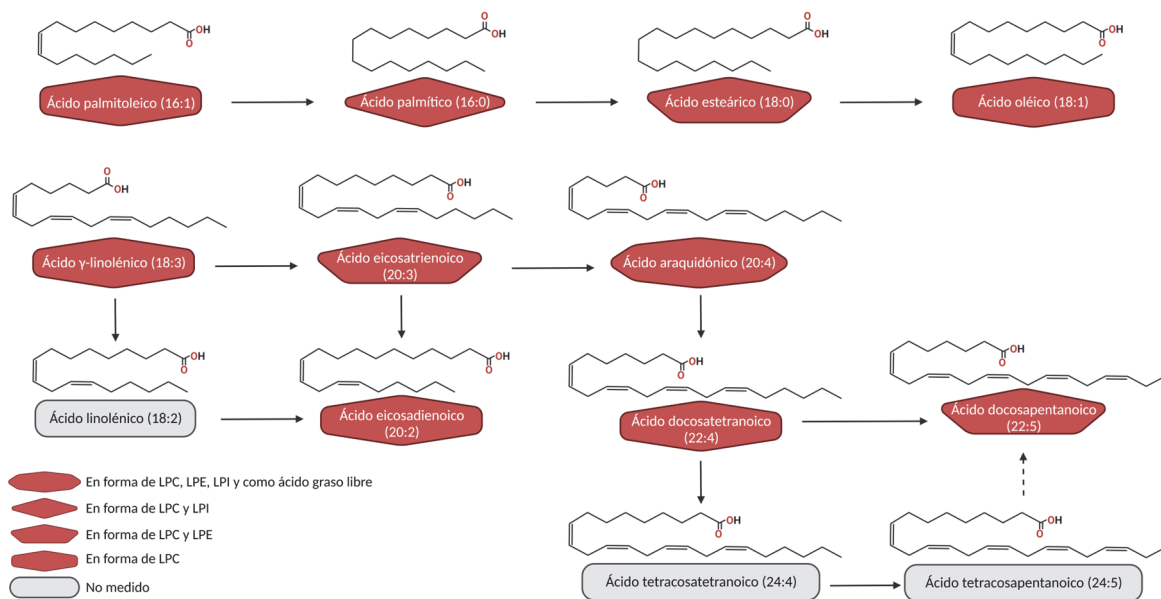


**Figura 21.** Rutas metabólicas relacionadas con los lisofosfolípidos y ácidos grasos encontrados. Se muestra el nombre de cada ácido graso, así como su estructura. El color rojo indica que se encontró aumentado en UCA, mientras que el gris se utiliza para los que no se vieron alterados. *LPC*: lisofosfatidilcolina; *LPE*: lisofosfatidiletanolamina; *LPI*: lisofosfatidilinositol.

En conjunto, el análisis metabolómico permitió diferenciar los grupos ICS y UCA. Estas diferencias se asociaron a un perfil alterado de, entre otros compuestos, lisofosfolípidos relacionados con rutas de inflamación.

### 4.2.3. Análisis proteómico

El análisis del perfil proteico de los pacientes ICS y UCA mediante Olink reveló que 8 de las 92 proteínas analizadas (cuyo listado puede consultarse en la **Tabla 9**) se encontraban significativamente alteradas entre los dos grupos (**Figura 22 A**). De éstas, 7 pudieron ser relacionadas mediante un análisis STRING (**Figura 22 B**). Particularmente, IFN $\gamma$  parecía ser el nexo entre la mayoría de ellas, ya que era la proteína que más relaciones directas tenía con el resto. ARG-1, CASP-8, CCL-13, IL-15 y TNFRSF12A se encontraron aumentadas en los pacientes UCA, mientras que CCL-19, CD4 soluble (sCD4) e IFN $\gamma$  se encontraron disminuidas (**Figura 22 C**).

Resultados

**Tabla 9.** Expresión diferencial de proteínas en suero entre ICS y UCA. Los valores de expresión de proteína normalizada (NPX) entre ICS y UCA fueron analizados mediante una prueba estadística de t-test

Proteína	p-valor	FDR	logFC (UCA)	Proteína	p-valor	FDR	logFC (UCA)
CASP-8	0.0019	0.1722	<b>0.8887</b>	CAIX	0.4602	0.8764	<b>-0.1663</b>
ARG1	0.0095	0.3219	<b>0.6945</b>	CCL20	0.4647	0.8764	<b>0.2925</b>
IFN $\gamma$	0.0150	0.3219	<b>-1.0880</b>	CD27	0.4668	0.8764	<b>-0.1079</b>
CCL19	0.0160	0.3219	<b>-0.8013</b>	PD-L1	0.4808	0.8847	<b>-0.1106</b>
CCL13	0.0175	0.3219	<b>0.6027</b>	GZMH	0.4952	0.8859	<b>0.2153</b>
CD4	0.0282	0.379	<b>-0.2826</b>	CD40-L	0.5007	0.8859	<b>0.3346</b>
IL15	0.0288	0.379	<b>0.2786</b>	IL12RB1	0.5204	0.9034	<b>0.0520</b>
TNFRSF12A	0.0367	0.4222	<b>0.3939</b>	TNFRSF9	0.5323	0.9069	<b>-0.1042</b>
CD40	0.0583	0.5963	<b>0.2662</b>	DCN	0.5511	0.9218	<b>0.0619</b>
TIE2	0.0725	0.6059	<b>0.1675</b>	CD83	0.6067	0.9372	<b>-0.0637</b>
HGF	0.0778	0.6059	<b>0.2847</b>	KIR3DL1	0.6069	0.9372	<b>-0.2133</b>
FGF2	0.0796	0.6059	<b>0.0972</b>	MCP-2	0.6147	0.9372	<b>0.1473</b>
PDGF-B	0.0878	0.6059	<b>0.0820</b>	Gal-1	0.6168	0.9372	<b>0.0449</b>
CXCL12	0.0922	0.6059	<b>-0.0957</b>	CXCL9	0.6393	0.9372	<b>-0.1510</b>
ICOSLG	0.1013	0.6104	<b>0.2889</b>	TNF	0.6401	0.9372	<b>-0.1260</b>
TNFSF14	0.1159	0.6104	<b>0.3216</b>	CD70	0.6405	0.9372	<b>-0.1081</b>
IL13	0.1202	0.6104	<b>0.2609</b>	CD8A	0.6426	0.9372	<b>0.0857</b>
GZMB	0.1230	0.6104	<b>0.5404</b>	TNFRSF21	0.6597	0.9372	<b>0.0384</b>
IL8	0.1261	0.6104	<b>0.3042</b>	CXCL13	0.6886	0.9372	<b>-0.1233</b>
LAMP3	0.1700	0.7819	<b>-0.3742</b>	IL18	0.6958	0.9372	<b>0.0917</b>
CXCL1	0.1981	0.8525	<b>0.2798</b>	ANGPT2	0.7009	0.9372	<b>-0.0732</b>
VEGFA	0.2169	0.8525	<b>0.3049</b>	PD-L2	0.7227	0.9372	<b>-0.0488</b>
PTN	0.2224	0.8525	<b>0.3497</b>	CD5	0.7245	0.9372	<b>-0.0736</b>
FASLG	0.2305	0.8525	<b>0.2086</b>	CSF-1	0.7309	0.9372	<b>0.0322</b>
EGF	0.2464	0.8525	<b>0.4909</b>	IL12	0.7336	0.9372	<b>-0.0927</b>
MIC-A/B	0.2614	0.8525	<b>0.6787</b>	PDCD1	0.7375	0.9372	<b>0.0706</b>
CX3CL1	0.2643	0.8525	<b>0.1422</b>	LAP TGF $\beta$ -1	0.7437	0.9372	<b>0.0539</b>
CD244	0.2657	0.8525	<b>0.1485</b>	TNFRSF4	0.7549	0.9385	<b>-0.0516</b>
IL7	0.2707	0.8525	<b>0.2045</b>	LAG3	0.7671	0.941	<b>0.0602</b>
ADA	0.2879	0.8525	<b>0.1445</b>	MMP12	0.8168	0.9677	<b>0.0520</b>
CCL23	0.2890	0.8525	<b>0.2007</b>	TWEAK	0.8183	0.9677	<b>0.0360</b>
IL5	0.2965	0.8525	<b>-0.3551</b>	CXCL10	0.8219	0.9677	<b>0.0644</b>
IL2	0.3370	0.8764	<b>0.0362</b>	CXCL11	0.8486	0.9677	<b>0.0543</b>
CD28	0.3393	0.8764	<b>-0.0596</b>	CCL17	0.8524	0.9677	<b>0.0640</b>
VEGFR-2	0.3564	0.8764	<b>-0.0951</b>	IL10	0.8562	0.9677	<b>0.0373</b>
MCP-1	0.3692	0.8764	<b>0.1647</b>	HO-1	0.8628	0.9677	<b>-0.0292</b>
CXCL5	0.3789	0.8764	<b>-0.1786</b>	KLRD1	0.8731	0.9677	<b>-0.0379</b>
GZMA	0.3969	0.8764	<b>0.1487</b>	TRAIL	0.8924	0.9774	<b>-0.0202</b>
PGF	0.4114	0.8764	<b>-0.1782</b>	MCP-3	0.9123	0.9874	<b>0.0256</b>
IL6	0.4123	0.8764	<b>0.2100</b>	MUC-16	0.9304	0.9903	<b>0.0262</b>
IL-1 $\alpha$	0.4189	0.8764	<b>-0.0197</b>	CCL3	0.9365	0.9903	<b>0.0369</b>
CRTAM	0.4298	0.8764	<b>-0.1564</b>	NCR1	0.9653	0.9964	<b>0.0072</b>
ADGRG1	0.4366	0.8764	<b>0.2031</b>	NOS3	0.9692	0.9964	<b>0.0119</b>
MMP7	0.4433	0.8764	<b>0.0854</b>	CCL4	0.9781	0.9964	<b>0.0072</b>
ANGPT1	0.4466	0.8764	<b>0.1188</b>	IL4	0.9856	0.9964	<b>0.0037</b>
Gal-9	0.4495	0.8764	<b>0.0919</b>	IL33	1	1	<b>0</b>

FC: Fold change o incremento de la expresión en el grupo; FDR: tasa de falsos descubrimientos (*False Discovery Rate*). Es el p-valor tras aplicar la corrección de Benjamini-Hochberg.

## Resultados

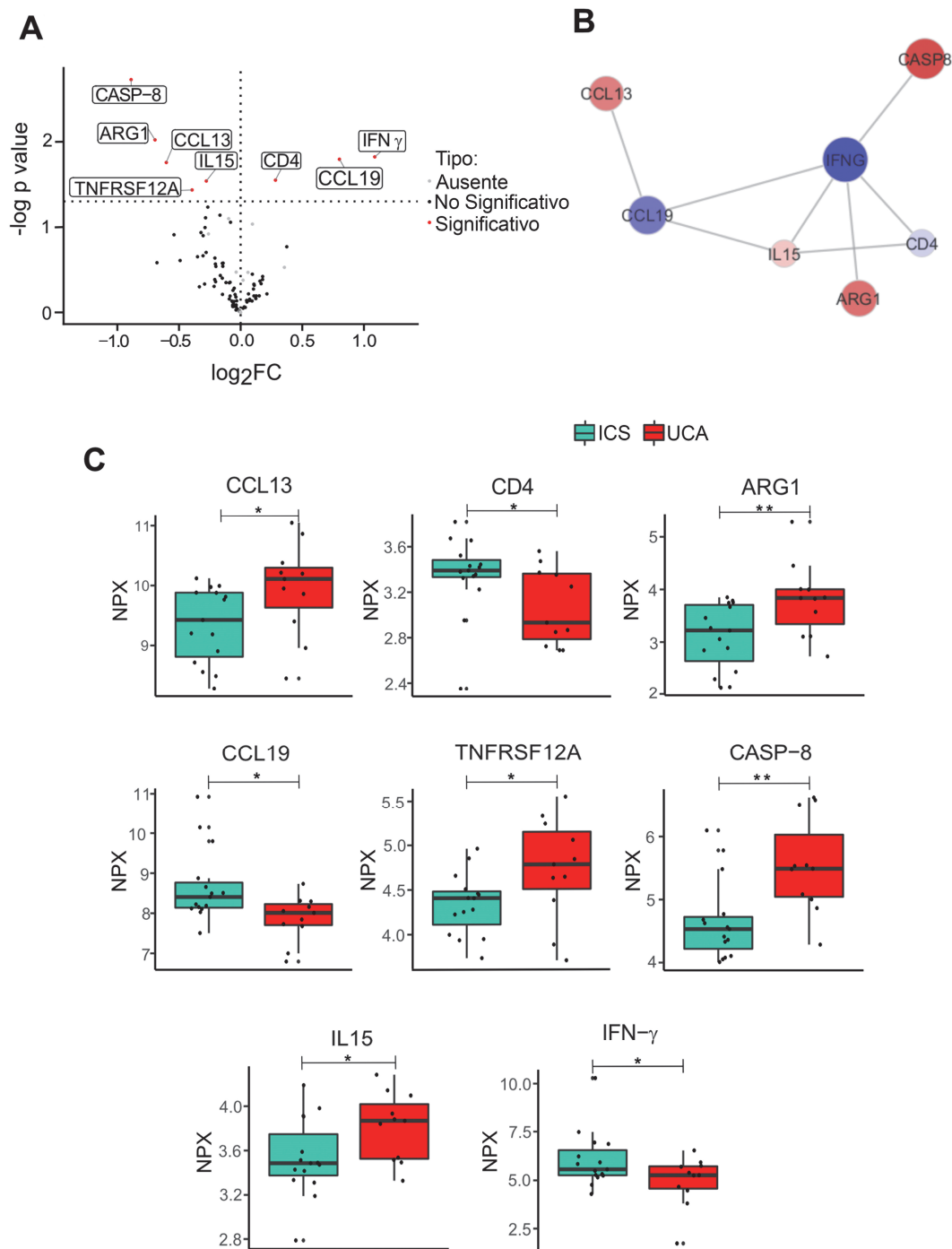


**Figura 22.** Análisis proteómico del suero de los pacientes ICS (azul) y UCA (rojo). **A.** Gráficos de volcán de las diferencias entre ambos grupos de pacientes. **B.** Análisis STRING de las proteínas significativas; en el que se muestran incrementos en los logFC mediante el aumento de la intensidad del color y del tamaño de los círculos. Además, el aumento o reducción en la expresión de una proteína en UCA se muestra en una escala rojo-azul; en la que el rojo indica un aumento y el azul una reducción. **C.** Trayectorias y valores individuales de expresión de proteína en los pacientes. \*:  $P < .05$ ; \*\*:  $P < .01$ . **NPX:** expresión de proteína normalizada.

Por otra parte, el análisis GO descubrió más de 200 posibles rutas alteradas; de estas, las 25 rutas más significativas se recogen en la **Tabla 10**. En general, se encontró una alteración de la respuesta inmunológica, con procesos tales como la respuesta a citoquinas, la adhesión y diferenciación de leucocitos, y la activación de linfocitos T. También se observó una alteración en



## Resultados

el metabolismo del nitrógeno y la respuesta inmune a lípidos, procesos que ya se vieron alterados en el análisis metabolómico.

**Tabla 10.** Listado de los 25 procesos biológicos de GO más asociados a la expresión de las proteínas significativamente diferentes entre grupos.

#ID	Ruta	Genes observados	Genes de fondo	FDR
GO:0034097	Respuesta a citoquinas	11	1035	1.46E-11
GO:1902107	Regulación positive de la diferenciación de leucocitos	7	139	2.70E-10
GO:0071345	Respuesta celular al estímulo con citoquinas	10	953	4.21E-10
GO:0048584	Regulación positive de la respuesta a estímulos	11	2054	4.43E-09
GO:0051707	Respuesta a otros organismos	9	835	5.43E-09
GO:0071310	Respuesta celular a sustancias orgánicas	11	2219	5.56E-09
GO:1903037	Regulación de la adhesión célula-célula en leucocitos	7	278	5.56E-09
GO:0097191	Ruta de señalización de apoptosis extrínseca	5	93	7.98E-08
GO:0033993	Respuesta a lípidos	8	825	8.91E-08
GO:0050776	Regulación de la respuesta inmune	8	873	1.29E-07
GO:0002684	Regulación positiva de procesos del sistema inmune	8	882	1.35E-07
GO:0007166	Ruta de señalización de receptores de superficie celular	10	2198	1.63E-07
GO:0045597	Regulación positiva de diferenciación celular	8	908	1.63E-07
GO:0050863	Regulación de la activación de linfocitos T	6	302	2.78E-07
GO:0034612	Respuesta a TNF ( <i>tumor necrosis factor</i> )	5	217	2.01E-06
GO:0032268	Regulación de procesos celulares metabólicos de proteínas	9	2486	6.02E-06
GO:0043123	Regulación positiva de señalización IKK/NF-κB	4	122	7.81E-06
GO:0046425	Regulación de la ruta de señalización de receptor via JAK-STAT	4	151	1.57E-05
GO:0051173	Regulación positiva de procesos metabólicos de compuestos de nitrógeno	9	2946	2.09E-05
GO:0070374	Regulación positiva de las cascadas de señalización ERK1 y ERK2	4	196	3.78E-05
GO:0006959	Respuesta inmune humoral	4	252	8.97E-05
GO:0032879	Regulación de localización	8	2524	8.97E-05
GO:0032700	Regulación negativa de la producción de IL-17	2	12	2.30E-04
GO:0035723	Ruta de señalización de IL-15	2	13	2.60E-04
GO:0045834	Regulación positiva del metabolismo de lípidos	3	135	4.10E-04

*FDR*: tasa de falsos descubrimientos (*False Discovery Rate*). Es el *p*-valor tras aplicar la corrección de Benjamini-Hochberg.

#### 4.2.4. Construcción de modelos de predicción y aprendizaje automático

Con el objetivo de crear un algoritmo capaz de separar los pacientes en función de su gravedad, se construyeron tres modelos  $k$ -NN: uno incluyendo solamente las variables clínicas, uno incluyendo solamente las variables metabólicas, y uno integrando todas las variables con los datos de los pacientes ICS y UCA. No se encontró un codo (es decir, un valor  $k$  óptimo) para los modelos construidos con las variables clínicas o metabólicas por separado; mientras que, para la combinación de ambos conjuntos de datos, se encontró que el valor de  $k$  óptimo era de 2 o 3 (**Figura 23**); por lo que se construyó un modelo con cada valor. Ambos modelos se comportaron de manera idéntica.

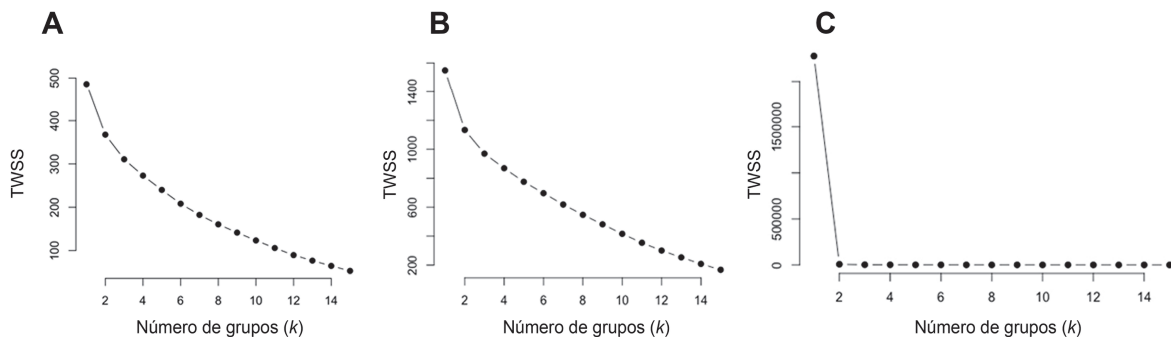


**Figura 23.** Representación gráfica del método del codo para los modelos que utilizaban solamente variables clínicas (A) o metabólicas (B), y para el método que combina ambos tipos de variables (C).

Los modelos construidos utilizaron 39 (16 clínicas y 23 metabólicas) de las 136 variables posibles. Una vez generados, los modelos se utilizaron para clasificar a aquellos pacientes de los grupos ICS y UCA del set de evaluación, cuyos datos no se habían utilizado para su construcción. Estos fueron capaces de predecir con éxito todos los pacientes menos uno (precisión del 87.5%). Además, su especificidad fue del 75%; la sensibilidad, del 100%; y los valores predictivos positivo (*Positive Predictive Value*, PPV) y negativo (*Negative Predictive Value*, NPV), del 80% y 100%, respectivamente (**Figura 24**).

Por último, se intentó reducir el número de variables utilizadas; sin embargo, los modelos resultantes tuvieron peores valores predictivos, por lo que se descartaron.

## Resultados

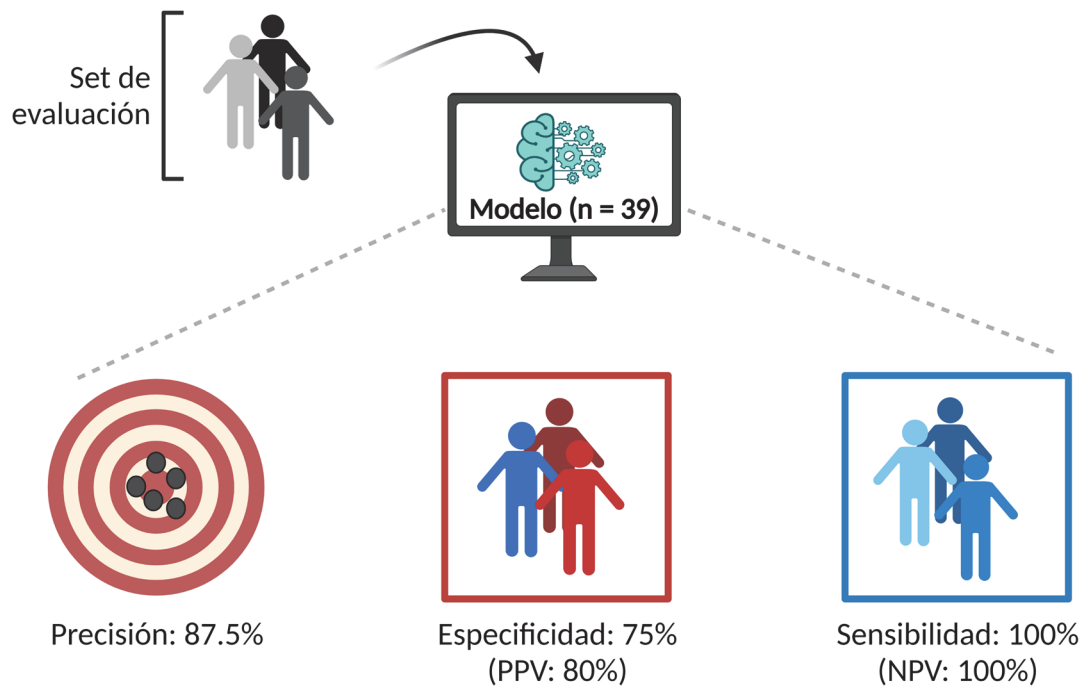


**Figura 24.** Resultados de los dos modelos de aprendizaje automático ( $k = 2$  y  $k = 3$ , respectivamente) creados con el algoritmo  $k$ -NN. En la imagen se muestran sus valores de precisión, especificidad y sensibilidad, así como su valor predictivo positivo (PPV) y negativo (NPV).

En conclusión, la integración de las diferencias clínicas y metabolómicas encontradas entre los grupos permitió clasificar a los pacientes, y podría ser una herramienta de utilizad en la práctica clínica.

### 4.3. BLOQUE II. Estudio del papel de la alergia en pacientes asmáticos graves no controlados

#### 4.3.1. Descripción de la población de estudio

De los 100 pacientes asmáticos incluidos en esta tesis, 23 tenían un asma no controlado con la medicación disponible en el momento de la inclusión. De éstos, 9 pacientes eran alérgicos a ácaros (UCA), mientras que 14 presentaron una prueba cutánea negativa frente a todos los ácaros y alérgenos testados (UCNA). Los datos de estos 23 pacientes se recogen en la **Tabla 11**.

**Tabla 11.** Características clínicas de los pacientes del estudio

	UCNA	UCA
N	14	9
Edad	62.1 ± 2.8	47 ± 4.7**
Edad de aparición	29.4 ± 2.9	9.6 ± 2.1****
Sexo (F/M)	13 / 1	6 / 3
IMC	29.7 ± 1.4	27.3 ± 1.4
Fumadores	0	0
IgE total	257.9 ± 138.2	683.2 ± 222.2 **
EREA (%)	7 (50%)	0

*IMC*: Índice de Masa Corporal; *EREA*: Enfermedad Respiratoria exacerbada por la aspirina. \*:  $P < .05$ ; \*\*:  $P < .01$ ; \*\*\*:  $P < .001$ ; \*\*\*\*:  $P < .0001$ .

De los pacientes UCNA, el 64% (9/14) presentaban intolerancia a AINES y/o pólipos nasales, y 7 de ellos tenían ambas (EREA). En cambio, sólo uno de los pacientes UCA (18%) presentaba intolerancia a AINES, y ninguno tenía pólipos nasales ni EREA.

No se encontraron diferencias significativas en relación con el sexo o el IMC entre los grupos; sin embargo, sí que se encontraron diferencias en cuanto a la edad (62.1 ± 2.8 en UCNA vs 47 ± 4.7 en UCA;  $P < .01$ ) y a la edad de aparición de la enfermedad (29.4 ± 2.9 vs 9.6 ± 2.1;  $P < .0001$ ), siendo ambas mayores en UCNA; y en los valores de IgE total (257.9 ± 138.2 vs 683.2 ± 222.2;  $P < .01$ ), que estaban aumentados en los pacientes UCA. Ningún paciente fumaba en el momento de la recolección de las muestras.

#### 4.3.2. Análisis metabolómico

Se obtuvieron 1327 señales (734 en ESI+ y 593 en ESI-) del análisis del suero, tras el pertinente procesamiento de los datos. La calidad de los datos se comprobó con el agrupamiento de las muestras QC en un primer análisis PCA (**Figura 25**).

## Resultados

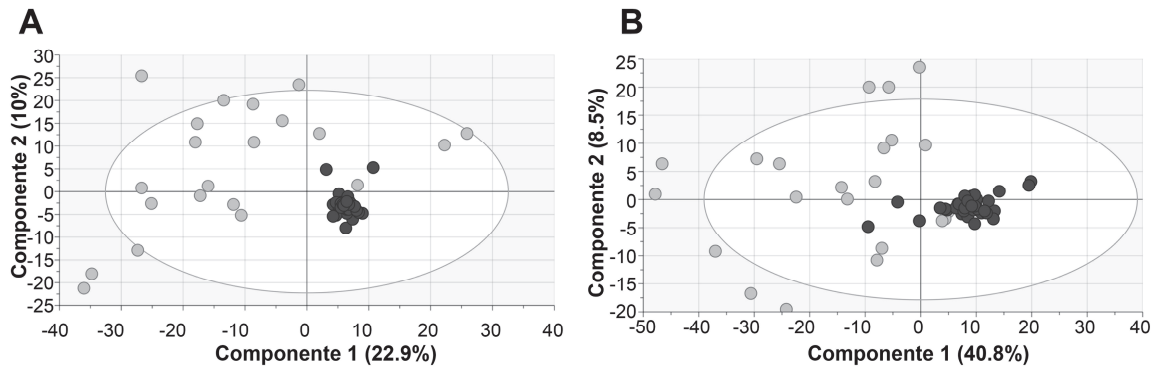


**Figura 25.** Análisis PCA de las muestras para comprobar la calidad de los datos en las polaridades ESI+ (A) y ESI- (B). La agrupación de las muestras QC (en negro) prueba que las diferencias que puedan encontrarse en las muestras (en gris) son debidas a las diferencias entre grupos, y no a las técnicas analíticas.

A continuación, se realizó un análisis multivariante para comparar ambos grupos, incluyendo las muestras de pacientes (Figura 26).

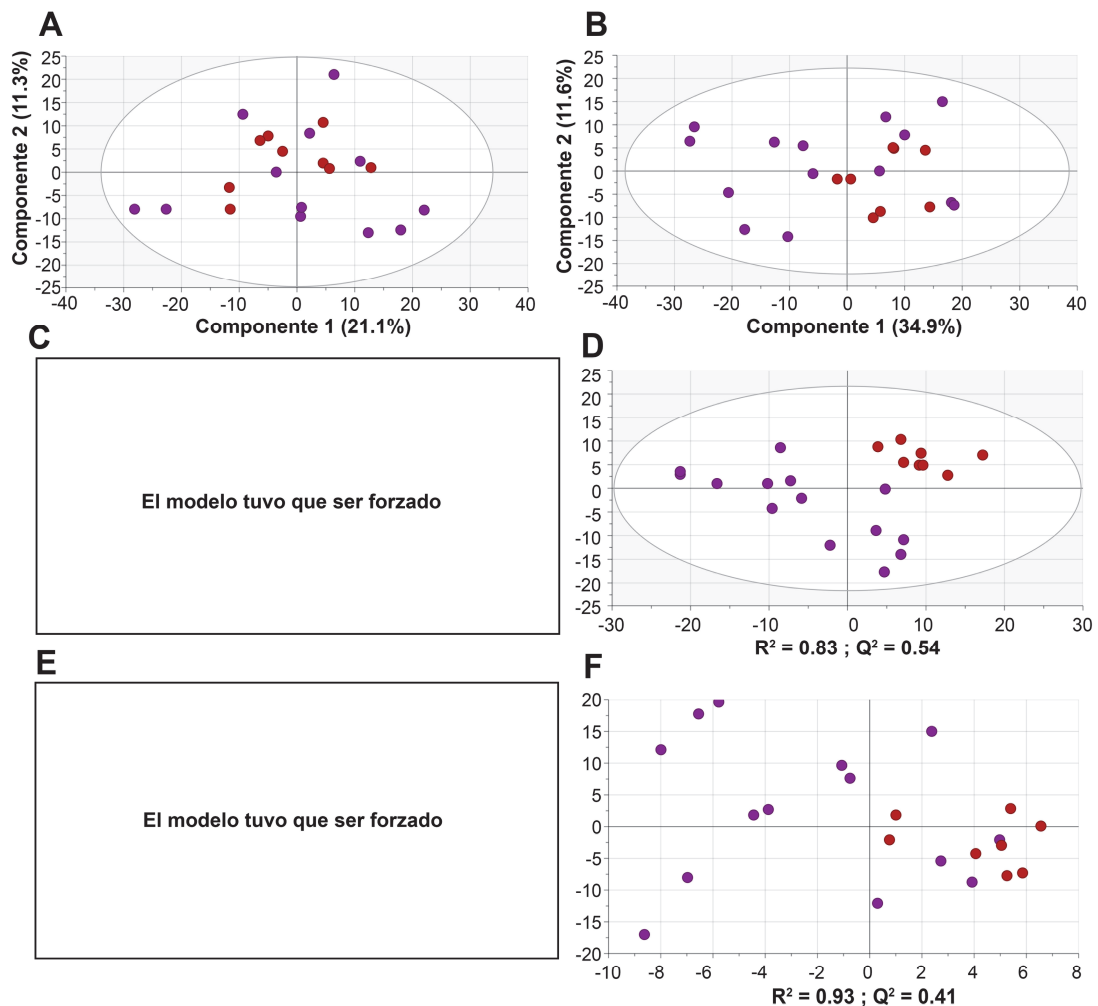


**Figura 26.** Análisis multivariante para la comparación de los 23 pacientes UCA y UCNA. Se muestran los resultados para un análisis no supervisado PCA de los dos grupos utilizando las 833 señales que cumplieron con los estándares de calidad en polaridad positiva (ESI+) (A) y las 565 de la polaridad negativa (ESI-) (B). Dado que no se observó una agrupación clara, aunque sí una tendencia para los grupos más extremos, se realizó un análisis PLS-DA en ESI+ (B) y ESI- (C) y un OPLS-DA, también en ambas polaridades ESI+ (E) y ESI- (F). Sin embargo, para la polaridad ESI+, no se encontraron modelos supervisados. UCA: rojo; UCNA: morado.  $R^2$  hace referencia a la capacidad de clasificación del modelo; y  $Q^2$ , a la capacidad de predicción.

## Resultados

No se observaron diferencias claras entre UCA y UCNA en un análisis PCA (**Figura 26 A-B**). Para ESI-, se obtuvieron modelos PLS-DA, con parámetros de  $R^2$  de 0.85 y  $Q^2$  de 0.55 (**Figura 26 D**) y OPLS-DA, con  $R^2$  y  $Q^2$  de 0.91 y 0.4 (**Figura 26 F**). En cambio, los modelos obtenidos con los algoritmos dirigidos en polaridad ESI+ tuvieron que ser forzados; lo que significa que los valores de  $R^2$  y/o  $Q^2$  fueron negativos o muy bajos y, por tanto, que esas señales no permitían diferenciar ambos grupos (**Figura 26 C, E**).

Después se realizó un análisis univariante no paramétrico de U de Mann-Whitney. Se encontraron un total de 103 señales con abundancias significativamente distintas entre ambos grupos (20 para ESI+ y 83 para ESI-). La mayor parte de ellas (97) estaban aumentadas en los pacientes UCA con respecto a los UCNA. Estas 103 señales se utilizaron para construir un *heatmap* mediante un análisis HCA (**Figura 27**), que logró clasificar adecuadamente 21 de los 23 pacientes analizados; agrupando correctamente todos los pacientes UCA, junto a dos pacientes UCNA.

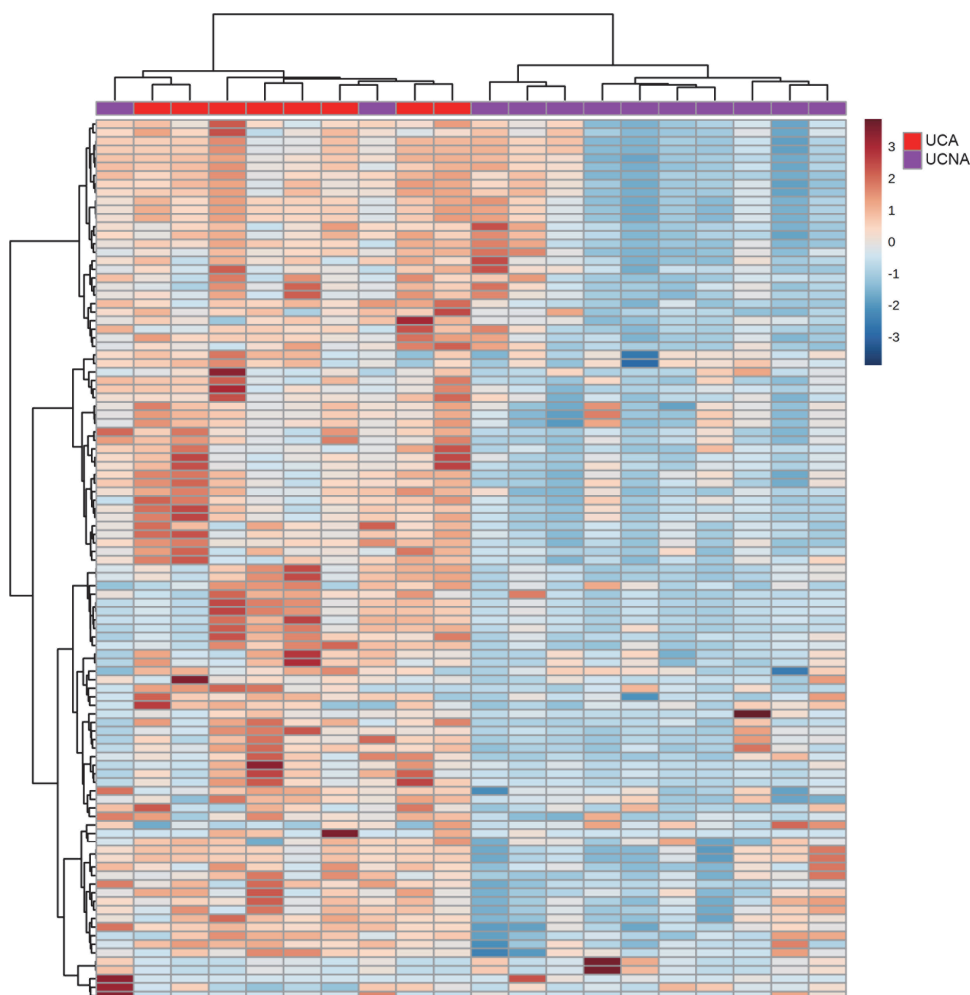


**Figura 27.** *Heatmap* creado tras el análisis de agrupamiento jerárquico de los pacientes (en columnas), utilizando los 103 metabolitos significativamente distintos (en filas). El color de las celdas representa una expresión disminuida (azul) o aumentada (rojo). Los pacientes y los metabolitos se agruparon según su similitud (izquierda).

## Resultados

Para identificar los metabolitos con abundancias significativamente distintas, se realizó un nuevo análisis de espectrometría de masas en tándem. Se pudieron identificar 14 de las 103 señales encontradas (**Tabla 12**). Los metabolitos identificados incluían esteroides (hormonas, ácidos biliares, vitaminas), varios LPC y una carnitina. Sólo dos de los compuestos (palmitoleil carnitina y ácido deoxicólico) se encontraron disminuidos en los pacientes UCA; el resto estaban aumentados en comparación al grupo UCNA (**Figura 28**).

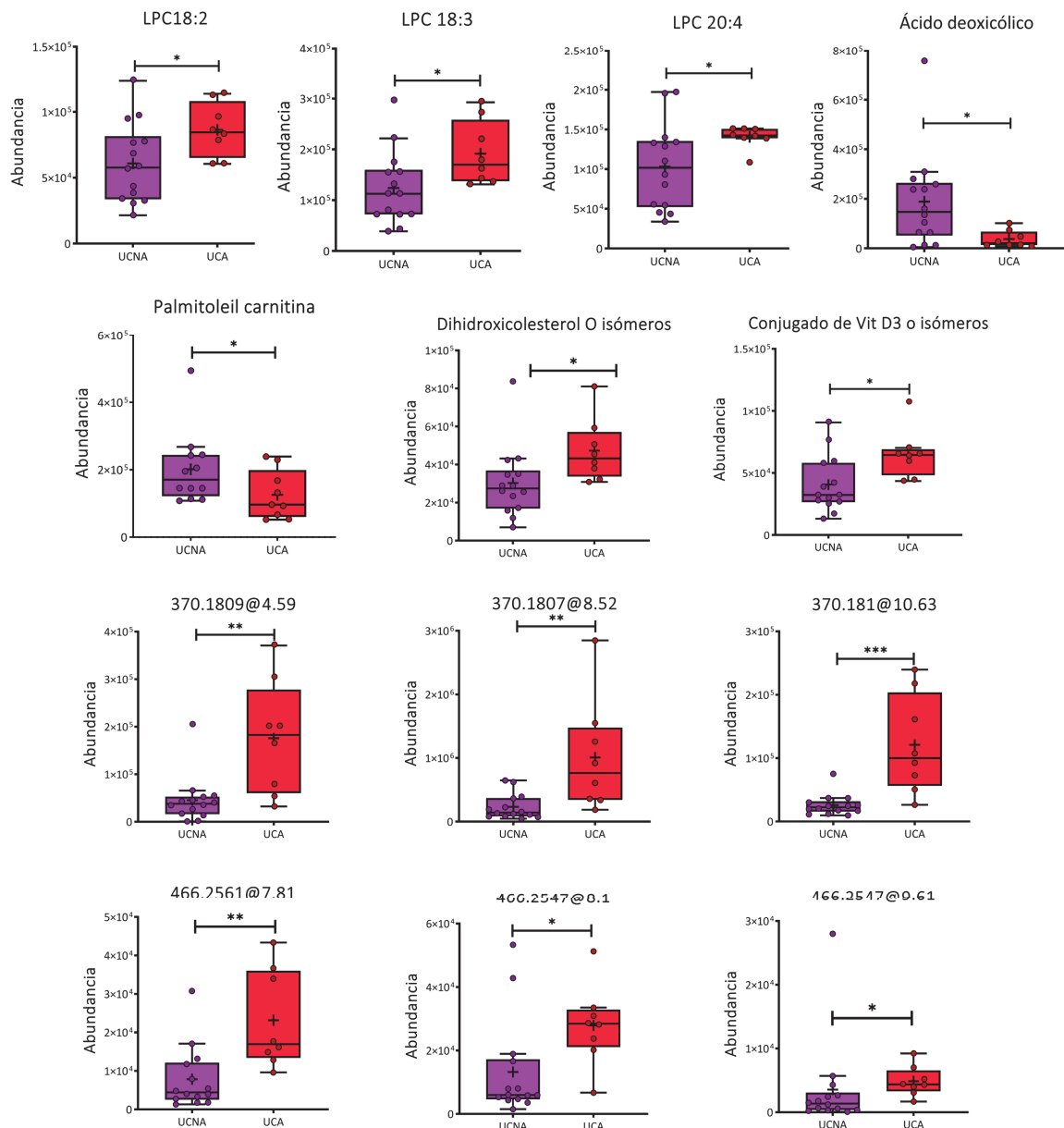


**Figura 28.** Trayectorias de los metabolitos significativamente distintos entre UCA (en rojo) y UCNA (en morado). La media se muestra como '+' dentro de las cajas. Se seleccionaron los  $m/z$  más abundantes para aquellos metabolitos en los que se detectó más de un  $m/z$ . Para aquellos metabolitos con una misma identidad, pero distintos tiempos de retención, se identificaron con su valor  $m/z@RT$  en lugar de con sus identificaciones. \*:  $P < .05$ ; \*\*:  $P < .01$ ; \*\*\*:  $P < .001$ . LPC: lisofosfatidilcolina.

Resultados

**Tabla 12.** Características fisicoquímicas y valores estadísticos de las señales anotadas mediante LC-MS/MS significativamente distintas en la comparación UCA vs UCNA.

Nº Técnica	Compuesto	m/z	Masa (Da)	RT (min)	Fórmula	Error (ppm)	Aducto	CV en QCs (%)	% cambio (UCA)	p-valor	FDR
1 LC-MS-	1 $\alpha$ ,25-dihidroxi-2 $\alpha$ -(3-hidroxiopropoxi)-vitamina D3 O isómeros	489.3552	490.363	30.47	C30H50O5	-5.7	M-H	6.7	37.3	0.0105	0.1298
2 LC-MS-	5 $\alpha$ -Dihydrotestosterone sulfate OR isomers	369.1738	370.1816	4.59	C19H30O5S	0.5	M-H	6.3	74.3	0.0070	0.1021
3 LC-MS-	5 $\alpha$ -Dihydrotestosterone sulfate OR isomers	369.1736	370.1814	8.52	C19H30O5S	0	M-H	5.7	77	0.0070	0.1021
4 LC-MS-	5 $\alpha$ -Dihydrotestosterone sulfato O isómeros	369.1738	370.1816	10.63	C19H30O5S	0.5	M-H	7.4	78.7	0.0007	0.0915
5 LC-MS-	17 $\alpha$ ,20 $\alpha$ -Dihidrocolesterol O isómeros	463.3426	418.3449	29.92	C27H46O3	0.5	M+FA-H	11.3	36	0.0154	0.1629
6 LC-MS-	Glucurónido-3 de androsterona O isómeros	465.2496	466.2574	7.81	C25H38O8	1.5	M-H	6.2	66.1	0.0030	0.0915
7 LC-MS-	Glucurónido-3 de androsterona O isómeros	465.2463	466.2541	8.1	C25H38O8	-5.6	M-H	6.2	52.6	0.0127	0.1453
8 LC-MS-	Glucurónido-3 de androsterona O isómeros	465.2474	466.2552	9.61	C25H38O8	-3.2	M-H	9.8	27	0.0154	0.1629
9 LC-MS-	Ácido deoxicólico O Isómeros	437.2901	392.2924	14.73	C24H40O4	-0.5	M+FA-H	5.4	-385.8	0.0222	0.2053
10 LC-MS-	LPC 18:2 sn-1	504.3085	519.332	16.97	C26H50NO7P	-0.9	M-CH3	9.6	29.5	0.0374	0.2862
11 LC-MS-	LPC 18:3 sn-1	562.3137	517.316	15.63	C26H48NO7P	-1.5	M+FA-H	12.7	35.3	0.0374	0.2862
12 LC-MS-	LPC 20:4 sn-1	656.3182	543.3332	17.12	C28H50NO7P	1.2	M+TFA-H	27.1	26.8	0.0222	0.2053
13 LC-MS-	LPC 20:4 sn-2	656.3182	543.3332	17.12	C28H50NO7P	1.2	M+TFA-H	27.4	26.6	0.0265	0.2272
14 LC-MS+	Palmitoleil carnitina	398.3269	397.3191	15.95	C23H43NO4	-0.3	M+H	11.3	-60.5	0.0428	0.9027

LPC: lisofosfatidilcolina; FA: ácido fórmico, TFA: ácido trifluoroacético; CV: coeficiente de variación; QC: control de calidad. La medida del CV en las muestras QC es una forma de asegurar que los metabolitos han sido medidos de forma reproducible y constante a lo largo de todo el experimento. Se fijan variaciones inferiores al 30% como criterio de calidad; FDR: tasa de falsos descubrimientos (False Discovery Rate), correspondiente al p-valor tras aplicar la corrección de Benjamini-Hochberg.



## Resultados

Posteriormente, se realizó un análisis del enriquecimiento por categoría de metabolito. Este análisis se hace mediante el cálculo de la ratio de enriquecimiento, obtenido al dividir el número de metabolitos con abundancias diferentes para una estructura química concreta entre el número de metabolitos cuya abundancia se esperaría encontrar alterada. Se encontró que los esteroides y los LPC fueron los dos grupos de compuestos con una mayor ratio de enriquecimiento (**Figura 29**).

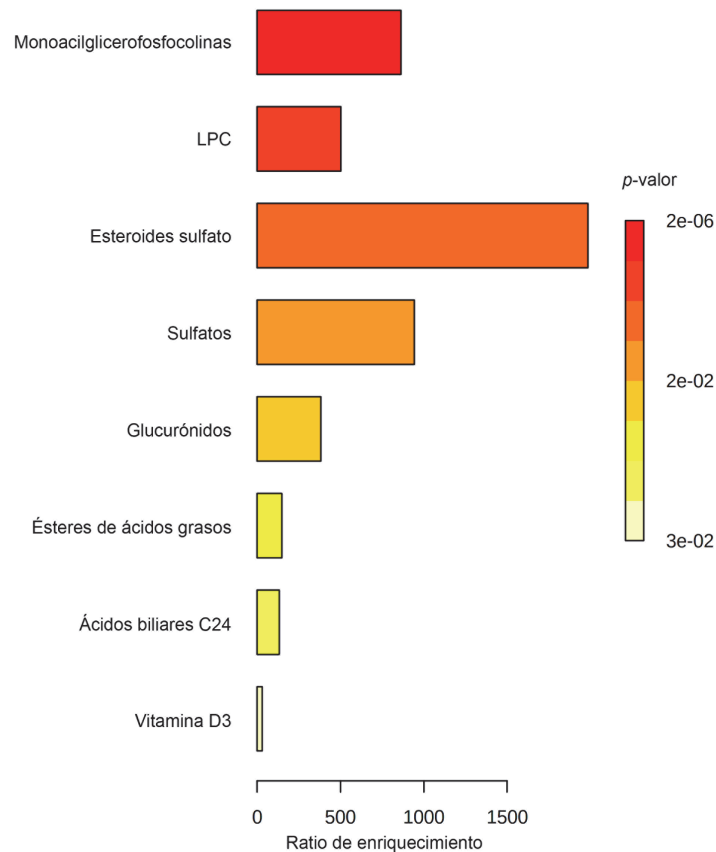


**Figura 29.** Análisis de enriquecimiento para la comparación UCA vs UCNA. En este análisis se representan las categorías de metabolitos que sufren más cambios al comparar ambos grupos.

Por último, con el fin de asociar estos cambios a una posible función biológica, se realizó un análisis de rutas metabólicas (**Tabla 13**). Se encontraron 44 rutas con diferencias significativas, incluyendo la ruta PLA<sub>2</sub>, rutas de biosíntesis de hormonas esteroideas, catabolismo y remodelado de fosfatidilcolinas, y metabolismo lipídico.

En conjunto, los resultados obtenidos apuntan a la existencia de diferencias metabólicas en el asma grave no controlado en función de la presencia o ausencia de alergia. Estas diferencias son, mayoritariamente, en la abundancia de esteroides y LPC; y se relacionan con rutas inflamatorias (PLA<sub>2</sub>) y de síntesis de estos compuestos.

## Resultados

**Tabla 13.** Rutas metabólicas enriquecidas significativamente en los pacientes UCA ( $P < .05$ ).

Ruta metabólica	$p$ -valor	FDR	Metabolitos de la ruta	Fuente
Señalización osteoblástica	0.00383	1	1	Wikipathways
Señalización mediada por receptores del ácido retinoico	0.00383	1	1	PID
Señalización mediada por la familia Hedgehog	0.00383	1	1	PID
Artritis reumatoide en <i>Homo sapiens</i>	0.00574	1	1	KEGG
Ruta STING en enfermedad similar a Kawasaki y COVID-19	0.00765	1	1	Wikipathways
Biosíntesis de hormonas esteroides ( <i>Homo sapiens</i> )	0.0103	1	2	KEGG
Remodelado de cardiolipina por cadenas acilo	0.0115	1	3	Reactome
Remodelado de fosfatidilcolinas por cadenas acilo	0.0115	1	3	Reactome
Hidrólisis de LPC	0.0115	1	3	Reactome
Catabolismo de fosfatidilcolina	0.0115	1	3	Wikipathways
Heterodimerización de RXR y RAR con otros receptores nucleares	0.0115	1	1	PID
Tráfico retrógrado de Golgi a RE independiente de COPI	0.0133	1	3	Reactome
Ruta de la fosfolipasa A <sub>2</sub> (PLA <sub>2</sub> )	0.0133	1	3	Reactome
Mecanismos de acción de las vitaminas A y D	0.0133	1	1	Wikipathways
Metabolismo de vitamina D (calciferol)	0.0152	1	1	Reactome
Transporte retrógrado de Golgi a ER	0.0171	1	3	Reactome
Metabolismo de esteroides	0.0171	1	2	Reactome
Metabolismo de vitamina D	0.0171	1	1	Wikipathways
Señalización <i>downstream</i> de GPCR	0.0185	1	4	Reactome
Biosíntesis de 1,25-dihydroxyvitamin D <sub>3</sub>	0.019	1	1	HumanCyc
Metabolismo de colina en cáncer ( <i>Homo sapiens</i> )	0.019	1	3	KEGG
Remodelado HDL	0.019	1	3	Reactome
Remodelado de lipoproteínas plasmáticas	0.019	1	3	Reactome
Metabolismo de lípido	0.0197	1	5	Reactome
Eventos dependientes de Ca <sup>2+</sup>	0.0209	1	3	Reactome
Tráfico intra-Golgi y de Golgi a RE	0.0209	1	3	Reactome
Vitaminas	0.0209	1	1	Reactome
Metabolismo de vitamina D3 (coleciferol)	0.0228	1	1	EHMN
Ensamblaje, remodelado y limpieza de lipoproteína plasmática	0.0247	1	3	Reactome
Señalización de calcio en Vitamina D en depresión	0.0247	1	1	Wikipathways
Señalización por GPCR	0.0264	1	4	Reactome
Rutas RAS y bradiquinina en COVID-19	0.0266	1	1	Wikipathways
Eventos mediados por proteína G	0.0303	1	3	Reactome
Eventos mediados por PLCβ	0.0303	1	3	Reactome
Síndrome de delección proximal de 16p11.2	0.0322	1	3	Wikipathways
Ruta de ácido biliar inducida por medicamentos	0.034	1	1	Wikipathways
Tráfico de membrana	0.0378	1	3	Reactome
Señalización por opioides	0.0378	1	3	Reactome
Reciclado de ácidos y sales biliares	0.0378	1	1	Reactome

## Resultados

Metabolismo de linoleato	0.0396	1	3	EHMN
Metabolismo de vitamina A y carotenoides	0.0396	1	1	Wikipathways
Producción de citoquinas antiinflamatorias mediada por ADORA2B	0.0415	1	1	Reactome
Eventos de señalización G- $\alpha$ (I)	0.047	1	1	Reactome
Metabolismo de glicerofosfolípidos ( <i>Homo sapiens</i> )	0.047	1	3	KEGG

---

*FDR*: tasa de falsos descubrimientos (*False Discovery Rate*). Es el *p*-valor tras aplicar la corrección de Benjamini-Hochberg.

## 4.4. BLOQUE III. Estudio del papel de la alergia en la poliposis nasosinusal

### 4.4.1. Descripción de la población de estudio

Los 22 pacientes reclutados fueron clasificados en función de su sensibilización alérgica respiratoria, diagnosticada mediante la técnica ImmunoCAP™ ISAC. Trece pacientes (59.1%) resultaron negativos frente a todos los alérgenos testados y se clasificaron como poliposis no alérgica, mientras que 9 de ellos (40.9%) estaban sensibilizados a uno o varios alérgenos y se clasificaron como poliposis alérgica. El alérgeno al que más pacientes se encontraban sensibilizados fue Fel d 1; además, la mayoría también estaban sensibilizados a gramíneas (Phl p 1 y Phl p 5) (**Figura 30**).

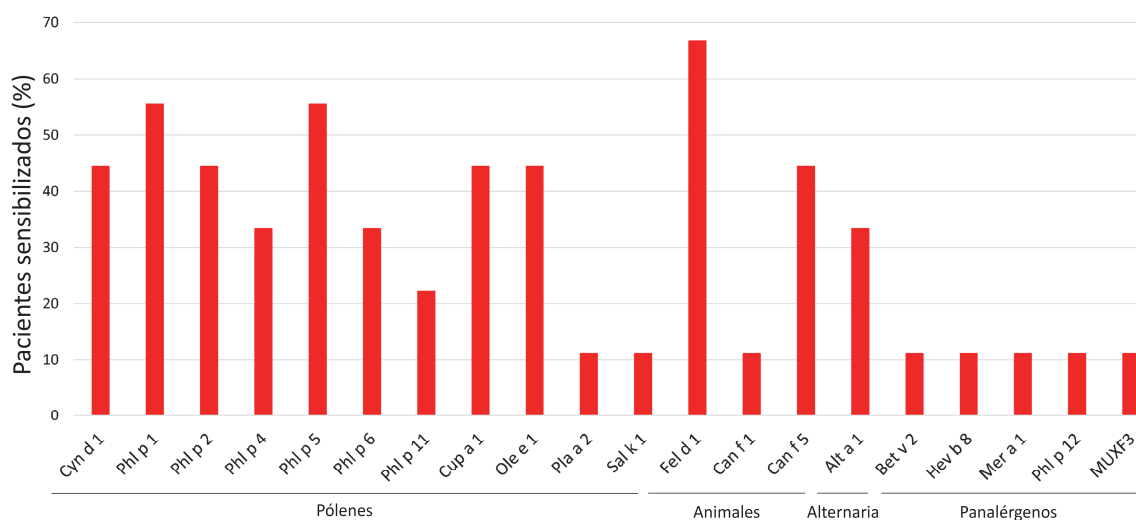


**Figura 30.** Porcentaje de pacientes del total de alérgicos sensibilizados a cada uno de los aeroalérgenos estudiados.

### 4.4.2. Análisis metabólico sistémico en suero

Tras el filtrado y el procesamiento de datos, se obtuvieron 535 señales para ESI+ y 429 para ESI- que cumplieran con los estándares de calidad, lo que se comprobó mediante la proyección de las 19 muestras incluidas en el análisis metabólico en un modelo PCA (**Figura 31**). Este modelo reveló una buena agrupación de las muestras QC (en verde); sin embargo, no se observaron grandes diferencias entre los grupos en este análisis multivariante. Por otra parte, el análisis supervisado PLS-DA no generó ningún modelo.

## Resultados

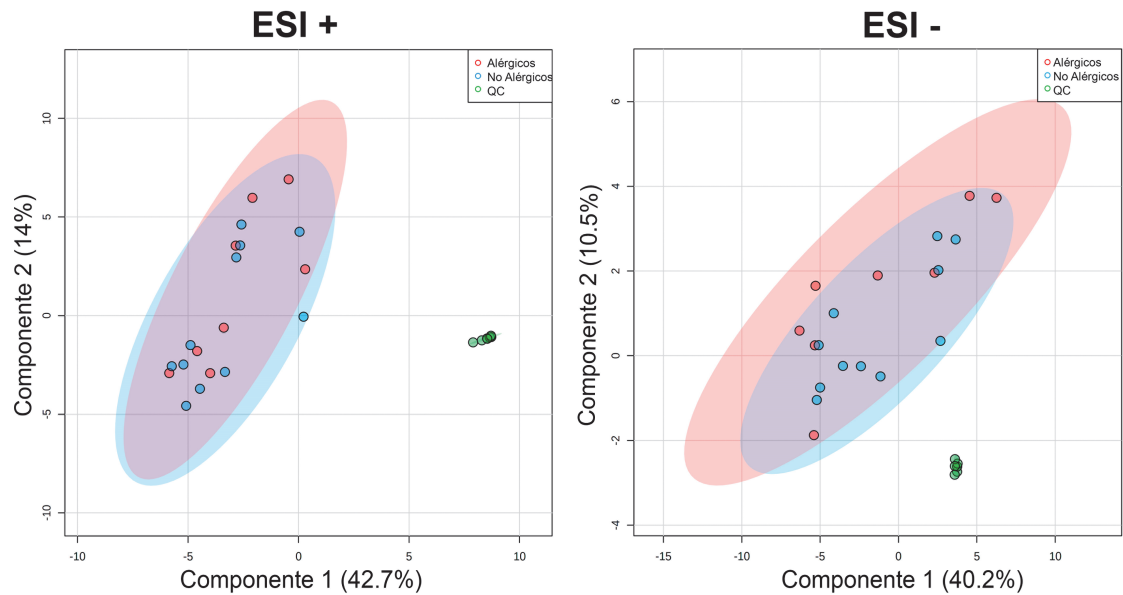


**Figura 31.** Análisis multivariante PCA de las muestras de plasma en ambas polaridades. El agrupamiento de las muestras QC (en verde) demuestra la calidad de los datos. Ambos grupos (poliposis con alergia, en rojo, y poliposis sin alergia, en azul) se agrupaban juntos, por lo que se intentaron construir modelos supervisados PLS-DA. Sin embargo, no se obtuvieron modelos.

A continuación, se realizó un análisis univariante, en el que se encontraron un total de 13 (ESI+) y 26 (ESI-) metabolitos con abundancias significativamente distintas entre ambos grupos. Para verificar que estas diferencias eran realmente debidas a la variación biológica, y no a interferencias analíticas o a artefactos estadísticos, se comprobó que el porcentaje de cambio entre los grupos fuera 1) mayor que el CV entre las muestras QC, y 2) superior al 20%, o bien (para aquellos metabolitos que pueden cargarse tanto en ESI+ como en ESI-) que aparecieran en ambas polaridades. Estas señales se utilizaron para construir un *heatmap* mediante HCA para cada polaridad (**Figura 32**), los cuales permitieron separar las muestras correctamente en el 100% (19/19) de los casos para ESI+, y en el 85% (16/19) para ESI-.

Los metabolitos significativos se identificaron mediante cotejo con bases de datos y posterior fragmentación en experimentos de LC-MS/MS. De los 39, 14 pudieron ser identificadas, encontrándose un total de 8 metabolitos únicos (**Tabla 14**). Estos metabolitos fueron la bilirrubina, el cortisol, el LPC 16:0, el LPC 18:0, el LPC 20:4 y el LPI 20:4, que se encontraban aumentados en el grupo de pacientes con poliposis no alérgica frente al grupo de poliposis alérgica.

## Resultados

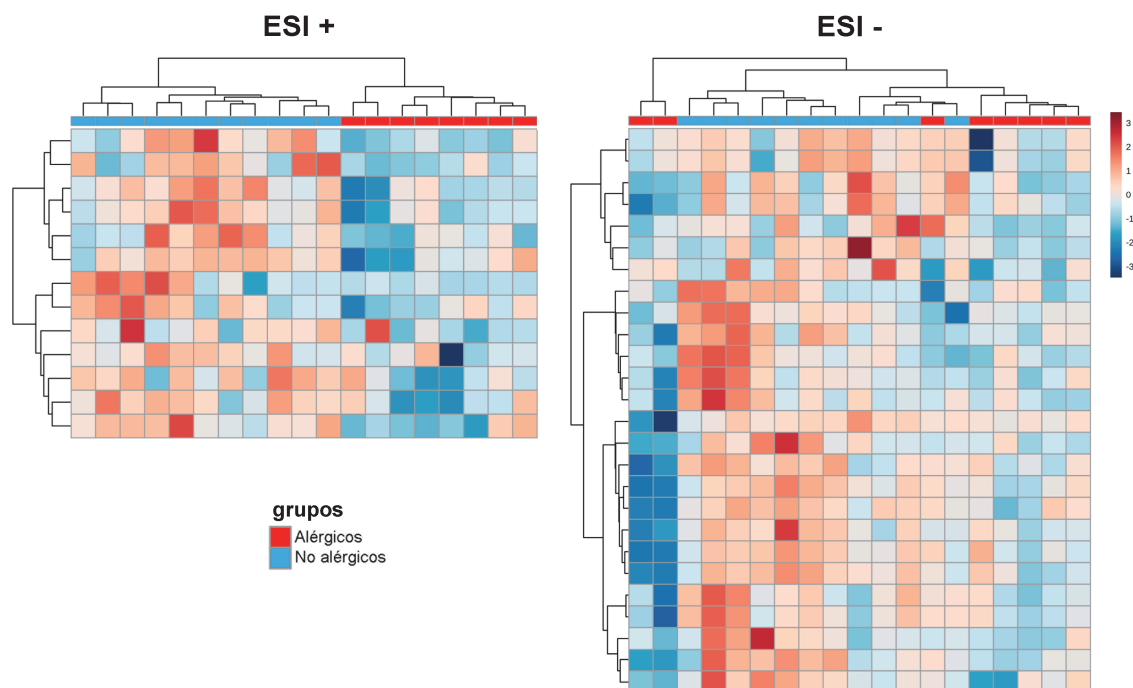


**Figura 32.** *Heatmap* de los metabolitos obtenidos para la comparación de poliposis alérgica (rojo) y no alérgica (azul) en ESI+ (izquierda) y ESI- (derecha). El color de las celdas indica si los metabolitos (en filas) se encuentran aumentados (rojo) o disminuidos (azul) en cada muestra (en columnas). Las muestras se agrupan en función de su similitud.

**Tabla 14.** Compuestos encontrados en la comparación de pacientes de poliposis no alérgica y alérgica.

Nº	Técnica	Compuesto	Aducto	$m/z$ (Da)	Masa (Da)	RT (min)	Error (ppm)	CV en QCs (%)	FC (NA)	% cambio (NA)	$p$ -valor	FDR
1	LC-MS-	Bilirrubina	[M-H] <sup>-</sup>	583.2549	584.2621	32.94	2	16.9	2.03	103.28	0.041	0.049
	LC-MS+		[M+H] <sup>+</sup>	585.2702	584.2630	32.90	1	11.4	1.96	95.56	0.033	0.039
2	LC-MS+	Cortisol	[M+H] <sup>+</sup>	363.2171	362.2099	3.66	1	12.4	2.20	119.55	0.026	0.034
3	LC-MS-	LPC 16:0 sn-1	[M+FA] <sup>-</sup>	540.3301	495.3324	19.42	1	8.8	1.23	23.49	0.026	0.038
	LC-MS+		[M+H] <sup>+</sup>	496.3402	495.3330	19.36	1	13.5	1.27	27.17	0.036	0.042
4	LC-MS-	LPC 16:0 sn-2	[M+FA] <sup>-</sup>	540.3305	495.3324	20.20	1	6.2	1.17	16.94	0.041	0.049
	LC-MS+		[M+H] <sup>+</sup>	496.3403	495.3331	20.14	1	10.5	1.25	25.45	0.018	0.032
5	LC-MS-	LPC 18:0 sn-2	[M+FA] <sup>-</sup>	568.3623	523.3642	23.74	1	9.1	1.33	32.80	0.007	0.029
	LC-MS+		[M+H] <sup>+</sup>	524.3713	523.3641	23.66	0	12.6	1.36	36.19	0.005	0.025
6	LC-MS-	LPC 18:0 sn-1	[M+FA] <sup>-</sup>	568.3618	523.3637	24.58	1	6.2	1.23	22.55	0.041	0.049
	LC-MS+		[M+H] <sup>+</sup>	524.3719	523.3647	24.52	2	11.1	1.30	30.01	0.010	0.031
7	LC-MS-	LPC 20:4 sn-2	[M+Cl] <sup>-</sup>	578.3016	543.3324	18.59	1	10.8	1.42	42.11	0.026	0.034
	LC-MS+		[M+H] <sup>+</sup>	544.3401	543.3329	18.49	1	23.7	1.49	49.03	0.054	0.071
8	LC-MS-	LPI 20:4 sn-1	[M-H] <sup>-</sup>	619.2880	620.2952	19.59	1	6.1	1.38	38.01	0.020	0.034

FC: *fold change*, calculado como la media del área bajo la curva en no alérgicos / media del área en alérgicos; el % cambio se calculó como (FC-1) x 100; FDR: Benjamini-Hochberg.

En general, se observó una reducción a nivel sistémico en una serie de metabolitos relacionados con la inflamación en pacientes con poliposis y alergia comparado con los pacientes con poliposis no alérgicos.

### 4.4.3. Análisis metabolómico local en pólipo

Para analizar el fenotipo local en el pólipo, se analizaron mediante metabolómica dirigida muestras de tejido de pólipo nasal procedentes de 6 pacientes (3 de cada grupo). En este análisis se incluyeron aquellos metabolitos significativamente distintos en plasma de los que se disponía un estándar comercial (**Tabla 3**). No se obtuvieron diferencias significativas para ninguno de los metabolitos analizados (**Figura 33**), si bien la tendencia parece ser similar a la observada en el plasma.

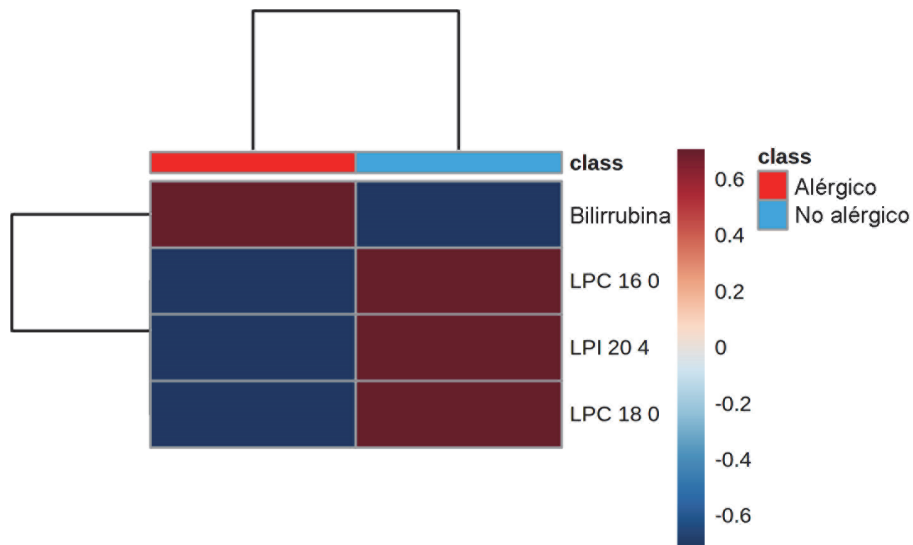


**Figura 33.** Heatmap de las abundancias medias de cada metabolito en los grupos.

Las trayectorias de los metabolitos analizados en cada tipo de muestra pueden observarse en la

**Figura 34.**

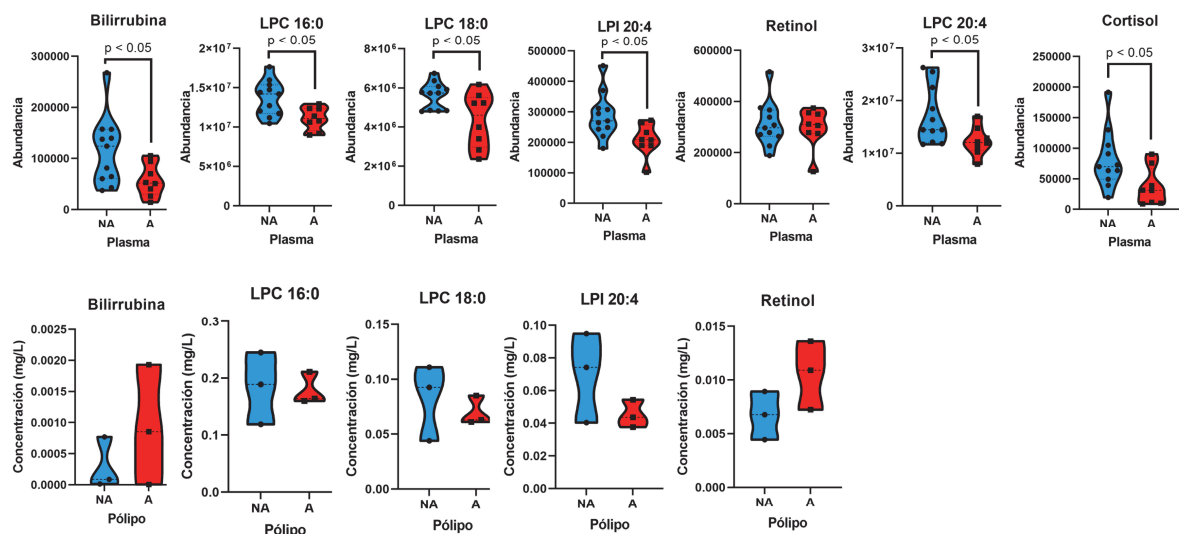


**Figura 34.** Trayectorias de los metabolitos identificados en el análisis no dirigido en plasma (parte superior) y en el análisis dirigido en pólipo (parte inferior) para los pacientes con poliposis no alérgicos (en azul) y alérgicos (en rojo).

#### 4.4.4. Análisis histológico en pólipo y mucosa nasal

Con el fin de analizar en profundidad el fenotipo local del pólipo y la mucosa, se analizaron la infiltración de células inflamatorias (recuento de eosinófilos, neutrófilos y células CD3<sup>+</sup> y CD11c<sup>+</sup>) y el remodelado tisular (la deposición de fibras de colágeno y la hiperplasia de células caliciformes).

La cuantificación de eosinófilos (**Figura 35 A**) reveló que se encontraban aumentados en los pólipos de todos los pacientes con respecto a sus respectivas mucosas ( $9.7 \pm 2.3$  células/área vs  $0.71 \pm 0.41$  células/área,  $P < .001$ ). Además, se demostró que los pólipos de pacientes con alergia presentaban una mayor infiltración de eosinófilos que los de los pacientes sin alergia ( $16.6 \pm 3.6$  células/área vs  $4.5 \pm 1.4$  células/área,  $P < .05$ ) (**Figura 35 B**).

En el caso de los neutrófilos (**Figura 36 A**), estos también estaban aumentados en los pólipos de los pacientes con respecto a sus mucosas ( $0.60 \pm 0.10$  células/área vs  $0.31 \pm 0.10$  células/área,  $P < .01$ ). Los pacientes alérgicos presentaban en sus pólipos los valores más altos de neutrófilos, encontrándose significativamente aumentados en comparación con sus propias mucosas nasales ( $0.70 \pm 0.17$  células/área vs  $0.16 \pm 0.060$  células/área,  $P < .01$ ). No se encontraron diferencias entre los pólipos y las mucosas de los pacientes no alérgicos, o entre los pólipos de pacientes alérgicos y no alérgicos ( $p > 0.41$ ) (**Figura 36 B**).

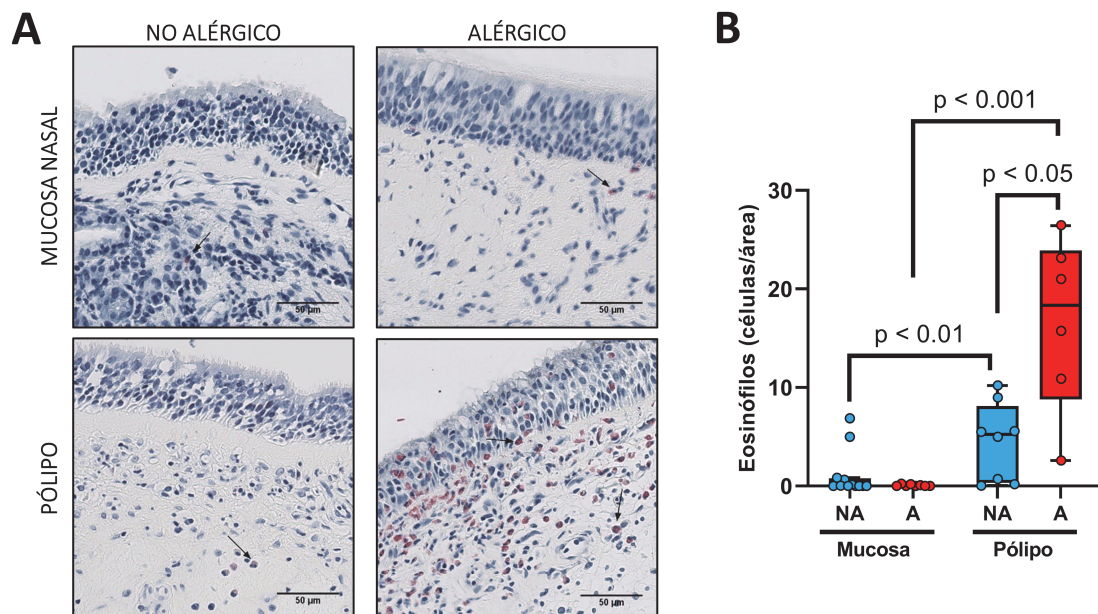


**Figura 35. A.** Imágenes representativas de tejido de mucosa nasal (parte superior) y pólipo (parte inferior) de pacientes con poliposis no alérgicos (izquierda) y alérgicos (derecha) para la tinción de Luna. Las flechas negras señalan la posición de los eosinófilos (teñidos en rojo), y las barras de escala indican 50  $\mu$ m. **B.** Análisis estadístico del infiltrado de eosinófilos en las muestras de tejido anteriores. NA: no alérgico, en azul, A: alérgico, en rojo.



## Resultados

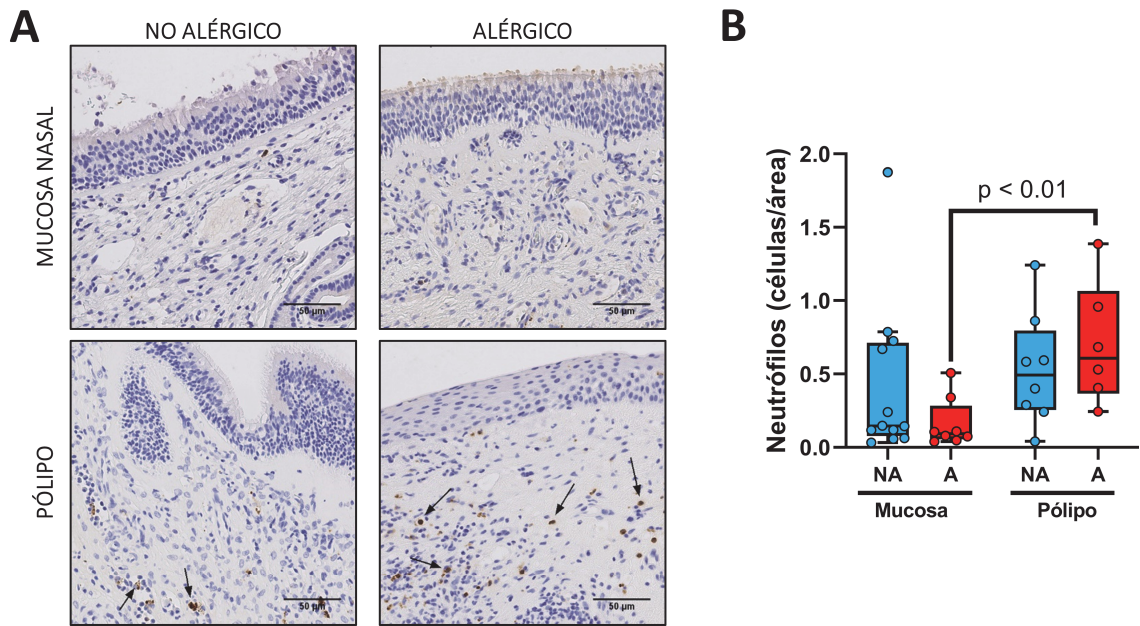


**Figura 36. A.** Imágenes representativas de tejido de mucosa nasal (parte superior) y pólipo (parte inferior) de pacientes con poliposis no alérgicos (izquierda) y alérgicos (derecha) para la tinción con anti-elastasa de neutrófilos. Las flechas negras señalan la posición de los neutrófilos (teñidos en marrón), y las barras de escala indican 50  $\mu$ m. **B.** Análisis estadístico del infiltrado de neutrófilos en las muestras de tejido anteriores. NA: no alérgico, en azul, A: alérgico, en rojo.

No se encontraron diferencias significativas en cuanto a la infiltración de células CD3<sup>+</sup> (**Figura 37**) o CD11c<sup>+</sup> (**Figura 38**) entre los pólipos de los pacientes alérgicos y no alérgicos; ni entre las mucosas y los pólipos de ninguno de los grupos.

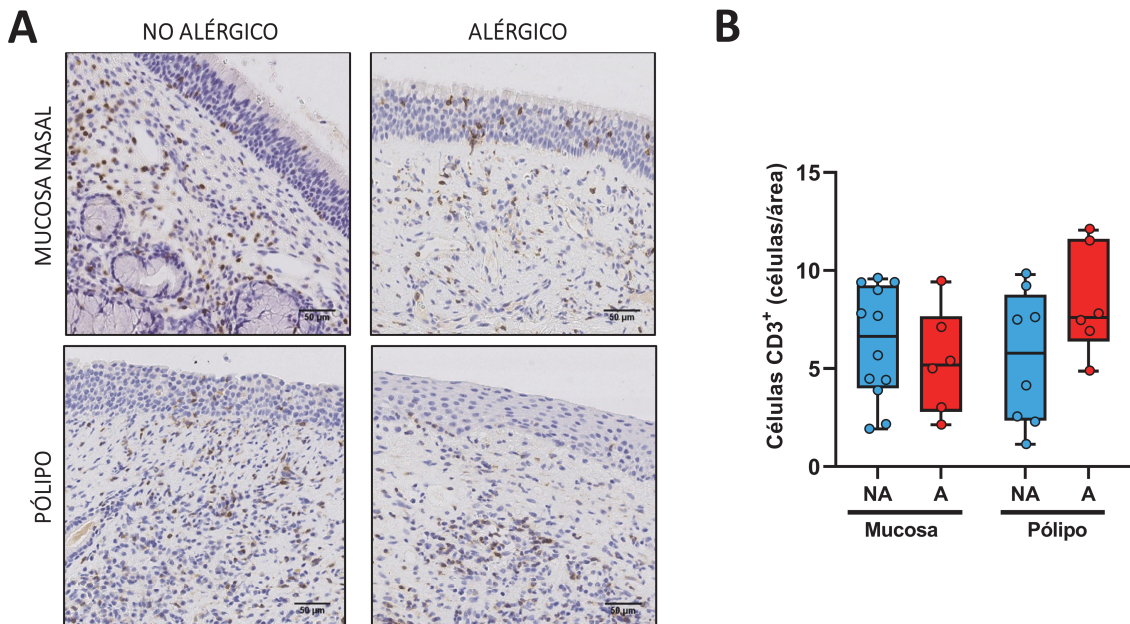


**Figura 37. A.** Imágenes representativas de tejido de mucosa nasal (parte superior) y pólipo (parte inferior) de pacientes con poliposis no alérgicos (izquierda) y alérgicos (derecha) para la tinción con anti-CD3. Las flechas negras señalan la posición de las células CD3<sup>+</sup> (teñidos en marrón), y las barras de escala indican 50  $\mu$ m. **B.** Análisis estadístico del infiltrado de células CD3<sup>+</sup> en las muestras de tejido anteriores. NA: no alérgico, en azul, A: alérgico, en rojo.

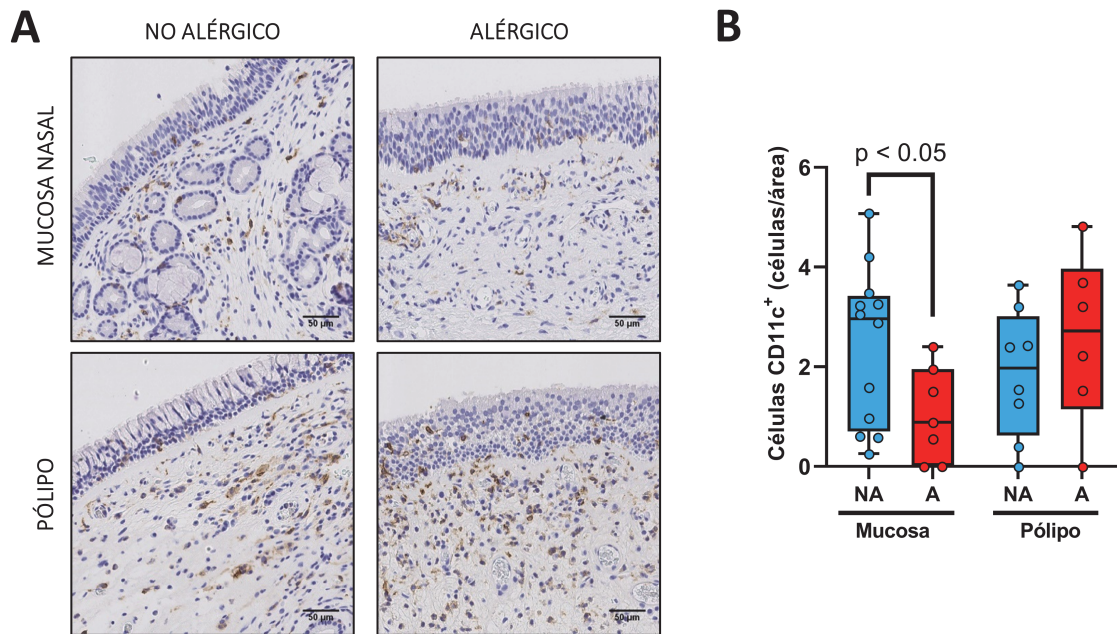


**Figura 38. A.** Imágenes representativas de tejido de mucosa nasal (parte superior) y pólipo (parte inferior) de pacientes con poliposis no alérgicos (izquierda) y alérgicos (derecha) para la tinción con anti-CD11c. Las flechas negras señalan la posición de las células CD11c<sup>+</sup> (teñidas en marrón), y las barras de escala indican 50 µm. **B.** Análisis estadístico del infiltrado de células CD11c<sup>+</sup> en las muestras de tejido anteriores. NA: no alérgico, en azul, A: alérgico, en rojo.

Tampoco fueron significativas las diferencias en la deposición de fibras de colágeno (**Figura 39**) o la hiperplasia de células caliciformes (**Figura 40**) entre los pólipos de los pacientes alérgicos y no alérgicos. No obstante, se observó una tendencia a la reducción en el número de fibras de colágeno en los pólipos con respecto a las mucosas, lo que podría indicar que los pólipos de los pacientes reclutados eran edematosos. De hecho, la diferencia entre las mucosas y los pólipos fue significativa para los pacientes no alérgicos ( $P < .001$ ) (**Figura 39 B**). También se observó que, en algunos pacientes, existía un aumento del área teñida con tinción de PAS en el epitelio, lo que sugiere una hiperplasia de las células caliciformes, si bien la diferencia no fue significativa ni en los pacientes alérgicos ( $p = 0.41$ ) ni en los no alérgicos ( $p = 0.29$ ) (**Figura 40 B**).

## Resultados

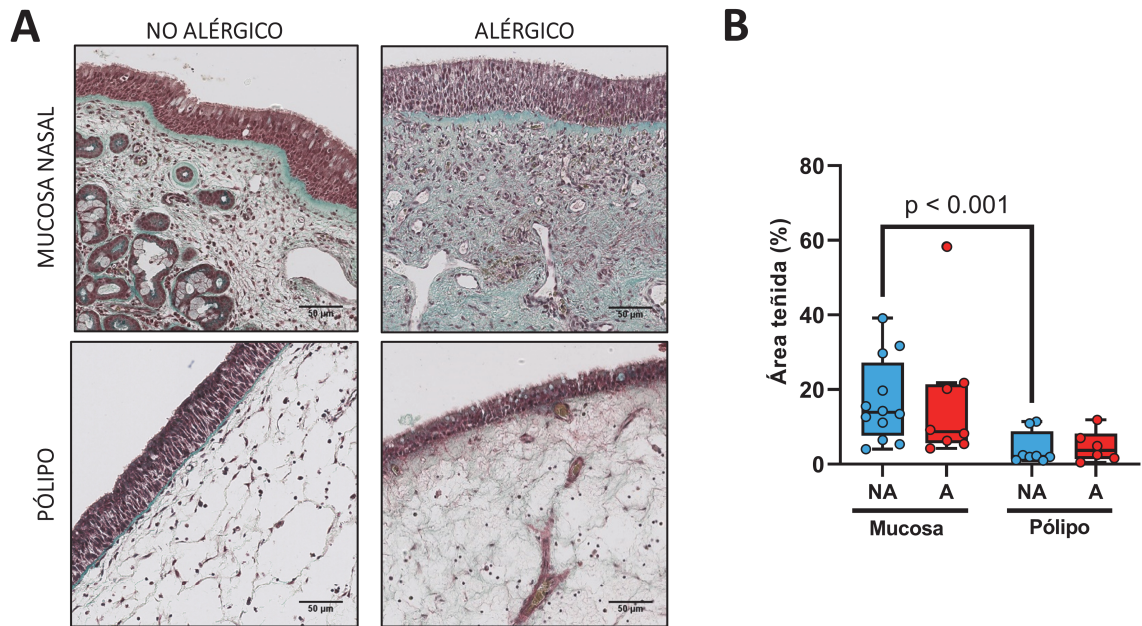


**Figura 39. A.** Imágenes representativas de tejido de mucosa nasal (parte superior) y pólipo (parte inferior) de pacientes con poliposis no alérgicos (izquierda) y alérgicos (derecha) para la tinción de Masson. Con ella, las fibras de colágeno se tiñen de color verde; los citoplasmas, de color rojo/marrón, y los eritrocitos, de color dorado. Las barras de escala indican 50  $\mu\text{m}$ . **B.** Análisis estadístico del área teñida en verde en las muestras de tejido anteriores. NA: no alérgico, en azul, A: alérgico, en rojo.

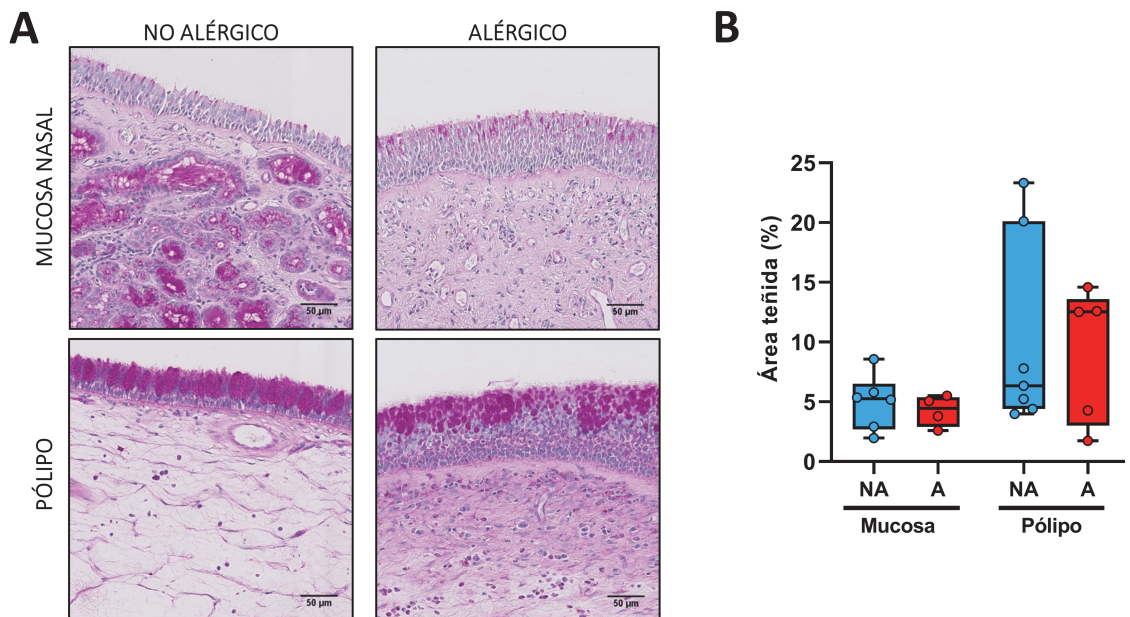


**Figura 40. A.** Imágenes representativas de tejido de mucosa nasal (parte superior) y pólipo (parte inferior) de pacientes con poliposis no alérgicos (izquierda) y alérgicos (derecha) para la tinción PAS. Con ella, los polisacáridos, y particularmente las glándulas y células calciformes del epitelio, se tiñen de rosa fucsia intenso, mientras que los citoplasmas se tiñen de morado/azul. Las barras de escala indican 50  $\mu\text{m}$ . **B.** Análisis estadístico del área teñida en rosa en el epitelio en las muestras de tejido anteriores. NA: no alérgico, en azul, A: alérgico, en rojo.

En conjunto, los pólipos de pacientes alérgicos presentan un mayor infiltrado de eosinófilos que los pólipos de pacientes no alérgicos, pero no existen entre ellos diferencias significativas en cuanto

## Resultados

al infiltrado de otras células inflamatorias (neutrófilos, CD3, CD11c) o marcadores de remodelado (deposición de fibras de colágeno, hiperplasia de células caliciformes).

## 5. Discusión

El objetivo principal de esta tesis es la identificación de biomarcadores asociados con los mecanismos subyacentes del asma grave no controlado tanto alérgico como no alérgico; además de en poliposis nasosinusal, patología que se asocia con el asma grave, para la estratificación de pacientes.

El asma afecta a un 1-18% de la población a nivel mundial; en concreto, en Europa ese porcentaje varía entre el 5 y el 15% (102). Alrededor de un 50% del asma grave es alérgico. En los últimos años, se está produciendo un incremento en la incidencia de asma, particularmente de los fenotipos alérgicos y graves (26). A día de hoy, aún existen muchas incógnitas con respecto a los mecanismos subyacentes a esta patología. No obstante, entenderlos es fundamental, tanto para mejorar la calidad de vida de los pacientes como para reducir la carga que supone el tratamiento de aquellos con asma grave no controlado en los sistemas de salud, ya que conlleva un importante gasto económico (44,45,102,103). En la actualidad, se estima que hasta un 90% de los pacientes con asma se encuentran sin tratar o con un tratamiento inadecuado, que no permite controlar los síntomas en su totalidad (45).

Para lograr controlar el asma grave, el primer paso es identificar a los pacientes que presentan este fenotipo, algo sumamente complejo debido a la heterogeneidad de esta enfermedad. No obstante, la estratificación de los pacientes es una estrategia clave para mejorar su calidad de vida, ya que la identificación temprana del asma no controlado permitiría reducir el tiempo entre el diagnóstico y el control de los síntomas del paciente (72) y, por tanto, conseguir una medicina personalizada y de precisión. En este proceso, el primer paso es el desarrollo de herramientas analíticas para la búsqueda de biomarcadores, algo para lo que las ciencias ómicas resultan de gran utilidad (74).

La búsqueda de biomarcadores, además de ser fundamental para la estratificación de pacientes, también puede ser útil en el desarrollo de nuevas terapias, otro de los puntos clave en el control de la enfermedad. Hasta la fecha, las terapias para el asma alérgico incluyen una combinación de glucocorticoides, la inmunoterapia específica contra alérgeno (único tratamiento capaz de modificar el curso de la enfermedad alérgica) y medicamentos biológicos que bloquean rutas fundamentales de la respuesta inmune alérgica, tales como las rutas de IgE, IL-5 o IL-4R. Aunque, a la fecha de inclusión de este estudio, solamente existía un biológico aprobado para el tratamiento de asma (omalizumab, anti-IgE), otros como mepolizumab (anti-IL5) y dupilumab (anti-IL-4R $\alpha$ ) han sido aprobados posteriormente. En algunos casos, estos biológicos funcionan en pacientes que no respondían a omalizumab (104,105), o son más efectivos que otros tratamientos (106). Sin

## Discusión

embargo, siguen existiendo pacientes que no responden a estos tratamientos; además, elegir cuál es más apropiado para tratar a un determinado paciente es complejo (107). Para hacerlo de forma exitosa, predecir la respuesta al tratamiento es fundamental. En el caso del asma no alérgico, en el que existen pocos tratamientos efectivos, esta problemática es aún más acuciante (108).

Dentro de las ciencias ómicas, la metabolómica en la búsqueda de biomarcadores es muy prometedora, al ser capaz de detectar cambios dinámicos asociados con la patología, además de estar altamente relacionada con el fenotipo de la enfermedad (80). La elección de la técnica analítica depende de varios factores, como el tipo de metabolitos que se quieran medir. Por ejemplo, el uso de LC-MS permite la detección de una gran variedad de metabolitos en cada muestra. Sin embargo, el número máximo de muestras que se pueden medir en un único experimento de LC-MS es de 100, aproximadamente. Dado que en este análisis se incluyeron inicialmente 165 muestras, fue necesario el desarrollo de un método de normalización para poder integrar los datos generados tras la medida secuencial de muestras en lotes separados. Este método de normalización podrá ser utilizado en futuros estudios con cohortes numerosas.

En el desarrollo de esta tesis se estudió a pacientes asmáticos alérgicos y no alérgicos, residentes en la isla de Gran Canaria y estratificados por gravedad en función de su respuesta al tratamiento, considerándose leves a aquellos pacientes que respondían a tratamientos con corticosteroides tópicos o inhalados (ICS), y graves no controlados a aquellos en los que no se producía una mejora en la sintomatología del paciente con ninguno de los medicamentos disponibles (incluyendo corticosteroides orales, inmunoterapia o biológicos) (UCA). Una de las principales ventajas de este modelo clínico es que es muy homogéneo, ya que la inclusión de pacientes fue realizada por un único grupo clínico con más de 30 años de experiencia, que ha realizado un seguimiento médico a los pacientes durante, al menos, 5 años antes de su inclusión en este estudio.

También el exposoma de estos pacientes es muy homogéneo. Las islas Canarias se localizan cerca de la costa norteafricana y del desierto del Sáhara; por lo que se ven afectadas por la calima durante aproximadamente un tercio del año (109). Además, por sus condiciones climatológicas, existe una gran prevalencia de los ácaros *Dermatophagoides pteronyssinus* y *Blomia tropicalis*, ambos relacionados con el desarrollo de asma (32,33). Estos factores se relacionan con una prevalencia de alergia y rinitis persistente mayor a la de la península (31,42), y similar a la de otras regiones con condiciones climatológicas de humedad y/o temperatura parecidas, como Reino Unido, Australia, Nueva Zelanda o Tailandia (32,43,110). En conjunto, estos factores hacen que este modelo de enfermedad sea extrapolable a otras regiones, sin dejar de ser muy homogéneo en cuanto a los niveles de exposición a alérgenos, estilo de vida, clima, u otras variables.

## Discusión

Usando este modelo, en el **BLOQUE I** se realizó un análisis metabolómico y proteómico en pacientes con asma alérgico a ácaros estratificados de acuerdo con su gravedad y control de la enfermedad (ICS, IT, BIO y UCA). En estos experimentos se detectaron cambios a nivel metabolómico y proteómico que apuntan a una activación en los pacientes UCA de las rutas de inflamación de PLA<sub>2</sub> y ácido araquidónico, así como en la activación, proliferación y migración a tejido de linfocitos T.

El análisis metabolómico reveló un aumento en una serie de lisofosfolípidos, incluyendo LPC 16:0, LPC 18:0, LPC 18:1 y LPC 20:4. Éstos son, junto al LPC 18:2, los LPC más abundantes en el plasma humano (111). Existen estudios previos que describen niveles aumentados de LPC 16:0 y LPC 18:0 en el BAL de pacientes asmáticos moderados con respecto a los de pacientes leves y sujetos control, asociados a un aumento de la actividad de PLA<sub>2</sub> (112). También se relacionan con esta ruta otros LPC aumentados en los pacientes UCA, como los LPC 20:4, LPC 20:5, LPC 22:5 y LPC 22:6.

PLA<sub>2</sub> es una enzima que actúa sobre los fosfolípidos, liberando tanto lisofosfolípidos como ácidos grasos libres (113–115), entre los que se encuentran el ácido araquidónico (20:4), el ácido eicosapentanoico (20:5) o el ácido docosapentanoico (22:5). Éstos son precursores de eicosanoides, docosanoides y derivados oxidados; lípidos bioactivos que incluyen a las prostaglandinas, leucotrienos, tromboxanos, ácidos hidroxieicosatetraenoicos (HETES) y lipoxinas, que se relacionan con la resolución de la inflamación (116,117). La acumulación de ácido araquidónico, precursor de estos metabolitos, podría ser indicativa de un bloqueo en esta ruta, que impediría la síntesis de mediadores reguladores e interrumpiría la correcta resolución de la inflamación, lo que podría explicar por qué existe el fenotipo grave (118). De hecho, alteraciones en los niveles de estos mediadores lipídicos han sido descritos previamente en asma y alergia (116,119–123).

Por otra parte, los LPC 16:0, 18:0 y 18:1 se han relacionado con la activación, migración y adhesión de eosinófilos (124,125). Existen estudios que describen un incremento del LPC 18:1 en el suero de pacientes asmáticos con un fenotipo eosinofílico comparado con pacientes sin eosinofilia (119). Teniendo en cuenta que los niveles de eosinófilos son biomarcadores de la efectividad del tratamiento y predicen la respuesta a mepolizumab (126), estos marcadores podrían actuar de forma similar.

Además, PLA<sub>2</sub> también se relaciona con la producción de ácido lisofosfatídico (LPA) (117). Los LPC 22:5 y LPC 22:6, que en esta tesis se encontraron aumentados en UCA, pueden actuar como sustrato para generar LPA 22:5 y LPA 22:6, los cuales favorecen a su vez la inflamación de las vías aéreas, la hiperreactividad bronquial y el remodelado (127).

Los cambios metabólicos asociados con los fenotipos de asma alérgico grave como resultado de la activación de PLA<sub>2</sub> se resumen en la **Figura 41**.

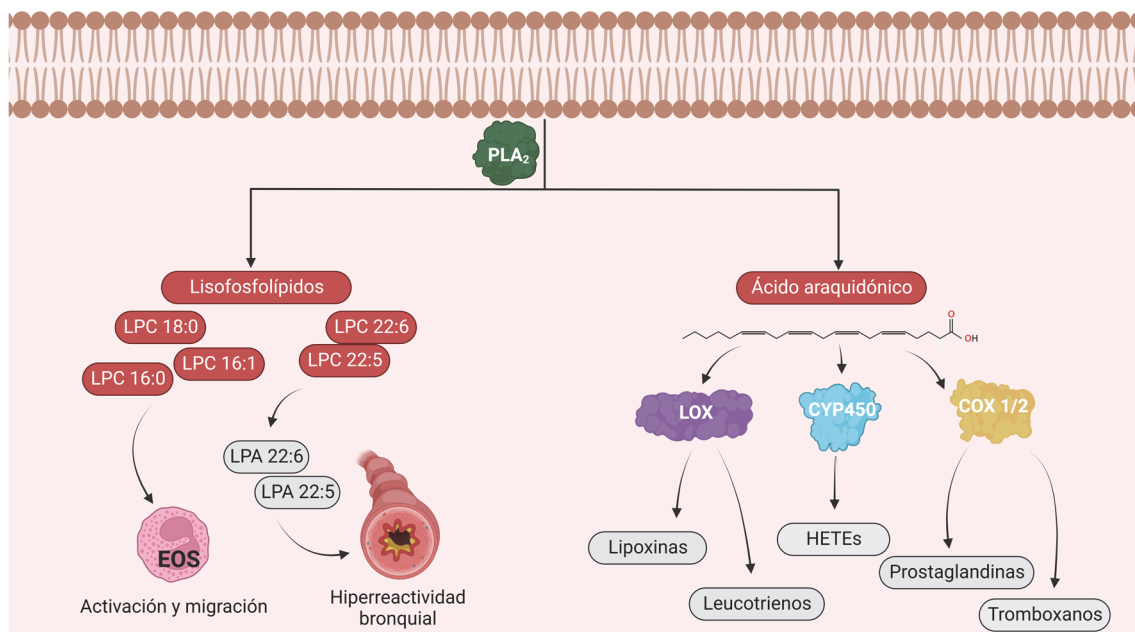


**Figura 41.** Perfil metabólico asociado a cPLA<sub>2</sub> en pacientes con asma alérgico grave no controlado. PLA<sub>2</sub> actúa sobre los fosfolípidos de la membrana plasmática liberando lisofosfolípidos y ácidos grasos libres. Los lisofosfolípidos, como las LPC, pueden actuar sobre células diana (eosinófilos) induciendo su activación y causando hiperreactividad bronquial. Entre los ácidos grasos, el ácido araquidónico puede servir como sustrato a distintas enzimas que producen mediadores inflamatorios y de resolución de la inflamación. En la figura, se muestran en rojo aquellos metabolitos que se encontraron incrementados en los pacientes graves en este estudio. EOS: eosinófilos, COX: ciclooxigenasa, CYP450: citocromo P450, LOX: lisil oxidasa, LPC: lisofosfolcolina, HETEs: ácidos hidroxieicosatetraenoicos.

Otro fosfolípido con reconocida función moduladora del sistema inmune es la esfingosina-1-fosfato (S1P) (117). Este mediador inflamatorio actúa sobre diversos tipos celulares, incluyendo los linfocitos T, favoreciendo su reclutamiento al tejido, así como su supervivencia al inhibir la degradación mitocondrial (128–130). Además, es un elemento clave en la señalización inflamatoria de mastocitos en respuestas alérgicas (131–133). La síntesis de S1P está regulada por la proteína reguladora de biosíntesis de esfingolípidos ORMDL 3 (ORMDL3), una proteína transmembrana que regula la síntesis *de novo* de S1P (134). De hecho, existe un polimorfismo en esta proteína asociado con un mayor riesgo de asma alérgico infantil (135). S1P ya se había descrito aumentada en pacientes asmáticos con respecto a sujetos control, así como en pacientes asmáticos graves (120,136–139). Resultados del grupo en estudios previos a esta tesis en pacientes alérgicos estratificados por gravedad también hallaron niveles aumentados en los pacientes más graves, además de asociarlo a otras características de plaquetas (140). Se ha encontrado un aumento de S1P en pacientes con asma no controlado con mayores niveles de eosinófilos adherentes a plaquetas (141). También se ha descrito su rol en la enfermedad inflamatoria intestinal; algunos



## Discusión

estudios apuntan a que el tratamiento con reguladores de S1P podrían ser efectivos para tratarla (142). En conjunto, el incremento en S1P indicaría una activación de linfocitos T en los pacientes UCA, que podrían jugar un papel en el control del asma.

Éste rol de los linfocitos T se ve apoyado, además, por el incremento de leucina, que se asocia con la activación, proliferación y diferenciación de linfocitos T por medio de la activación de la ruta mTORC1 (143), así como por la disminución de bilirrubina, metabolito conocido por su potente efecto antiinflamatorio (144) que es capaz de detener la migración de leucocitos a los tejidos mediante la disrupción de la molécula 1 de adhesión a células vasculares (*Vascular Cell Adhesion Molecule-1*, VCAM-1) (145). La bilirrubina y otros metabolitos biliares se están destacando progresivamente como mediadores en la respuesta inflamatoria (146). Su rol en asma será discutido más adelante.

El estudio proteómico del suero procedente de los pacientes UCA e ICS refuerza las conclusiones anteriores. Se observó un aumento en CCL13 e IL-15 en los pacientes UCA, dos proteínas que se relacionan con la atracción de monocitos y linfocitos y con la proliferación de linfocitos T (147–149). Este aumento estuvo acompañado de una reducción de CCL19, que se relaciona con la migración de linfocitos T a órganos linfoides (150–152), y de sCD4, que puede funcionar como un inhibidor competitivo del CD4 de los linfocitos T (153). Por su parte, TNFRSF12A y ARG1, aumentados en UCA, participan en el aumento en la permeabilidad y crecimiento epitelial y endotelial (154,155). ARG1 se relaciona con la ruta del óxido nítrico (NO) mediante la regulación de la enzima NOS. El NO es un mediador fundamental de la hiperreactividad en las vías aéreas, y se utiliza como marcador diagnóstico del asma a través de la medida de FeNO (156). En asma, NO induce la vasodilatación, aumentando la permeabilidad, la infiltración de células inmunes, la secreción de moco y la activación de linfocitos T (157). Además, la producción de NO se relaciona con el metabolismo de arginina (158), la cual también induce la proliferación de linfocitos T (159). La arginina, que en otros estudios ya se había relacionado con asma (138,160–162), se encontró asimismo elevada en los pacientes UCA.

Estos hallazgos indicarían que los pacientes UCA presentan una mayor respuesta proinflamatoria de linfocitos T, localizada fundamentalmente en la mucosa. Además, dada la reducción en los niveles de IFN $\gamma$ , es probable que esta respuesta tuviera un perfil tipo Th2. De hecho, se sabe que la señalización mediada por TNFRSF12A induce una respuesta tipo Th2 en un modelo de colitis crónica con fibrosis (163). Además, los niveles aumentados de CASP-8 apuntan a una respuesta mantenida en el tiempo, puesto que esta proteína es fundamental en el mantenimiento de la proliferación de linfocitos T (164).

## Discusión

En resumen, los datos metabolómicos y proteómicos muestran que los pacientes UCA presentan una respuesta inflamatoria sistémica y crónica, caracterizada por un aumento de la proliferación y activación de linfocitos T unida a un metabolismo exacerbado de mediadores lipídicos, S1P y arginina, lo que se relaciona con una activación de las rutas del ácido araquidónico, la esfingosina y el NO. Existen estudios que apuntan a que las rutas del ácido araquidónico y linoleico, junto al metabolismo de esfingolípidos, podrían ser buenos predictores para el control del asma (120); el presente estudio refuerza esos datos, además de ampliar el abanico de biomarcadores que podrían utilizarse para la estratificación de asma en función de la gravedad.

Sin embargo, en una enfermedad tan compleja como el asma se hace necesaria la generación de un panel de biomarcadores multidimensional que incluya distintos tipos de datos ómicos y los datos clínicos (22,76,165).

En asma existen tentativas previas para la integración de distintas ómicas (120,166,167). La construcción de modelos predictivos de aprendizaje automático puede ser muy útil en este proceso (168). Por ello, en este proyecto se creó un algoritmo *k*-NN con el objetivo de que clasificara a los pacientes en grupos. El algoritmo *k*-NN es uno de los más simples y eficientes de aprendizaje automático (169). Para ello, se utilizaron los datos clínicos y metabolómicos, y el modelo construido fue capaz de clasificar a los pacientes con una precisión superior al 80%.

Este estudio muestra que el asma grave no controlado alérgico se diferencia del asma controlado alérgico por una marcada respuesta inflamatoria, que conlleva una activación de los linfocitos Th2 (caracterizada por un aumento en los niveles de CCL13, IL-15, CASP-8, S1P y leucina, así como una reducción de CCL-19, IFN $\gamma$  y bilirrubina) y de las rutas del ácido araquidónico, la PLA<sub>2</sub> y la ruta de NO (caracterizadas por un incremento en los niveles de diversos LPC, LPE y LPI, así como un aumento en los niveles de arginina y ARG1).

En este análisis, debido al número de muestras inicial, se decidió utilizar una única técnica metabolómica que fuera capaz de medir un amplio abanico de moléculas. No obstante, ciertos metabolitos, como lípidos de alto peso molecular, moléculas muy pequeñas o compuestos volátiles no fueron medidos. Utilizar otras técnicas podría revelar otras rutas biológicas de interés que complementen estos resultados. Además, el modelo de aprendizaje automático fue construido con un total de diez pacientes; dado el limitado número de pacientes, hubo que excluir algunas variables que no fueron medidas en este grupo de muestras, pero que podrían ser biomarcadores de interés en esta enfermedad, como son las variables proteómicas. Es importante entender que estos resultados fueron obtenidos en el contexto de un estudio piloto. La validación en cohortes más numerosas es imprescindible para confirmar estos hallazgos, y la realización de ensayos

funcionales permitiría comprender el mecanismo molecular concreto por el que estos pacientes no controlan la enfermedad.

Uno de los paradigmas del asma alérgico es dilucidar cuál es la contribución de la patología alérgica y cuál la del asma en el desarrollo de la enfermedad. En este sentido, resulta sorprendente que, en una zona de alta exposición a ácaros, los que, como se ha descrito anteriormente, tienen características que favorecen el desarrollo de asma tras la sensibilización alérgica, existan pacientes en los que la patología asmática sea independiente de la alergia. Por ello, en el **BLOQUE II**, se reclutaron pacientes no controlados alérgicos (UCA) y no alérgicos (UCNA) de esta zona de alta exposición. Ser capaces de identificar los mecanismos de contribución de la alergia al asma permitiría una mejor estratificación de los pacientes, así como el descubrimiento de nuevas dianas terapéuticas. Esto es particularmente interesante en el caso del asma grave no alérgico, un fenotipo que históricamente ha sido menos estudiado (48,170).

Los pacientes UCNA eran mayores, tenían una edad de aparición de la enfermedad más tardía y unos niveles de IgE más bajos que los pacientes UCA, lo que concuerda con estudios previos que describen las diferencias clínicas entre estos fenotipos (3,23). Estas observaciones pueden relacionarse con la evolución de la enfermedad. Los pacientes graves no controlados presentan un tiempo de evolución de la patología mayor que los pacientes controlados, puesto que, para clasificarlos como no controlados, se les ha prescrito todo el abanico de medicaciones disponibles, y ninguna de ellas ha sido exitosa. Dado que en los pacientes no alérgicos la edad de aparición es más tardía (23), es lógico pensar que también lo es la media de edad, puesto que los tiempos de evolución deberían de ser similares independientemente de la alergia.

Los cambios detectados mediante el análisis metabolómico se relacionan con una activación de la ruta PLA<sub>2</sub>, similar a la observada entre los pacientes alérgicos no controlados (UCA) y los controlados (ICS), y una desregulación de los ácidos biliares, que recientemente se han destacado como reguladores de la inflamación (146).

Los pacientes UCA presentaban niveles aumentados de los LPC 18:2, LPC 18:3 y LPC 20:4 en los pacientes UCA con respecto a los UCNA. Un aumento en los LPC 18:2 y LPC 20:4 se han descrito previamente entre asma eosinofílico y no eosinofílico (171). Estos LPC se relacionan con la activación de PLA<sub>2</sub> y la ruta del ácido araquidónico (111), que se ha descrito previamente.

Específicamente, el LPC 18:2 forma parte de las lipoproteínas de alta densidad (*High-Density Lipoprotein*, HDL). Se ha descrito que, tras la provocación con alérgeno, los mastocitos, macrófagos alveolares y neutrófilos pueden secretar sPLA<sub>2</sub> (172), la cual es capaz, a su vez, de alterar la composición de las HDL y liberar los LPC que contienen. Existen estudios que describen que las HDL

## Discusión

se encuentran enriquecidas en LPC durante procesos inflamatorios. Estos LPC pueden actuar como mediadores y, entre otras funciones, alterar la agregación plaquetaria (173). El rol de las plaquetas en la inflamación está siendo cada vez más estudiado, y existen evidencias que apoyan su papel en asma y alergia (140,174,175). De hecho, el pulmón es un lugar de síntesis y almacenamiento plaquetario (176). Curiosamente, se ha descrito un aumento del ácido graso 18:2 en pacientes asmáticos con respecto a pacientes con EPOC (177). La EPOC, al igual que el asma no-Th2, se caracteriza por una infiltración de neutrófilos (178), por lo que las diferencias de este LPC en ambos fenotipos pueden deberse a las diferencias en cuanto al perfil inflamatorio subyacente.

En cuanto al LPC 18:3, no existen muchos estudios que lo relacionen con el asma. Sin embargo, se ha visto que éste y otros fosfolípidos se encuentran aumentados en la fase de recuperación de EPOC (179), lo que podría ser indicativo de un posible rol en neutrófilos, asociados al asma no alérgico. Se sabe que otros LPC, como los LPC 16:0 y 18:0 promueven la activación de neutrófilos y agravan la hipersensibilidad por contacto (180). Por último, la palmitoleil carnitina (16:1) se encontró disminuida en los pacientes UCA. La suplementación con L-carnitina se asocia con una reducción de mediadores inflamatorios tales como la proteína C reactiva, la IL-6 o el TNF- $\alpha$  (181), lo que apunta al rol regulador de estos mediadores. Una disminución en carnitinas acompañada de un aumento en LPC ha sido descrito previamente en alergia grave (140).

En conjunto, los datos sugieren que la alergia en asma no controlado conlleva una alteración en el metabolismo de los mediadores LPC y de las carnitinas, junto con una activación de la ruta del ácido araquidónico, lo que indicaría que estos factores juegan un papel relevante.

La biosíntesis de esteroides se encontró, asimismo, aumentada en pacientes UCA en comparación con los UCNA, lo cual ya había sido descrito en pacientes con asma alérgico en comparación con sujetos control (182). Los esteroides participan en la activación del sistema inmune y el desarrollo de asma, existiendo una relación, por ejemplo, entre las hormonas esteroideas femeninas y una activación de la inflamación, y las hormonas esteroideas masculinas y una inmunosupresión (5). Algunos estudios han relacionado la toma de glucocorticoides con una supresión de la glándula adrenal que podría explicar una reducción en los niveles de esteroides (183). No obstante, todos los pacientes no controlados tomaban, en el momento de la inclusión en este estudio, una combinación de corticosteroides inhalados y LABA, y no existían diferencias en cuanto al uso de corticosteroides tópicos u orales entre los dos grupos.

Por último, se encontró un perfil alterado de ácidos biliares, particularmente de ácido deoxicólico, entre los dos grupos. Alteraciones en el perfil de ácidos biliares se han relacionado con enfermedades inflamatorias (146). En concreto, existe una relación entre el desarrollo de

## Discusión

enfermedades inflamatorias respiratorias (particularmente en asma no alérgico) y el reflujo gastroesofágico, que puede ser debida al daño que los jugos gástricos pueden producir, o a la estimulación debido al origen vagal común del esófago y los bronquios (53). Estudios recientes apuntan a que ambas enfermedades actúan retroalimentándose la una a la otra (54). Algunos ácidos biliares se han visto aumentados en asma con reflujo gastroesofágico (139). El ácido deoxicólico se encontró reducido en los pacientes UCA con respecto a los UCNA, lo cual también se observó en la comparación de UCA con respecto a ICS. Este ácido biliar estimula la producción de citoquinas inflamatorias tales como IL-1 $\beta$  e IL-6 *in vitro* e *in vivo* en modelos animales (184); también es capaz de activar el inflammasoma (185) y produce disbiosis en la microbiota intestinal (186) en modelos animales. En conjunto, los datos señalarían que un perfil esteroideo alterado podría ser responsable de la inflamación en el asma no alérgico.

En resumen, dentro de los pacientes graves no controlados, los pacientes alérgicos presentan niveles alterados de LPC y ácidos biliares con respecto a los pacientes no alérgicos, lo que apunta a mecanismos de enfermedad diferentes entre ambos fenotipos.

En este análisis, no fue posible incluir otras técnicas ómicas, como sí lo fue para la estratificación por gravedad. Complementar estos resultados con otros análisis ómicos y su integración en modelos predictivos permitiría obtener una perspectiva más completa y entender en mayor profundidad el rol de la alergia en la patología asmática.

Otro de los hallazgos relevantes en pacientes con asma no alérgico fue que el 50% de ellos tenían EREA, una asociación que ha sido previamente descrita en diversos estudios (69,187). Una de las características de la EREA es la aparición de pólipos nasales.

La CRSwNP es, al igual que el asma, una enfermedad muy heterogénea que presenta diversos endofenotipos que se diferencian en cuanto a sus características clínicas, como el número de recidivas o el tratamiento efectivo (64). Sin embargo, el fenotipado de los pólipos nasales se basa en el análisis histológico tras la extracción por cirugía. La búsqueda de biomarcadores mediante ciencias ómicas junto al análisis de las características clínicas e histológicas de estos pacientes permitiría identificar mejor los mecanismos inflamatorios que tienen lugar en los distintos fenotipos, y facilitaría la clasificación previa, lo que ayudaría a elegir el tratamiento de la enfermedad (188). Su relación con la alergia es controvertida, y existen estudios tanto a favor como en contra de ésta (59,66). Por ello, en el **BLOQUE III** de esta tesis se planteó analizar la contribución de la alergia al desarrollo de pólipos. Además, por su relación con el asma, se planteó un análisis de los mecanismos implicados tanto a nivel local como a nivel sistémico. El análisis reveló que los pacientes con poliposis no alérgica presentaban niveles sistémicos elevados de mediadores

## Discusión

inflamatorios, tales como LPC 16:0, LPC 18:0 y LPC 20:4, mientras que, a nivel local, presentaban una disminución en el número de eosinófilos con respecto a los pacientes alérgicos con poliposis, lo que sugiere que los mecanismos por los que se establece la patología en ambos grupos son diferentes.

En el análisis metabolómico sistémico se encontraron niveles aumentados de los LPC 16:0, LPC 18:0 y LPC 20:4, además del LPI 20:4, en los pacientes no alérgicos con poliposis nasal. Estos LPC también se vieron alterados en el análisis de los pacientes asmáticos estratificados por gravedad, y su papel en la inflamación tanto por su acción como mediadores inflamatorios como por su relación con las rutas de PLA<sub>2</sub> y del ácido araquidónico, ya ha sido discutido previamente. En cuanto al LPI 20:4 es uno de los más abundantes en plasma, y se ha relacionado con el establecimiento de una respuesta proinflamatoria en modelos animales de enfermedad intestinal (189) y en diabetes tipo 2 (190).

Por otra parte, los pacientes con poliposis no alérgicos presentaban también un aumento en la hormona cortisol. Se ha descrito que el cortisol actúa como un inhibidor temprano de la inflamación; no obstante, si no es capaz de controlarla por sí mismo, actúa sobre las células para prepararlas para los procesos inflamatorios subsecuentes (191). Un estudio en saliva describió que los pacientes con poliposis nasal tienen los ritmos circadianos de cortisol alterados (192). Además, las células epiteliales desarrolladas a partir de pólipos nasales son capaces de producir cortisol, lo que quizá se relaciona con la respuesta al tratamiento de glucocorticoides que reciben estos pacientes (193). En conjunto, el aumento de cortisol en el plasma de pacientes no alérgicos puede relacionarse con una estrategia de control de la inflamación, que podría estar actuando a nivel local.

Con el fin de descubrir si existían, de hecho, características inflamatorias específicas para cada fenotipo a nivel local, se desarrolló un nuevo método de análisis metabolómico dirigido en muestras de tejido de pólipo nasal. El análisis metabolómico en muestras de tejido es un campo bastante novedoso, que está experimentando un crecimiento estable (194). No obstante, la mayoría de los análisis se basan en estudios de tumores, y el uso de pólipo nasal como matriz resulta novedoso. Cuando se realizó este análisis, no existía ningún otro estudio que utilizara esta matriz; sin embargo, casi de forma paralela, se publicó uno centrado en el análisis de tejido de pólipos clasificados en función de su grado de eosinofilia (195). Los autores encontraron una reducción en ácido araquidónico (20:4) y ácido  $\gamma$ -linolénico (18:3) en los pólipos con mayores niveles de eosinófilos, lo que podría estar relacionado con la reducción en el LPC 20:4 y el LPI 20:4 en los pólipos de pacientes alérgicos que se describe en esta tesis, cuyos pólipos presentaban una infiltración de eosinófilos significativamente mayor. No obstante, el reducido número de muestras del que se disponía para este análisis impidió obtener resultados estadísticamente significativos, si bien los niveles de los

## Discusión

mediadores inflamatorios encontrados en plasma parecen consistentes con los encontrados en los pólipos.

A día de hoy, son pocos los estudios de CRSwNP que utilizan la metabolómica, tanto a nivel sistémico, en suero o plasma (188), como a nivel local, en tejido (195,196); y ninguno de ellos combina ambos tipos de análisis. Además, éste es el primero que utiliza esta metodología para tratar de evaluar el papel de la alergia en la enfermedad. En conjunto, el uso de esta nueva metodología puede ser muy interesante en estudios futuros para entender mejor la respuesta inflamatoria del pólipo a nivel local en función del estado alérgico.

El análisis metabolómico local se combinó con un estudio histológico de los pólipos nasales y el tejido de mucosa nasal circundante. El análisis histológico resulta, a día de hoy, la manera más fiable de diferenciar los distintos endofenotipos de los pólipos (56,64).

En primer lugar, se encontró que los pólipos de los pacientes alérgicos presentaban una mayor infiltración de eosinófilos que los pólipos de los pacientes no alérgicos. Los eosinófilos son células efectoras características de la inflamación tipo Th2 (197), cuyo rol en distintas enfermedades inflamatorias, como el asma o la CRSwNP, se relaciona con su capacidad de inducir un remodelado del tejido (198). El aumento del número de eosinófilos, tanto a nivel local como sistémico, ha sido descrito previamente en CRSwNP, en patologías alérgicas y en asma. Un aumento en los niveles de eosinófilos y/o sus proteínas en tejido o plasma se ha relacionado con la gravedad y permanencia de los síntomas (199,200) y con la recidiva de los pólipos (63,201). De hecho, el tratamiento con mepolizumab (anti-IL5) es capaz de reducir significativamente los pólipos nasales, así como el número de eosinófilos en sangre, produciendo una mejoría de los síntomas y un mejor pronóstico (202).

Su papel en la inflamación viene condicionado, además de por las proteínas características de estas células, como la proteína básica principal (*Major Basic Protein*, MBP) o la proteína catiónica de eosinófilos (*Eosinophil Cationic Protein*, ECP), por la producción de mediadores inflamatorios a partir de ácido araquidónico (203). Por otra parte, se ha descrito que los eosinófilos procedentes de pólipo presentan alteraciones en los metabolitos de la ruta del ácido araquidónico (204). Así, la diferencias en los números de eosinófilos entre los pacientes con y sin alergia podría estar ligada a las diferencias metabolómicas encontradas.

El número de neutrófilos, sin embargo, fue similar en los pólipos de pacientes alérgicos y no alérgicos. Pese a que algunos autores describen una relación inversamente proporcional entre los niveles de eosinófilos y neutrófilos en pólipos (57), estudios más recientes desvelan resultados similares a los descritos en este estudio, ligando el papel de los neutrófilos en la poliposis nasal a la

## Discusión

oncostatina M (OSM), una citoquina responsable de la disfunción de la barrera epitelial (205,206). Este tipo de inflamación “mixta” ha sido descrita en asma previamente, particularmente en asma no alérgico, que se relaciona con la presencia de poliposis nasosinusal.

Por último, la reducción en la deposición de fibras de colágeno en los pólipos con respecto a las mucosas, si bien no es significativa, es un indicativo de que los pólipos incluidos en este estudio tienen un perfil edematoso, no fibrótico (64).

Estos resultados apuntan que los pólipos de pacientes alérgicos y no alérgicos tienen un perfil metabolómico diferencial y una infiltración de eosinófilos distinta que permitiría clasificarlos de forma más precisa.

No obstante, este estudio piloto presenta ciertas limitaciones en cuanto al método diagnóstico de la alergia y al número de muestras. Es importante remarcar que este estudio es un análisis exploratorio; el análisis combinado del perfil local y sistémico en cohortes más numerosas con fenotipos definidos permitirá validar estos resultados y lograr definir endotipos más concretos que permitan un mejor tratamiento de la CRSwNP (207–209).

En conjunto, los resultados de esta tesis han permitido entender mejor los mecanismos de inflamación en el asma grave no controlado, así como el papel de la alergia en la patogénesis del asma y la poliposis nasal. Algunos de los mecanismos descritos son compartidos entre los distintos modelos, lo que sugiere que el mecanismo de inflamación es común. En esta tesis, utilizando técnicas de alto rendimiento, se ha logrado encontrar biomarcadores con potencial para ser usados en la estratificación de los pacientes y una mejor comprensión de las rutas biológicas asociadas a la contribución de la patología alérgica, lo que supone completar con éxito la primera etapa del largo proceso de descubrimiento de biomarcadores (**Figura 9**). Además, los metabolitos encontrados gracias al trabajo descrito en esta tesis, conjuntamente con otros candidatos encontrados en distintos modelos de alergia de fenotipos graves (140,210,211), han permitido el desarrollo de un método analítico de metabolómica dirigida que permitirá validar la utilidad de estos metabolitos como biomarcadores predictivos en cohortes más grandes (212); lo que supone, en conjunto, tanto el desarrollo de nuevas metodologías para la identificación de biomarcadores de estratificación en nuevas cohortes de pacientes en vida real como una mejor comprensión de la biología subyacente a estas patologías, fundamental en el proceso de identificación de nuevas dianas terapéuticas y la generación de nuevas estrategias de intervención.



## 6. Conclusiones

1. Se ha implementado un método de normalización que permite integrar datos metabolómicos no dirigidos procedentes de muestras medidas en lotes independientes.
2. Los pacientes con asma alérgico grave no controlado presentan un perfil metabolómico diferencial, caracterizado por el incremento de LPC 16:0, LPC 18:0, LPC 18:1, LPC 20:4, LPC 22:5 y LPC 22:6, asociados a las rutas del ácido araquidónico y la fosfolipasa A2.
3. Los pacientes con asma alérgico grave no controlado presentan una alteración de la proliferación y activación de linfocitos Th2, que se refleja en una alteración del perfil proteómico y metabolómico, con niveles incrementados de CCL13, IL-15, CASP-8, esfingosina-1-fosfato y leucina, y una reducción de CCL-19, IFN $\gamma$  y bilirrubina.
4. Los pacientes con asma alérgico grave no controlado presentan una activación de la ruta del óxido nítrico, caracterizada por niveles incrementados de arginina y ARG1.
5. El modelo de aprendizaje automático permite diferenciar a los pacientes con asma grave alérgico no controlado cuando se utiliza una combinación de los datos metabolómicos y clínicos.
6. La comparación de asma grave no controlado alérgico y no alérgico demuestra una alteración en el perfil de lisofosfolípidos y esteroides asociada con el fenotipo alérgico, incluyendo un aumento de los LPC 18:2, LPC 18:3 y LPC 20:4 y una reducción del ácido deoxicólico. Esta alteración se relaciona con las rutas de la fosfolipasa A2 y de ácidos biliares.
7. Los pacientes con poliposis nasosinusal y alergia presentan una reducción en los niveles de LPC 16:0, LPC 18:0, LPC 20:4, LPI 20:4, cortisol y bilirrubina con respecto a los pacientes con poliposis sin alergia, lo que indicaría una reducción de la inflamación a nivel sistémico.
8. A nivel local, los pacientes con poliposis y alergia presentan un mayor infiltrado de eosinófilos en sus pólipos con respecto a los pacientes con poliposis sin alergia.
9. Se ha implementado una metodología para medir metabolitos de forma dirigida en tejido de pólipo nasal que podría utilizarse en futuros estudios.



## 7. Conclusions

1. A normalization method that allows the integration of untargeted metabolomic data obtained after the analysis of samples in independent batches has been developed.
2. Severe uncontrolled allergic asthmatic patients display a differential metabolomic profile, characterized by an increased in LPC 16:0, LPC 18:0, LPC 18:1, LPC 20:4, LPC 22:5 and LPC 22:6, which are related with the arachidonic acid and the phospholipase A2 pathways.
3. Severe uncontrolled allergic asthmatic patients display enhanced activation and proliferation of Th2 cells, as shown by the increase of CCL13, IL-15, CASP-8, sphingosine-1-phosphate and leucine, and the reduction of CCL-19, IFN $\gamma$  and bilirubin.
4. Severe uncontrolled allergic asthmatic patients have an enhanced activation of the nitric oxide pathway, characterized by increased levels of arginine and ARG1.
5. The machine learning classifier that includes both metabolomic and clinical data can correctly predict the severe uncontrolled allergic asthmatic patients.
6. Severe uncontrolled allergic asthmatic patients, when compared to severe uncontrolled non-allergic asthmatic patients, present an altered lipophilic and steroid fingerprint, characterized by an increase in LPC 18:2, LPC 18:3 and LPC 20:4, and a reduction in deoxycholic acid. These are related with the phospholipase A2 and bile acid pathways.
7. Patients with nasal polyps and allergy have reduced levels of LPC 16:0, LPC 18:0, LPC 20:4, LPI 20:4, cortisol, and bilirubin compared to non-allergic nasal polyp patients, which points towards a reduced systemic inflammation.
8. Patients with nasal polyps and allergy present higher numbers of eosinophils in their polyps than patients with nasal polyps without allergy.
9. A novel methodology for the targeted metabolomic analysis of nasal polyps tissue has been implemented in this study, and could be used in future studies.



## 8. Bibliografía

1. Global Initiative for Asthma. Global strategy for asthma management and prevention. 2022;:209.
2. Holgate ST. A Brief History of Asthma and Its Mechanisms to Modern Concepts of Disease Pathogenesis. *Allergy, Asthma Immunol Res* 2010;**2**:165–171.
3. Wenzel SE. Asthma phenotypes: the evolution from clinical to molecular approaches. *Nat Med* 2012;**18**:716–725.
4. Vos T, Lim SS, Abbafati C, Abbas KM, Abbasi M, Abbasifard M et al. Global burden of 369 diseases and injuries in 204 countries and territories, 1990–2019: a systematic analysis for the Global Burden of Disease Study 2019. *Lancet* 2020;**396**:1204–1222.
5. Fuseini H, Newcomb DC. Mechanisms Driving Gender Differences in Asthma. *Curr Allergy Asthma Rep* 2017;**17**:19.
6. van den Berge M, Heijink HI, van Oosterhout AJM, Postma DS. The role of female sex hormones in the development and severity of allergic and non-allergic asthma. *Clin Exp Allergy* 2009;**39**:1477–1481.
7. Holgate ST, Wenzel S, Postma DS, Weiss ST, Renz H, Sly PD. Asthma. *Nat Rev Dis Prim* 2015;**1**:15025.
8. Lambrecht BN, Hammad H. The airway epithelium in asthma. *Nat Med* 2012;**18**:684–692.
9. Vignola AM, Kips J, Bousquet J. Tissue remodeling as a feature of persistent asthma. *J Allergy Clin Immunol* 2000;**105**:1041–1053.
10. Escribese MM, Gómez-Casado C, Barber D, Díaz-Perales A. Immune Polarization in Allergic Patients: Role of the Innate Immune System. *J Investig Allergol Clin Immunol* 2015;**25**:251–258.
11. Licona-Limón P, Kim LK, Palm NW, Flavell RA. TH2, allergy and group 2 innate lymphoid cells. *Nat Immunol* 2013;**14**:536–542.
12. Lambrecht BN, Hammad H. The immunology of asthma. *Nat Immunol* 2015;**16**:45–56.
13. Shamji MH, Boyle RJ. Biomarkers in asthma and allergic diseases. *Clin Exp Allergy* 2021;**51**:982–984.
14. Woodruff PG, Modrek B, Choy DF, Jia G, Abbas AR, Ellwanger A et al. T-helper Type 2–driven Inflammation Defines Major Subphenotypes of Asthma. *Am J Respir Crit Care Med*

## Bibliografía

- 2009;**180**:388–395.
15. Gans MD, Gavrilova T. Understanding the immunology of asthma: Pathophysiology, biomarkers, and treatments for asthma endotypes. *Paediatr Respir Rev* 2020;**36**:118–127.
  16. Agache I, Akdis C, Jutel M, Virchow JC. Untangling asthma phenotypes and endotypes. *Allergy* 2012;**67**:835–846.
  17. Campo P, Rodríguez F, Sánchez-García S, Barranco P, Quirce S, Pérez-Francés C et al. Phenotypes and endotypes of uncontrolled severe asthma: new treatments. *J Investig Allergol Clin Immunol* 2013;**23**:76–88; quiz 1 p. follow 88.
  18. Platts-Mills TAE. The allergy epidemics: 1870-2010. *J Allergy Clin Immunol* 2015;**136**:3–13.
  19. Lambrecht BN, Hammad H. The immunology of the allergy epidemic and the hygiene hypothesis. *Nat Immunol* 2017;**18**:1076–1083.
  20. Akdis CA. Does the epithelial barrier hypothesis explain the increase in allergy, autoimmunity and other chronic conditions? *Nat Rev Immunol* 2021;**21**:739–751.
  21. Schett G, Neurath MF. Resolution of chronic inflammatory disease: universal and tissue-specific concepts. *Nat Commun* 2018;**9**:3261.
  22. Agache I. Severe asthma phenotypes and endotypes. *Semin Immunol* 2019;**46**:101301.
  23. Pakkasela J, Ilmarinen P, Honkamäki J, Tuomisto LE, Andersén H, Piirilä P et al. Age-specific incidence of allergic and non-allergic asthma. *BMC Pulm Med* 2020;**20**:9.
  24. Akar-Ghibril N, Casale T, Custovic A, Phipatanakul W. Allergic Endotypes and Phenotypes of Asthma. *J Allergy Clin Immunol Pract* 2020;**8**:429–440.
  25. Baos S, Calzada D, Cremades-Jimeno L, Sastre J, Picado C, Quiralte J et al. Nonallergic Asthma and Its Severity: Biomarkers for Its Discrimination in Peripheral Samples. *Front Immunol* 2018;**9**:1416.
  26. Backman H, Räsänen P, Hedman L, Stridsman C, Andersson M, Lindberg A et al. Increased prevalence of allergic asthma from 1996 to 2006 and further to 2016-results from three population surveys. *Clin Exp Allergy* 2017;**47**:1426–1435.
  27. Kennedy JL, Heymann PW, Platts-Mills TAE. The role of allergy in severe asthma. *Clin Exp Allergy* 2012;**42**:659–669.
  28. Wang J-Y. The Innate Immune Response in House Dust Mite-Induced Allergic Inflammation. *Allergy Asthma Immunol Res* 2013;**5**:68.

## Bibliografía

29. Sánchez-Borges M, Fernandez-Caldas E, Thomas WR, Chapman MD, Lee BW, Caraballo L et al. International consensus (ICON) on: clinical consequences of mite hypersensitivity, a global problem. *World Allergy Organ J* 2017;**10**:14.
30. Miller JD. The Role of Dust Mites in Allergy. *Clin Rev Allergy Immunol* 2019;**57**:312–329.
31. Julià Serdà G, Cabrera Navarro P, Acosta Fernández O, Martín Pérez P, Batista Martín J, Alamo Santana F et al. High Prevalence of Asthma Symptoms in the Canary Islands: Climatic Influence? *J Asthma* 2005;**42**:507–511.
32. Juliá-Serdá G, Cabrera-Navarro P, Acosta-Fernández O, Martín-Pérez P, Losada-Cabrera P, García-Bello MA et al. High prevalence of asthma and atopy in the Canary Islands, Spain. *Int J Tuberc Lung Dis* 2011;**15**:536–541.
33. Juliá-Serdá G, Cabrera-Navarro P, Acosta-Fernández O, Martín-Pérez P, García-Bello MA, Antó-Boqué J. Prevalence of Sensitization to *Blomia tropicalis* among Young Adults in a Temperate Climate. *J Asthma* 2012;**49**:349–354.
34. Barber D, Arias J, Boquete M, Cardona V, Carrillo T, Gala G et al. Analysis of mite allergic patients in a diverse territory by improved diagnostic tools. *Clin Exp Allergy* 2012;**42**:1129–1138.
35. Menzies-Gow AN, McBrien C, Unni B, Porsbjerg CM, Al-Ahmad M, Ambrose CS et al. Real World Biologic Use and Switch Patterns in Severe Asthma: Data from the International Severe Asthma Registry and the US CHRONICLE Study. *J Asthma Allergy* 2022;**2022**:63–78.
36. Pelaia C, Pelaia G, Crimi C, Maglio A, Gallelli L, Terracciano R et al. Tezepelumab: A Potential New Biological Therapy for Severe Refractory Asthma. *Int J Mol Sci* 2021;**22**:4369.
37. Jones TL, Neville DM, Chauhan AJ. Diagnosis and treatment of severe asthma: a phenotype-based approach. *Clin Med (Northfield Il)* 2018;**18**:s36–s40.
38. Bernstein JA, Panettieri R. Treatment of severe, uncontrolled eosinophilic asthma: Where we are heading. *J Asthma* 2019;**56**:459–472.
39. Holgate ST, Polosa R. Treatment strategies for allergy and asthma. *Nat Rev Immunol* 2008;**8**:218–230.
40. Quirce S, Plaza V, Picado C, Vennera M, Casafont J. Prevalence of uncontrolled severe persistent asthma in pneumology and allergy hospital units in Spain. *J Investig Allergol Clin Immunol* 2011;**21**:466–471.
41. Peters SP, Ferguson G, Deniz Y, Reisner C. Uncontrolled asthma: A review of the prevalence,

## Bibliografía

- disease burden and options for treatment. *Respir Med* 2006;**100**:1139–1151.
42. Suárez-Lorenzo I, Cruz-Niesvaara D, Rodríguez-Gallego C, Rodríguez de Castro F, Carrillo-Díaz T. Epidemiological Study of the Allergic Population in the North of Gran Canaria. *J Investig Allergol Clin Immunol* 2018;**28**:212–215.
  43. European Respiratory Society. Chapter 12 - Adult Asthma. In: Gibson GJ, Loddenkemper R, Sibille Y, Lundbäck B, editors. *The European Lung White Book: Respiratory Health and Disease in Europe*. 2013: 138–147.
  44. Bahadori K, Doyle-Waters MM, Marra C, Lynd L, Alasaly K, Swiston J et al. Economic burden of asthma: a systematic review. *BMC Pulm Med* 2009;**9**:24.
  45. Zuberbier T, Lötvald J, Simoens S, Subramanian S V., Church MK. Economic burden of inadequate management of allergic diseases in the European Union: a GA 2 LEN review. *Allergy* 2014;**69**:1275–1279.
  46. Tliba O, Panettieri RA. Paucigranulocytic asthma: Uncoupling of airway obstruction from inflammation. *J Allergy Clin Immunol* 2019;**143**:1287–1294.
  47. Hinks TSC, Levine SJ, Brusselle GG. Treatment options in type-2 low asthma. *Eur Respir J* 2021;**57**:2000528.
  48. Seys SF, Lokwani R, Simpson JL, Bullens DMA. New insights in neutrophilic asthma. *Curr Opin Pulm Med* 2019;**25**:113–120.
  49. Esmaeilzadeh H, Sanaei Dashti A, Mortazavi N, Fatemian H, Vali M. Persistent cough and asthma-like symptoms post COVID-19 hospitalization in children. *BMC Infect Dis* 2022;**22**:1–8.
  50. Boulet LP, Boulay MÈ. Asthma-related comorbidities. *Expert Rev Respir Med* 2011;**5**:377–393.
  51. Bantulà M, Roca-Ferrer J, Arismendi E, Picado C. Asthma and Obesity: Two Diseases on the Rise and Bridged by Inflammation. *J Clin Med* 2021;**10**:169.
  52. Liu Y, Zheng J, Zhang HP, Zhang X, Wang L, Wood L et al. Obesity-Associated Metabolic Signatures Correlate to Clinical and Inflammatory Profiles of Asthma: A Pilot Study. *Allergy Asthma Immunol Res* 2018;**10**:628–647.
  53. Paoletti G, Melone G, Ferri S, Puggioni F, Baiardini I, Racca F et al. Gastroesophageal reflux and asthma: when, how, and why. *Curr Opin Allergy Clin Immunol* 2021;**21**:52–58.
  54. Grandes XA, Talanki Manjunatha R, Habib S, Sangaraju SL, Yopez D. Gastroesophageal Reflux



## Bibliografía

- Disease and Asthma: A Narrative Review. *Cureus* 2022;**14**:e24917.
55. Fokkens WJ, Lund VJ, Hopkins C, Hellings PW, Kern R, Reitsma S et al. European Position Paper on Rhinosinusitis and Nasal Polyps 2020. *Rhinology* 2020;**58**:1–464.
56. Brescia G, Alessandrini L, Giacomelli L, Parrino D, Zanotti C, Tealdo G et al. A classification of chronic rhinosinusitis with nasal polyps based on structured histopathology. *Histopathology* 2020;**76**:296–307.
57. Schleimer RP. Immunopathogenesis of Chronic Rhinosinusitis and Nasal Polyposis. *Annu Rev Pathol Mech Dis* 2017;**12**:331–357.
58. Ferreira Couto LG, Fernades AM, Brandão DF, de Santi Neto D, Pereira Valera FC, Anselmo-Lima WT. Histological Aspects of Rhinosinusal Polyps. *Braz J Otorhinolaryngol* 2008;**74**:207–212.
59. Chen S, Zhou A, Emmanuel B, Thomas K, Guiang H. Systematic literature review of the epidemiology and clinical burden of chronic rhinosinusitis with nasal polyposis. *Curr Med Res Opin* 2020;**36**:1897–1911.
60. Georgy MS, Peters AT. Chapter 7: Nasal polyps. *Allergy Asthma Proc* 2012;**33**:22–23.
61. Lund VJ. Fortnightly Review: Diagnosis and treatment of nasal polyps. *BMJ* 1995;**311**:1411–1414.
62. Wynn R, Har-El G. Recurrence Rates after Endoscopic Sinus Surgery for Massive Sinus Polyposis. *Laryngoscope* 2004;**114**:811–813.
63. Tos M, Larsen PL, Larsen K, Caye-Thomasen P. Pathogenesis and Pathophysiology of Nasal Polyps. In: Önerci TM, Ferguson BJ, editors. *Nasal Polyposis*. Berlin, Heidelberg: Springer Berlin Heidelberg 2010: 53–63.
64. Brescia G, Alessandrini L, Marioni G. Structured histopathology for endotyping and planning rational treatment in chronic rhinosinusitis. *Am J Otolaryngol* 2021;**42**:102795.
65. Brescia G, Zanotti C, Parrino D, Barion U, Marioni G. Nasal polyposis pathophysiology: Endotype and phenotype open issues. *Am J Otolaryngol* 2018;**39**:441–444.
66. Wilson KF, McMains KC, Orlandi RR. The association between allergy and chronic rhinosinusitis with and without nasal polyps: an evidence-based review with recommendations. *Int Forum Allergy Rhinol* 2014;**4**:93–103.
67. Marnett LJ, Rowlinson SW, Goodwin DC, Kalgutkar AS, Lanzo CA. Arachidonic Acid Oxygenation by COX-1 and COX-2. *J Biol Chem* 1999;**274**:22903–22906.

## Bibliografía

68. Kennedy JL, Stoner AN, Borish L. Aspirin-Exacerbated Respiratory Disease: Prevalence, Diagnosis, Treatment, and Considerations for the Future. *Am J Rhinol Allergy* 2016;**30**:407–413.
69. Taniguchi M, Mitsui C, Hayashi H, Ono E, Kajiwara K, Mita H et al. Aspirin-exacerbated respiratory disease (AERD): Current understanding of AERD. *Allergol Int* 2019;**68**:289–295.
70. Wan XC, Woodruff PG. Biomarkers in Severe Asthma. *Immunol Allergy Clin North Am* 2016;**36**:547–557.
71. Kunc P, Fabry J, Lucanska M, Pecova R. Biomarkers of Bronchial Asthma. *Physiol Res* 2020;**69**:S29–S34.
72. Willis JCD, Lord GM. Immune biomarkers: the promises and pitfalls of personalized medicine. *Nat Rev Immunol* 2015;**15**:323–329.
73. Quezada H, Guzmán-Ortiz AL, Díaz-Sánchez H, Valle-Rios R, Aguirre-Hernández J. Omics-based biomarkers: current status and potential use in the clinic. *Boletín Médico Del Hosp Infant México (English Ed)* 2017;**74**:219–226.
74. Galeone C, Scelfo C, Bertolini F, Caminati M, Ruggiero P, Facciolongo N et al. Precision Medicine in Targeted Therapies for Severe Asthma: Is There Any Place for “Omics” Technology? *Biomed Res Int* 2018;**2018**:1–15.
75. Abdel-Aziz MI, Neerincx AH, Vijverberg SJ, Kraneveld AD, Maitland-van der Zee AH. Omics for the future in asthma. *Semin Immunopathol* 2020;**42**:111–126.
76. Hasin Y, Seldin M, Lusis A. Multi-omics approaches to disease. *Genome Biol* 2017;**18**:83.
77. Salzberg SL. Open questions: How many genes do we have? *BMC Biol* 2018;**16**:94.
78. Aebersold R, Agar JN, Amster IJ, Baker MS, Bertozzi CR, Boja ES et al. How many human proteoforms are there? *Nat Chem Biol* 2018;**14**:206–214.
79. Wishart DS, Guo A, Oler E, Wang F, Anjum A, Peters H et al. HMDB 5.0: the Human Metabolome Database for 2022. *Nucleic Acids Res* 2022;**50**:D622–D631.
80. Villaseñor A, Rosace D, Obeso D, Pérez-Gordo M, Chivato T, Barbas C et al. Allergic asthma: an overview of metabolomic strategies leading to the identification of biomarkers in the field. *Clin Exp Allergy* 2017;**47**:442–456.
81. Smith L, Villaret-Cazadamont J, Claus SP, Canlet C, Guillou H, Cabaton NJ et al. Important Considerations for Sample Collection in Metabolomics Studies with a Special Focus on Applications to Liver Functions. *Metabolites* 2020;**10**:104.

## Bibliografía

82. Segers K, Declerck S, Mangelings D, Heyden Y Vander, Eeckhaut A Van. Analytical techniques for metabolomic studies: a review. *Bioanalysis* 2019;**11**:2297–2318.
83. Crestani E, Harb H, Charbonnier L-M, Leirer J, Motsinger-Reif A, Rachid R et al. Untargeted metabolomic profiling identifies disease-specific signatures in food allergy and asthma. *J Allergy Clin Immunol* 2020;**145**:897–906.
84. Cambiaghi A, Ferrario M, Masseroli M. Analysis of metabolomic data: tools, current strategies and future challenges for omics data integration. *Brief Bioinform* 2016;**18**:bbw031.
85. Gil-de-la-Fuente A, Godzien J, Saugar S, Garcia-Carmona R, Badran H, Wishart DS et al. CEU Mass Mediator 3.0: A Metabolite Annotation Tool. *J Proteome Res* 2019;**18**:797–802.
86. Gil de la Fuente A, Godzien J, Fernández López M, Rupérez FJ, Barbas C, Otero A. Knowledge-based metabolite annotation tool: CEU Mass Mediator. *J Pharm Biomed Anal* 2018;**154**:138–149.
87. Shanmuganathan M, Kroezen Z, Gill B, Azab S, de Souza RJ, Teo KK et al. The maternal serum metabolome by multisegment injection-capillary electrophoresis-mass spectrometry: a high-throughput platform and standardized data workflow for large-scale epidemiological studies. *Nat Protoc* 2021;**16**:1966–1994.
88. Rodríguez-Coira J, Delgado-Dolset M, Obeso D, Dolores-Hernández M, Quintás G, Angulo S et al. Troubleshooting in Large-Scale LC-ToF-MS Metabolomics Analysis: Solving Complex Issues in Big Cohorts. *Metabolites* 2019;**9**:247.
89. Gromski P, Xu Y, Kotze H, Correa E, Ellis D, Armitage E et al. Influence of Missing Values Substitutes on Multivariate Analysis of Metabolomics Data. *Metabolites* 2014;**4**:433–452.
90. Kuligowski J, Sánchez-Illana Á, Sanjuán-Herráez D, Vento M, Quintás G. Intra-batch effect correction in liquid chromatography-mass spectrometry using quality control samples and support vector regression (QC-SVRC). *Analyst* 2015;**140**:7810–7817.
91. Sánchez-Illana Á, Piñeiro-Ramos JD, Sanjuan-Herráez JD, Vento M, Quintás G, Kuligowski J. Evaluation of batch effect elimination using quality control replicates in LC-MS metabolite profiling. *Anal Chim Acta* 2018;**1019**:38–48.
92. Triba MN, Le Moyec L, Amathieu R, Goossens C, Bouchemal N, Nahon P et al. PLS/OPLS models in metabolomics: the impact of permutation of dataset rows on the K-fold cross-validation quality parameters. *Mol Biosyst* 2015;**11**:13–19.

## Bibliografía

93. Mamani-Huanca M, de la Fuente AG, Otero A, Gradillas A, Godzien J, Barbas C et al. Enhancing confidence of metabolite annotation in Capillary Electrophoresis-Mass Spectrometry untargeted metabolomics with relative migration time and in-source fragmentation. *J Chromatogr A* 2021;**1635**:461758.
94. García CA, Gil-de-la-Fuente A, Barbas C, Otero A. Probabilistic metabolite annotation using retention time prediction and meta-learned projections. *J Cheminform* 2022;**14**:33.
95. Gonzalez-Riano C, Gradillas A, Barbas C. Exploiting the formation of adducts in mobile phases with ammonium fluoride for the enhancement of annotation in liquid chromatography-high resolution mass spectrometry based lipidomics. *J Chromatogr Open* 2021;**1**:100018.
96. Demarque DP, Crotti AEM, Vessecchi R, Lopes JLC, Lopes NP. Fragmentation reactions using electrospray ionization mass spectrometry: an important tool for the structural elucidation and characterization of synthetic and natural products. *Nat Prod Rep* 2016;**33**:432–455.
97. Tsugawa H, Ikeda K, Takahashi M, Satoh A, Mori Y, Uchino H et al. MS-DIAL 4: accelerating lipidomics using an MS/MS, CCS, and retention time atlas. *bioRxiv* 2020;:2020.02.11.944900.
98. Mitamura Y, Schulz D, Oro S, Li N, Kolm I, Lang C et al. Cutaneous and systemic hyperinflammation drives maculopapular drug exanthema in severely ill COVID-19 patients. *Allergy* 2022;**77**:595–608.
99. Calinski T, Harabasz J. A dendrite method for cluster analysis. *Commun Stat - Theory Methods* 1974;**3**:1–27.
100. Kodinariya T, Makwana PR. Review on determining number of Cluster in K-Means Clustering. *Int J Adv Res Comput Sci Manag Stud* 2013;**1**:90–95.
101. Akshay S, Megha YJ, Shetty CB. Machine Learning Algorithm to Identify Eye Movement Metrics using Raw Eye Tracking Data. In: *2020 Third International Conference on Smart Systems and Inventive Technology (ICSSIT)*. IEEE 2020: 949–955.
102. European Academy of Allergy and Clinical Immunology. *Global Atlas of Asthma*. 2nd ed. European Academy of Allergy and Clinical Immunology 2021www.eaaci.org
103. Yaghoubi M, Adibi A, Safari A, FitzGerald JM, Sadatsafavi M. The Projected Economic and Health Burden of Uncontrolled Asthma in the United States. *Am J Respir Crit Care Med* 2019;**200**:1102–1112.
104. Liu MC, Chipps B, Munoz X, Devouassoux G, Bergna M, Smith SG et al. Benefit of switching

## Bibliografía

- to mepolizumab from omalizumab in severe eosinophilic asthma based on patient characteristics. *Respir Res* 2021;**22**:144.
105. Chapman KR, Albers FC, Chipps B, Muñoz X, Devouassoux G, Bergna M et al. The clinical benefit of mepolizumab replacing omalizumab in uncontrolled severe eosinophilic asthma. *Allergy* 2019;**74**:1716–1726.
  106. Bateman ED, Khan AH, Xu Y, Guyot P, Chao J, Kamat S et al. Pairwise indirect treatment comparison of dupilumab versus other biologics in patients with uncontrolled persistent asthma. *Respir Med* 2022;**191**:105991.
  107. Rupani H, Murphy A, Bluer K, Renwick C, McQuitty P, Jackson DJ et al. Biologics in severe asthma: Which one, When and Where? *Clin Exp Allergy* 2021;**51**:1225–1228.
  108. Edwards MR, Saglani S, Schwarze J, Skevaki C, Smith JA, Ainsworth B et al. Addressing unmet needs in understanding asthma mechanisms. *Eur Respir J* 2017;**49**:1602448.
  109. Menéndez I, Derbyshire E, Carrillo T, Caballero E, Engelbrecht JP, Romero LE et al. Saharan dust and the impact on adult and elderly allergic patients: the effect of threshold values in the northern sector of Gran Canaria, Spain. *Int J Environ Health Res* 2017;**27**:144–160.
  110. Katel P, Pinkaew B, Talek K, Tantilipikorn P. Pattern of Aeroallergen Sensitization and Quality of Life in Adult Thai Patients With Allergic Rhinitis. *Front Allergy* 2021;**2**. doi:10.3389/falgy.2021.695055
  111. Liu P, Zhu W, Chen C, Yan B, Zhu L, Chen X et al. The mechanisms of lysophosphatidylcholine in the development of diseases. *Life Sci* 2020;**247**:117443.
  112. Yoder M, Zhuge Y, Yuan Y, Holian O, Kuo S, van Breemen R et al. Bioactive Lysophosphatidylcholine 16:0 and 18:0 Are Elevated in Lungs of Asthmatic Subjects. *Allergy Asthma Immunol Res* 2014;**6**:61–65.
  113. Balgoma D, Astudillo AM, Perez-Chacon G, Montero O, Balboa MA, Balsinde J. Markers of Monocyte Activation Revealed by Lipidomic Profiling of Arachidonic Acid-Containing Phospholipids. *J Immunol* 2010;**184**:3857–3865.
  114. Arita M. Eosinophil polyunsaturated fatty acid metabolism and its potential control of inflammation and allergy. *Allergol Int* 2016;**65**:S2–S5.
  115. Bennett M, Gilroy DW. Lipid Mediators in Inflammation. *Microbiol Spectr* 2016;**4**:MCHD-0035-2016.
  116. Sokolowska M, Rovati GE, Diamant Z, Untersmayr E, Schwarze J, Lukasik Z et al. Current

## Bibliografía

- perspective on eicosanoids in asthma and allergic diseases: EAACI Task Force consensus report, part I. *Allergy* 2021;**76**:114–130.
117. Peebles RS, Boyce JA. Lipid Mediators of Hypersensitivity and Inflammation. In: *Middleton's Allergy*. Elsevier 2014: 139–161.
118. Izquierdo E, Rodriguez-Coira J, Delgado-Dolset M, Gomez-Casado C, Barber D, Escribese M. Epithelial Barrier: Protector and Trigger of Allergic Disorders. *J Investig Allergy Clin Immunol* 2022;**32**:81–96.
119. Pang Z, Wang G, Wang C, Zhang W, Liu J, Wang F. Serum Metabolomics Analysis of Asthma in Different Inflammatory Phenotypes: A Cross-Sectional Study in Northeast China. *Biomed Res Int* 2018;**2018**:1–14.
120. McGeachie MJ, Dahlin A, Qiu W, Croteau-Chonka DC, Savage J, Wu AC et al. The metabolomics of asthma control: a promising link between genetics and disease. *Immunity, Inflamm Dis* 2015;**3**:224–238.
121. Sokolowska M, Chen L-Y, Liu Y, Martinez-Anton A, Logun C, Alsaaty S et al. Dysregulation of lipidomic profile and antiviral immunity in response to hyaluronan in patients with severe asthma. *J Allergy Clin Immunol* 2017;**139**:1379–1383.
122. Nie X, Wei J, Hao Y, Tao J, Li Y, Liu M et al. Consistent Biomarkers and Related Pathogenesis Underlying Asthma Revealed by Systems Biology Approach. *Int J Mol Sci* 2019;**20**:4037.
123. Miyata J, Arita M. Role of omega-3 fatty acids and their metabolites in asthma and allergic diseases. *Allergol Int* 2015;**64**:27–34.
124. Knuplez E, Curcic S, Theiler A, Bärnthaler T, Trakaki A, Trieb M et al. Lysophosphatidylcholines inhibit human eosinophil activation and suppress eosinophil migration in vivo. *Biochim Biophys Acta - Mol Cell Biol Lipids* 2020;**1865**:158686.
125. Zhu X, Learoyd J, Butt S, Zhu L, Usatyuk P V., Natarajan V et al. Regulation of Eosinophil Adhesion by Lysophosphatidylcholine via a Non–Store–Operated Ca<sup>2+</sup> Channel. *Am J Respir Cell Mol Biol* 2007;**36**:585–593.
126. Ortega HG, Yancey SW, Mayer B, Gunsoy NB, Keene ON, Bleecker ER et al. Severe eosinophilic asthma treated with mepolizumab stratified by baseline eosinophil thresholds: a secondary analysis of the DREAM and MENSA studies. *Lancet Respir Med* 2016;**4**:549–556.
127. Ackerman SJ, Park GY, Christman JW, Nyenhuis S, Berdyshev E, Natarajan V. Polyunsaturated lysophosphatidic acid as a potential asthma biomarker. *Biomark Med* 2016;**10**:123–135.

## Bibliografía

128. Mendelson K, Evans T, Hla T. Sphingosine 1-phosphate signalling. *Development* 2014;**141**:5–9.
129. Chang C-H, Randolph GJ. Sphingosine-1-Phosphate as the Lymphocyte's Ticket to Ride and Survive. *Dev Cell* 2017;**41**:576–578.
130. Mendoza A, Fang V, Chen C, Serasinghe M, Verma A, Muller J et al. Lymphatic endothelial S1P promotes mitochondrial function and survival in naive T cells. *Nature* 2017;**546**:158–161.
131. Olivera A. Unraveling the complexities of sphingosine-1-phosphate function: The mast cell model. *Prostaglandins Other Lipid Mediat* 2008;**86**:1–11.
132. Kulinski JM, Muñoz-Cano R, Olivera A. Sphingosine-1-phosphate and other lipid mediators generated by mast cells as critical players in allergy and mast cell function. *Eur J Pharmacol* 2016;**778**:56–67.
133. Saluja R, Kumar A, Jain M, Goel SK, Jain A. Role of Sphingosine-1-Phosphate in Mast Cell Functions and Asthma and Its Regulation by Non-Coding RNA. *Front Immunol* 2017;**8**:587.
134. Levy BD. Sphingolipids and Susceptibility to Asthma. *N Engl J Med* 2013;**369**:976–978.
135. James B, Milstien S, Spiegel S. ORMDL3 and allergic asthma: From physiology to pathology. *J Allergy Clin Immunol* 2019;**144**:634–640.
136. Chiurchiù V, Leuti A, Maccarrone M. Bioactive Lipids and Chronic Inflammation: Managing the Fire Within. *Front Immunol* 2018;**9**:38.
137. Petrache I, Berdyshev E V. Ceramide Signaling and Metabolism in Pathophysiological States of the Lung. *Annu Rev Physiol* 2016;**78**:463–480.
138. Reinke SN, Gallart-Ayala H, Gómez C, Checa A, Fauland A, Naz S et al. Metabolomics analysis identifies different metabotypes of asthma severity. *Eur Respir J* 2017;**49**:1601740.
139. Comhair SAA, McDunn J, Bennett C, Fettig J, Erzurum SC, Kalhan SC. Metabolomic Endotype of Asthma. *J Immunol* 2015;**195**:643–650.
140. Obeso D, Mera-Berriatua L, Rodríguez-Coira J, Rosace D, Fernández P, Martín-Antoniano IA et al. Multi-omics analysis points to altered platelet functions in severe food-associated respiratory allergy. *Allergy* 2018;**73**:2137–2149.
141. Kim S, Jung H, Kim M, Moon J, Ban G, Kim SJ et al. Ceramide/sphingosine-1-phosphate imbalance is associated with distinct inflammatory phenotypes of uncontrolled asthma. *Allergy* 2020;**75**:1991–2004.

## Bibliografía

142. Peyrin-Biroulet L, Christopher R, Behan D, Lassen C. Modulation of sphingosine-1-phosphate in inflammatory bowel disease. *Autoimmun Rev* 2017;**16**:495–503.
143. Ananieva EA, Powell JD, Hutson SM. Leucine Metabolism in T Cell Activation: mTOR Signaling and Beyond. *Adv Nutr An Int Rev J* 2016;**7**:798S-805S.
144. Peng Y-F, Goyal H, Xu G-D. Serum bilirubin has an important role in multiple clinical applications. *J Lab Precis Med* 2017;**2**:82–82.
145. Vogel ME, Zucker SD. Bilirubin acts as an endogenous regulator of inflammation by disrupting adhesion molecule-mediated leukocyte migration. *Inflamm Cell Signal* 2016;**3**:e1178.
146. Chen ML, Takeda K, Sundrud MS. Emerging roles of bile acids in mucosal immunity and inflammation. *Mucosal Immunol* 2019;**12**:851–861.
147. Garcia-Zepeda EA, Combadiere C, Rothenberg ME, Sarafi MN, Lavigne F, Hamid Q et al. Human monocyte chemoattractant protein (MCP)-4 is a novel CC chemokine with activities on monocytes, eosinophils, and basophils induced in allergic and nonallergic inflammation that signals through the CC chemokine receptors (CCR)-2 and -3. *J Immunol* 1996;**157**:5613–5626.
148. Li CW, Zhang KK, Li TY, Lin ZB, Li YY, Curotto de Lafaille MA et al. Expression profiles of regulatory and helper T-cell-associated genes in nasal polyposis. *Allergy* 2012;**67**:732–740.
149. Morris SR, Chen B, Mudd JC, Panigrahi S, Shive CL, Sieg SF et al. ‘Inflammascent’ CX3CR1+CD57+ CD8 T cells are generated and expanded by IL-15. *JCI Insight* 2020;**5**:e132963.
150. He H, Suryawanshi H, Morozov P, Gay-Mimbrera J, Del Duca E, Kim HJ et al. Single-cell transcriptome analysis of human skin identifies novel fibroblast subpopulation and enrichment of immune subsets in atopic dermatitis. *J Allergy Clin Immunol* 2020;**145**:1615–1628.
151. Kaiser A, Donnadieu E, Abastado J-P, Trautmann A, Nardin A. CC Chemokine Ligand 19 Secreted by Mature Dendritic Cells Increases Naive T Cell Scanning Behavior and Their Response to Rare Cognate Antigen. *J Immunol* 2005;**175**:2349–2356.
152. Takamura K, Fukuyama S, Nagatake T, Kim D-Y, Kawamura A, Kawauchi H et al. Regulatory Role of Lymphoid Chemokine CCL19 and CCL21 in the Control of Allergic Rhinitis. *J Immunol* 2007;**179**:5897–5906.



## Bibliografía

153. Tseng W-Y, Huang Y-S, Chiang N-Y, Chou Y-P, Wu Y-JJ, Luo S-F et al. Increased Soluble CD4 in Serum of Rheumatoid Arthritis Patients Is Generated by Matrix Metalloproteinase (MMP)-Like Proteinases. *PLoS One* 2013;**8**:e63963.
154. Mendez-Barbero N, Yuste-Montalvo A, Nuñez-Borque E, Jensen BM, Gutiérrez-Muñoz C, Tome-Amat J et al. The TNF-like weak inducer of the apoptosis/fibroblast growth factor–inducible molecule 14 axis mediates histamine and platelet-activating factor–induced subcutaneous vascular leakage and anaphylactic shock. *J Allergy Clin Immunol* 2020;**145**:583-596.e6.
155. Suwanpradid J, Shih M, Pontius L, Yang B, Birukova A, Guttman-Yassky E et al. Arginase1 Deficiency in Monocytes/Macrophages Upregulates Inducible Nitric Oxide Synthase To Promote Cutaneous Contact Hypersensitivity. *J Immunol* 2017;**199**:1827–1834.
156. Chapman DG, Irvin CG. Mechanisms of airway hyper-responsiveness in asthma: the past, present and yet to come. *Clin Exp Allergy* 2015;**45**:706–719.
157. Prado CM, Martins MA, Tibério IFLC. Nitric Oxide in Asthma Physiopathology. *ISRN Allergy* 2011;**2011**:1–13.
158. Moncada S, Higgs A. The L-Arginine-Nitric Oxide Pathway. *N Engl J Med* 1993;**329**:2002–2012.
159. O’Neill LAJ, Kishton RJ, Rathmell J. A guide to immunometabolism for immunologists. *Nat Rev Immunol* 2016;**16**:553–565.
160. Farraia M, Cavaleiro Rufo J, Paciência I, Castro Mendes F, Delgado L, Laerte Boechat J et al. Metabolic interactions in asthma. *Eur Ann Allergy Clin Immunol* 2019;**51**:196–205.
161. Jung J, Kim S-H, Lee H-S, Choi GS, Jung Y-S, Ryu DH et al. Serum metabolomics reveals pathways and biomarkers associated with asthma pathogenesis. *Clin Exp Allergy* 2013;**43**:425–433.
162. Kertys M, Grendar M, Kosutova P, Mokra D, Mokry J. Plasma based targeted metabolomic analysis reveals alterations of phosphatidylcholines and oxidative stress markers in guinea pig model of allergic asthma. *Biochim Biophys Acta - Mol Basis Dis* 2020;**1866**:165572.
163. Son A, Oshio T, Kawamura YI, Hagiwara T, Yamazaki M, Inagaki-Ohara K et al. TWEAK/Fn14 pathway promotes a T helper 2-type chronic colitis with fibrosis in mice. *Mucosal Immunol* 2013;**6**:1131–1142.
164. Bell BD, Leverrier S, Weist BM, Newton RH, Arechiga AF, Luhrs KA et al. FADD and caspase-

## Bibliografía

- 8 control the outcome of autophagic signaling in proliferating T cells. *Proc Natl Acad Sci* 2008;**105**:16677–16682.
165. Jung ES, Park HM, Hyun SM, Shon JC, Lakshmanan M, Noh M et al. Integrative metabolomic analysis reveals diet supplementation with green tea alleviates UVB-damaged mouse skin correlated with ascorbate metabolism and urea cycle. *Metabolomics* 2017;**13**:82.
166. Ried JS, Baurecht H, Stücker F, Krumsiek J, Gieger C, Heinrich J et al. Integrative genetic and metabolite profiling analysis suggests altered phosphatidylcholine metabolism in asthma. *Allergy* 2013;**68**:629–636.
167. Pecak M, Korošec P, Kunej T. Multiomics Data Triangulation for Asthma Candidate Biomarkers and Precision Medicine. *Omi A J Integr Biol* 2018;**22**:392–409.
168. Reel PS, Reel S, Pearson E, Trucco E, Jefferson E. Using machine learning approaches for multi-omics data analysis: A review. *Biotechnol Adv* 2021;**49**:107739.
169. Venables WN, Ripley BD. *Modern Applied Statistics with S-Plus*. New York: Springer 2013
170. Trejo Bittar HE, Yousem SA, Wenzel SE. Pathobiology of Severe Asthma. *Annu Rev Pathol Mech Dis* 2015;**10**:511–545.
171. Gai XY, Zhang LJ, Chang C, Guo CL, Abulikemu M, Li WX et al. Metabolomic Analysis of Serum Glycerophospholipid Levels in Eosinophilic and Neutrophilic Asthma. *Biomed Environ Sci* 2019;**32**:96–106.
172. Bansal P, Gaur SN, Arora N. Lysophosphatidylcholine plays critical role in allergic airway disease manifestation. *Sci Rep* 2016;**6**:27430.
173. Curcic S, Holzer M, Pasterk L, Knuplez E, Eichmann TO, Frank S et al. Secretory phospholipase A2 modified HDL rapidly and potently suppresses platelet activation. *Sci Rep* 2017;**7**:8030.
174. Yue M, Hu M, Fu F, Ruan H, Wu C. Emerging Roles of Platelets in Allergic Asthma. *Front Immunol* 2022;**13**:846055.
175. Gomez-Casado C, Villaseñor A, Rodriguez-Nogales A, Bueno J, Barber D, Escribese M. Understanding Platelets in Infectious and Allergic Lung Diseases. *Int J Mol Sci* 2019;**20**:1730.
176. Lefrançois E, Ortiz-Muñoz G, Caudrillier A, Mallavia B, Liu F, Sayah DM et al. The lung is a site of platelet biogenesis and a reservoir for haematopoietic progenitors. *Nature* 2017;**544**:105–109.
177. Liang Y, Gai XY, Chang C, Zhang X, Wang J, Li TT. Metabolomic Profiling Differences among Asthma, COPD, and Healthy Subjects: A LC-MS-based Metabolomic Analysis. *Biomed Environ*

## Bibliografía

- Sci* 2019;**32**:659–672.
178. Singh D. Chronic Obstructive Pulmonary Disease, Neutrophils and Bacterial Infection: A Complex Web Involving IL-17 and IL-22 Unravels. *EBioMedicine* 2015;**2**:1580–1581.
  179. Gai X, Guo C, Zhang L, Zhang L, Abulikemu M, Wang J et al. Serum Glycerophospholipid Profile in Acute Exacerbation of Chronic Obstructive Pulmonary Disease. *Front Physiol* 2021;**12**:1–8.
  180. Song MH, Gupta A, Kim HO, Oh K. Lysophosphatidylcholine aggravates contact hypersensitivity by promoting neutrophil infiltration and IL17 expression. *BMB Rep* 2021;**54**:203–208.
  181. Haghghatdoost F, Jabbari M, Hariri M. The effect of L-carnitine on inflammatory mediators: a systematic review and meta-analysis of randomized clinical trials. *Eur J Clin Pharmacol* 2019;**75**:1037–1046.
  182. Zheng P, Bian X, Zhai Y, Li C, Li N, Hao C et al. Metabolomics reveals a correlation between hydroxyeicosatetraenoic acids and allergic asthma: Evidence from three years' immunotherapy. *Pediatr Allergy Immunol* 2021;**32**:1654–1662.
  183. Kachroo P, Stewart ID, Kelly RS, Stav M, Mendez K, Dahlin A et al. Metabolomic profiling reveals extensive adrenal suppression due to inhaled corticosteroid therapy in asthma. *Nat Med* 2022;**28**:814–822.
  184. Chung SJ, Lee CH, Lee HS, Kim ST, Sohn UD, Park ES et al. The role of phosphatidylcholine and deoxycholic acid in inflammation. *Life Sci* 2014;**108**:88–93.
  185. Zhao S, Gong Z, Zhou J, Tian C, Gao Y, Xu C et al. Deoxycholic Acid Triggers NLRP3 Inflammasome Activation and Aggravates DSS-Induced Colitis in Mice. *Front Immunol* 2016;**7**:00536.
  186. Xu M, Cen M, Shen Y, Zhu Y, Cheng F, Tang L et al. Deoxycholic Acid-Induced Gut Dysbiosis Disrupts Bile Acid Enterohepatic Circulation and Promotes Intestinal Inflammation. *Dig Dis Sci* 2021;**66**:568–576.
  187. Quiralte J, Blanco C, Castillo R, Ortega N, Carrillo T. Anaphylactoid Reactions due to Nonsteroidal Antiinflammatory Drugs: Clinical and Cross-Reactivity Studies. *Ann Allergy, Asthma Immunol* 1997;**78**:293–296.
  188. Xie S, Zhang H, Liu Y, Gao K, Zhang J, Fan R et al. The Role of Serum Metabolomics in Distinguishing Chronic Rhinosinusitis With Nasal Polyp Phenotypes. *Front Mol Biosci*

## Bibliografía

- 2021;**7**:593976.
189. Grill M, Högenauer C, Blesl A, Haybaeck J, Golob-Schwarzl N, Ferreirós N et al. Members of the endocannabinoid system are distinctly regulated in inflammatory bowel disease and colorectal cancer. *Sci Rep* 2019;**9**:2358.
  190. Lu Y, Wang Y, Ong C-N, Subramaniam T, Choi HW, Yuan J-M et al. Metabolic signatures and risk of type 2 diabetes in a Chinese population: an untargeted metabolomics study using both LC-MS and GC-MS. *Diabetologia* 2016;**59**:2349–2359.
  191. Yeager MP, Guyre CA, Sites BD, Collins JE, Pioli PA, Guyre PM. The Stress Hormone Cortisol Enhances Interferon- $\gamma$ -Mediated Proinflammatory Responses of Human Immune Cells. *Anesth Analg* 2018;**127**:556–563.
  192. Fidan V, Alp HH, Kalkandelen S, Cingi C. Melatonin and cortisol rhythm in patients with extensive nasal polyposis. *Am J Otolaryngol* 2013;**34**:61–64.
  193. Kook JH, Kim HJ, Kim KW, Park SJ, Kim TH, Lim SH et al. The Expression of 11 $\beta$ -Hydroxysteroid Dehydrogenase Type 1 and 2 in Nasal Polyp-Derived Epithelial Cells and its Possible Contribution to Glucocorticoid Activation in Nasal Polyp. *Am J Rhinol Allergy* 2015;**29**:246–250.
  194. Saoi M, Britz-McKibbin P. New Advances in Tissue Metabolomics: A Review. *Metabolites* 2021;**11**:672.
  195. Ma Y, Wei Y, Liu X, Dang H, Zou H, Tian P et al. Metabolomics analysis of metabolic patterns in chronic rhinosinusitis with nasal polyps. *Allergy* 2022;**77**:653–656.
  196. Li J-X, Wang Z-Z, Zhai G-T, Chen C-L, Zhu K-Z, Yu Z et al. Untargeted metabolomic profiling identifies disease-specific and outcome-related signatures in chronic rhinosinusitis. *J Allergy Clin Immunol* 2022;**150**:727-735.e6.
  197. Rosenberg HF, Dyer KD, Foster PS. Eosinophils: changing perspectives in health and disease. *Nat Rev Immunol* 2013;**13**:9–22.
  198. Kariyawasam HH, Robinson DS. The role of eosinophils in airway tissue remodelling in asthma. *Curr Opin Immunol* 2007;**19**:681–686.
  199. Sun C, Ouyang H, Luo R. Distinct characteristics of nasal polyps with and without eosinophilia. *Braz J Otorhinolaryngol* 2017;**83**:66–72.
  200. Erbek SS, Erbek S, Topal O, Cakmak O. The Role of Allergy in the Severity of Nasal Polyposis. *Am J Rhinol* 2007;**21**:686–690.

## Bibliografía

201. Van Zele T, Holtappels G, Gevaert P, Bachert C. Differences in Initial Immunoprofiles between Recurrent and Nonrecurrent Chronic Rhinosinusitis with Nasal Polyps. *Am J Rhinol Allergy* 2014;**28**:192–198.
202. Bachert C, Sousa AR, Lund VJ, Scadding GK, Gevaert P, Nasser S et al. Reduced need for surgery in severe nasal polyposis with mepolizumab: Randomized trial. *J Allergy Clin Immunol* 2017;**140**:1024-1031.e14.
203. Bochner BS, Stevens WW. Biology and function of eosinophils in chronic rhinosinusitis with or without nasal polyps. *Allergy, Asthma Immunol Res* 2021;**13**:8–22.
204. Miyata J, Fukunaga K, Kawashima Y, Watanabe T, Saitoh A, Hirosaki T et al. Dysregulated fatty acid metabolism in nasal polyp-derived eosinophils from patients with chronic rhinosinusitis. *Allergy* 2019;**74**:1113–1124.
205. Pothoven KL, Norton JE, Suh LA, Carter RG, Harris KE, Biyasheva A et al. Neutrophils are a major source of the epithelial barrier disrupting cytokine oncostatin M in patients with mucosal airways disease. *J Allergy Clin Immunol* 2017;**139**:1966-1978.e9.
206. Kong IG, Kim DW. Pathogenesis of Recalcitrant Chronic Rhinosinusitis: The Emerging Role of Innate Immune Cells. *Immune Netw* 2018;**18**:1–12.
207. Brescia G, Barion U, Zanotti C, Giacomelli L, Martini A, Marioni G. The prognostic role of serum eosinophil and basophil levels in sinonasal polyposis. *Int Forum Allergy Rhinol* 2017;**7**:261–267.
208. Kim DW, Cho SH. Emerging Endotypes of Chronic Rhinosinusitis and Its Application to Precision Medicine. *Allergy Asthma Immunol Res* 2017;**9**:299.
209. Bachert C, Zhang N, Hellings PW, Bousquet J. Endotype-driven care pathways in patients with chronic rhinosinusitis. *J Allergy Clin Immunol* 2018;**141**:1543–1551.
210. Perales-Chorda C, Obeso D, Twomey L, Rojas-Benedicto A, Puchades-Carrasco L, Roca M et al. Characterization of anaphylaxis reveals different metabolic changes depending on severity and triggers. *Clin Exp Allergy* 2021;**51**:1295–1309.
211. Barker-Tejeda TC, Bazire R, Obeso D, Mera-Berriatua L, Rosace D, Vazquez-Cortes S et al. Exploring novel systemic biomarker approaches in grass-pollen sublingual immunotherapy using omics. *Allergy* 2021;**76**:1199–1212.
212. Obeso D, Contreras N, Dolores-Hernández M, Carrillo T, Barbas C, Escribese MM et al. Development of a Novel Targeted Metabolomic LC-QqQ-MS Method in Allergic

## Bibliografía

Inflammation. *Metabolites* 2022;**12**:592.

# ANEXOS





## I. Publicaciones científicas derivadas de esta tesis doctoral

- **Delgado-Dolset, M. I.**, Obeso, D., Rodríguez-Coira, J., Villaseñor, A., González-Cuervo, H., Arjona, A., Barbas, C., Barber, D., Carrillo, T., Villaseñor, & Escribese, M. M. (2022). *Contribution of allergy in the acquisition of uncontrolled severe asthma*. *Frontiers in Medicine*, 9, 1009324. <https://doi.org/10.3389/fmed.2022.1009324>
- **Delgado-Dolset, M. I.**, Obeso, D., Rodríguez-Coira, J., Tarin, C., Tan, G., Cumplido, J. A., Cabrera, A., Angulo, S., Barbas, C., Sokolowska, M., Barber, D., Carrillo, T., Villaseñor, A., & Escribese, M. M. (2022). *Understanding uncontrolled severe allergic asthma by integration of omic and clinical data*. *Allergy*, 77(6), 1772–1785. <https://doi.org/10.1111/all.15192>
- **Delgado-Dolset, M. I.**, Obeso, D., Sánchez-Solares, J., Mera-Berriatua, L., Fernández, P., Barbas, C., Fresnillo, M., Chivato, T., Barber, D., Escribese, M. M., & Villaseñor, A. (2021). *Understanding Systemic and Local Inflammation Induced by Nasal Polyposis: Role of the Allergic Phenotype*. *Frontiers in Molecular Biosciences*, 8, 662792. <https://doi.org/10.3389/fmolb.2021.662792>
- Rodríguez-Coira, J., **Delgado-Dolset, M. I.**, Obeso, D., Dolores-Hernández, M., Quintás, G., Angulo, S., Barber, D., Carrillo, T., Escribese, M. M., & Villaseñor, A. (2019). *Troubleshooting in Large-Scale LC-ToF-MS Metabolomics Analysis: Solving Complex Issues in Big Cohorts*. *Metabolites*, 9(11), 247. <https://doi.org/10.3390/metabo9110247>





## OPEN ACCESS

## EDITED BY

Girolamo Pelaia,  
Magna Græcia University, Italy

## REVIEWED BY

Victor Matheu,  
Canary Islands University  
Hospital, Spain  
Francesco Perna,  
Federico II University Hospital, Italy

## \*CORRESPONDENCE

María M. Escribese  
mariamarta.escribesealonso@ceu.es

## SPECIALTY SECTION

This article was submitted to  
Pulmonary Medicine,  
a section of the journal  
Frontiers in Medicine

RECEIVED 01 August 2022

ACCEPTED 22 August 2022

PUBLISHED 21 September 2022

## CITATION

Delgado Dolset MI, Obeso D,  
Rodriguez-Coira J, Villaseñor A,  
González Cuervo H, Arjona A,  
Barbas C, Barber D, Carrillo T and  
Escribese MM (2022) Contribution of  
allergy in the acquisition of  
uncontrolled severe asthma.  
*Front. Med.* 9:1009324.  
doi: 10.3389/fmed.2022.1009324

## COPYRIGHT

© 2022 Delgado Dolset, Obeso,  
Rodriguez-Coira, Villaseñor, González  
Cuervo, Arjona, Barbas, Barber, Carrillo  
and Escribese. This is an open-access  
article distributed under the terms of  
the [Creative Commons Attribution  
License \(CC BY\)](https://creativecommons.org/licenses/by/4.0/). The use, distribution  
or reproduction in other forums is  
permitted, provided the original  
author(s) and the copyright owner(s)  
are credited and that the original  
publication in this journal is cited, in  
accordance with accepted academic  
practice. No use, distribution or  
reproduction is permitted which does  
not comply with these terms.

# Contribution of allergy in the acquisition of uncontrolled severe asthma

María Isabel Delgado Dolset<sup>1</sup>, David Obeso<sup>1,2</sup>,  
Juan Rodriguez-Coira<sup>1,2</sup>, Alma Villaseñor<sup>1,2</sup>,  
Heleia González Cuervo<sup>3</sup>, Ana Arjona<sup>3</sup>, Coral Barbas<sup>2</sup>,  
Domingo Barber<sup>1</sup>, Teresa Carrillo<sup>3,4</sup> and María M. Escribese<sup>1,5\*</sup>

<sup>1</sup>Institute for Applied Molecular Medicine Nemesio Díez, School of Medicine, Universidad San Pablo-CEU, CEU Universities, Urbanización Montepríncipe, Boadilla del Monte, Spain, <sup>2</sup>Centre of Metabolomics and Bioanalysis (CEMBO), School of Pharmacy, Universidad San Pablo-CEU, CEU Universities, Urbanización Montepríncipe, Boadilla del Monte, Spain, <sup>3</sup>Allergy Service, Hospital Universitario de Gran Canaria Doctor Negrin, Las Palmas de Gran Canaria, Spain, <sup>4</sup>Department of Medical and Surgical Sciences, School of Health Sciences, Universidad de Las Palmas de Gran Canaria, Las Palmas de Gran Canaria, Spain, <sup>5</sup>Department of Basic Medical Sciences, School of Medicine, Universidad San Pablo-CEU, CEU Universities, Urbanización Montepríncipe, Boadilla del Monte, Spain

Asthma is a multifactorial, heterogeneous disease that has a challenging management. It can be divided in non-allergic and allergic (usually associated with house dust mites (HDM) sensitization). There are several treatments options for asthma (corticosteroids, bronchodilators, antileukotrienes, anticholinergics,...); however, there is a subset of patients that do not respond to any of the treatments, who can display either a T2 or a non-T2 phenotype. A deeper understanding of the differential mechanisms underlying each phenotype will help to decipher the contribution of allergy to the acquisition of this uncontrolled severe phenotype. Here, we aim to elucidate the biological pathways associated to allergy in the uncontrolled severe asthmatic phenotype. To do so, twenty-three severe uncontrolled asthmatic patients both with and without HDM-allergy were recruited from Hospital Universitario de Gran Canaria Dr. Negrin. A metabolomic fingerprint was obtained through liquid chromatography coupled to mass spectrometry, and identified metabolites were associated with their pathways. 9/23 patients had uncontrolled HDM-allergic asthma (UCA), whereas 14 had uncontrolled, non-allergic asthma (UCNA). 7/14 (50%) of the UCNA patients had Aspirin Exacerbated Respiratory Disease. There were no significant differences regarding gender or body mass index; but there were significant differences in age and onset age, which were higher in UCNA patients; and in total IgE, which was higher in UCA. The metabolic fingerprint revealed that 103 features were significantly different between UCNA and UCA ( $p < 0.05$ ), with 97 being increased in UCA and 6 being decreased. We identified lysophosphocholines (LPC) 18:2, 18:3 and 20:4 (increased in UCA patients); and deoxycholic acid and palmitoleoylcarnitine (decreased in UCA). These metabolites were related with a higher activation of phospholipase A2 (PLA2) and other phospholipid metabolism pathways. Our results show that allergy induces the activation of specific inflammatory pathways, such as the PLA2 pathway, which supports its role in the development of an uncontrolled

asthma phenotype. There are also clinical differences, such as higher levels of IgE and earlier onset ages for the allergic asthmatic group, as expected. These results provide evidences to better understand the contribution of allergy to the establishment of a severe uncontrolled phenotype.

#### KEYWORDS

asthma, metabolomics, allergy, lysophospholipids, bile acids (BAs), HDM-allergy

## Introduction

Asthma is a heterogenous, multifactorial respiratory disease that is characterized by wheezing, shortness of breath, chest tightness and coughing (1). It affects around 1–18% of the population worldwide, significantly reducing their quality of life (2).

Asthma management is a challenge due to its complexity. In fact, there are multiple phenotypes, which are defined according to the clinical manifestation of the disease, as well as endotypes defined according to the underlying mechanisms. Thus, efforts to define homogenous phenotypes of asthma based on their underlying characteristics, have been pushed in the last years (3–5).

Allergic asthma has been deeply studied over the years. Around 80% of childhood-onset asthma and more than 50% of asthmatic adult patients suffer from allergic asthma (6). It has an early onset, usually in childhood, that commonly persists throughout life (3, 7), and is characterized by a type 2 inflammatory profile, dominated by IL-4, IL-5, IL-9 and IL-13, Th2 cells, eosinophils, and IgE producing plasma cells (8). On the other hand, non-allergic or intrinsic asthma is poorly understood (9). It usually appears in adulthood, normally around 30–40 years old (10). Inflammatory profiles vary among patients, which can be type 2-high or low; and multiple effector cells might be involved, including eosinophils, neutrophils, both, or none (paucigranulocytic asthma) (4, 11). Moreover, it is usually associated with aspirin-exacerbated respiratory disease (AERD), a non-allergic intolerance to non-steroidal anti-inflammatory drugs (NSAIDs) related to cyclooxygenase (COX)-1. Patients with AERD experiment worsened asthma symptoms while taking this kind of medications, and they usually present nasal polyyps (12, 13).

Treatment for asthmatic patients is complex and is prescribed in a step by step approach regarding GINA guidelines (1). Mild allergic asthmatic patients' symptoms control involves either topical or inhaled corticosteroids, usually in combination with short- and long-acting bronchodilators, antileukotrienes, anticholinergics, among other pharmacological drugs, and/or allergen-specific immunotherapy (AIT); while for the more severe ones, systemic corticosteroids and add-on biological therapy targeting type 2 inflammation mediators are also needed. Currently, anti-IgE (omalizumab), anti-IL-5

(mepolizumab, reslizumab), anti-IL-5R $\alpha$  (benralizumab) and anti-IL-4R $\alpha$  (dupilumab) are approved for asthmatic patients (14), and others, such as anti-TSLP (tezepelumab) are currently under research. Still, there is a subset of asthmatic patients that do not respond to any of these treatments and remain uncontrolled, suffering several exacerbations and hospitalizations every year, which leads to a very low quality of life. In fact, this subset of patients involves allergic and non-allergic patients.

On the other hand, type 2-low non-allergic asthmatic patients do not have any medication that specifically targets their underlying characteristics. Although macrolides have used to treat these patients, they have shown limited success; and a continued use is frowned upon due to antibiotic resistance dangers (15).

Overall, uncontrolled asthma remains a concern, as these patients usually present more comorbidities, a lower quality of life and higher mortality rates (16). Additionally, evidence regarding the role of allergy in the evolution of asthmatic severity is still lacking.

Allergic asthma usually presents sensitization to house dust mites (HDM). There are reports that up to 85% of asthmatic patients are sensitized to HDM (17). It has been recently shown that sensitization to HDM is associated with asthma severity and a lack of disease control in children (18). HDM are arachnids that live in tropical areas with high humidity and temperate climates (19, 20); but are present worldwide and widely populate clothes and bed linens (21). Their association with asthma is hypothesized to be related to the physicochemical properties of HDM allergens (such as Der p 1, Der p 2, Der p 21), which include proteases and immune system mimickers that can activate TLR4 responses (22). Thus, these proteins might be able to, first, damage the epithelium, and then, activate the immune system, eliciting an immune response, especially in children with an immature epithelial barrier. In fact, respiratory infections in childhood are associated with a higher risk of developing asthma (7). Moreover, it has been recently described that Der p 1 elicits a differential metabolic response in an *in vitro* model of lung epithelium between underdeveloped (2 days of culture) and mature (7 days of culture) tissue (23).

However, despite the fact that allergic asthma is the most common phenotype of asthma, and that sensitization to HDM

is the most common among these patients, there are asthmatic patients that do not have concomitant allergy, even in areas where HDM exposure is high, such as tropical climates (24) or high-humidity areas such as islands. One of these regions is the Canary Islands, in Spain, where the HDM exposome has been characterized in depth (19, 20, 25, 26). The reason why some patients do not get sensitized to HDM, but do develop severe uncontrolled asthma without allergy, is unknown; although the fact that lots of these patients have a family history of asthma might be related. Also unknown are the implications of allergy in the development and evolution of asthma. Thus, we aim to decipher the role of allergic inflammation in the pathogenesis of uncontrolled asthma.

## Materials and methods

### Patients

The study was approved by the Ethics Committee of the Hospital on 4<sup>th</sup>/February/2016 (code: 160009). Twenty-three severe uncontrolled asthmatic patients with and without allergy were recruited in the Hospital Universitario de Gran Canaria doctor Negrin (Las Palmas de Gran Canaria, Spain). Allergic status was assessed by skin-prick test to a set of HDM allergens (*Dermatophagoides pteronyssinus*, *Dermatophagoides farinae*, *Blomia tropicalis*, *Acarus siro*, *Lepidoglyphus destructor* and *Tyrophagus putrescentiae*) and the analysis of clinical history; and patients were classified as allergic, if they were sensitized to HDM (and, possibly, to other allergens) and as non-allergic if they had no known sensitizers. Severity was defined according to the GINA guidelines; patients included were at least on step 4–5 of medication and did not respond to the treatments approved at the date of inclusion (including high doses of inhaled and systemic corticosteroids and/or anti-IgE). They also had around 5 exacerbations per year.

Differences in age, onset age, BMI and total IgE in patients were analyzed using Mann-Whitney U test, as the allergic group had <10 patients, while gender, number of smokers and number of patients with AERD were analyzed by Fisher's Exact, using GraphPad Prism v9.3.1 for Windows (GraphPad Software, San Diego, California USA, [www.graphpad.com](http://www.graphpad.com)).

### Metabolomic analysis

The metabolomic analysis has already been thoroughly described elsewhere (27, 28). Briefly, serum samples were measured in batches using an Agilent High Performance Liquid Chromatography system (Agilent 1200 series) coupled with a quadrupole-time of flight (QTOF) analyser system (Q-ToF MS 6520) (Agilent Technologies, Waldbronn, Germany), in positive and negative ionization modes (ESI + and ESI -, respectively). A

TABLE 1 Clinical characteristics of the recruited patients.

	UCNA	UCA
<i>n</i>	14	9
Age	62.1 ± 2.8	47 ± 4.7**
Onset age	29.4 ± 2.9	9.6 ± 2.1****
Sex (F/M)	13/1	6 / 3
BMI	29.7 ± 1.4	27.3 ± 1.4
Current smokers	0	0
Total IgE	257.9 ± 138.2	683.2 ± 222.2**
AERD (%)	7 (50%)	0

BMI, body mass index; AERD, Aspirin Exacerbated Respiratory Disease.

\**p*-value < 0.05; \*\**p*-value < 0.01; \*\*\**p*-value < 0.001; \*\*\*\**p*-value < 0.0001.

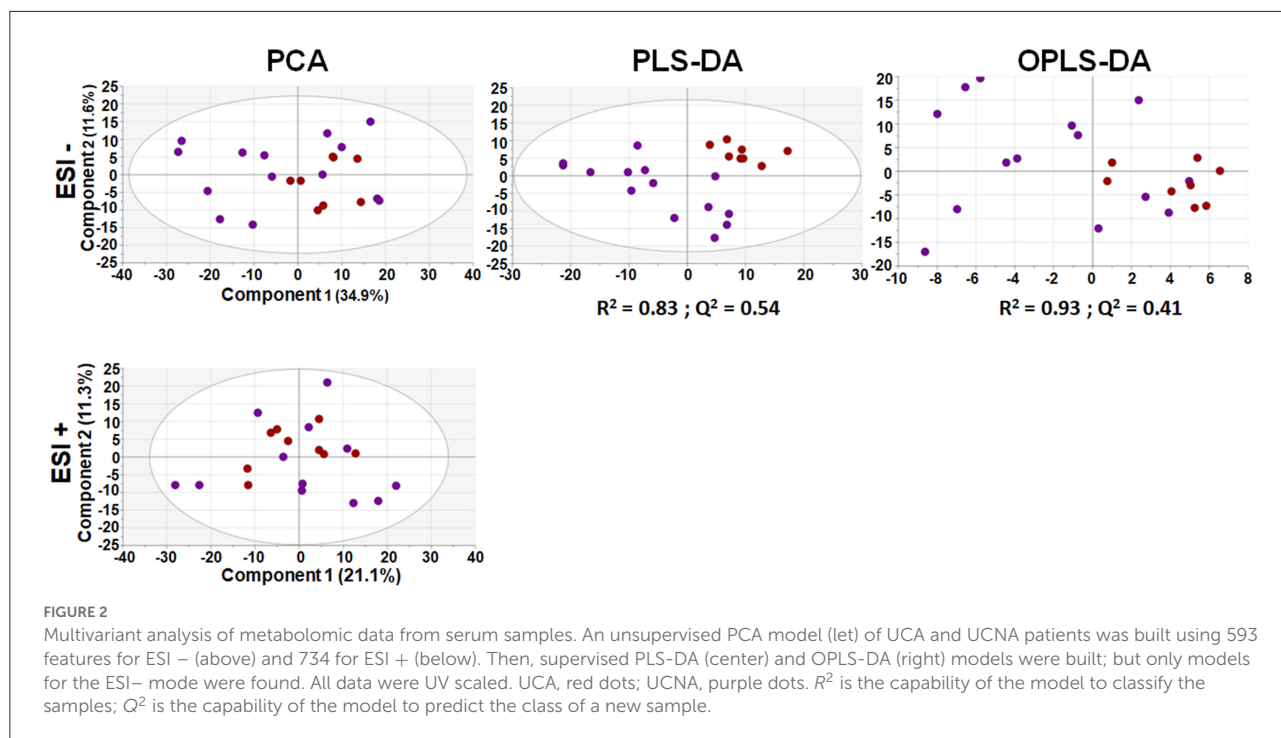
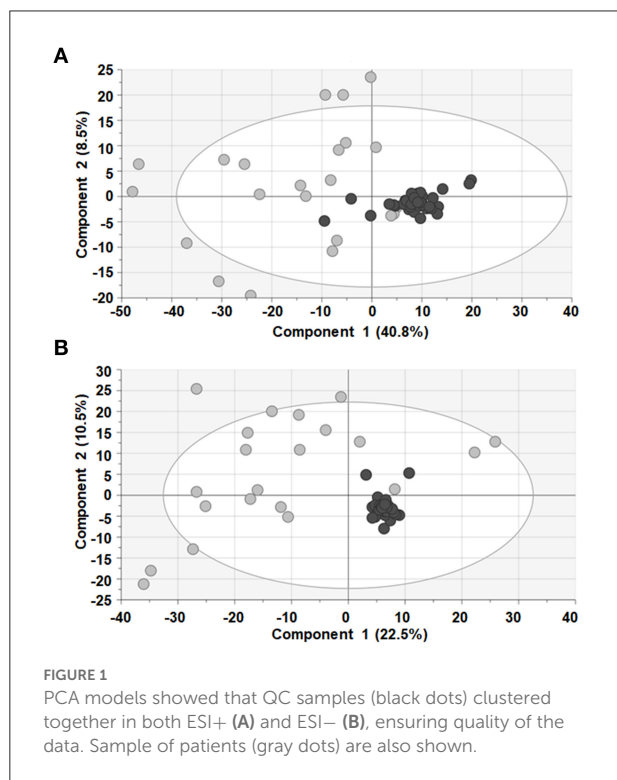
quality control sample (QC) prepared by mixing equal volumes of a set of samples was measured throughout the analytical run. The HPLC system was equipped with a degasser, two binary pumps, and a thermostated autosampler. For the analysis, 10 μL of sample were injected into a Discovery HS C18 (2.1 × 150 mm, 3.0 μm; Supelco, Sigma Aldrich, Germany), maintained at 40°C. The flow rate was set at 0.6 mL/min. The elution gradient involved a mobile phase consisting of: (A) 0.1% v/v formic acid (FA) in water and (B) 0.1% v/v FA in acetonitrile. The initial conditions were set at 25% phase B, which increased linearly to 95% phase B in 35 min, and then returned to the initial conditions in 1 min, which were held for 9 min for column reconditioning. Samples were analyzed in both ESI+ and ESI- modes. The capillary voltage was set at 3500 for ESI+ and 4000V for ESI-. The drying gas flow rate was 10.5 L/min at 330°C and gas nebulizer at 52 psi; fragmentor voltage was 175 V; skimmer and octopole radio frequency voltages were set to 65 and 750 V, respectively. A full scan from 100 to 1200 *m/z* for both modes was performed. MS spectra were collected in the centroid mode at a scan rate of 1.2 Hz. Automatic MS recalibration during batch analysis was carried out introducing a reference standard into the source via a reference sprayer valve. Reference masses for ESI+ were purine (*m/z* = 121.0508) and HP-0921 (*m/z* = 922.0097), whereas for ESI- TFA were NH4 (*m/z* = 119.0363) and HP-0921 (*m/z* = 966.0007).

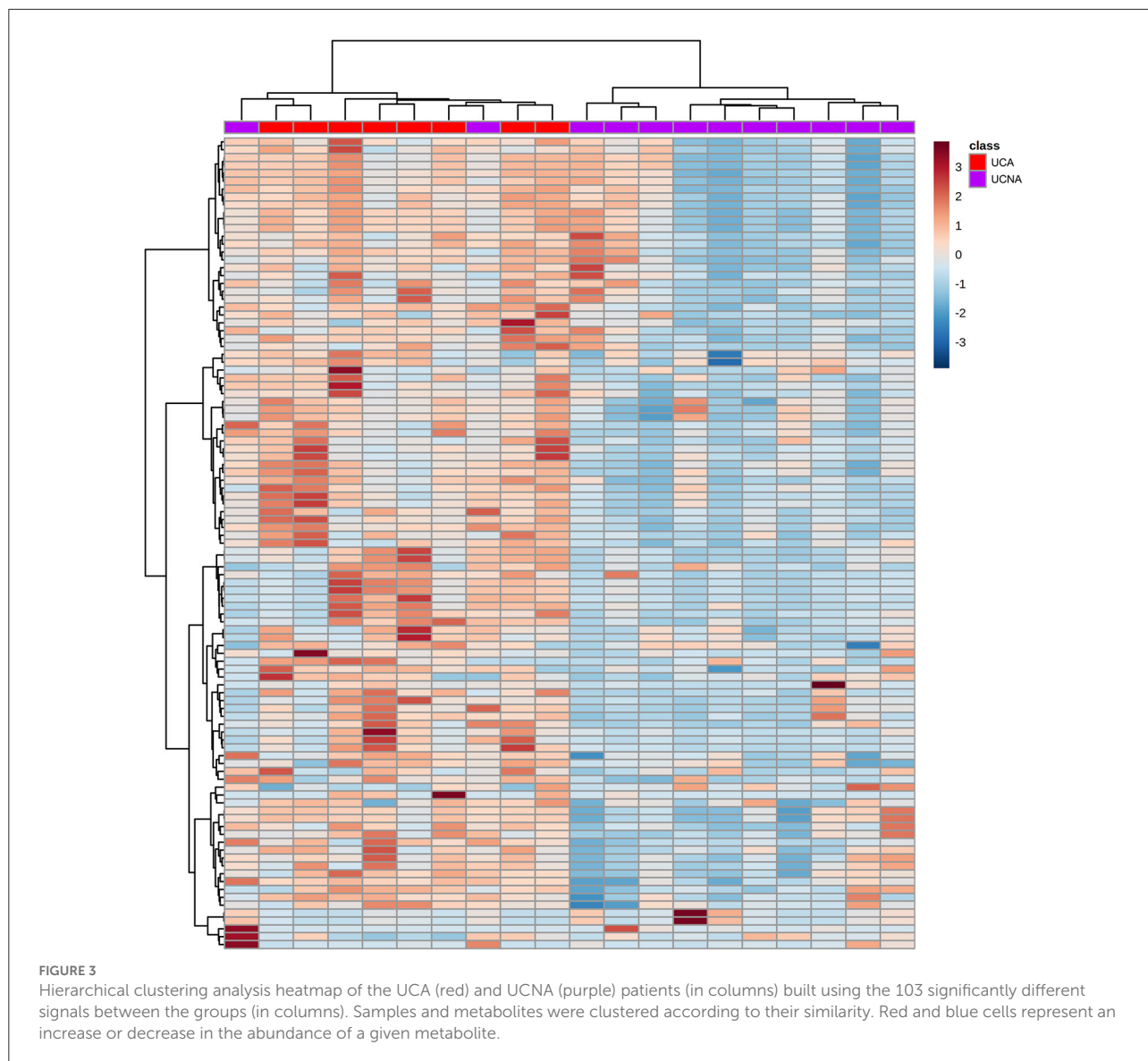
Multivariate analysis was performed using SIMCA v.16.0 (Sartorius Stedim Data Analytics). A Principal Component Analysis (PCA) model was used to evaluate data quality and find patterns in samples. Likewise, Partial Least Square Discriminant Analysis (PLS-DA) and Orthogonal Projections to Latent Structures Discriminant Analysis (OPLS-DA) supervised models were used to classify the samples and to evaluate differences between groups. Models were evaluated using R<sup>2</sup> and Q<sup>2</sup> parameters which are the classification and prediction capacity, respectively.

Significant features were selected after pair-wise comparisons using two-tailed Mann-Whitney U test with an FDR correction using an in-house script for Matlab R2015a

software (Mathworks, Natick, Massachusetts, USA); and used to build a Hierarchical Clustering Heatmap (HCA), with MetaboAnalyst 5.0 online tool (<https://www.metaboanalyst.ca>).

Metabolite annotation was performed by comparison with online platform CEU Mass Mediator 3.0 (29–32) for data bases, and confirmed through tandem mass spectrometry (MS/MS). LC-MS/MS was performed in a similar LC-Q-ToF-MS instrument than the original experiment (Agilent series 1290 HPLC and series 6550 Q-ToF, respectively); and the method for the new equipment, which has been previously described (33, 34), was adapted to be as close as possible to the original method used. In this analysis, the HPLC system was equipped with a degasser, two binary pumps, and a thermostated autosampler. Briefly, 2  $\mu$ L of sample were injected into a Zorbax C18-Extend USH BD06804 column (2.1  $\times$  150 mm, 5.0  $\mu$ m; Agilent Technologies), maintained at 60  $^{\circ}$ C. The flow rate was set at 0.6 mL/min. The elution gradient involved a mobile phase with the same components than those of the previous analysis, and the initial conditions were set at 5% phase B, which increased linearly to 80% phase B in 7 min, and then to 100% phase B in 4.5 min. Then it returned to the initial conditions in 0.5 min, which were held for 3 min. The capillary voltage was set at 3000 for ESI+ and 4000V for ESI-. The drying gas flow rate was 12 L/min at 250 $^{\circ}$ C. and gas nebulizer, fragmentor voltage, skimmer and octupole radio frequency were set as in the LC-MS analysis. MS/MS spectra were collected in the centroid mode; ions were targeted using the narrow  $m/z$  window (1.3 Da) and 20 eV of energy for fragmentation on the quadrupole. To obtain the newer retention time (RT) for this shorter method, samples were first run for LC-MS; then,  $m/z$  were matched with their newer RT. Some of the peaks could not be matched





with the new RTs. Finally, comparison of the structure proposed against the obtained fragments led to the confirmation of the identity.

An enrichment analysis was performed using MetaboAnalyst 5.0 online tool (<https://www.metaboanalyst.ca>). Moreover, pathways of the significant identified compounds were obtained using IMPaLA (v 12.0) online tool (<http://impala.molgen.mpg.de/>).

## Results

### Patients

A total of 23 patients, 9 allergic to HDM and 14 non-allergic, were recruited for metabolomic analysis.

Clinical characteristics of the groups can be found on [Table 1](#).

Non-allergic uncontrolled asthmatic patients (UCNA) were older and had a later onset of asthma than allergic uncontrolled asthmatic patients (UCA) ( $62.1 \pm 2.8$  vs.  $47 \pm 4.7$ ,  $p < 0.01$ , and  $29.4 \pm 2.9$  vs.  $9.6 \pm 2.1$ ,  $p < 0.0001$ , respectively). UCNA also had lower levels of total IgE ( $257.9 \pm 138.2$  vs.  $683.2 \pm 222.2$ ,  $p < 0.01$ ), as expected. None of the patients were active smokers.

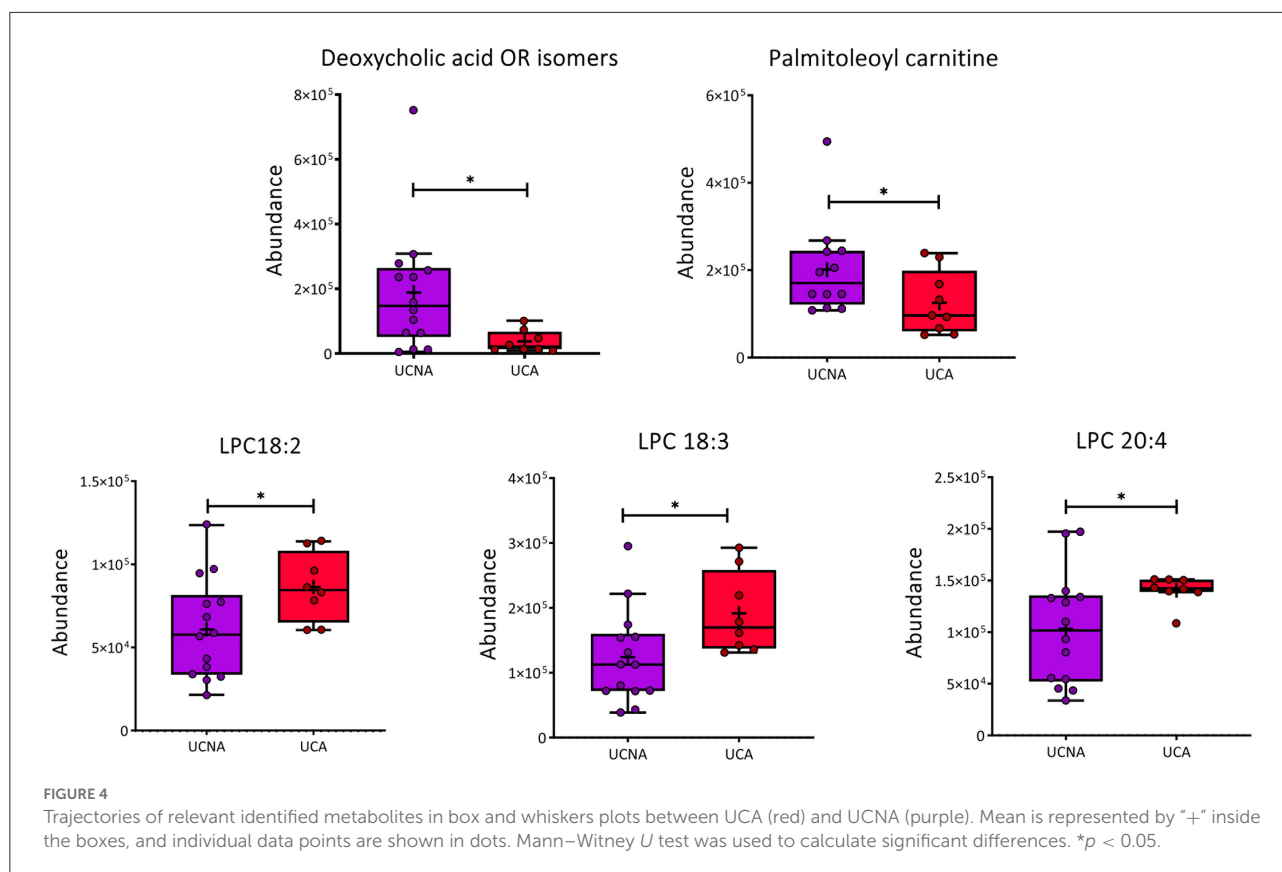
Moreover, 7 (50%) of the UCNA patients suffered AERD, 1 (7%) reported nasal polyps without NSAIDs hypersensitivity besides asthma, and 1 (7%) suffered from NSAIDs hypersensitivity without nasal polyps. On the other hand, from UCA patients, only 1 (11%) had NSAIDs hypersensitivity, and none had nasal polyps.

TABLE 2 Physicochemical characteristics of significant annotated signals in metabolomics through LC-MS/MS between UCNA and UCA groups.

No.	Technique	Biological category	Compound	m/z	Mass (Da)	RT (min)	Formula	Error (ppm)	Adduct	CV in QCs (%)	% Change (UCA)	p-value	p-value (BH)
1	LC-MS-	Vitamins	1 $\alpha$ ,25-dihydroxy-2 $\alpha$ -(3-hydroxypropoxy)vitamin D3 OR isomers	489.3552	490.363	30.47	C30H50O5	-5.7	M-H	6.7	37.3	0.0105	0.1298
2	LC-MS-	Steroids	5 $\alpha$ -Dihydrotestosterone sulfate OR isomers	369.1738	370.1816	4.59	C19H30O5S	0.5	M-H	6.3	74.3	0.0070	0.1021
3	LC-MS-	Steroids	5 $\alpha$ -Dihydrotestosterone sulfate OR isomers	369.1736	370.1814	8.52	C19H30O5S	0	M-H	5.7	77	0.0070	0.1021
4	LC-MS-	Steroids	5 $\alpha$ -Dihydrotestosterone sulfate OR isomers	369.1738	370.1816	10.63	C19H30O5S	0.5	M-H	7.4	78.7	0.0007	0.0915
5	LC-MS-	Steroids	17 $\alpha$ ,20 $\alpha$ -Dihydroxycholesterol OR isomers	463.3426	418.3449	29.92	C27H46O3	0.5	M+FA-H	11.3	36	0.0154	0.1629
6	LC-MS-	Steroids	Androsterone 3-glucuronide OR isomers	465.2496	466.2574	7.81	C25H38O8	1.5	M-H	6.2	66.1	0.0030	0.0915
7	LC-MS-	Steroids	Androsterone 3-glucuronide OR isomers	465.2463	466.2541	8.1	C25H38O8	-5.6	M-H	6.2	52.6	0.0127	0.1453
8	LC-MS-	Steroids	Androsterone 3-glucuronide OR isomers	465.2474	466.2552	9.61	C25H38O8	-3.2	M-H	9.8	27	0.0154	0.1629
9	LC-MS-	Bile acids	Deoxycholic acid OR isomers	437.2901	392.2924	14.73	C24H40O4	-0.5	M+FA-H	5.4	-385.8	0.0222	0.2053
10	LC-MS-	Phospholipids	Phosphocholine (18:2/0:0)	504.3085	519.332	16.97	C26H50NO7P	-0.9	M-CH3	9.6	29.5	0.0374	0.2862
11	LC-MS-	Phospholipids	Phosphocholine (18:3/0:0)	562.3137	517.316	15.63	C26H48NO7P	-1.5	M+FA-H	12.7	35.3	0.0374	0.2862
12	LC-MS-	Phospholipids	Phosphocholine (20:4/0:0)	656.3182	543.3332	17.12	C28H50NO7P	1.2	M+TFA-H	27.4	26.6	0.0265	0.2272
13	LC-MS-	Phospholipids	Phosphocholine (0:0/20:4)	614.3483	569.3506	18.59	C30H52NO7P	4.4	M+FA-H	20.9	35.7	0.0265	0.2272
14	LC-MS+	Carnitines	Palmitoleoyl carnitine	398.3269	397.3191	15.95	C23H43NO4	-0.3	M+H	11.3	-60.5	0.0428	0.9027

FA, Formic Acid; TFA, Trifluoroacetic acid; CV, Coefficient of variation; QC, Quality control. The CV in the injections of the QC sample assures that the metabolites were measured throughout the experiment in a constant and reproducible manner. In this sense, if the variations in QCs are lower than 30%, it means that the variations found in a particular metabolite are due to the true increase or decrease between the comparison groups. Thus, the % of CV in QCs should be always less than the % change between groups for each metabolite, which assesses that the results of this experiment are reliable.





Overall, our findings, as expected, demonstrate significant differences in clinical and demographic features between both groups.

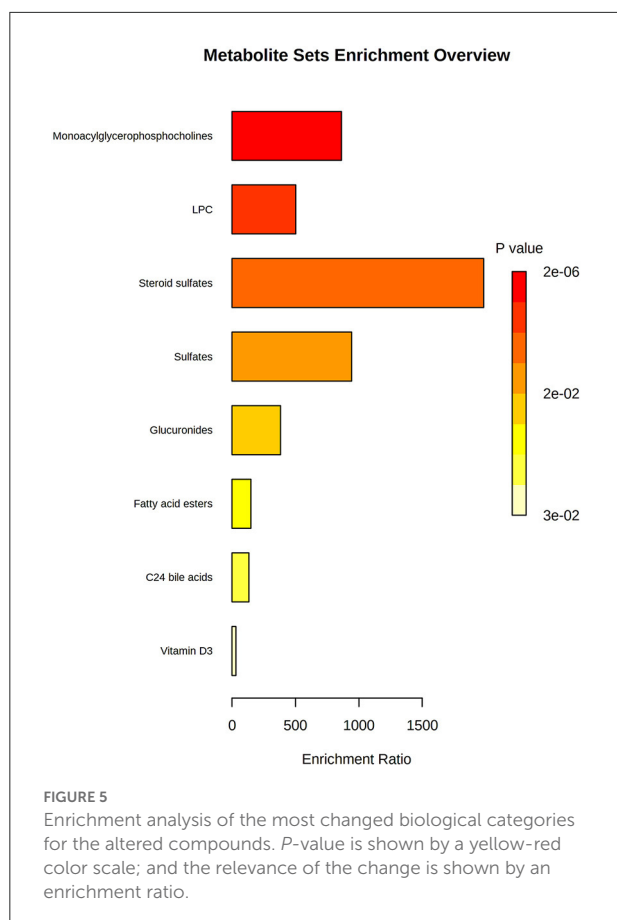
## Metabolomic analysis reveals distinct phenotypes for allergic and non-allergic uncontrolled asthma

After appropriate data processing, a total number of 1,327 features (593 for ESI<sup>-</sup> and 734 for ESI<sup>+</sup>) were obtained for the metabolomic profiling of serum. Quality of the data was assessed by grouping of QC samples on a non-supervised PCA model (Figure 1) proving that the variability of the samples was biological and not due to the technique. Then, both groups were compared using a multivariate analysis (Figure 2). We found that UCA patients tended to cluster in the ESI<sup>-</sup> plot (Figure 2, left) even if the PCA models did not completely separate both groups. As for the PLS-DA and OPLS-DA supervised models, only the ones obtained with the ESI<sup>-</sup> mode data were valid (upper part of Figure 2); and they had  $R^2$  and  $Q^2$  parameters of 0.85 and 0.55, for the PLS-DA mode (Figure 2, center), and 0.91 and 0.4, on the OPLS-DA model, where 100% of UCA samples and 64% of UCNA were correctly classified (Figure 2, right).

Afterwards, we performed an univariate analysis with Mann–Whitney–U (as the allergic group had <10 patients) and obtained a total of 83 (for ESI<sup>-</sup>) and 20 (for ESI<sup>+</sup>) significantly different signals. Most of them (97) were increased in UCA patients compared to UCNA patients. These 103 features were used to build HCA heatmap (Figure 3). As shown, this model was able to correctly classify most of the patients (21 out of 23), grouping all UCA + 2 UCNA patients together (on the left) and the rest of the UCNA patients on the other branch.

## Lipid metabolism, specifically for steroids and phosphocholines, lead the differences among groups

We wanted to identify which were the specific features responsible for the separation of these groups. Thus, we performed a tandem MS/MS analysis and compared the obtained fragmented features with fragmentation spectra when available. In addition, manual identification was performed based on previous publications (35–37). From the 103 features, we were able to identify 14, with 13 of them having a unique  $m/z@RT$  (Table 2). These included steroids (hormones, bile acids, vitamins), lysophosphocholines, and a carnitine,



which were all increased in UCA compared to UCNA, with the exception of deoxycholic acid and palmitoleylcarnitine, which were decreased in UCA. Trajectories of some relevant metabolites can be found in [Figure 4](#).

Finally, we performed an enrichment analysis to obtain the chemical subclasses that were changed in our samples ([Figure 5](#)); where the more changed classes were lysophosphocholines (LPC) and steroids.

Moreover, we tried to relate these specific compounds to the pathways in which they are involved using IMPALA ([Table 3](#)). We found 155 possible related pathways, 44 of them being significantly different, including the phospholipase A2 (PLA2) pathway, steroid hormone biosynthesis, phosphatidyl choline catabolism and acyl chain remodeling, or lipids metabolism, among others.

## Discussion

The stratification of asthma in groups with the idea of finding the underlying mechanisms has been pursued since a long time ago. Particularly, finding the endotypes of uncontrolled severe asthma is crucial, as the therapeutic options

for these patients are limited and often do not work ([38](#)). Particularly, in non-allergic asthma, there are limited available options, as this phenotype has been understudied ([39](#), [40](#)). Here, we aimed to elucidate the contribution of allergy to the uncontrolled severe allergic phenotype.

Clinical differences in allergic and non-allergic non-Th2 asthma have been already described in previous publications ([3](#), [10](#)). In our research, we found that UCNA patients were older, had a later onset age, and lower levels of total IgE than UCA patients, which is consistent with these previous publications. Nonetheless, this should be taken into account, as these could act as confounding factors given the complexity of this asthma model. Moreover, AERD was clearly associated with non-allergic asthma, as has been already described ([3](#), [13](#)). It is known that NSAIDs intolerance is not related to an increase in atopy ([41](#)). Despite the risk of AERD patients to develop a systemic reaction and the worsening of symptoms after NSAIDs intake, there is a lack of studies on the underlying mechanisms of this syndrome. Interestingly, it has been described that AERD was associated with an increase in eicosanoids compared to aspirin-tolerant asthma ([42](#)). However, the allergic status of non-AERD patients was not described; thus, it remains unclear if AERD and allergy activate similar pathways in asthma, and further studies investigating this should be pursued.

Regarding the metabolomic analysis, we found a distinctive metabolic profile between UCA and UCNA patients, which was characterized by a substantial increase in a set of LPCs, including LPC 18:2 and LPC 20:4, two of the most abundant LPCs in plasma ([43](#)). These LPCs are related to the PLA2 pathway, which, together with a reduction in palmitoleylcarnitine, point toward the arachidonic acid pathway as critical to understand the contribution of allergy to these settings.

Changes in LPCs have already been described in asthma and allergy ([44–47](#)) and extensively associated with inflammatory response ([48](#)). Increases in LPC 18:2 and 20:4 have been observed in the active group compared with the placebo treatment in grass-pollen allergic patients after 2 years of sublingual immunotherapy ([49](#)), pointing toward an induction of inflammation.

It has been described that mast cells, alveolar macrophages and neutrophils can secrete sPLA2, a process that is triggered by allergen challenge ([50](#)). Moreover, during inflammation, sPLA2 is associated with high-density lipoproteins (HDL), and can significantly alter HDL composition, which, in inflammation, are enriched in LPCs, including LPC 18:2. It has been demonstrated that these LPCs can act as mediators and impair platelet aggregation ([51](#)). There is increasing evidence of platelets playing a role in asthma ([52](#)) and allergy ([53](#), [54](#)).

LPC 20:4 has been associated with increased release of inflammatory cytokines in endothelial cells, triggering M2 or alternative macrophage polarization ([55](#)). Furthermore, PLA2 hydrolyses phospholipids and releases LPC and free fatty acids; including arachidonic acid ([56–58](#)).

TABLE 3 Significantly enriched metabolic pathways in UCA patients compared to UCNA ( $p < 0.05$ ).

Pathway name	<i>p</i> -value	<i>p</i> -value (BH)	Number of genes identified in pathway	Pathway source
Osteoblast signaling	0.00383	1	1	Wikipathways
Retinoic acid receptors-mediated signaling	0.00383	1	1	PID
Signaling events mediated by the hedgehog family	0.00383	1	1	PID
Rheumatoid arthritis - Homo sapiens (human)	0.00574	1	1	KEGG
STING pathway in kawasaki-like disease and COVID-19	0.00765	1	1	Wikipathways
Steroid hormone biosynthesis - homo sapiens (human)	0.0103	1	2	KEGG
Acyl chain remodeling of CL	0.0115	1	1	Reactome
Acyl chain remodeling of PC	0.0115	1	1	Reactome
Hydrolysis of LPC	0.0115	1	1	Reactome
Phosphatidylcholine catabolism	0.0115	1	1	Wikipathways
RXR and RAR heterodimerization with other nuclear receptor	0.0115	1	1	PID
COPI-independent golgi-to-ER retrograde traffic	0.0133	1	1	Reactome
phospho-PLA2 pathway	0.0133	1	1	Reactome
Vitamins A and D - action mechanisms	0.0133	1	1	Wikipathways
Vitamin D (calciferol) metabolism	0.0152	1	1	Reactome
Golgi-to-ER retrograde transport	0.0171	1	1	Reactome
Metabolism of steroids	0.0171	1	2	Reactome
Vitamin D metabolism	0.0171	1	1	Wikipathways
GPCR downstream signalling	0.0185	1	2	Reactome
1_25-dihydroxyvitamin D <sub>3</sub> biosynthesis	0.019	1	1	HumanCyc
Choline metabolism in cancer - homo sapiens (human)	0.019	1	1	KEGG
HDL remodeling	0.019	1	1	Reactome
Plasma lipoprotein remodeling	0.019	1	1	Reactome
Metabolism of lipids	0.0197	1	3	Reactome
Ca-dependent events	0.0209	1	1	Reactome
Intra-Golgi and retrograde Golgi-to-ER traffic	0.0209	1	1	Reactome
Vitamins	0.0209	1	1	Reactome
Vitamin D3 (cholecalciferol) metabolism	0.0228	1	1	EHMN
Plasma lipoprotein assembly_ remodeling_ and clearance	0.0247	1	1	Reactome
Vitamin D-sensitive calcium signaling in depression	0.0247	1	1	Wikipathways
Signaling by GPCR	0.0264	1	2	Reactome
RAS and bradykinin pathways in COVID-19	0.0266	1	1	Wikipathways
G-protein mediated events	0.0303	1	1	Reactome
PLC beta mediated events	0.0303	1	1	Reactome
16p11.2 proximal deletion syndrome	0.0322	1	1	Wikipathways
Drug Induction of Bile Acid Pathway	0.034	1	1	Wikipathways
Membrane Trafficking	0.0378	1	1	Reactome
Opioid Signaling	0.0378	1	1	Reactome
Recycling of bile acids and salts	0.0378	1	1	Reactome
Linoleate metabolism	0.0396	1	1	EHMN
Vitamin A and carotenoid metabolism	0.0396	1	1	Wikipathways
ADORA2B mediated anti-inflammatory cytokines production	0.0415	1	1	Reactome
G alpha (s) signalling events	0.047	1	1	Reactome
Glycerophospholipid metabolism - Homo sapiens (human)	0.047	1	1	KEGG

Arachidonic acid (AA, C 20:4), which was found increased in its LPC form in UCA, is a precursor of eicosanoids (prostaglandins, lipoxins, leukotrienes), resolvins, and protectins, all of them involved in the regulation of immune response (59). These are known to play a role in asthma, allergy, and other inflammatory pathologies (60, 61).

Interestingly, we found that palmitoleoylcarnitine was decreased in UCA patients. A decrease in carnitines together with an increase in LPCs has been described in severe allergy compared to controls (53).

Overall, our results show that allergic inflammation in uncontrolled asthma leads to a significant alteration of various inflammatory routes, including the AA pathway, along with a dysregulation of LPC mediators, pointing toward these two factors as allergic contributors in asthma.

Steroid biosynthesis was also found increased in UCA patients, which has also been described in allergic asthma compared to healthy controls (47). Steroids have been demonstrated to play a role in the activation of immune system and in the development of asthma (62); thus this might be related with the higher activation shown. Some studies have linked inhaled corticosteroids with a suppression of the adrenal gland (63). However, all our patients were treated with a combination of inhaled corticosteroids and a long-acting bronchodilators; and there were no differences in topical or oral corticosteroid intake among groups. Moreover, there also seemed to be an involvement of bile acids. The role of bile acids in inflammatory diseases is becoming increasingly clearer (64); in particular, there seems to be a connection between respiratory diseases and gastroesophageal reflux; and bile acid increases have been reported previously (45).

Interestingly, deoxycholic acid was found reduced in UCA patients compared to UCNA. We have previously reported a decrease in deoxycholic acid in asthma according to severity (28). This secondary bile acid has been demonstrated to stimulate the production of inflammatory cytokines in an *in vitro* epithelial airway cell culture; and to promote inflammation in animal models either by inducing inflammatory cytokine production (65), activation of the inflammasome (66) and inducing the dysbiosis of gut microbiota (67). Thus, steroid metabolism seems to be differential and a key player in inflammation for non-allergic asthma.

Nonetheless, it is important to consider that this is an exploratory study. Future projects including more samples that explore other aspects of asthma are needed. For example, there is increasing evidence that sensitization to *Staphylococcus aureus* enterotoxins is related with the development of severe asthma and disease exacerbations (68), and with nasal polyps (69). Thus, sensitization to staphylococcal enterotoxins might play a role in non-allergic asthma pathogenesis, and its analysis could be helpful in understanding the influence of asthma in this disease.

## Conclusions

Overall, we found that allergic inflammation elicits a differential inflammatory phenotype in severe uncontrolled asthma patients. This inflammation is related to the arachidonic acid and the PLA2 pathways and is marked by a distinctive metabolomic profile in both groups. Moreover, this study highlights the need of further studies to better elucidate the underlying pathways in non-allergic asthma, as novel therapeutic targets unrelated to type 2 inflammation are needed for a better treatment in these patients.

## Data availability statement

The datasets presented in this study can be found in online repositories. The names of the repository/repositories and accession number(s) can be found below: <https://www.ebi.ac.uk/metabolights/>, MTBLS1133.

## Ethics statement

The studies involving human participants were reviewed and approved by Comité de ética de la Investigación Hospital Universitario de Gran Canaria Check dot after Dr. Negrin Hospital Barranco de la Ballena s/n. Hospital Universitario de Gran Canaria Dr. Negrin, Edificio de Investigación, Planta principal. 35019 Las Palmas de Gran Canaria (study code: 160009). The patients/participants provided their written informed consent to participate in this study.

## Author contributions

ME was the PI and together with DB and AV designed the study and supervised the research. TC, AA, and HG recruited the patients and obtained the samples. MD, DO, JR-C, AV, and CB performed the metabolomic analysis and data treatment. MD performed analysis of the results together with DO. All authors contributed to the writing of the manuscript and have given approval to the final version of the manuscript.

## Funding

This work was supported by ISCIII (PI19/00044 and PI18/01467), cofounded by FEDER Investing in your future for the thematic network and cooperative research centers ARADyAL (RD16/0006/0015) and RICORS Red de Enfermedades Inflammatorias (REI) (RD21/0002/0008), the Ministry of Science and innovation in Spain (PCI2018-092930) co-funded by the European program ERA HDHL – Nutrition & the Epigenome, Project Dietary Intervention in Food Allergy: Microbiome, Epigenetic and Metabolomic

Interactions DIFAMEM and Fundación Mutua Madrileña (AP177712021). MD and JR-C were supported by FPI-CEU predoctoral fellowships and DO was funded by a postdoctoral research fellowship from the European program ERA HDHL – Nutrition & the Epigenome, Project Dietary Intervention in Food Allergy: Microbiome, Epigenetic and Metabolomic Interactions DIFAMEM.

## Acknowledgments

We would like to thank all institutions involved: Institute of Applied Molecular Medicine (IMMA, Universidad CEU San Pablo, CEU Universities, Madrid), Center of Metabolomics and Bioanalysis (CEMPIO, Universidad CEU San Pablo, CEU Universities, Madrid), and the Hospital Universitario de Gran Canaria Dr. Negrín (Las Palmas de Gran Canaria, Spain).

## References

1. Global Initiative for Asthma. *Global Strategy for Asthma Management and Prevention*. (2022). Available online at: [www.ginasthma.org](http://www.ginasthma.org) (accessed June 26, 2022).
2. Vos T, Lim SS, Abbafati C, Abbas KM, Abbasi M, Abbasifard M, et al. Global burden of 369 diseases and injuries in 204 countries and territories, 1990–2019: a systematic analysis for the Global Burden of Disease Study 2019. *Lancet*. (2020) 396:1204–22. doi: 10.1016/S0140-6736(20)30925-9
3. Wenzel SE. Asthma phenotypes: the evolution from clinical to molecular approaches. *Nat Med*. (2012) 18:716–25. doi: 10.1038/nm.2678
4. Agache I, Akdis C, Jutel M, Virchow JC. Untangling asthma phenotypes and endotypes. *Allergy*. (2012) 67:835–46. doi: 10.1111/j.1398-9995.2012.02832.x
5. Campo P, Rodríguez F, Sánchez-García S, Barranco P, Quirce S, Pérez-Francés C, et al. Phenotypes and endotypes of uncontrolled severe asthma: new treatments. *J Investig Allergol Clin Immunol*. (2013) 23:76–88.
6. Akar-Ghibril N, Casale T, Custovic A, Phipatanakul W. Allergic endotypes and phenotypes of asthma. *J Allergy Clin Immunol Pract*. (2020) 8:429–40. doi: 10.1016/j.jaip.2019.11.008
7. Holgate ST, Wenzel S, Postma DS, Weiss ST, Renz H, Sly PD. Asthma. *Nat Rev Dis Prim*. (2015) 1:1–22. doi: 10.1016/B978-0-12-415847-4.00096-3
8. Licona-Limón P, Kim LK, Palm NW, Flavell RA. TH2, allergy and group 2 innate lymphoid cells. *Nat Immunol*. (2013) 14:536–42. doi: 10.1038/ni.2617
9. Edwards MR, Saglani S, Schwarze J, Skevaki C, Smith JA, Ainsworth B, et al. Addressing unmet needs in understanding asthma mechanisms. *Eur Respir J*. (2017) 49:1602448. doi: 10.1183/13993003.02448-2016
10. Pakkasaala J, Ilmarinen P, Honkamäki J, Tuomisto LE, Andersén H, Piirilä P, et al. Age-specific incidence of allergic and non-allergic asthma. *BMC Pulm Med*. (2020) 20: 9. doi: 10.1186/s12890-019-1040-2
11. Tliba O, Panettieri RA. Paucigranulocytic asthma: uncoupling of airway obstruction from inflammation. *J Allergy Clin Immunol*. (2019) 143:1287–94. doi: 10.1016/j.jaci.2018.06.008
12. Kennedy JL, Stoner AN, Borish L. Aspirin-exacerbated respiratory disease: prevalence, diagnosis, treatment, and considerations for the future. *Am J Rhinol Allergy*. (2016) 30:407–13. doi: 10.2500/ajra.2016.30.4370
13. Taniguchi M, Mitsui C, Hayashi H, Ono E, Kajiwara K, Mita H, et al. Aspirin-exacerbated respiratory disease (AERD): current understanding of AERD. *Allergol Int*. (2019) 68:289–95. doi: 10.1016/j.alit.2019.05.001
14. Menzies-Gow AN, McBrien C, Unni B, Porsbjerg CM, Al-Ahmad M, Ambrose CS, et al. Real world biologic use and switch patterns in severe asthma: data from the international severe asthma registry and the US CHRONICLE study. *J Asthma Allergy*. (2022) 15:63–78. doi: 10.2147/JAA.S328653

## Conflict of interest

The authors declare that the research was conducted in the absence of any commercial or financial relationships that could be construed as a potential conflict of interest.

## Publisher's note

All claims expressed in this article are solely those of the authors and do not necessarily represent those of their affiliated organizations, or those of the publisher, the editors and the reviewers. Any product that may be evaluated in this article, or claim that may be made by its manufacturer, is not guaranteed or endorsed by the publisher.

15. Hinks TSC, Levine SJ, Brusselle GG. Treatment options in type-2 low asthma. *Eur Respir J*. (2021) 57:1–36. doi: 10.1183/13993003.00528-2020
16. Peters SP, Ferguson G, Deniz Y, Reisner C. Uncontrolled asthma: a review of the prevalence, disease burden and options for treatment. *Respir Med*. (2006) 100:1139–51. doi: 10.1016/j.rmed.2006.03.031
17. Wang JY. The innate immune response in house dust mite-induced allergic inflammation. *Allergy, Asthma Immunol Res*. (2013) 5:68–74. doi: 10.4168/air.2013.5.2.68
18. Okasha NM, Sarhan AA, Ahmed EO. Association between house dust mites sensitization and level of asthma control and severity in children attending Mansoura University Children's Hospital. *Egypt J Bronchol*. (2021) 15:36. doi: 10.1186/s43168-021-00082-x
19. Juliá-Serdà G, Cabrera-Navarro P, Acosta-Fernández O, Martín-Pérez P, Losada-Cabrera P, García-Bello MA, et al. High prevalence of asthma and atopy in the Canary Islands, Spain. *Int J Tuberc Lung Dis*. (2011) 15:536–41. doi: 10.5588/ijtld.10.0303
20. Juliá Serdà G, Cabrera Navarro P, Acosta Fernández O, Martín Pérez P, Batista Martín J, Alamo Santana F, et al. High prevalence of asthma symptoms in the Canary Islands: climatic influence? *J Asthma*. (2005) 42:507–11. doi: 10.1081/JAS-67621
21. Miller JD. The role of dust mites in allergy. *Clin Rev Allergy Immunol*. (2019) 57:312–29. doi: 10.1007/s12016-018-8693-0
22. Sánchez-Borges M, Fernandez-Caldas E, Thomas WR, Chapman MD, Lee BW, Caraballo L, et al. International consensus (ICON) on: clinical consequences of mite hypersensitivity, a global problem. *World Allergy Organ J*. (2017) 10:14. doi: 10.1186/s40413-017-0145-4
23. López-Rodríguez JC, Rodríguez-Coira J, Benedé S, Barbas C, Barber D, Villalba MT, et al. Comparative metabolomics analysis of bronchial epithelium during barrier establishment after allergen exposure. *Clin Transl Allergy*. (2021) 11:1–10. doi: 10.1002/ct2.12051
24. Pumhirun P, Towiwat P, Mahakit P. Aeroallergen sensitivity of Thai patients with allergic rhinitis. *Asian Pacific J Allergy Immunol*. (1997) 15:183–5.
25. Juliá-Serdà G, Cabrera-Navarro P, Acosta-Fernández O, Martín-Pérez P, García-Bello MA, Antó-Boqué J. Prevalence of sensitization to *Blomia tropicalis* among young adults in a temperate climate. *J Asthma*. (2012) 49:349–54. doi: 10.3109/02770903.2012.672611
26. Menéndez I, Derbyshire E, Carrillo T, Caballero E, Engelbrecht JP, Romero LE, et al. Saharan dust and the impact on adult and elderly allergic patients: the effect of threshold values in the northern sector of Gran Canaria, Spain. *Int J Environ Health Res*. (2017) 27:144–60. doi: 10.1080/09603123.2017.1292496
27. Rodríguez-Coira J, Delgado-Dolset M, Obeso D, Dolores-Hernández M, Quintás G, Angulo S, et al. Troubleshooting in large-scale LC-ToF-MS

- metabolomics analysis: solving complex issues in big cohorts. *Metabolites*. (2019) 9:247. doi: 10.3390/metabo9110247
28. Delgado-Dolset MI, Obeso D, Rodríguez-Coira J, Tarin C, Tan G, Cumplido JA, et al. Understanding uncontrolled severe allergic asthma by integration of omic and clinical data. *Allergy*. (2022) 77:1772–85. doi: 10.1111/all.15192
29. Gil-de-la-Fuente A, Godzien J, Saugar S, García-Carmona R, Badran H, Wishart DS, et al. CEU mass mediator 3.0: a metabolite annotation tool. *J Proteome Res*. (2019) 18:797–802. doi: 10.1021/acs.jproteome.8b00720
30. Gil de la Fuente A, Godzien J, Fernández López M, Rupérez FJ, Barbas C, Otero A. Knowledge-based metabolite annotation tool: CEU mass mediator. *J Pharm Biomed Anal*. (2018) 154:138–49. doi: 10.1016/j.jpba.2018.02.046
31. Mamani-Huanca M, de la Fuente AG, Otero A, Gradillas A, Godzien J, Barbas C, et al. Enhancing confidence of metabolite annotation in Capillary Electrophoresis-Mass Spectrometry untargeted metabolomics with relative migration time and in-source fragmentation. *J Chromatogr A*. (2021) 1635:461758. doi: 10.1016/j.chroma.2020.461758
32. García CA, Gil-de-la-Fuente A, Barbas C, Otero A. Probabilistic metabolite annotation using retention time prediction and meta-learned projections. *J Cheminformatics*. (2022) 14:1–23. doi: 10.1186/s13321-022-00613-8
33. Soldevilla B, López-lópez A, Lens-pardo A, Carretero-puche C, Lopez-gonzalez A, La Salvia A, et al. Comprehensive plasma metabolomic profile of patients with advanced neuroendocrine tumors (Nets): diagnostic and biological relevance. *Cancers*. (2021) 13:2634. doi: 10.3390/cancers13112634
34. Gil de la Fuente A, Traldi F, Siroka J, Kretowski A, Ciborowski M, Otero A, et al. Characterization and annotation of oxidized glycerophosphocholines for non-targeted metabolomics with LC-QTOF-MS data. *Anal Chim Acta*. (2018) 1037:358–68. doi: 10.1016/j.aca.2018.08.005
35. Gonzalez-Riano C, Gradillas A, Barbas C. Exploiting the formation of adducts in mobile phases with ammonium fluoride for the enhancement of annotation in liquid chromatography-high resolution mass spectrometry based lipidomics. *J Chromatogr Open*. (2021) 1:100018. doi: 10.1016/j.jcoa.2021.100018
36. Demarque DP, Crotti AEM, Vessecchi R, Lopes JLC, Lopes NP. Fragmentation reactions using electrospray ionization mass spectrometry: an important tool for the structural elucidation and characterization of synthetic and natural products. *Nat Prod Rep*. (2016) 33:432–55. doi: 10.1039/C5NP00073D
37. Tsugawa H, Ikeda K, Takahashi M, Satoh A, Mori Y, Uchino H, et al. MS-DIAL 4: accelerating lipidomics using an MS/MS, CCS, and retention time atlas. *bioRxiv*. (2020). doi: 10.1101/2020.02.11.944900
38. Agache I. Severe asthma phenotypes and endotypes. *Semin Immunol*. (2019) 46:101301. doi: 10.1016/j.smim.2019.101301
39. Seys SF, Lokwani R, Simpson JL, Bullens DMA. New insights in neutrophilic asthma. *Curr Opin Pulm Med*. (2019) 25:113–20. doi: 10.1097/MCP.0000000000000543
40. Bittar HET, Yousem SA, Wenzel SE. Pathobiology of severe asthma. *Annu Rev Pathol Mech Dis*. (2015) 10:511–45. doi: 10.1146/annurev-pathol-012414-040343
41. Quiralte J, Blanco C, Castillo R, Ortega N, Carrillo T. Anaphylactoid reactions due to nonsteroidal antiinflammatory drugs: clinical and cross-reactivity studies. *Ann Allergy, Asthma Immunol*. (1997) 78:293–6. doi: 10.1016/S1081-1206(10)63184-5
42. Ban GY, Cho K, Kim SH, Yoon MK, Kim JH, Lee HY, et al. Park HS. Metabolomic analysis identifies potential diagnostic biomarkers for aspirin-exacerbated respiratory disease. *Clin Exp Allergy*. (2017) 47:37–47. doi: 10.1111/cea.12797
43. Liu P, Chen C, Chen X. The mechanisms of lysophosphatidylcholine in the development of diseases. *Life Sci*. (2020) 247:117443. doi: 10.1016/j.lfs.2020.117443
44. Jung J, Kim S-H, Lee H-S, Choi GS, Jung Y-S, Ryu DH, et al. Serum metabolomics reveals pathways and biomarkers associated with asthma pathogenesis. *Clin Exp Allergy*. (2013) 43:425–33. doi: 10.1111/cea.12089
45. Comhair SAA, McDunn J, Bennett C, Fettig J, Erzurum SC, Kalhan SC. Metabolomic endotype of asthma. *J Immunol*. (2015) 195:643–50. doi: 10.4049/jimmunol.1500736
46. Ried JS, Baurecht H, Stücker F, Krumsiek J, Gieger C, Heinrich J, et al. Integrative genetic and metabolite profiling analysis suggests altered phosphatidylcholine metabolism in asthma. *Allergy*. (2013) 68:629–36. doi: 10.1111/all.12110
47. Zheng P, Bian X, Zhai Y, Li C, Li N, Hao C, et al. Metabolomics reveals a correlation between hydroxyeicosatetraenoic acids and allergic asthma: evidence from three years' immunotherapy. *Pediatr Allergy Immunol*. (2021) 32:1654–62. doi: 10.1111/pai.13569
48. Chiurchiù V, Leuti A, Maccarrone M. Bioactive lipids and chronic inflammation: managing the fire within. *Front Immunol*. (2018) 9:38. doi: 10.3389/fimmu.2018.00038
49. Barker-Tejeda TC, Bazire R, Obeso D, Mera-Berriatua L, Rosace D, Vazquez-Cortes S, et al. Exploring novel systemic biomarker approaches in grass-pollen sublingual immunotherapy using omics. *Allergy*. (2021) 76:1199–212. doi: 10.1111/all.14565
50. Bansal P, Gaur SN, Arora N. Lysophosphatidylcholine plays critical role in allergic airway disease manifestation. *Sci Rep*. (2016) 6:2–11. doi: 10.1038/srep27430
51. Curcic S, Holzer M, Pasterk L, Knuplez E, Eichmann TO, Frank S, et al. Secretory phospholipase A2 modified HDL rapidly and potently suppresses platelet activation. *Sci Rep*. (2017) 7:1–12. doi: 10.1038/s41598-017-08136-1
52. Yue M, Hu M, Fu F, Ruan H, Wu C. Emerging roles of platelets in allergic asthma. *Front Immunol*. (2022) 13:846055. doi: 10.3389/fimmu.2022.846055
53. Obeso D, Mera-Berriatua L, Rodríguez-Coira J, Rosace D, Fernández P, Martín-Antoniano IA, et al. Multi-omics analysis points to altered platelet functions in severe food-associated respiratory allergy. *Allergy*. (2018) 73:2137–49. doi: 10.1111/all.13563
54. Gomez-Casado C, Villaseñor A, Rodriguez-Nogales A, Bueno JL, Barber D, Escribese MM. Understanding platelets in infectious and allergic lung diseases. *Int J Mol Sci*. (2019) 20:1730. doi: 10.3390/ijms20071730
55. Assunção LS, Magalhães KG, Carneiro AB, Molinaro R, Almeida PE, Atella GC, et al. Schistosomal-derived lysophosphatidylcholine triggers M2 polarization of macrophages through PPAR $\gamma$  dependent mechanisms. *Biochim Biophys Acta Mol Cell Biol Lipids*. (2017) 1862:246–54. doi: 10.1016/j.bbalip.2016.11.006
56. Bennett M, Gilroy DW. Lipid mediators in inflammation. *Microbiol Spectr*. (2016) 4:MCHD-0035-2016. doi: 10.1128/microbiolspec.MCHD-0035-2016
57. Arita M. Eosinophil polyunsaturated fatty acid metabolism and its potential control of inflammation and allergy. *Allergol Int*. (2016) 65:S2–5. doi: 10.1016/j.alit.2016.05.010
58. Balgoma D, Astudillo AM, Perez-Chacon G, Montero O, Balboa MA, Balsinde J. Markers of monocyte activation revealed by lipidomic profiling of arachidonic acid-containing phospholipids. *J Immunol*. (2010) 184:3857–65. doi: 10.4049/jimmunol.0902883
59. Sokolowska M, Rovati GE, Diamant Z, Untersmayr E, Schwarze J, Lukasik Z, et al. Current perspective on eicosanoids in asthma and allergic diseases - EAACI Task Force consensus report, part I. *Allergy*. (2021) 76:114–30. doi: 10.1111/all.14295
60. Pecak M, Korošec P, Kunej T. Multiomics data triangulation for asthma candidate biomarkers and precision medicine. *Omi A J Integr Biol*. (2018) 22:392–409. doi: 10.1089/omi.2018.0036
61. Nie X, Wei J, Hao Y, Tao J, Li Y, Liu M, et al. Consistent biomarkers and related pathogenesis underlying asthma revealed by systems biology approach. *Int J Mol Sci*. (2019) 20:4037. doi: 10.3390/ijms20164037
62. Fuseini H, Newcomb DC. Mechanisms driving gender differences in asthma. *Curr Allergy Asthma Rep*. (2017) 17:19. doi: 10.1007/s11882-017-0686-1
63. Kachroo P, Stewart ID, Kelly RS, Stav M, Mendez K, Dahlin A, et al. Metabolomic profiling reveals extensive adrenal suppression due to inhaled corticosteroid therapy in asthma. *Nat Med*. (2022) 28:814–22. doi: 10.1038/s41591-022-01714-5
64. Chen ML, Takeda K, Sundrud MS. Emerging roles of bile acids in mucosal immunity and inflammation. *Mucosal Immunol*. (2019) 12:851–61. doi: 10.1038/s41385-019-0162-4
65. Chung SJ, Lee CH, Lee HS, Kim ST, Sohn UD, Park ES, et al. The role of phosphatidylcholine and deoxycholic acid in inflammation. *Life Sci*. (2014) 108:88–93. doi: 10.1016/j.lfs.2014.05.013
66. Zhao S, Gong Z, Zhou J, Tian C, Gao Y, Xu C, et al. Deoxycholic acid triggers nlrP3 inflammasome activation and aggravates Dss-induced colitis in mice. *Front Immunol*. (2016) 7:536. doi: 10.3389/fimmu.2016.00536
67. Xu M, Cen M, Shen Y, Zhu Y, Cheng F, Tang L, et al. Deoxycholic acid - induced gut dysbiosis disrupts bile acid enterohepatic circulation and promotes intestinal inflammation. *Dig Dis Sci*. (2021) 66:568–76. doi: 10.1007/s10620-020-06208-3
68. Flora M, Perna F, Abbadessa S, Garziano F, Maffucci R, Maniscalco M, et al. Basophil activation test for *Staphylococcus aureus* enterotoxins in severe asthmatic patients. *Clin Exp Allergy*. (2021) 51:536–45. doi: 10.1111/cea.13772
69. Cui XY, Miao JL, Lu HQ, Qi QH, Chen XI, Xu J, et al. Serum levels of specific IgE to *Staphylococcus aureus* enterotoxins in patients with chronic rhinosinusitis. *Exp Ther Med*. (2015) 9:1523–7. doi: 10.3892/etm.2015.2247

## ORIGINAL ARTICLE

## Basic and Translational Allergy Immunology

# Understanding uncontrolled severe allergic asthma by integration of omic and clinical data

María Isabel Delgado-Dolset<sup>1,2</sup>  | David Obeso<sup>1,2</sup>  | Juan Rodríguez-Coira<sup>1,2,3</sup>  | Carlos Tarin<sup>1</sup> | Ge Tan<sup>3</sup>  | José A. Cumplido<sup>4</sup> | Ana Cabrera<sup>4</sup> | Santiago Angulo<sup>5</sup>  | Coral Barbas<sup>2</sup>  | Milena Sokolowska<sup>3</sup>  | Domingo Barber<sup>1</sup>  | Teresa Carrillo<sup>4</sup> | Alma Villaseñor<sup>1</sup>  | María M. Escribese<sup>1</sup> 

<sup>1</sup>Institute of Applied Molecular Medicine (IMMA), Department of Basic Medical Sciences, Facultad de Medicina, Universidad San Pablo CEU, CEU Universities, Urbanización Montepríncipe, Madrid, Spain

<sup>2</sup>Centre for Metabolomics and Bioanalysis (CEMBO), Department of Chemistry and Biochemistry, Facultad de Farmacia, Universidad San Pablo CEU, CEU Universities, Urbanización Montepríncipe, Madrid, Spain

<sup>3</sup>Swiss Institute of Allergy and Asthma Research (SIAF), University of Zurich, Zurich, Switzerland

<sup>4</sup>Hospital Universitario de Gran Canaria Doctor Negrin, Las Palmas de Gran Canaria, Spain

<sup>5</sup>Department of Applied Mathematics and Statistics, Universidad San Pablo-CEU, CEU Universities, Madrid, Spain

## Correspondence

María M. Escribese, Department of Basic Medical Sciences, Faculty of Medicine, San Pablo CEU University, Campus Montepríncipe, Crtra, Boadilla del Monte km 5.3, CP 28668 Boadilla del Monte, Madrid, Spain.  
Email: mariamarta.escribesealonso@ceu.es

## Funding information

Ministerio de Ciencia, Innovación y Universidades, Grant/Award Number: PCI2018-092930; ISCIII, Grant/Award Number: PI18/01467 and PI19/00044; Ministerio de Ciencia, Innovación y Universidades, Grant/Award Number: RTI2018-095166-B-I00; Swiss National Science Foundation (SNFS), Grant/Award Number: 310030\_189334/1

## Abstract

**Background:** Asthma is a complex, multifactorial disease often linked with sensitization to house dust mites (HDM). There is a subset of patients that does not respond to available treatments, who present a higher number of exacerbations and a worse quality of life. To understand the mechanisms of poor asthma control and disease severity, we aim to elucidate the metabolic and immunologic routes underlying this specific phenotype and the associated clinical features.

**Methods:** Eighty-seven patients with a clinical history of asthma were recruited and stratified in 4 groups according to their response to treatment: corticosteroid-controlled (ICS), immunotherapy-controlled (IT), biologicals-controlled (BIO) or uncontrolled (UC). Serum samples were analysed by metabolomics and proteomics; and classifiers were built using machine-learning algorithms.

**Results:** Metabolomic analysis showed that ICS and UC groups cluster separately from one another and display the highest number of significantly different metabolites among all comparisons. Metabolite identification and pathway enrichment analysis highlighted increased levels of lysophospholipids related to inflammatory pathways in the UC patients. Likewise, 8 proteins were either upregulated (CCL13, ARG1, IL15 and TNFRSF12A) or downregulated (sCD4, CCL19 and IFN $\gamma$ ) in UC patients compared to ICS, suggesting a significant activation of T cells in these patients. Finally, the machine-learning model built including metabolomic and clinical data was able to classify the patients with an 87.5% accuracy.

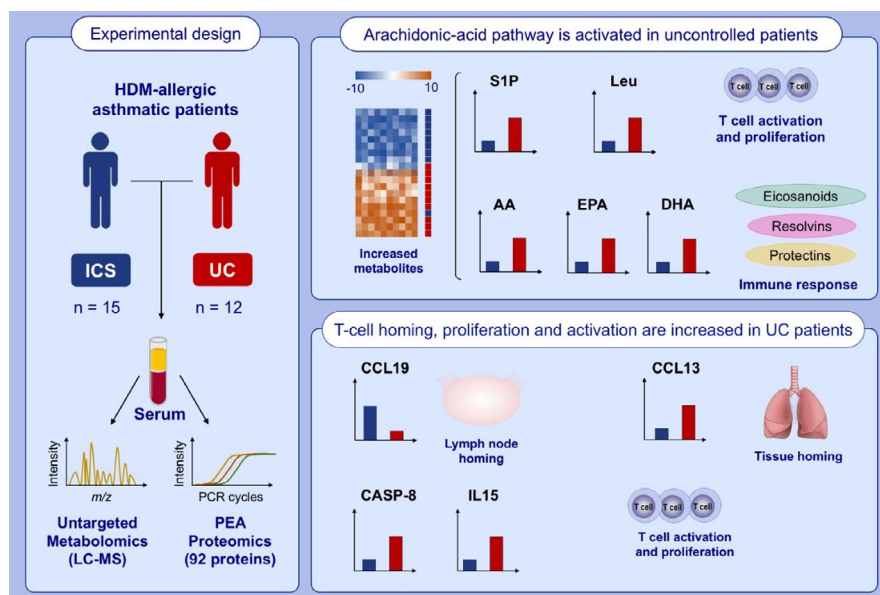
This is an open access article under the terms of the Creative Commons Attribution-NonCommercial-NoDerivs License, which permits use and distribution in any medium, provided the original work is properly cited, the use is non-commercial and no modifications or adaptations are made.

© 2021 The Authors. *Allergy* published by European Academy of Allergy and Clinical Immunology and John Wiley & Sons Ltd.

**Conclusions:** UC patients display a unique fingerprint characterized by inflammatory-related metabolites and proteins, suggesting a pro-inflammatory environment. Moreover, the integration of clinical and experimental data led to a deeper understanding of the mechanisms underlying UC phenotype.

**KEYWORDS**

allergy, asthma, machine learning, metabolomics, proteomics



**GRAPHICAL ABSTRACT**

Severe uncontrolled HDM-allergic asthma (UC) displays an increased T-cell activation and proliferation (IL-15, CASP-8, S1P, Leu) and an increased T-cell tissue recruitment (CCL13) compared to corticosteroid-controlled HDM-allergic asthma (ICS). UC shows an exacerbated inflammatory response with increased levels of inflammatory mediators (AA, EPA, DHA, ...). Integration of clinical and metabolomic data is the best strategy to stratify patients by severity.

**1 | INTRODUCTION**

Asthma is a heterogeneous disease characterized by chronic airway inflammation and a clinical history of respiratory symptoms such as wheeze, shortness of breath, chest tightness and cough that vary over time and in intensity, together with variable expiratory airflow limitation.<sup>1</sup>

Asthma can have multiple phenotypes and endotypes, depending on the clinical features, histopathology, genetics or response to treatment, along with other characteristics.<sup>2</sup> We can distinguish between allergic, intrinsic, neutrophilic, aspirin-intolerant and extensive remodelling asthma,<sup>3</sup> among others. Patients with allergic asthma are usually sensitized to house dust mites (HDM). In fact, IgE titres to HDM correlate with exacerbations in asthma.<sup>4</sup>

HDM are the most relevant inducers of allergic diseases worldwide.<sup>5</sup> HDM allergens include cysteine-proteases (Der p 1, Blo t 1) and chitin-associated proteins (Der p 23), involved in epithelial disruption and remodelling; proteins able to activate TLR4 (Der p 2, Eur

m 2), and lipid-binding proteins (Der p 5, Der p 7 and Der p 21), linked with the establishment of the Th2 response.<sup>5</sup> The Canary Islands in Spain is one of the regions in Europe with higher mite exposure levels and sensitization prevalence to HDM due to its almost tropical climate of high humidity and warm temperatures.<sup>6,7</sup> These features are common with other high-exposure HDM areas like Singapore or New Zealand.<sup>5</sup> Additionally, the exposome in the Canary Islands has been deeply studied<sup>8</sup>; and it is very stable along the island, which makes it a perfect model to minimize variability in the study.

Due to the complexity of asthma, effective treatment is also a challenge. The GINA guideline sets a step-by-step approach, in which treatment with increasing doses and add-on medications are given to patients. For allergic asthma, therapeutic strategies include corticosteroids, bronchodilators, immunotherapy and biological drugs (*i.e.*, anti-IgE or anti-IL5).<sup>1</sup>

Classification of asthmatic allergic patients is a difficult task. Several endotypes and phenotypes have been described. According to their response to treatment, patients have severe asthma if they



either needed treatment from steps 4–5 of the GINA,<sup>1</sup> or 5–6 of the GEMA<sup>9</sup> guidelines (which includes inhaled corticosteroids coupled to long term acting beta-agonists (inhaled CS/LABA) in high doses + antileukotrienes (LTRA) + theophylline (T)) or had to take systemic corticosteroids to achieve control in the previous year.

However, despite having received the treatment previously mentioned, around 3%–10% of patients display severe uncontrolled asthma. These patients often present comorbidities such as obesity, nasal polyposis, allergic rhinitis or food allergy; resulting in a worse quality of life and higher mortality rates.<sup>1,10</sup>

Particularly, in the Canary Islands several studies report frequent respiratory problems in children and high rates of asthma prevalence (69.6%). Moreover, 16% of the asthmatic patients have severe uncontrolled asthma,<sup>11</sup> which is similar to other European countries, such as the United Kingdom where it is close to 18%.<sup>12</sup>

Regardless of this significant prevalence, there is no available effective treatment for these patients. Their treatment options rely on the development of new personalized medicine strategies.

In this study, all the patients were included by the Allergy Service at Hospital Universitario de Gran Canaria Dr Negrin, a group with deep knowledge on asthma management that works in an area with high HDM exposure and with a well-known exposome, resulting in a very homogenous cohort of asthmatic patients stratified according to their response to treatment. This is a unique clinical model to study a complex disease such as allergic asthma.

Here, we used untargeted metabolomics and a bioinformatic analysis, in addition to a proteomics approach, to generate a specific fingerprint associated with uncontrolled allergic asthma that conforms a set of biomarkers with a potential use to develop the personalized intervention strategies that these patients need.

## 2 | METHODS

### 2.1 | Patients

Patient recruitment was conducted within one full year. Eighty-seven patients with a clinical history of asthma, classified by the GINA guideline<sup>1</sup> and with a positive skin-prick test to HDM were enrolled in the Allergy Department of Hospital Universitario de Gran Canaria Dr Negrin (Las Palmas de Gran Canaria, Spain).

Recruited patients were characterized by a very complete clinical history, since they were monitored for at least 5 years prior to the study. Detailed information about patient sensitization profiling and clinical characteristics can be found in Supplementary. All patients signed informed consent and the study was approved by the Ethics Committee of the hospital on the 4th/February/2016 (code: 160009). Serum samples were obtained as described in Supplementary.

Clinical characteristics were compared between the 4 groups. For continuous variables, Shapiro-Wilk test was applied to assess normality of the data. Age and BMI passed the normality test, so we performed ANOVA test with Tukey's post hoc. Onset age and total

IgE, however, did not pass the Shapiro-Wilk test, and were therefore analysed using Kruskal-Wallis with Dunn's post hoc. For categorical variables, chi-square analysis was performed, and for groups with data lower than 5, Fisher's exact was used.

### 2.2 | Metabolomic analysis

Serum samples were prepared and measured in batches, in a randomized order using a liquid chromatography coupled to mass spectrometry (LC-MS) with a quadrupole-time of flight (Q-TOF) analyser (Agilent series 6520). The experiment, as previously described,<sup>13</sup> was measured in electrospray ionization in positive and negative modes (ESI+ and ESI-, respectively). A quality control (QC) sample was prepared by mixing equal volumes of a representative set of samples and was analysed throughout the analyses to ensure instrumental reproducibility. Metabolite annotation was performed using CEU Mass Mediator 3.0 online data base<sup>14</sup> and confirmed through tandem mass experiments (MS/MS) with a fragmentation energy of 20 eV. Full description of sample preparation, instrumental characteristics, data quality, data treatment, statistical analysis and metabolite annotation are stated in Supplementary.

### 2.3 | Proteomic analysis

Serum proteins were analysed by Proximity Extension Assay (PEA) (Olink<sup>®</sup>, Uppsala). PEA is based on the probes linked to paired antibodies recognizing the same protein. Upon the antibodies binding to the target, the primers hybridize and create a PCR product, which is then amplified as the read-out, giving the Normalized Protein Expression (NPX) as result. For this assay, 10 µl of serum of corticosteroid-controlled (ICS) ( $n = 15$ ) and uncontrolled (UC) patients ( $n = 11$ ) were analysed by Olink. Therefore, proteomic analysis was not performed in all samples. We used Target 96 Immuno-Oncology panel (95311, Olink<sup>®</sup>, Uppsala) consisting in 92 proteins involved in processes such as promotion and inhibition of tumour immunity, chemotaxis, vascular & tissue remodelling, apoptosis & cell killing and metabolism & autophagy. Detailed information about quality control, data treatment and statistical analysis can be found in Supplementary.

### 2.4 | Machine-learning model construction

To gather novel insights about the molecular mechanisms involved in the UC allergic asthma phenotype, we employed multi-omic data analysis. The integration and analysis of omics and clinical data with machine-learning (ML) methods offer novel techniques enabling the discovery of new biomarkers.<sup>15</sup> After data pre-processing and down sampling, clinical (50 variables after the exclusion of medication) and metabolomic (86 identified significant metabolites) data were mixed

to create a ML predictor that could classify ICS and UC patients in separate groups. For the ML model, *caret*, *mlbench*, *sjmisc* and *class* R packages were used for k-Nearest Neighbour (k-NN) algorithm. Proteomic data were not included in this analysis because the samples used for metabolomics and proteomics were not always the same. Full description of the data treatment steps, training and testing can be found in Supplementary.

### 3 | RESULTS

#### 3.1 | Patient classification

Patients were classified in 4 groups according to the medication that controlled their symptoms: (1) Mild asthma patients controlled with inhaled or topic corticosteroids, and never with systemic corticosteroids (ICS,  $n = 15$ ); (2) mild-moderate asthma controlled with immunotherapy (IT,  $n = 44$ ); (3) moderate-severe asthma patients controlled with omalizumab (anti-IgE) (BIO,  $n = 16$ ); and (4) severe asthma patients that do not respond to any treatment, or

uncontrolled patients (UC,  $n = 12$ ). More information about these groups can be found in Supplementary.

Moreover, their clinical history was thoroughly analysed. There were no differences related to sex, ethnicity, BMI, smoking status, total IgE levels and type of HDM sensitization among the groups ( $p > 0.05$ ) (Table 1). However, age was found to be significantly higher in the UC group than in the ICS.

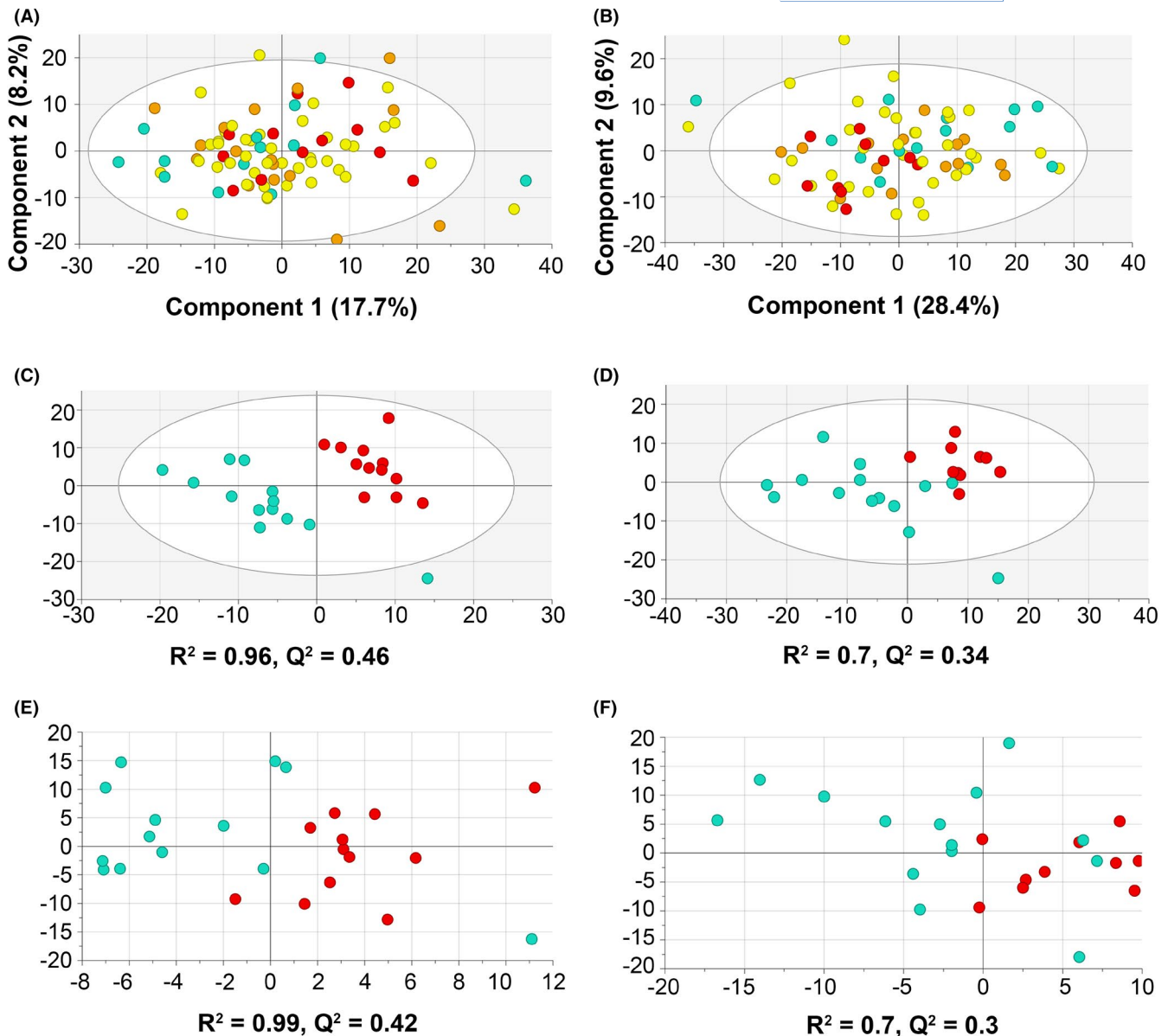
Looking at the medication, patients from the ICS group were treated with antihistamine (AH) and topical corticosteroids (Topic CS), and most of them (93%) administered inhaled CS/LABA. Three of these patients were prescribed LTRA and/or short-effect bronchodilators (SABA). IT patients had a medication pattern like that of ICS patients, although only about a third of them were taking inhaled CS/LABA, while most of them (75%) were prescribed SABA. BIO patients, on the other hand, had more in common with the UC, although the percentage of patients taking topic CS doubled that of UC patients taking this drug (68.8%). The exact treatment and sensitizations of each patient are shown in Table S1. Regarding the UC, all patients were taking both inhaled CS/LABA and SABA, and most of them (75%) were taking LTRA as well. 50% of these

TABLE 1 Clinical information of the patients

	ICS	IT	BIO	UC
N	15	44	16	12
Age (years)	37.2 ± 2.3	37.3 ± 1.5 <sup>†</sup>	43.3 ± 2.4	48.5 ± 3.6*
Onset Age (years)	15.8 ± 2.9	16.1 ± 1.7	12.1 ± 1.8	11.9 ± 2.7
Gender (%F/%M)	66.7/33.3	77.3/22.7	87.5/12.5	58.3/41.7
BMI	26.7 ± 1.4	26.0 ± 0.6	26.8 ± 1.1	28.0 ± 1.2
Smoker (%)	13.3	0	6.3	0
Ex-smoker (%)	6.7	2.3	6.3	25
Total IgE (U)	483.7 ± 164.7	396.2 ± 64.6	503.9 ± 161.5	536.3 ± 181.7
AC (%)	0	0 <sup>†</sup>	43.8*	50*
AH (%)	100	90.9 <sup>†</sup>	37.5*	41.7*
LTRA (%)	13.3	11.4 <sup>†</sup>	75*	75*
Inhaled CS (%)	0	2.3	0	0
Inhaled CS/LABA (%)	93.3	34.1* <sup>†</sup>	100	100
Oral CS (%)	0	0	0	16.7
Topic CS (%)	100	97.7 <sup>†</sup>	68.8*	33.3*
SABA (%)	20	75*	93.8*	100*
T (%)	0	0	0	8.3
NSAID-HS (%)	13.3	6.8	6.3	16.7
<i>D. pteronyssinus</i> (%)	93.3	97.7	93.8	91.7
<i>D. farinae</i> (%)	93.3	93.2	87.5	91.7
<i>L. destructor</i> (%)	66.7	50	43.8	58.3
<i>B. tropicalis</i> (%)	86.7	77.3	81.3	66.7
<i>A. siro</i> (%)	26.7	20.5	0	8.3
<i>T. putrescentiae</i> (%)	53.3	45.5	56.3	58.3

Abbreviations: AC, anticholinergic; AH, antihistaminic; BMI, Body mass index; CS, corticosteroids; Inhaled CS/LABA, inhaled corticosteroids combined with Long-acting beta-adrenoceptor agonist; LTRA, antileukotriene; NSAID-HS, NSAID-hypersensitivity; SABA, short-acting beta-adrenoceptor agonist; T, theophylline; U, ISAC units.

\* $p < .05$  against ICS. <sup>†</sup> $p < .05$  against UC.



**FIGURE 1** Serum metabolomic profile of all patients. A. Unsupervised PCA model of all groups (ICS, IT, Bio, UC) built using the 833 signals for ESI+ that complied with quality criteria. B. Unsupervised PCA model of all groups built using the 565 signals for ESI- that complied with quality criteria. C. PLS-DA model for patients controlled with non-systemic corticosteroids (ICS) vs patients with uncontrolled asthma (UC) comparison in LC-MS (ESI+). D. PLS-DA model for ICS vs UC comparison in LC-MS (ESI-). E. OPLS-DA model for ICS vs UC comparison in LC-MS (ESI+). F. OPLS-DA model for ICS vs UC comparison in LC-MS (ESI-). All data were UV scaled. (Key: 'ICS': blue, 'IT': yellow, 'BIO': orange, 'UC': red).  $R^2$  is the capability of the model to classify the samples;  $Q^2$  is the capability of the model to predict the class of a new sample

patients were prescribed with anticholinergics (AC); 41.7%, with AH; and 16.7% were having oral corticosteroid (Oral CS), while 8.3% were having theophylline (T). 33.3% were taking topic CS.

### 3.2 | Severe uncontrolled asthmatic patients display a unique metabolic fingerprint

The metabolomic signature of each patient was obtained by LC-MS. A total of 833 signals for ESI+ and 565 for ESI- complied with the quality criteria for metabolomics. Clustering of the QC injections in

the non-supervised (PCA) model indicated the high quality of the data, while dispersion of the samples showed the biological variability of the patients (Figure S1).

Patterns of the groups were analysed by PCA models for ESI+ and ESI- modes, respectively (Figure 1A,B). UC patients clustered together, especially in the ESI- mode. Additionally, we performed PCA models to see the differences between the UC group and the others, but only differences between ICS and UC patients were observed (Figure S2).

More restrictive analysis was performed to assess the metabolic differences between ICS and UC patients, the ones that differed most

in terms of asthma control. To evaluate real differences between ICS and UC groups, PLS-DA and OPLS-DA models were performed (Figure 1C–F). The robustness of OPLS-DA models was assessed by a seven-fold cross-validation.<sup>16</sup> The resulting models showed good quality parameters:  $R^2$  (0.70–0.96) for the variance explained, and  $Q^2$  (0.3–0.46) for the prediction capability by the model. The cross-validated OPLS-DA scores plot showed that the percentage of accuracy was of 84% and 75% for ESI+ and ESI– modes (Figure 1D–E), respectively. From these models two ICS patients were observed to be outliers (bottom right in the panels from Figure 1C,F). The outlier patient from the ESI+ mode has the lowest FEV1 and FVC of the group ( $\approx 70\%$ ), while the outlier patient from the ESI– mode has hypersensitivity to NSAIDs drugs. However, we did not find any remarkable reason to exclude these patients from the study.

Furthermore, as age was found significant between ICS and UC groups, PCA models were performed to illustrate their significance (Figure S3). We found that only for the ESI– mode there is a slightly trend of clustering inside ICS group between younger or older than 35 years old.

Together, these results reveal that the UC group is different from the ICS group in terms of their metabolic fingerprint. However, potential differences with IT and BIO might be expected.

### 3.3 | Severe uncontrolled asthma metabolic fingerprint is characterized by increased levels of lipid mediators

Univariate analysis was carried out to obtain significant metabolic signals in the ICS vs UC comparison, finding 280 with  $p < 0.05$  (204 of them had a FDR  $< 0.2$ ). Using MS/MS fragmentation experiments, we could annotate (identify) 89 of these metabolites. Most of them had a FDR  $< 0.2$  (83 out of 89); which is valid in exploratory studies as it allows to find more potential biomarkers.<sup>17–19</sup>

Next, aiming to see if the metabolic signals were able to stratify the patients according to their group, we built a heatmap with hierarchical clustering analysis (HCA) (Figure 2) using the 280 statistically significant signals ( $p < 0.05$ ). We found that ICS patients (in light blue) are stratified at the bottom of the heatmap, while UC patients (in red) are located in the top. Accordingly, ICS and UC patients are able to be clustered separately using these 280 signals, as expected. IT and BIO patients did not cluster in any specific part of the heatmap, although most BIO patients seemed to be closer to UC patients. Therefore, we demonstrate significant metabolic features that differentiate ICS and UC and point out specific features for IT and BIO patients, although no significant clustering was demonstrated.

Since age was significant between ICS and UC groups (Table 1 and Figure S2), ANCOVA was used to remove those metabolites that were affected by age. Therefore, we ended up with 86 annotated metabolites that were not affected by age. ANCOVA test, physico-chemical and statistical details of annotated metabolites are shown in Tables S2–S4, respectively. From these, we obtained 33 metabolites that were uniquely identified.

Among the significant annotated metabolites there were amino acids, bile acids, fatty acids, phospholipids, sphingolipids and vitamins; with phospholipids being the greatest group. Changes in the abundance of compounds between ICS and UC are presented in Figure 3 and Figure S4.

Most of these compounds, such as lysophosphocholines (LPC), lysophosphoethanolamines (LPE), lysophosphatidylinositols (LPI), leucine, arginine, arachidonic acid, sphingosine-1-phosphate (S1P) and retinol were increased in the UC group; with the exception of bilirubin, deoxycholic acid (Figure S4) and phosphocholine 16:0/20:5 (Figure 3), which were decreased in the UC group.

We then performed a pathway analysis of the unique annotated metabolites ( $n = 33$ ) to look for the routes in which they are involved (Table S5). We found an altered phospholipase A2 (PLA2) pathway (100% of affected metabolites in this route, whose changes are shown in Figure 4), along with arachidonic acid metabolism (79.81%), lipoprotein remodelling (52%), phospholipid biosynthesis (95.83%), sphingolipid metabolism (100%) and biosynthesis (82.86%), and other lipid-related routes (Table S5). There are also changes in signalling and transport pathways. Interestingly, there is an increase in metabolites related to a deficiency in leukotriene C4 production (91.5%). These routes are significantly enriched in the UC compared to the ICS patients.

Figure 5 represents metabolites from oleic acid and arachidonic acid pathways. We observed that all measured metabolites that participate in these pathways are increased in UC patients. Thus, we conclude that UC patients have an altered lipid metabolism, with increased levels of lipid mediators in serum compared to the ICS group.

### 3.4 | UC patients have a distinctive expression of inflammatory-related proteins

In addition to the metabolic fingerprint, we studied the protein serum profile in ICS and UC patients. We measured the expression of 92 proteins (Table S6) and found that 8 of them were significantly different between ICS and UC ( $p < 0.05$ ) (Figure 6A). From these, one of them (CASP-8) also had FDR  $< 0.2$  (Table S6). A STRING analysis was performed in order to find relations between the differentially expressed proteins. We were able to link 7 out of the 8 proteins (Figure 6B). We found that CCL13, ARG1, IL15, TNFRSF12A and CASP-8 were increased in the UC patients, whereas sCD4, CCL19 and IFN $\gamma$  were decreased (Figure 6C).

Finally, we looked for biological processes in which these proteins were involved using gene ontology (GO) pathway enrichment analysis (Table S7). We found that these proteins are linked to immune response including cytokine response, leukocyte differentiation and adhesion, T cell activation, and nitrogen metabolism, among other pathways.

Therefore, proteomic results support that UC patients have an altered inflammatory response, and point out immune cell activation as a possible key mechanism.

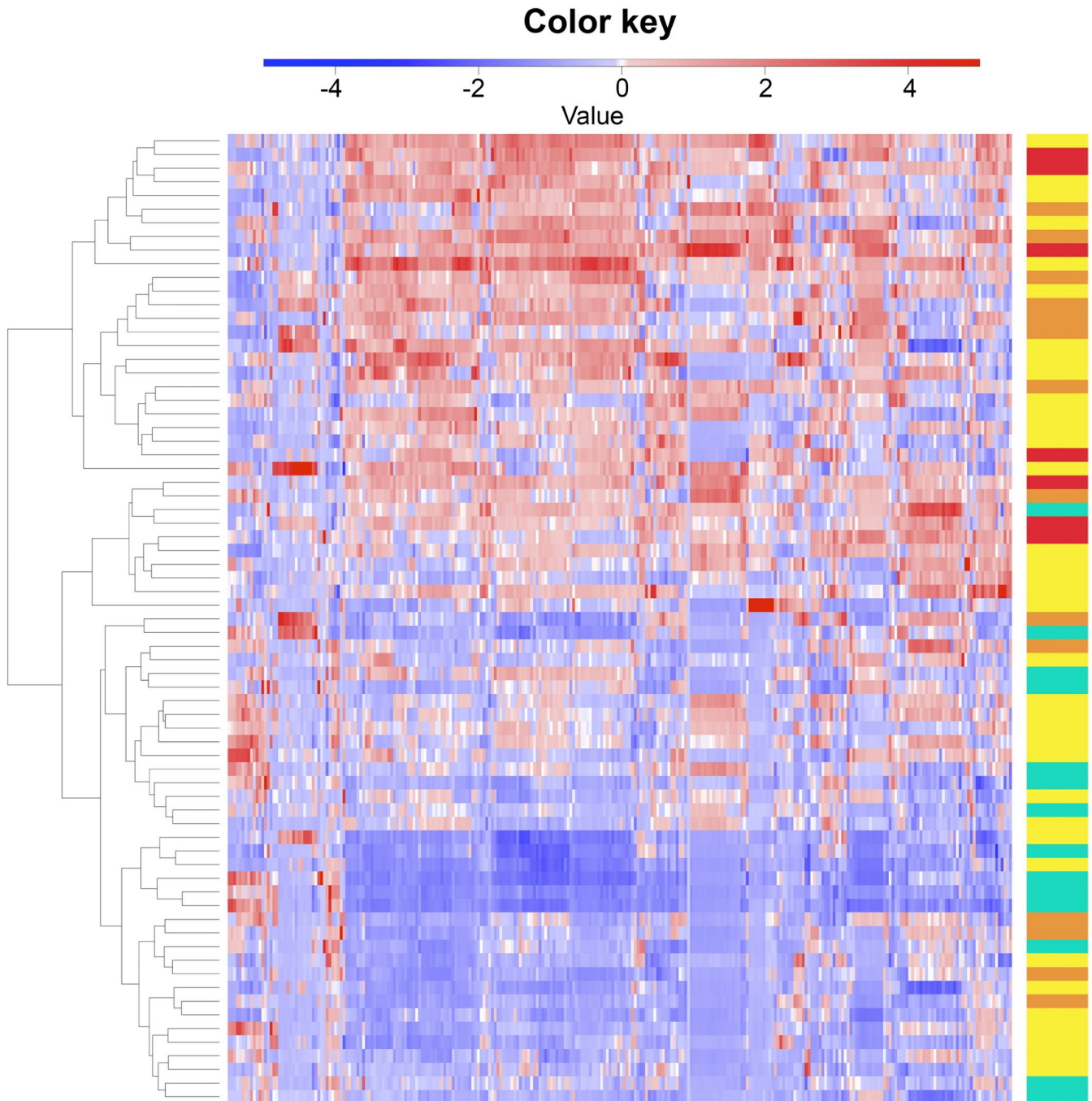


**FIGURE 2** Hierarchical clustering heatmap of the patients from the four groups (in rows) and the 280 significant metabolites between ICS and UC (in columns). Red cells represent an increase of the specific metabolite in that sample, whereas blue cells represent decreased metabolites. Samples and metabolites are clustered according to their similarity, and the group they belong to is showed with colours at the right. (Key: 'ICS': light blue; 'IT': yellow; 'BIO': orange; 'UC': red)

### 3.5 | Machine-learning models for UC classification

Aiming to obtain a more accurate profile of the UC asthmatic phenotype, we integrated both the metabolomic and clinical data in a ML model. Since the proteomic analysis was performed in a limited number of samples, it could not be included in the model. The ML model aim was to find which variables could be used to classify UC and ICS patients. The k-NN model is a ML algorithm that classify a sample

based on all the variables given, which has been tested for breast cancer prediction model.<sup>20</sup> The k-NN learning algorithm requires us to specify how many neighbours ( $k$ ) are going to be considered. To obtain this parameter we used the elbow method. The lack of elbow when using only clinical or metabolomic data alone suggests that these datasets are not good enough to predict classification of UC and ICS patients on their own. When using both datasets combined, the elbow test suggested that the  $k$  parameter should be either 2 or

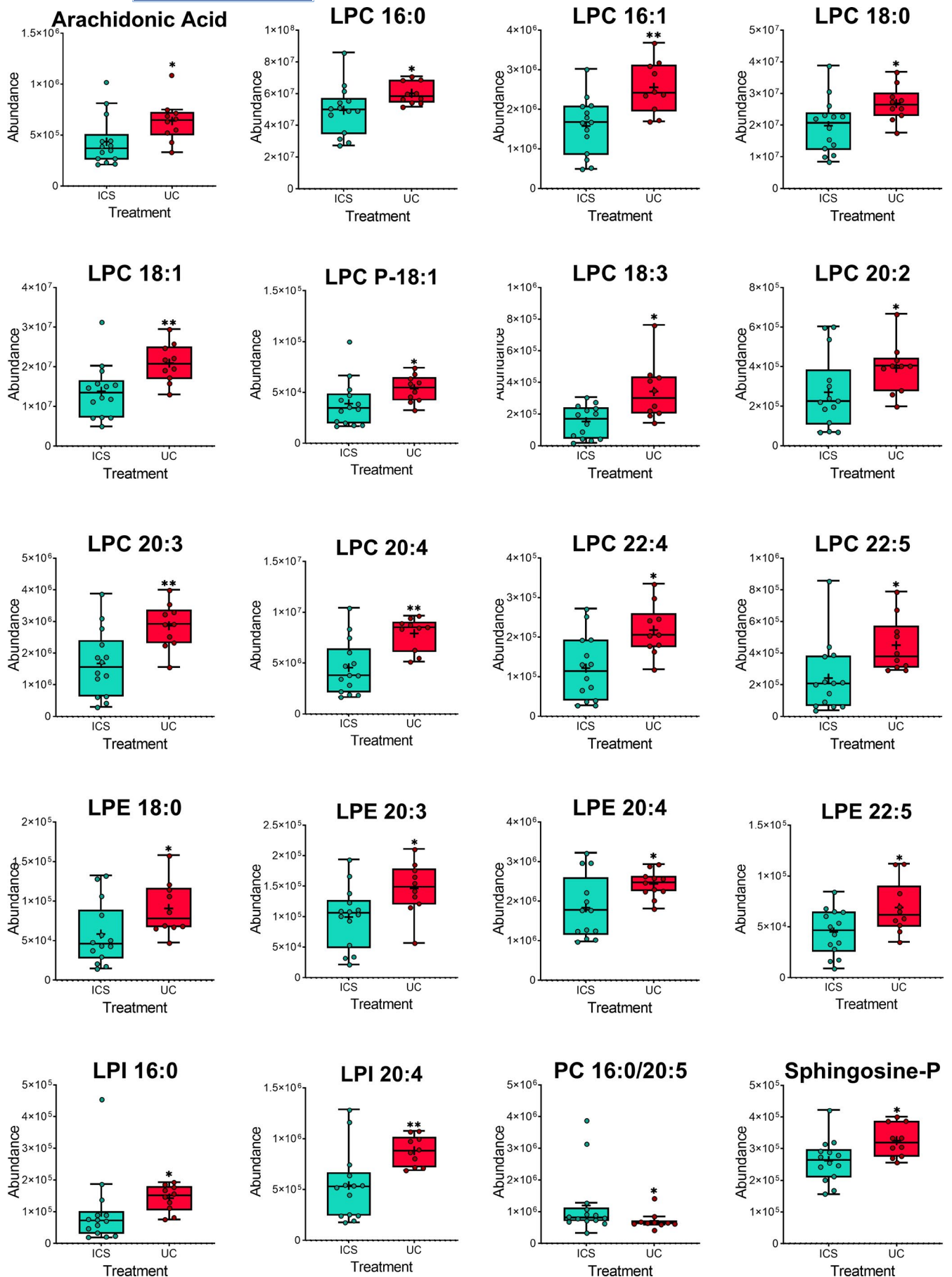
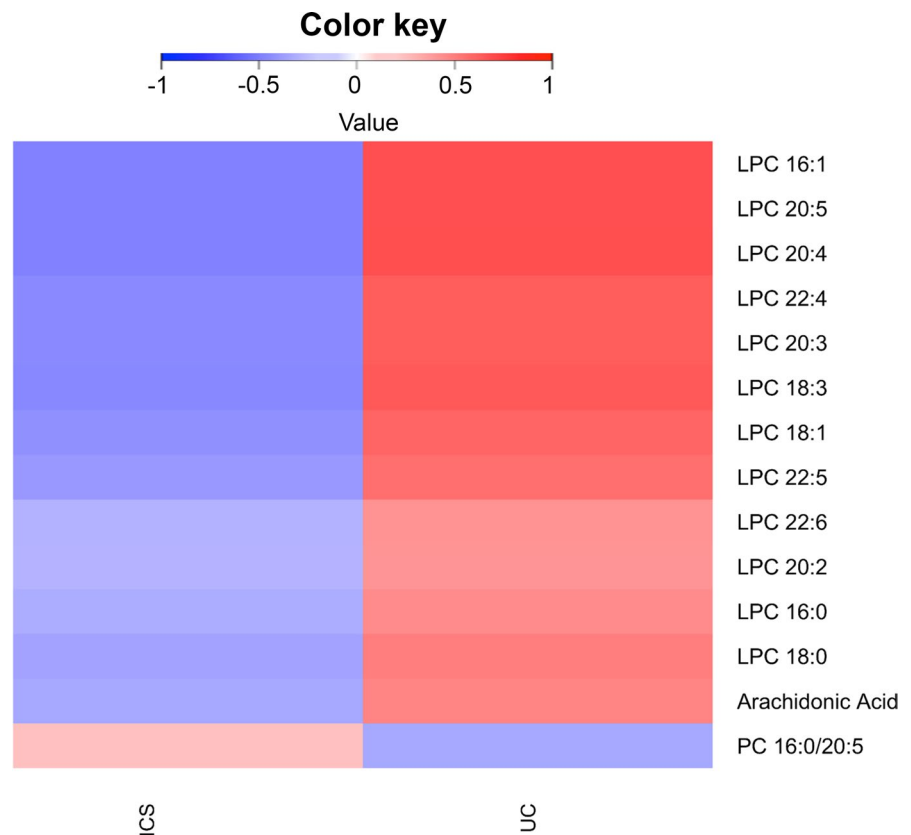


FIGURE 3 Legend on next page

**FIGURE 3** Trajectories of the most relevant identified compounds. Box and whiskers plots with mean are represented for corticosteroid-controlled (ICS, blue) and uncontrolled (UC, red) groups. For metabolites that had more than one  $m/z$  or that were detected in both ESI modes, the most abundant  $m/z$  overall was represented. Mean is represented with '+' inside the boxes and individual data points are shown as blue (ICS) or red (UC) dots. Mann-Witney  $U$  test was used to calculate significant differences. \* $p < .05$ ; \*\* $p < .01$ . Other trajectories can be found in Figure S4

**FIGURE 4** Changes in the abundance of metabolites in the PLA2 pathway between ICS and UC patients. Red cells represent an increase in the amount of a metabolite, whereas blue cells represent a decrease. LPC: lysophosphocholine, PC: phosphocholine



3, so we built one model with each value to select the one with a better performance. However, both models ended up being identical.

From the original 136 variables (50 clinical variables and 86 metabolites), we ended with a k-NN model that used 39 (16 clinical and 23 metabolomic variables). This model was able to correctly classify all patients but one. The accuracy, specificity, sensibility, positive predicted value (PPV) and negative predicted value (NPV) were all  $\geq 0.75$  (Table S8). We also performed a variable selection analysis, but the resultant model had worst performance (data not shown).

#### 4 | DISCUSSION

Management of uncontrolled severe asthma entails a significant challenge for healthcare professionals. These patients are difficult to identify in the first place and need personalized treatment because they do not respond to conventional pharmacological interventions. We believe that a better knowledge regarding the metabolic, proteomic and biological pathways associated with this specific phenotype will provide new insights and will be helpful towards the management of these patients.

Here, we studied a cohort of HDM-allergic asthmatic patients from a high-exposure HDM region. The Canary Islands are located near the west coast of North Africa, close to the Sahara Desert, and thus, are impacted by Saharan Dust (calima) during approximately 30% of the year. The most common HDM sensitizers in the Canary Islands are *Dermatophagoides pteronyssinus* and *Blomia tropicalis*, which are linked to asthma prevalence.<sup>7,21</sup> Moreover, prevalence of persistent rhinitis and asthma is higher in this area than in the mainland of Spain, as previously reported,<sup>6,11</sup> probably due to the higher sensitization profile to perennial allergens and favourable ecological conditions supporting mite growth. Similar conditions have been described in other insular areas like the United Kingdom, Australia or New Zealand.<sup>7,12</sup> Thus, even if this study was carried out in a specific region, the results can be extrapolated to many Atlantic climate areas.

Moreover, this cohort of patients is characterized by a well-known exposome and a recruitment process by a single clinical group with more than 30 years of experience in the field, which assures the uniformity of inclusion criteria and treatment strategy. This fact minimizes variability factors, making this a unique asthma model that is representative of the severe allergic asthma phenotype.

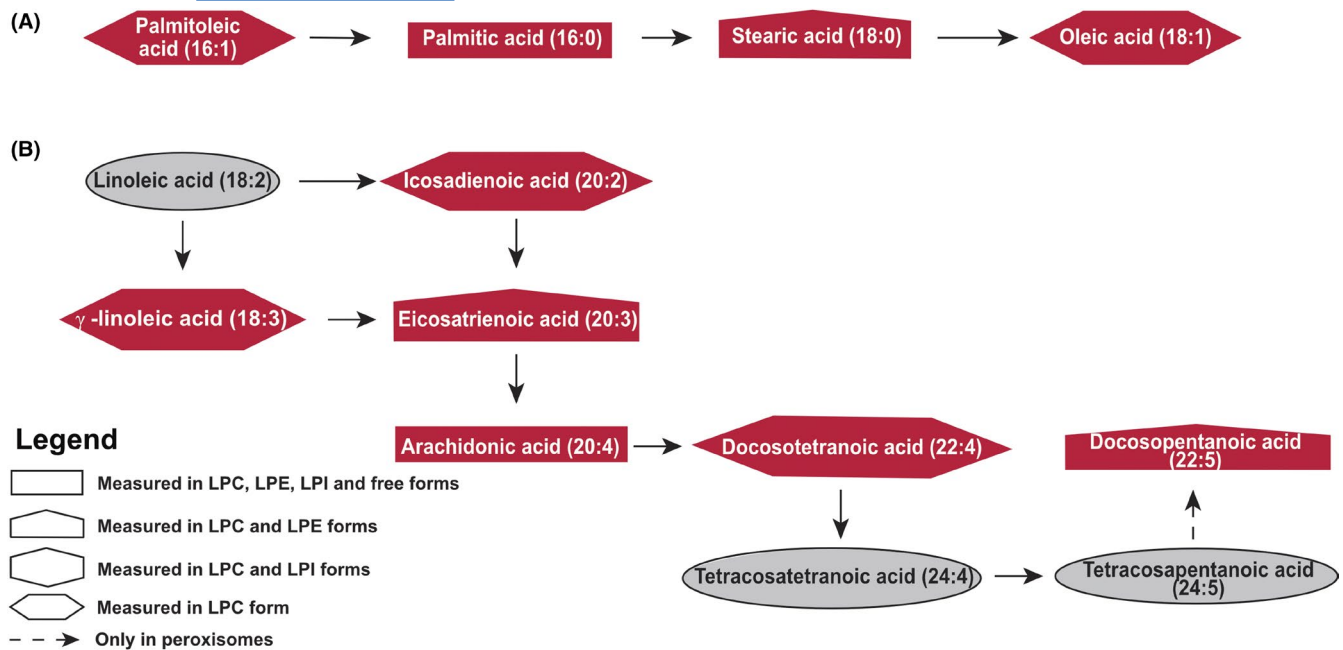


**FIGURE 5** Pathways of lipid metabolism in uncontrolled patients. A. Oleic acid pathway; B. Arachidonic acid pathway. In red, metabolites increased in uncontrolled patients (UC) with respect to corticosteroid-controlled patients (ICS); in grey, metabolites that were not significantly changed between UC and ICS patients

According to their response to treatment, patients were classified into 4 groups. Patients that controlled asthma with non-systemic CS were considered mild HDM-allergic asthmatic patients (ICS); and patients that do not respond to none of the available treatments are considered uncontrolled HDM-allergic asthmatic patients (UC). Additionally, patients controlled with IT and biological drugs were also included, showing a disperse distribution probably due to several factors, like time of treatment, administration pathway or response to treatment, that might need further analysis. Moreover, BIO patients were only treated with omalizumab, since it was the only biological drug approved for the treatment of asthma in the Canary Islands at the time. Therefore, it will be relevant to perform further studies considering other biologics such as mepolizumab or benralizumab.

Here, we combine an appropriate clinical classification, focusing on disease control, with a wide range of techniques to identify metabolites and proteins.

Metabolomics is a promising tool in the detection of dynamic changes and alterations in the metabolism associated to a pathology.<sup>22</sup> In fact, the metabolome has been described to be closely linked to the phenotype of a disease and can be an extremely useful tool when evaluating the effect of treatments. From a practical point of view, it uses very sensitive and specific techniques, such as LC-MS, which allows the simultaneous detection of a great variety of metabolites in each biological sample.<sup>23,24</sup>

In this study, we performed an untargeted metabolomic analysis in all samples from each experimental group, what results, after a complex and laborious statistical analysis, into the identification of several significant signals that conform the metabolomic signature of UC group. Therefore, this study should be understood as

exploratory. In addition to the metabolites, we have also identified the biological pathways associated to those metabolic changes. However, further analyses in prospective studies are needed to validate these metabolites as potential biomarkers in a new and larger cohort of patients, including other subtypes of asthma.

Most of the identified compounds (94%) have a FDR < 0.2. For exploratory studies, setting higher cut-offs allows them to find more potential biomarkers resulting in a more extensive knowledge<sup>17-19</sup>; although validation in further studies is critical to ensure that the resulting biomarkers can properly classify the patients.<sup>25</sup>

Our metabolomic results show that LPC, LPE and LPI, along with arachidonic acid, are increased in the UC compared to the ICS. Lipid metabolism has been previously associated with asthma, as lipid mediators are related to inflammatory signalling pathways. Yoder *et al*<sup>26</sup> previously reported increased levels of LPC 16:0 and LPC 18:0 in the bronchoalveolar lavage fluid (BALF) of patients with moderate asthma compared to non-asthmatic or mild-asthmatic patients. This was also accompanied by an increase in PLA2 activity, a pathway that we report increased in UC patients as well. Moreover, Pang *et al*<sup>27</sup> compared eosinophilic and non-eosinophilic asthma, finding that LPC 18:1 was increased in the eosinophilic phenotype. As a matter of fact, LPC have been reported to have a role in eosinophil regulation.<sup>28-30</sup> Therefore, the observed increase in LPC seems to be directly associated with an exacerbated inflammatory response taking place in UC patients.

LPC have also been associated to arachidonic acid release in human derived monocytes.<sup>31</sup> Arachidonic acid (C 20:4; AA), eicosapentaenoic acid (C 20:5; EPA) and docosahexaenoic acid (C 22:6; DHA) were detected either as free fatty acids or in LPC, LPE and/or LPI forms. An enrichment of these metabolites and their implied



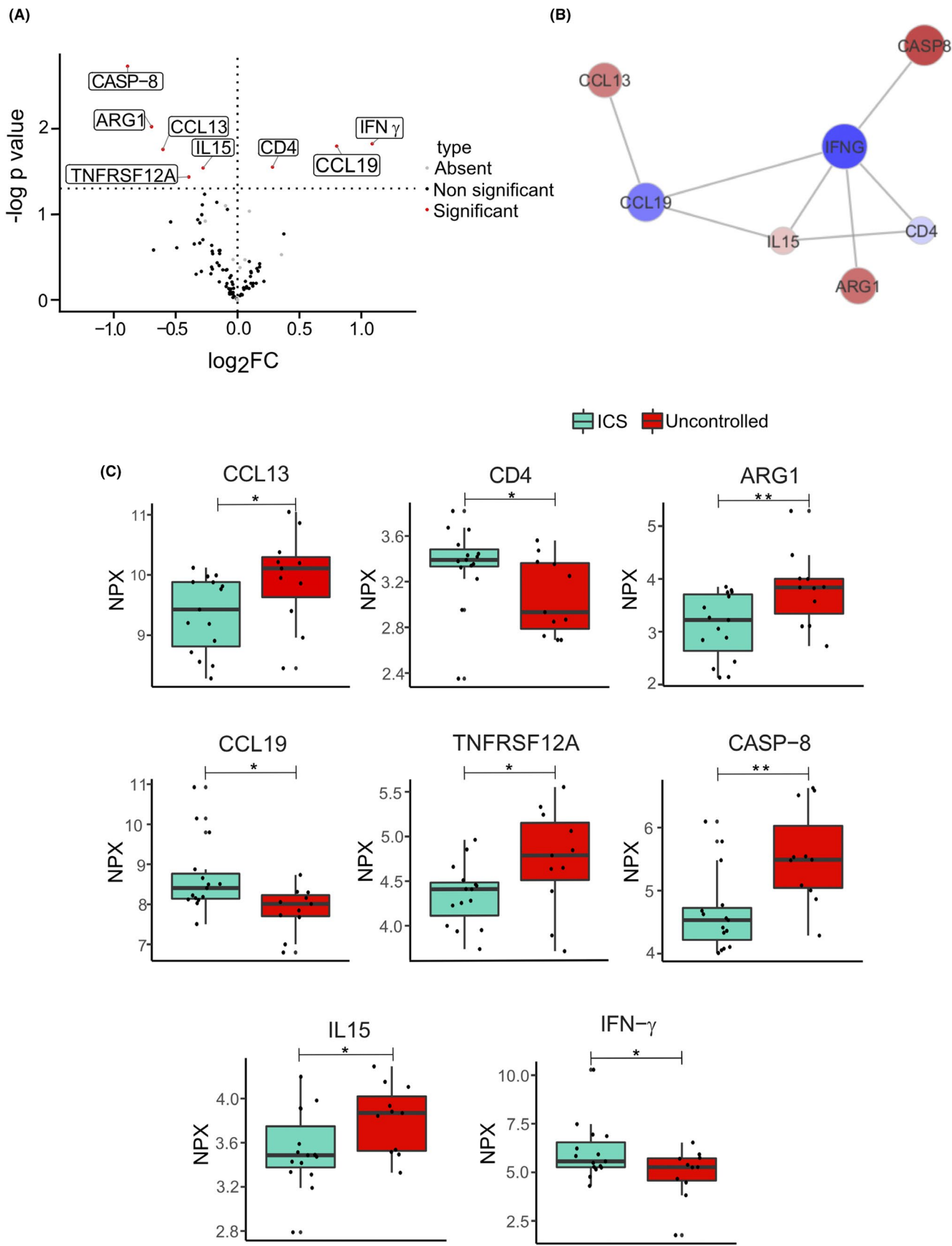


**FIGURE 6** Specific serum proteomic profile of ICS and UC patients. A. Volcano plot of the differences in proteomic profile between ICS and uncontrolled patients. B. STRING analysis of significant proteins. An increase in the size of the circles and intensity of colour signals an increase in  $\log_2FC$ . Red signals an increase of the protein expression, while blue means that the protein is decreased. C. Boxplot of the relative abundances of significant proteins between ICS (light blue) and UC (red). Significance \* $p < .05$ , \*\* $p < .01$

pathways has been previously reported in asthma.<sup>27,32-34</sup> These fatty acids act as precursors of eicosanoids (prostaglandins, leukotrienes, lipoxins), resolvins and protectins through the activity of enzymes such as cyclooxygenase (COX), lipoxygenase (LOX) or cytochrome P450.<sup>35,36</sup> This suggests that UC patients have a significant activation of these pathways, which are involved in the regulation of the immune response.

S1P was also increased in UC patients. This metabolite has been previously associated with asthma and other lung inflammatory diseases,<sup>37</sup> along with asthma severity.<sup>32,38</sup> Interestingly, we have reported an increase of S1P levels in plasma of patients with severe allergy.<sup>39</sup> Moreover, S1P also plays a key role in regulation of T cells lifespan and recruitment.<sup>40</sup> Thus, this increase might point to the activation of T cells in UC patients, which may play a role in uncontrolled asthma pathogenesis.

Other metabolites significantly altered in UC patients are arginine, which is related to the nitric oxide (NO) pathway<sup>38,41-44</sup>, and leucine, associated with the activation of mTORC1 pathways responsible for T cells activation, proliferation and differentiation.<sup>45</sup>

Furthermore, proteomic analysis reveal that UC patients seems to have an increased pro-inflammatory T cell response, which is also supported but the changes in S1P and leucine abovementioned. We found an increase in CCL13 and IL-15 in the UC patients, which have been shown to attract monocytes and lymphocytes and promote T cell proliferation, suggesting an activation of the immune response.<sup>46-49</sup> This activation would be mainly produced in the mucosa, as there was a reduction of CCL19, responsible of lymphoid organ homing, and soluble CD4.<sup>50-52</sup> Moreover, this is a type 2 response, as shown by the decrease of IFN $\gamma$ . This inflammation was accompanied by complementary epithelial and endothelial permeability and growth, as shown in the increase of proangiogenic factor TNFRSF12A and ARG 1, which regulates NOS activity.<sup>53,54</sup> Finally, this inflammation might be maintained in time by the increased levels of CASP-8, as this caspase is important to maintain T cell proliferation and has been shown to inactivate RIPK1, which limits TNF and inflammatory responses.<sup>55,56</sup>

Together, metabolomic and proteomic data demonstrate unique biological mechanisms associated with HDM-allergic asthmatic uncontrolled asthma patients (UC) when compare with the mild phenotype (ICS), which are mainly associated with a pro-inflammatory environment and T cell activation and proliferation.

Next, aiming to integrate clinical and demographical with metabolic data and to identify potential classifiers for UC patients, we performed a ML approach. K-NN algorithm is one of the simplest ML algorithms, but it has a very efficient performance.<sup>57</sup> Using this model, we could properly classify UC patients with more than 80% of accuracy. In fact, our results demonstrate that inclusion of clinical data in the ML model significantly improved patient's classification, demonstrating the need to develop more bioinformatic models that allow the integration of clinical and omics data to generate a complete picture of the patient phenotype.

Currently, high throughput techniques are already being used in other disciplines, like cancer or even in allergy (e.g. protein arrays).

The next step in precision medicine will be to have a more detailed and accurate vision of the patient through the integration of data from one or more high throughput techniques (multi-omics) with clinical and demographical data. This type of analysis will provide a better comprehension of the pathology, and will help develop better systems to classify patients, design personalized treatments and reach a more accurate diagnosis.

Together, these data show a set of specific biological features associated with the UC phenotype. Metabolomics, proteomics and clinical data all point towards a systemic and sustained inflammatory response, underlined by an exacerbated lipid, S1P and NO metabolism, and an increase in T cells activation and proliferation. Moreover, our results support the need of exhaustive clinical criteria to better characterize and classify these patients. These observations shed light into the molecular and cellular mechanisms underlying this phenotype and provide a starting point to design novel personalized treatments for these patients.

## ACKNOWLEDGEMENTS

We would like to thank all institutions involved: Institute of Applied Molecular Medicine (IMMA, Universidad CEU San Pablo, CEU Universities, Madrid), Centre of Metabolomics and Bioanalysis (CEMBIO, Universidad CEU San Pablo, CEU Universities, Madrid), and Swiss Institute of Allergy and Asthma Research (SIAF); as well as the Hospital Universitario de Gran Canaria Dr Negrín (Las Palmas de Gran Canaria, Spain). This work was supported by ISCIII (PI18/01467 and PI19/00044), cofounded by FEDER 'Investing in your future' for the thematic network and co-operative research centres ARADyAL RD16/0006/0015; as well as by the grant from Ministerio de Ciencia, Innovación y Universidades co-financed with FEDER RTI2018-095166-B-I00. This work was also supported by the Ministry of Science, Innovation and Universities in Spain (PCI2018-092930) co-funded by the European program ERA HDHL - Nutrition & the Epigenome, project Dietary Intervention in Food Allergy: Microbiome, Epigenetic and Metabolomic interactions DIFAMEM. M.I.D.D. and J.R.-C. are supported by FPI-CEU predoctoral fellowships, D.O. is funded by JPI-DIFAMEM PCI2018-092930 and A.V. is funded by a postdoctoral research fellowship from ARADyAL. MS is funded by the Swiss National Science Foundation (SNFS) grant 310030\_189334/1.

## CONFLICT OF INTEREST


Delgado-Dolset has nothing to disclose. Dr. Obeso has nothing to disclose. Rodríguez-Coira has nothing to disclose. Dr. Tarín has nothing to disclose. Dr. Tan has nothing to disclose. Dr. Cumplido Bonny has nothing to disclose. Dr. Cabrera Santana has nothing to disclose. Dr. Angulo Díaz-Parreño has nothing to disclose. Dr. Barbas reports grants from Ministerio de Ciencia, Innovación y Universidades co-financed with FEDER RTI2018-095166-B-I00, during the conduct of the study. Dr. Sokolowska reports grants from Swiss National Science Foundation (SNSF), grants from GSK, outside the submitted work. Dr. Barber reports grants from ALK, Allero Therapeutics, personal fees from ALK, AIMMUNE, outside the submitted work and

the grant from the Ministry of Science, Innovation and Universities in Spain (PCI2018-092930) co-funded by the European program ERA HDHL - Nutrition & the Epigenome, project Dietary Intervention in Food Allergy: Microbiome, Epigenetic and Metabolomic interactions DIFAMEM. Dr. Carrillo has nothing to disclose. Dr. Villaseñor has nothing to disclose. Dr. Escribese has nothing to disclose.

## AUTHOR CONTRIBUTIONS

MME was the PI and together with DB, AV, CB and MS designed and supervised the research. TC, JAC and AC recruited the patients and obtained the samples. MIDD, JR-C, AV and DO performed the metabolomics analysis and data treatment. JR-C and GT performed the proteomic analysis and data treatment. MIDD performed analysis of the results together with CT and SA. All authors contributed to the writing of the manuscript and have given approval to the final version of the manuscript.

## ORCID

María Isabel Delgado-Dolset  <https://orcid.org/0000-0001-7924-5454>

David Obeso  <https://orcid.org/0000-0001-7875-7327>

Juan Rodríguez-Coira  <https://orcid.org/0000-0003-0517-7078>

Ge Tan  <https://orcid.org/0000-0003-0026-8739>

Santiago Angulo  <https://orcid.org/0000-0002-7868-7442>

Coral Barbas  <https://orcid.org/0000-0003-4722-491X>

Milena Sokolowska  <https://orcid.org/0000-0001-9710-6685>

Domingo Barber  <https://orcid.org/0000-0002-5488-5700>

Alma Villaseñor  <https://orcid.org/0000-0002-6652-2739>

María M. Escribese  <https://orcid.org/0000-0001-5057-5150>

## REFERENCES

- Global Initiative for Asthma. *Global strategy for asthma management and prevention*. 2020. [www.ginasthma.org](http://www.ginasthma.org)
- Campo P, Rodríguez F, Sánchez-García S, et al. Phenotypes and endotypes of uncontrolled severe asthma: new treatments. *J Investig Allergol Clin Immunol*. 2013;23:76-88. quiz 1 p. follow 88.
- Agache I, Akdis C,utel M, Virchow JC. Untangling asthma phenotypes and endotypes. *Allergy*. 2012;67:835-846.
- Kennedy JL, Heymann PW, Platts-Mills TAE. The role of allergy in severe asthma. *Clin Exp Allergy*. 2012;42:659-669.
- Sánchez-Borges M, Fernandez-Caldas E, Thomas WR, et al. International consensus (ICON) on: clinical consequences of mite hypersensitivity, a global problem. *World Allergy Organ J*. 2017;10:14.
- Julià Serdà G, Cabrera Navarro P, Acosta Fernández O, et al. High prevalence of asthma symptoms in the Canary Islands: climatic influence? *J Asthma*. 2005;42:507-511.
- Julià-Serdà G, Cabrera-Navarro P, Acosta-Fernández O, et al. High prevalence of asthma and atopy in the Canary Islands, Spain. *Int J Tuberc Lung Dis*. 2011;15:536-541.
- Barber D, Arias J, Boquete M, et al. Analysis of mite allergic patients in a diverse territory by improved diagnostic tools. *Clin Exp Allergy*. 2012;42:1129-1138.
- Plaza MV. GEMA4.0. Guía española para el manejo del asma. *Arch Bronconeumol*. 2015;51:2-54.
- Peters SP, Ferguson G, Deniz Y, Reisner C. Uncontrolled asthma: a review of the prevalence, disease burden and options for treatment. *Respir Med*. 2006;100:1139-1151.
- Suárez-Lorenzo I, Cruz-Niesvaara D, Rodríguez-Gallego C, Rodríguez de Castro F, Carrillo-Díaz T. Epidemiological study of the allergic population in the north of Gran Canaria. *J Investig Allergol Clin Immunol*. 2018;28:212-215.
- European Respiratory Society. *European Lung White Book*. 2003;16-25.
- Rodríguez-Coira J, Delgado-Dolset M, Obeso D, et al. Troubleshooting in large-scale LC-ToF-MS metabolomics analysis: solving complex issues in big cohorts. *Metabolites*. 2019;9:247.
- Gil-de-la-Fuente A, Godzien J, Saugar S, et al. CEU mass mediator 3.0: a metabolite annotation tool. *J Proteome Res*. 2019;18:797-802.
- Reel PS, Reel S, Pearson E, Trucco E, Jefferson E. Using machine learning approaches for multi-omics data analysis: a review. *Biotechnol Adv*. 2021;49:107739.
- Triba MN, Le Moyec L, Amathieu R, et al. PLS/OPLS models in metabolomics: the impact of permutation of dataset rows on the K-fold cross-validation quality parameters. *Mol Biosyst*. 2015;11:13-19.
- Chen M, Zhou K, Chen X, et al. Metabolomic analysis reveals metabolic changes caused by bisphenol a in rats. *Toxicol Sci*. 2014;138:256-267.
- Fiehn O, Garvey WT, Newman JW, Lok KH, Hoppel CL, Adams SH. Plasma metabolomic profiles reflective of glucose homeostasis in non-diabetic and type 2 diabetic obese African-American women. *PLoS One*. 2010;5:e15234.
- Putluri N, Shojaie A, Vasu VT, et al. Metabolomic profiling reveals potential markers and bioprocesses altered in bladder cancer progression. *Cancer Res*. 2011;71:7376-7386.
- Hajiloo M, Damavandi B, HooshSadat M, et al. Breast cancer prediction using genome wide single nucleotide polymorphism data. *BMC Bioinformatics*. 2013;14:S3.
- Julià-Serdà G, Cabrera-Navarro P, Acosta-Fernández O, Martín-Pérez P, García-Bello MA, Antó-Boqué J. Prevalence of sensitization to *Blomia tropicalis* among young adults in a temperate climate. *J Asthma*. 2012;49:349-354.
- Villaseñor A, Rosace D, Obeso D, et al. Allergic asthma: an overview of metabolomic strategies leading to the identification of biomarkers in the field. *Clin Exp Allergy*. 2017;47:442-456.
- Crestani E, Harb H, Charbonnier L-M, et al. Untargeted metabolomic profiling identifies disease-specific signatures in food allergy and asthma. *J Allergy Clin Immunol*. 2020;145:897-906.
- Delgado-Dolset MI, Obeso D, Sánchez-Solares J, et al. Understanding systemic and local inflammation induced by nasal polyposis: role of the allergic phenotype. *Front Mol Biosci*. 2021;8:409.
- Vinaixa M, Samino S, Saez I, Duran J, Guinovart JJ, Yanes O. A guideline to univariate statistical analysis for LC/MS-based untargeted metabolomics-derived data. *Metabolites*. 2012;2:775-795.
- Yoder M, Zhuge Y, Yuan Y, et al. Bioactive lysophosphatidylcholine 16:0 and 18:0 are elevated in lungs of asthmatic subjects. *Allergy Asthma Immunol Res*. 2014;6:61.
- Pang Z, Wang G, Wang C, Zhang W, Liu J, Wang F. Serum metabolomics analysis of asthma in different inflammatory phenotypes: a cross-sectional study in Northeast China. *Biomed Res Int*. 2018;2018:1-14.
- Knuplex E, Curcic S, Theiler A, et al. Lysophosphatidylcholines inhibit human eosinophil activation and suppress eosinophil migration in vivo. *Biochim Biophys Acta - Mol Cell Biol Lipids*. 2020;1865:158686.
- Zhu X, Learoyd J, Butt S, et al. Regulation of eosinophil adhesion by lysophosphatidylcholine via a non-store-operated Ca<sup>2+</sup> channel. *Am J Respir Cell Mol Biol*. 2007;36:585-593.
- Kariyawasam HH, Robinson DS. The role of eosinophils in airway tissue remodelling in asthma. *Curr Opin Immunol*. 2007;19:681-686.
- Oestvang J, Anthonsen MW, Johansen B. LysoPC and PAF trigger arachidonic acid release by divergent signaling mechanisms in monocytes. *J Lipids*. 2011;2011:1-11.

32. McGeachie MJ, Dahlin A, Qiu W, et al. The metabolomics of asthma control: a promising link between genetics and disease. *Immunity, Inflamm Dis*. 2015;3:224-238.
33. Nie X, Wei J, Hao Y, et al. Consistent biomarkers and related pathogenesis underlying asthma revealed by systems biology approach. *Int J Mol Sci*. 2019;20:4037.
34. Sokolowska M, Chen L-Y, Liu Y, et al. Dysregulation of lipidomic profile and antiviral immunity in response to hyaluronan in patients with severe asthma. *J Allergy Clin Immunol*. 2017;139:1379-1383.
35. Miyata J, Arita M. Role of omega-3 fatty acids and their metabolites in asthma and allergic diseases. *Allergol Int*. 2015;64:27-34.
36. Sokolowska M, Rovati GE, Diamant Z, et al. Current perspective on eicosanoids in asthma and allergic diseases - EAACI Task Force consensus report, part I. *Allergy*. 2021;76(1):114-130. 10.1111/all.14295
37. Petrache I, Berdyshev EV. Ceramide signaling and metabolism in pathophysiological states of the lung. *Annu Rev Physiol*. 2016;78:463-480.
38. Reinke SN, Gallart-Ayala H, Gómez C, et al. Metabolomics analysis identifies different metabolotypes of asthma severity. *Eur Respir J*. 2017;49:1601740.
39. Obeso D, Mera-Berriatua L, Rodríguez-Coira J, et al. Multi-omics analysis points to altered platelet functions in severe food-associated respiratory allergy. *Allergy*. 2018;73:2137-2149.
40. Mendelson K, Evans T, Hla T. Sphingosine 1-phosphate signalling. *Development*. 2014;141:5-9.
41. Kertys M, Grendar M, Kosutova P, Mokra D, Mokry J. Plasma based targeted metabolomic analysis reveals alterations of phosphatidylcholines and oxidative stress markers in guinea pig model of allergic asthma. *Biochim Biophys Acta - Mol Basis Dis*. 2020;1866:165572.
42. Comhair SAA, McDunn J, Bennett C, Fettig J, Erzurum SC, Kalhan SC. Metabolomic endotype of asthma. *J Immunol*. 2015;195:643-650.
43. Jung J, Kim S-H, Lee H-S, et al. Serum metabolomics reveals pathways and biomarkers associated with asthma pathogenesis. *Clin Exp Allergy*. 2013;43:425-433.
44. Farraia M, Cavaleiro Rufo J, Paciência I, et al. Metabolic interactions in asthma. *Eur Ann Allergy Clin Immunol*. 2019;51:196.
45. Ananieva EA, Powell JD, Hutson SM. Leucine metabolism in T cell activation: mTOR signaling and beyond. *Adv Nutr Int Rev J*. 2016;7:798S-805S.
46. Garcia-Zepeda EA, Combadiere C, Rothenberg ME, et al. Human monocyte chemoattractant protein (MCP)-4 is a novel CC chemokine with activities on monocytes, eosinophils, and basophils induced in allergic and nonallergic inflammation that signals through the CC chemokine receptors (CCR)-2 and -3. *J Immunol*. 1996;157:5613-5626.
47. Li CW, Zhang KK, Li TY, et al. Expression profiles of regulatory and helper T-cell-associated genes in nasal polyposis. *Allergy*. 2012;67:732-740.
48. Morris SR, Chen B, Mudd JC, et al. 'Inflammascent' CX3CR1+CD57+CD8 T cells are generated and expanded by IL-15. *JCI Insight*. 2020;5. 10.1172/jci.insight.132963
49. Grabstein K, Eisenman J, Shanebeck K, et al. Cloning of a T cell growth factor that interacts with the beta chain of the interleukin-2 receptor. *Science*. 1994;264:965-968.
50. He H, Suryawanshi H, Morozov P, et al. Single-cell transcriptome analysis of human skin identifies novel fibroblast subpopulation and enrichment of immune subsets in atopic dermatitis. *J Allergy Clin Immunol*. 2020;145:1615-1628.
51. Kaiser A, Donnadieu E, Abastado J-P, Trautmann A, Nardin A. CC chemokine ligand 19 secreted by mature dendritic cells increases naive T cell scanning behavior and their response to rare cognate antigen. *J Immunol*. 2005;175:2349-2356.
52. Takamura K, Fukuyama S, Nagatake T, et al. Regulatory role of lymphoid chemokine CCL19 and CCL21 in the control of allergic rhinitis. *J Immunol*. 2007;179:5897-5906.
53. Mendez-Barbero N, Yuste-Montalvo A, Nuñez-Borque E, et al. The TNF-like weak inducer of the apoptosis/fibroblast growth factor-inducible molecule 14 axis mediates histamine and platelet-activating factor-induced subcutaneous vascular leakage and anaphylactic shock. *J Allergy Clin Immunol*. 2020;145:583-596.e6.
54. Suwanpradit J, Shih M, Pontius L, et al. Arginase1 deficiency in monocytes/macrophages upregulates inducible nitric oxide synthase to promote cutaneous contact hypersensitivity. *J Immunol*. 2017;199:1827-1834.
55. Oberst A, Dillon CP, Weinlich R, et al. Catalytic activity of the caspase-8-FLIP L complex inhibits RIPK3-dependent necrosis. *Nature*. 2011;471:363-368.
56. Bell BD, Leverrier S, Weist BM, et al. FADD and caspase-8 control the outcome of autophagic signaling in proliferating T cells. *Proc Natl Acad Sci USA*. 2008;105:16677-16682.
57. Venables WN, Ripley BD. *Modern Applied Statistics with S-Plus*. Springer; 2013.

## SUPPORTING INFORMATION

Additional supporting information may be found in the online version of the article at the publisher's website.

**How to cite this article:** Delgado-Dolset MI, Obeso D, Rodríguez-Coira J, et al. Understanding uncontrolled severe allergic asthma by integration of omic and clinical data. *Allergy*. 2021;00:1-14. doi:[10.1111/all.15192](https://doi.org/10.1111/all.15192)



# Understanding Systemic and Local Inflammation Induced by Nasal Polyposis: Role of the Allergic Phenotype

María Isabel Delgado-Dolset<sup>1</sup>, David Obeso<sup>1,2</sup>, Javier Sánchez-Solares<sup>1</sup>, Leticia Mera-Berriatua<sup>1</sup>, Paloma Fernández<sup>1</sup>, Coral Barbas<sup>2</sup>, Miguel Fresnillo<sup>3</sup>, Tomás Chivato<sup>1,4</sup>, Domingo Barber<sup>1</sup>, María M. Escribese<sup>1,5\*†</sup> and Alma Villaseñor<sup>1\*†</sup>

<sup>1</sup>Department of Basic Medical Sciences, Faculty of Medicine, Institute of Applied Molecular Medicine (IMMA), San Pablo CEU Universities, Madrid, Spain, <sup>2</sup>Centre for Metabolomics and Bioanalysis (CEMBIO), Department of Chemistry and Biochemistry, Faculty of Pharmacy, San Pablo CEU Universities, Madrid, Spain, <sup>3</sup>Otorhinolaryngology Service, HM Montepríncipe Hospital, Madrid, Spain, <sup>4</sup>Department of Clinic Medical Sciences, Faculty of Medicine, San Pablo CEU Universities, Madrid, Spain, <sup>5</sup>Department of Basic Medical Sciences, Faculty of Medicine, San Pablo CEU Universities, Madrid, Spain

## OPEN ACCESS

### Edited by:

Serge Rudaz,  
Université de Genève, Switzerland

### Reviewed by:

Monica Cala,  
University of Los Andes, Colombia  
Gino Marioni,  
University of Padua, Italy

### \*Correspondence:

Alma Villaseñor  
alma.villaseñor@ceu.es  
María M. Escribese  
mariamarta.escribesealonso@  
ceu.es

<sup>†</sup>These authors share last authorship

### Specialty section:

This article was submitted to  
Metabolomics,  
a section of the journal  
Frontiers in Molecular Biosciences

**Received:** 01 February 2021

**Accepted:** 27 April 2021

**Published:** 14 May 2021

### Citation:

Delgado-Dolset MI, Obeso D, Sánchez-Solares J, Mera-Berriatua L, Fernández P, Barbas C, Fresnillo M, Chivato T, Barber D, Escribese MM and Villaseñor A (2021) Understanding Systemic and Local Inflammation Induced by Nasal Polyposis: Role of the Allergic Phenotype. *Front. Mol. Biosci.* 8:662792. doi: 10.3389/fmolb.2021.662792

Chronic rhinosinusitis with nasal polyps (CRSwNP) is characterized by persistent symptoms associated to the development of nasal polyps. To this day, the molecular mechanisms involved are still not well defined. However, it has been suggested that a sustained inflammation as allergy is involved in its onset. In this exploratory study, the aim was to investigate the effect of the allergic status in the development of CRSwNP. To achieve this, we recruited 22 patients with CRSwNP and classified them in non-allergic and allergic using ImmunoCAP ISAC molecular diagnosis. Plasma samples were analyzed using liquid chromatography coupled to mass spectrometry (LC-MS). Subsequently, significant metabolites from plasma that were commercially available were then analyzed by targeted analysis in some nasal polyps. Additionally, nasal polyp and nasal mucosa samples were examined for eosinophils, neutrophils, CD3<sup>+</sup> and CD11c<sup>+</sup> cells, as well as collagen deposition and goblet cell hyperplasia. We found that 9 out of the 22 patients were sensitized to some aeroallergens (named as allergic CRSwNP). The other 13 patients had no sensitizations (non-allergic CRSwNP). Regarding metabolomics, bilirubin, cortisol, lysophosphatidylcholines (LPCs) 16:0, 18:0 and 20:4 and lysophosphatidylinositol (LPI) 20:4, which are usually related to a sustained allergic inflammation, were unexpectedly increased in plasma of non-allergic CRSwNP compared to allergic CRSwNP. LPC 16:0, LPC 18:0 and LPI 20:4 followed the same trend in nasal polyp as they did in plasma. Comparison of nasal polyps with nasal mucosa showed a significant increase in eosinophils ( $p < 0.001$ ) and neutrophils ( $p < 0.01$ ) in allergic CRSwNP. There were more eosinophils in polyps of non-allergic CRSwNP than in their nasal mucosa ( $p < 0.01$ ). Polyps from non-allergic CRSwNP had less eosinophils than the polyps of allergic CRSwNP ( $p < 0.05$ ) and reduced amounts of collagen compared to their nasal mucosa ( $p < 0.001$ ). Our data suggests that there is a systemic inflammatory response associated to CRSwNP in the absence of allergy, which could be accountable for the nasal polyp development. Allergic CRSwNP presented a higher number of eosinophils in nasal polyps,

suggesting that eosinophilia might be connected to the development of nasal polyps in this phenotype.

**Keywords:** metabolomics, nasal polyps, allergy, targeted analysis, untargeted analysis

## INTRODUCTION

Chronic rhinosinusitis with nasal polyps (CRSwNP) is a disease characterized by persistent inflammatory symptoms in nasal and paranasal mucosa that result in the development of a nasal polyp (Fokkens et al., 2012). This is an outgrowth of tissue that arises into the nasal cavity (Schleimer, 2017). The prevalence of the disease is estimated between 1–4% of the population (Fokkens et al., 2012; Chen et al., 2020). Symptoms include nasal blockage and itching, rhinorrhea, sneezing, facial pain, headache and smell impairment or loss (Georgy and Peters, 2012; Chen et al., 2020). Treatment starts with intranasal topic corticosteroids in the milder cases, followed by surgical extirpation or biological drugs, such as omalizumab, in the most severe ones (Lund, 1995; Georgy and Peters, 2012).

CRSwNP presents several endotypes, which are subtypes of diseases defined either by having the same molecular mechanism or because they respond to the same treatment (Anderson, 2008). In this sense, the analysis of cells and molecules involved in inflammation and the underlying pathophysiological mechanism is essential in CRSwNP (Brescia et al., 2020).

There are several comorbidities associated to CRSwNP appearance and recurrence, including asthma, allergic rhinitis, cystic fibrosis or aspirin-exacerbated respiratory disease (AERD) (Lund, 1995; Wynn and Har-El, 2004; Pearlman et al., 2010). In addition, nasal polyps relapse in up to 60–70% of the patients (Wynn and Har-El, 2004).

There are significant differences in histological features between nasal mucosa and nasal polyps, such as the development of oedema or fibrosis, goblet cell hyperplasia and/or squamous metaplasia; the thickening of the basal membrane; and the infiltration of inflammatory cells, including lymphocytes, eosinophils and neutrophils (Ferreira Couto et al., 2008).

However, the molecular mechanisms involved in the development of nasal polyps are still not well defined (Hopkins, 2019). Due to the inflammatory features described in several cohorts of CRSwNP (Brescia et al., 2018), most of the hypothesis agree that long-term maintained inflammation plays a key role in this process (Tos et al., 2010; Chojnowska et al., 2013; Brescia et al., 2021) and, therefore, inflammatory diseases such as allergy and/or asthma might be associated with its onset.

The role of allergy in CRSwNP development has been extensively discussed. In their 2014 review, Wilson *et al* (Wilson et al., 2014) examined the existing evidence both for and against an association of these two diseases. Although the role of allergy in CRSwNP was inconclusive, the review showed a higher rate of positive skin prick test among CRSwNP patients; and greater improvement in patients with negative skin prick tests compared to those with positive ones. These differences suggest that allergic inflammation might play a role in nasal polyposis.

Metabolomics is one of the most promising tools in the identification of biomarkers. It allows the detection of dynamic changes and alterations in the metabolism that point to a given pathological state (Villaseñor et al., 2017). The metabolome is closely linked to the phenotype and can be an extremely useful tool for diagnosing diseases and evaluating the effect of treatments. From a practical point of view, it uses very sensitive and specific techniques, such as liquid chromatography coupled to mass spectrometry (LC-MS), which allows the simultaneous detection of a great variety of metabolites in a biological sample (Crestani et al., 2020). Once the study subjects are well characterized, these results should be validated in a new and larger cohort of patients in subsequent studies. Compared to other omics, such as transcriptomics or genomics, the validation of metabolites found after exploratory studies is carried out through the development of analytical methodologies. This process is usually laborious depending on the number of metabolites and their physicochemical properties, and is conditioned by the availability of commercial standards.

Previous reports show that allergic inflammation has both systemic and local effects. As for the systemic role of allergy, we have previously demonstrated that severe allergic phenotypes induce significant changes in the plasma metabolome (Obeso et al., 2018). Similarly, allergic inflammation also induces local remodeling in oral mucosa (Aceves and Ackerman, 2009; Samitas et al., 2018; Rosace et al., 2019). In fact, this remodeling might result in the formation of the nasal polyp (Tos et al., 2010). However, to our knowledge, no metabolomic analysis has been performed for CRSwNP.

Here, our aim is to determine the role of allergic inflammation in patients with CRSwNP and how it affects both systemic and local features. Thus, we performed: 1) a systemic analysis, using a non-targeted metabolomics approach to achieve an overall picture of the metabolic profile in CRSwNP patients with and without allergy, and 2) a local analysis using both a targeted metabolomic analysis of the nasal polyps to evaluate if the systemic potential metabolites found are associated specifically to the nasal polyp, and a histological analysis to better characterize the local polyp environment. Our results support the idea that the nasal polyp has a specific inflammatory environment characterized by immune cells infiltrates, epithelial damage and the presence of inflammatory-related metabolites.

## MATERIALS AND METHODS

### Patients and Sample Collection

Twenty-two adult patients diagnosed with CRSwNP within an age range of  $48 \pm 8$  years that arrived for the first time to the Otorhinolaryngology Service of the Hospital Madrid Montepíncipe (Spain) were included in this study. Patients

underwent a basic allergy history questionnaire. The inclusion criteria were: patients older than 18 years of age, with nasal polyps that needed to undergo a surgery to remove following their clinician's diagnosis. Patients received the same pharmacological pre-surgery treatment and their corticosteroid medication was removed two weeks prior the procedure. The exclusion criteria were: patients with concomitant inflammatory diseases such as autoimmune diseases or cancer. The ethical committee approved the study protocol and all subjects were informed and provided written consent prior to any procedure. Data were anonymized.

During endoscopic surgical procedures to remove the polyp, 5 mm biopsies of nasal polyp and nasal mucosa were obtained and either kept in RNAlater at  $-80^{\circ}\text{C}$  or fixed in 4% paraformaldehyde (PFA) for 24–48 h. PFA-fixed samples were dehydrated and included in paraffin using Leica TP 1020 tissue processor. From these, 3  $\mu\text{m}$  sections were obtained and used for histological and immunohistochemical analysis. Additionally, from the twenty-two patients, a blood sample from nineteen was obtained. About 20 ml of heparinized blood were collected to obtain plasma using a Ficoll-Paque (GE Healthcare™) density gradient centrifugation. Supernatants were stored at  $-80^{\circ}\text{C}$  until their use.

## ImmunoCAP ISAC

To determine the sensitization profile of the patients, ImmunoCAP ISAC® (Phadia, Uppsala, Sweden) with chips for 112 allergens assays were performed to detect specific IgE (sIgE) as described in the manufacturer protocol. Values above 0.3 ISU-E were considered positive.

## Untargeted Plasma Metabolomic Analysis

Plasma samples were measured using a Liquid Chromatography coupled to Mass Spectrometry (LC-QTOF-MS Agilent series 6520). We followed previously described methodologies developed in our group (Ciborowski et al., 2010). Principal component analysis and heatmaps with hierarchical clustering were obtained using MetaboAnalyst v 5.0 webpage (<https://www.metaboanalyst.ca>).

Full descriptions are available in the Supplementary Information. Metabolite annotation was carried out using the online advanced CEU Mass Mediator tool (Godzien et al., 2015; Dudzik et al., 2018; Gil-de-la-Fuente et al., 2019). Statistical analysis was performed using non-parametric Mann Whitney *U* test, with statistical significance set at 95% ( $p < 0.05$ ) with a Benjamini-Hochberg (also known as False Discovery Rate, FDR). Annotation was confirmed through LC-MS/MS experiments using 20 eV for fragmentation. Data were uploaded to Metabolomics Workbench webpage (ID study: ST001733 and ST001734).

## Target Method for Nasal Polyps Sample Preparation

Three nasal polyp samples of each group collected in RNAlater were used to measure the metabolites from plasma that were commercially available. RNAlater solvent was removed by washing the tissue 3 times with PBS 1X. Then, the nasal polyp

was frozen in liquid nitrogen for 30 s. The frozen sample was put in cryoPREPTMCP02 (Covaris, MA, United States) plastic bags and submerged again for 30 s in liquid nitrogen. Once the plastic bag was inside the automated cryoPREPTMCP02, two consecutive impact forces of levels 2 and 4 out of 6 were applied. The resultant powder was gathered and weighted. Then, 100  $\mu\text{L}$  of cold methanol:ethanol (1:1, v/v) and 0.5  $\mu\text{L}$  of internal standard (LPC 18:1-d7; 0.01 mM) were added per each 10 mg of tissue for metabolite extraction and protein precipitation. Samples were then vortex-mixed and homogenized using Tissue-Lyser LT homogenizer (Qiagen, Germany) for 5 min at 50 Hz, 3 times. Supernatant containing the metabolites was separated from the pellet by centrifugation (2,000 rcf for 10 min at  $4^{\circ}\text{C}$ ). Then, an aliquot of 70  $\mu\text{L}$  was transferred to an LC vial and diluted with 490  $\mu\text{L}$  of mobile phase (5% water: 95% acetonitrile; both with 7.5 mM ammonium acetate and 0.1% acetic acid). All samples were randomized before metabolite extraction and for the corresponding analytical run.

## Analysis of Nasal Polyp by Liquid Chromatography Coupled to Triple Quadrupole Mass Spectrometry (LC-QqQ-MS)

Samples were measured using Dynamic Molecular Reaction Monitoring (dMRM) in LC-QqQ-MS for the analysis of metabolites. We used HPLC system (1260 Infinity, Agilent Technologies) coupled to an ESI(AJS)-QqQ-MS (6470 Agilent Technologies). The metabolites were separated on a Kinetex hydrophilic interaction liquid chromatography (HILIC) silica column (150 mm  $\times$  2.1 mm, particle size 100Å, Phenomenex, United States) maintained at  $25^{\circ}\text{C}$ . The mobile phases consisted of: A) water, and B) acetonitrile, both with 7.5 mM ammonium acetate and 0.1% acetic acid, with a final pH of 4.0 in the aqueous phase. The flow rate was 0.5 ml/min with an injection volume of 5  $\mu\text{L}$ . Gradient started with 5% of A for 2 min, then increased up to 50% until 12 min, and back to initial conditions until 22 min. The MS conditions were: 5500 V of capillary voltage in positive ESI mode, a nebulizer gas flow rate of 11.0 L/min; a source temperature of  $250^{\circ}\text{C}$ ; and a source pressure of 60 psi. The sample tray temperature was maintained at  $4^{\circ}\text{C}$ . Each transition was optimized adjusting the fragmentor and collision energy voltages, which can be seen in **Table 1**.

## Data Acquisition, Pre-processing and Treatment

Data were acquired in MassHunter Workstation B.05.00 (Agilent Technologies), and re-processed using MassHunter QQQ Quantitative Analysis B.08.00 (Agilent) where peak areas were integrated. Concentration of metabolites were calculated using external calibration curves with the standard addition method. Once the concentrations were obtained, all data treatment and statistical comparisons was performed using Excel 2016, MATLAB R 2018b and GraphPad Prism v8.1.2.

## Immune Cell Quantification Tissue Staining

We quantified eosinophils, neutrophils, CD3<sup>+</sup> and CD11c<sup>+</sup> cells, and checked for collagen deposition and goblet cell hyperplasia,

**TABLE 1** | Optimized MS transitions and parameters for the targeted analysis. LPC: Lysophosphatidylcholine, LPI: Lysophosphatidylinositol, RT: Retention time, V: Volt, eV: Electronvolt.

Compound name	Precursor ion ( <i>m/z</i> )	Product ion ( <i>m/z</i> )	RT (min)	Fragmentor (V)	Collision energy (eV)	Polarity
Bilirubin	585.3	299.1	0.91	131	25	+
LPC 16:0	496.3	183.9	9.95	100	28	+
LPC 18:0	524.4	183.8	9.80	100	28	+
LPI 20:4	621.3	361.3	7.83	84	17	+

in nasal polyps and nasal mucosa samples. For eosinophil quantification, we adapted a Luna staining protocol. Samples were stained with a working solution prepared with 0.9 parts of homemade Weigert's Iron Hematoxylin, and 0.1 parts of commercial Brierlich-Scarlett solution (Sigma Aldrich, ref. HT151) for 5 min. Slides were then differentiated in 1% acid alcohol and 0.25% lithium carbonate solutions, and preparations were mounted.

Regarding goblet cell hyperplasia, we optimized a Periodic Acid-Schiff (PAS) staining. Briefly, samples were kept in a 0.5% periodic acid solution, then stained with Schiff's reactive (Merck, ref. 109033) and washed. Nuclei were stained with a 1:4 Harris Hematoxylin solution and differentiated with a 1% acid alcohol (1% of HCl in 70% ethanol) solution and a saturated lithium carbonate (Sigma-Aldrich, ref. 62470) solution. Preparations were mounted with DPX medium.

Regarding neutrophil, CD3<sup>+</sup> cells and CD11c<sup>+</sup> cells quantification, we performed immunohistochemical staining with anti-human neutrophil elastase (ab68672, ABCAM), anti-CD3 (MCA 1477, AbD Serotec) and anti-CD11c (NCL-L-CD11c-563, Novocastra) using the automatized system Leica Bond Max (Leica Biosystems), as previously described (Sanchez-Solares et al., 2019). For negative controls, the antibody was substituted with antibody diluent Bond<sup>TM</sup> (Leica Biosystems) for incubation.

Masson Trichrome staining (Sigma-Aldrich, ref HT15-1KT) was performed following the manufacturer's instructions.

### Image Analysis

All slides were scanned with Leica SCN400 scanner (Leica Biosystems). Images were obtained for each staining using the Leica Scan Viewer software. Luna and neutrophil elastase-positive cells were counted in the whole sample, while CD3<sup>+</sup> cells and CD11c<sup>+</sup> cells were counted in five representative areas on the sample. Areas were measured using ImageJ v1.51j8 by at least two independent observers. Results are presented as number of cells per area. For goblet cell hyperplasia, PAS<sup>+</sup> stained areas in the epithelium were measured, while for collagen deposition, green areas of Masson staining were measured in the whole sample using Image-Pro Plus v4.5.0.29 for Windows (Media Cybernetics) software.

### Statistical Analysis

GraphPad Prism v8.1.2 for Windows (GraphPad Software) was used for statistical analysis. We checked data distribution and then used *t*-test or Mann-Whitney *U* test to determine significant

differences between the means accordingly. Statistical significance was set at 95% ( $p < 0.05$ ).

## RESULTS

### Patient Classification

Patients with CRSwNP were classified according to their allergic sensitization phenotype by ImmunoCAP ISAC (Figure 1). As observed in the figure, 13 patients (59.1%) had undetectable sIgE levels and were classified as non-allergic CRSwNP. On the other hand, 9 (40.9%) had significant levels of sIgE. They were sensitized to either one or more perennial allergen sources (*i.e.* cat, dog, mites or *Alternaria*) and/or to a group of seasonal allergen sources. Thus, we consider them to be perennial allergic patients and classified them as allergic CRSwNP patients.

### Untargeted Plasma Metabolomic Analysis

The plasma metabolic profile of each patient with CRSwNP with or without allergic sensitization was acquired. After data treatment, 535 features for LC-MS positive and 429 for LC-MS negative ionization modes in each plasma sample were obtained. These features passed the different quality filters (blank subtraction, presence in quality control samples (QCs; >50%) and patients (>75%), and coefficient of variation in QCs (<30%)).

To assess the correct performance of the LC-MS equipment and the quality of the acquired data, samples were projected on a PCA model (Figure 2A). Clustering of the QC injections in the non-supervised plot indicated the high quality of the data, while dispersion of the samples showed the biological variability of the patients. The groups were compared using a discriminant PLS-DA analysis, obtaining no model. Thus, a Mann Whitney-*U* test was used for the selection of significant features, finding a total of 13 and 26 features from LC-MS in positive and negative ionization modes, respectively. For these significant features, we assessed that they had a coefficient of variation (CV) on QCs lower than the percentage of change between the non-allergic CRSwNP compared to the allergic CRSwNP group. Additionally, we checked that metabolites had a % of change higher than 20% or that the feature matched the complementary polarity. These features were represented using a heatmap with hierarchical clustering for each ionization mode (Figures 2B,C). As observed, the significant features from the positive ionization mode were able to define a specific metabolic signature for each group, accurately clustering all the samples. On the other hand,



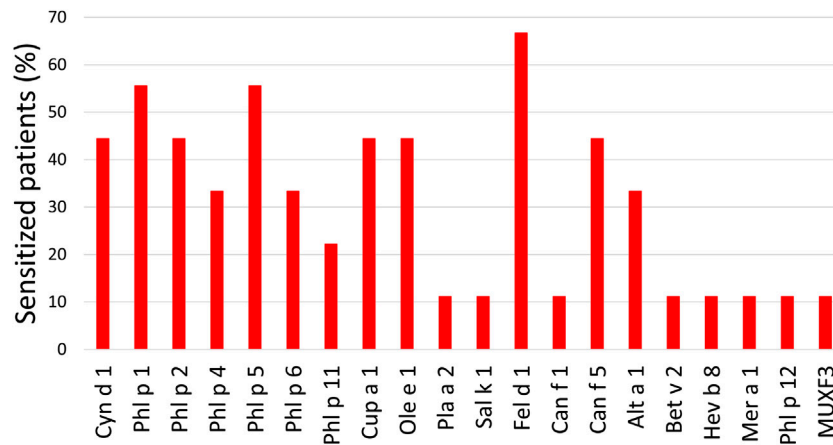


**FIGURE 1** | Percentage of allergic patients sensitized to each allergen. Cyn d: *Cynodon dactylon* (Bermuda grass); Phl p: *Phleum pratense* (timothy); Cup a: *Cupressus arizonica* (cypress); Ole e: *Olea europaea* (olive); Pla a: *Platanus acerifolia* (London plane tree); Sal k: *Salsola kali* (saltwort); Fel d: *Felis domesticus* (cat); Can f: *Canis familiaris* (dog); Alt a: *Alternaria alternata* (*Alternaria* plant rot fungus); Bet v: *Betula verrucosa* (European white birch); Hev b: *Hevea brasiliensis* (latex); Mer a: *Mercurialis annua* (annual mercury); MUXF3: Bromelain.

the significant features from the negative ionization mode were able to correctly cluster around 85% of the samples (16 out of 19).

We carried out an annotation for all the significant features. After tentative annotation and confirmation by MS/MS fragmentation experiments, we were able to annotate 14 features. Taking into account both polarities, eight metabolites had a unique annotation—comprising sn-1 and sn-2 for lysophospholipids— (Table 2). We found increased levels of lysophosphatidylcholines (LPC 16:0, LPC 18:0 and LPC 20:4), a lysophosphatidylinositol (LPI 20:4), cortisol and bilirubin in the non-allergic CRSwNP compared to the allergic CRSwNP group.

Overall, specific systemic metabolic changes were defined for non-allergic and allergic CRSwNP patients.

## Targeted Metabolomic Analysis of Nasal Polyps

The significant metabolites found in plasma that had available commercial standards were used to test their presence in the nasal polyp. Therefore, nasal polyp samples from six CRSwNP patients (three non-allergic and three allergic) were analyzed to confirm the results found in plasma. We applied univariate statistical analysis between the two groups, obtaining no statistically significant changes in any metabolite ( $p > 0.05$ , Mann Whitney  $U$  test). However, to study the metabolite patterns, these were represented in a heatmap using the average per group (Figure 2D). We observe that, despite the low number of samples, the LPC 16:0, LPC 18:0 and LPI 20:4 followed the same increasing trend in the non-allergic CRSwNP patients as we described in plasma samples. Finally, these metabolites in plasma and in the nasal polyps from untargeted and targeted analyses were represented using trajectories in Figure 3.

## Histological Features

To better characterize the specific local features of nasal polyps and mucosa associated to allergy, we analyzed the infiltration of eosinophils, neutrophils, CD3<sup>+</sup> and CD11c<sup>+</sup>; along with the

hyperplasia of goblet cells and the abundance of collagen fibers in all of them.

Eosinophil quantification (Figure 4A) revealed that the number of these cells in nasal polyps was higher than in the nasal mucosa samples ( $9.7 \pm 2.3$  cells/area vs  $0.71 \pm 0.41$  cells/area,  $p < 0.001$ ). Importantly, the highest number of eosinophils was detected in nasal polyps from allergic CRSwNP patients (Figure 4B). In fact, polyps of non-allergic CRSwNP patients had significantly less eosinophils than those of allergic CRSwNP patients ( $16.6 \pm 3.6$  cells/area vs  $4.5 \pm 1.4$  cells/area,  $p < 0.05$ ).

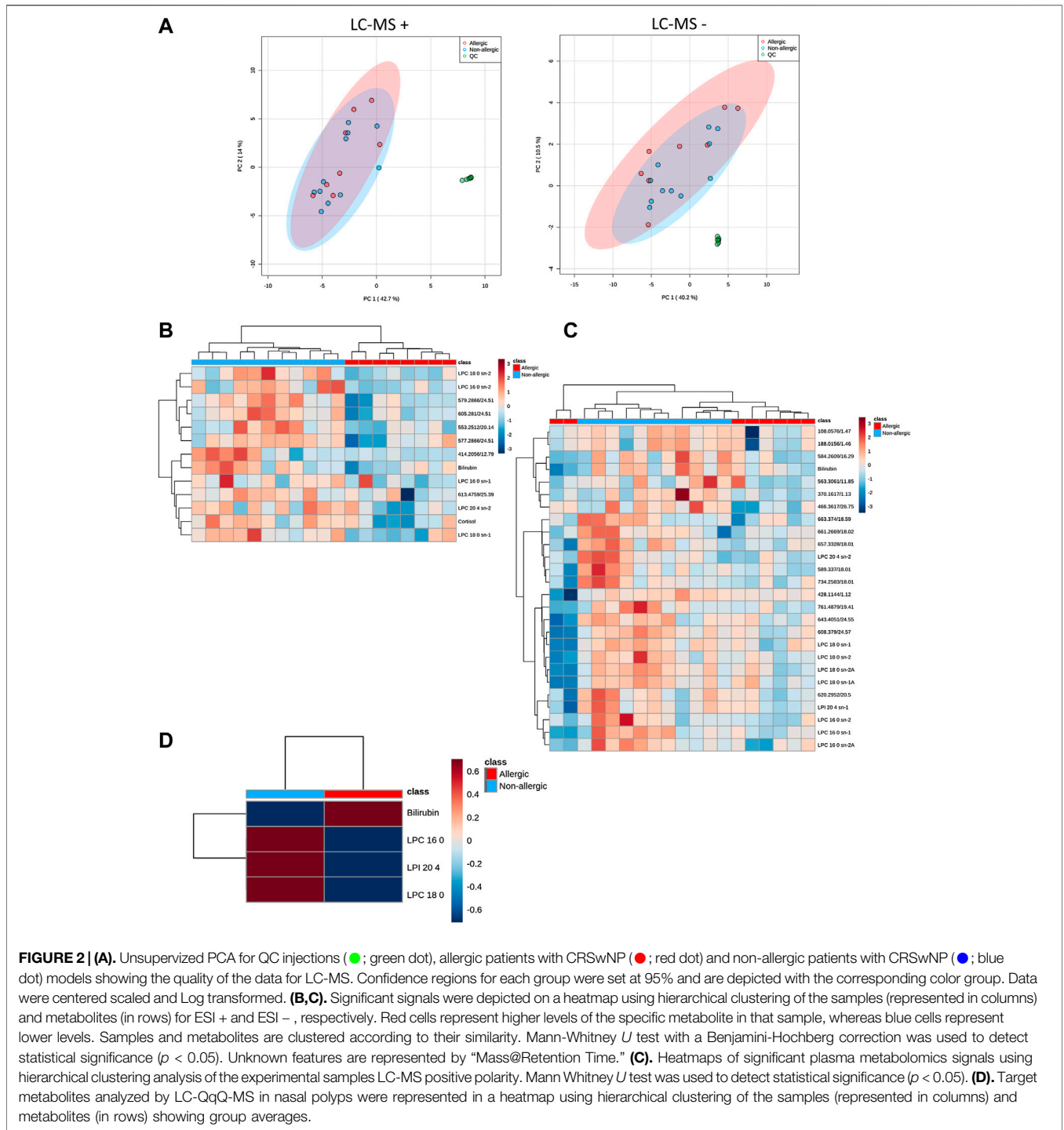
We also found more neutrophils (Figure 5A) in nasal polyps than in the nasal mucosa ( $0.60 \pm 0.10$  cells/area vs  $0.31 \pm 0.10$  cells/area,  $p < 0.01$ ). Nasal polyps of allergic CRSwNP patients had the highest number of neutrophils (Figure 5B), being significantly different to their own nasal mucosa ( $0.70 \pm 0.17$  cells/area vs  $0.16 \pm 0.060$  cells/area,  $p < 0.01$ ). However, there were no significant differences in the number of neutrophils in nasal polyps between non-allergic and allergic CRSwNP patients ( $p > 0.41$ ).

No statistical differences were observed between the nasal polyps of non-allergic CRSwNP and those of allergic CRSwNP regarding collagen deposition (Figure 6,  $p > 0.66$ ), goblet cell hyperplasia (Figure 7,  $p < 0.87$ ), infiltration of CD3<sup>+</sup> (Figure 8,  $p < 0.22$ ) and CD11c<sup>+</sup> cells (Figure 9,  $p > 0.41$ ).

However, more collagen deposition was observed in the nasal mucosa compared to the nasal polyps in the non-allergic CRSwNP ( $p < 0.001$ ). Moreover, the same trend was found for the allergic CRSwNP patients, although the difference was not significant ( $p > 0.059$ ) (Figure 6B).

There also seemed to be a higher area stained with PAS in the epithelium of nasal polyps compared to the nasal mucosa for both allergic and non-allergic CRSwNP groups (Figure 7). Although the difference was not significant ( $p > 0.29$  for non-allergic CRSwNP and  $p > 0.41$  for allergic CRSwNP patients), this fact suggests the presence of goblet cell hyperplasia.

Finally, for the infiltration of CD3<sup>+</sup> and CD11c<sup>+</sup> cells (Figures 8,9, respectively), no statistical differences were obtained between



nasal mucosa and nasal polyp for both allergic and non-allergic CRSwNP groups.

In summary, we found that nasal polyps present a higher immune cell infiltration (eosinophils and neutrophils) than nasal mucosa for both allergic and non-allergic CRSwNP patients. Moreover, allergic CRSwNP patients were characterized by eosinophilia in their nasal polyps compared to non-allergic CRSwNP patients. In the case of non-allergic CRSwNP

patients, more collagen deposition in their nasal mucosa than in their nasal polyp was observed.

## DISCUSSION

Nasal polyps are growths of inflamed nasal tissue that have been well-known for a long time. However, the molecular mechanisms

**TABLE 2** | Pairwise comparisons showing the significant identified metabolites.

Non-allergic CRSwNP vs allergic CRSwNP												
N°	Technique	Compound	Adduct	m/z (Da)	Mass (Da)	RT (min)	Error (ppm)	%CV on QCs	FC in non-allergic	% Change in non-allergic	p-Value	p-BH
1	LC - MS -	Bilirubin	[M-H] <sup>-</sup>	583.2549	584.2621	32.94	2	16.9	2.03	103.28	0.041	0.049
	LC - MS +		[M+H] <sup>+</sup>	585.2702	584.2630	32.90	1	11.4	1.96	95.56	0.033	0.039
2	LC - MS -	Cortisol	[M+H] <sup>+</sup>	363.2171	362.2099	3.66	1	12.4	2.20	119.55	0.026	0.034
	LC - MS +		[M+FA] <sup>+</sup>	540.3301	495.3324	19.42	1	8.8	1.23	23.49	0.026	0.038
3	LC - MS -	LPC 16:0 sn-1	[M+H] <sup>+</sup>	496.3402	495.3330	19.36	1	13.5	1.27	27.17	0.036	0.042
	LC - MS +		[M+FA] <sup>+</sup>	540.3305	495.3324	20.20	1	6.2	1.17	16.94	0.041	0.049
4	LC - MS -	LPC 16:0 sn-2	[M+H] <sup>+</sup>	496.3403	495.3331	20.14	1	10.5	1.25	25.45	0.018	0.032
	LC - MS +		[M+FA] <sup>+</sup>	568.3623	523.3642	23.74	1	9.1	1.33	32.80	0.007	0.029
5	LC - MS -	LPC 18:0 sn-2	[M+H] <sup>+</sup>	524.3713	523.3641	23.66	0	12.6	1.36	36.19	0.005	0.025
	LC - MS +		[M+FA] <sup>+</sup>	568.3618	523.3637	24.58	1	6.2	1.23	22.55	0.041	0.049
6	LC - MS -	LPC 18:0 sn-1	[M+H] <sup>+</sup>	524.3719	523.3647	24.52	2	11.1	1.30	30.01	0.010	0.031
	LC - MS +		[M+Cl] <sup>+</sup>	578.3016	543.3324	18.59	1	10.8	1.42	42.11	0.026	0.034
7	LC - MS -	LPC 20:4 sn-2	[M+H] <sup>+</sup>	544.3401	543.3329	18.49	1	23.7	1.49	49.03	0.054	0.071
	LC - MS +		[M-H] <sup>-</sup>	619.2880	620.2952	19.59	1	6.1	1.38	38.01	0.020	0.034

LC-MS: Liquid Chromatography coupled to Mass Spectrometry; RT: retention time; ppm: part per million; FC: fold change, was calculated as average of area in Non-allergic/average of area in Allergic; % change was calculated as (FC-1) x 100; LPC: Lysophosphatidylcholine; LPI: Lysophosphatidylinositol; FA: formic acid; BH: Benjamini-Hochberg (False Discovery Rate).

involved in the development of nasal polyps remain unclear. Additionally, even though allergy and CRSwNP have been traditionally linked, whether there is a connection between allergy and the development of nasal polyps or not is yet to be described. Here, we perform an original experimental design, aiming to elucidate systemic metabolic differences in CRSwNP patients with and without allergy.

From our patient cohort, 40% (9 out of 22) of the patients were allergic, close to the levels in average population which is around 30% (Bauchau and Durham, 2004; Bousquet et al., 2008).

A metabolic fingerprint in plasma of patients with CRSwNP was obtained. Non-allergic CRSwNP patients displayed an increase of LPCs (LPC 16:0, LPC 18:0, LPC 20:4) together with LPI 20:4, compared to allergic CRSwNP. These LPCs have been previously associated with systemic inflammation (Chiurchiù et al., 2018; Obeso et al., 2018). Moreover, they have been described in asthma (Ried et al., 2013; Comhair et al., 2015; Villaseñor et al., 2017) as arachidonic acid (AA) precursors. The free fatty acids from the LPCs are released after the action of lipase A2 to synthesize inflammatory mediators, that participate as precursors in the AA pathway (Balgoma et al., 2010; Arita, 2016; Bennett and Gilroy, 2016). Interestingly, LPI 20:4, which is one of the more abundant LPIs in plasma, has been related to a potent pro-inflammatory signaling in intestinal bowel disease and colorectal cancer in animal models (Grill et al., 2019) and in type 2 diabetes (Lu et al., 2016). Overall, the LPI 20:4 metabolite seems to be involved in the inflammatory response.

On the other hand, there is growing evidence that bilirubin exerts potent anti-inflammatory effects. Bilirubin is able to suppress inflammatory responses by preventing the migration of leukocytes into target tissues through the disruption of vascular cell adhesion molecule-1 (VCAM-1)-dependent cell signaling. In a previous study, bilirubin was shown to alleviate colitis (Vogel and Zucker, 2016). Additionally, nanoparticles containing bilirubin were used for the treatment of allergic lung inflammation disease in a mouse model obtaining amelioration of the disease (Kim et al., 2017). Therefore, bilirubin has been demonstrated that has anti-oxidative, anti-inflammatory and immunosuppressive functions in various diseases such as inflammatory bowel disease, cardiovascular disease, autoimmune disorders, cancer and type 2 diabetes mellitus (Peng et al., 2017). Mildly elevation of this metabolite is associated with better prognosis; thus, the decrease we observe in allergic CRSwNP patients might be related with a worse outcome. As bilirubin can be measured in a laboratory standard test, this metabolite can be compared in future studies in these patients.

Finally, cortisol has been described as a hormone which acts suppressing early inflammatory responses; however, when cortisol is not enough to control inflammation, it prepares immune cells for major subsequent inflammatory episodes (Yeager et al., 2018). Interestingly, circadian rhythms of salivary cortisol were found to be disrupted in patients with extensive nasal polyposis compared to controls (Fidan et al., 2013). The authors suggest that a therapy with cortisol-based drugs might be useful in the treatment of CRSwNP (Fidan et al., 2013). In this line, intrapolyp steroid injections appear to

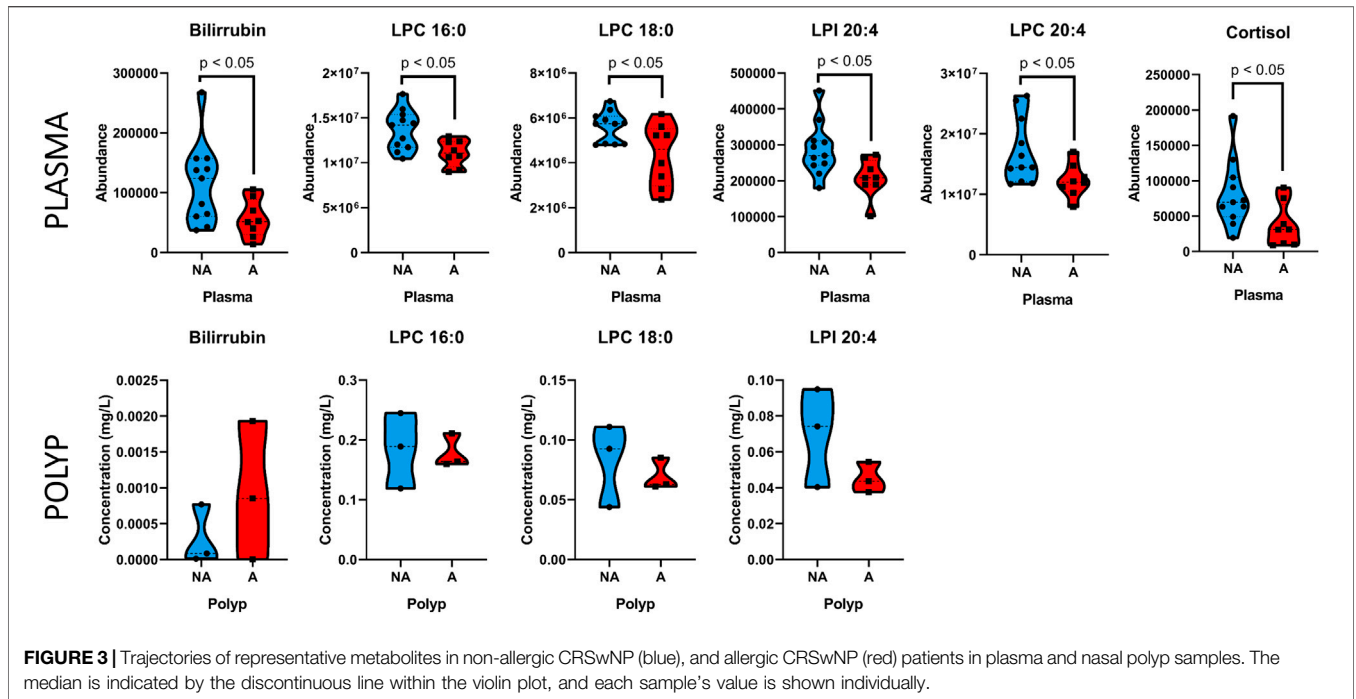


**FIGURE 3** | Trajectories of representative metabolites in non-allergic CRSwNP (blue), and allergic CRSwNP (red) patients in plasma and nasal polyp samples. The median is indicated by the discontinuous line within the violin plot, and each sample's value is shown individually.

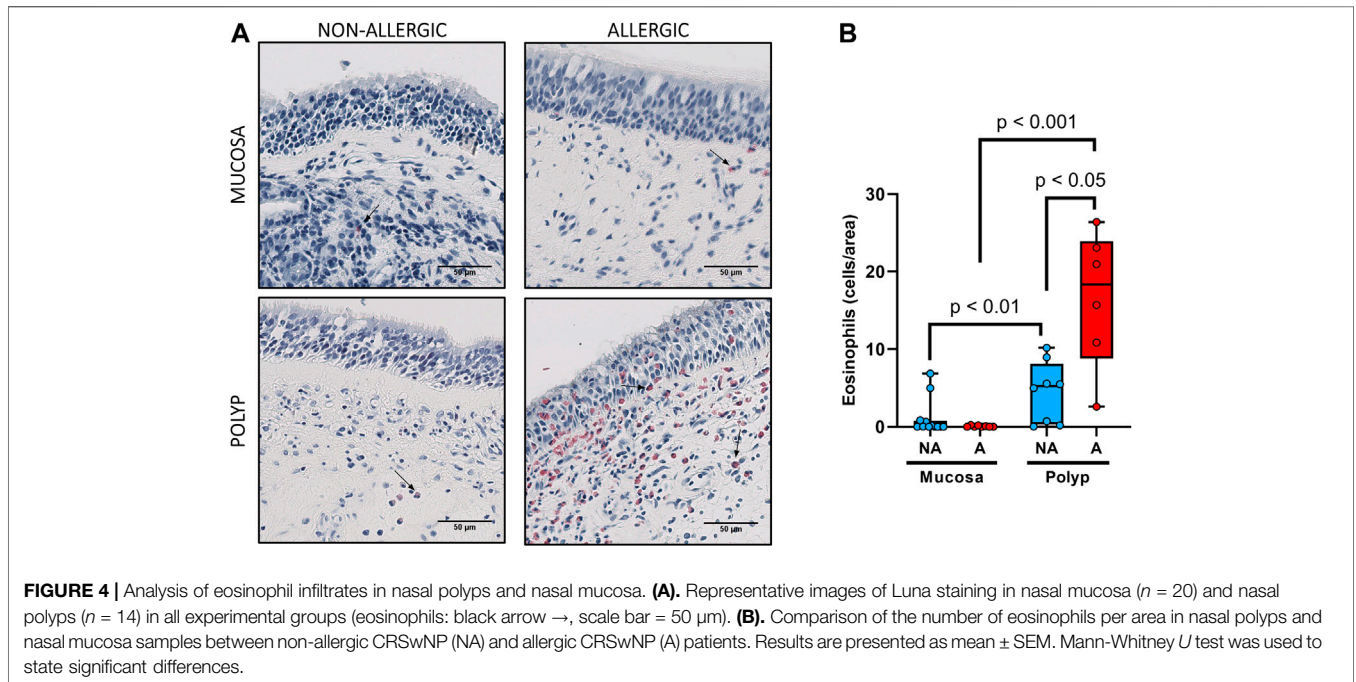
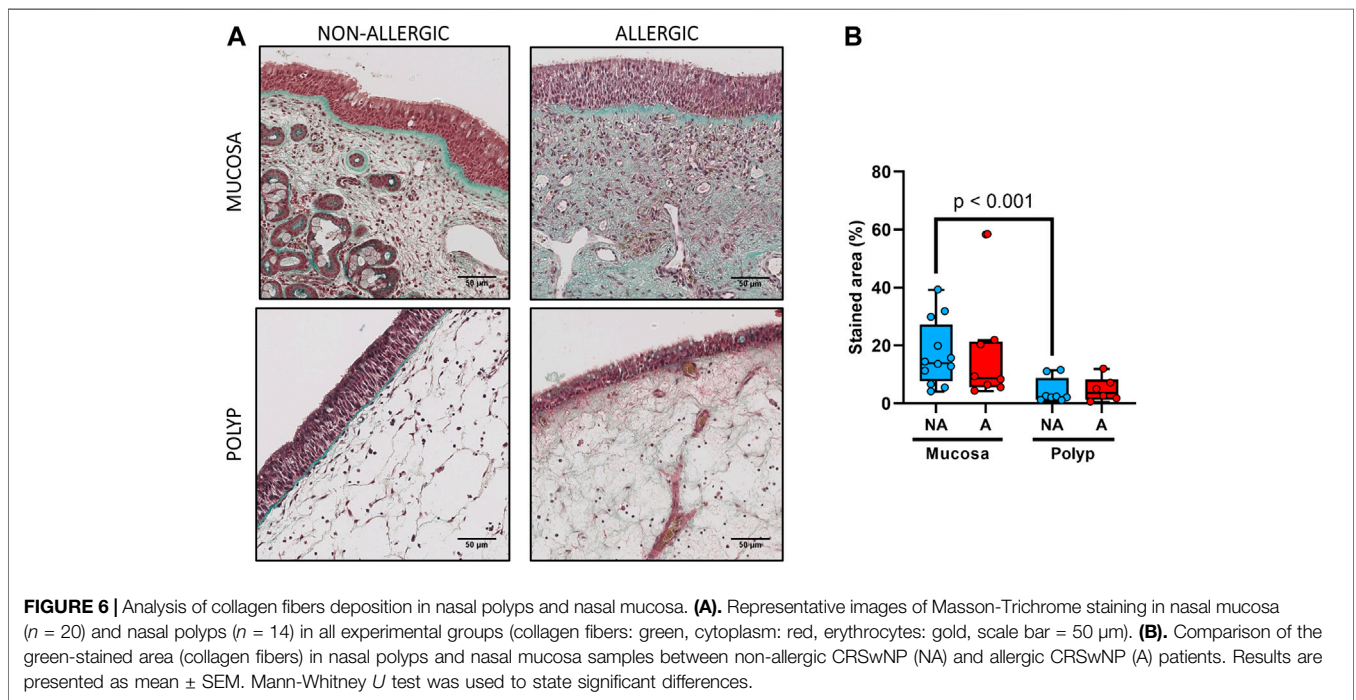
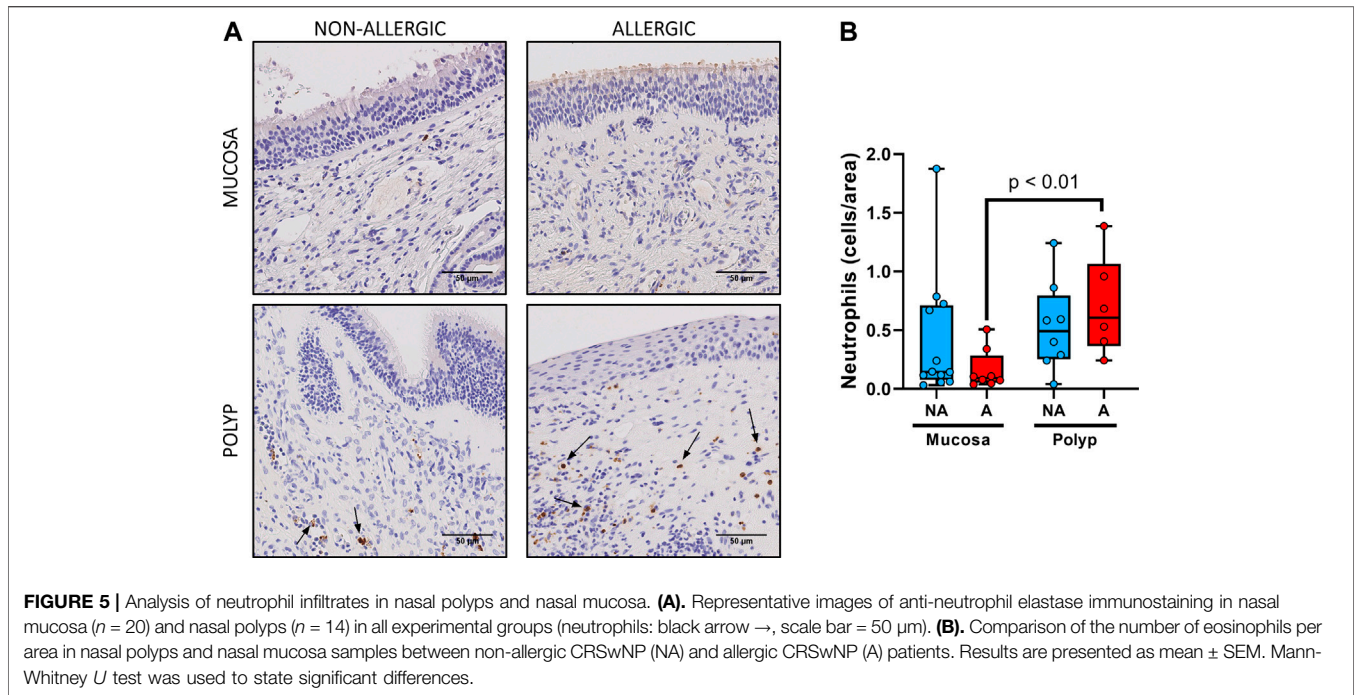


**FIGURE 4** | Analysis of eosinophil infiltrates in nasal polyps and nasal mucosa. **(A)**. Representative images of Luna staining in nasal mucosa ( $n = 20$ ) and nasal polyps ( $n = 14$ ) in all experimental groups (eosinophils: black arrow  $\rightarrow$ , scale bar = 50  $\mu\text{m}$ ). **(B)**. Comparison of the number of eosinophils per area in nasal polyps and nasal mucosa samples between non-allergic CRSwNP (NA) and allergic CRSwNP (A) patients. Results are presented as mean  $\pm$  SEM. Mann-Whitney  $U$  test was used to state significant differences.

be effective and safe for the treatment of nasal polyps (Kiris et al., 2016). Additionally, it has been shown that polyp-derived epithelial cells produce cortisol, which may be involved in the anti-inflammatory response established when patients receive treatment with glucocorticoid for nasal polyps (Kook et al., 2015). The elevation of this metabolite in the non-allergic CRSwNP patients might point

to a specific pathway to cope with inflammation. Additionally, this suggests that, in allergic CRSwNP patients, the cortisol acts by recruiting immune cells instead of solving the inflammation by itself.

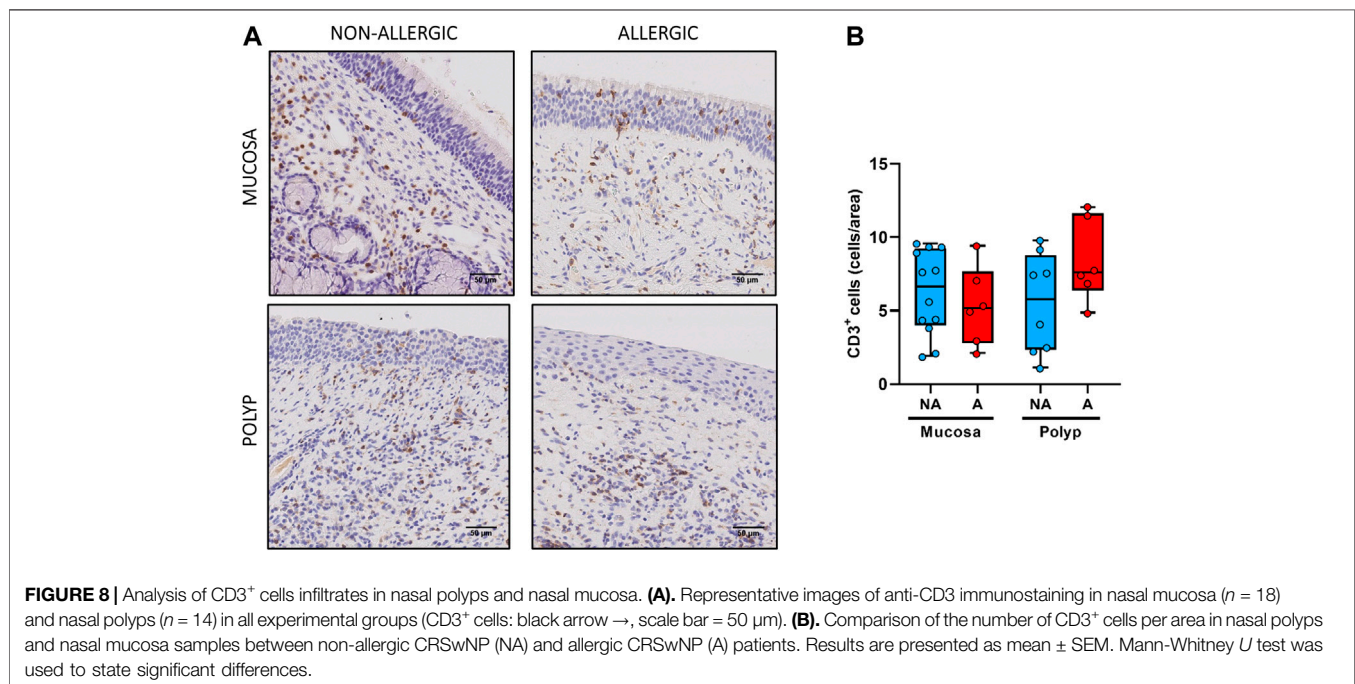
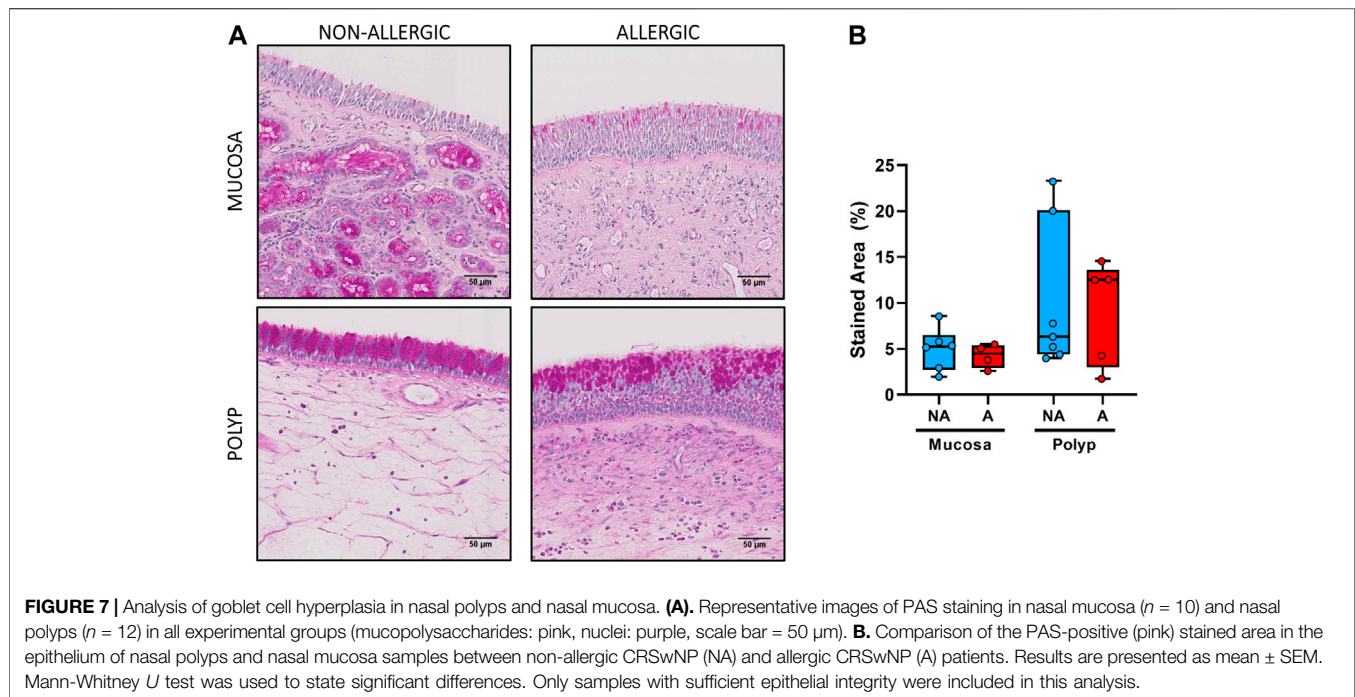
Our results demonstrate that allergy produces metabolic changes in plasma in patients with CRSwNP. The increase of LPC 16:0, LPC 18:0, LPC 20:4, LPI 20:4, cortisol and



bilirubin metabolites in the plasma of non-allergic CRSwNP patients points toward a systemic inflammatory response in the absence of allergy. These metabolites might participate in the development of a characteristic tissue environment, responsible for the differences observed at the histological and inflammatory infiltration levels. Therefore, we

hypothesized that they might be also altered in the nasal polyp in the same way.

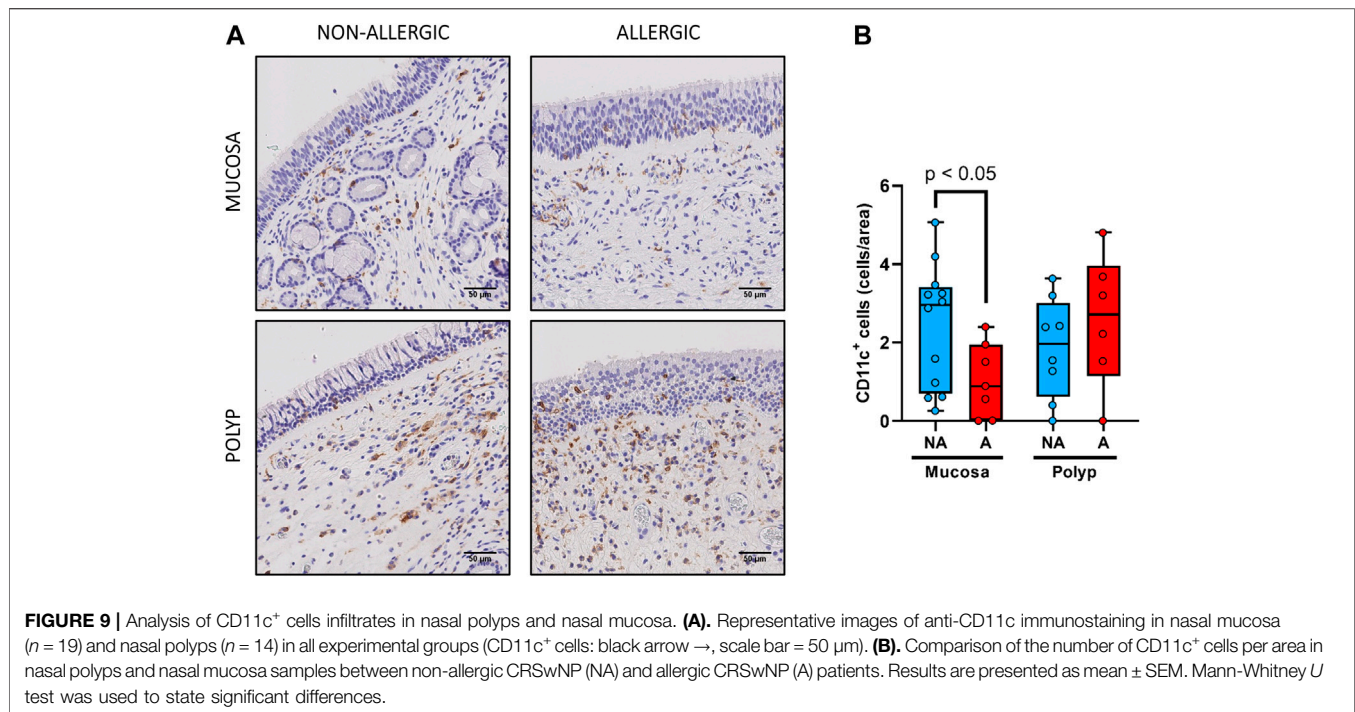
Consequently, we implemented a novel target methodology to analyze these significant metabolites from plasma that were commercially available in the nasal polyp, obtaining good analytical parameters. We observed that the trends of the LPC



16:0, LPC 18:0 and LPI 20:4 metabolites are similar in plasma and nasal polyps samples. However, further studies are needed, including a higher number of tissue samples to validate these results.

Together, the metabolomic results demonstrate that allergy induces specific metabolic changes in CRSwNP patients. These

are LPC 16:0, LPC 18:0, LPC 20:4, LPI 20:4, cortisol and bilirubin. Most of these metabolites were measured in nasal polyp, a biological sample that has not been previously analyzed by metabolomics. We showed that LPC 16:0, LPC 18:0 and LPI 20:4 follow the same trend in the nasal polyp than in plasma. This novel methodological procedure could be used in future studies to



better understand the local metabolomic environment of nasal polyps.

Histological characteristics in the nasal polyp and their nasal mucosa of these patients was also analyzed. Tissue eosinophils have been described both in nasal polyps and in allergic pathologies. In fact, treatment with anti-IL5 (mepolizumab) has shown a reduction in both nasal polyp and blood eosinophils, and a significant improvement in CRSwNP patients, resulting in better prognosis (Bachert et al., 2017). Eosinophils have been also measured locally and systemically. Therefore, a high number of tissue eosinophils and/or their proteins in nasal polyps have been related to more severe and maintained symptoms (Sun et al., 2017) and recurrence (Tos et al., 2010; Van Zele et al., 2014; Yang et al., 2018). High numbers of eosinophils in plasma correlate with higher allergy incidence and worse symptomatology as well (Erbek et al., 2007). Thus, it seems clear that eosinophils might play a role in the development and prognosis of allergic CRSwNP.

On the other hand, neutrophil quantification showed a similar distribution pattern between non-allergic CRSwNP and allergic CRSwNP patients, which was independent of the presence or absence of eosinophils. Although there are studies describing lower numbers of neutrophils in eosinophilic CRSwNP compared to the non-eosinophilic polyps (Schleimer, 2017); other authors (Pothoven et al., 2017; Kong and Kim, 2018) have recently reported similar results, linking the role of neutrophils in this disease to their expression of oncostatin M (OSM), a cytokine that has been found elevated in CRSwNP and that induces barrier dysfunction.

Additionally, a lower collagen deposition in nasal polyps compared to nasal mucosa for both allergic and non-allergic

CRSwNP patients, suggest that the polyps of the study are edematous, rather than a fibrous (Brescia et al., 2021).

In brief, immune cell infiltration analysis revealed differential features between nasal polyp and nasal mucosa and suggest that a maintained allergy would enhances the inflammatory response mediated by eosinophils in nasal polyps but, surprisingly, not in nasal mucosa for allergic CRSwNP patients.

Separately, according to Brescia *et al* (Brescia et al., 2021), CRS appears to be a very heterogeneous inflammatory condition, with various emerging endotypes. Molecular and cellular screening together with clinical phenotyping in CRSwNP could be useful to define endotypes, and thus clarify the inflammatory mechanisms and allow the establishment of a more precise treatment. However, because of the aim of this exploratory study was to use allergy as the main classifying criterion, we are not able to describe our data in terms of CRS endotypes. This limitation should be addressed in the future including a more complete immunological, histopathological and clinical phenotyping approach, what will lead to an improvement in the endotyping capability, as it has been reported (Brescia et al., 2017; Kim and Cho, 2017; Bachert et al., 2018). In this sense, metabolomics could offer help in both 1) the endotyping of patients with CRSwNP, along with cellular and other molecular analysis; and 2) the understanding of the molecular mechanisms that underlay the endotypes.

Our findings suggest that the two phenotypes (non-allergic CRSwNP and allergic CRSwNP), although sharing histological features such as cellular infiltration, have distinctive metabolomic fingerprints and eosinophilia, which point toward different mechanisms of formation.

Previous studies from our group have followed this metabolomics approach in other respiratory allergy models and have found alterations in the AA pathway, as we report in this manuscript (Obeso et al., 2018; Barker-Tejeda et al., 2020). Although, surprisingly, this route was downregulated in allergic CRSwNP patients, an increased recruitment of eosinophils in the nasal polyp was observed. Therefore, we hypothesized that the development of the phenotype CRSwNP without allergy requires a great underlying uncontrolled systemic inflammation, which is different in the allergic phenotype. Thus, eosinophils seem to be accountant for the inflammation leading to CRSwNP development in the allergic phenotype, while non-allergic CRSwNP phenotype would be characterized by higher levels of AA precursors and other inflammatory mediators needed to develop the nasal polyp. The reason of the increase in these biological pathways is, however, yet to be defined.

This is an exploratory study, where the design is innovative and aimed to understand the effect of respiratory allergy in the development of CRSwNP; however, it has some limitations. Although the sample size was small, the samples (nasal polyps, nasal mucosa and plasma) were extensively characterized by metabolomics and histology. Moreover, despite the metabolic alterations that were observed between these two groups of patients not being able to generate a discriminant model (i.e. PLS-DA) capable of predicting new samples, the findings are promising in this field and would shed light on the mechanism by which patients without allergy develop CRSwNP. Therefore, in further studies, the validation of these results in a bigger cohort is needed.

Overall, CRSwNP is a pathology of high level of clinic-pathological complexity where the collection of biopsies is not an easy task. Although the role of histological study of biopsies is a complementary approach for the endotyping of nasal polyps, the inclusion of a metabolomic analysis has allowed us to identify biological processes associated with the allergic or non-allergic phenotypes and, therefore, could be helpful in the design of novel, less invasive treatments for these patients.

## CONCLUSION

Our results demonstrate that patients with CRSwNP with and without allergy display systemic metabolic changes. Surprisingly, these metabolites (LPC 16:0, LPC 18:0, LPC 20:4, LPI 20:4, cortisol and bilirubin), which are associated with inflammation, appear to be increased in the absence of allergy, suggesting that non-allergic CRSwNP patients develop the nasal polyp after a sustained systemic inflammation. We have developed a new method for the analysis of nasal polyps using targeted metabolomics. With this, we spotted the same trends of LPC 16:0, LPC 18:0 and LPI 20:4 that were observed in plasma. The increased numbers of eosinophils in the nasal polyp of allergic CRSwNP patients hints that nasal polyps might develop by a local immune effector cell recruitment that ends in tissue remodeling. Finally, this is an exploratory study, where the significant metabolites were obtained by a semi-quantitative comparison between the groups. Thus, interpretation of these results should be made taking into account these limitations. Further validation studies in new cohort of samples using targeted quantitative methods must be carried out.

## DATA AVAILABILITY STATEMENT

The datasets presented in this study can be found in online repositories. The names of the repository/repositories and accession number(s) can be found below: <https://www.metabolomicsworkbench.org/ST001733>; <https://www.metabolomicsworkbench.org/ST001734>.

## ETHICS STATEMENT

The studies involving human participants were reviewed and approved by the ethical committee of Hospital Madrid Montepincipe (Spain). The patients/participants provided their written informed consent to participate in this study.

## AUTHOR CONTRIBUTIONS

TC was the PI and together with DB, ME and AV, which designed and supervised the research. MID-D, JS-S, LM-B and PF performed the immunohistochemical analysis. DO and AV performed the metabolomic analysis. MID-D, DO, CB, DB and AV contributed to the metabolomics interpretation. MF included all study patients. CB and ME supervised the metabolomic and immunohistochemical analysis, respectively. All authors contributed to the writing of the manuscript and have given approval to the final version of the manuscript.

## FUNDING

This work was supported by Instituto de Salud Carlos III (project numbers PI19/00044 and PI18/01467) co-funded by European Regional Development Fund “Investing in your future” for the thematic network and co-operative research centers ARADyAL RD16/0006/0015. This work was also supported by the grant from Ministerio de Ciencia, Innovacion y Universidades RTI 2018–095166-B-100. MID-D, JS-S, LM-B were supported by FPI-CEU predoctoral fellowships and A.V. is funded by a postdoctoral research fellowship from ARADyAL. Data have been presented at EAACI Congress 2018 (Munich, Germany) and EAACI Congress 2019 (Lisbon, Portugal).

## ACKNOWLEDGMENTS

We would like to thank Virginia Garcia and Javier Moratinos of the Histology Core Facility at the Institute of Applied Molecular Medicine, Faculty of Medicine, San Pablo CEU University, Madrid, Spain, for their advice and expertise in this study, as well as Tomás Clive Barker Tejeda for his asserted comments.

## SUPPLEMENTARY MATERIAL

The Supplementary Material for this article can be found online at: <https://www.frontiersin.org/articles/10.3389/fmolb.2021.662792/full#supplementary-material>



## REFERENCES

- Aceves, S. S., and Ackerman, S. J. (2009). Relationships between Eosinophilic Inflammation, Tissue Remodeling, and Fibrosis in Eosinophilic Esophagitis. *Immunol. Allergy Clin. North America* 29 (1), 197–211. doi:10.1016/j.iac.2008.10.003
- Anderson, G. P. (2008). Endotyping Asthma: New Insights into Key Pathogenic Mechanisms in a Complex, Heterogeneous Disease. *The Lancet* 372 (9643), 1107–1119. doi:10.1016/s0140-6736(08)61452-x
- Arita, M. (2016). Eosinophil Polyunsaturated Fatty Acid Metabolism and its Potential Control of Inflammation and Allergy. *Allergol. Int.* 65 (Suppl. 1), S2–S5. doi:10.1016/j.alit.2016.05.010
- Bachert, C., Sousa, A. R., Lund, V. J., Scadding, G. K., Gevaert, P., Nasser, S., et al. (2017). Reduced Need for Surgery in Severe Nasal Polyposis with Mepolizumab: Randomized Trial. *J. Allergy Clin. Immunol.* 140 (4), 1024–1031. doi:10.1016/j.jaci.2017.05.044
- Bachert, C., Zhang, N., Hellings, P. W., and Bousquet, J. (2018). Endotype-driven Care Pathways in Patients with Chronic Rhinosinusitis. *J. Allergy Clin. Immunol.* 141 (5), 1543–1551. doi:10.1016/j.jaci.2018.03.004
- Balgoma, D., Astudillo, A. M., Pérez-Chacón, G., Montero, O., Balboa, M. A., and Balsinde, J. (2010). Markers of Monocyte Activation Revealed by Lipidomic Profiling of Arachidonic Acid-Containing Phospholipids. *J.L.* 184 (7), 3857–3865. doi:10.4049/jimmunol.0902883
- Barker-Tejeda, T. C., Bazire, R., Obeso, D., Mera-Berriatua, L., Rosace, D., Vazquez-Cortes, S., et al. (2020). Exploring Novel Systemic Biomarker Approaches in Grass-Pollen Sublingual Immunotherapy Using Omics. *Allergy* 76 (4), 1199–1212. doi:10.1111/all.14565
- Bauchau, V., and Durham, S. R. (2004). Prevalence and Rate of Diagnosis of Allergic Rhinitis in Europe. *Eur. Respir. J.* 24 (5), 758–764. doi:10.1183/09031936.04.00013904
- Bennett, M., and Gilroy, D. W. (2016). Lipid Mediators in Inflammation. *Microbiol. Spectr.* 4 (6), 4. doi:10.1128/microbiolspec.MCHD-0035-2016
- Bousquet, J., Khaltaev, N., Cruz, A. A., Denburg, J., Fokkens, W. J., Togias, A., et al. (2008). Allergic Rhinitis and its Impact on Asthma (ARIA) 2008 Update (In Collaboration with the World Health Organization, GA(2)LEN and AllerGen). *Allergy* 63 Suppl 86, 8–160. doi:10.1111/j.1398-9995.2007.01620.x
- Brescia, G., Alessandrini, L., Giacomelli, L., Parrino, D., Zanotti, C., Tealdo, G., et al. (2020). A Classification of Chronic Rhinosinusitis with Nasal Polyps Based on Structured Histopathology. *Histopathology* 76 (2), 296–307. doi:10.1111/his.13969
- Brescia, G., Alessandrini, L., and Marioni, G. (2021). Structured Histopathology for Endotyping and Planning Rational Treatment in Chronic Rhinosinusitis. *Am. J. Otolaryngol.* 42 (1), 102795. doi:10.1016/j.amjoto.2020.102795
- Brescia, G., Barion, U., Zanotti, C., Giacomelli, L., Martini, A., and Marioni, G. (2017). The Prognostic Role of Serum Eosinophil and Basophil Levels in Sinonasal Polyposis. *Int. Forum Allergy Rhinol.* 7 (3), 261–267. doi:10.1002/alf.21885
- Brescia, G., Zanotti, C., Parrino, D., Barion, U., and Marioni, G. (2018). Nasal Polyposis Pathophysiology: Endotype and Phenotype Open Issues. *Am. J. Otolaryngol.* 39 (4), 441–444. doi:10.1016/j.amjoto.2018.03.020
- Chen, S., Zhou, A., Emmanuel, B., Thomas, K., and Guiang, H. (2020). Systematic Literature Review of the Epidemiology and Clinical Burden of Chronic Rhinosinusitis with Nasal Polyposis. *Curr. Med. Res. Opin.* 36 (11), 1897–1911. doi:10.1080/03007995.2020.1815682
- Chiurchiù, V., Leuti, A., Maccarrone Bioactive Lipids, M., and Inflammation, Chronic. (2018). Managing the Fire within. *Front. Immunol.* 9, 38. doi:10.3389/fimmu.2018.00038
- Chojnowska, S., Kępk, A., Waszkiewicz, N., Zp, K., Duchnowska, E., Ościłowicz, K., et al. (2013). Etiopathogenesis of Nasal Polyps. *Prog. Heal Sci.* 3 (2), 151–159.
- Ciborowski, M., Javier Rupérez, F., Martínez-Alcázar, M. P., Angulo, S., Radziwon, P., Olszanski, R., et al. (2010). Metabolomic Approach with LC–MS Reveals Significant Effect of Pressure on Diver's Plasma. *J. Proteome Res.* 9 (8), 4131–4137. doi:10.1021/pr100331j
- Comhair, S. A. A., McDunn, J., Bennett, C., Fetting, J., Erzurum, S. C., and Kalhan, S. C. (2015). Metabolomic Endotype of Asthma. *J.L.* 195 (2), 643–650. doi:10.4049/jimmunol.1500736
- Crestani, E., Harb, H., Charbonnier, L.-M., Leirer, J., Motsinger-Reif, A., Rachid, R., et al. (2020). Untargeted Metabolomic Profiling Identifies Disease-specific Signatures in Food Allergy and Asthma. *J. Allergy Clin. Immunol.* 145 (3), 897–906. doi:10.1016/j.jaci.2019.10.014
- Dudzík, D., Barbas-Bernardos, C., García, A., and Barbas, C. (2018). Quality Assurance Procedures for Mass Spectrometry Untargeted Metabolomics. A review. *Journal of Pharmaceutical and Biomedical Analysis*. a review, *J. Pharm. Biomed. Anal.* 147, 149–173. doi:10.1016/j.jpba.2017.07.044
- Erbek, S. S., Erbek, S., Topal, O., and Cakmak, O. (2007). The Role of Allergy in the Severity of Nasal Polyposis. *Am. J. Rhinology* 21 (6), 686–690. doi:10.2500/ajr.2007.21.3062
- Ferreira Couto, L. G., Fernandes, A. M., Brandão, D. F., de Santi Neto, D., Pereira Valera, F. C., and Anselmo-Lima, W. T. (2008). Histological Aspects of Rhinosinusal Polyps. *Braz. J. Otorhinolaryngol.* 74 (2), 207–212. doi:10.1016/s1808-8694(15)31090-9
- Fidan, V., Alp, H. H., Kalkandelen, S., and Cingi, C. (2013). Melatonin and Cortisol Rhythm in Patients with Extensive Nasal Polyposis. *Am. J. Otolaryngol.* 34 (1), 61–64. doi:10.1016/j.amjoto.2012.09.001
- Fokkens, W. J., Lund, V. J., Mullol, J., Bachert, C., Alobid, I., Baroody, F., et al. (2012). EPOS 2012: European Position Paper on Rhinosinusitis and Nasal Polyps 2012. A Summary for Otorhinolaryngologists. *Rhin* 50 (1), 1–12. doi:10.4193/rhino50e2
- Georgy, M. S., and Peters, A. T. (2012). Chapter 7: Nasal Polyps. *Allergy Asthma Proc.* 33 (Suppl. 1), S22–S23. doi:10.2500/aap.2012.33.3537
- Gil-de-la-Fuente, A., Godzien, J., Saugar, S., Garcia-Carmona, R., Badran, H., Wishart, D. S., et al. (2019). CEU Mass Mediator 3.0: A Metabolite Annotation Tool. *J. Proteome Res.* 18 (2), 797–802. doi:10.1021/acs.jproteome.8b00720
- Godzien, J., Alonso-Herranz, V., Barbas, C., and Armitage, E. G. (2015). Controlling the Quality of Metabolomics Data: New Strategies to Get the Best Out of the QC Sample. *Metabolomics* 11 (3), 518–528. doi:10.1007/s11306-014-0712-4
- Grill, M., Högenauer, C., Blesl, A., Haybaeck, J., Golob-Schwarzl, N., Ferreirós, N., et al. (2019). Members of the Endocannabinoid System Are Distinctly Regulated in Inflammatory Bowel Disease and Colorectal Cancer. *Sci. Rep.* 9 (1), 2358. doi:10.1038/s41598-019-38865-4
- Hopkins, C. (2019). “Chronic Rhinosinusitis with Nasal Polyps,” Editor C. G. Solomon, N. Engl. J. Med 381 (1), 55–63. doi:10.1056/nejmcp1800215
- Kim, D. E., Lee, Y., Kim, M., Lee, S., Jon, S., and Lee, S.-H. (2017). Bilirubin Nanoparticles Ameliorate Allergic Lung Inflammation in a Mouse Model of Asthma. *Biomaterials* 140, 37–44. doi:10.1016/j.biomaterials.2017.06.014
- Kim, D. W., and Cho, S. H. (2017). Emerging Endotypes of Chronic Rhinosinusitis and its Application to Precision Medicine. *Allergy Asthma Immunol. Res.* 9 (4), 299. doi:10.4168/aa.2017.9.4.299
- Kong, I. G., and Kim, D. W. (2018). Pathogenesis of Recalcitrant Chronic Rhinosinusitis: The Emerging Role of Innate Immune Cells. *Immune Netw.* 18 (2), 1–12. doi:10.4110/in.2018.18.e6
- Kook, J. H., Kim, H. J., Kim, K. W., Park, S. J., Kim, T. H., Lim, S. H., et al. (2015). The Expression of 11 $\beta$ -Hydroxysteroid Dehydrogenase Type 1 and 2 in Nasal Polyp-Derived Epithelial Cells and its Possible Contribution to Glucocorticoid Activation in Nasal Polyp. *Am. J. Rhinol. Allergy* 29 (4), 246–250. doi:10.2500/ajra.2015.29.4185
- Kırıs, M., Muderris, T., Yalçın, G., Bercin, S., Sevil, E., and Gul, F. (2016). Intrapoly Steroid Injection for Nasal Polyposis: Randomized Trial of Safety and Efficacy. *Laryngoscope* 126 (8), 1730–1735. doi:10.1002/lary.25945
- Lu, Y., Wang, Y., Ong, C.-N., Subramaniam, T., Choi, H. W., Yuan, J.-M., et al. (2016). Metabolic Signatures and Risk of Type 2 Diabetes in a Chinese Population: an Untargeted Metabolomics Study Using Both LC-MS and GC-MS. *Diabetologia* 59 (11), 2349–2359. doi:10.1007/s00125-016-4069-2
- Lund, V. J. (1995). Fortnightly Review: Diagnosis and Treatment of Nasal Polyps. *BMJ* 311 (7017), 1411–1414. doi:10.1136/bmj.311.7017.1411
- Obeso, D., Mera-Berriatua, L., Rodríguez-Coira, J., Rosace, D., Fernández, P., Martín-Antoniano, I. A., et al. (2018). Multi-omics Analysis Points to Altered Platelet Functions in Severe Food-Associated Respiratory Allergy. *Allergy* 73 (11), 2137–2149. doi:10.1111/all.13563
- Pearlman, A. N., Chandra, R. K., Conley, D. B., and Kern, R. C. (2010). “Epidemiology of Nasal Polyps,” in *Nasal Polyposis*. Editors T. M. Önerci and B. J. Ferguson (Heidelberg, Berlin: Springer), 9–15. doi:10.1007/978-3-642-11412-0\_2
- Peng, Y.-F., Goyal, H., and Xu, G.-D. (2017). Serum Bilirubin Has an Important Role in Multiple Clinical Applications. *J. Lab. Precis. Med.* 2, 82. doi:10.21037/jlpm.2017.09.08








- Pothoven, K. L., Norton, J. E., Suh, L. A., Carter, R. G., Harris, K. E., Biyasheva, A., et al. (2017). Neutrophils Are a Major Source of the Epithelial Barrier Disrupting Cytokine Oncostatin M in Patients with Mucosal Airways Disease. *J. Allergy Clin. Immunol.* 139 (6), 1966–1978. doi:10.1016/j.jaci.2016.10.039
- Ried, J. S., Baurecht, H., Stücker, F., Krumsiek, J., Gieger, C., Heinrich, J., et al. (2013). “Integrative Genetic and Metabolite Profiling Analysis Suggests Altered Phosphatidylcholine Metabolism in Asthma,” Editor H-U. Simon and Allergy, 68 (5), 629–636. doi:10.1111/all.12110
- Rosace, D., Gomez-Casado, C., Fernandez, P., Perez-Gordo, M., Dominguezdel, M. d. C. C., Vega, A., et al. (2019). Profilin-mediated Food-Induced Allergic Reactions Are Associated with Oral Epithelial Remodeling. *J. Allergy Clin. Immunol.* 143 (2), 681–690. doi:10.1016/j.jaci.2018.03.013
- Samitas, K., Carter, A., Kariyawasam, H. H., and Xanthou, G. (2018). Upper and Lower Airway Remodelling Mechanisms in Asthma, Allergic Rhinitis and Chronic Rhinosinusitis: The One Airway Concept Revisited. *Allergy* 73 (5), 993–1002. doi:10.1111/all.13373
- Sanchez-Solares, J., Delgado-Dolset, M. I., Mera-Berriatua, L., Hormias-Martin, G., Cumplido, J. A., Saiz, V., et al. (2019). Respiratory Allergies with No Associated Food Allergy Disrupt Oral Mucosa Integrity. *Allergy*. 74 (11), 2261–2265. doi:10.1111/all.13860
- Schleimer, R. P. (2017). Immunopathogenesis of Chronic Rhinosinusitis and Nasal Polyposis. *Annu. Rev. Pathol. Mech. Dis.* 12 (1), 331–357. doi:10.1146/annurev-pathol-052016-100401
- Sun, C., Ouyang, H., and Luo, R. (2017). Distinct Characteristics of Nasal Polyps with and without Eosinophilia. *Braz. J. Otorhinolaryngol.* 83 (1), 66–72. doi:10.1016/j.bjorl.2016.01.012
- Tos, M., Larsen, P. L., Larsen, K., and Caye-Thomasen, P. (2010). “Pathogenesis and Pathophysiology of Nasal Polyps,” in *Nasal Polyposis*. Editors T. M. Önerci and B. J. Ferguson (Heidelberg, Berlin: Springer), 53–63. doi:10.1007/978-3-642-11412-0\_7
- Van Zele, T., Holtappels, G., Gevaert, P., and Bachert, C. (2014). Differences in Initial Immunoprofiles between Recurrent and Nonrecurrent Chronic Rhinosinusitis with Nasal Polyps. *Am. J. Rhinol. allergy* 28 (3), 192–198. doi:10.2500/ajra.2014.28.4033
- Villaseñor, A., Rosace, D., Obeso, D., Pérez-Gordo, M., Chivato, T., Barbas, C., et al. (2017). Allergic Asthma: an Overview of Metabolomic Strategies Leading to the Identification of Biomarkers in the Field. *Clin. Exp. Allergy* 47 (4), 442–456. doi:10.1111/cea.12902
- Vogel, M. E., and Zucker, S. D. (2016). Bilirubin Acts as an Endogenous Regulator of Inflammation by Disrupting Adhesion Molecule-Mediated Leukocyte Migration. *Inflamm. Cel Signal* 3 (1), e1178. doi:10.14800/ics.1178
- Wilson, K. F., McMains, K. C., and Orlandi, R. R. (2014). The Association between Allergy and Chronic Rhinosinusitis with and without Nasal Polyps: an Evidence-Based Review with Recommendations. *Int. Forum Allergy Rhinology* 4 (2), 93–103. doi:10.1002/alr.21258
- Wynn, R., and Har-El, G. (2004). Recurrence Rates after Endoscopic Sinus Surgery for Massive Sinus Polyposis. *The Laryngoscope* 114 (5), 811–813. doi:10.1097/00005537-200405000-00004
- Yang, H. H., Fang, H., You, Q. J., Han, L., Yang, Z. F., Yu, L. L., et al. (2018). [Predictive Study on Recurrence of Chronic Sinusitis with Nasal Polyps by Tissue Eosinophils and Sinus CT]. *Zhonghua Er Bi Yan Hou Tou Jing Wai Ke Za Zhi* 53 (11), 842–846. doi:10.3760/cma.j.issn.1673-0860.2018.11.009
- Yeager, M. P., Guyre, C. A., Sites, B. D., Collins, J. E., Pioli, P. A., and Guyre, P. M. (2018). The Stress Hormone Cortisol Enhances Interferon- $\nu$ -Mediated Proinflammatory Responses of Human Immune Cells. *Anesth. Analgesia* 127 (2), 556–563. doi:10.1213/ane.0000000000003481

**Conflict of Interest:** The authors declare that the research was conducted in the absence of any commercial or financial relationships that could be construed as a potential conflict of interest.

Copyright © 2021 Delgado-Dolset, Obeso, Sánchez-Solares, Mera-Berriatua, Fernández, Barbas, Fresnillo, Chivato, Barber, Escribese and Villaseñor. This is an open-access article distributed under the terms of the Creative Commons Attribution License (CC BY). The use, distribution or reproduction in other forums is permitted, provided the original author(s) and the copyright owner(s) are credited and that the original publication in this journal is cited, in accordance with accepted academic practice. No use, distribution or reproduction is permitted which does not comply with these terms.

Article

# Troubleshooting in Large-Scale LC-ToF-MS Metabolomics Analysis: Solving Complex Issues in Big Cohorts

Juan Rodríguez-Coira <sup>1,2</sup>, María I Delgado-Dolset <sup>1,2</sup>, David Obeso <sup>1,2</sup>,  
Mariana Dolores-Hernández <sup>1,3</sup>, Guillermo Quintás <sup>4,5</sup>, Santiago Angulo <sup>6</sup>,  
Domingo Barber <sup>2</sup>, Teresa Carrillo <sup>7</sup>, María M. Escribese <sup>2,8,\*</sup> and Alma Villaseñor <sup>2,\*</sup>

<sup>1</sup> CEMBIO, Centro de Excelencia en Metabolómica y Bioanálisis, Facultad de Farmacia, Universidad San Pablo CEU, 28668 Madrid, Spain; juan.rodriiguezwillanueva@ceu.es (J.R.-C.); maria.delgadodolset@beca.ceu.es (M.I.D.-D.); david.obesomontero@beca.ceu.es (D.O.); may34@comunidad.unam.mx (M.D.-H.)

<sup>2</sup> IMMA, Instituto de Medicina Molecular Aplicada, Facultad de Medicina, Universidad San Pablo CEU, 28668 Madrid, Spain; domingo.barberhernandez@ceu.es

<sup>3</sup> Laboratorio de Ensayos de Desarrollo Farmacéutico (LEDEFAR), Facultad de Estudios Superiores Cuautitlán, Universidad Nacional Autónoma de México, Estado de México CP.54714, Mexico

<sup>4</sup> Health and Biomedicine, Leitat Technological Center, 08028 Barcelona, Spain; gquintas@leitat.org

<sup>5</sup> Analytical Unit, Health Research Institute Hospital La Fe, 46026 Valencia, Spain

<sup>6</sup> Departamento de Matemática Aplicada y Estadística, Universidad San Pablo CEU, 28668 Madrid, Spain; sangulo@ceu.es

<sup>7</sup> Servicio de Alergia, “Hospital Universitario de Gran Canaria, Dr. Negrin”, 35010 Las Palmas de G.C., Spain; tcardia@gobiernodecanarias.org

<sup>8</sup> Departamento de Ciencias Médicas Básicas, Facultad de Medicina, Universidad San Pablo CEU, 28668 Madrid, Spain

\* Correspondence: mariamarta.escribesealonso@ceu.es (M.M.E.); alma.villasenor@ceu.es (A.V.); Tel.: +34-91-372-47-00 (ext. 15057) (M.M.E.); +34-91-372-47-00 (ext. 4769) (A.V.)

Received: 26 July 2019; Accepted: 21 October 2019; Published: 24 October 2019



**Abstract:** Metabolomics, understood as the science that manages the study of compounds from the metabolism, is an essential tool for deciphering metabolic changes in disease. The experiments rely on the use of high-throughput analytical techniques such as liquid chromatography coupled to mass spectrometry (LC-ToF MS). This hyphenation has brought positive aspects such as higher sensitivity, specificity and the extension of the metabolome coverage in a single run. The analysis of a high number of samples in a single batch is currently not always feasible due to technical and practical issues (i.e., a drop of the MS signal) which result in the MS stopping during the experiment obtaining more than a single sample batch. In this situation, careful data treatment is required to enable an accurate joint analysis of multi-batch data sets. This paper summarizes the analytical strategies in large-scale metabolomic experiments; special attention has been given to QC preparation troubleshooting and data treatment. Moreover, labeled internal standards analysis and their aim in data treatment, and data normalization procedures (intra- and inter-batch) are described. These concepts are exemplified using a cohort of 165 patients from a study in asthma.

**Keywords:** large-scale; metabolomics; LC-QToF-MS; normalization; asthma

## 1. Introduction

The application of “omics” sciences for deciphering the mechanisms involved in complex diseases has succeeded, showing a great impact in the recent years not only in the number of publications,

but also in the advance of medical treatments [1,2]. Metabolomics has gained attention due to its capability to inquire into the metabolism of living organisms.

Asthma is a prevalent disease that currently affects almost 25% of the population worldwide [3]. The number of cases increases every year, as well as its severity, creating a high economic burden and severely impacting health, especially in children. It is a multifactorial disease in which the clinical phenotypes are not clearly defined; partially because the underlying molecular mechanisms are still largely unknown [3]. In addition, it is associated with secondary comorbidities such as obesity and allergy.

Metabolomics experiments rely on the use of high-throughput analytical techniques, such as nuclear magnetic resonance (NMR) and mass spectrometry (MS) based techniques. The use of high-resolution MS, particularly with a quadrupole-time of flight analyzer coupled to liquid chromatography (LC-QToF-MS), has dramatically increased the sensitivity and specificity of the technique enabling the extension of the metabolome coverage in a single run. Therefore, it obtains a very complete picture of the metabolic fingerprint of a patient.

Usually, the instrumental analysis consists on the measurement of a small number of samples—less than a hundred—in a single batch. However, in large-scale studies samples need to be analyzed across multiple batches. This is required due to different reasons including the shift in the instrument response associated with the contamination of the ionization source after repeated injections of samples. Every time a batch is run, the instrument is cleaned, calibrated and conditioned, leading to minor changes in the analytical response. This introduces a between-batch systematic error that needs to be properly addressed to enable the joint analysis of multi-batch data.

For this purpose, the development of algorithms for a post-acquisition correction of both intra- and inter-batch effects is an active field of research [4–6]. On the other hand, additional aspects in large-scale studies, such as the use of internal standards (ISs), the preparation of the quality control samples (QCs), the strategy for sample preparation, the instrumental analysis and the batch design are an integral part of the study design and must be clearly established in advance [7].

The “IS” is a compound (or a group of them) with the closest chemical nature possible to the target metabolites found in the sample and that is not naturally present in it. ISs are widely used in quantitative (targeted) LC-MS methods to assess the effects of the matrix on ion suppression or enhancement, as well as to test the extraction efficiency [8]. In untargeted metabolomic studies, ISs should be carefully selected to avoid interference with the a priori unknown metabolites. Thus, isotopically labeled analogues (often with  $^2\text{H}$  or  $^{13}\text{C}$ ) are frequently selected due to their nearly identical physico-chemical properties to the unlabeled metabolites. The ISs selected should provide a broad coverage of the different classes of metabolites that are expected to be found in the samples. However, their use in untargeted LC-QToF-MS is limited to the assessment of instrument performance, as the IS intensity should not be used to correct between batch systematic errors since the metabolites present in the samples can influence the IS estimates by cross contribution [4,7,9]. Currently, different normalization strategies to correct the instrumental drift have been developed, and most of them rely on the information contented in QCs [10–12].

Furthermore, the preparation of the QCs in large-scale studies is not obvious. Ideally, the QC should be prepared by pooling a small volume of all samples; however, in large-scale studies sometimes this is not feasible. Moreover, even when this is possible, if the time of sample thawing for QC preparation is extensive, it may induce the enzymes in blood samples to activate, leading to a change in the original sample. Therefore, alternative strategies have been suggested, i.e., the use of a pool of randomly selected samples that could represent the sample population [13]. Nonetheless, the exact number of samples needed to represent the whole population should be defined beforehand. Additional factors increasing the complexity of large-scale studies have not been addressed, such as if samples should be prepared all at once or in different sets, and how could this impact the retrieved metabolomic profiles. These “naïve” aspects are essential. Additionally, randomization of the complete

set of samples into the batches is the statistically correct approach; however, there is no warrant that batches will be accurately normalized after integration.

Large-scale studies are mostly unavoidable when working with heterogeneous diseases like asthma, where hundreds of samples are collected, analyzed together and later compared to extract useful biological information. In this work, we propose a series of strategies and troubleshooting suggestions for large-scale LC-QToF-MS metabolomic studies. Special attention is given to the experimental design and to methodological checkpoints required to achieve a proper analysis and integration of a large set of samples.

This work exemplifies from begging to the end the process to be followed in a large-scale analysis in metabolomics. We show for the first time the inclusion of a deuterated lysophosphocholine, sphingolipid and fatty acid, apart from carnitine and isoleucine in the IS mix to cover the complete retention time span in a reverse phase analysis, which is one of the most common analysis in metabolomic fingerprinting studies. Regarding this IS mix, we describe its response in a large-scale sequence in different ways, and we show its utility in the analysis. In addition, we present the comparison of different normalization strategies such as IS, total useful signal (TUS), QC-SVRC normalization and QC-norm. The novelty of this work relies on an experimental strategy to prove that a robust normalization is possible in large-scale studies by using replicates of case samples. This paper highlights the issues found when working with hundreds of samples and shows a way to overcome them and succeed in the integration of the data from multiple batches.

## 2. Results

### 2.1. Instrumental Analysis Considerations

For this study, some analytical conditions were taken into account before analysis. Mobile phase volumes for the complete analysis in each mode were calculated beforehand, preparing 5 L of each, to avoid instrumental variability during the experiment. As the bottles for the mobile phases, needle and needle-seat cleaning and those for the extra pipelines of the pump did not fit on top of the HPLC, one of the 5 L bottles was randomly selected and placed on a separate stool. The rest were arranged on top of the equipment (see Figure S1). Samples were prepared in small sets ( $n = 32$  per day) as the equipment required to analyze them as fresh as possible. Once the samples were prepared, they were kept on the autosampler tray until the end of the analysis. Between modes, samples were centrifuged before measurement to settle down any precipitate. The MS ionization source was cleaned between batches, but the chromatographic column was not, to avoid any potential column de-conditioning which could modify its chromatographic performance. The computer of the equipment was rebooted at the beginning and between the modes of analysis.

### 2.2. Sample Measurement

For this project, a total of 165 serum samples were measured in multiple batches. Two subsets of 7 samples among them were randomly selected to be analyzed in all batches in electrospray source ionization (ESI) in both positive (ESI+) and negative (ESI-) modes, respectively. The samples, blanks and QCs were analyzed following this worklist in each batch: first, 3 no-injection runs, 3 injections of extracting solvent (methanol: ethanol 1:1 (*v/v*)), 10 QC injections for system conditioning, one QC injection followed by 5 experimental samples until all were measured and finally, after the last QC injection, 3 no-injection runs. The no-injection runs were characterized by passing mobile phase through the column without injection in the port of the instrument. They were done with the aim of cleaning and starting the conditioning of the chromatographic conditions. Additionally, extracting solvent injections were used as blanks to identify and exclude signals coming from the experimental samples. The no-injection runs allowed the identification of signals from the column carry-over while the blank runs contained the injector carry-over as well. Regarding the ESI+, the analysis of the samples was done in two batches (see Figure 1A). On the other hand, in the case of

ESI<sup>-</sup>, the samples were measured in three batches as the equipment stopped due to technical issues (an injection failure stopped the analysis) while measuring batch 2. As a result, batch 2 was subdivided into two: batch 2 and 3. Furthermore, batch 3 stopped due to an ‘instrument communication error’ that caused the worklist to fail, impeding sample acquisition. As a result, complementary samples were not measured, including a sample selected to be measured in both batches (see Figure 1B). To sum up, 183 and 178 experimental samples were measured in ESI<sup>+</sup> and ESI<sup>-</sup> mode, respectively.

### 2.3. Analysis of the Labeled IS Mix

IS mix was used to monitor the performance of the system in LC-QTOF-MS experiments (7). For this study, the selection of the compounds for the IS was focused on different physicochemical properties including a lysophosphocholine (LPC), a sphingolipid, a fatty acid, an amino acid and a carnitine with a wide range of *m/z* values and retention times (RTs) (see Figure S2). Carnitine-D<sub>3</sub> and sphingosine-D<sub>7</sub> were detected only in ESI<sup>+</sup> while stearic acid-D<sub>5</sub> was only detected in ESI<sup>-</sup> mode. LPC18:1-D<sub>7</sub>—which showed two peaks at RT 19.3 and 20.0 min—and isoleucine <sup>13</sup>C,<sup>15</sup>N were detected in both modes.

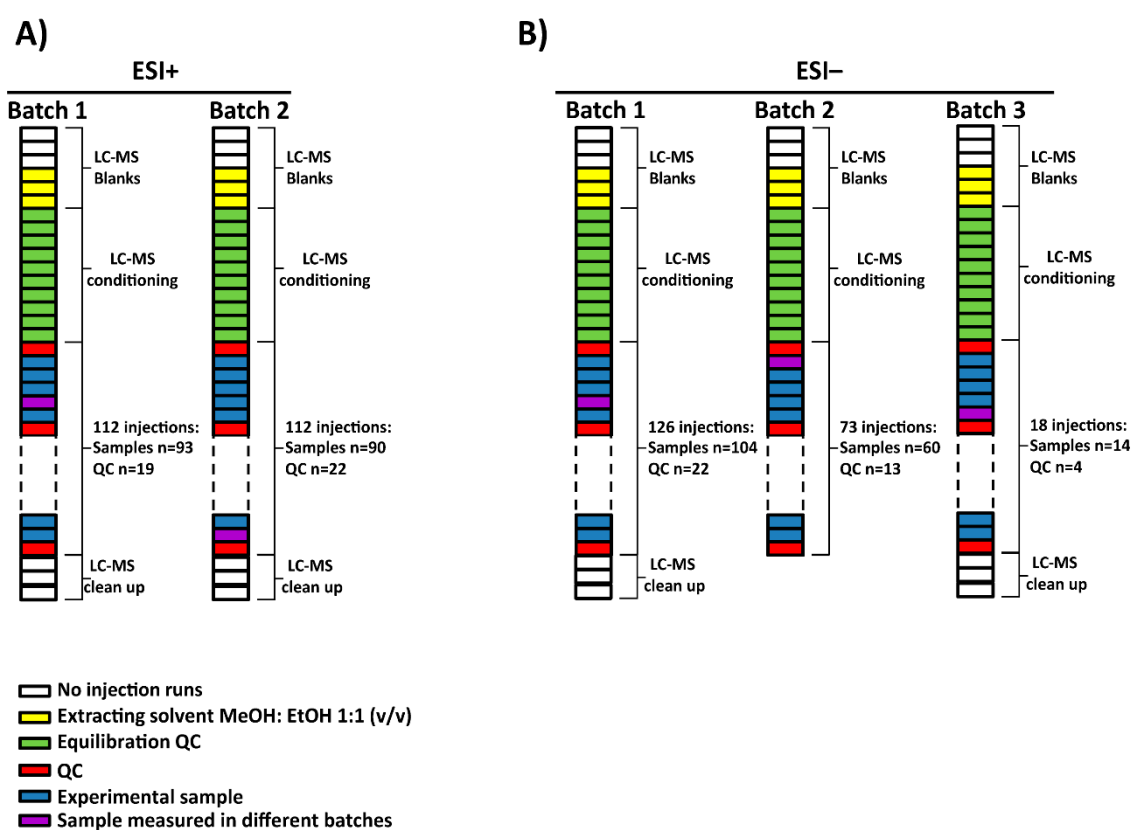


**Figure 1.** Experimental worklists and batches followed for (A) ESI<sup>+</sup> and (B) ESI<sup>-</sup> modes. (A) Experimental samples were measured into two batches for ESI<sup>+</sup> while (B) in the case of ESI<sup>-</sup> mode, 3 batches were obtained due to an ‘instrument communication error’. NOTE. The source of the equipment was not cleaned up between batches 2 and 3 in ESI<sup>-</sup> mode.

Figure S3 depicts the variation in the relative IS intensities in the experimental samples and QCs as a function of the injection order, in order to evaluate the presence and composition of the IS mix. The IS mix was detected in all samples for both modes of analysis. Additionally, fluctuations in the abundances of the IS compounds were observed. Regarding the ESI<sup>+</sup> mode, the most abundant compound was sphingosine-D<sub>7</sub>, while for ESI<sup>-</sup> mode it was LPC 18:1-D<sub>7</sub>—the peak at RT 20.00 min.

Besides, the abundance of each IS compound was plotted along the injection order to observe their pattern in both modes of analysis (Figures 2 and 3). Regarding the ESI<sup>+</sup> mode, the plot showed that each

IS had a distinct pattern within each sample (Figure 2). LPC 18-D<sub>7</sub> can exemplify this, as it presented two peaks at 19.30 and 20.00 min and each of them followed a different pattern. Moreover, from the IS compounds that eluted at the beginning of the chromatogram, L-carnitine-D<sub>3</sub> showed a trend to decrease the signal and such trend was not observed in isoleucine-<sup>13</sup>C, <sup>15</sup>N. Finally, lower relative standard deviation (RSD%) values were observed in isoleucine-<sup>13</sup>C, <sup>15</sup>N, sphingosine-D<sub>7</sub>, LPC 18:1-D<sub>7</sub> RTs 19.3 and 20.0 with RSD of 8.40%, 5.15%, 7.04% and 8.82%, respectively, compared to L-carnitine-D<sub>3</sub> with a RSD of 22.95%.

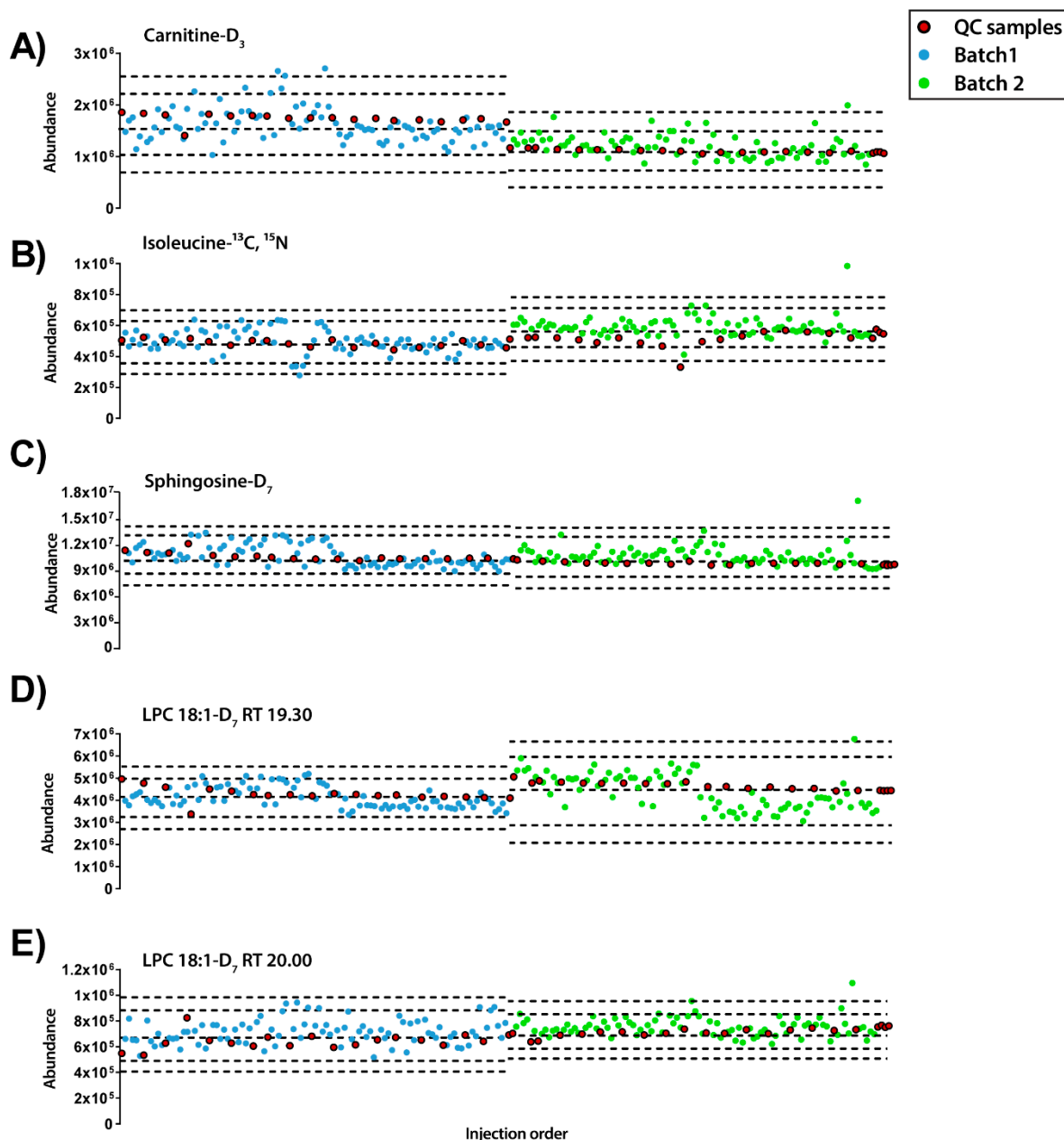


**Figure 2.** Quality control charts of the abundance of IS compounds in each sample according to the injection order for ESI+ mode. (A) Carnitine-D<sub>3</sub> RT 0.70 min, RSD = 22.95%. (B) Isoleucine-<sup>13</sup>C, <sup>15</sup>N RT 0.77 min, RSD = 8.40%. (C) Sphingosine-D<sub>7</sub> RT 14.38 min, RSD = 5.15%. (D) LPC18:1-D<sub>7</sub> RT 19.30 min, RSD = 7.04%. (E) LPC18:1-D<sub>7</sub> RT 20.00 min, RSD = 8.82%. **Legend.** Y-axis: Abundance. X-axis: Sample order. Red circles: QCs; blue and green circles: Experimental samples measured in batch 1 and batch 2, respectively. Dotted lines represent the mean  $\pm$  2 and 3 SD for each batch independently.

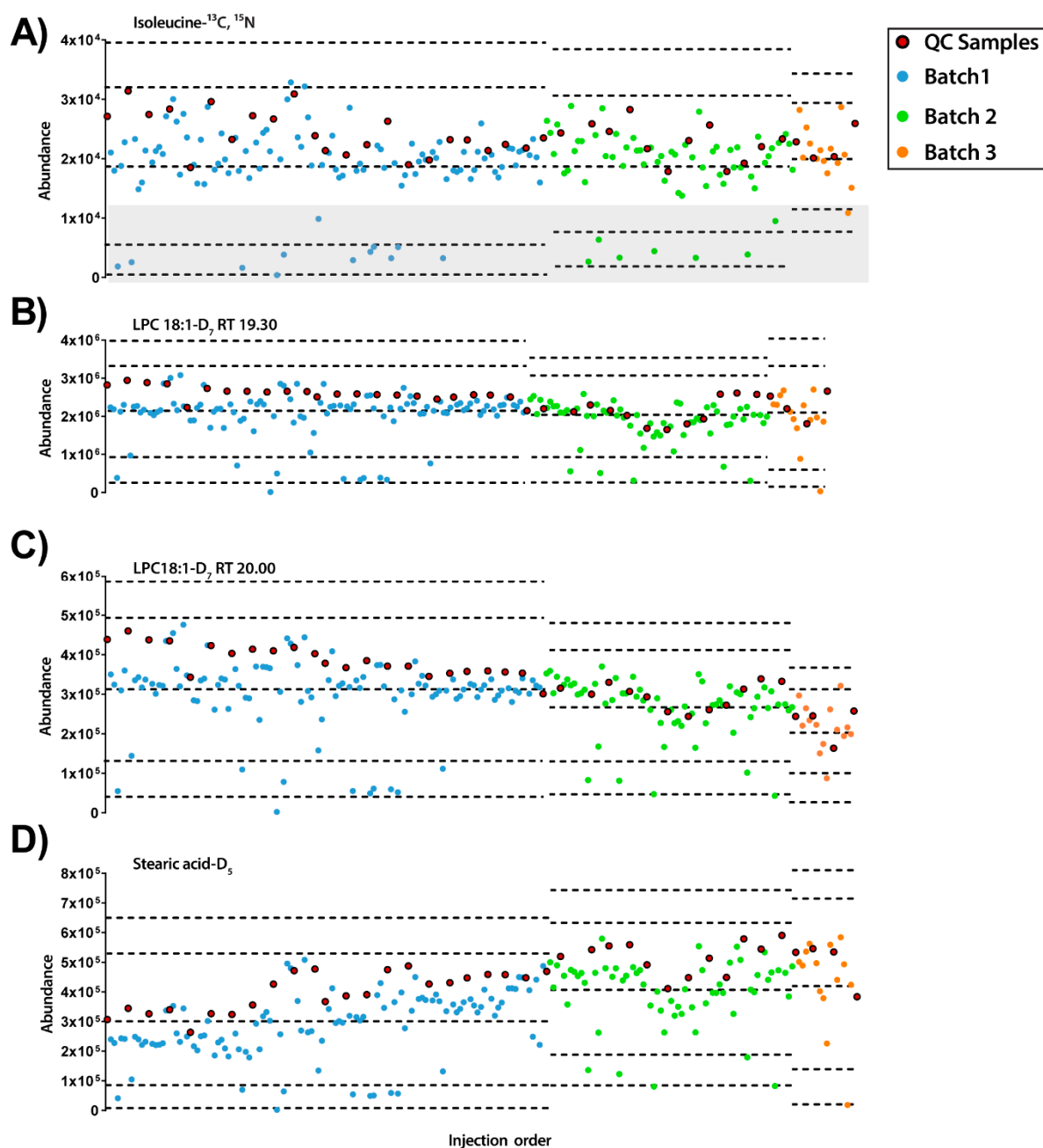


**Figure 3.** Quality control charts of the abundance of IS compounds in each sample according to the injection order for ESI<sup>−</sup> mode. (A) Isoleucine-<sup>13</sup>C, <sup>15</sup>N at RT 0.77 min, RSD = 25.01%. Grey rectangle signals samples with low levels of IS mix. (B) LPC18:1-D<sub>7</sub> RT 19.30 min, RSD = 23.93%. (C) LPC18:1-D<sub>7</sub> RT 20.00 min, RSD = 21.22%. (D) Stearic acid-D<sub>5</sub> RT 34.54 min, RSD = 30.03%. Legend. Y-axis: Abundance. X-axis: Sample order. Red circles: QCs; blue and green circles: experimental samples measured in batch 1 and batch 2, respectively. Dotted lines represent the mean  $\pm$  2 and 3 SD for each batch independently.

On the other hand, in ESI<sup>−</sup> mode, it was detected that some of the experimental samples presented low abundance for all the IS compounds (see Figure 3). Furthermore, as observed previously with ESI<sup>+</sup> mode, each IS compound had different inter- and intra-batch variability along the experiment. Interestingly, while stearic acid-D<sub>5</sub> had a trend to increase its signal along the experiment, LPC18:1-D<sub>7</sub> showed the opposite trend. Excluding the samples with low IS mix abundance (lower than the



mean minus 2 standard deviation (SD),  $n = 20$ ), the RSDs of the IS compounds were LPC 18:1-D<sub>7</sub>: 23.93% and 21.22% for 19.3 and 20.0 min, respectively, isoleucine-<sup>13</sup>C, <sup>15</sup>N 25.01% and stearic acid-D<sub>5</sub> 30.03%.

To sum up, the use of IS with different physicochemical and biological properties has proved that each one may provide different information about the instrument performance and the presence of both intra- and inter-batch effects. Furthermore, results show that the information provided by the different IS is complementary, as the observed trends did not necessarily correlate with each other.

#### 2.4. Initial Quality of the Data

Data was pre-processed by eliminating the signals from the blanks, filtering by presence on QCs, replacing missing values using the k-nearest neighbors (kNN) algorithm, and calculating the RSD% on QCs to exclude those LC-MS features showing RSD > 30%. As a result, the initial number of features for ESI+ and ESI- modes were 991 and 370, respectively. Therefore, a plot of total useful signal (TUS) following the injection order was performed to evaluate the response of each sample in the experiment (Figure S4). We observed that the trend followed by the samples in ESI+ mode was similar to the ISs: LPC18:1-D<sub>7</sub> at RT 20.00 min (see Figure 2D). Moreover, in the case of ESI- mode, an increasing signal from QCs along the experiment was observed. Interestingly, the experimental samples that showed low abundance of IS mix in ESI- mode did not show lower TUS signal.

Moreover, an unsupervised PCA model was built with the data excluding those samples with a TUS higher than 3 SD of the mean or lower than -3 SD to observe initial patterns of the samples (Figure S5). As we can observe in ESI+ mode the first component (PC1), which accounts for the 20.8% of the variability in the data set, separates both batches. There is a clustering of QCs within each batch. In the case of ESI- mode, the same pattern was observed with the exception that batch 2 and 3 were clustering together and that QCs showed a higher variation within each batch (Figure S6). In this case, PC1 and PC2 were investigated independently along with injection order (Figure S7). As it can be observed, batch separation was determined by the second component which accounted for 10.0% of total data variation while the variation in the first component, accounting for 35.9% of the total variance, was associated to the analytical drift. Finally, in ESI- the clustering of a group of samples in the left end of the plot (grey circle) matched with those samples with lower abundances of ISs.

Together, the initial quality checking indicated that the normalization between batches is necessary before the start of the statistical analysis of the metabolomic profiles.

#### 2.5. Normalization of Data

The strategy of normalization for data from different batches is critical, as there are no warranties that intra- and/or inter-batch effects will be accurately corrected afterwards. Two of the most common normalization approaches in metabolomics were initially applied: (1) Normalization by the sum of the IS mix compounds and (2) normalization by the TUS of each sample. These normalization approaches were evaluated using both a TUS plot represented according to the injection order and a principal component analysis (PCA) model (Figures S6 and S8). Regarding the normalization by IS mix, TUS plots for both modes showed a clear trend to increase the signal along the injection order. This correlates with the PCA plot which displayed an analytical drift on the first PC. Moreover, separation of batches was still observed in both modes. Therefore, it is clear that normalization by IS mix does not correct the analytical drift observed in the experiment. The normalization by TUS showed similar QC abundance levels for all batches. However, PCA models showed comparable results as the IS mix normalization in terms of analytical drift and batch separation.

An algorithm called QC-SVRC for intra-batch effect correction based on the information contained on QCs was recently developed (10). This method was applied to correct the intra-batch effect for both modes (Figure 4). As shown by Figure 4A, the QC draw a straight constant line between batches for both modes. Regarding the PCA models, the QC clustering between batches was observed (Figure 4B).

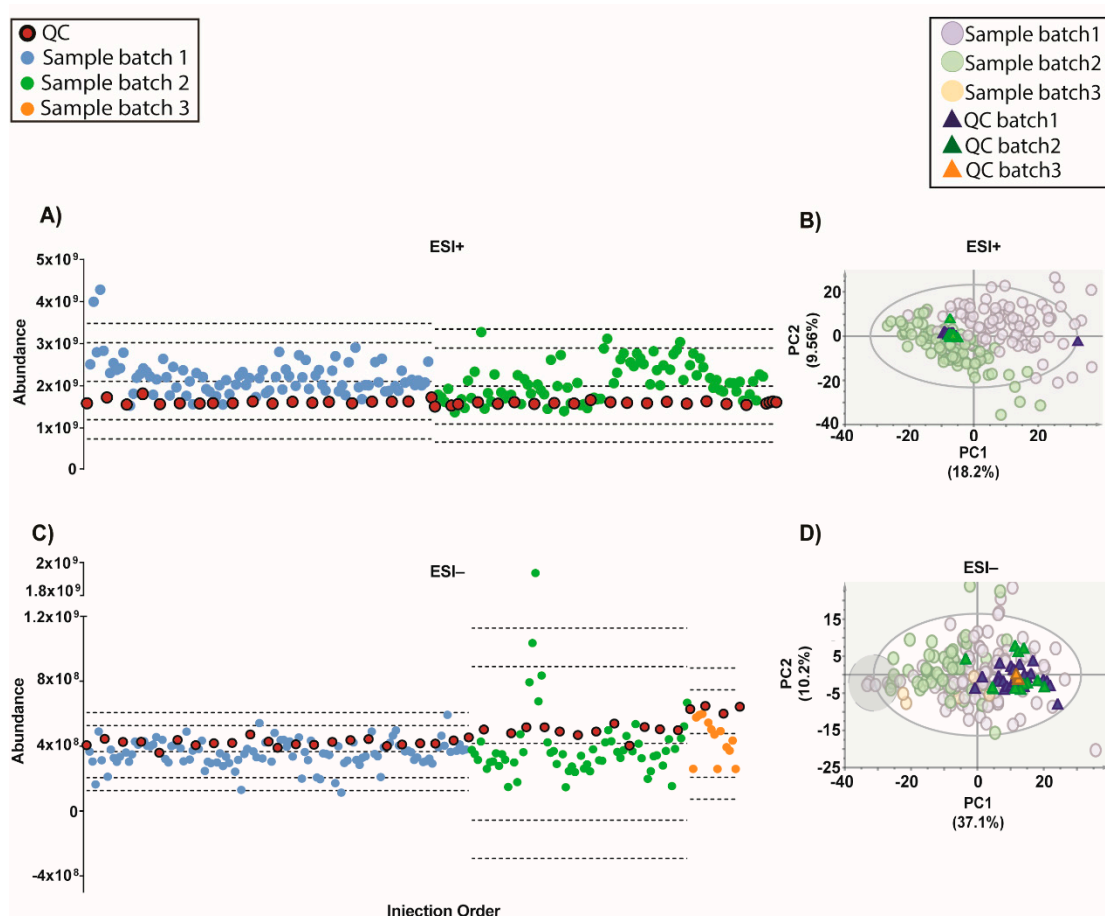


**Figure 4.** Outcome of the data normalization strategy after QC-SVRC algorithm for both ESI+ and ESI- modes. (A,C) Quality control chart of ESI+ and ESI- modes. Samples with a TUS higher than 3 SD of the mean or lower than  $-3$  SD were removed from PCA model. (B,D) PCA plots of ESI+ and ESI- mode, respectively. Signals with %RSD < 30% on QCs were kept, and UV scaling was used. Features in ESI+ and ESI- modes, respectively: 1056 and 394. **Legend.** TUS plot: Blue and green dots: samples of batch1 and batch2, respectively, red dots: QCs. Dotted lines represent the mean  $\pm$  2 and 3 SD for each batch independently. PCA: Blue dots and dark blue triangles are samples and QCs measured in batch1, respectively; green dots and dark green triangles are samples and QCs from batch2, respectively. Grey circle are samples with low levels of IS mix.

Moreover, a recent strategy to normalize the inter-batch variation on top of QC-SVRC algorithm was used to obtain a complete integration of the data [4]. This method, called QC-norm, is based on the shift of QC median within and between batches [7]. The results are shown in Figure 5 and compared to the previous normalization we can observe the complete clustering of the QCs and the mix of the samples between batches. Results showed that a two-step combination of QC-SVRC algorithm followed by QC-norm enabled a successful correction of within and between systematic errors, thus facilitating the joint analysis of metabolic profiles acquired in independent batches.

Interestingly, the PCA model for ESI- raw data and after most normalization procedures (except by IS) showed a group of samples clustering together (marked within a grey circle). These samples presented a normal total ion chromatogram (TIC), TUS intensity values and clinical parameters comparable to the rest of the samples. However, as these samples presented low intensity of IS mix, they can be excluded from further statistics. Without the information of the IS mix, these samples could not have been excluded and would lead into the misinterpretation of the data.

To sum up, all the normalization strategies tested were compared and the RSD% of all the features in QCs for both positive and negative ionization modes was plotted (Figure 6). As it can be observed, the combination of QC-SVRC +QC-norm showed the highest number of features with RSD < 30%.

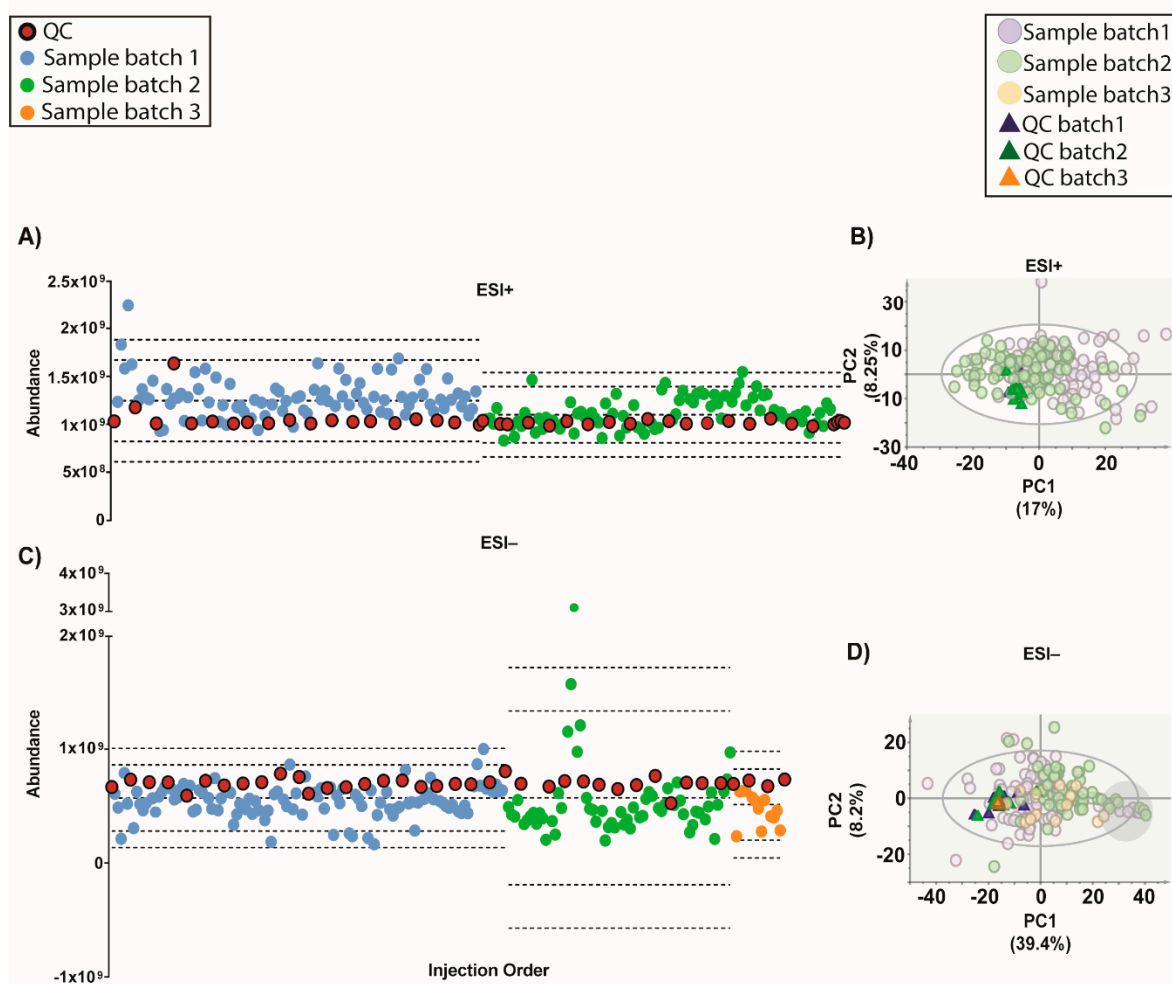


**Figure 5.** Outcome of the data normalization strategy after QC-SVRC algorithm and QC-norm for both: ESI+ and ESI- modes. (A,C) Quality control chart of ESI+ and ESI- modes, respectively. Samples with a TUS higher than 3 SD of the mean or lower than  $-3$  SD were removed from the PCA model. (B,D) PCA plots of ESI+ and ESI- mode, respectively. Signals with %RSD < 30% on QCs were kept, and UV scaling was used. Features in ESI+ and ESI- modes respectively: 880 and 525. **Legend.** TUS plot: Blue and green dots: samples of batch1 and batch2, respectively, red dots: QCs. Dotted lines represent the mean  $\pm$  2 and 3 SD for each batch independently. PCA: Blue dots and dark blue triangles are samples and QCs measured in batch1, respectively; green dots and dark green triangles are samples and QCs from batch2, respectively. Grey circle signals samples with low levels of IS mix.

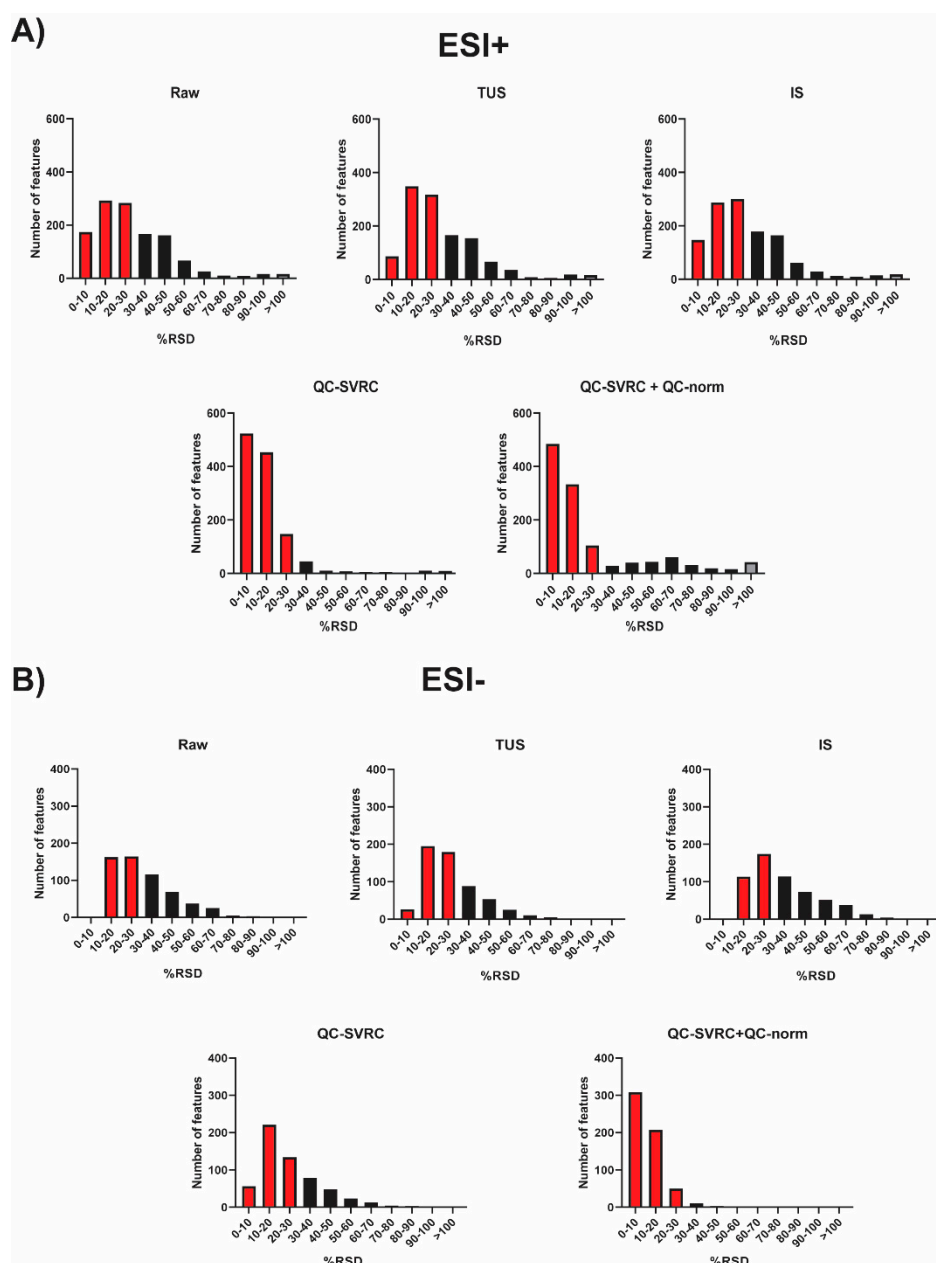


**Figure 6.** RSD distribution across QC samples from the complete dataset after each normalization method. (A) ESI+ mode and (B) ESI− mode. The red and grey bars indicate peaks that fall under RSD < 30% and RSD > 100%, respectively.

## 2.6. Assessment of Normalization Quality

In order to test the quality of the QC-SVRC normalization followed by QC-norm, four tests were used. First, PCA plots without QCs were evaluated in both modes for raw data (before normalization) and after normalization by QC-SVRC and by QC-SVRC + QC-norm (Figure S9). The latter procedure successfully integrated the samples measured in the multiple batches in both ionization modes. Moreover, in ESI− mode, the clustering of the samples with low IS mix abundance was still observed (grey circle).

Second, replicates of experimental samples were measured in different batches to assess the impact of the normalization strategy. This was done based on a PCA model again for raw data (before normalization) and after normalization, by QC-SVRC and QC-SVRC + QC-norm for both ionization modes (Figure S10). Once again, the intra- and inter-batch normalization procedure brought

together the replicate samples in the PCA plots. Additionally, the distances of the repeated samples in these plots were calculated before and after normalization (QC-SVRC + QC-norm). The results were plotted and tested using a paired *t*-test (Figure S11). In the data from ESI+ mode, the difference in distances from the replicates was significantly lower (from 31.2 to 22.5) with a *p* value = 0.022 after normalization. Regarding the ESI- mode, the difference in distance was lower (from 12.8 to 9.1) but not significant (*p* value = 0.149).

Furthermore, hierarchical clustering analysis (HCA) was also performed to the same datasets (Figure 7). In ESI+ mode, no pairs of repeated samples were clustered before normalization, one pair clustered after QC-SVRC method and three pairs clustered after QC-SVRC+QC-norm. Regarding the ESI- mode, two pairs clustered in the HCA before normalization, three pairs after QC-SVRC and four after QC-SVRC+QC-norm. Moreover, the pairs that did not cluster together at the end of the normalization process were joined together in the proximal nodes of the tree (Figure 7C,F).

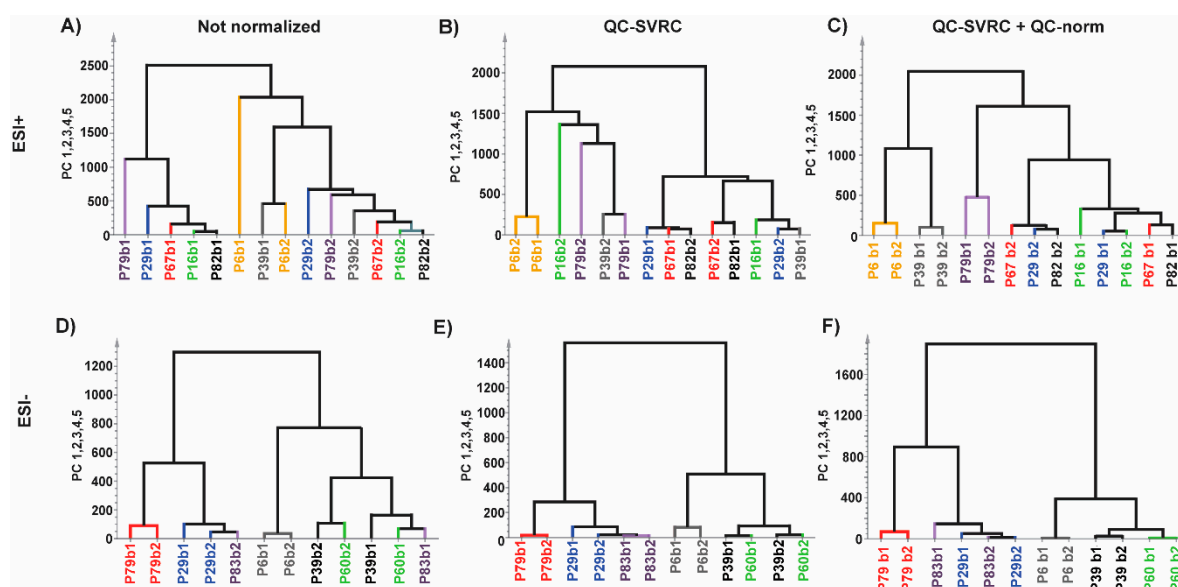


**Figure 7.** Normalization impact evaluated by HCA test on repeated experimental samples for (A,D) raw data; (B,E) after normalization by QC-SVRC and; (C,F) QC-SVRC + QC-norm for both, ESI+ and ESI- modes, respectively. **Legend.** Every pair of samples represents one patient and is depicted in a different color for each polarity mode.

Third, the effects of the normalization in a metabolite were analyzed depicting its signal along the injection order before and after normalization (QC-SVRC followed by QC norm). Lysophosphocholine 20:0 (LPC 20:0, RT 29.50 min) was chosen as it was detected in both modes (Figure S12). Results in ESI+ mode showed minimal changes in the samples and QC, while in ESI- mode the correction of the signal from LPC 20:0 was observed. To conclude, these tests demonstrated that a normalization strategy can be easily implemented for the correction of systematic intra- and inter-batch effects.

Finally, two clinical groups were selected and compared before and after normalization. Statistically significant features were compared using Venn diagrams (Figure S13). The total amount of significant features highly increased for both ionization modes.

### 3. Discussion

The execution of large-scale metabolomic studies is a complex task, specially using LC-QToF-MS, as the analysis of samples is typically distributed across different batches. The main issue is that differences in the instrument response across batches introduce a systematic error in the datasets that may lead to underpowered or even incorrect results in downstream analysis, leading ultimately to

false discoveries. The aim of this study was to present a strategy to troubleshoot the integration of the data from different batches.

In this study, analytical conditions for the large-scale experiment were described. We considered several aspects that should be taken into consideration before the analysis, such as the total mobile phase volume needed and their placement. Complete volume preparation will avoid changes in the ionization and chromatographic separation during the experiment. Additional factors we consider important and are mentioned in this study are: rebooting the computer before the experiment to ensure enough memory to complete the whole experiment, avoiding communication errors between computer and equipment; preparation of samples in subsets and centrifugation of sample vials before each analysis. Batches should also be designed to ensure that study groups are evenly distributed across batches. Accordingly, in this study, samples were split in two batches, and each batch included approximately the same number of cases and controls.

Regarding QC preparation, this is not an obvious task. We considered that a quarter of the samples from each experimental group were necessary to obtain a representative sample of our experimental population (i.e., 46 samples in this study). Following this approach, the resultant QC was representative of the tested population and fulfilled the objective of evaluating the performance and stability of the analytical technique. Moreover, in order to avoid repeated freeze-thaw cycles, the selected experimental samples for the QC were assigned to be measured in the first batch and as the first set of samples, with the idea of preparing at the same time each experimental sample and QC. This QC was pooled into different tubes with the aim to thaw new QCs as needed. After the preparation of this first set of samples, we calculated the samples analyzed per day. As a consequence, we prepared a new set of samples each day to maintain a comparable time span to the first sample set.

Peak areas from the IS mix were assessed for a preliminary analysis of data quality after acquisition. Traditionally, the main use of a IS in metabolic fingerprinting in other separation techniques (such as gas chromatography and capillary electrophoresis) has been to correct the volume of injection and the MS signal of each sample [14–16]. In the case of LC-QToF-MS, especially in large-scale experiments, IS are useful for the monitoring of performance of the system [7]. In this study, a combination of 5 ISs was employed: L-carnitine-D<sub>3</sub>, isoleucine-<sup>13</sup>C, <sup>15</sup>N, sphingosine-D<sub>7</sub>, LPC 18:1-D<sub>7</sub> and stearic acid-D<sub>5</sub>. The aim of this IS mix was to cover not only the complete RTs of the chromatogram (from 0.6 to 34.5 min) but also a wide spectrum of biochemical and physicochemical properties. The results markedly showed that each signal from the IS mix followed a different trend for the same sample in both ionization modes. Moreover, these independent trends did not correlate with compound abundances, the RT in the chromatogram or the nature of the IS. This fact suggests the idea that each biological sample has an intrinsic matrix effect.

In case of the IS mix in ESI<sup>−</sup> mode, we found that some samples presented very low intensities of all IS peaks. These samples were not present together in a specific time point of the experiment but were throughout all the batches. This issue is intriguing since it might suggest technical issues in metabolite extraction, but no differences were observed on the TUS values of these samples. Additional experiments are needed to understand this effect.

Moving forward, the quality of the initial data (after filtration of blanks, missing values and %RSD in QCs) showed that although on the TUS were comparable among batches, they were different indeed in the PCA plots (Figure 4 and Figure S4). This evidence proves that a normalization strategy is necessary to integrate the data from the whole experiment.

In the case of data normalization, we tried two common strategies applied in metabolomics: the normalization by IS (in this case the sum of all IS compounds) and the normalization by TUS. The results show that both approaches did not achieve the integration of the data and, in the case of TUS normalization, increased the drift of the QC by the injection order.

However, in the latest years the normalization methods based on the information contained on QCs has gain great interest to correct the instrumental drift, especially in large-scale studies [10–12]. Most of these, have showed the application of support vector regression (SVR) for the modeling of

the instrumental drift, such as the strategy proposed by Kuligowski et al. in 2015 [10], which uses a radial basis function (RBF) kernel to correct the instrumental drift. This algorithm applied to our data, resulted in a good clustering of QCs from all batches in both modes. Moreover, following Sánchez-Illana et al. in 2018 an inter-batch correction was applied [4]. The resulting outcome improved the complete integration of QCs in both modes (Figure 6). The samples with low IS mix in ESI<sup>-</sup> mode grouped together in one end of most PCAs (Figures 3–7, Figures S5–S7 on grey circles) from the different normalization strategies. This demonstrates the importance of adding multiple IS to the samples. Otherwise, it could be thought that these samples shared a common biological condition.

The assessment of the QC-SVRC normalization followed by QC-norm, compared to raw data and with QC-SVRC alone, was tested by the analysis of the PCA models of complete set of samples and the comparison of samples measured in multiple batches (Figures S10 and S11, respectively). This last strategy has not been explored previously and proves the feasibility of the normalization strategy. After testing the reduction in distance of the replicates by the normalization we corroborate these findings by HCA where the clustered pairs increased after every normalization (intra and inter) for both modes (Figure 7). Additionally, the extent of normalization was checked by exploring the outcome in one of the metabolites common to both modes. We detected that the normalization process only corrects the effects that are necessary as in ESI<sup>+</sup> mode there was no visual change compared to ESI<sup>-</sup> mode. To sum up, these tests demonstrate the full integration and the high quality of the data from multiple batches. This would result in the further reliable comparison of the clinical groups of the study. This was depicted by the significant number of features increased after normalization between two clinical groups, which otherwise would lead to false negative results.

To conclude, this work illustrates a strategy to generate high-quality data from untargeted large-scale metabolomics studies. This strategy considers the stability of the equipment and the normalization of the data to assess a correct integration of the batches. We have addressed different issues that should be taken into consideration in these types of studies. Together, we have generated a guideline to integrate data for different batches that could be useful in any metabolomics study with more than a single batch.

## 4. Materials and Methods

### 4.1. Patients and Sample Collection

140 adult patients with a clinical history of asthma, and 25 non-allergic and non-asthmatic subjects were enrolled as control population at the allergy department, “Hospital Universitario de Gran Canaria, Dr. Negrin”, Las Palmas de G.C., Spain. Participants were recruited as they arrived to daily practice. All participants read and signed an informed consent. The study was conducted in accordance with the Declaration of Helsinki, and the protocol was approved by the Ethics Committee of “Hospital Universitario de Gran Canaria, Dr. Negrin” on the 4th of February 2016 (code: 160009).

Whole blood was collected and incubated with a clotting agent in Vacutainer™ SST II tube (Becton Dickinson S.A., Spain). The sample was placed at room temperature for 40 min. Afterwards, it was centrifuged at  $2000 \times g$  for 10 min at room T. Then, serum was collected and stored at  $-80 \text{ }^{\circ}\text{C}$  until the metabolomic analysis was performed.

### 4.2. Sample Randomization

Due to the large number of samples, the sample set was split into 2 batches according to clinical parameters to obtain half of each experimental group in each batch. Thus, 83 and 82 samples were included in batches 1 and 2, respectively. In addition, to assess the correction of systematic between-batch effects, a subset of randomly selected samples was measured in both batches (7 and 6 samples in ESI<sup>+</sup> and ESI<sup>-</sup> modes). Samples within batch were randomized for sample preparation and instrumental analysis.

#### 4.3. Metabolomic Analysis

Serum samples were measured using an Agilent HPLC system (1200 series) coupled with quadrupole-time of flight analyzer system (Q-ToF MS 6520) (Agilent Technologies, Waldbronn, Germany), as previously described [17,18].

#### 4.4. Sample Treatment

Serum proteins were removed adding 300  $\mu$ L of cold ( $-20$  °C) methanol: ethanol (1:1) to 100  $\mu$ L of sample. For the analysis, 20  $\mu$ L of a mix of five labelled IS were added to each sample. The IS mix was selected to cover a wide range of different RTs and physico-chemical properties. This was composed of: (1) Carnitine-D<sub>3</sub> (C<sub>7</sub>H<sub>12</sub>D<sub>3</sub>NO<sub>3</sub>, mass = 144.1454 Da, RT: 0.70 min, 0.02 mM); (2) Isoleucine-<sup>13</sup>C, <sup>15</sup>N (C<sub>6</sub>H<sub>13</sub><sup>15</sup>NO<sub>2</sub>, molecular mass=138.1118 Da, RT: 0.77 min, 0.18 mM); (3) Sphingosine-D<sub>7</sub> (C<sub>18</sub>H<sub>30</sub>D<sub>7</sub>NO<sub>2</sub>, molecular mass = 306.3264 Da, RT: 14.38 min, 0.02 mM); (4) LPC 18:1-D<sub>7</sub> (C<sub>26</sub>H<sub>45</sub>D<sub>7</sub>NO<sub>7</sub>P, molecular mass = 528.3921 Da, 2 peaks at RTs = 19.30 and 20.00 min, 0.01 mM) and (5) Stearic acid-D<sub>5</sub> (C<sub>18</sub>H<sub>31</sub>D<sub>5</sub>O<sub>2</sub>, molecular mass = 289.3029 Da, RT: 34.54 min, 0.17 mM). All detected adducts are present in Table S1. Samples were then vortex-mixed and kept on ice for 5 min. Supernatant was separated by centrifugation (16110  $\times g$  for 20 min at 4 °C) and transferred into LC vials for analysis. Extraction solvent used as blank for the analysis was prepared mixing 400  $\mu$ L of cold ( $-20$  °C) methanol: ethanol (1:1) and 20  $\mu$ L of ISs. The blank followed the same steps as the samples.

#### 4.5. QC Preparation

QC was prepared by pooling equal volumes of serum from the first 46 samples of the first batch. Then, the QC was aliquoted into different tubes to preserve it from freezing-thawing cycles. Every time QC was needed, fresh QC was prepared. The QCs clean-up steps followed the same procedure applied for the experimental samples. QCs were analyzed throughout the run to provide a measurement of system stability, performance and reproducibility of the LC-QToF-MS system.

#### 4.6. LC-Quadrupole Time of Flight-MS Analysis

The HPLC system was equipped with a degasser, two binary pumps, and a thermostated autosampler. Briefly, 10  $\mu$ L of sample were injected into a Discovery HS C18 column (2.1  $\times$  150 mm, 3.0  $\mu$ m; Supelco, Sigma Aldrich, Germany), with a guard column Discovery<sup>®</sup> HS C18 (2.1  $\times$  20 mm, 3  $\mu$ m; Supelco), both maintained at 40 °C. The flow rate was set at 0.6 mL/min. The elution gradient involved a mobile phase consisting of: (A) 0.1% *v/v* formic acid (FA) in water and (B) 0.1% *v/v* FA in acetonitrile. The initial conditions were set at 25% phase B, which increased linearly to 95% phase B in 35 min. Then it returned to the initial conditions in 1 min, which were held for 9 min for column reconditioning. Samples were analyzed in both ESI+ and ESI- modes in separate injections. The capillary voltage was set at 3500 for ESI+ and 4000V for ESI-. The drying gas flow rate was 10.5 L/min at 330 °C and gas nebulizer at 52 psi; fragmentor voltage was 175 V; skimmer and octopole radio frequency voltages were set to 65 and 750 V, respectively. MS spectra were collected in the centroid mode at a scan rate of 1.2 Hz. The MS detection window was performed in full scan from 100 to 1200 *m/z* for both modes. Automatic MS recalibration during batch analysis was carried out introducing a reference standard into the source via a reference sprayer valve. Reference masses for ESI+ were purine (*m/z* = 121.0508) and HP-0921 (*m/z* = 922.0097), whereas for ESI- TFA NH<sub>4</sub> (*m/z* = 119.0363) and HP-0921 (*m/z* = 966.0007).

#### 4.7. Raw Data Availability

Metabolomics data have been deposited to the EMBL-EBI MetaboLights database (DOI: 10.1093/nar/gks1004. PubMed PMID: 23109552) with the identifier MTBLS1133. The complete dataset can be accessed here <https://www.ebi.ac.uk/metabolights/MTBLS1133> [19].



#### 4.8. Data Treatment

Acquired signals were processed to provide structured raw data in an appropriate format for analysis. Collected data from all batches were put and cleaned together in a single analysis of background and unrelated ions using MassHunter Profinder (B.08.00; SP3, Agilent Technologies) software. Molecular feature extraction (MFE) algorithm was used to reduce the size and complexity of data. Furthermore, Find by Ion (FbI) algorithm was applied to improve the reliability of the features found in the data. In the end, 1382 and 887 chemical signals for LC-MS positive and negative ionization modes were obtained respectively. Afterwards, raw data was filtered by keeping all features that were not present in the blanks, were detected in >50% of all QCs and >75% in the experimental samples. The rest of the signals were excluded from the analyses. Missing values were replaced using the kNN algorithm using an in-house script developed in Matlab® [20].

The IS compounds were extracted in a targeted manner using a file containing the formula, mass and RT in MassHunter Profinder.

#### 4.9. Data Normalization and Analysis

Different normalization strategies were used to pre-process the raw data matrix containing data acquired from the independent batches. For intra-batch normalization, the following methods were used: (1) Normalization of each signal (i.e., LC-MS feature) to the total area of the IS mix; (2) normalization of each signal by the TUS of each sample; (3) intra-batch effect correction using the QC-SVRC (10) algorithm using the information contained in the QCs to correct the drift of the MS signal within the batch. This algorithm requires the selection of the tolerance threshold ( $\epsilon$ ), the kernel width ( $\gamma$ ) and the error penalty parameter (C). The values used were  $\epsilon = 5\%$ ,  $\gamma = [2^{-3}, 2^{-2}, \dots, 2^6]$ , and  $C = 50\%$ . In addition to intra-batch normalization using QC-SVRC, a sequential inter-batch effect correction called QC-norm was tested. It is a ratio-based method which normalizes the intensity of each signal in each sample using as scaling factor the ratio of the median intensity in the QC of the corresponding batch over the median QC intensity across batches (4). Moreover, after each normalization, features were filtered by keeping those with a RSD < 30% in QCs.

To monitor the performance of each data pre-processing strategy, the abundance of TUS as a function of the injection order was depicted before and after each normalization approach. In each of them, the mean plus/minus 2 and 3 times the SD were calculated and depicted for each batch independently.

Multivariate and HCA were performed using SIMCA® v.15.0 (Umetrics, Umeå, Sweden). PCA, a non-supervised model, was used to identify patterns across samples associated to the injection order and batch after the data normalization. Autoscaling was used for all the models. HCA was performed for the samples analyzed in all batches to assess the similarity after normalization using Ward's method to calculate the similarity between clusters. The trees were sorted by size.

The distances in the PCA models of the repeated experimental samples were calculated and compared before and after normalization (QC-SVRC followed by QC-norm). Afterwards, using a paired t-student test the distances were tested. Moreover, the reduction of the distance between the pair of repeated samples after normalization was plotted calculating the Euclidean distance of the pairs in Matlab®.

To prove the relevance of data normalization, two clinical groups were compared before (using raw data) and after the normalization using QC-SVRC followed by QC-norm. The number of samples of each group were 9 and 17, and the applied statistical test was non-parametric Mann-Whitney U test using an in-house script developed in Matlab®.

**Supplementary Materials:** The following are available online at <http://www.mdpi.com/2218-1989/9/11/247/s1>, Figure S1: Scheme of the mobile phase position during large-scale experiment, Figure S2: Extracted ion chromatogram (EIC) of IS mix in A) ESI+ and B) ESI- modes, Figure S3: Relative abundance of the IS mix in all experimental samples and QCs according with the injection order for ESI+ and ESI- modes, Figure S4: Quality control charts of the total useful signal (TUS) using the initial data (before normalization) for each sample

according to the injection order, Figure S5: PCA models of initial data (before normalization), Figure S6: Outcome of the data normalization strategy by the IS mix for both: ESI+ and ESI− modes, Figure S7: Contribution of PC1 and PC 2 along with injection order in ESI− mode after normalization by IS mix, **Figure S8**: Outcome of the data normalization strategy by the TUS for both: ESI+ and ESI− modes, Figure S9: Normalization impact evaluated by PCA models of all experimental samples in the study, Figure S10: Normalization assessment by PCA of repeated experimental samples for raw data; after normalization by QC-SVRC and QC-SVRC + QC-norm., Figure S11: Euclidean distances plots of repeated experimental samples, Figure S12: Abundance plots before and after normalization of LPC 20:0, RT 29.5 min, Figure S13: Venn diagram comparing the number of significant features between two groups of the clinical study before normalization (raw data) and after QC-SVRC + QC-norm normalization., Table S1: IS mix adducts detected in the experiment.

**Author Contributions:** M.M.E. was the PI and together with D.B., A.V. designed and supervised the research. A.V., J.R.-C., M.D.-H., and D.O. performed the metabolomics analysis and data treatment. M.I.D.-D. performed data treatment and analysis of results. T.C. recruited the patients from the study. S.A. and G.Q. supervised data treatment and the statistical analysis. All authors contributed to the writing of the manuscript and have given approval to the final version of the manuscript.

**Funding:** This work was supported by ISCIII (PI15/02256, PI16/00249 and PI18/01467) cofounded by FEDER for the thematic network and co-operative research centers ARADyAL RD16/0006/0015, RD16/0006/009. D.O., M.I.D.-D. and J.R.-C. are supported by FPI-CEU predoctoral fellowships and A.V. is funded by a postdoctoral research fellowship from ARADyAL.

**Acknowledgments:** We would like to thank all institutions and hospitals involved: Centre for Metabolomics and Bioanalysis (CEMBIO, San Pablo CEU University, Madrid), Institute of Applied Molecular Medicine (IMMA, San Pablo CEU University, Madrid), Negrin University Hospital (Las Palmas de G.C.). Authors also acknowledge Tomás Clive Barker-Tejeda, for his asserted comments.

**Conflicts of Interest:** The authors declare no conflict of interest. The funders had no role in the design of the study; in the collection, analyses, or interpretation of data; in the writing of the manuscript, or in the decision to publish the results.

## References

1. Puchades-Carrasco, L.; Pineda-Lucena, A. Metabolomics Applications in Precision Medicine: An Oncological Perspective. *Curr. Top. Med. Chem.* **2017**, *17*, 2740–2751. [[CrossRef](#)] [[PubMed](#)]
2. Phelps, D.L.; Balog, J.; Gildea, L.F.; Bodai, Z.; Savage, A.; El-Bahrawy, M.A.; Speller, A.V.; Rosini, F.; Kudo, H.; McKenzie, J.S.; et al. The surgical intelligent knife distinguishes normal, borderline and malignant gynaecological tissues using rapid evaporative ionisation mass spectrometry (REIMS). *Br. J. Cancer* **2018**, *118*, 1349–1358. [[CrossRef](#)]
3. Global Initiative for Asthma. Available online: <http://ginasthma.org/gina-reports/> (accessed on 27 July 2019).
4. Sánchez-Illana, Á.; Piñeiro-Ramos, J.D.; Sanjuan-Herráez, J.D.; Vento, M.; Quintás, G.; Kuligowski, J. Evaluation of batch effect elimination using quality control replicates in LC-MS metabolite profiling. *Anal. Chim. Acta* **2018**, *1019*, 38–48. [[CrossRef](#)]
5. Dunn, W.B.; Broadhurst, D.; Begley, P.; Zelena, E.; Francis-McIntyre, S.; Anderson, N.; Brown, M.; Knowles, J.D.; Halsall, A.; Haselden, J.N.; et al. Procedures for large-scale metabolic profiling of serum and plasma using gas chromatography and liquid chromatography coupled to mass spectrometry. *Nat. Protoc.* **2011**, *6*, 1060–1083. [[CrossRef](#)] [[PubMed](#)]
6. Lewis, M.R.; Pearce, J.T.; Spagou, K.; Green, M.; Dona, A.C.; Yuen, A.H.; David, M.; Berry, D.J.; Chappell, K.; Horneffer-van der Sluis, V.; et al. Development and Application of Ultra-Performance Liquid Chromatography-TOF MS for Precision Large Scale Urinary Metabolic Phenotyping. *Anal. Chem.* **2016**, *88*, 9004–9013. [[CrossRef](#)] [[PubMed](#)]
7. Broadhurst, D.; Goodacre, R.; Reinke, S.N.; Kuligowski, J.; Wilson, I.D.; Lewis, M.R.; Dunn, W.B. Guidelines and considerations for the use of system suitability and quality control samples in mass spectrometry assays applied in untargeted clinical metabolomic studies. *Metabolomics* **2018**, *14*. [[CrossRef](#)] [[PubMed](#)]
8. U.S. FOOD&DRUG ADMINISTRATION. Available online: <https://www.fda.gov/files/drugs/published/Bioanalytical-Method-Validation-Guidance-for-Industry> (accessed on 27 June 2018).
9. Redestig, H.; Fukushima, A.; Stenlund, H.; Moritz, T.; Arita, M.; Saito, K.; Kusano, M. Compensation for systematic cross-contribution improves normalization of mass spectrometry based metabolomics data. *Anal. Chem.* **2009**, *81*, 7974–7980. [[CrossRef](#)] [[PubMed](#)]

10. Kuligowski, J.; Sánchez-Illana, Á.; Sanjuán-Herráez, D.; Vento, M.; Quintás, G. Intra-batch effect correction in liquid chromatography-mass spectrometry using quality control samples and support vector regression (QC-SVRC). *Analyst* **2015**, *140*, 7810–7817. [[CrossRef](#)] [[PubMed](#)]
11. Zhu, X.; Gong, X.; Cai, Y. Normalization and integration of large-scale metabolomics data using support vector regression. *Metabolomics* **2016**, *12*. [[CrossRef](#)]
12. Wang, S.-Y.; Kuo, C.-H.; Tseng, Y.J. Batch Normalizer: A Fast Total Abundance Regression Calibration Method to Simultaneously Adjust Batch and Injection Order Effects in Liquid Chromatography/Time-of-Flight Mass Spectrometry-Based Metabolomics Data and Comparison with Current Calibration Met. *Anal. Chem.* **2013**, *85*, 1037–1046. [[CrossRef](#)] [[PubMed](#)]
13. Dunn, W.B.; Wilson, I.D.; Nicholls, A.W.; Broadhurst, D. The importance of experimental design and QC samples in large-scale and MS-driven untargeted metabolomic studies of humans. *Bioanalysis* **2012**, *4*, 2249–2264. [[CrossRef](#)] [[PubMed](#)]
14. Garcia, A.; Barbas, C. Gas chromatography-mass spectrometry (GC-MS)-based metabolomics. *Methods Mol. Biol.* **2011**, *708*, 191–204. [[PubMed](#)]
15. Mastrangelo, A.; Ferrarini, A.; Rey-Stolle, F.; Garcia, A.; Barbas, C. From sample treatment to biomarker discovery: A tutorial for untargeted metabolomics based on GC-(EI)-Q-MS. *Anal. Chim. Acta* **2015**, *900*, 21–35. [[CrossRef](#)] [[PubMed](#)]
16. Lopez-Gonzalvez, A.; Godzien, J.; Garcia, A.; Barbas, C. Capillary Electrophoresis Mass Spectrometry as a Tool for Untargeted Metabolomics. *Methods Mol. Biol.* **2019**, *1978*, 55–77. [[PubMed](#)]
17. Ciborowski, M.; Javier Ruperez, F.; Martínez-Alcázar, M.P.; Angulo, S.; Radziwon, P.; Olszanski, R.; Kloczko, J.; Barbas, C. Metabolomic approach with LC-MS reveals significant effect of pressure on diver's plasma. *J. Proteome Res.* **2010**, *9*, 4131–4137. [[CrossRef](#)] [[PubMed](#)]
18. Dudzik, D.; Zorawski, M.; Skotnicki, M.; Zarzycki, W.; Kozłowska, G.; Bibik-Malinowska, K.; Vallejo, M.; García, A.; Barbas, C.; Ramos, M.P. Metabolic fingerprint of gestational diabetes mellitus. *J. Proteomics* **2014**, *103*, 57–71. [[CrossRef](#)] [[PubMed](#)]
19. Haug, K.; Salek, R.M.; Conesa, P.; Hastings, J.; de Matos, P.; Rijnbeek, M.; Mahendraker, T.; Williams, M.; Neumann, S.; Rocca-Serra, P.; et al. MetaboLights—An open-access general-purpose repository for metabolomics studies and associated meta-data. *Nucleic Acids Res.* **2013**, *41*, D781–D786. [[CrossRef](#)] [[PubMed](#)]
20. Gromski, P.; Xu, Y.; Kotze, H.; Correa, E.; Ellis, D.; Armitage, E.; Turner, M.; Goodacre, R. Influence of missing values substitutes on multivariate analysis of metabolomics data. *Metabolites* **2014**, *4*, 433–452. [[CrossRef](#)] [[PubMed](#)]



© 2019 by the authors. Licensee MDPI, Basel, Switzerland. This article is an open access article distributed under the terms and conditions of the Creative Commons Attribution (CC BY) license (<http://creativecommons.org/licenses/by/4.0/>).



## II. Otras publicaciones

### A) Artículos de investigación original

- Pablo-Torres, C.\* **Delgado-Dolset, M. I.\***, Sanchez-Solares, J., Mera-Berriatua, L., Núñez Martín Buitrago, L., Reaño Martos, M., Bueno, J. L., Escribese, M. M., Barber, D., & Gomez-Casado, C. (2022). *A method based on plateletpheresis to obtain functional platelet, CD3+ and CD14+ matched populations for research immunological studies*. Clinical and experimental Allergy, Advance online publication. <https://doi.org/10.1111/cea.14192>
- Sanchez-Solares, J., **Delgado-Dolset, M. I.**, Mera-Berriatua, L., Hormias-Martin, G., Cumplido, J. A., Saiz, V., Carrillo, T., Moreno-Aguilar, C., Escribese, M. M., Gomez-Casado, C., & Barber, D. (2019). *Respiratory allergies with no associated food allergy disrupt oral mucosa integrity*. Allergy, 74(11), 2261–2265. <https://doi.org/10.1111/all.13860>

### B) Artículos de revisión bibliográfica






- Tan, T. J.\* , **Delgado-Dolset, M. I.\***, Escribese, M. M., Barber, D., Layhadi, J. A., & Shamji, M.H. *Biomarkers of AIT: Models of prediction of efficacy*. Submitted to Allergologie Select
- López-Sanz, C., Jiménez-Saiz, R., Esteban, V., **Delgado-Dolset, M. I.**, Perales-Chorda, C., Villaseñor, A., Barber, D., & Escribese, M. M. (2022). *Mast Cell Desensitization in Allergen Immunotherapy*. Frontiers in allergy, 3, 898494. <https://doi.org/10.3389/falgy.2022.898494>
- **Delgado-Dolset, M. I.\***, Rodríguez-Coira, J.\* , & Sánchez-Solares, J.\* (2022). *Word of mouth: Oral mucosa composition in health and immune disease*. Allergy, 77(5), 1641–1643. <https://doi.org/10.1111/all.15219>
- Izquierdo, E., Rodríguez-Coira, J., **Delgado-Dolset, M. I.**, Gomez-Casado, C., Barber, D., & Escribese, M. M. (2022). *Epithelial Barrier: Protector and Trigger of Allergic Disorders*. Journal of investigational allergology & clinical immunology, 32(2), 81–96. <https://doi.org/10.18176/jiaci.0779>

---

\* Autores con igual contribución a la publicación.



# A method based on plateletpheresis to obtain functional platelet, CD3<sup>+</sup> and CD14<sup>+</sup> matched populations for research immunological studies

Carmela Pablo-Torres MSc<sup>1</sup>  | María Isabel Delgado-Dolset MSc<sup>1,2</sup>  |  
 Javier Sanchez-Solares PhD<sup>1</sup> | Leticia Mera-Berriatua PhD<sup>1</sup> |  
 Lucía Núñez Martín Buitrago MD<sup>3</sup> | Mar Reaño Martos MD<sup>4</sup> | José Luis Bueno MD<sup>3</sup> |  
 María M. Escribese PhD<sup>1</sup>  | Domingo Barber PhD<sup>1</sup>  | Cristina Gomez-Casado PhD<sup>1,5</sup> 

<sup>1</sup>Institute of Applied Molecular Medicine (IMMA) Nemesio Díez, Department of Basic Medical Sciences, School of Medicine, San Pablo-CEU University, CEU Universities, Boadilla del Monte, Spain

<sup>2</sup>Centre for Metabolomics and Bioanalysis (CEMBO), Department of Chemistry and Biochemistry, School of Pharmacy, San Pablo-CEU University, CEU Universities, Boadilla del Monte, Spain

<sup>3</sup>Department of Hematology and Hemotherapy, Puerta de Hierro-Majadahonda University Hospital, Madrid, Spain

<sup>4</sup>Department of Allergy and Immunology, Puerta de Hierro-Majadahonda University Hospital, Madrid, Spain

<sup>5</sup>Department of Dermatology, Medical Faculty, University Hospital Düsseldorf, Heinrich-Heine-University Düsseldorf, Düsseldorf, Germany

## Correspondence

Cristina Gomez-Casado, Institute of Applied Molecular Medicine (IMMA) Nemesio Díez, Department of Basic Medical Sciences, School of Medicine, San Pablo-CEU University, CEU Universities, Urbanización Montepríncipe, Boadilla del Monte, 28660, Spain.

Email: [cristina.gomezcasado@med.uni-duesseldorf.de](mailto:cristina.gomezcasado@med.uni-duesseldorf.de)

## Funding information

This work was supported by ISCIII (PI18/01467 and PI19/00044), co-funded by FEDER 'Investing in your future' for the thematic network and co-operative research centres ARADyAL RD16/0006/0015 and RICORS Red de Enfermedades Inflammatorias (REI) RD21 0002 0008. This work was also supported by the Ministry of Science, Innovation and Universities in Spain (PCI2018-092930) co-funded by the European program ERA HDHL- Nutrition & the Epigenome, project Dietary Intervention in Food Allergy: Microbiome, Epigenetic and Metabolomic interactions DIFAMEM, Junta de Andalucía (PC-0278-2017) and Fundación Mutua Madrileña (AP177712021). CP-T,

## Abstract

**Background:** In previous studies with peripheral blood cells, platelet factors were found to be associated with severe allergic phenotypes. A reliable method yielding highly concentrated and pure platelet samples is usually not available for immunological studies. Plateletpheresis is widely used in the clinics for donation purposes. In this study, we designed a protocol based on plateletpheresis to obtain Platelet-Rich Plasma (PRP), Platelet-Poor Plasma (PPP) as well as CD3<sup>+</sup> and CD14<sup>+</sup> cells matched samples from a waste plateletpheresis product for immunological studies.

**Methods:** Twenty-seven subjects were voluntarily subjected to plateletpheresis. PRP, PPP and blood cell concentrate contained in a leukocyte reduction system chamber (LRSC) were obtained in this process. CD3<sup>+</sup> and CD14<sup>+</sup> cells were isolated from the LRSC by density-gradient centrifugation and positive magnetic bead isolation. RNA was isolated from PRP, CD3<sup>+</sup> and CD14<sup>+</sup> cell samples and used for transcriptomic studies by Affymetrix. PRP and PPP samples were used for platelet protein quantification by multiplex assays.

**Results:** A reliable high yield method to obtain matched samples of PRP, PPP, CD3<sup>+</sup> and CD14<sup>+</sup> from a single donor for RNA and protein analyses has been designed. The RNA quality indicators (RQI) routinely used for other cell types were not suitable for platelet RNA characterization. Despite this, the platelet RNA was valid for

Carmela Pablo-Torres and María Isabel Delgado-Dolset were equally contributed.

This is an open access article under the terms of the [Creative Commons Attribution-NonCommercial](https://creativecommons.org/licenses/by-nc/4.0/) License, which permits use, distribution and reproduction in any medium, provided the original work is properly cited and is not used for commercial purposes.

© 2022 The Authors. *Clinical & Experimental Allergy* published by John Wiley & Sons Ltd.

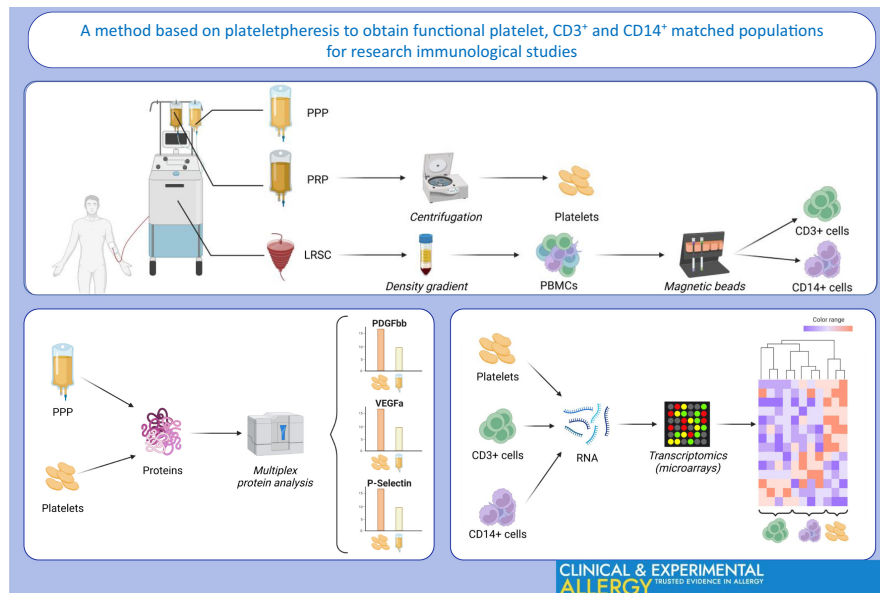
JS-S, MID-D and LM-B were supported by FPI-CEU predoctoral fellowships. CG-C was awarded an 'Atracción de talento investigador' contract from Community of Madrid (2017–2020).

transcriptomic studies by Affymetrix, as platelet transcripts obtained in our previous studies were confirmed in PRP samples. Platelet samples were enriched in platelet factors as determined in protein multiplex analysis.

**Conclusions:** We have developed a method that yields not only high content and pure platelet samples from a single donor but also CD3<sup>+</sup> and CD14<sup>+</sup> matched samples that can be used for RNA and protein analyses in immunological studies.

#### KEYWORDS

leukocyte reduction system chamber (LRSC), multiplex, plateletpheresis, platelet-rich plasma (PRP), platelets, transcriptomics



## GRAPHICAL ABSTRACT

We describe a platelet isolation method based on plateletpheresis that allows to obtain pure, highly concentrated and functional platelet samples from a single donor. Additionally, matched CD3<sup>+</sup> and CD14<sup>+</sup> populations can be obtained from a waste product of plateletpheresis procedure. All the samples are suitable for *omics* studies.

## 1 | INTRODUCTION

Platelets are anucleate blood cells generated from megakaryocytes. They are loaded with a wide range of mediators contained in secretory granules, which not only have coagulation-related functions, but also play a key role in inflammation.<sup>1,2</sup> There is increasing evidence supporting the potential of platelets as a source of biomarkers in inflammatory diseases.<sup>3</sup> This is particularly interesting in the field of allergy, in which severe allergy management often represents a difficult challenge.

Platelet activation markers, such as  $\beta$ -thromboglobulin ( $\beta$ -TG) and platelet factor 4 (PF4), have been found increased in allergic asthmatic patients after allergen challenge.<sup>4</sup> This is also the case for patients with atopic dermatitis, which also presented increased plasma levels of such markers.<sup>5,6</sup> In our previous studies, alteration of the platelet function was found to be associated with severe allergic phenotypes.<sup>7</sup> Severe allergic patients do not respond to treatment, suffer exacerbations and present a reduced quality of life.<sup>8</sup>

### Key Messages

- A high yield method to obtain platelets from a single donor based on plateletpheresis.
- Matched samples of other peripheral blood mononuclear cell populations are also obtained with this procedure.
- All the cell samples are suitable for RNA and protein analyses in research studies.

The mechanisms that explain the acquisition of a severe phenotype are still poorly understood.

The study of platelets and their role in inflammation requires pure, non-activated platelet isolates. A single leukocyte possesses 12,500-fold higher mRNA content and 65-fold higher protein content than one platelet.<sup>9,10</sup> Therefore, even very low numbers of



contaminating leukocytes could shed misleading results in transcriptomic and proteomic platelet studies. Currently, a reliable method yielding highly concentrated and pure platelet samples for immunological studies is not commonly available.

The most used techniques for isolating pure platelets are based on multiple centrifugation steps, which cause physical stress leading to platelet activation and granule content release.<sup>11</sup> This mechanical activation could lead to a misinterpretation in the quantification of protein and mRNA. In addition, protocols based on successive centrifugation steps require large blood volumes and pooling samples from multiple subjects to obtain sufficient mRNA concentration for performing platelet gene expression studies.<sup>12</sup> This requirement makes these techniques impractical for use in clinical research and underlies why many studies use pools of platelets from different donors.<sup>13</sup>

Plateletpheresis is a technique mainly used for platelet donation purposes that allows the generation of a platelet-rich plasma (PRP) product from a single donor with no leukocyte or red blood cell contamination. Whole blood is processed by a cell separator, which separates the blood components based on centrifugation parameters. Platelets are retained and collected as PRP, while the remaining blood components are returned to the donor through automated circulation.<sup>11</sup> Although the process is highly efficient, a remaining of highly concentrated blood sample is collected in a leukocyte reduction chamber system (LRCS), which is usually discarded as a waste product. This technique is not commonly used in basic research since specialized equipment and training are required. However, its advantages over platelet isolation methods based on centrifugation make plateletpheresis an attractive alternative for performing multi-omics assays, in which concentration and purity of samples are essential.

In this study, we describe a protocol based on plateletpheresis to obtain PRP as well as CD3<sup>+</sup> and CD14<sup>+</sup> matched cell samples. The PRP and cell samples obtained by plateletpheresis are suitable for transcriptomic and protein analyses. Therefore, this methodology could be used for phenotyping platelets as well as other cell populations in immune diseases in order to elucidate their role in inflammation.

## 2 | MATERIAL AND METHODS

### 2.1 | Study subjects

Twenty-seven individuals were recruited between October 2018 and February 2021 at the blood bank and the Allergy Service of the Puerta de Hierro-Majadahonda University Hospital. The protocol was approved by the Ethics Research Committee from the hospital, and written informed consent was obtained from all study subjects. Individuals younger than 18 years old, with cancer or haematological diseases were excluded from the study.

### 2.2 | Plateletpheresis

Plateletpheresis donor's standard exclusion criteria were used to select participants. Plateletpheresis was performed in the Apheresis Unit of the Haematology department of the hospital. Trima Accel machine (Terumo BCT) was set to obtain PRP (85 ml) and platelet-poor plasma (PPP) (50 ml) samples using Adenine Citrate Dextrose-A (ACD-A) as anticoagulant. PRP and PPP samples were collected sterile and transferred to two different storage bags (Paediatric Transfer Bags, Grifols). After plateletpheresis, samples were allowed to rest at room temperature (RT) for 2 h. After resting, a hemogram of both samples was performed to assess cell counts. A minimum concentration of 500x10<sup>9</sup>platelets/L was considered a quality requirement for PRP. Moreover, the content of other cell types was negligible. We also obtained the LRSC and used it for peripheral blood mononuclear cell (PBMC) isolation.

### 2.3 | Isolation of PBMCs from the LRSC

Blood contained in the LRSC (7–9 ml) was diluted 1:1 in RPMI medium (Thermo Fisher Scientific). The total volume of diluted blood was carefully dispensed onto 1 V of Ficoll (Thermo Fisher Scientific) and centrifuged for 20 min, 500g with no brake at RT. The PBMC fraction was collected from the buffy layer. Two washing steps with PBS (Thermo Fisher Scientific) and centrifugation for 5 min, 300g at 4°C were performed. Supernatant was discarded, and cells were re-suspended in 5 ml PBS to quantify cell numbers with a N-20 Sysmex (Roche).

### 2.4 | CD3<sup>+</sup> and CD14<sup>+</sup> isolation with magnetic beads

CD14<sup>+</sup> and CD3<sup>+</sup> cells were sequentially isolated from the PBMC fraction with magnetic MicroBeads (Miltenyi Biotec) following manufacturer instructions. Once isolated, cell populations were stored in Rneasy Lysis (RLT) buffer containing 1% β-mercaptoethanol at –20°C until transcriptomic analysis.

### 2.5 | CD3<sup>+</sup> and CD14<sup>+</sup> RNA extraction

RNA was extracted from CD3<sup>+</sup> and CD14<sup>+</sup> cells using Rneasy® Mini Kit (Qiagen) with Dnase treatment following manufacturer procedure. RNA concentration was determined using a NanoDrop™ 2000/2000c Spectrophotometer, and its integrity was assessed with Experion RNA StdSens analysis kit (Bio-Rad Laboratories Inc.), establishing an RNA quality indicator (RQI) ≥ 7 as a requisite for transcriptomic analysis.

## 2.6 | PPP and PRP processing for transcriptomic analysis and protein quantification

Two different methods to process PRP samples for transcriptomic analyses were used. PRP and PPP samples PL-1 to PL-14 were aliquoted in 50 ml tubes and directly frozen at  $-80^{\circ}\text{C}$ . For subsequent samples, the protocol described by Amisten et al.<sup>12</sup> with modifications was followed. From samples PL-15 to PL-27, 45 ml PRP were distributed into three previously weighed tubes (each tube containing 15 ml PRP). The process was repeated for PPP, but tubes were not weighed in this case. Weighed tubes containing PRP were centrifuged for 10 min, 300g at RT, with full acceleration and no brake. Supernatant was discarded and tubes were again weighed to assess the pellet mass. One ml of TRIzol (Sigma) was added to every 100 mg of platelet pellet. Resuspended pellet was divided into 1 ml aliquots and stored at  $-80^{\circ}\text{C}$  until RNA extraction.

Seventy-five  $\mu\text{l}$  of the remaining PPP and PRP volumes were collected for multiplex protein assays and stored at  $-80^{\circ}\text{C}$  until assay performance.

## 2.7 | Platelet RNA isolation, quantification and quality control

Directly frozen PRP and PPP samples (PL-1 to PL-14) were thawed and RNA was isolated using different methods (TRIzol [Sigma] and Rneasy kits [Qiagen]). The amount of RNA obtained was in every case insufficient for further experiments ( $<10\text{ ng}/\mu\text{l}$ ). Therefore, the protocol was changed for subsequent samples.

Samples PL-15 to PL-27 (frozen in TRIzol) were thawed and maintained at RT for 5 min. Then, 200  $\mu\text{l}$  of cold chloroform (Panreac) were added to each tube containing 1 ml TRIzol. After mixing by inverting the tubes 5 times, they were left to rest for 3 min at RT and later centrifuged for 15 min, 14,000g at  $4^{\circ}\text{C}$ . Approximately 400  $\mu\text{l}$  of supernatant were transferred to new tubes containing 10  $\mu\text{g}$  of ultra-pure glycogen (Thermo Fisher). 500  $\mu\text{l}$  of cold isopropanol (Panreac) were added to each tube and mixed by inversion. Samples were stored overnight at  $-20^{\circ}\text{C}$ . Next, samples were centrifuged for 15 min, 14,000g at  $4^{\circ}\text{C}$ . Supernatant was discarded and pellets of the same study subject were pooled and resuspended in 1 ml of ethanol 70% (Panreac). After 10 min of 5500g centrifugation at  $4^{\circ}\text{C}$ , supernatant was discarded. Pellets were dried out at  $35\text{--}37^{\circ}\text{C}$  in a thermoblock for 2 min with open tube lids. RNA pellets were resuspended in 30  $\mu\text{l}$  of water, mixed by vortex and frozen at  $-80^{\circ}\text{C}$ . Finally, RNA isolation was performed following MinElute Cleanup (Qiagen) kit instructions. RNA contamination with proteins and salts was assessed and RNA was quantified with a NanoDrop™ 2000/2000c Spectrophotometer. RNA integrity was evaluated for two samples (PL-15 and PL-16) by Experion RNA StdSens Starter Kit (Bio-Rad Laboratories Inc.), following manufacturer instructions.

## 2.8 | Affymetrix

Transcriptomic analysis of  $\text{CD}3^{+}$ ,  $\text{CD}14^{+}$  cell and PRP samples ( $n = 13$ ) was performed using GeneChip Human Gene 2.1 ST strips (Affymetrix, Thermo Fisher Scientific). Following manufacturer instructions, 100 ng RNA from each sample were hybridized using GeneChip™ WT PLUS Reagent Kit. Hybridization details can be found elsewhere.<sup>7</sup>

## 2.9 | Multiplex protein analysis

Three platelet-associated proteins, P-Selectin, platelet-derived growth factor  $\beta\beta$  (PDGF $\beta\beta$ ) and vascular endothelial growth factor a (VEGF-a), were measured using Luminex technology in undiluted PPP and PRP samples. Proteins were quantified in duplicate in 96-well plates following manufacturer instructions (Thermo Fisher). The plate was analysed on a LUMINEX 200 (Luminex Corp) equipment and xPONENT software (Luminex corp). Samples with a low number of counts ( $<70$ ) were discarded.

## 2.10 | Statistical analysis

Mean and standard deviation (SD) were calculated for continuous demographic variables. Affymetrix results were analysed with TAC software (Thermo Fisher). EBayes ANOVA method was used for comparing gene expression between the three different cell types. Genes were filtered by selecting those with a gene-level fold change  $<-2$  or  $>2$ . Statistical significance was set at  $p$ -value  $<.05$ , and multiple correction was performed using FDR  $<0.1$ . Luminex results were analysed with GraphPad Prism 9 software. Protein concentrations in PPP and PRP were compared by paired-Wilcoxon Test, setting statistical significance at  $p$ -value  $<.05$ .

# 3 | RESULTS

## 3.1 | Characteristics of study subjects

Twenty-seven individuals were recruited and subjected to plateletpheresis donation. Of those, three individuals were excluded of the study for different reasons: PL-1 was excluded because  $\text{CD}3^{+}$  and  $\text{CD}14^{+}$  were not isolated; PL-6 did not complete the plateletpheresis process due to vein rupture during the procedure; and PL-12 PRP did not reach the minimum platelet concentration.

Some of the subjects experienced sickness or dizziness along the process due to the hypocalcaemia caused by the action of the ACD-A anticoagulant. In these cases, a calcium supplement was administered without further incidences.

Of the 24 included study subjects, only 4 were male. The study population was aged 29.5 years (median), ranging between 21 and 53 years (minimum and maximum). Demographics and blood

TABLE 1 Demographics and blood parameters of the study subjects before plateletpheresis

Subject	Sex	Age	Weight (kg)	Height (cm)	WBC (10 <sup>9</sup> /L)	RBC (10 <sup>9</sup> /L)	HGB/g/dL	HCT (%)	MCV (fL)	MCH (pg)	MCHC (g/dL)	PLT (10 <sup>9</sup> /L)	NEUT (10 <sup>9</sup> /L)	LYMPH (10 <sup>9</sup> /L)	MONO (10 <sup>9</sup> /L)	EO (10 <sup>9</sup> /L)	BASO (10 <sup>9</sup> /L)
PL-02	F	36	74	159	6.23	4.89	13.6	40.2	82.2	27.8	33.8	240	3.18	2.5	0.47	0.05	0.02
PL-03	M	43	87	170	7.63	5.31	16.10	45.90	86.40	30.30	35.10	255.00	4.94	1.86	0.61	0.15	0.05
PL-04	F	35	64	161	6.38	4.59	13.60	39.40	85.80	29.60	34.50	262.00	3.19	2.69	0.40	0.07	0.02
PL-05	F	29	58	164	6.54	4.38	12.70	38.80	88.60	29.00	32.70	311.00	3.79	2.13	0.44	0.10	0.07
PL-07	F	23	61	158	5.38	4.48	13.10	38.50	85.90	29.20	34.00	304.00	3.27	1.59	0.27	0.19	0.02
PL-08	F	26	54	162	7.98	4.81	13.90	40.90	85.00	28.90	34.00	316.00	4.41	2.50	0.67	0.32	0.06
PL-09	F	35	54	167	5.09	5.04	14.80	43.60	86.50	29.40	33.90	161.00	2.79	1.91	0.32	0.05	0.02
PL-10	M	38	76	175	5.85	4.48	14.90	42.50	94.90	33.30	35.10	199.00	3.71	1.34	0.69	0.06	0.03
PL-11	F	26	55	167	5.77	4.29	12.90	39.20	91.40	30.10	32.90	254.00	2.43	2.56	0.57	0.13	0.05
PL-13	F	30	67	160	5.14	4.37	13.00	38.80	88.80	29.70	33.50	206.00	2.77	1.83	0.37	0.12	0.04
PL-14	F	53	73	158	6.35	4.81	13.40	42.10	87.50	27.90	31.80	210.00	3.51	2.12	0.34	0.27	0.09
PL-15	F	46	63	168	4.27	4.54	13.90	40.90	90.10	30.60	34.00	244.00	2.27	1.45	0.30	0.16	0.08
PL-16	F	28	75	168	5.06	4.23	11.80	35.70	84.40	27.90	33.10	203.00	2.57	1.90	0.43	0.11	0.04
PL-17	F	28	68	165	7.06	4.49	13.60	41.10	91.50	30.30	33.10	313.00	3.76	1.88	0.90	0.45	0.06
PL-18	F	40	68	166	11.01	3.91	11.40	34.80	89.00	29.20	32.80	288.00	8.35	1.88	0.55	0.15	0.04
PL-19	M	24	77	178	6.85	5.95	17.70	53.20	89.40	29.70	33.30	194.00	3.25	2.76	0.64	0.14	0.05
PL-20	F	21	56	156	5.70	5.12	14.20	42.90	83.80	27.70	33.10	326.00	2.68	1.86	0.47	0.61	0.07
PL-21	F	27	114	172	7.38	4.13	12.40	36.90	89.30	30.00	33.60	299.00	3.75	2.89	0.49	0.20	0.03
PL-22	F	22	75	163	8.18	4.68	13.20	38.80	82.90	28.20	34.00	263.00	4.58	2.78	0.55	0.16	0.03
PL-23	M	50	85	170	10.79	4.47	13.20	38.80	86.80	29.50	34.00	334.00	6.92	2.79	0.60	0.28	0.05
PL-24	F	41	60	171	7.01	4.50	13.60	41.40	92.00	30.20	32.90	355.00	4.27	2.25	0.31	0.13	0.04
PL-25	F	26	70	168	7.86	4.69	12.60	39.40	84.00	26.90	32.00	225.00	5.32	1.77	0.45	0.22	0.06
PL-26	F	36	52	160	7.63	4.01	12.10	36.80	91.80	30.20	32.90	222.00	4.76	1.94	0.61	0.21	0.07
PL-27	F	26	58	160	7.39	4.41	13.50	40.10	90.90	30.60	33.70	200.00	5.55	1.13	0.50	0.17	0.03
Mean ± SD or frequency	84% F/16%M	32.64 ± 8.91	68.48 ± 13.51	165.44 ± 5.7	6.76 ± 1.66	4.58 ± 0.45	13.49 ± 1.34	40.24 ± 3.76	96.79 ± 45.15	31.92 ± 12.48	33.4 ± 1.03	243.68 ± 68.43	3.92 ± 1.47	2.08 ± 0.48	0.49 ± 0.14	0.18 ± 0.12	0.04 ± 0.01

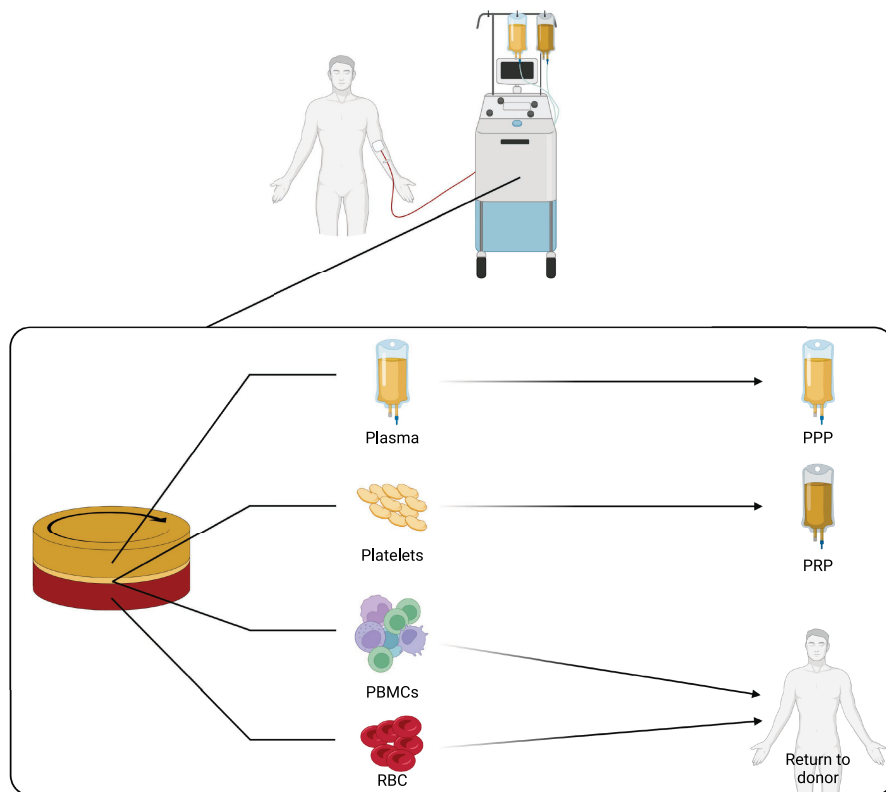


**FIGURE 1** Simplified diagram of plateletpheresis. Whole blood is collected from the subject and separated by centrifugation into plasma, red blood cells (RBC) and platelets + white blood cells (WBC). Plasma (or PPP: platelet-poor plasma) is collected in donation bags. Platelets are separated from WBC using Leukoreduction system chambers (LRSC). Purified platelets are then collected in donation bags as PRP (platelet-rich plasma). Finally, RBC and WBC are transferred back to the donor via the same puncture point. Some RBC and WBC remain in the LRSC, usually discarded as a waste plateletpheresis product. PBMCs can be then isolated from it

parameters of the study subjects before the plateletpheresis process are shown in Table 1.

### 3.2 | Plateletpheresis yielded pure, highly concentrated platelet samples from single donors

Once completed the plateletpheresis process (Figure 1) and after 2 h resting at RT without shaking, PRP samples were analysed on a haemocytometer to assess platelet concentration (Table 2). All the individual samples yielded at least  $500 \times 10^9$  platelets/L. However, the duration of the process and the processed volume of blood were different for each study subject. The duration of the plateletpheresis procedure mainly depends on the blood platelet counts of the donor before the procedure (Table 1). Other minor affecting factors are the donor's haematocrit levels and the vein access flow. In our study, the average time to complete the donation was  $32.14 \pm 6.57$  min (mean  $\pm$  SD), and the processed volume of blood was  $1127 \pm 166.6$  ml (mean  $\pm$  SD) (Table 2).

### 3.3 | CD3<sup>+</sup> and CD14<sup>+</sup> cell populations were isolated from a waste product of plateletpheresis process

The cell content of the PBMC fraction obtained from the LRSC was analysed on a haemocytometer. The numbers of total white blood cells (WBC), lymphocytes, monocytes and platelets are collected in Table 3. From those, 10 million monocytes and the corresponding number of

lymphocytes were sequentially isolated by positive selection with magnetic beads from each subject. CD3<sup>+</sup> and CD14<sup>+</sup> fractions were subsequently used for RNA isolation. The purity of the isolated ranged 97.6–98.9% for CD3<sup>+</sup> and 96.9–98.8% for CD14<sup>+</sup> cells (data not shown). The remaining PBMCs that were not used for CD3<sup>+</sup> and CD14<sup>+</sup> isolation were frozen and stored for future experiments.

### 3.4 | Platelet RNA obtained with TRIzol is suitable for Affymetrix transcriptomic analysis and enriched in platelet transcripts compared to CD3<sup>+</sup> and CD14<sup>+</sup> cell populations

Once all the cell populations (PRP, CD3<sup>+</sup> and CD14<sup>+</sup>) were collected, RNA was isolated by established procedures. We could not obtain valid platelet RNA samples for further transcriptomic analyses from PL-2 to PL-14, as PRP samples were directly frozen after plateletpheresis. Freezing/thawing cycles lyse platelets releasing all their components to the medium. For PRP samples PL-15 to PL-27, the protocol developed by Amisten et al<sup>12</sup> based on TRIzol extraction was used. When assessing the quality of the platelet RNA, the ratios obtained on the Nanodrop were low (Figure 2A). Moreover, the RNA integrity of two platelet samples was analysed by Experion. Neither of them complied with the minimum RQI = 7, established as a quality requirement for transcriptomic studies (Figure 2B–E). This is because the composition of 18s/28s is different in platelets, resulting in a lower RQI than that from nucleated cells<sup>13</sup>; therefore, we did not evaluate more samples with this technique. Nevertheless, we decided to continue further processing platelet RNA samples and analysed their

TABLE 2 Characteristics of plateletpheresis and obtained PRP samples after 2 h resting

Subject	Process duration (min)	Processed blood volume (ml)	PRP volume (ml)	PLT ( $10^9/L$ )	PDW (fL)	MPV (fL)	P-LCR (%)	Platelet mass ( $\mu$ l)
PL-02	27	1074	83	1419	10.80	10.00	24.20	15,240.06
PL-03	32	1080	83	1100	9.80	9.60	20.20	11,404.80
PL-04	29	1056	83	1687	9.80	9.70	21.50	17,280.28
PL-05	26	953	83	1310	10.70	10.10	24.70	12,609.14
PL-07	27	964	83	1346	8.80	8.90	15.20	11,548.14
PL-08	28	945	84	1213	10.70	10.00	25.10	11,462.85
PL-09	50	1519	83	561	9.20	9.20	17.30	7839.86
PL-10	38	1406	84	903	7.50	8.40	9.70	10,664.79
PL-11	42	1096	83	700	7.80	8.40	10.40	6444.48
PL-13	35	1286	84	1164	9.30	9.30	18.50	13,921.21
PL-14	32	1228	84	1085	10.40	10.00	23.80	13,323.80
PL-15	35	1151	83	1113	7.40	8.10	8.60	10,376.61
PL-16	-	1275	84	670	8.90	9.00	14.80	7688.25
PL-17	28	955	83	1390	9.00	9.20	17.40	12,212.54
PL-18	29	1035	80	1053	10.80	10.00	24.20	10,898.55
PL-19	40	1358	83	869	8.20	8.80	13.40	10,384.90
PL-20	28	943	83	1189	8.40	8.90	14.30	9978.92
PL-21	-	1072	118	1366	9.10	9.30	18.20	13,618.47
PL-22	26	1035	84	1124	8.40	8.90	15.00	10,353.73
PL-23	22	985	110	1157	7.20	8.10	8.20	9231.12
PL-24	26	903	85	1500	8.50	9.00	15.50	12,190.50
PL-25	35	1208	83	1098	8.40	8.90	14.50	11,804.82
PL-26	36	1236	84	706	8.90	9.00	15.40	7853.54
PL-27	36	1276	83	1256	10.90	10.00	25.00	16,026.56
Mean $\pm$ SD	32.13 $\pm$ 6.57	1126.62 $\pm$ 166.57	85.83 $\pm$ 8.80	1124.12 $\pm$ 278.98	9.12 $\pm$ 1.15	9.20 $\pm$ 0.61	17.29 $\pm$ 5.35	11,431.58 $\pm$ 2661.27

**TABLE 3** Concentration and total counts of white blood cells (WBC), lymphocytes, monocytes and platelets collected in the PBMC fraction isolated from the LRSC

Subject	WBC count	LYMPH (10 <sup>9</sup> /L)	MONO (10 <sup>9</sup> /L)	PLT (10 <sup>9</sup> /L)	Total WBC	Total lymph	Total Mono	Total PLT
PL-02	40.60	31.54	8.84	64	2.03E+08	1.58E+08	4.42E+07	3.20E+08
PL-03	20.50	15.68	4.68	137	1.03E+08	7.84E+07	2.34E+07	6.85E+08
PL-04	58.54	50.06	8.15	121	2.93E+08	2.50E+08	4.08E+07	6.05E+08
PL-05	45.18	36.79	8.18	206	2.26E+08	1.84E+08	4.09E+07	1.03E+09
PL-07	14.11	11.03	2.86	5	7.06E+07	5.52E+07	1.43E+07	2.50E+07
PL-08	10.84	7.80	2.82	192	5.42E+07	3.90E+07	1.41E+07	9.60E+08
PL-09	47.05	37.71	8.90	242	2.35E+08	1.89E+08	4.45E+07	1.21E+09
PL-10	96.97	57.08	37.22	333	4.85E+08	2.85E+08	1.86E+08	1.67E+09
PL-11	59.68	46.12	13.27	184	2.98E+08	2.31E+08	6.64E+07	9.20E+08
PL-13	23.19	16.11	6.74	39	1.16E+08	8.06E+07	3.37E+07	1.95E+08
PL-14	55.98	42.34	13.15	411	2.80E+08	2.12E+08	6.58E+07	2.06E+09
PL-15	85.20	66.49	17.99	353	4.26E+08	3.32E+08	9.00E+07	1.77E+09
PL-16	71.08	58.65	11.39	267	3.55E+08	2.93E+08	5.70E+07	1.34E+09
PL-17	24.38	16.10	7.38	259	1.22E+08	8.05E+07	3.69E+07	1.30E+09
PL-18	16.03	12.31	3.39	246	8.02E+07	6.16E+07	1.70E+07	1.23E+09
PL-19	76.43	64.64	11.38	526	3.82E+08	3.23E+08	5.69E+07	2.63E+09
PL-20	37.73	28.71	8.69	670	1.89E+08	1.44E+08	4.35E+07	3.35E+09
PL-21	71.60	71.60	13.27	685	3.58E+08	3.58E+08	6.64E+07	3.43E+09
PL-22	64.18	47.68	16.02	641	3.21E+08	2.38E+08	8.01E+07	3.21E+09
PL-23	88.38	62.00	24.14	1071	4.42E+08	3.10E+08	1.21E+08	5.36E+09
PL-24	7.07	4.91	1.92	52	3.54E+07	2.46E+07	9.60E+06	2.60E+08
PL-25	32.81	19.43	12.82	101	1.64E+08	9.72E+07	6.41E+07	5.05E+08
PL-26	26.33	14.57	14.57	135	1.32E+08	7.29E+07	7.29E+07	6.75E+08
PL-27	23.38	10.35	11.04	100	1.17E+08	5.18E+07	5.52E+07	5.00E+08
Mean±SD	26.33±23.38	14.57±10.35	14.57±11.04	135±100	1.31E+8± 1.16E+8	7.28E+7± 5.17E+7	7.28E+7± 5.52E+7	6.75E+8± 5E+8

transcriptome on the Affymetrix platform, together with CD3<sup>+</sup> and CD14<sup>+</sup> samples, whose RNA was optimal for further transcriptomic analysis, as determined by the purity ratios and the RQI (Figure 2F,G).

When RNA isolated from PRP, CD3<sup>+</sup> and CD14<sup>+</sup> cell samples was analysed on the Affymetrix platform, the different cell types were clustered apart from the others in a non-supervised principal component analysis (PCA) (Figure 3A). Moreover, it was confirmed that platelet-related transcripts obtained in previous studies with PBMC samples (presumably containing platelets)<sup>7</sup> were enriched in the PRP (Figure 3B) when compared to the CD3<sup>+</sup> and CD14<sup>+</sup> cell populations. Among these transcripts were those involved in different platelet functions, such as formation of adhesion complexes (*GP1BA* and *SELP*), aggregation of complexes (*ITGA2B*) or granule secretion and trafficking (*RAB27B*).

CD3<sup>+</sup> and CD14<sup>+</sup> populations also depicted classical transcriptomic profiles for these populations (Figure S1).

### 3.5 | PDGFββ, VEGF-a and P-Selectin proteins are increased in the PRP fraction

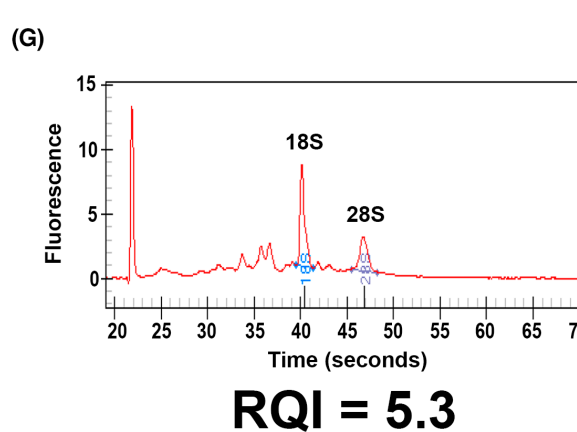
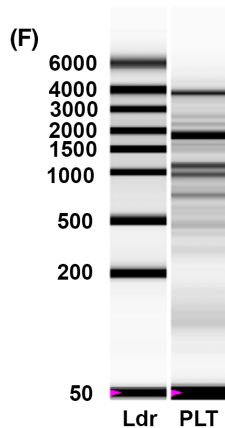
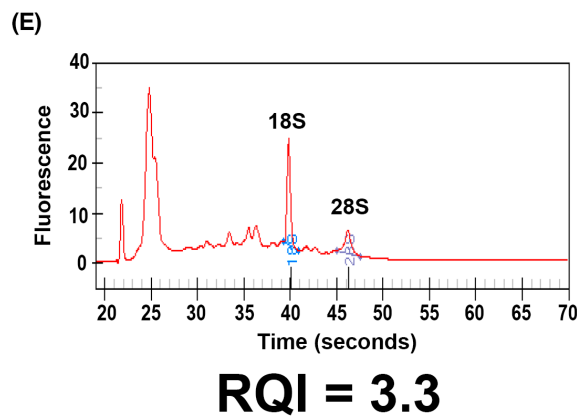
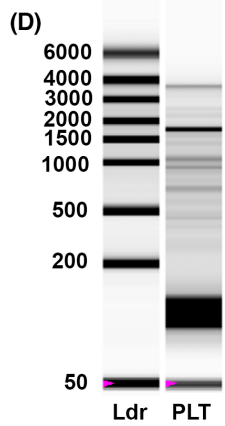
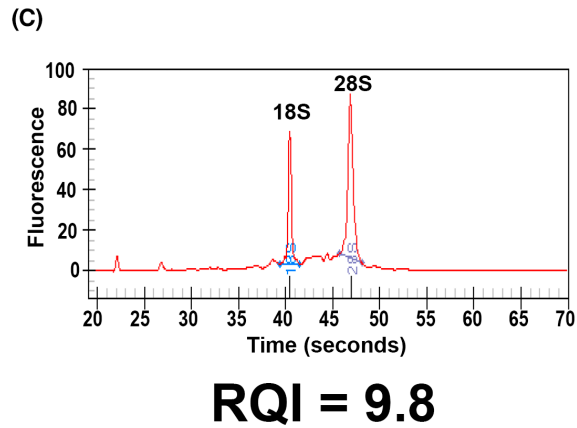
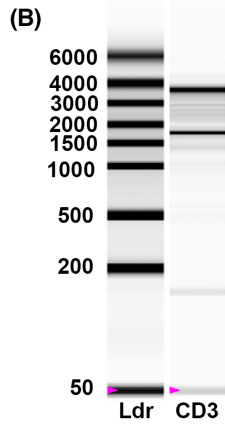
Finally, we assessed whether PRP and PPP samples could be used for protein measurements. We quantified the content of proteins described to be related to platelets, such as PDGFββ, VEGF-a and P-Selectin by multiplexing assays. We could confirm that PRP samples were enriched in platelet-associated proteins when compared to their matched PPP samples (Figure 4).

## 4 | DISCUSSION

There is increasing evidence that platelets can no longer be considered as mere mediators of coagulation, but as important players in

**FIGURE 2** RNA quality assessment. Concentration and contamination of platelet RNA was analysed by NanoDrop® before and after amplification for Affymetrix (A). Quality and integrity of platelet RNA was analysed by Experion® before (B, C) and after (D, E) treatment with a CleanUp column (Qiagen). RNA from CD3<sup>+</sup> cells was analysed as a control (F, G). RQI: RNA Quality Indicator; Ldr: ladder; PLT: platelet sample

Subject	PLATELETS					
	[RNA] (ng/ml)	260/280	260/230	[ss-cDNA] (ng/ml)	260/280	260/230
PL-17	115.3	1.96	0.75	492	2.04	1.99
PL-18	81.3	1.52	0.51	354.8	2.07	1.89
PL-19	41.1	1.74	0.75	313.7	2.09	1.88
PL-20	39.8	1.77	0.36	312.7	2.05	1.84
PL-21	167.1	2.01	0.79	303.5	2.1	1.96
PL-22	54.9	1.82	1.07	321.1	2.09	1.9
PL-23	102.2	1.89	1.18	333.4	2.07	1.91
PL-24	25.1	1.3	0.14	115.9	1.88	1.44
PL-25	18.4	1.44	0.05	130.6	1.98	2.32
PL-26	35.9	1.59	0.07	91.1	1.92	2.35
PL-27	42.4	1.7	0.31	65.8	1.9	2.45



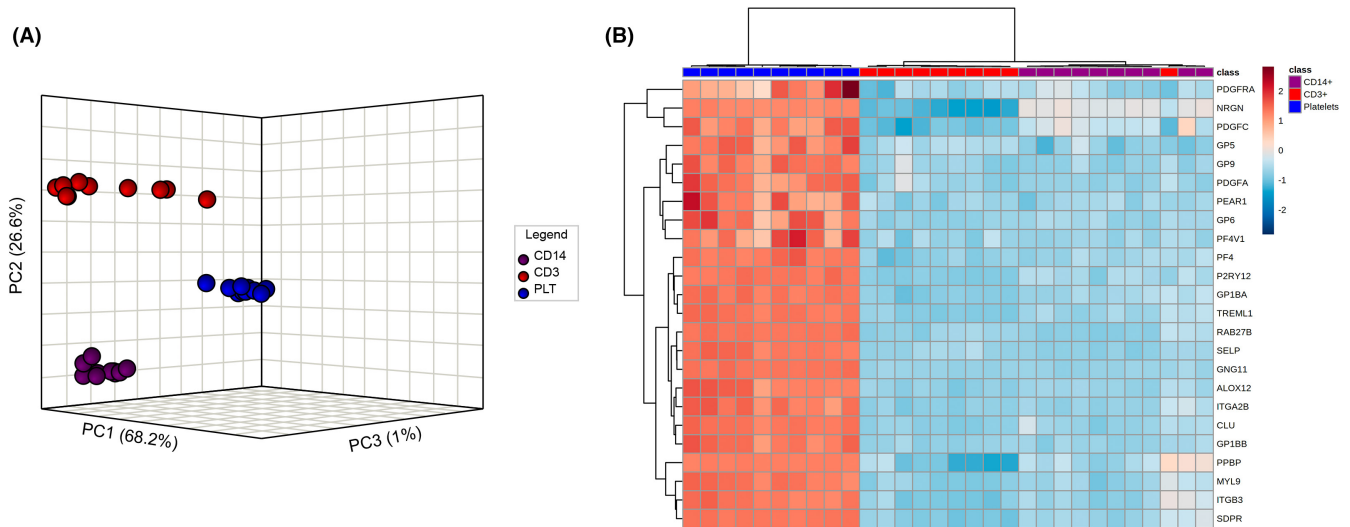


**FIGURE 3** Transcriptomic differences between platelets, CD3<sup>+</sup> and CD14<sup>+</sup> samples. (A). Unsupervised multivariate analysis of transcriptomic data was used to analyse the clustering of platelet (blue), CD3<sup>+</sup> (purple) and CD14<sup>+</sup> (red) samples. (B) Heatmap of platelet-related genes expressed in platelet (blue), CD3<sup>+</sup> (purple) and CD14<sup>+</sup> (red) samples. Upregulated genes are represented in red and downregulated genes are shown in blue. ANOVA *p*-value <.05. FDR *p*-value <.05

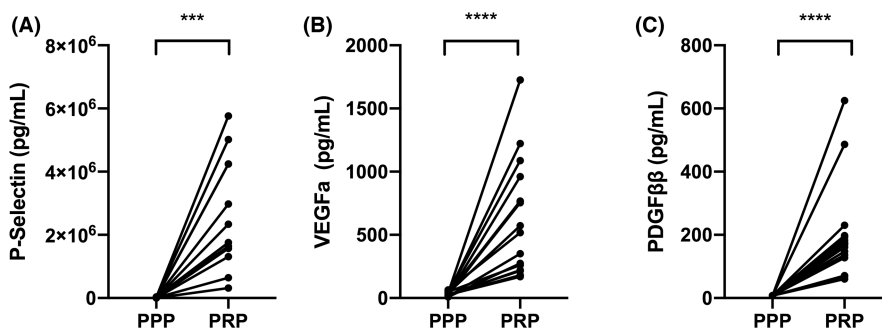


**FIGURE 4** Platelet-associated molecules are increased in PRP samples. P-Selectin (A), VEGF-a (B) and PDGFβ (C) quantification by Luminex in PPP and PRP samples. \*\*\*Paired-Wilcoxon Test *p*-value <.005, \*\*\*\* Paired-Wilcoxon Test *p*-value <.001

inflammatory and immune-modulatory processes.<sup>2</sup> The transcriptional landscape of human platelets has been reported altered during sepsis.<sup>14</sup> Several studies have pointed out modifications on platelet functions in inflammatory diseases such as Chronic Obstructive Pulmonary Disease (COPD)<sup>15</sup> or COVID-19 severity and mortality.<sup>16</sup> Moreover, increased levels of platelet-derived mediators have been noted in peripheral blood and bronchoalveolar lavage fluid (BALF) of asthmatic patients, suggesting increased levels of platelet activation.<sup>17</sup> We previously found that severe food-associated respiratory allergy could be associated with the alteration of platelet functions.<sup>7</sup> Since then, our aim had been to study platelet phenotype and role in severe allergic patients. However, the lack of an optimized method to obtain pure and functional platelet samples from single donors has made their characterization so far difficult or inaccurate. Here, we describe a high-yielding method for the collection of a pure platelet-rich product from single donors based on plateletpheresis for multi-omic studies.

Plateletpheresis is not commonly used for research purposes. Efficient platelet collection is nevertheless routinely performed by plateletpheresis in blood donation centres for donation purposes.<sup>18,19</sup> Since specialized equipment and staff training are required, few research studies have so far used this technique.<sup>20</sup> The most commonly used technique for isolating pure platelets is based on successive

centrifugation steps. As previously discussed, this technique requires large blood volumes<sup>12</sup>; thus, many studies report using pools of samples from different donors, instead of individual samples.<sup>13</sup> Moreover, platelets suffer mechanical stress during the multiple centrifugation steps, which leads to platelet activation and release of molecules contained in platelet granules.<sup>11</sup> Therefore, the interpretation of results could be altered. Nevertheless, this activation can be minimized by allowing the isolated platelets to rest, as it is described in our protocol for PRP samples obtained by plateletpheresis.

General research has traditionally focused on the study of blood leukocyte populations. For that, density-gradient centrifugation has been widely applied for the isolation of these cell types. However, due to their density, platelets are also retained in the cell layer after blood centrifugation together with leukocytes. This was the case in our previous study,<sup>7</sup> where we identified a set of transcripts involved in platelet functions contained in PBMC samples. This highlights the fact that the extraction of pure platelet samples is difficult using classical laboratory techniques.

In contrast, plateletpheresis allows the collection of pure rich platelet samples from a single donor.<sup>18</sup> Hence, plateletpheresis not only provides a higher purity of the collected platelet samples, but also a higher yield when compared to traditional blood



centrifugation. This opens an avenue to perform platelet research studies without contamination with other blood cell populations and without the need of pooling samples.

Moreover, plateletpheresis allows collecting acellular plasma (PPP) and functional leukocytes from the LRSC, usually discarded as a waste product of the plateletpheresis procedure.<sup>21</sup> Therefore, from a single donor we can obtain matched samples of PRP, PPP and leukocytes, simplifying sampling and minimizing sample contamination.

In the present study, we have validated the suitability of platelet samples obtained by plateletpheresis for omic studies. With the method described here, PRP samples can be used for protein determination by multiplex and RNA isolation for transcriptomic studies.

We described that the protein levels of platelet-related factors such as VEGF-a, PDGF $\beta$  and P-Selectin are higher in PRP samples than in their PPP counterparts. Previous studies have reported platelet-rich concentrates as a source of platelets and growth factors, including transforming growth factor-beta (TGF-beta) and PDGF.<sup>22</sup> VEGF-a is a member of the PDGF/VEGF family.<sup>23</sup> Current evidence implies that platelets not only contribute structurally but instructively to vascular remodelling. In this sense, platelets are major storage and delivery vehicles for pro- and anti-angiogenic growth factors including VEGF-a.<sup>24</sup> PDGF $\beta$  is involved in the recruitment and differentiation of pericytes that are smooth muscle-like cells found in close contact with the endothelium in capillaries, where they regulate the morphology and function of the vessels during vessel formation.<sup>25</sup> Recent research has also implicated PDGF $\beta$  as a potential contributing factor to cell signalling pathway of mesenchymal stem cells, human dermal fibroblasts, pericytes and smooth muscle cells, among others, in various interrelated diseases.<sup>26</sup> In turn, P-selectin is one of the most bioactive molecules contained in  $\alpha$ -granules and involved in inflammation. It promotes platelet aggregation and platelet interactions with both leukocytes and endothelial cells.<sup>27</sup>

At the transcriptional level, we have observed an enrichment in platelet-related transcripts in PRP samples compared to their matched CD3<sup>+</sup> and CD14<sup>+</sup> counterparts. The transcriptomic results presented here, therefore, validate plateletpheresis as a suitable method for obtaining pure platelet samples and suggest that the findings involving platelet transcripts previously obtained from PBMCs were most presumably due to platelet presence in the cell layer fraction obtained by density-gradient centrifugation.<sup>7,28</sup> This set of platelet transcripts includes those involved in the following platelet functions: formation of adhesion complexes (GP1BA and SELP)<sup>29,30</sup>; receptors (GP6, P2RY12)<sup>31</sup>; aggregation of complexes (ITGA2B)<sup>31</sup>; granule secretion and trafficking (RAB27B)<sup>32-34</sup> and activation and response to elevated platelet cytosolic Ca<sup>2+</sup> (PF4).<sup>35</sup>

It is worth mentioning that RNA of PRP samples was valid and used for transcriptomic analysis, regardless of the integrity and quality determinations. In this regard, it can be concluded that the methods usually employed to assess RNA quality are not suitable for platelet RNA. Platelets are known to have a complex transcriptome including mRNA and miRNA, among others.<sup>36</sup> RNA was detected in platelets over 30 years ago; however, we are currently only beginning to unravel the complexity of the platelet transcriptome.<sup>37</sup>

The use of RNA sequencing or genome-wide studies with platelet RNA has enabled us to expand our knowledge on platelet biology and functions since a rising number of studies have been dedicated to this topic.<sup>13,38-40</sup> Therefore, it is essential to use standardized and appropriate tools for isolating, quantifying and characterizing the complex and rich platelet RNA repertoire.

In this study, we have developed a protocol based on plateletpheresis to obtain pure PRP samples, as well as PPP, CD3<sup>+</sup> and CD14<sup>+</sup> matched cell samples from single donors. These samples are suitable for protein and transcriptomic studies. Therefore, this methodology could be used for phenotyping platelets as well as other cell populations in immune diseases and contribute to unravel their role in inflammatory diseases such as allergy.

## AUTHOR CONTRIBUTION

CG-C and JLB designed the study and together with DB and MME supervised the research. JLB supervised sample collection and together with LNMB and MRM recruited the study subjects. JS-S, LM-B, MID-D and CP-T processed the samples and performed the experiments. CP-T, MID-D and CG-C drafted the manuscript. All authors approved the final version of the manuscript.

## CONFLICT OF INTEREST

The authors declare that they do not have any conflict of interest in relation to this study.

## DATA AVAILABILITY STATEMENT

The data that support the findings of this study are openly available in GEO (Gene Expression Omnibus) at <https://www.ncbi.nlm.nih.gov/geo/query/acc.cgi?acc=GSE203196>, reference number GSE203196.

## ORCID

Carmela Pablo-Torres  <https://orcid.org/0000-0003-2861-5763>

María Isabel Delgado-Dolset  <https://orcid.org/0000-0001-7924-5454>

org/0000-0001-7924-5454

Maria M. Escribese  <https://orcid.org/0000-0001-5057-5150>

Domingo Barber  <https://orcid.org/0000-0002-5488-5700>

Cristina Gomez-Casado  <https://orcid.org/0000-0002-7707-6367>

## REFERENCES

1. Luo L, Zhang J, Lee J, Tao A. Platelets, not an insignificant player in development of allergic asthma. *Cell*. 2021;10(8):2038.
2. Gomez-Casado C, Villaseñor A, Rodriguez-Nogales A, Bueno JL, Barber D, Escribese MM. Understanding platelets in infectious and allergic lung diseases. *Int J Mol Sci*. 2019;20(7):1730.
3. Chen Y, Zhong H, Zhao Y, Luo X, Gao W. Role of platelet biomarkers in inflammatory response. *Biomark Res*. 2020;8(1):28. doi:10.1186/s40364-020-00207-2
4. Kowal K, Pampuch A, Kowal-Bielecka O, DuBuske LM, Bodzentek-Łukaszuk A. Platelet activation in allergic asthma patients during allergen challenge with Dermatophagoides pteronyssinus. *Clin Exp Allergy*. 2006;36(4):426-432.
5. Nastafek M, Potaczek DP, Wojas-Pelc A, Undas A. Plasma platelet activation markers in patients with atopic dermatitis and concomitant allergic diseases. *J Dermatol Sci*. 2011;64(1):79-82. doi:10.1016/j.jdermsci.2011.07.001

6. Tamagawa-Mineoka R, Katoh N, Ueda E, Masuda K, Kishimoto S. Elevated platelet activation in patients with atopic dermatitis and psoriasis: increased plasma levels of  $\beta$ -thromboglobulin and platelet factor 4. *Allergol Int*. 2008;57(4):391-396.
7. Obeso D, Mera-Berriatua L, Rodríguez-Coira J, et al. Multi-omics analysis points to altered platelet functions in severe food-associated respiratory allergy. *Allergy Eur J Allergy Clin Immunol*. 2018;73(11):2137-2149.
8. Barber D, Villaseñor A, Escribese MM. Metabolomics strategies to discover new biomarkers associated to severe allergic phenotypes. *Asia Pac Allergy*. 2019;9(4):e37. doi:10.5415/apallergy.2019.9.e37
9. Amisten S, Braun OÖ, Bengtsson A, Erlinge D. Gene expression profiling for the identification of G-protein coupled receptors in human platelets. *Thromb Res*. 2008;122(1):47-57. doi:10.1016/j.thromres.2007.08.014
10. Bugert P, Dugrillon A, Günaydin A, Eichler H, Klüter H. Messenger RNA profiling of human platelets by microarray hybridization. *Thromb Haemost*. 2003;90(4):738-748.
11. Jang C-S, Kim S-I, Kim H-K, et al. Plateletpheresis: the process, devices, and indicators of product quality. *J Life Sci*. 2014;30(24):1030-1038.
12. Amisten S. A rapid and efficient platelet purification protocol for platelet gene expression studies. In: Gibbins JM, Mahaut-Smith MP, eds. *Platelets and Megakaryocytes: Volume 3, Additional Protocols and Perspectives*. Springer New York; 2012:155-172. doi:10.1007/978-1-61779-307-3\_12
13. Rowley JW, Oler AJ, Tolley ND, et al. Genome-wide RNA-seq analysis of human and mouse platelet transcriptomes. *Blood*. 2011;118(14):e101-e111. doi:10.1182/blood-2011-03-339705
14. Middleton EA, Rowley JW, Campbell RA, et al. Sepsis alters the transcriptional and translational landscape of human and murine platelets. *Blood*. 2019;134(12):911-923. doi:10.1182/blood.2019000067
15. Maclay JD, McAllister DA, Johnston S, et al. Increased platelet activation in patients with stable and acute exacerbation of COPD. *Thorax*. 2011;66(9):769-774. <http://thorax.bmj.com/content/66/9/769.abstract>
16. Hottz ED, Azevedo-Quintanilha IG, Palhinha L, et al. Platelet activation and platelet-monocyte aggregate formation trigger tissue factor expression in patients with severe COVID-19. *Blood*. 2020;136(11):1330-1341. doi:10.1182/blood.2020007252
17. Turkalj M. The role of platelets in allergic inflammation and asthma. In: IBE-C P, ed. *Asthma*. IntechOpen; 2019:Ch. 5. doi:10.5772/intechopen.85114
18. Bueno JL, García F, Castro E, Barea L, González R. A randomized crossover trial comparing three plateletpheresis machines. *Transfusion*. 2005;45(8):1373-1381.
19. Bueno JL, Barea L, García F, Castro E. A comparison of PLT collections from two apheresis devices. *Transfusion*. 2004;44(1):119-124.
20. Bueno JL, Ynigo M, de Miguel C, et al. Growth differentiation factor 11 (GDF11) - a promising anti-ageing factor - is highly concentrated in platelets. *Vox Sang*. 2016;111(4):434-436.
21. Pfeiffer IA, Zinser E, Strasser E, et al. Leukoreduction system chambers are an efficient, valid, and economic source of functional monocyte-derived dendritic cells and lymphocytes. *Immunobiology*. 2013;218(11):1392-1401.
22. Mehta S, Watson JT. Platelet rich concentrate: basic science and current clinical applications. *J Orthop Trauma*. 2008;22(6):432-438. [https://journals.lww.com/jorthotrauma/Fulltext/2008/07000/Platelet\\_Rich\\_Concentrate\\_\\_Basic\\_Science\\_and.12.aspx](https://journals.lww.com/jorthotrauma/Fulltext/2008/07000/Platelet_Rich_Concentrate__Basic_Science_and.12.aspx)
23. Shibuya M. Vascular endothelial growth factor and its receptor system: physiological functions in angiogenesis and pathological roles in various diseases. *J Biochem*. 2013;153(1):13-19. doi:10.1093/jb/mvs136
24. Rafii DC, Psaila B, Butler J, Jin DK, Lyden D. Regulation of vasculogenesis by platelet-mediated recruitment of bone marrow-derived cells. *Arterioscler Thromb Vasc Biol*. 2008;28(2):217-222.
25. Hellberg C, Ostman A, Heldin C-H. PDGF and vessel maturation. *Recent Results Cancer Res*. 2010;180:103-114.
26. Wang C, Liu Y, He D. Diverse effects of platelet-derived growth factor-BB on cell signaling pathways. *Cytokine*. 2019;113:13-20. <https://www.sciencedirect.com/science/article/pii/S1043466618304071>
27. Nurden AT. Platelets, inflammation and tissue regeneration. *Thromb Haemost*. 2011;105(S 06):S13-S33.
28. Uerpmann-Witzack R. European Directorate for the Quality of Medicines and Healthcare (EDQM). *The Council of Europe: Its Law and Policies*. European Directorate for the Quality of Medicines & HealthCare; 2017:394-406.
29. Othman M, Emsley J. Gene of the issue: GP1BA gene mutations associated with bleeding. *Platelets*. 2017;28(8):832-836.
30. Rondina MT, Voora D, Simon LM, et al. Longitudinal RNA-seq analysis of the repeatability of gene expression and splicing in human platelets identifies a platelet SELP splice QTL. *Circ Res*. 2020;126(4):501-516. doi:10.1161/CIRCRESAHA.119.315215
31. Rumbaut RE, Thiagarajan P. No Title. San Rafael (CA); 2010.
32. Tanya T, Magnus Å, Futter CE, Authi KS, Seabra MC. Rab27b regulates number and secretion of platelet dense granules. *Proc Natl Acad Sci*. 2007;104(14):5872-5877. doi:10.1073/pnas.0609879104
33. Tiwari S, Italiano JEJ, Barral DC, et al. A role for Rab27b in NF-E2-dependent pathways of platelet formation. *Blood*. 2003;102(12):3970-3979.
34. Chen D, Guo J, Miki T, Tachibana M, Gahl WA. Molecular cloning and characterization of rab27a and rab27b, novel human Rab proteins shared by melanocytes and platelets. *Biochem Mol Med*. 1997;60(1):27-37.
35. Sikara MP, Vlachoyiannopoulos PG. FRI0273 plasma levels of PF-4var/cxcl411, a nonallelic variant of platelet factor-4 (PF-4/CXCL4), are elevated in patients with antiphospholipid syndrome (APS). *Ann Rheum Dis*. 2013;72(Suppl 3):A466 LP-A466. [http://ard.bmj.com/content/72/Suppl\\_3/A466.3.abstract](http://ard.bmj.com/content/72/Suppl_3/A466.3.abstract)
36. Davizon-Castillo P, Rowley JW, Rondina MT. Megakaryocyte and platelet transcriptomics for discoveries in human health and disease. *Arterioscler Thromb Vasc Biol*. 2020;40(6):1432-1440. doi:10.1161/ATVBAHA.119.313280
37. Rowley JW, Schwertz H, Weyrich AS. Platelet mRNA: the meaning behind the message. *Curr Opin Hematol*. 2012;19(5):385-391.
38. Ranucci M, Ballotta A, Di Dedda U, et al. The procoagulant pattern of patients with COVID-19 acute respiratory distress syndrome. *J Thromb Haemost*. 2020;18(7):1747-1751. doi:10.1111/jth.14854
39. Sol N, Wurdinger T. Platelet RNA signatures for the detection of cancer. *Cancer Metastasis Rev*. 2017;36(2):263-272.
40. Supernat A, Popęda M, Pastuszek K, Best MG, Grešner P, et al. Transcriptomic landscape of blood platelets in healthy donors. *Sci Rep*. 2021;11(1):15679. doi:10.1038/s41598-021-94003-z

## SUPPORTING INFORMATION

Additional supporting information can be found online in the Supporting Information section at the end of this article.

**How to cite this article:** Pablo-Torres C, Delgado-Dolset MI, Sanchez-Solares J, et al. A method based on plateletpheresis to obtain functional platelet, CD3<sup>+</sup> and CD14<sup>+</sup> matched populations for research immunological studies. *Clin Exp Allergy*. 2022;00:1-12. doi: [10.1111/cea.14192](https://doi.org/10.1111/cea.14192)

# Respiratory allergies with no associated food allergy disrupt oral mucosa integrity

To the Editor,

Respiratory allergy is the most common allergy worldwide. Studies in Europe have shown that up to 30% of the population suffers from allergic rhinoconjunctivitis, while up to 20% suffer from asthma. This group of allergic diseases is characterized by an aberrant immune response to aeroallergens. The prevalence of aeroallergens varies in different regions depending on the climate.<sup>1</sup> Patients overexposed to grass pollen are frequently sensitized to the pan-allergen profilin. In fact, we have recently demonstrated that a fraction of these patients develops severe profilin-mediated food reactions that are associated with intense oral mucosa remodeling,<sup>2</sup> and with unique metabolic and transcriptomic signatures.<sup>3</sup>

In the present study, we aim to investigate whether oral mucosa is compromised in the absence of food allergy. We formulated the hypothesis that an intense systemic inflammation could induce structural changes in the oral mucosa after respiratory sensitization.

To test this hypothesis, we took advantage of respiratory phenotypes associated with olive pollen (seasonal allergy) and mites (perennial allergy), previously described.<sup>4,5</sup> We recruited patients with respiratory allergy to olive pollen from Cordoba, Spain ( $n = 5$ ), defined by clinical history and with positive skin prick test (SPT) to olive allergens Ole e1 and/or Ole e7, and patients with allergy to house dust mites (HDM) from Gran Canaria, Spain ( $n = 6$ ), who experienced urticaria, respiratory distress or pruritus after ingestion of mite-contaminated flours. Clinical and demographic data of allergic participants are summarized in Table 1. Oral mucosa biopsies were obtained from the cheek lining of the subjects by using a scalpel or punch and used for histological and immunohistochemical analyses (Appendix S1). We analyzed structural components and cell infiltrate in oral mucosal samples from these patients compared with a control group of nonallergic subjects ( $n = 5$ ).

First, we studied whether the oral mucosal barrier integrity was compromised. For this purpose, we determined tight junction (TJ) and adherens junction (AJ) protein expression. We observed a significant and similar decrease in occludin and E-cadherin expression in both groups of allergic patients in accordance with previous results<sup>2</sup> (Figure 1A-D). However, we could not find significant differences in claudin-1 expression (Figure 1E,F) as previously reported.<sup>2</sup> Next, we studied fibrosis in the oral connective tissue of these patients. Augmented fibrosis has been previously associated with epithelial

disruption.<sup>2,6</sup> We observed increased collagen deposition in olive pollen and HDM-allergic patients (Figure 1G,H). An affected epithelial barrier together with increased fibrosis of the oral mucosa suggest that extensive structural changes are taking place in respiratory phenotypes associated with olive pollen and mites.

Increased angiogenesis has been previously described in the oral mucosa of patients with inflammatory pathologies.<sup>7</sup> No significant differences were found in this study for the angiogenic factor VEGFa (data not shown). However, when measuring capillary density, an increased number of blood vessels was observed in HDM-allergic patients (Figure 1I). Regarding immune recruitment to the oral mucosal tissue, we could not find major differences in immune cell counts when comparing allergic groups with nonallergic controls. We focused on phagocytes, mast cells, innate lymphoid cells and lymphocytes. For this purpose, the expression of langerin, MCT, FcεRI, CRTH2, CD3, CD4 and FoxP3 was determined. Numbers of langerin+ cells among the experimental groups were similar; however, FcεRI expression in these cells tended to be higher in the oral epithelium of allergic patients (data not shown). Regarding the connective tissue, MCT+ cells represented almost 100% of the FcεRI-expressing cells in nonallergic subjects. In contrast, FcεRI/MCT ratio revealed that other cell types were also FcεRI+ in the allergic populations (Figure 1J). CD3+ and CD4+ counts were higher in the connective tissue of nonallergic subjects (data not shown). The majority of CD3+ cells were also CD4+ (Figure 1K). Among the CD3+ cells, HDM patients showed a significantly increased proportion of regulatory T cells (Tregs). Although not significant, this trend was also found for olive pollen allergic patients (Figure 1L). We also stained for eosinophils (Figure 1M) and neutrophils (Figure 1N) but found hardly any positively stained cell.

Based on these results, we conclude that oral mucosal integrity is compromised in respiratory phenotypes in the absence of food allergy. Moreover, oral mucosa structural changes take place with no associated local recruitment of inflammatory infiltrate, which is presumably directed to the airway mucosa, but higher numbers of Tregs. In this sense, Morita et al reported that IL-33-stimulated mast cells promoted expansion of Tregs in a mouse model of papain-induced allergic inflammation.<sup>8</sup> In this model, IL-2 produced by IL-33-stimulated mast cells promoted Tregs expansion, which suppressed papain-induced airway inflammation. Tregs have been described to contribute to tissue homeostasis by promoting wound healing and repair processes. Thus, we hypothesize that the increased numbers of Tregs we observed in allergic patients are recruited to protect against tissue damage and maintain barrier integrity.

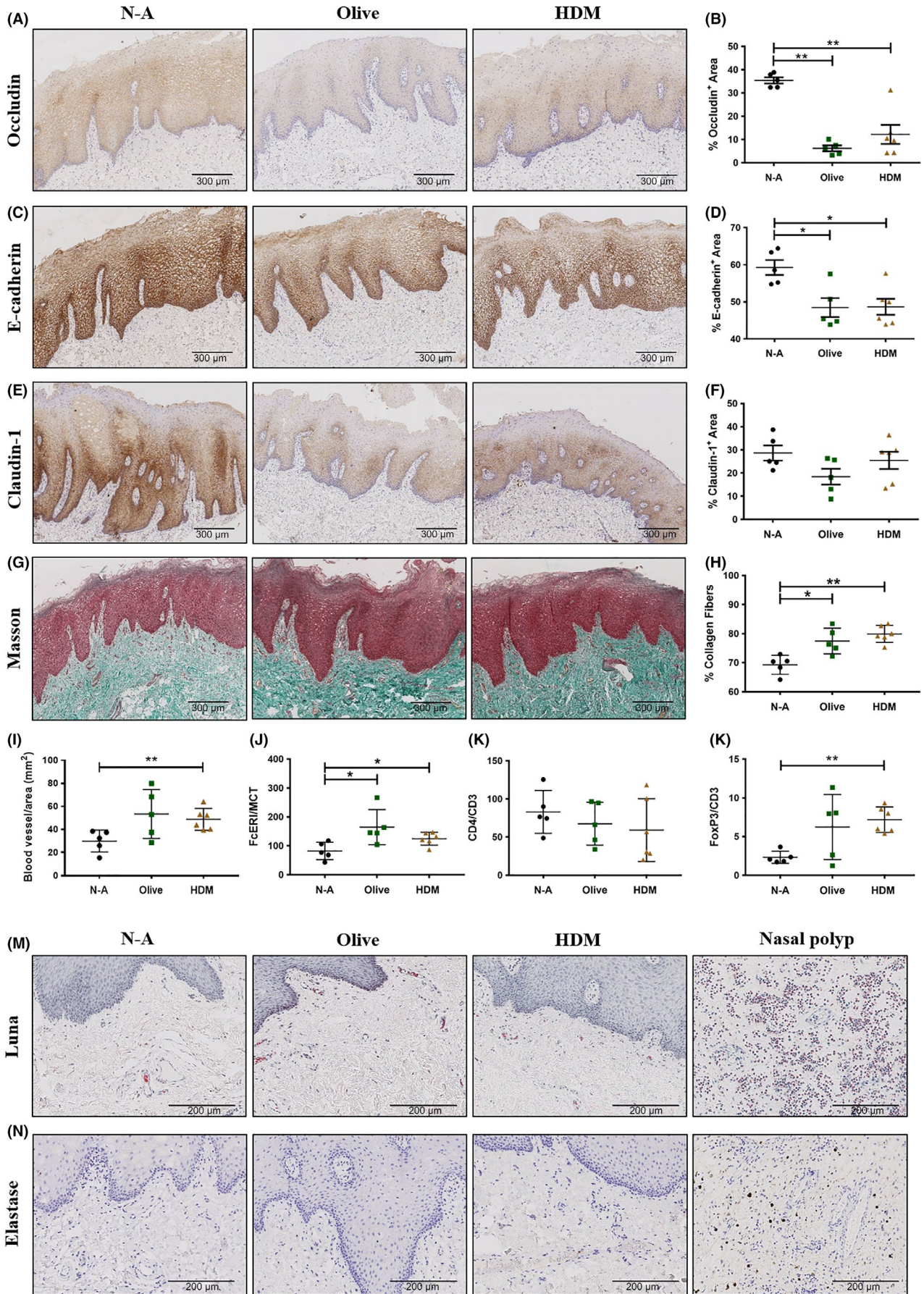
**Abbreviations:** AJ, adherens junction; CRTH2, chemoattractant receptor-homologous molecule expressed on Th2 cells; FFPE, formalin-fixed paraffin embedded; HDM, house dust mites; ILC, innate lymphoid cell; MCT, mast cell tryptase; S1P, sphingosine-1-phosphate; SPT, skin prick test; TJ, tight junction; Treg, regulatory T cell; VEGFa, vascular endothelial growth factor A.

**TABLE 1** Detailed information on study allergic patients

Age	Sex	Specific IgE (kU/L)							Positive SPT	FEV1/ FVC	FVC	FEV1	BT	Self-re- ported reactions <sup>A</sup>	NSAID intol- erance
		Total IgE (kU/L)	<i>Ole</i> <i>e1</i>	<i>Ole</i> <i>e7</i>	<i>Ole</i> <i>e9</i>	<i>D Pte</i>	<i>D</i> <i>Farinae</i>	<i>L</i> <i>Destructor</i>							
Olive															
25	M	193	0	79.40	0	Nd	Nd	Nd	Ole	90	134	118	NEG	NC, RHI, RESP	No
18	M	193	0	85.50	0	Nd	Nd	Nd	Ole, lol, cyp	102	99	98	NEG	NC, RHI, RESP, PRU	No
40	F	Nd	8.05	72.20	0	0.82	Nd	0	Ole, pte	98	125	123	NEG	NC, RHI, RESP	No
18	F	3301	241	696	181	Nd	Nd	Nd	Ole, lol, sal, cyp, alt, cat, dog	95	115	111	NEG	NC, RHI, RESP	No
31	M	240	7.47	19.60	0	Nd	Nd	0	Ole, lol, cyp, cat, lepi	94	81	75	POS	NC, RHI, RESP	No
HDM															
39	F	1113	Nd	Nd	Nd	22	14	5	Pte, far, lepi, tyro, blo	107	95	99	POS	UR, EE, RESP, DIZZ	Yes
39	F	47	Nd	Nd	Nd	1.57	1.42	0.70	Pte, far, lepi, tyro, blo	92	85	74	POS	RHI, RESP, PRU, EE, UR	Yes
36	F	Nd	Nd	Nd	Nd	Nd	Nd	Nd	Pte, far, lepi, tyro, blo, a siro	106	79	86	NEG	RHI, RESP, PRU, CG	Yes
44	F	180	Nd	Nd	Nd	4	4	0.80	Pte, far, lepi, blo, a siro	105	88	91	POS	RHI, RESP, PRU, AE, CG	Yes
40	F	116	Nd	Nd	Nd	20	13	1.60	Pte, far, lepi, tyro, blo, a siro	93	97	87	POS	NC, ABP, DI, VO, DIZZ, PRU	Yes
37	F	67	Nd	Nd	Nd	8.50	Nd	1.30	Pte, far, lepi, tyro, blo	96	111	102	NEG	CG, TO, AE, PRU, HY, F	Yes

Abbreviations: M/F, male/female; Nd, nondetermined parameter; NSAID, nonsteroidal anti-inflammatory drugs. Test: FEV1/FVC: Tiffeneau-Pinelli index. FVC: forced vital capacity. FEV1: first second of forced expiration volume. B.T: bronchodilation test. SPT: ole: *Olea europea*, lol: *Lolium perenne*, sal: *Salsola kali*, cyp: *Cupressus arizonica*, alt: *Alternaria alternata*; pte: *Dermatophagoides pteronyssinus*, far: *Dermatophagoides farinae*, lepi: *Lepidoglyphus destructor*, tyro: *Tyrophagus putrescentiae*, blo: *Blomia tropicalis*, a siro: *Acarus siro*. Reactions<sup>A</sup> Olive pollen allergy: reactions reported during pollen-season/HDM allergy: reported during last anaphylactic episode. ABP: abdominal pain, AE: angioedema, CG: cough, DI: diarrhea, DIZZ: dizziness, EE: eyelid edema, F: fainting, HY: hypotension, NC: nasal congestion, PRU: pruritus, RESP: respiratory difficulties, RHI: rhinitis, TO: thorax oppression, UR: urticaria, VO: vomit.

**FIGURE 1** Histological and immunohistochemical analyses of FFPE oral mucosal sections from nonallergic subjects (N-A) and patients allergic to olive pollen (Olive) or HDM (HDM). Staining and quantification for occludin (A-B), E-cadherin (C-D), claudin-1 (E-F), and collagen fiber deposition (Masson trichrome) (G-H) in all groups. Quantification is the percentage-stained area (mm<sup>2</sup>) of epithelial (B, D, and F), or connective tissue area (H). Capillary density (blood vessel/mm<sup>2</sup>) in the connective tissue (I). FcεRI + cells in the connective tissue expressed as the percentage of total MCT+ cells (J). Frequency of CD4+ (K) and FoxP3+ (L) cells expressed as the percentage of total CD3+ cells in the whole tissue. Luna (M) and elastase (N) representative images for each experimental group. Nasal polyp was used as a positive control. Images were captured at 8X (A, C, E, and G), and 20X (M, N) magnification. Scatter plots show mean ± SD \*P < 0.05, \*\*P < 0.01



Since we could not find increased recruitment of inflammatory cells in the oral mucosa of respiratory allergic patients, we hypothesize that systemic changes could account for the altered oral mucosal features observed in these phenotypes. Under inflammatory conditions, epithelial cells can release IL-33. This alarmin disrupts epithelial barrier and activates type 2 innate lymphoid cells (ILC2s). ILC2s and Th2 cells, and their associated cytokines, play major roles in type 2 inflammation. It has been reported that Th2 cytokines, such as IL-4 and IL-13, induced impaired barrier function in bronchial epithelial cells. IL-13 appeared to be a key effector cytokine in ILC2-induced bronchial epithelial leakiness in the study by Sugita et al.<sup>9</sup> This cytokine has TJ disruptive effects and induces IgE production. Although we could not find differences in Th2- or ILC2-associated markers locally, in the multi-omics study of severe profilin-mediated food allergy, Obeso et al described increased sphingosine-1-phosphate (S1P) and lysophospholipids synthesis along with altered platelet functionality systemically.<sup>3</sup> We believe that systemic changes may also reflect the leaky oral mucosal barrier found in the patients of the current study.

To our knowledge, this is the first study describing an affected oral mucosa in the absence of food allergy and opens new ways of understanding barrier alterations associated with respiratory allergy. A disrupted barrier could be responsible for the progression to food allergy when the affected oral mucosa gets in direct contact with a trigger.<sup>2</sup> In fact, many food allergies are associated with previous respiratory sensitizations (PR10, lipid transfer proteins, profilins).<sup>10</sup>

These reports highlight the need to understand how systemic inflammatory factors affect the integrity of TJs and to further investigate common metabolic and transcriptomic fingerprints that might be useful for the identification of new therapeutic targets to prevent allergic progression.

## ACKNOWLEDGMENTS

We acknowledge Francisco Muñoz del Castillo for his collaboration in biopsy sampling, Otorhinolaryngology (ORL) Unit of Reina Sofia University Hospital, Cordoba, Spain; Virginia Garcia and Javier Moratinos for their expertise in histological and immunohistochemical staining, Histology Core Facility, and Tomas Barker for English proofreading, Institute of Applied Molecular Medicine, Faculty of Medicine, San Pablo CEU University, Madrid, Spain.



## CONFLICTS OF INTEREST

The authors declare that they have no conflicts of interest.

## FUNDING INFORMATION

This work was supported by ISCIII (Project number PI16/00249) co-funded by European Regional Development Fund "Investing in your future" for the thematic network and co-operative research centers ARADyAL RD16/0006/0015, RD16/0006/0018. Javier

Sanchez-Solares, Maria I Delgado-Dolset and Leticia Mera-Berriatua were supported by FPI-CEU predoctoral fellowships. Cristina Gomez-Casado was supported by a postdoctoral contract co-funded by the competitive Program "Attracting Talent," Community of Madrid, Spain.

Javier Sanchez-Solares<sup>1</sup>  
Maria I. Delgado-Dolset<sup>1</sup>  
Leticia Mera-Berriatua<sup>1</sup>  
Gonzalo Hormias-Martin<sup>2</sup>  
Jose A. Cumplido<sup>3</sup>  
Vanesa Saiz<sup>4</sup>  
Teresa Carrillo<sup>3</sup>  
Carmen Moreno-Aguilar<sup>4</sup>  
Maria M. Escribese<sup>1</sup>  
Cristina Gomez-Casado<sup>1</sup>   
Domingo Barber<sup>1</sup> 

<sup>1</sup>Department of Basic Medical Sciences, Faculty of Medicine, Institute of Applied Molecular Medicine, San Pablo CEU University, Madrid, Spain

<sup>2</sup>Technical School of Food, Agronomic and Biosystems Engineering, Technical University of Madrid, Madrid, Spain

<sup>3</sup>Allergology Service, Dr Negrin University Hospital of Gran Canaria, Las Palmas de Gran Canaria, Spain

<sup>4</sup>Unit of Clinical Immunology and Allergology, Maimonides Institute for Research in Biomedicine, Reina Sofia University Hospital, Cordoba, Spain

## Correspondence

Cristina Gomez-Casado, Instituto de Medicina Molecular Aplicada (IMMA), Departamento de Ciencias Médicas Básicas, Facultad de Medicina. Campus Montepríncipe, Universidad San Pablo-CEU, 28925 Alcorcón, Madrid, Spain.

Email: cristina.gomezcasado@ceu.es

## ORCID

Cristina Gomez-Casado  <https://orcid.org/0000-0002-7707-6367>

Domingo Barber  <https://orcid.org/0000-0002-5488-5700>

## REFERENCES

1. Cecchi L, D'Amato G, Annesi-Maesano I. External exposome and allergic respiratory and skin diseases. *J Allergy Clin Immunol.* 2018;141:846-857.
2. Rosace D, Gomez-Casado C, Fernandez P, et al. Profilin-mediated food-induced allergic reactions are associated with oral epithelial remodeling. *J Allergy Clin Immunol.* 2018;18:30611.
3. Obeso D, Mera-Berriatua L, Rodríguez-Coira J, et al. Multi-omics analysis points to altered platelet functions in severe food-associated respiratory allergy. *Allergy* 2018;73:2137-2149.
4. Barber D, de la Torre F, Feo F, et al. Understanding patient sensitization profiles in complex pollen areas: a molecular epidemiological study. *Allergy* 2008;63:1550-1558.

5. Blanco C, Quiralte J, Castillo R, et al. Anaphylaxis after ingestion of wheat flour contaminated with mites. *J Allergy Clin Immunol.* 1997;99:308-313.
6. Van Bruaene N, Derycke L, Perez-Novo CA, et al. TGF- $\beta$  signaling and collagen deposition in chronic rhinosinusitis. *J Allergy Clin Immunol.* 2009;124(2):253-259.
7. Ribatti D, Crivellato E. Immune cells and angiogenesis. *J Cell Mol Med.* 2009;13:2822-2833.
8. Morita H, Arae K, Unno H, et al. An interleukin-33-mast cell-interleukin-2 axis suppresses papain-induced allergic inflammation by promoting regulatory T cell numbers. *Immunity* 2015;43:175-186.
9. Sugita K, Steer CA, Martinez-Gonzalez I, et al. Type 2 innate lymphoid cells disrupt bronchial epithelial barrier integrity by targeting

tight junctions through IL-13 in asthmatic patients. *J Allergy Clin Immunol.* 2018;141(1):300-310.

10. Popescu F-D. Cross-reactivity between aeroallergens and food allergens. *World J Methodol.* 2015;5:31.

#### SUPPORTING INFORMATION

Additional supporting information may be found online in the Supporting Information section at the end of the article.







# Mast Cell Desensitization in Allergen Immunotherapy

Celia López-Sanz<sup>1</sup>, Rodrigo Jiménez-Saiz<sup>1,2,3,4</sup>, Vanesa Esteban<sup>5,6</sup>,  
María Isabel Delgado-Dolset<sup>7</sup>, Carolina Perales-Chorda<sup>7,8</sup>, Alma Villaseñor<sup>7,8</sup>,  
Domingo Barber<sup>7</sup> and María M. Escribese<sup>7\*</sup>

<sup>1</sup> Department of Immunology, Instituto de Investigación Sanitaria Hospital Universitario de La Princesa (IIS-Princesa), Madrid, Spain, <sup>2</sup> Department of Immunology and Oncology, Centro Nacional de Biotecnología (CNB)-CSIC, Madrid, Spain, <sup>3</sup> Faculty of Experimental Sciences, Universidad Francisco de Vitoria (UFV), Madrid, Spain, <sup>4</sup> McMaster Immunology Research Centre (MIRC), Department of Medicine, McMaster University, Hamilton, ON, Canada, <sup>5</sup> Department of Allergy and Immunology, Instituto de Investigación Sanitaria Fundación Jiménez Díaz (IIS-FJD), Universidad Autónoma de Madrid (UAM), Madrid, Spain, <sup>6</sup> Faculty of Medicine and Biomedicine, Alfonso X El Sabio University, Madrid, Spain, <sup>7</sup> Department of Basic Medical Sciences, Facultad de Medicina, Institute of Applied Molecular Medicine Nemesio Díez, Universidad San Pablo-CEU, CEU Universities, Urbanización Montepríncipe, Madrid, Spain, <sup>8</sup> Centre for Metabolomics and Bioanalysis (CEMBIO), Department of Chemistry and Biochemistry, Facultad de Farmacia, Universidad San Pablo CEU, CEU Universities, Urbanización Montepríncipe, Madrid, Spain

## OPEN ACCESS

### Edited by:

Linda Cox,  
Wyoming, United States

### Reviewed by:

Mariana C. Castells,  
Brigham and Women's Hospital and  
Harvard Medical School,  
United States  
Marek Jutel,  
Wroclaw Medical University, Poland

### \*Correspondence:

María M. Escribese  
mariamarta.escribesealonso@ceu.es

### Specialty section:

This article was submitted to  
Allergen Immunotherapy,  
a section of the journal  
Frontiers in Allergy

**Received:** 17 March 2022

**Accepted:** 16 May 2022

**Published:** 16 June 2022

### Citation:

López-Sanz C, Jiménez-Saiz R,  
Esteban V, Delgado-Dolset MI,  
Perales-Chorda C, Villaseñor A,  
Barber D and Escribese MM (2022)  
Mast Cell Desensitization in Allergen  
Immunotherapy.  
Front. Allergy 3:898494.  
doi: 10.3389/falgy.2022.898494

Allergen immunotherapy (AIT) is the only treatment with disease-transforming potential for allergic disorders. The immunological mechanisms associated with AIT can be divided along time in two phases: short-term, involving mast cell (MC) desensitization; and long-term, with a regulatory T cell (Treg) response with significant reduction of eosinophilia. This regulatory response is induced in about 70% of patients and lasts up to 3 years after AIT cessation. MC desensitization is characteristic of the initial phase of AIT and it is often related to its success. Yet, the molecular mechanisms involved in allergen-specific MC desensitization, or the connection between MC desensitization and the development of a Treg arm, are poorly understood. The major AIT challenges are its long duration, the development of allergic reactions during AIT, and the lack of efficacy in a considerable proportion of patients. Therefore, reaching a better understanding of the immunology of AIT will help to tackle these shortcomings and, particularly, to predict responder-patients. In this regard, omics strategies are empowering the identification of predictive and follow-up biomarkers in AIT. Here, we review the immunological mechanisms underlying AIT with a focus on MC desensitization and AIT-induced adverse reactions. Also, we discuss the identification of novel biomarkers with predictive potential that could improve the rational use of AIT.

**Keywords:** allergen immunotherapy, mast cell, desensitization, Treg, anaphylaxis, IgE

## INTRODUCTION

Allergic diseases are a heterogeneous group of immunological disorders characterized by a detrimental reaction to a given allergen. The onset of allergy occurs at the sensitization phase, which entails induction of a T helper (Th) 2 response and production of interleukin (IL)-4, IL-13 or IL-5, and immunoglobulin (Ig) E. Following sensitization, the effector phase is triggered by allergen re-exposure (1, 2). Effector allergic reactions are complex and often classified - according to the timing of the reaction- in acute and late phase (3, 4). The former is largely (but not

exclusively) mediated by IgE (5–8) and its binding to the high-affinity IgE receptor (FcεRI), which is expressed on eosinophils (9, 10), monocytes (11), dendritic cells (12, 13) platelets (14), and specifically on basophils (15, 16) and mast cells (MCs) (17–19). IgE-FcεRI cross-linking leads to MC degranulation and the rapid release of vasoactive and pro-inflammatory mediators (e.g., histamine, tryptase or prostaglandins), which underlies clinical manifestations associated with acute allergic reactions, such as angioedema, hypotension or even anaphylaxis (1, 2, 5, 20, 21). Of these, anaphylaxis is defined as a life-threatening condition that compromises patient's airway, breathing, and/or circulation, and may occur without typical skin features or the presence of cardiovascular collapse (22).

The standard of care is allergen avoidance, when possible, together with the urgent treatment of an allergic reaction upon accidental allergen exposure (23). Allergen immunotherapy (AIT) is the most promising therapeutic approach as it is the only clinical intervention with disease-transforming capacity. AIT has been proven to confer long-term protection and to prevent disease progression and exacerbation. AIT operates in two phases: an early or escalation phase, headed by MC hypo-responsiveness on allergen provocation and an increase of Th2 cells and IgE; and a late or consolidation phase that takes 2–3 years of treatment and is dominated by regulatory T cells (Treg) (24–26). Nevertheless, effector cell activation and adverse side effects can happen at any time during AIT, compromising patients' safety and compliance. Thus, it is essential to discover reliable biomarkers to monitor immunological changes, to prevent side effects and to identify AIT-responder patients that can benefit from intervention.

Recent studies support that AIT efficacy relies on MC desensitization during the initial phase (24, 27, 28). However, the molecular mechanisms underlying AIT-induced MC hypo-responsiveness are controversial (29). Given that MC degranulation is a common driver of anaphylaxis (30), understanding MC desensitization is key, not only for preventing these life-threatening reactions, but also for improving current intervention strategies, including AIT. Here, we review the immunological mechanisms underlying AIT with a focus on MC desensitization and AIT-induced adverse reactions. Also, we discuss the identification of novel biomarkers with predictive potential that could improve the rational use of AIT.

## THE IMMUNE RESPONSE UNDERLYING AIT

AIT constitutes a pivotal pharmacological intervention aiming to control allergic diseases such as allergic rhinitis, allergic asthma,

**Abbreviations:** AIT, allergen immunotherapy; BAT, basophil activation test; ELIFAB, enzyme-linked immunosorbent-facilitated antigen binding assay; FcεRI, high-affinity IgE receptor; FcεRII, low-affinity IgE receptor; FoxP3, Forkhead box protein 3; IgE-FAB, IgE-facilitated allergen; Ig, immunoglobulin; IL, interleukin; ITAM, immunoreceptor tyrosine-based activation motif; MC, mast cell; MoAb, monoclonal antibodies; MRGPRX2, Mas-related G protein-coupled receptor X2; PAF, platelet activating factor; sIg, specific immunoglobulin; SPT, skin prick test; STAT6, signal transducer and activator of transcription 6; Th, T helper cells; tIgE, total IgE; TNF-α, tumor necrosis factor alpha; Treg, regulatory T cells.

atopic dermatitis, insect venom hypersensitivity (31) or food allergy (29, 32). It consists of the administration of subsequent increasing doses of allergen until an adequate dose is reached, which induces immunological tolerance (31). The efficacy of AIT relies on changes in both innate and adaptive immune cells and is associated with a shift from a Th2 toward a Th1 and Treg phenotype. However, despite being in use for 110 years, the immunological mechanisms of AIT remain poorly understood (33).

A 3-year-follow-up study demonstrated that the immunological changes induced by sublingual AIT come about in two sequential phases (**Figure 1**). First, an early desensitization phase which takes place in the first 4 months. This stage is accompanied by an initial but short invigoration of Th2 immunity, with an increase in both allergen-specific Ig (sIg) E and IL4<sup>+</sup> cells (24). In addition, AIT has been demonstrated to impair MC degranulation in this early stage (29, 32, 34). Finally, there is a later augmentation in sIgG/sIgG<sub>4</sub> levels, which compete with sIgE and inhibit sIgE, thus preventing MC and basophil activation and their production of Th2-related cytokines (29).

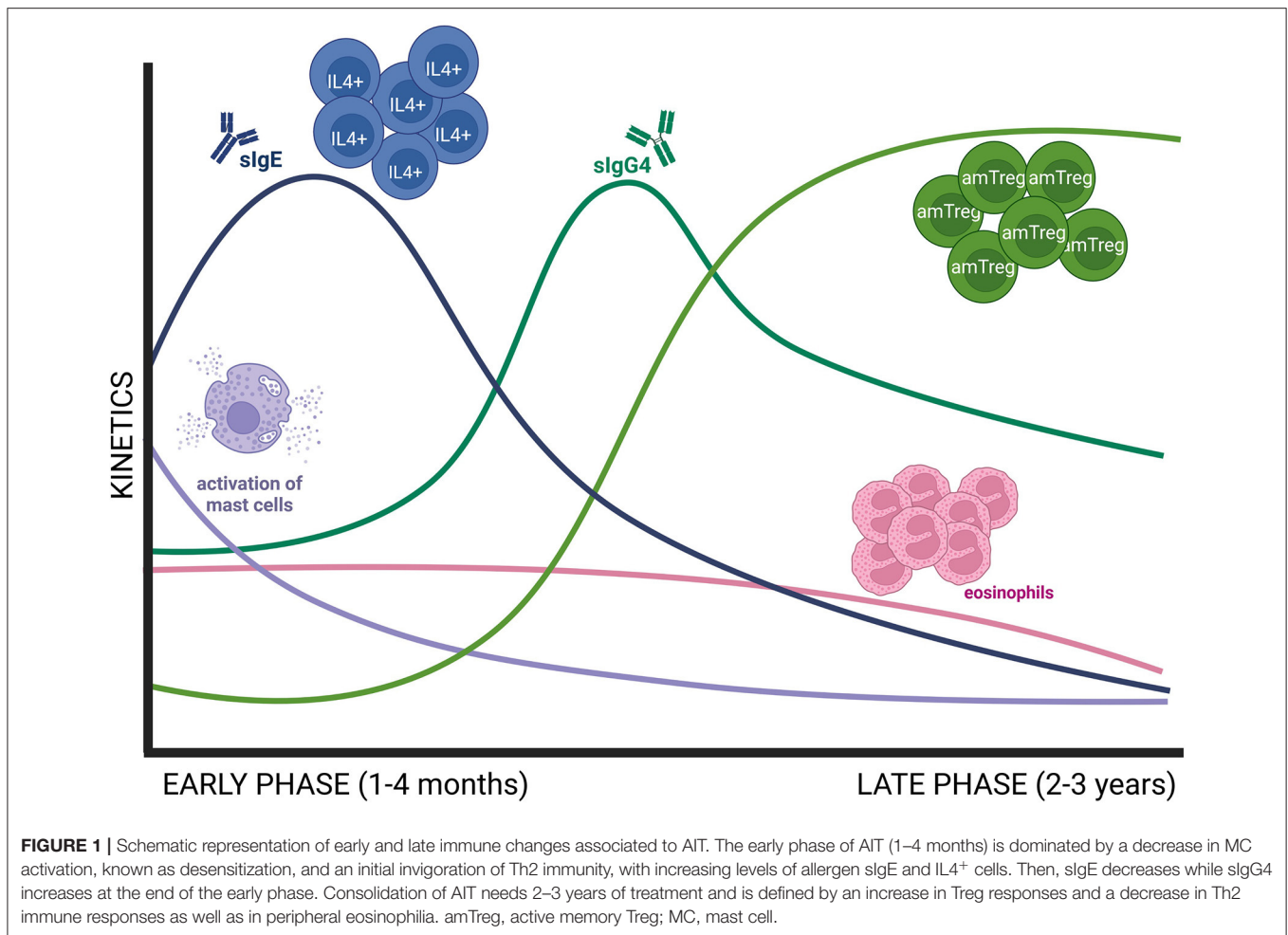
Next comes the consolidation of the regulatory response, which needs at least 3 years of AIT (24). During this period there is a contraction of IL4<sup>+</sup> cells, a downregulation of sIgE levels and a decrease in blood eosinophilia (24). In parallel, there is an increase in Treg responses, particularly activated memory Treg cells (24). Recent studies have pointed out that there is a regulatory network between MCs and Tregs. On the one hand, Treg suppresses MC activation by different mechanisms (i.e., IL-10 secretion, MC anergy via OX40L engagement) (29). On the other hand, in a food allergy model, desensitized MCs facilitated a Treg cell expansion in a IL-2-dependent manner (32).

Altogether, MCs appear to play key roles in both early and late phase AIT. As previous reports demonstrated strong benefits only few months after starting treatment (24), MC desensitization seems to be a key mechanism in keeping AIT efficacy.

## AIT-INDUCED ANAPHYLAXIS

Local and systemic adverse reactions have been observed during AIT (22, 35). Of these, systemic reactions are described in ~1–4% of patients and can be mild to severe, anaphylaxis being the gravest (31). Over the years, diverse definitions of anaphylaxis have appeared in the literature with the purpose of improving its diagnosis and patients' management. Lately, the World Allergy Organization (WAO) depicted anaphylaxis as a potential life-threatening compromise of airways, breathing, and/or circulation, which may occur without typical skin symptoms or the presence of circulatory shock (22). These symptoms are usually developed within the first 30 min after AIT administration (31).

While the occurrence of adverse reactions in AIT is influenced by factors such as viral infections, fever, physical activity, non-steroidal anti-inflammatory drug use, hormonal changes, *etc.*, the route of administration and allergen type are determinant. AIT with aeroallergens is usually administered subcutaneously and is less likely to induce anaphylactic reactions (36, 37). On the



other hand, adverse allergic reactions including anaphylaxis are more common in AIT with food allergens (38). In terms of the route, subcutaneous AIT with peanut allergy is highly associated with anaphylaxis (39), but oral and sublingual AIT for peanut (and other food allergens) are clearly safer (40–44). Despite being safer, a recent systematic review and meta-analysis showed that the risk of anaphylaxis was significantly higher in peanut-allergic patients undergoing oral AIT than in those following allergen avoidance (45).

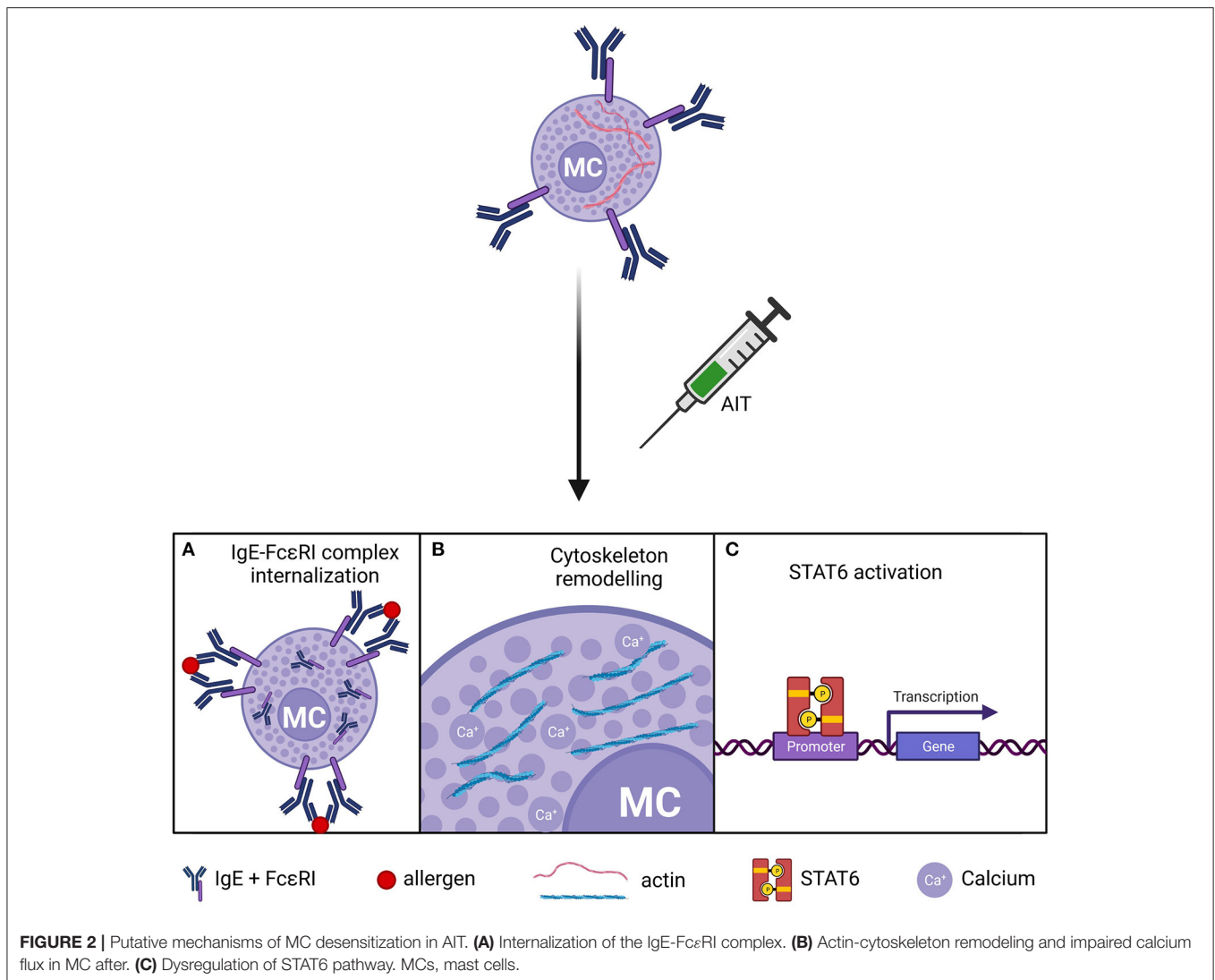
The classical pathway of anaphylaxis is IgE-mediated and involves MCs and basophils (5–8) and recently, omalizumab in combination with AIT has been proven to improve patients' outcome (46). However, IgE-independent mechanisms have also been described in murine models, and there is growing evidence of their importance in humans (5, 8, 47). These mechanisms involve IgG and platelet activating factor (PAF) release by neutrophils, basophils and macrophages (5), or complement activation. Non-immunological anaphylaxis can also occur through the direct stimulation of MC degranulation (48, 49) or by Mas-related G protein-coupled receptor X2 (MRGPRX2) expressed in MCs. In addition, the differential contribution of the endothelium to the pathophysiology of the anaphylaxis is being

increasingly recognized, which adds another layer of complexity to this clinical manifestation (50).

Anaphylaxis severity is correlated to MC degranulation and the release of pro-inflammatory mediators (50–52). Intriguingly, anaphylactic mediators such as histamine are released during AIT without induction of anaphylaxis (53, 54), which insinuates that a certain level of MC activation may be required to achieve desensitization. MC desensitization is accomplished during the early-phase of AIT, and studies in murine models support that this process directs the immunological outcome of AIT (30). However, the molecular mechanisms of AIT involve several effector cell types (55, 56). Therefore, it is likely that different cellular and molecular microenvironments created between immune and non-immune cells modify the threshold of a detrimental inflammatory MC response during AIT.

## MC DESENSITIZATION MECHANISMS

MCs are key effector cells in allergic disease for different reasons. They are immune sentinels located in mucosal and epithelial



tissues, close to the vascular and lymphatic endothelium (57, 58). Because of this strategic distribution, MCs sense and respond promptly to allergens or pathogens (59, 60). Furthermore, MCs have a long lifespan as compared to its mobile analog, the basophil (61); retain surface IgE for months (62, 63); and can react to minute amounts of allergen (64). On activation, MCs degranulate rapidly because they are equipped with cytoplasmic granules (50–200 per MC) that contain preformed allergic mediators (60, 65).

In sensitized individuals, IgE-FcεRI complex clustering causes MC activation and degranulation. FcεRI activates several pathways through the immunoreceptor tyrosine-based activation motif in its cytoplasmic domain, e.g., Syk, PI3K/Akt, ERK and STAT6 (66, 67). These routes increase the intracellular calcium flux, which is crucial for exocytosis of preformed inflammatory mediators such as histamine or tryptase. Also, they activate the *de novo* synthesis of late-phase inflammatory cytokines (e.g., IL-6, TNF- $\alpha$ ), prostaglandins, leukotrienes, and PAF, among others (29). The rapid release of these vasoactive

and inflammatory mediators underlies clinical manifestations associated with acute allergic reactions (i.e., angioedema, hypotension or cardiovascular collapse and anaphylaxis) (5, 20, 21).

The IgE-MC pathway has long been a target for therapeutic intervention, and some drugs and biologicals have been developed to interfere with it (20, 29, 68). In this regard, AIT has been shown to dampen this axis (24, 26). Several *in vitro* and *in vivo* studies in mice have demonstrated that MC become hypo-responsive to allergen exposures after desensitization (34). MC desensitization appears to be allergen-specific (69, 70) and reversible (71, 72). Yet, the molecular mechanisms underlying AIT-induced MC desensitization remain controversial (29) (Figure 2).

Different *in vitro* studies support that increasing doses of allergen induce IgE-FcεRI complex internalization, rendering MCs unresponsive to allergen challenge (70, 73). In contrast, others report a partial IgE reduction in desensitized MCs (69, 72, 74, 75). In these studies, primary MCs of different origins

were assayed, including murine and rat peritoneal MCs (70, 73), murine bone marrow-derived MCs (69, 74), and human lung MCs (72), which may explain this inconsistency. Moreover, MC sensitization was performed with different IgE clones such as SPE-7 (69, 74) and  $\epsilon$ -26 (70). However, experiments with the same clone yielded divergent results (69, 70). Other experimental variables may have contributed to the discrepancy in IgE internalization. For instance, Oka et al. (70) used lower MC cellularity and a higher target dose of allergen than Sancho-Serra et al. (69), which may have facilitated IgE saturation and internalization in the former. Despite the variable results on IgE internalization, all these experimental approaches induced MC desensitization. In other words, MC desensitization is accomplished whether the loss of IgE is total or partial. Hence, mechanisms other than IgE-Fc $\epsilon$ RI internalization might be at play during MC desensitization. The recent research of Nagata et al. (75) report that the size of the IgE-Fc $\epsilon$ RI internalization complexes are responsible of MC desensitization success.

Another line of inquiry on the mechanisms of MC desensitization focused on the STAT6 pathway. Morales *et al.* reported that murine STAT6-deficient bone marrow-derived MCs failed to get desensitized (76), although they also showed that MC desensitization did not induce STAT6 phosphorylation (69). Additional experiments in peritoneal MCs from STAT6-null mice demonstrated that STAT6 was redundant for desensitization (70). STAT6 affects different aspects of MC biology, and its deficiency may cause unspecific effects depending on the maturity of MCs. For example, STAT6 is required for IL4-dependent responses (77), which increase Fc $\epsilon$ RI expression on MCs (18). Besides STAT6, recent studies are shedding light on the cytoskeletal dynamics that drive MC activation and desensitization (66, 78, 79). Gladys Ang et al. (74) showed that desensitized MCs had an atypical but stable redistribution of the actin cytoskeleton, which precluded calcium flux from intracellular stores and abrogated exocytosis of inflammatory granules.

There are some questions remaining on the mechanisms of MC desensitization. The notion that IgE-Fc $\epsilon$ RI complex internalization occurs to some degree during MC desensitization is well established, but how this process is regulated is largely unknown. In this regard, recent studies in murine MCs suggested that sIgG binding to Fc $\gamma$ RIIB is required for IgE downregulation (80), and other MC inhibitory signaling pathways such as gp49B1/LILRB4 (81) may be also involved in MC desensitization. Nevertheless, *in vitro* experimentation supporting IgE-Fc $\epsilon$ RI complex internalization was conducted in the absence of IgG (69, 70, 74). Moreover, the role of STAT6 in MC desensitization is controversial (69, 76) and the kinetics of STAT6 phosphorylation during desensitization are not clearly defined.

From a broader perspective, the current mechanistic knowledge on MC desensitization can explain how it occurs at the cellular or local level. However, the fact that minute amounts of allergen can desensitize systemically in AIT, even by sublingual route (82–84), is certainly intriguing and points toward the participation of widespread, fast-acting systems. Further studies are necessary to understand how allergen desensitization operates at the level of an entire organism, as

well as to identify biomarkers to monitor/predict successful MC desensitization in AIT.

## IDENTIFICATION OF BIOMARKERS IN AIT

A biomarker is any substance objectively measured that can be used as an indicator of biological/pathological processes, or pharmacologic responses to a therapeutic intervention. There is a lack of reliable biomarkers that can accurately reflect the clinical course or predict a positive response to AIT (85–87). Despite this dearth, there are some *in vivo* and *in vitro* biomarkers applied to monitor AIT safety and efficacy.

In the clinical practice, *in vivo* biomarkers such as skin prick test (SPT), intradermoreaction, nasal provocation and controlled exposure tests in chambers evaluate allergen-specific reactivity, which is expected to decrease after AIT (88). *In vitro* biomarkers are based on the cellular and humoral events that take place during AIT (89). Some widespread biomarkers are the determination of total IgE (tIgE) and sIgE. The latter is the gold-standard test for AIT patient selection. A high sIgE/tIgE ratio is predictive of positive responses to AIT (90, 91), although it has not been properly validated. AIT-induced desensitization correlates with a CD4<sup>+</sup> T cell shift from Th2 towards a Th1 and Treg phenotype (Table 1). Also, sIgE increases during up-dosing but decreases during the maintenance phase, in parallel with a higher production of sIgG4, which suggests the development of a Treg response (24). AIT has also been shown to increase sIgA (113) and IL-10-producing innate-like lymphoid cells 2 (98).

Other biomarkers for AIT efficacy are the assessment of the serum inhibitory activity of IgE, which can be measured by IgE-facilitated allergen binding (IgE-FAB) (85) or enzyme-linked immunosorbent-facilitated antigen binding assay (ELIFAB). IgE-FAB determines the binding of allergen-IgE complexes to B cells via the low-affinity IgE receptor (Fc $\epsilon$ R2 or CD23). The decrease of IgE-FAB correlates with a positive clinical response to AIT (87). It has been reported that serum IgE-inhibitory activity persists for several years and is associated with long-term clinical efficacy (114). Moreover, *in vitro* assays, like the basophil activation test (BAT) (115), which measures lysosomal-associated proteins indicative of degranulation (e.g., CD63, CD203c) have been used to evaluate basophil suppression in AIT (85, 91, 116). Also, cytokines, chemokines and cellular markers have been applied for the study of AIT (Table 1).

During the last several years, omics have been applied in AIT research. Omics are techniques that use high-throughput approaches, each one correlating with a specific level of the system biology. Genomics, epigenomics, transcriptomics, proteomics, metabolomics (including lipidomics) and microbiomics could empower the identification of new diagnostic strategies for AIT (117) (Table 1). Genomics has been applied for the discovery of genetic variants that predispose to atopy (118) or affect asthma severity (119). Genetic variants that associate with good AIT outcomes could be used as biomarkers moving forward to stratify patients prior to treatment (28). Epigenomics studies have suggested that DNA methylation patterns, specifically in gene promoter regions associated

**TABLE 1** | Potential biomarkers in AIT.

Domains	Biomarkers	Effect after AIT	References
<b>In vivo biomarkers</b>	Allergen provocation test	SPT ID NPT EEC	↓ (92–94)
<b>Antibodies</b>	IgE	slgE tlgE slgE/tlgE	↓ (95)
	IgG	Total IgG <sub>4</sub> tlgG/IgG <sub>4</sub>	↑ ↑ ↓ (95)
	IgA	slgA	↑ (96)
<i>Serum inhibitory activity for IgE</i>	IgE FAB ELIFAB		↓ (95)
<b>Cellular biomarkers</b>	Treg cells Breg cells DC	DC2 (GATA3) DCreg (C1qA1)	↑ ↑ ↓ ↑ (97)
	IL10 <sup>+</sup> KLR <sup>+</sup> ILC2		↑ (98)
<i>Basophil activation</i>	CD63 CD203c Intracellular DAO Basophil histamine release		↓ ↓ ↑ ↓ (99–101)
<i>MC activation</i>			↓ (102)
<i>Eosinophil activation</i>			↓
<b>Cytokines and chemokines</b>	Th2	IL-4 IL-13 IL-9 IL-17 Eotaxin TNF- $\alpha$	↓ (103)
	Th1	IL-12 INF $\gamma$	↑ (104)
	Treg	IL-10 TGF $\beta$	↑ (105)
<b>Omics science</b>	<b>Biomarkers</b>		<b>Reference</b>
<i>Genomics</i>	Identification of functional variants in atopy and asthma severity		(106)
<i>Epigenomics</i>	DNA methylation of FoxP3 DNA methylation of Th cytokine genes		(107) (108)
<i>Transcriptomics</i>	Th and Treg cytokine and chemokine transcripts		(109)
<i>Proteomics</i>	Molecular markers for four different monocyte-derived DC subclasses		(97)
<i>Metabolomics</i>	Hydroxyeicosatetraenoic acids (HETEs) during subcutaneous immunotherapy Effect of patient sensitization on the metabolic profile during sublingual immunotherapy		(110) (26)
<i>Microbiomics</i>	Influence susceptibility to allergic diseases		(111)
<b>Others</b>	<b>Biomarkers</b>		<b>Reference</b>
<i>Immunophenotyping</i>	Th and Treg cells, IgG subclass and IgE expressing B cells, Breg		(112)

SPT, skin prick test; ID, intradermal test; NPT, nasal provocation test; EEC, Environmental exposure chamber; DC, dendritic cells; IL, interleukin; TNF, tumor necrosis factor; INF, interferons; TGF $\beta$ , Transforming growth factor beta; forkhead box protein 3 (FoxP3); ILC, innate lymphoid cells.

with Forkhead box protein 3 (FoxP3), could inform of AIT progress (120, 121). Additionally, it has been proposed that the microbiota composition could influence AIT efficacy

(111), which is another potential source of AIT biomarkers. Furthermore, transcriptomics and proteomics have been used to improve AIT patient selection through the characterization

of allergen extracts, along with a profiling of IgE reactivity (113, 122, 123). Regarding metabolomics, a recent study demonstrated that the type of the patient's sensitization (mono- or poli-sensitized) is key in the clinical response to AIT (26). A different study focused on eicosanoid profiles showed that they increased at the beginning of AIT and then decreased after 1 to 3 years of AIT, decreasing at year 3 to levels below than baseline (110). Finally, techniques such as immunophenotyping using flow cytometry and mass spectrometry have allowed the parallel analysis of all cell subpopulations in a sample during AIT (124).

## CONCLUSION AND REMARKS

Despite the widespread use of AIT for more than 110 years, MC desensitization has just recently been identified as a key mechanism during the first 2 years of AIT. Yet, fundamental mechanisms associated with desensitization remain obscure. How a MC gets desensitized in an allergen-specific manner and how the desensitization pattern is transmitted throughout all barrier systems is certainly intriguing. MCs have a broad repertoire of signaling pathways. Due to the potential for inducing life-threatening reactions, research focus has always been on MC degranulation, perhaps overlooking their role as lipid-secreting mediators such as prostaglandins or leukotrienes. Moreover, MCs hypo-responsiveness, even without dampening Th2 responses, is effective not only in anaphylaxis prevention, but also for the control of allergic symptoms and reduction of medication usage (83, 125). This supports the key role of MC activation in allergic inflammation.

The sustained and disease-modifying effect of AIT is linked to the acquisition and epigenetic fixation of a regulatory phenotype. However, how the initial MC control predates the Treg response is unclear. Understanding this link is pivotal for the design of new AIT strategies aiming to avoid IgE-mediated reactivity. To date, no study with strict focus on Treg induction has proven to be effective. If effector cell desensitization governs AIT during the first 2 years of intervention, studies aiming to bypass effector cell activation should be planned for at least 3 years of intervention.

Different inflammatory routes have been described in anaphylaxis. AIT reduces IgE and likely impairs the classical

pathway of anaphylaxis, but its effect on allergic reactions mediated by alternative pathways is debatable. Alternative routes could be activated during allergic sensitization (126), and might be relevant in pediatric anaphylaxis and AIT to foods. Should this be the case, AIT patient selection may benefit from novel biomarkers that classify patients according to the dominant inflammatory routes (127).

## AUTHOR CONTRIBUTIONS

MME and DB designed the manuscript structure and participated in the writing and discussion. CLS, VE, and RJS participated in the design, writing, and discussion of the manuscript. CLS, RJS, CPC, AV, and MIDD collaborated in the writing, correction, and discussion of the manuscript. AV and CPC prepared the table. MME and MIDD participated in the design and preparations of the figures.

## FUNDING

This work was supported by ISCIII (PI18/01467 and PI19/00044), cofounded by FEDER Investing in your future for the thematic network and co-operative research centers and the thematic network RICORS “Red de Enfermedades Inflamatorias” (REI) RD21 0002 0008. This work was also supported by the Ministry of Science, Innovation and Universities in Spain (PCI2018-092930) co-funded by the European program ERA HDHL – Nutrition & the Epigenome, project Dietary Intervention in Food Allergy: Microbiome, Epigenetic and Metabolomic interactions DIFAMEM. MIDD is supported by FPI-CEU predoctoral fellowships. RJS's laboratory acknowledges the support received by the Severo Ochoa Program (AEI/SEV-2017-0712), FSE/FEDER through the Instituto de Salud Carlos III (ISCIII; CP20/00043), The Nutricia Research Foundation (NRF-2021-13), New Frontiers in Research Fund (NFRFE- 2019-00083), and SEAIC (BECA20A9). VE laboratory was supported by ISCIII (PI21/00158) cofounded by FEDER Investing in your future for the thematic network and co-operative research centres ARADyAL RD16/0006/0013 and SEAIC (19\_A08).

## REFERENCES

- Breiteneder H, Diamant Z, Eiwegger T, Fokkens WJ, Traidl-Hoffmann C, Nadeau K et al. Future research trends in understanding the mechanisms underlying allergic diseases for improved patient care. *Allergy*. (2019) 74:2293–311. doi: 10.1111/all.13851
- Escribese MM, Gómez-Casado C, Barber D, Diaz-Perales A. Immune polarization in allergic patients: role of the innate immune system. *J Investig Allergol Clin Immunol*. (2015) 25:251–8.
- Jiménez-Saiz R, Chu DK, Waserman S, Jordana M. Initiation, Persistence and Exacerbation of Food Allergy. In: Schmidt-Weber C, editor. *Allergy Prevention and Exacerbation. Birkhäuser Advances in Infectious Diseases*. Springer, Cham (2017): 121–144. doi: 10.1007/978-3-319-69968-4\_7
- Valenta R, Hochwaller H, Linhart B, Pahr S. Food allergies: the basics. *Gastroenterology*. (2015) 148:1120–31.e4. doi: 10.1053/j.gastro.2015.02.006
- Finkelman FD, Khodoun M V, Strait R. Human IgE-independent systemic anaphylaxis. *J Allergy Clin Immunol*. (2016) 137:1674–80. doi: 10.1016/j.jaci.2016.02.015
- Godon O, Hechler B, Jönsson F. The role of IgG subclasses and platelets in experimental anaphylaxis. *J Allergy Clin Immunol*. (2021) 147:1209–11. doi: 10.1016/j.jaci.2021.01.009
- Elieh Ali Komi D, Wöhrl S, Bielory L. Mast cell biology at molecular level: a comprehensive review. *Clin Rev Allergy Immunol*. (2020) 58:342–65. doi: 10.1007/s12016-019-08769-2
- Jönsson F, De Chaisemartin L, Granger V, Gouel-Chéron A, Gillis CM, Zhu Q et al. An IgG-induced neutrophil activation pathway contributes to human drug-induced anaphylaxis. *Sci Transl Med*. (2019) 11:1479. doi: 10.1126/scitranslmed.aat1479
- Rosenberg HF, Dyer KD, Foster PS. Eosinophils: changing perspectives in health and disease. *Nat Rev Immunol*. (2013) 13:9–22. doi: 10.1038/nri3341
- Lee JJ, Jacobsen EA, Ochkur SI, McGarry MP, Condjella RM, Doyle AD et al. Human vs. mouse eosinophils: ‘that which we call an eosinophil,

- by any other name would stain as red'. *J Allergy Clin Immunol.* (2012) 130:572–84. doi: 10.1016/j.jaci.2012.07.025
11. Shin JS, Greer AM. The role of FcεRI expressed in dendritic cells and monocytes. *Cell Mol Life Sci.* (2015) 72:2349–60. doi: 10.1007/s00018-015-1870-x
  12. Wang B, Rieger A, Kilgus O, Ochiai K, Maurer D, Födinger D et al. Epidermal Langerhans cells from normal human skin bind monomeric IgE via Fc epsilon RI. *J Exp Med.* (1992) 175:1353–65. doi: 10.1084/jem.175.5.1353
  13. Bieber T, Salle HD, La, Wollenberg A, Hakimi J, Chizzonite R, Ring J, et al. Human epidermal Langerhans cells express the high affinity receptor for immunoglobulin E (Fc epsilon RI). *J Exp Med.* (1992) 175:1285–90. doi: 10.1084/jem.175.5.1285
  14. Hasegawa S, Pawankar R, Suzuki K, Nakahata T, Furukawa S, Okumura K, et al. Functional expression of the high affinity receptor for IgE (FcεRI) in Human platelets and its' intracellular expression in human megakaryocytes. *Blood.* (1999) 93:2543–51. doi: 10.1182/blood.V93.8.2543
  15. Malveaux FJ, Conroy MC, Adkinson NF. IgE receptors on human basophils. Relationship to serum IgE concentration. *J Clin Invest.* (1978) 62:176–81. doi: 10.1172/JCI109103
  16. Maclashan D, McKenzie-White J, Chichester K, Bochner BS, Davis FM, Schroeder JT, et al. *In vitro* regulation of FcRIα expression on human basophils by IgE antibody. *Blood.* (1998) 91:1633–43. doi: 10.1182/blood.V91.5.1633
  17. Matsuda A, Okayama Y, Ebihara N, Yokoi N, Gao P, Hamuro J et al. High-affinity IgE receptor-β chain expression in human mast cells. *J Immunol Methods.* (2008) 336:229–34. doi: 10.1016/j.jim.2008.05.006
  18. Ra, Hano Toru C, Nonoyama S, Suzuki K, Yata J, Nakahata T, et al. Induction of the high-affinity IgE receptor (FcεRI) on human mast cells by IL-4. *Int Immunol.* (1996) 8:1367–73. doi: 10.1093/intimm/8.9.1367
  19. Bax HJ, Bowen H, Dodev TS, Sutton BJ, Gould HJ. Mechanism of the antigen-independent cytokinergic SPE-7 IgE activation of human mast cells *in vitro*. *Sci Rep.* (2015) 5:9538. doi: 10.1038/srep09538
  20. Dahlin JS, Maurer M, Metcalfe DD, Pejler G, Sagi-Eisenberg R, Nilsson G. The ingenious mast cell: contemporary insights into mast cell behavior and function. *Allergy.* (2022) 77:83–99. doi: 10.1111/all.14881
  21. Galli SJ, Tsai M. IgE and mast cells in allergic disease. *Nat Med.* (2012) 18:693–704. doi: 10.1038/nm.2755
  22. Cardona V, Ansotegui JJ, Ebisawa M, El-Gamal Y, Fernandez Rivas M, Fineman S, et al. World allergy organization anaphylaxis guidance 2020. *World Allergy Organ J.* (2020) 13:100472. doi: 10.1016/j.waojou.2020.100472
  23. Yu W, Freeland DMH, Nadeau KC. Food allergy: immune mechanisms, diagnosis and immunotherapy. *Nat Rev Immunol.* (2016) 16:751–65. doi: 10.1038/nri.2016.111
  24. Varona R, Ramos T, Escribese MM, Jimeno L, Galán A, Würtzen PA, et al. Persistent regulatory T-cell response 2 years after 3 years of grass tablet SLIT: links to reduced eosinophil counts, sIgE levels, and clinical benefit. *Allergy.* (2019) 74:349–60. doi: 10.1111/all.13553
  25. Suárez-Fueyo A, Ramos T, Galán A, Jimeno L, Würtzen PA, Marin A, et al. Grass tablet sublingual immunotherapy downregulates the TH2 cytokine response followed by regulatory T-cell generation. *J Allergy Clin Immunol.* (2014) 133:43. doi: 10.1016/j.jaci.2013.09.043
  26. Barker-Tejeda TC, Bazire R, Obeso D, Mera-Berriatua L, Rosace D, Vazquez-Cortes S et al. Exploring novel systemic biomarker approaches in grass-pollen sublingual immunotherapy using omics. *Allergy.* (2021) 76:1199–212. doi: 10.1111/all.14565
  27. Drazdauskaite G, Layhadi JA, Shamji MH. Mechanisms of allergen immunotherapy in allergic Rhinitis. *Curr Allergy Asthma Rep.* (2021) 21:2. doi: 10.1007/s11882-020-00977-7
  28. Zelm MC, McKenzie CI, Varese N, Rolland JM, O'Hehir RE. Recent developments and highlights in immune monitoring of allergen immunotherapy. *Allergy.* (2019) 74:2342–54. doi: 10.1111/all.14078
  29. Tontini C, Bullfone-Paus S. Novel approaches in the inhibition of IgE-induced mast cell reactivity in food allergy. *Front Immunol.* (2021) 12:2725. doi: 10.3389/fimmu.2021.613461
  30. Woo HY, Kim YS, Kang NI, Chung WC, Song CH, Choi IW et al. Mechanism for acute oral desensitization to antibiotics. *Allergy.* (2006) 61:954–8. doi: 10.1111/j.1398-9995.2006.01147.x
  31. Moote W, Kim H, Ellis AK. Allergen-specific immunotherapy. *Allergy, Asthma Clin Immunol.* (2018) 14:53. doi: 10.1186/s13223-018-0282-5
  32. Takasato Y, Kurashima Y, Kiuchi M, Hirahara K, Murasaki S, Arai F et al. Orally desensitized mast cells form a regulatory network with Treg cells for the control of food allergy. *Mucosal Immunol.* (2020) 143:14:640–51. doi: 10.1038/s41385-020-00358-3
  33. Pfaar O, Bousquet J, Durham SR, Kleine-Tebbe J, Larché M, Roberts G et al. 110 years of Allergen immunotherapy: a journey from empiric observation to evidence. *Allergy.* (2022) 77:454–68. doi: 10.1111/all.15023
  34. Zhao W, Gomez G, Macey M, Kepley CL, Schwartz LB. *In vitro* desensitization of human skin mast cells. *J Clin Immunol.* (2012) 32:150–60. doi: 10.1007/s10875-011-9605-8
  35. Simons FER, Arduzzo LRF, Bilò MB, El-Gamal YM, Ledford DK, Ring J, et al. World allergy organization guidelines for the assessment and management of anaphylaxis. *World Allergy Organ J.* (2011) 4:13–37. doi: 10.1097/WOX.0b013e318211496c
  36. Incorvaia C, Ridolo E, Mauro M, Pucciarini F, Heffler E, Canonica GW. Venom immunotherapy and aeroallergen immunotherapy: how do their outcomes differ? *Front Allergy.* (2022) 0:14. doi: 10.3389/falgy.2022.854080
  37. Nelson HS. Allergy immunotherapy for inhalant allergens: strategies to minimize adverse reactions. *Allergy Asthma Proc.* (2020) 41:38–44. doi: 10.2500/aap.2020.41.190014
  38. Mori F, Giovannini M, Barni S, Jiménez-Saiz R, Munblit D, Biagioni B, et al. Oral immunotherapy for food-allergic children: a pro-con debate. *Front Immunol.* (2021) 12:3861. doi: 10.3389/fimmu.2021.636612
  39. NELSON H, LAHR J, RULE R, BOCK A, LEUNG D. Treatment of anaphylactic sensitivity to peanuts by immunotherapy with injections of aqueous peanut extract1. *J Allergy Clin Immunol.* (1997) 99:744–51. doi: 10.1016/S0091-6749(97)80006-1
  40. Staden U, Rolinck-Werninghaus C, Brewe F, Wahn U, Niggemann B, Beyer K. Specific oral tolerance induction in food allergy in children: efficacy and clinical patterns of reaction. *Allergy.* (2007) 62:1261–9. doi: 10.1111/j.1398-9995.2007.01501.x
  41. Longo G, Barbi E, Berti I, Meneghetti R, Pittalis A, Ronfani L et al. Specific oral tolerance induction in children with very severe cow's milk-induced reactions. *J Allergy Clin Immunol.* (2008) 121:343–7. doi: 10.1016/j.jaci.2007.10.029
  42. O'B Hourihane J, Beyer K, Abbas A, Fernández-Rivas M, Turner PJ, Blumchen K et al. Efficacy and safety of oral immunotherapy with AR101 in European children with a peanut allergy (ARTEMIS): a multicentre, double-blind, randomised, placebo-controlled phase 3 trial. *Lancet Child Adolesc Heal.* (2020) 4:728–39. doi: 10.1016/S2352-4642(20)30234-0
  43. Anagnostou K, Islam S, King Y, Foley L, Pasea L, Bond S et al. Assessing the efficacy of oral immunotherapy for the desensitisation of peanut allergy in children (STOP II): a phase 2 randomised controlled trial. *Lancet.* (2014) 383:1297–304. doi: 10.1016/S0140-6736(13)62301-6
  44. AR101 Oral immunotherapy for peanut allergy. *N Engl J Med.* (2018) 379:1991–2001. doi: 10.1056/NEJMoa1812856
  45. Chu DK, Wood RA, French S, Fiocchi A, Jordana M, Wasserman S, et al. Oral immunotherapy for peanut allergy (PACE): a systematic review and meta-analysis of efficacy and safety. *Lancet.* (2019) 393:2222–32. doi: 10.1016/S0140-6736(19)30420-9
  46. Giannetti M, Silver J, Hufdhri R, Castells M. One-day ultrarush desensitization for Hymenoptera venom anaphylaxis in patients with and without mast cell disorders with adjuvant omalizumab. *J Allergy Clin Immunol Pract.* (2020) 8:1431–5. doi: 10.1016/j.jaip.2019.10.022
  47. Jiménez-Saiz R. Drug-induced IgG-neutrophil-mediated anaphylaxis in humans: uncovered! *Allergy.* (2020) 75:484–5. doi: 10.1111/all.14118
  48. Bruhns P, Chollet-Martin S. Mechanisms of human drug-induced anaphylaxis. *J Allergy Clin Immunol.* (2021) 147:1133–42. doi: 10.1016/j.jaci.2021.02.013
  49. Montañez MI, Mayorga C, Bogas G, Barrionuevo E, Fernandez-Santamaria R, Martin-Serrano A, et al. Epidemiology, mechanisms, and diagnosis of drug-induced anaphylaxis. *Front Immunol.* (2017) 8:614. doi: 10.3389/fimmu.2017.00614
  50. Galli SJ. The mast cell-IgE paradox. *Am J Pathol.* (2016) 186:212–24. doi: 10.1016/j.ajpath.2015.07.025



51. van der Linden PWG, Hack CE, Poortman J, Vivié-Kipp YC, Struyvenberg A, van der Zwan JK. Insect-sting challenge in 138 patients: relation between clinical severity of anaphylaxis and mast cell activation. *J Allergy Clin Immunol.* (1992) 90:110–8. doi: 10.1016/S0091-6749(06)80017-5
52. Vadas P, Perelman B, Liss G. Platelet-activating factor, histamine, and tryptase levels in human anaphylaxis. *J Allergy Clin Immunol.* (2013) 131:144–9. doi: 10.1016/j.jaci.2012.08.016
53. Eberlein-König B, Ullmann S, Thomas P, Przybilla B. Tryptase and histamine release due to a sting challenge in bee venom allergic patients treated successfully or unsuccessfully with hyposensitization \*. *Clin Exp Allergy.* (1995) 25:704–12. doi: 10.1111/j.1365-2222.1995.tb00007.x
54. Nuñez-Borque E, Fernandez-Bravo S, Yuste-Montalvo A, Esteban V. Pathophysiological, cellular, and molecular events of the vascular system in anaphylaxis. *Front Immunol.* (2022) 0:700. doi: 10.3389/fimmu.2022.836222
55. Akdis CA, Akdis M. Mechanisms of allergen-specific immunotherapy and immune tolerance to allergens. *World Allergy Organ J.* (2015) 8:17. doi: 10.1186/s40413-015-0063-2
56. Wachholz PA, Durham SR. Mechanisms of immunotherapy: IgG revisited. *Curr Opin Allergy Clin Immunol.* (2004) 4:313–8. doi: 10.1097/01.all.0000136753.35948.c0
57. Cheng LE, Hartmann K, Roers A, Krummel MF, Locksley RM. Perivascular mast cells dynamically probe cutaneous blood vessels to capture immunoglobulin E. *Immunity.* (2013) 38:166–75. doi: 10.1016/j.immuni.2012.09.022
58. Kunder CA, St John AL, Abraham SN. Mast cell modulation of the vascular and lymphatic endothelium. *Blood.* (2011) 118:5383–93. doi: 10.1182/blood-2011-07-358432
59. Abraham SN, St. John AL. Mast cell-orchestrated immunity to pathogens. *Nat Rev Immunol.* (2010) 10:440–52. doi: 10.1038/nri2782
60. Krystal-Whittemore M, Dileepan KN, Wood JG. Mast cell: a multi-functional master cell. *Front Immunol.* (2016) 6:620. doi: 10.3389/fimmu.2015.00620
61. Yamanishi Y, Karasuyama H. Basophils and mast cells in immunity and inflammation. *Semin Immunopathol.* (2016) 38:535–7. doi: 10.1007/s00281-016-0582-0
62. Jiménez-Saiz R, Chu DK, Mandur TS, Walker TD, Gordon ME, Chaudhary R, et al. Lifelong memory responses perpetuate humoral TH2 immunity and anaphylaxis in food allergy. *J Allergy Clin Immunol.* (2017) 140:1604–15. doi: 10.1016/j.jaci.2017.01.018
63. Kubo S, Nakayama T, Matsuoka K, Yonekawa H, Karasuyama H. Long term maintenance of IgE-mediated memory in mast cells in the absence of detectable serum IgE. *J Immunol.* (2003) 170:775–80. doi: 10.4049/jimmunol.170.2.775
64. Khodoun M V, Strait R, Armstrong L, Yanase N, Finkelman FD. Identification of markers that distinguish IgE- from IgG-mediated anaphylaxis. *Proc Natl Acad Sci.* (2011) 108:12413–8. doi: 10.1073/pnas.1105695108
65. da Silva EZM, Jamur MC, Oliver C. Mast cell function: a new vision of an old cell. *J Histochem Cytochem.* (2014) 62:698–738. doi: 10.1369/0022155414545334
66. Ménasché G, Longé C, Bratti M, Blank U. Cytoskeletal transport, reorganization, and fusion regulation in mast cell-stimulus secretion coupling. *Front Cell Dev Biol.* (2021) 9:316. doi: 10.3389/fcell.2021.652077
67. Malaviya R, Uckun FM. Role of STAT6 in IgE receptor/FcεRI-mediated late phase allergic responses of mast cells. *J Immunol.* (2002) 168:421–6. doi: 10.4049/jimmunol.168.1.421
68. Khodoun MV, Morris SC, Angerman E, Potter C, Schuman R, Wunderlich M, et al. Rapid desensitization of humanized mice with anti-human FcεRIα monoclonal antibodies. *J Allergy Clin Immunol.* (2020) 145:907–21. doi: 10.1016/j.jaci.2019.12.003
69. Sancho-Serra M, del C, Simarro M, Castells M. Rapid IgE desensitization is antigen specific and impairs early and late mast cell responses targeting FcεRI internalization. *Eur J Immunol.* (2011) 41:1004–13. doi: 10.1002/eji.201040810
70. Oka T, Rios EJ, Tsai M, Kalesnikoff J, Galli SJ. Rapid desensitization induces internalization of antigen-specific IgE on mouse mast cells. *J Allergy Clin Immunol.* (2013) 132:922–32. doi: 10.1016/j.jaci.2013.05.004
71. Mendoza GR, Orner FB. Reversibility of IgE-mediated rat mast cell desensitization. *Int Arch Allergy Immunol.* (1982) 69:50–5. doi: 10.1159/000233145
72. Lewis A, MacGlashan DW, Suvarna SK, Peachell PT. Recovery from desensitization of IgE-dependent responses in human lung mast cells. *Clin Exp Allergy.* (2017) 47:1022–31. doi: 10.1111/cea.12912
73. Shalit M, Levi-Schaffer F. Challenge of mast cells with increasing amounts of antigen induces desensitization. *Clin Exp Allergy.* (1995) 25:896–902. doi: 10.1111/j.1365-2222.1995.tb00033.x
74. Gladys Ang WX, Church AM, Kulis M, Choi HW, Wesley Burks A, Abraham SN. Mast cell desensitization inhibits calcium flux and aberrantly remodels actin. *J Clin Invest.* (2016) 126:4103–18. doi: 10.1172/JCI87492
75. Nagata Y, Suzuki R. FcεRI cluster size determines effective mast cell desensitization without effector responses *in vitro*. *Int Arch Allergy Immunol.* (2022) 183:453–61. doi: 10.1159/000520132
76. Morales AR, Shah N, Castells M. Antigen-IgE desensitization in signal transducer and activator of transcription 6-deficient mast cells by suboptimal doses of antigen. *Ann Allergy, Asthma Immunol.* (2005) 94:575–80. doi: 10.1016/S1081-1206(10)61136-2
77. Sherman MA, Secor VH, Brown MA. IL-4 preferentially activates a novel STAT6 isoform in mast cells. *J Immunol.* (1999) 162:2703–8.
78. Navinés-Ferrer A, Ainsua-Enrich E, Serrano-Candelas E, Proaño-Pérez E, Muñoz-Cano R, Gastaminza G, et al. MYO1F regulates IgE and MRGPRX2-dependent mast cell exocytosis. *J Immunol.* (2021) 206:2277–89. doi: 10.4049/jimmunol.2001211
79. Dispenza MC, Krier-Burris RA, Chhiba KD, Udem BJ, Robida PA, Bochner BS. Bruton's tyrosine kinase inhibition effectively protects against human IgE-mediated anaphylaxis. *J Clin Invest.* (2020) 130:4759–70. doi: 10.1172/JCI138448
80. Uermösi C, Zabel F, Manolova V, Bauer M, Beerli RR, Senti G et al. IgG-mediated down-regulation of IgE bound to mast cells: a potential novel mechanism of allergen-specific desensitization. *Allergy.* (2014) 69:338–47. doi: 10.1111/all.12327
81. Castells MC, Klickstein LB, Hassani K, Cumplido JA, Lacouture ME, Austen KF et al. gp49B1-αvβ3 interaction inhibits antigen-induced mast cell activation. *Nat Immunol.* (2001) 2:436–42. doi: 10.1038/87749
82. Jin JJ, Li JT, Klimek L, Pfaar O. Sublingual Immunotherapy Dosing Regimens: What Is Ideal? *J Allergy Clin Immunol Pract.* (2017) 5:1–10. doi: 10.1016/j.jaip.2016.09.027
83. Barber D, Rico P, Blanco C, Fernandez-Rivas M, Ibañez MD, Escribese MM. GRAZAX®: a sublingual immunotherapy vaccine for Hay fever treatment: from concept to commercialization. *Hum Vaccin Immunother.* (2019) 15:2887–95. doi: 10.1080/21645515.2019.1622976
84. Hoover H, Leatherman B, Ryan M, McMains K, Veling M. Evidence-based dosing of maintenance subcutaneous immunotherapy: a contemporary review of state-of-the-art practice. *Int Forum Allergy Rhinol.* (2018) 8:806–16. doi: 10.1002/alr.22118
85. Pitsios C. Allergen immunotherapy: biomarkers and clinical outcome measures. *J Asthma Allergy.* (2021) 14:141–8. doi: 10.2147/JAA.S267522
86. Moingeon P. Biomarkers for allergen immunotherapy: a 'panoramic' view. *Immunol Allergy Clin North Am.* (2016) 36:161–79. doi: 10.1016/j.iac.2015.08.004
87. Kouser L, Kappen J, Walton RP, Shamji MH. Update on biomarkers to monitor clinical efficacy response during and post treatment in allergen immunotherapy. *Curr Treat Options Allergy.* (2017) 4:43–53. doi: 10.1007/s40521-017-0117-5
88. Breiteneder H, Peng YQ, Agache I, Diamant Z, Eiwegger T, Fokkens WJ et al. Biomarkers for diagnosis and prediction of therapy responses in allergic diseases and asthma. *Allergy.* (2020) 75:3039–68. doi: 10.1111/all.14582

89. Hardy LC, Smeekens JM, Kulis MD. Biomarkers in food allergy immunotherapy. *Curr Allergy Asthma Rep.* (2019) 19:61. doi: 10.1007/s11882-019-0894-y
90. Pfaar O, Bonini S, Cardona V, Demoly P, Jakob T, Jutel M et al. Perspectives in allergen immunotherapy: 2017 and beyond. *Allergy.* (2018) 73:5–23. doi: 10.1111/all.13355
91. Shamji MH, Kappen JH, Akdis M, Jensen-Jarolim E, Knol EF, Kleine-Tebbe J, et al. Biomarkers for monitoring clinical efficacy of allergen immunotherapy for allergic rhinoconjunctivitis and allergic asthma: an EAACI position paper. *Allergy.* (2017) 72:1156–73. doi: 10.1111/all.13138
92. Agache I, Bilò M, Braunstahl GJ, Delgado L, Demoly P, Eigenmann P, et al. *In vivo* diagnosis of allergic diseases—allergen provocation tests. *Allergy.* (2015) 70:355–65. doi: 10.1111/all.12586
93. Nolte H, Maloney J, Nelson HS, Bernstein DI, Lu S, Li Z, et al. Onset and dose-related efficacy of house dust mite sublingual immunotherapy tablets in an environmental exposure chamber. *J Allergy Clin Immunol.* (2015) 135:1494–501. doi: 10.1016/j.jaci.2014.12.1911
94. Horak F, Zieglmayer P, Zieglmayer R, Lemell P, Devillier P, Montagut A, et al. Early onset of action of a 5-grass-pollen 300-IR sublingual immunotherapy tablet evaluated in an allergen challenge chamber. *J Allergy Clin Immunol.* (2009) 124:471–7. doi: 10.1016/j.jaci.2009.06.006
95. Shamji MH, Ljørring C, Francis JN. A Calderon M, Larché M, Kimber I, et al. Functional rather than immunoreactive levels of IgG4 correlate closely with clinical response to grass pollen immunotherapy. *Allergy.* (2012) 67:217–26. doi: 10.1111/j.1398-9995.2011.02745.x
96. Pilette C, Nouri-Aria KT, Jacobson MR, Wilcock LK, Detry B, Walker SM, et al. Grass pollen immunotherapy induces an allergen-specific IgA2 antibody response associated with mucosal TGF- $\beta$  expression. *J Immunol.* (2007) 178:4658–66. doi: 10.4049/jimmunol.178.7.4658
97. Gueguen C, Bouley J, Moussu H, Luce S, Duchateau M, Chamot-Rooke J, et al. Changes in markers associated with dendritic cells driving the differentiation of either TH2 cells or regulatory T cells correlate with clinical benefit during allergen immunotherapy. *J Allergy Clin Immunol.* (2016) 137:545–58. doi: 10.1016/j.jaci.2015.09.015
98. Golebski K, Layhadi JA, Sahiner U, Steveling-Klein EH, Lenormand MM, Li RCY et al. Induction of IL-10-producing type 2 innate lymphoid cells by allergen immunotherapy is associated with clinical response. *Immunity.* (2021) 54:291–307. doi: 10.1016/j.immuni.2020.12.013
99. Shamji MH, Layhadi JA, Scadding GW, Cheung DKM, Calderon MA, Turka LA, et al. Basophil expression of diamine oxidase: a novel biomarker of allergen immunotherapy response. *J Allergy Clin Immunol.* (2015) 135:913–21. doi: 10.1016/j.jaci.2014.09.049
100. Caruso M, Cibella F, Emma R, Campagna D, Tringali G, Amaradio MD et al. Basophil biomarkers as useful predictors for sublingual immunotherapy in allergic rhinitis. *Int Immunopharmacol.* (2018) 60:50–8. doi: 10.1016/j.intimp.2018.04.034
101. Tsai M, Mukai K, Chinthrajah RS, Nadeau KC, Galli SJ. Sustained successful peanut oral immunotherapy associated with low basophil activation and peanut-specific IgE. *J Allergy Clin Immunol.* (2020) 145:885–96. doi: 10.1016/j.jaci.2019.10.038
102. Palaniyandi S, Watanabe K, Ma M, Tachikawa H, Kodama M, Aizawa Y. Inhibition of mast cells by interleukin-10 gene transfer contributes to protection against acute myocarditis in rats. *Eur J Immunol.* (2004) 34:3508–15. doi: 10.1002/eji.200425147
103. Cosmi L, Santarlasci V, Angeli R, Liotta F, Maggi L, Frosali F, et al. Sublingual immunotherapy with Dermatophagoides monomeric allergoid down-regulates allergen-specific immunoglobulin E and increases both interferon- $\gamma$ - and interleukin-10-production. *Clin Exp Allergy.* (2006) 36:261–72. doi: 10.1111/j.1365-2222.2006.02429.x
104. Ebner C, Siemann U, Bohle B, Willheim M, Wiedermann U, Schenk S, et al. Immunological changes during specific immunotherapy of grass pollen allergy: reduced lymphoproliferative responses to allergen and shift from TH2 to TH1 in T-cell clones specific for Phi p 1, a major grass pollen allergen. *Clin Exp Allergy.* (1997) 27:1007–15. doi: 10.1111/j.1365-2222.1997.tb01252.x
105. Bohle B, Kinaciyan T, Gerstmayr M, Radakovics A, Jahn-Schmid B, Ebner C. Sublingual immunotherapy induces IL-10-producing T regulatory cells, allergen-specific T-cell tolerance, and immune deviation. *J Allergy Clin Immunol.* (2007) 120:707–13. doi: 10.1016/j.jaci.2007.06.013
106. Zhu Z, Lee PH, Chaffin MD, Chung W, Loh P-R, Lu Q, et al. A genome-wide cross-trait analysis from UK Biobank highlights the shared genetic architecture of asthma and allergic diseases. *Nat Genet.* (2018) 50:857–64. doi: 10.1038/s41588-018-0121-0
107. Mondoulet L, Dioszeghy V, Busato F, Plaquet C, Dhelft V, Bethune K, et al. Gata3 hypermethylation and Foxp3 hypomethylation are associated with sustained protection and bystander effect following epicutaneous immunotherapy in peanut-sensitized mice. *Allergy.* (2019) 74:152–64. doi: 10.1111/all.13479
108. Hwang SS, Jang SW, Lee KO, Kim HS, Lee GR. RHS6 coordinately regulates the Th2 cytokine genes by recruiting GATA3, SATB1, and IRF4. *Allergy.* (2017) 72:772–82. doi: 10.1111/all.13078
109. Croote D, Darmanis S, Nadeau KC, Quake SR. High-affinity allergen-specific human antibodies cloned from single IgE B cell transcriptomes. *Science (80-).* (2018) 362:1306–9. doi: 10.1126/science.aau2599
110. Zheng P, Bian X, Zhai Y, Li C, Li N, Hao C et al. Metabolomics reveals a correlation between hydroxyeicosatetraenoic acids and allergic asthma: evidence from 3 years' immunotherapy. *Pediatr Allergy Immunol.* (2021) 32:1654–62. doi: 10.1111/pai.13569
111. Ohnmacht C, Park JH, Cording S, Wing JB, Atarashi K, Obata Y, et al. The microbiota regulates type 2 immunity through ROR $\gamma$ T+ T cells. *Science (80-).* (2015) 349:989–93. doi: 10.1126/science.aac4263
112. Tsai YG, Yang KD, Niu DM, Chien JW, Lin CY. TLR2 Agonists enhance CD8 + Foxp3 + regulatory T cells and suppress Th2 immune responses during allergen immunotherapy. *J Immunol.* (2010) 184:7229–37. doi: 10.4049/jimmunol.1000083
113. Lam HY, Tergaonkar V, Ahn KS. Mechanisms of allergen-specific immunotherapy for allergic rhinitis and food allergies. *Biosci Rep.* (2020) 40:256. doi: 10.1042/BSR20200256
114. James LK, Shamji MH, Walker SM, Wilson DR, Wachholz PA, Francis JN, et al. Long-term tolerance after allergen immunotherapy is accompanied by selective persistence of blocking antibodies. *J Allergy Clin Immunol.* (2011) 127:509–16. doi: 10.1016/j.jaci.2010.12.1080
115. Knol EF, Mul FPJ, Jansen H, Calafat J, Roos D. Monitoring human basophil activation via CD63 monoclonal antibody 435. *J Allergy Clin Immunol.* (1991) 88:328–38. doi: 10.1016/0091-6749(91)90094-5
116. Patil SU, Steinbrecher J, Calatroni A, Smith N, Ma A, Ruiter B, et al. Early decrease in basophil sensitivity to Ara h 2 precedes sustained unresponsiveness after peanut oral immunotherapy. *J Allergy Clin Immunol.* (2019) 144:1310–9. doi: 10.1016/j.jaci.2019.07.028
117. Barber D, Escribese MM. Predictive biomarkers in allergen specific immunotherapy. *Allergol Immunopathol.* (2017) 45:12–4. doi: 10.1016/j.aller.2017.09.003
118. Irvine AD, McLean WHI, Leung DYM. Filaggrin mutations associated with skin and allergic diseases. *N Engl J Med.* (2011) 365:1315–27. doi: 10.1056/NEJMra1011040
119. Kim KW, Ober C. Lessons learned from GWAS of asthma. *Allergy Asthma Immunol Res.* (2019) 11:170. doi: 10.4168/aaair.2019.11.2.170
120. Bunning BJ, DeKruyff RH, Nadeau KC. Epigenetic changes during food-specific immunotherapy. *Curr Allergy Asthma Rep.* (2016) 16:87. doi: 10.1007/s11882-016-0665-y
121. Sindher SB, Long A, Acharya S, Sampath V, Nadeau KC. The use of biomarkers to predict aero-allergen and food immunotherapy responses. *Clin Rev Allergy Immunol.* (2018) 55:190–204. doi: 10.1007/s12016-018-8678-z
122. Waldron R, McGowan J, Gordon N, McCarthy C, Mitchell EB, Fitzpatrick DA. Proteome and allergenome of the European house dust mite dermatophagoides pteronyssinus. *PLoS ONE.* (2019) 14:e0216171. doi: 10.1371/journal.pone.0216171
123. Glesner J, Filep S, Vailes LD, Wünschmann S, Chapman MD, Birrueta G, et al. Allergen content in German cockroach extracts and sensitization profiles to a new expanded set of cockroach allergens determine *in vitro*

- extract potency for IgE reactivity. *J Allergy Clin Immunol.* (2019) 143:1474–81. doi: 10.1016/j.jaci.2018.07.036
124. Ihara F, Sakurai D, Yonekura S, Iinuma T, Yagi R, Sakurai T, et al. Identification of specifically reduced Th2 cell subsets in allergic rhinitis patients after sublingual immunotherapy. *Allergy.* (2018) 73:1823–32. doi: 10.1111/all.13436
125. Durham SR, Emminger W, Kapp A, de Monchy JGR, Rak S, Scadding GK et al. SQ-standardized sublingual grass immunotherapy: confirmation of disease modification 2 years after 3 years of treatment in a randomized trial. *J Allergy Clin Immunol.* (2012) 129:717–25.e5. doi: 10.1016/j.jaci.2011.12.973
126. Jiménez-Saiz R, Ellenbogen Y, Koenig JFE, Gordon ME, Walker TD, Rosace D, et al. IgG1 + B-cell immunity predates IgE responses in epicutaneous sensitization to foods. *Allergy.* (2019) 74:165–75. doi: 10.1111/all.13481
127. Perales-Chorda C, Obeso D, Twomey L, Rojas-Benedicto A, Puchades-Carrasco L, Roca M, et al. Characterization of anaphylaxis reveals different metabolic changes depending on severity and triggers. *Clin Exp Allergy.* (2021) 51:1295–309. doi: 10.1111/cea.13991

**Conflict of Interest:** The authors declare that the research was conducted in the absence of any commercial or financial relationships that could be construed as a potential conflict of interest.

**Publisher's Note:** All claims expressed in this article are solely those of the authors and do not necessarily represent those of their affiliated organizations, or those of the publisher, the editors and the reviewers. Any product that may be evaluated in this article, or claim that may be made by its manufacturer, is not guaranteed or endorsed by the publisher.

Copyright © 2022 López-Sanz, Jiménez-Saiz, Esteban, Delgado-Dolset, Perales-Chorda, Villaseñor, Barber and Escribese. This is an open-access article distributed under the terms of the Creative Commons Attribution License (CC BY). The use, distribution or reproduction in other forums is permitted, provided the original author(s) and the copyright owner(s) are credited and that the original publication in this journal is cited, in accordance with accepted academic practice. No use, distribution or reproduction is permitted which does not comply with these terms.



## Word of mouth: Oral mucosa composition in health and immune disease

Oral mucosa is composed of a multilayered squamous cell epithelium that acts as a barrier that is constantly exposed to external threats, such as allergens, pathogens or mastication forces. There are structural differences in oral mucosa: while lining (buccal) mucosa is composed of lightly keratinized epithelium, masticatory mucosa (gingiva) is highly keratinized. There are also other areas of specialized tissue like the dorsal tongue, which has taste buds.<sup>1</sup>

Oral gingiva is commonly affected by periodontitis, a highly prevalent inflammatory disease that affects ~10% of the general population. It is caused by dysbiosis of the oral microbiome that triggers aberrant immune activation.

Recently, Williams et al<sup>2</sup> have investigated the composition, function and crosstalk between the stromal and immune cells in healthy oral mucosa and gingival mucosa suffering from periodontitis. They performed single-cell RNA sequencing and validated their results by histology and flow cytometry. They found that, compared with other mucosal tissues, gingival mucosa had a unique expression of neutrophil-related genes in the epithelial compartment, while buccal mucosa had increased endothelium development. Moreover, they observed that periodontitis induced inflammatory cell infiltration (neutrophils and IgG<sup>+</sup> plasma cells) and a shift in the epithelial and stromal compartments towards a pro-inflammatory environment, marked by increased immune cell adhesion and chemokine secretion. Fibroblasts and epithelial cells specifically promoted neutrophil recruitment via cytokine biosynthesis (IL-8), and fibroblasts also expressed several neutrophil-recruiting chemokine ligands (CXCL1, 2, 5, 8) in periodontitis, thus suggesting a role of stromal cells in the establishment of the pro-inflammatory environment (Figure 1).

These results go in line with what has been observed in respiratory allergic diseases. It is widely accepted that the oral mucosa presents a unique pro-tolerogenic environment. However, a systemic Th2 response has been shown to impair oral tolerance by

shifting the phenotype of Tregs towards a Th2-like phenotype in animal models,<sup>3</sup> thus promoting allergy. The mechanisms behind the loss of oral tolerance are not completely understood, but the impairment of the oral mucosal barrier might play a pivotal role on it.<sup>4</sup> Interestingly, the epithelial disruption observed in the oral mucosa of patients suffering from respiratory allergies with no associated food allergy was not associated with an increase in the infiltration of immune cells.<sup>4</sup> However, there is a lack of knowledge regarding the mechanisms behind this change of phenotype or how that could affect the oral mucosa in the long term. One possibility could be the affectation of basal cells. It has been shown that extensive local Th2 activity is able to block productive basal cell differentiation in chronic allergic rhinitis and other pathologies even after the Th2 environment is removed, promoting the barrier disruption.<sup>5</sup>

In celiac disease (CD), oral mucosa has been shown to have an increased abundance of Treg cells that was inversely correlated with E-cadherin expression and positively correlated with peripheral amphiregulin expression. Thus, we hypothesize that the Treg cells observed in CD patients are recruited to protect against further tissue damage and maintain barrier integrity.<sup>6</sup>

These publications advance the knowledge of the immune system of the oral mucosa in health and disease. The role of neutrophils seems to not be significant in the buccal mucosa for other inflammatory diseases, although this might be due to the location of the tissue (gingiva vs buccal mucosa).<sup>2,4,6</sup> In this regard, oral mucosa is affected in periodontal, allergic and celiac disease, among others; thus, a full characterization of neutrophil, Th2 and Treg response in the oral mucosa could serve as a powerful, accessible tool to understand local and systemic disease. Moreover, other cell populations, such as innate lymphoid cells, and the function of the many antigen-presenting cells of the human oral mucosa should be further investigated to understand their role when oral tolerance is lost.

**Abbreviations:** Tregs, regulatory T cells.

© 2022 European Academy of Allergy and Clinical Immunology and John Wiley & Sons Ltd.

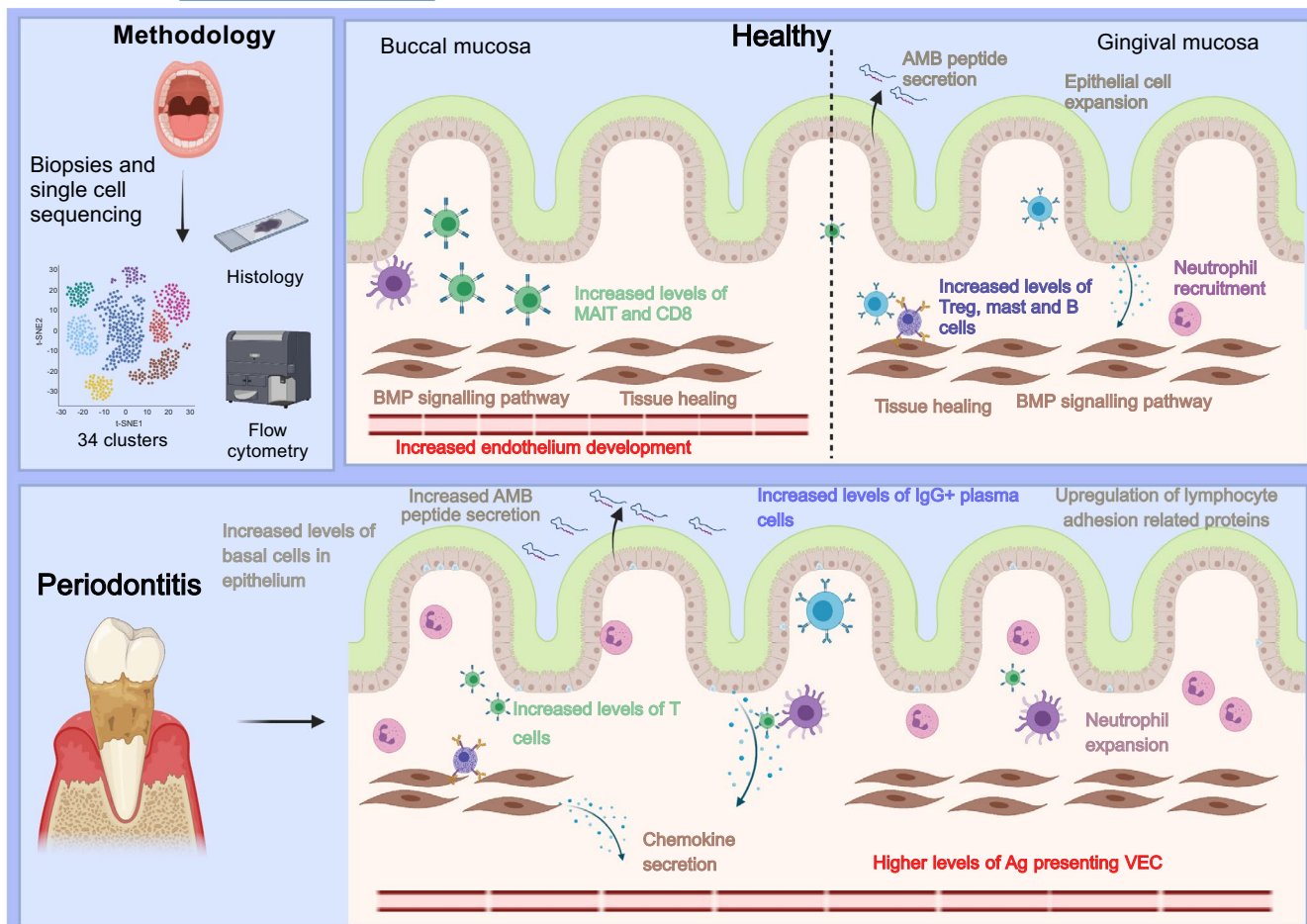


**FIGURE 1** Main differences in healthy buccal and gingival mucosa, and in gingival mucosa with periodontitis. Summary of the findings of Williams et al<sup>2</sup> about oral mucosa composition. Briefly, biopsies from the buccal and gingival mucosa were isolated from healthy individuals and patients suffering from periodontitis. Characterization of cells was performed by single-cell sequencing, histology and flow cytometry experiments. Upper figure: the main findings in composition of buccal and gingival mucosa in healthy individuals are displayed. Buccal mucosa presented higher levels of MAIT and CD8<sup>+</sup> cells, increased endothelium development and regenerative fibroblast phenotypes. On the contrary, gingival mucosa was characterized by inflammatory preparedness signatures such as antimicrobial peptide secretion, neutrophil recruitment and increased mast cells and B cells numbers. Lower figure: the inflammatory changes associated with periodontitis in the gingiva involve T cell and neutrophil infiltration and an increase in Ag presentation to immune cells. Figure created with <http://www.biorender.com>. Ag: antigen; AMB: antimicrobial peptides; MAIT: mucosa-associated lymphoid T cells; CD: cluster of differentiation; VEC: vascular endothelial cells; Treg: regulatory T cell; and Ig: immunoglobulin

#### ACKNOWLEDGMENTS



The authors recognize Dr. Anna Globinska for graphical abstract design and Dr. Rodrigo Jiménez-Saiz for critical review of the manuscript.

#### CONFLICT OF INTEREST

The authors have no conflicts of interest to declare.

#### FUNDING INFORMATION

M.I.D.D. and J.R.-C. are supported by FPI-CEU predoctoral fellowships.

María Isabel Delgado-Dolset   
 Juan Rodríguez-Coira   
 Javier Sánchez-Solares


*Instituto de Medicina Molecular Aplicada (IMMA),  
 Departamento de Ciencias Médicas Básicas, Facultad de  
 Medicina, Universidad San Pablo-CEU, CEU Universities,  
 Madrid, Spain*

#### Correspondence

María Isabel Delgado-Dolset, Instituto de Medicina Molecular Aplicada (IMMA), Departamento de Ciencias Médicas Básicas, Facultad de Medicina, Universidad San Pablo-CEU, CEU Universities, Campus Montepríncipe, Crtra, Boadilla del Monte km 5.3, CP 28668 Boadilla del Monte, Madrid, Spain.  
 Email: maria.delgadodolset@ceu.es

María Isabel Delgado-Dolset, Juan Rodríguez-Coira and Javier Sánchez-Solares contributed equally.

#### ORCID

María Isabel Delgado-Dolset  <https://orcid.org/0000-0001-7924-5454>

Juan Rodríguez-Coira  <https://orcid.org/0000-0003-0517-7078>

#### REFERENCES

1. Squier C, Brogden KA. *Human oral mucosa: development, structure and function*. John Wiley & Sons, Ltd; 2013, ISBN 9781118710470.
2. Williams DW, Greenwell-Wild T, Brenchley L, et al. Human oral mucosa cell atlas reveals a stromal-neutrophil axis regulating tissue immunity. *Cell*. 2021;184(15):4090-4104.e15. doi:10.1016/j.cell.2021.05.013
3. Noval Rivas M, Burton OT, Wise P, et al. Regulatory T cell reprogramming toward a Th2-cell-like lineage impairs oral tolerance and promotes food allergy. *Immunity*. 2015;42(3):512-523. doi:10.1016/j.immuni.2015.02.004
4. Sanchez-Solares J, Delgado-Dolset MI, Mera-Berriatua L, et al. Respiratory allergies with no associated food allergy disrupt oral mucosa integrity. *Allergy*. 2019;74(11):2261-2265. doi:10.1111/all.13860
5. Ordovas-Montanes J, Dwyer DF, Nyquist SK, et al. Allergic inflammatory memory in human respiratory epithelial progenitor cells. *Nature*. 2018;560(7720):649-654. doi:10.1038/s41586-018-0449-8
6. Sanchez-Solares J, Sanchez L, Pablo-Torres C, et al. Celiac disease causes epithelial disruption and regulatory t cell recruitment in the oral mucosa. *Front Immunol*. 2021;12:623805. doi:10.3389/fimmu.2021.623805





# Epithelial Barrier: Protector and Trigger of Allergic Disorders

Izquierdo E<sup>1</sup>, Rodríguez-Coira J<sup>1</sup>, Delgado-Dolset MI<sup>1</sup>, Gomez-Casado C<sup>1,2</sup>, Barber D<sup>1</sup>, Escribese MM<sup>1</sup>

<sup>1</sup>Institute of Applied Molecular Medicine (IMMA) Nemesio Díez, Department of Basic Medical Sciences, Facultad de Medicina, Universidad San Pablo-CEU, CEU Universities, Boadilla del Monte, Madrid, Spain

<sup>2</sup>Department of Dermatology, University Hospital Düsseldorf, Düsseldorf, Germany

J Investig Allergol Clin Immunol 2022; Vol. 32(2): 81-96

doi: 10.18176/jiaci.0779

## ■ Abstract

The epithelial barrier has classically been considered as the only first line of defense against irritants, pathogens, and allergens. However, it is now known to play an essential role in the immune response to exogenous agents. In fact, recent reports postulate the epithelial barrier hypothesis as a possible explanation for the increasing incidence and severity of allergic diseases.

The epithelial barrier preserves the isolation of internal tissues from potential external threats. Moreover, a coordinated interaction between epithelial and immune cells ensures the unique immune response taking place in mucosal tissues, which is reported to be dysregulated in allergic diseases.

We and others have demonstrated that in severe allergic phenotypes, the epithelial barrier undergoes several histological modifications, with increased infiltration of immune cells, leading to dysfunction. This is common in atopic dermatitis, asthma, and food allergy. However, the precise role of the epithelial barrier in mucosal biology during progression of allergic diseases is not well understood.

In this review, we aim to compile recent knowledge regarding the histological structure and immunological function of the epithelial barrier and to shed light on the role of this compartment in the onset and progression of allergic diseases.

**Key words:** Epithelium. Mucosal immunity. Allergy. Antigen. Immunoglobulin (Ig) switch. Inflammation.

## ■ Resumen

La barrera epitelial se ha considerado clásicamente sólo como la primera línea de defensa contra los irritantes, patógenos y alérgenos, pero ahora sabemos que el epitelio también desempeña un papel esencial en la respuesta inmunológica frente los agentes exógenos. De hecho, informes recientes postulan la hipótesis de la barrera epitelial como una posible explicación de la creciente incidencia y la gravedad de las enfermedades alérgicas.

La barrera epitelial preserva el aislamiento de los tejidos internos de las posibles amenazas exteriores. Se sabe que las células epiteliales, además de un papel meramente protector, también tienen una función esencial en el desarrollo de la respuesta inmune en las mucosas, favoreciendo un ambiente tolerogénico. Sin embargo, en enfermedades alérgicas, estas características se ven afectadas como demuestra una repuesta exagerada ante antígenos inocuos. De hecho, en los fenotipos alérgicos graves, la barrera epitelial experimenta varias modificaciones histológicas que se asocian con pérdida de integridad y aumento de los infiltrados celulares, lo que conduce a una disfunción de la misma. Este proceso es común en la dermatitis atópica, el asma y/o la alergia alimentaria. Aunque todavía no se conoce bien la función exacta de la barrera epitelial en la biología de la mucosa durante las enfermedades alérgicas.

En esta revisión, pretendemos recopilar los conocimientos recientes sobre la estructura histológica y la función inmunológica de la barrera epitelial, y arrojar luz sobre el papel de este compartimento en la aparición y la progresión de las enfermedades alérgicas.

**Palabras clave:** Epitelio. Inmunidad de las mucosas. Alergia. Antígeno. Cambio de Inmunoglobulina (Ig). Inflamación.

## Introduction

The mucosa lines body cavities and passages (eg, in the gastrointestinal, respiratory, reproductive, and urinary tracts), which communicate directly or indirectly with the outside of the body. Mucosal tissues have 2 main features: (1) a specific histological conformation that preserves isolation of the inner tissues from external insult, and (2) privileged immunity. Together, these features enable specific and tight regulation of the immune response, which is essential for maintenance of homeostasis and participates in the development of several diseases, including allergic diseases and asthma [1].

Mucosal tissues are usually composed of conjunctive tissue and epithelium. Epithelial tissue in the mucosa is in contact with the external environment and underlined by a basal membrane and a lamina propria formed by connective tissue. This is highly vascularized and comprises different cell types (stromal and immune cells) and extracellular matrix proteins. Depending on its location in the body, mucosal tissue can be of several types, including oral, respiratory, and gastrointestinal. Each displays specific histological features [2-4].

The epithelium has classically been considered the first line of defense against inhaled irritants, pathogens, and allergens. However, in recent years, epithelial cells have been shown to play an essential role in the immune response and during the inflammatory process after tissue damage [5,6]. The epithelium consists of cells tightly attached to each other and arranged in several distinct layers. Junctional complexes such as tight junctions (TJs), adherent junctions, gap junctions, and desmosomes provide cohesion between cells. TJs form the closest cell-cell interactions in the apical area of oral epithelial cells, working as a restrictive gate for the passage of water, electrolytes, and other small molecules. They consist of transmembrane proteins, including occludin, claudin, and immunoglobulin-like surface proteins, as well as cytoplasmic molecules such as zonula occludens proteins [7]. Adherent junctions are protein complexes situated below TJs that bind strongly to cells. Adherent junctions are composed by cadherins that connect to the actin cytoskeleton [8]. Gap junctions are composed of hemichannels, called connexons, which are regulated by several factors including pH, calcium concentration, and posttranslational modifications. Thus, they provide direct communication between adjacent cells and regulate the exchange of small molecules and ions. Finally, desmosomes link 2 cells together by the intermediate filament cytoskeleton, becoming the adhesive bonds that give mechanical strength to tissues. Since the structure and functions of all the above-mentioned cell-cell junctions are key for preserving epithelial barrier integrity, their disruption has been linked to infections, autoimmune diseases, allergy, and cancer [9].

### Respiratory System

The respiratory system is divided anatomically into structures of the upper and the lower respiratory tract, which correspond to 2 functional components, namely, the conductive component and the respiratory component.

The conductive component, which involves the nasal cavity, pharynx, larynx, and trachea, is lined by a mucosal tissue formed by ciliated pseudostratified columnar epithelium.

Deeper into the respiratory system, the epithelium becomes thinner, and glands are less specialized and more abundant, passing from olfactory glands in the nasal cavity to seromucous glands in the trachea. These histological features in the upper airways enable isolation of the internal tissues and the humidification and conduction of the air into the lower respiratory tract, ie, the respiratory component.

The trachea bifurcates into the right and left primary bronchi, which enter the posterior side of each lung along with the pulmonary vessels, lymphatics, and nerves. Within each lung, the bronchus subdivides further to form the bronchial tree, the last component of the air conduction system. It is in the last parts of this component, the alveoli, where the gas exchange between air and blood occurs at the barrier membrane between an alveolus and the capillaries surrounding it.

The respiratory epithelium provides a physical barrier to infection, lining the respiratory tract from the nose to the alveoli with a wide range of cell types. Ciliated epithelial cells are important for propelling mucus up the airway, thereby removing particulate material. Ciliated cells line the respiratory tract down to the level of the respiratory bronchiole. The tracheobronchial glands are important sources of airway mucus, which serves to trap particulates. The respiratory epithelium also functions in the regulation of water and ion movement into the airway mucus. It secretes surfactant proteins A and D, lysozyme, lactoferrin, and antimicrobial peptides ( $\beta$ -defensins and cathelicidins) and releases reactive oxygen and nitrogen species to kill invading pathogens [5,10-13].

### Oral and Gastrointestinal Tracts

The gastrointestinal track comprises the oral cavity, esophagus, stomach, intestine, and anus in addition to associated glands. Its main function is to obtain the molecules necessary for the maintenance, growth, and energy needs of the body from ingested food.

Histologically, it is formed by 4 main layers: the mucosa, submucosa, muscularis, and serosa. We focus on the epithelial tissue that forms the mucosa [11]. The entrance to the gastrointestinal tract is the oral cavity. Here, the mucosal structure varies along its location within the oral cavity, although 3 main types of mucosa can be distinguished based on their morphology and specific pattern of differentiation: (1) keratinized stratified squamous epithelium or masticatory mucosa, which covers the hard palate and gingiva; (2) nonkeratinized stratified squamous epithelium or lining mucosa, on the underside of the tongue, inside the lips and cheeks, on the floor of the mouth, and on the alveolar ridge; and (3) the specialized mucosa of the dorsal surface of the tongue [9,10,14]. The oral epithelium is the superficial layer that separates the environment from underlying tissues. It comprises a stratified squamous epithelium consisting of cells tightly attached to each other and arranged in layers. The oral epithelium possesses structural properties, such as stratification and cornification of keratinocytes, and specific cell-to-cell interactions to maintain its barrier function. The keratinized type contains 4 layers of cells: the basal layer, the spinous layer, the granular layer, and the superficial layer (keratinized layer). Keratinocytes are born and proliferate in the basal layer and undergo terminal differentiation as they migrate to the surface, where they die. Thus, the outermost

cell layers are composed of dead cells. Conversely, the surface cells of nonkeratinized epithelia are living cells without keratin. Besides, the nonkeratinized oral epithelium has no granular layer [10,15].

The oral cavity is connected with the pharynx (oropharynx), followed by the esophagus, both of which are characterized by stratified squamous epithelium, which ends in the stomach and is replaced by simple columnar epithelium in glands and the intestine [11].

The small intestine is the site where the digestive processes are completed and where nutrients (production of digestion) are absorbed by the cells of the epithelial lining. This site has been studied in depth owing to its immune-privileged features. In the small intestine, the epithelium of the mucosal layer is made up of simple columnar epithelium with microvilli, which increase the surface of absorption, and goblet cells, which are responsible for mucus secretion. However, in the large intestine, the mucosa lacks microvilli, although it still presents goblet cells and absorptive cells involved in absorption of water and electrolytes [16-18].

### The Skin

The skin is the largest tissue in the body, comprising 3 layers: the epidermis, the dermis, and the hypodermis [11].

The epidermis presents a stratified squamous epithelium mainly formed by keratinocytes. It is the most external layer

of the skin and displays a high regeneration rate in response to exogenous factors (eg, detergents, environmental pollutants). Other less abundant cell types in the epidermis include melanocytes and Langerhans cells. The former are involved in the immune response taking place in this tissue. The epidermis is organized in several layers. The most external layer is the stratum corneum, made up of dead keratinocytes. Next is the stratum lucidum, a very thin layer found mainly in areas such as the palms and soles. The third layer is the stratum granulosum, formed by rhomboid cells containing large granules of keratin, which is followed by the stratum spinosum, a layer formed by polygonal cells with remarkable intracellular adhesions. Finally, the inner layer is the stratum basale, which contains a few layers of cubic cells with a high proliferative potential [11].

The middle layer of the skin, the dermis, is located beneath the epidermis. This layer mainly comprises connective tissue fibers (eg, collagen, elastin).

The last layer of the skin is the hypodermis, which comprises mainly loose connective tissue, thus enabling the skin to slide over subjacent organs.

### Mucosal Immune System

The need for permeability in the epithelial lining of mucous membranes (food absorption, gas exchange, reproduction) creates vulnerability to pathogens, making these

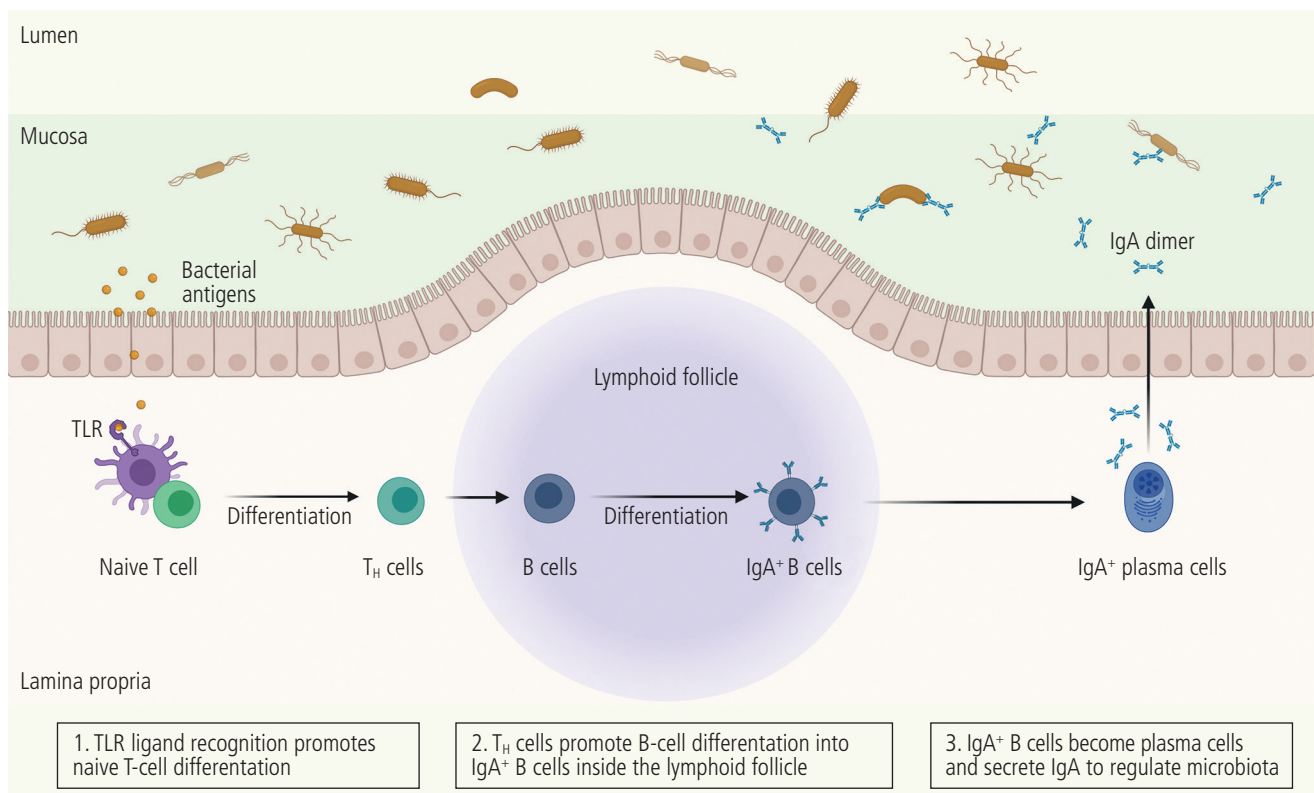


**Figure 1.** Immune protection by secretory IgA. (1) Antigen presenting cells of the mucosa can sense bacterial antigens through pattern recognition receptors such as toll-like receptors (TLRs) and induce naive T-cell differentiation to T helper (T<sub>H</sub>) cells. (2) T-cell activation can take place in special lymphatic tissue of the mucosa, where T<sub>H</sub> cells promote class switching in germinal center B cells to produce IgA (IgA<sup>+</sup> B cells). (3) The IgA<sup>+</sup> B cells differentiate to plasma cells that produce dimeric IgA (IgA<sup>+</sup> plasma cells), which becomes secretory IgA (sIgA) and is transported to the mucus to block entry of bacteria and regulate microbiota. Adapted from "IgA-mediated Gut Microbiota Regulation", by BioRender.com. Retrieved from <https://app.biorender.com/biorender-templates>.

regions a gateway for many infectious agents. Nonetheless, mucosal tissues rely on the larger part of the immune system (comprising mucus layers, epithelial cells, lymphoid tissues, and immune molecules situated in the mucosal membranes of the gut, the respiratory system, and the urogenital tract), thus providing a first line of defense for the internal body surfaces.

Mucosal tissues are continuously exposed to external stimuli, thus potentially leading to endless systemic proinflammatory responses. However, the mucosal immune system counts on 2 strategies to preserve homeostasis: (1) immune exclusion by secretory IgA antibodies, and (2) a confined tolerogenic immune response. Immunoglobulins (Igs) are the first barrier defense of mucosa tissues, in which polymeric IgA is the predominant isotype, except in the lower respiratory and genital tracts, where IgG is the major isotype [19,20]. Secreted IgA is synthesized by plasma cells derived from activated B cells in the lamina propria (Figure 1). Then, the antibody binds the polymeric Ig receptor expressed on the basolateral surfaces of epithelial cells, thus facilitating internalization of polymeric IgA, transport to the apical side, and release to the lumen. Subsequently, polymeric IgA blocks the access of antigens and pathogens to the epithelial barrier and enhances their agglutination [19,21]. Microorganisms become trapped in the mucus layer to be later eliminated by peristaltic and mucociliary events [22].

Alterations in epithelial barrier integrity could lead to invasion by pathogens. To avoid this, the mucosal immune system comprises inductive and effector sites, where the

immune response is initiated and manifested, respectively. The response to microorganisms is initiated by epithelial cells and antigen-presenting cells (APCs). The epithelial barrier is situated underneath the mucus layer, and contains different types of specialized epithelial cells that vary according to the organ and contribute to mucosal immune regulation [16] (Figure 2). Goblet cells secrete mucins and antimicrobial peptides, which play a critical role in antigen transfer from luminal tissue to the lamina propria, contributing to food tolerance [23]. Additionally, the human airway epithelium contains another type of secretory cell, club cells, which produce glycoproteins, lipids, and peptides to provide chemical and physical protection in the airway [24,25]. Club cells have been shown to be altered in inflammatory diseases, such as allergy [26]. Besides, in response to epithelial injury, club cells differentiate into ciliated and goblet cells [24]. Paneth cells are located in the epithelium of the small intestine and sustain homeostasis by releasing antimicrobial peptides and proteins that regulate the amount of commensal and pathogenic microorganisms [27,28] (Figure 2). Additionally, endocrine cells (eg, enteroendocrine and neuroendocrine cells) are found along the epithelial barrier and may secrete a wide range of peptide hormones and neuropeptides, such as serotonin, vasoactive intestinal peptide, and  $\gamma$ -aminobutyric acid, which influence the function of immune cells [29,30] (Figure 2). Individual chemosensory cells called tuft cells (also known as brush cells or microvillus cells) (Figure 2), which help to expel helminths and generate a type 2 immune response, are distributed along the mucosal epithelium [31]. Tuft cells produce IL-25 and stimulate the development of type 2 innate lymphoid cells (ILC2s), which could lead to intestinal eosinophilia [32,33]. However, the specific role of tuft cells in allergy remains to be clarified. Another highly specialized cell is the microfold (M) cell, which is a unique epithelial subtype that overlies the lymphoid tissue and plays a role in transepithelial antigen transport (Figure 2). M cells take up luminal microbes through phagocytosis, endocytosis, or transcytosis and deliver them to dendritic cells (DCs) located in the lamina propria (Figure 2). Moreover, M cells can express IgA receptor on their apical surface to bind and transport secretory IgA-bound antigens [19,34]. This antigen-transport function suggests that M cells may contribute to the genesis of allergy. Finally, epithelial cells present supplementary immune-regulatory features, such as class I and II major histocompatibility complex expression [35], which enables them to present antigens to T cells. This occurs concomitantly with CD23 expression (the low-affinity receptor for IgE, Fc $\epsilon$ RII), which enables the epithelial cells to transport IgE and IgE-immune complexes across the epithelial monolayer [36]. Although robust evidence supports a role for epithelial cells in the mucosal immune response, studies focusing on the specific involvement of individual epithelial cell subtypes in allergy are scarce.

Apart from the abovementioned luminal-antigen transference strategies of epithelial cells, antigens can be directly taken up by DCs with extending transepithelial dendrites and their own TJ proteins [37] (Figure 3). When the epithelial barrier is not damaged, antigens enter at specific sites underneath lymphoid follicles, composed mainly of clustered B-cell follicles interspersed with T-cell zones and a

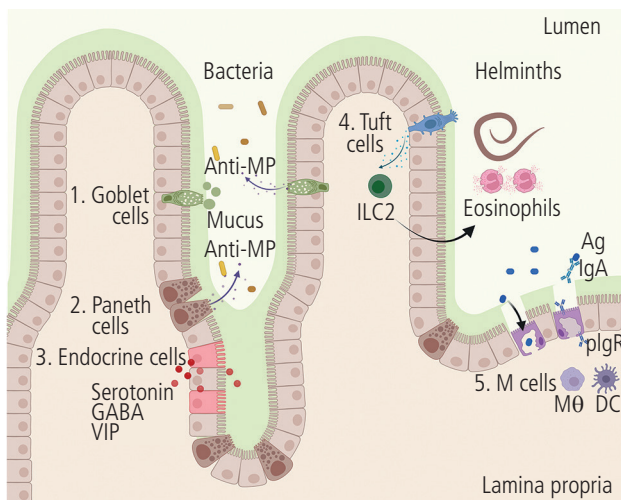


**Figure 2.** Mucosal epithelial cells. The epithelial cell barrier is home to specialized cell types with mucosa protective functions in the mucosa. The figure shows a section of the small intestine. (1) Goblet cells producing mucus and secreting antimicrobial peptides (Anti-MP); (2) Paneth cells releasing anti-MP; (3) Endocrine cells secreting neuropeptides such as serotonin, vasoactive intestinal peptide (VIP), and  $\gamma$ -aminobutyric acid (GABA); (4) Tuft cells participate in the response against helminths by stimulating type 2 innate lymphoid cells (ILC2s), which lead to intestinal eosinophilia; and (5) Microfold (M) cells capture luminal microbes and deliver them to dendritic cells (DCs) and macrophages (M $\Phi$ ) located in the lamina propria. M cells express the polymeric IgA receptor (pIgR) to bind and transport secretory IgA-bound antigens (Ag). Adapted from "Intestinal Epithelium (Background)", by BioRender.com. Retrieved from <https://app.biorender.com/biorender-templates>.

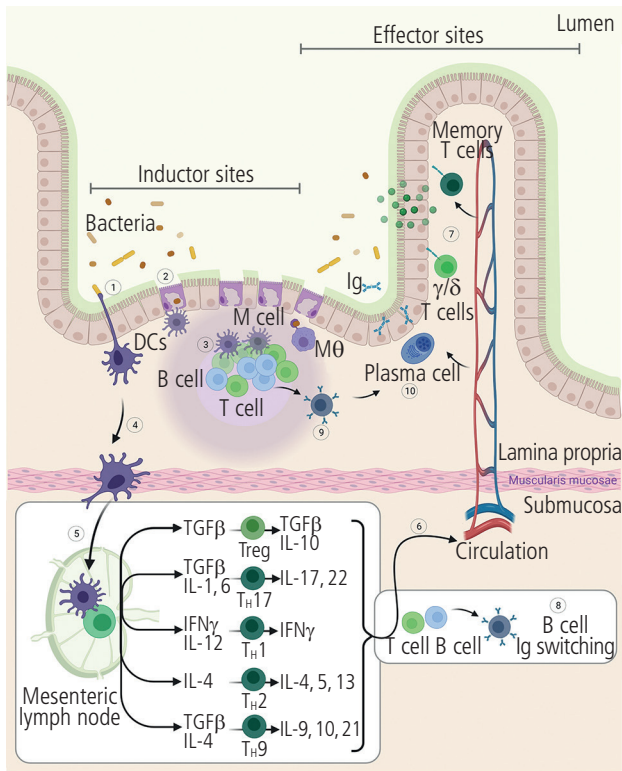


**Figure 3.** Mucosal immune system. The classic inductive sites consist of antigen-sampling M cells, T-cell areas, B-cell follicles, and antigen-presenting cells, which form mucosa-associated lymphoid tissue (MALT). Antigens can be captured by (1) dendritic cells (DCs) in the epithelium via dendrites extending directly into the lumen or (2) transported by M cells. Both cases induce DC maturation and migration to the T-cell zone (3) in MALT and (4) into draining mesenteric lymph nodes. (5) There, DCs trigger T-cell activation, which depends on the nature of the antigen and the local microenvironment. This results in T-cell differentiation and (6) homing to effector sites. (7) Activated T cells finish in the epithelium, where intraepithelial  $\gamma\delta$ -T cells are also situated. Class switching to IgA occurs in (8) mesenteric lymph nodes and in (9) MALT. (10) Then, primed B cells differentiate to plasma cells that migrate to the lamina propria, where they produce Igs, which can be secreted to the lumen. Adapted from "Intestinal Epithelium (Background)", by BioRender.com. Retrieved from <https://app.biorender.com/biorender-templates>.

variety of APCs. This organized structure is known as mucosa-associated lymphoid tissue (MALT), and, together with local lymph nodes, it is where the mucosal immune system is initiated (Figure 3) [38]. Mucosa-associated lymphoid tissue is classified according to its location as gut-associated lymphoid tissue, bronchial/tracheal-associated lymphoid tissue, nose-associated lymphoid tissue, and vulvovaginal-associated lymphoid tissue.

Epithelial cells and APCs are informed of the presence of microbes via pattern recognition receptors (Figures 1 and 3). Not all microorganisms are pathogenic (eg, microbiota). Thus, polar expression (apical versus basolateral side) of pattern recognition receptors is crucial for preventing unnecessary inflammatory responses. Under homeostatic conditions, interaction with microbiota induces transforming growth factor- $\beta$  (TGF- $\beta$ ), retinoic acid, and thymic stromal lymphopoietin (TSLP), which promote tolerogenic APCs and, together with IL-10, the induction of regulatory T cells

(Tregs) [39,40]. Tolerogenic APCs and Tregs stimulate B-cell class-switching to IgA production, which, after maturation, generates plasma cells able to migrate to the mucosa [41,42]. To achieve a successful IgA switch, ILC3s need to provide lymphotoxin- $\beta$  receptor-dependent signals to DCs and stromal cells [43]. ILC3s play a major role in maintaining tolerance in the gut mucosa by stimulating B-cell differentiation, the development of isolated lymphoid follicles, and the production of IL-22, IL-17, and GM-CSF [44]. A newly identified regulatory ILC (ILCreg) has been shown to participate in preserving gut homeostasis via the secretion of IL-10 and TGF- $\beta$  and relieving intestinal inflammation [45]. The role of ILC1s and ILC2s in the healthy gut is still unclear. In contrast, both subtypes are key to preservation of the epithelial barrier under pathogenic conditions [46,47].

Upon sampling antigens, conventional DCs migrate to draining lymph nodes to present them to naïve T lymphocytes (Figure 3). Depending on the antigen source and the cytokine environment, activated conventional DCs can polarize naïve T cells to T helper cell ( $T_H$ ) phenotypes, namely  $T_H1$ ,  $T_H17$ ,  $T_H2$ , and  $T_H9$  [48] (Figure 3). Pathogens that accumulate inside the vesicles of conventional DCs stimulate the differentiation of  $T_H1$  cells, whereas the prototypical response to helminths is characterized as  $T_H2$  [49]. Segmented filamentous bacteria lead to differentiation of  $T_H17$  cells in the small intestine [50], and the commensal *Staphylococcus aureus* and the opportunistic fungus *Candida albicans* are thought to induce polarization of  $T_H9$  cells [51]. Then, polarized T cells, together with antigen-activated conventional DCs, promote class switching of B cells, which prevent the spread of the infection. B and T cells subsequently migrate to the mucosa effector sites, where they express their effector functions, mainly releasing immunomodulatory cytokines.

In the event of infection, different types of immune cells are recruited through specialized vascular structures that allow lymphocytes to migrate into the tissue [52]. Bacterial and viral infections trigger a type 1 response (activation of  $T_H1$  cells, natural killer cells, ILC1,  $T_H17$  cells, and ILC3), which includes the release of proinflammatory cytokines (IL-1 $\beta$ , IL-18, IFN- $\gamma$ ) [53] and cytokines with protective functions (IL-23, IL-22, and IL-17) [54,55]. Then, neutrophils are recruited to produce a wide range of proinflammatory and anti-inflammatory effector molecules [56], which in turn contribute to the recruitment of other immune cells to control pathogen spread and later release the factors necessary for the resolution of inflammation.

Tick, insect, and snake bites and stings and helminth invasions trigger a type 2 response (activation of ILC2,  $T_H2$  cells, eosinophils, basophils, and mast cells). This is initiated by tuft cells, which release alarmins (TSLP, IL-25, and IL-33) that stimulate the production of IL-4, IL-5, and IL-13 and enhance B-cell class switching to IgE [57,58]. Similarly, allergic patients display a type 2 inflammatory response that is initiated after allergen exposure and results in the production of allergen-specific IgE, which might lead to airway hyperresponsiveness and mucus production [6,59].

The mucosal immune system also counts on intraepithelial  $\gamma\delta$ -T cells, ie, T cells that express the T-cell receptor  $\gamma\delta$  (TCR- $\gamma\delta$ ) and are located specifically in the epithelia of mucosal tissues. These T cells scan for signs of cellular stress

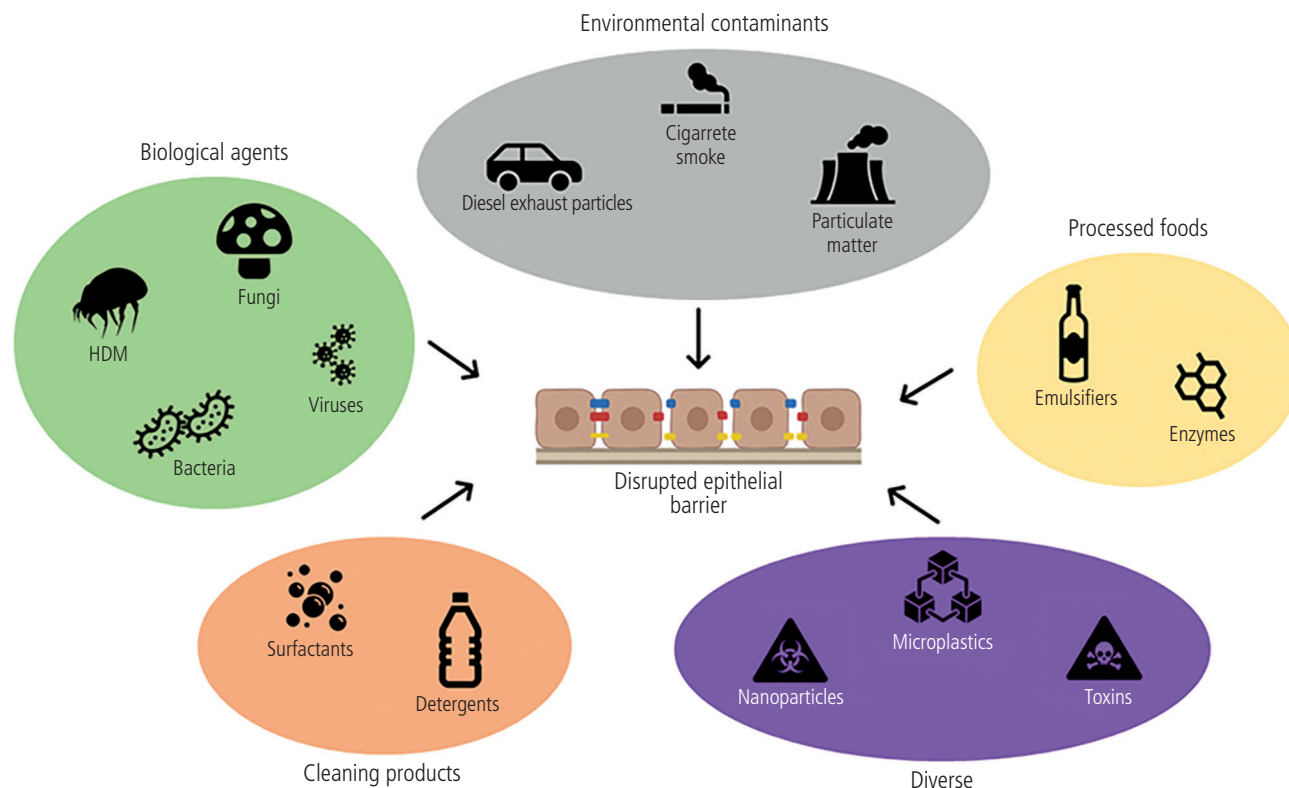


**Figure 4.** Environmental factors in epithelial barrier dysfunction. Human skin and mucosa are exposed daily to environmental contaminants (cigarette smoke, particulate matter, diesel exhaust particles, ozone, nanoparticles, and microplastics), airborne biological agents (house dust mites [HDM], bacteria, fungi, viruses) containing toxins and allergens, cleaning products containing surfactants and detergents, and processed food containing enzymes and emulsifiers, all of which have proven toxic for epithelial cells.

and respond with rapid effector functions (eg, lysing cells) when they detect infected or transformed host cells or if they sense critical information from other mucosal leukocyte populations. Recent data suggest that  $\gamma\delta$  T cells might be implicated in allergic airway diseases (asthma, rhinitis) and in intestinal hypersensitivity processes (food allergy, celiac disease), although the significance of this observation is not well known [60,61].

## Epithelial Barrier Remodeling in Allergy

Common allergic diseases in industrialized areas include allergic rhinitis (already common in the late 19th century), allergic asthma, atopic dermatitis (which reached epidemic proportions after the 1960s) [62-64], food allergy, eosinophilic esophagitis, and drug-induced anaphylaxis (considered epidemic since 2000) [65-67]. Many allergens derived from environmental agents such as dust mites, bacteria, fungi, viruses, and toxins are encountered daily by humans as a consequence of industrialization. In addition, human skin and mucosa are exposed daily to substances commonly used for laundry and household cleaning (eg, detergents and surfactants), enzymes and emulsifiers in processed food, cigarette smoke, particulate matter, diesel exhaust fumes,

ozone, nanoparticles, and microplastics. These agents have proven toxic for epithelial cells [68-71] (Figure 4).

The ability of the epithelium to control the balance between tissue damage and repair signals is essential if we are to limit epithelial damage, subsequent inflammation, and development of disease [72]. When the remodeling of epithelial barriers leads to increased leakiness, it also causes microbial dysbiosis and the translocation of bacteria to subepithelial areas, which induces tissue microinflammation [73] and sustained T-cell activation, with these alterations potentially underlying the onset of various allergic diseases [68].

Atopic dermatitis (AD) is an inflammatory skin disorder that affects 25% of children and 10% of adults and carries a higher risk of allergic rhinitis and asthma later in life. Filaggrin mutations and TJ protein deficiency (claudin-1, claudin-4, and claudin-6) have been described in the skin of patients with AD [74-80]. A recent gene expression analysis by RNA sequencing performed on matched lesional and nonlesional skin tissue biopsies from AD patients and healthy persons revealed that cell adhesion, cadherin signaling, and keratinization are the most differentially expressed gene groups in patients with AD. Of those, genetic expression levels of CLDN4 and TJP1 negatively correlated with *Staphylococcus aureus* in lesional samples [74]. A decrease in skin microbiota diversity due to an abundance of *S aureus* has been linked with the severity

of AD [74,81]. The role of *S aureus* in allergic diseases is controversial. A recent study on asthmatic patients showed that sensitization to *S aureus* enterotoxin B was associated with the presence of AD and with an increased risk of sensitization to common aeroallergens [82]. It is increasingly clear that the complex interaction between the skin microbiota, the epithelial barrier, and the immune system is key to our understanding of the development of AD.

AD is primarily a  $T_H2$  cell-driven disease, with variable numbers of eosinophils and where IgE is considered only to play a bystander role. Targeting the  $T_H2$  signature cytokines IL-4 and IL-13 with biological antagonists has proven effective for treatment of AD, indicating that both are major players in inducing skin inflammation in this disease [83-87]. In contrast, studies targeting the epithelial alarmins TSLP and IL-33 have not yet shown any effects on AD [88,89]. Emerging evidence shows that mast cells, eosinophils, and basophils are pivotal effector cells in causing pruritus in AD [90,91]. Chronic pruritus is a major clinical complaint in AD, since it considerably reduces quality of life and is difficult to treat [92]. Basophils and eosinophils infiltrate the skin in AD [93] and are located close to the nerves, thus providing a bridge between the neuronal and immune systems and amplifying local immune reactions [94]. Recent findings indicate that skin barrier defects support induction of pruritus [95]. In AD, chronic scratching worsens clinical symptoms. The impaired barrier function associated with the itch-scratch cycle further augments this positive feedback loop. IL-31 has recently emerged as one of the most effective approaches for treating pruritus in AD [96-99].

Allergic asthma is a heterogeneous lung disease characterized by chronic airway inflammation. It produces remodeling of the airway respiratory mucosa, causing airway obstruction and the subsequent loss of respiratory function [100,101]. Upon contact with a trigger (eg, viral infections, allergens, or pollution), asthma becomes exacerbated [102]. Given the ubiquitous presence of triggers and the heterogeneity of asthma patients, exacerbations cannot be fully prevented [103]. Airway mucosa remodeling in asthma can affect different layers of the epithelial barrier, namely, the airway smooth muscle below the epithelium, the extracellular matrix, the basal epithelial cell line, the epithelial layer itself, and even the lumen [101,104]. The airway smooth muscle tends to thicken with chronic inflammation, causing hypertrophy and hyperplasia, lowering the contractile potential of the airway tissue, and, hence, diminishing function [105,106]. This process often goes hand in hand with an increase in deposition of the extracellular matrix, which has been linked to an increase in arginase activity that releases precursors for synthesis of nitric oxide [107]. This process can be repressed by endogenous compounds such as asymmetric dimethylarginine, which inhibit nitric oxide synthase [107,108]. Interestingly, recent research has shown that in vitro culture of healthy epithelia incubated with Der p 1 produced higher amounts of asymmetric dimethylarginine than damaged epithelia [109]. Moreover, Der p 1 is a known proteolytic allergen that can cleave and disrupt TJs [110]. This disruption of TJs in the epithelial layer not only dysregulates epithelial cell differentiation, but also enables entry of other allergens and pathogens, which can then trigger continuous

exacerbations [111-113]. This process is characterized by decreased expression of structural proteins forming the TJs such as occludin, zonula occludens proteins, and claudin-18 in the epithelial cells [113,114]. Nevertheless, continuous release of histamine, IL-4, and TNF- $\alpha$  by basophils and T cells also promotes epithelial permeabilization in primary human bronchial epithelial cells and mouse models, thus suggesting the chronic  $T_H2$  allergic response as the main driver of the phenotype [115]. The loss of TJs is associated with changes in the type of cells that make up the epithelial layer. Remodeling is characterized by an increase in the number of goblet cells, which induces mucus overproduction and secretion to the airway lumen, reduces oxygen exchange, and obstructs the airway, thus impairing respiratory function [68]. It has recently been reported that microRNA 141 (miRNA141) may play a key role in this process. This miRNA is abundantly detected in the human airway epithelium, and its expression can be induced upon airway allergen challenge in asthma. Strikingly, inhibition of miRNA141 lowered airway hyperreactivity and suppressed mucus overproduction by IL-13 signaling [116].

Chronic inflammatory diseases can also influence the structure of the nasal mucosa. This is evident in chronic rhinosinusitis with nasal polyps (NP), in which the normal mucosa undergoes a remodeling process comprising rupture of the epithelial layer, proliferation of fibrotic tissue, deposition of the extracellular matrix, development of edema, and infiltration of immune cells and thin-wall vessels [117-119]. In this process,  $T_H2$ -related cytokines such as IL-4, IL-5, and IL-13 play a key role by recruiting eosinophils to the area; these would be responsible for causing edema and maintaining the inflammatory cascade over time [120,121]. Interestingly, recent research suggests that the basal epithelial cells may also play an important role in this process. Ordovas-Montanes et al [122] proposed that basal cells derived from NP may play a role in the reappearance of NP, in contrast with basal cells from healthy nasal mucosa, which constitutively maintain expression of the Wnt pathway in NP. Wnt genes are mostly induced by IL-4/IL-13 and limit basal cell differentiation to secretory cells. The authors showed that basal cells in NP could maintain Wnt expression without the presence of IL-4/IL-13 mirroring an inflammatory "memory" phenotype, inhibiting their differentiation, and promoting relapse of NP [122].

Remodeling also plays an important role in eosinophilic esophagitis, an antigen-driven  $T_H2$  disease in which chronic eosinophilic inflammation causes esophageal dysfunction [122,123]. Eosinophilic esophagitis is driven mainly by food allergens, although certain aeroallergens can also initiate the disease [124-127]. Interestingly, IgG4, rather than IgE, appears to be the main driver of the disease, as treatment with omalizumab (anti-IgE) is not effective and deposits of IgG4 and IgG4-expressing plasma cells were observed in biopsies from patients with eosinophilic esophagitis [128]. Eosinophilic esophagitis is defined by edema, exudates, longitudinal furrows, and esophageal narrowing in advanced disease. All these changes ultimately cause epithelial barrier dysfunction. At the structural level, the loss of several structural proteins, such as desmoglein 1, E-cadherin, occludin, and claudins 1 and 7, leads to decreased numbers of desmosomes and other intercellular junctions [129-132]. This promotes an

epithelial-to-mesenchymal transition, in which epithelial cells transdifferentiate to fibrotic cells, leading to remodeling of the mucosal layer [133].

Finally, little is known about the effect of food allergy on the remodeling of the mucosal layers. Recent reports show that individuals with severe allergic respiratory disease living in areas of high allergen exposure present remodeling in the oral mucosa mediated by allergic reactions characterized by impaired TJ formation, immune cell infiltration, and overproduction of extracellular matrix [134,135]. This suggests that the oral mucosa might play a key role in allergic sensitization, tolerance, and mucosal remodeling. This notion is supported by the tolerogenic properties of the secondary organs linked to the oral mucosa (tonsils) and the success of oral allergen immunotherapy [136-138]. However, gut mucosal remodeling in food allergy is a very unexplored field, probably owing to the continuous avoidance of antigen exposure as a common treatment. Nevertheless, the interplay between gut microbiota and intestinal eosinophils has been

hypothesized to cause intestinal alterations in the epithelial barrier [139]. In any case, these processes should be further investigated (Figure 5).

#### 4. Effect of the Inflammatory Response on the Epithelial Barrier

Once inflammation has fulfilled its purpose, it must be controlled to prevent it from becoming chronic. Thus, there is a change in proinflammatory factors, which are responsible for activation of the immune response, towards a proresolving environment, which is achieved by the production of proresolving agents (Figure 6).

Proresolving agents are anti-inflammatory mediators that meet a series of requirements [140], as follows: (1) limiting the recruitment, infiltration, and activation of leukocytes (particularly neutrophils, which are the first to enter the site of inflammation and initiate phagocytosis

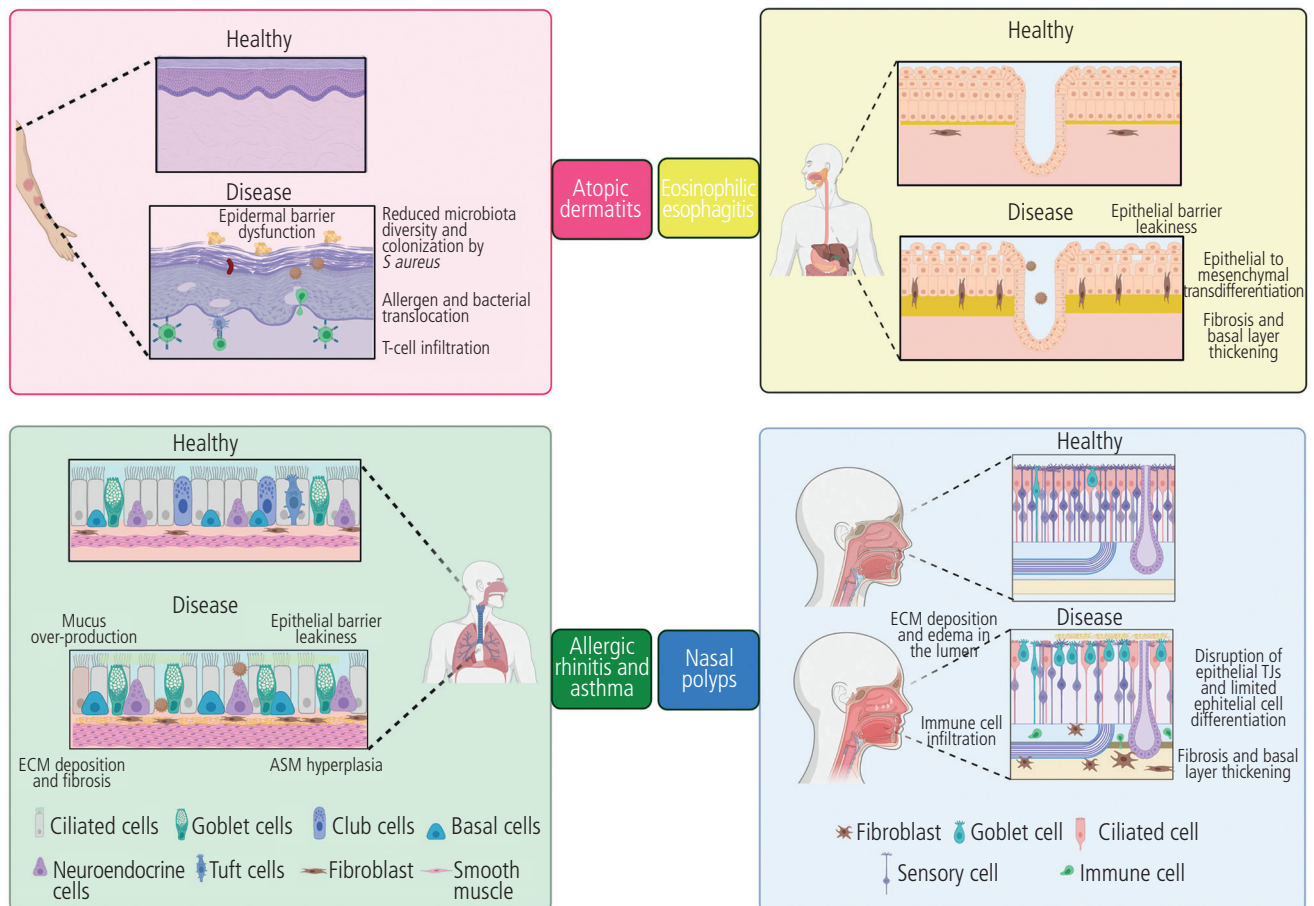


**Figure 5.** Epithelial remodeling in allergic diseases. Characteristic epithelial remodeling of mucosal surfaces in atopic dermatitis (top left, pink), eosinophilic esophagitis (top right, yellow), allergic rhinitis and asthma (bottom left, green), and nasal polyps (bottom right, blue). Remodeling in atopic dermatitis is characterized by dysfunction of the epithelial barrier, reduced diversity of skin microbiota, increased allergen translocation, and T-cell infiltration. Eosinophilic esophagitis is characterized by barrier leakiness, epithelial-to mesenchymal transdifferentiation, fibrosis, and basal layer thickening. Allergic rhinitis and asthma remodeling takes place in the airways and is defined by increased extracellular matrix (ECM) deposition and fibrosis, hyperplasia of the airway smooth muscle (ASM) layer, barrier leakiness, and overproduction of mucus. Nasal polyps are characterized by increased ECM deposition and edema in the lumen, limited cell differentiation and tight junction (TJ) disruption, immune cell infiltration, and basal layer thickening.



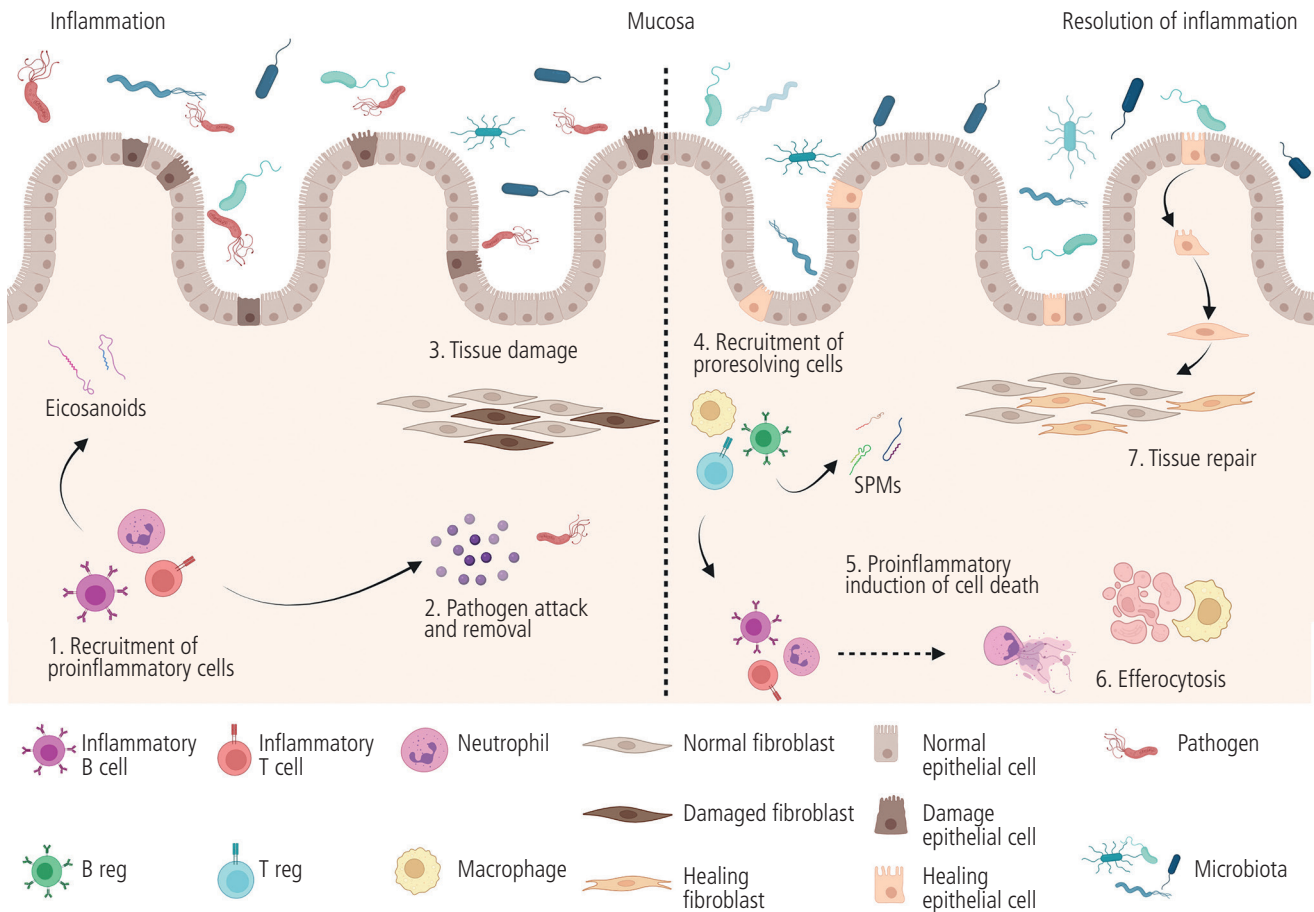


**Figure 6.** Comparison of the inflammatory response in the proinflammatory vs the resolution states. When a menace (eg, pathogens, injury, allergens) is encountered, a proinflammatory response ensues, starting with the recruitment of proinflammatory cells (1). These cells orchestrate the immune response using inflammatory mediators (eg, lipid mediators, such as eicosanoids and cytokines), with the aim of attacking and eliminating the threat (2). However, the inflammatory immune response might lead to tissue damage (3), which may remain chronic if inflammation is not appropriately resolved. Thus, after the threat is removed, the immune environment shifts towards a proresolving status via recruitment of regulatory immune cells (4). These cells ensure that homeostasis is restored using proresolving mediators (ie, anti-inflammatory cytokines and specialized proresolving mediators [SPMs]), which clear the inflammatory site of proinflammatory cells, both by stopping recruitment and by activating cell death (neutrophil extracellular trap, apoptosis) (5). Cell debris is eliminated by phagocytic cells, such as macrophages, in a process called efferocytosis (6), which prevents re-establishment of inflammation. Finally, tissue needs to be repaired, a process that is largely regulated by epithelial-mesenchymal transition (7).

of microbes [141]); (2) promotion of the recruitment of noninflammatory (nonphlogistic) immune cells; (3) induction of apoptosis and clearance of neutrophils (efferocytosis); (4) inhibition of proinflammatory mediators such as cytokines; (5) induction of an anti-inflammatory status; and (6) activation of tissue regeneration and healing, restoration of homeostasis [142,143]. Resolution of inflammation is tissue-specific, with both general and organ-specific characteristics [141], thus explaining differences in regeneration between locations (eg, skin, which generates scars upon repair vs the liver, which regains total function) [144,145]. It is important to note that the resolution phase is bound to happen from the onset of the inflammatory reaction [146] and comprises, like inflammation itself, 5 “pillars” of resolution: removal (of microbes, dead cells, and cellular debris), restoration (of vascular integrity), regeneration (of tissue), remission

(of fever and other inflammatory symptoms), and relief (of pain) [147].

First, proinflammatory cells and mediators must be depleted and substituted by others that can induce proresolving environments via nonphlogistic recruitment of cells, apoptosis of neutrophils, and evacuation of inflammatory cells from the tissue [148,149]. This process involves lipid mediators such as resolvins, protectins, and maresins, known as specialized proresolving mediators [140,150], which can target multiple cells (eg, neutrophils, macrophages, monocytes, T cells, and epithelial and endothelial cells) [140] and regulate apoptosis, efferocytosis, and tissue regeneration, thus preventing the activation of proinflammatory immune responses and fibrosis [140,147-152]. There is also evidence suggesting that proinflammatory mediators and cells play a role in the resolution of inflammation. For example, NFκB is a transcriptional factor that, during acute inflammation,

activates the production of proinflammatory cytokines; however, it also has a role in resolution of inflammation (eg, by increasing apoptosis of lymphocytes and neutrophils) [152], thus showing it to be a key regulator of the immune response.

The first steps in resolution of inflammation are directed towards stopping the recruitment of neutrophils and eliminating those that have already served their purpose. Neutrophils can undergo apoptosis, reverse migration, or lymphatic drainage [143]. Apoptosis is the main mechanism and is considered the desired form of cell death, being key in the regulation of resolution of inflammation. Other kinds of cell death, such as autophagy, pyroptosis, necrosis, and neutrophil extracellular traps usually lead to the maintenance of inflammation and tissue damage [143].

Efferocytosis of apoptotic neutrophils is essential for favorable resolution of inflammation. It is undertaken by phagocytic cells, especially monocytes and macrophages, which, upon recognition of apoptotic neutrophils, are skewed from a proinflammatory status towards an anti-inflammatory and proresolving status (from classic to alternately activated macrophages) [153]. Defects in efferocytosis usually delay resolution of inflammation and cause diseases such as systemic lupus erythematosus, where patients develop autoantibodies against intracellular components of the apoptotic cells released into the tissue [154].

Tissue repair is the next critical step in regaining homeostasis. It is directed mainly by the immune system (neutrophils and macrophages), although fibroblasts, epithelial and endothelial cells, and platelets are also needed for successful repair [155,156]. The numerous factors involved in resolution include growth factors and interleukins. Tissue repair requires proliferation and migration of epithelial cells, as well as proliferation of fibroblasts, usually through epithelial to mesenchymal transition [157], matrix deposition, and angiogenesis. While this process normally leads to remodeling of the tissue, final repair depends on the organ involved, as mentioned above [144,155].

Likewise, tissue repair mechanisms depend on the type of inflammation. For example, TGF- $\beta$  is critical after type 1 and type 17 inflammation, whereas IL-13 is responsible for tissue repair in type 2 cases [155].

Recent studies propose that, at the end of inflammation, tissue does not return to previous homeostasis, but rather achieves an adapted homeostatic state in which, despite recovery of organ architecture and function, there are changes in cellular composition and phenotype, thus affecting the severity of future inflammatory responses [143,158,159]. Consequently, at this stage, the risk of developing chronic inflammation or autoimmune diseases may outweigh the potential benefit of rapid response in the case of a new infection [158].

Chronic infections caused by opportunistic pathogens such as *Staphylococcus aureus* might develop after achievement of adaptive homeostasis, potentially leading to diseases such as asthma [68].

Inflammatory responses are needed against insults that might produce disease, such as pathogens. Under normal conditions, inflammation is usually stopped on time thanks to proresolving and anti-inflammatory mediators and cells, which are released from initiation of the response. Both proinflammatory and proresolving states are needed to ensure

successful tissue regeneration. However, it is necessary to strike a delicate balance, which is easily broken if any of the pieces are disturbed.

## Epithelial Barrier and Allergic Sensitization

An altered epithelial barrier may be critical to our understanding of allergic sensitization. Early viral infection significantly increases the risk of developing asthma. In fact, Kusel et al [160] stated that children who develop viral infections in the first 6 months of life had an OR of 4.1 of having asthma. In the same study, mite exposure was only associated with an OR of 2.3. Interestingly, both risk factors combined increased the risk of asthma to an OR of 9.0. Lopez-Rodriguez et al [109] recently explained this effect. The proteolytic activity of Der p 1 affects epithelial maturation and consolidates inflammation only if the epithelium is not well established, as is the case during early viral infection. Moreover, the same authors demonstrated that high endogenous levels of glutathione S-transferase, a phenotype that has been associated with asthma, promote the enzymatic activity of Der p 1 [161]. Interestingly, Barber et al [162] demonstrated that the prevalence of sensitization to Der p 1 was higher in children than in adults, while sensitization and sIgE levels to Der p 2 were higher in adults, suggesting early sensitization to mites and subsequent progression governed by Der p 2.

A second frequent respiratory sensitizer in children is *Alternaria* species. The reason for this is unclear, as other naturally abundant mold species present a lower sensitization rate in the population. Recently Garrido-Arandia et al [163] demonstrated that Alt a 1, the major *Alternaria* allergen, interacts with the epithelial SLC22A17 receptor, thus promoting allergic sensitization. Remarkably, *Alternaria* spores colonize dead grass and are aerosolized together. It has been demonstrated that there are Phl p 1-like allergens in *Alternaria* spores and that Alt a 1 and Phl p 1 interact; this promotes cosensitization and potentially explains the progression of sensitization to grass pollen. Interestingly, despite being of relatively low abundance [164], Phl p 1 is the leading grass pollen allergen sensitizer [165]. As in the case of Der p 2 in mites, the Phl p 5 grass pollen allergen is usually a marker of progression of grass allergy, not an early indicator of sensitization. A similar interaction has been described between Alt a 1 and thaumatin, a relevant plant allergen [166], suggesting a pivotal role of *Alternaria* in the onset of food allergy. Notably, in most cases, early sensitization to *Alternaria* resolves spontaneously later in life, although its effect as a “gate opener” for allergic sensitization to other sources should not be neglected [167].

Allergic sensitization to aeroallergens in the presence [135] or absence [134] of food allergy was recently shown to alter the mucosal barrier, suggesting a systemic barrier defect and an association with severity of allergic disease. This process seems to be associated with systemic signatures [168] that point to factors such as T-cell proliferation [169], sphingolipids [170], arachidonic route signaling, and platelet function [171]. Such findings might prove relevant to our understanding of allergic sensitization and disease

progression and reinforce our approach to allergic diseases, where barrier function is pivotal.

## Acknowledgments

We would like to thank the Institute of Applied Molecular Medicine (IMMA, Universidad CEU San Pablo, CEU Universities, Madrid). The figures were created with BioRender.com.

## Funding

This work was supported by ISCIII (PI18/01467 and PI19/00044), cofunded by FEDER “Investing in your future” for the thematic network and co-operative research centres ARADyAL RD16/0006/0015. This work was also supported by Agencia Estatal de Investigación, Ministry of Science and Innovation in Spain (PCI2018-092930), cofunded by the European program ERA HDHL - Nutrition & the Epigenome, project Dietary Intervention in Food Allergy: Microbiome, Epigenetic and Metabolomic interactions DIFAMEM. MID-D and JR-C are supported by FPI-CEU predoctoral fellowships.

## Conflicts of Interest

DB reports grants from ALK and Allero Therapeutics and personal fees from ALK and AIMMUNE. The remaining authors declare that they have no conflicts of interest.

## References

- McGhee JR, Fujihashi K. Inside the Mucosal Immune System. *PLOS Biol.* 2012;10:e1001397.
- Brizuela M, Winters R. Histology, Oral Mucosa. Treasure Island (FL): 2021.
- Hewitt RJ, Lloyd CM. Regulation of immune responses by the airway epithelial cell landscape. *Nat Rev Immunol.* 2021;21:347-62.
- Şenel S. An Overview of Physical, Microbiological and Immune Barriers of Oral Mucosa. *Int J Mol Sci.* 2021;22:7821.
- Gohy S, Hupin C, Ladjemi MZ, Hox V, Pilette C. Key role of the epithelium in chronic upper airways diseases. *Clin Exp Allergy.* 2020;50:135-46.
- Escribese MM, Gómez-Casado C, Barber D, Diaz-Perales A. Immune Polarization in Allergic Patients: Role of the Innate Immune System. *J Investig Allergol Clin Immunol.* 2015;25:251-8.
- Shin K, Fogg VC, Margolis B. Tight Junctions and Cell Polarity. *Annu Rev Cell Dev Biol.* 2006;22:207-35.
- Bergmeier LA. Oral Mucosa in Health and Disease. Cham: Springer International Publishing; 2018.
- Gomez-Casado C, Sanchez-Solares J, Izquierdo E, Díaz-Perales A, Barber D, Escribese MM. Oral mucosa as a potential site for diagnosis and treatment of allergic and autoimmune diseases. *Foods.* 2021;10:1-22.
- Hull J. Kendig's Disorders of the Respiratory Tract in Children. *Arch Dis Child.* 1998;79:292.
- Mescher A. Junqueira's Basic Histology: Text and Atlas, 12th Edition. vol. 12th Ed. 2009.
- Veres TZ. Visualizing immune responses of the airway mucosa. *Cell Immunol.* 2020;350:103865.
- Frey A, Lunding LP, Ehlers JC, Weckmann M, Zissler UM, Wegmann M. More Than Just a Barrier: The Immune Functions of the Airway Epithelium in Asthma Pathogenesis. *Front Immunol.* 2020;11:761.
- Shetty S, Gokul S. Keratinization and its disorders. *Oman Med J.* 2012;27:348-57.
- Groeger S, Meyle J. Oral Mucosal Epithelial Cells. *Front Immunol.* 2019;10:208.
- Ali A, Tan H, Kaiko GE. Role of the Intestinal Epithelium and Its Interaction With the Microbiota in Food Allergy. *Front Immunol.* 2020;11:604054.
- Rose EC, Odle J, Bliklager AT, Ziegler AL. Probiotics, Prebiotics and Epithelial Tight Junctions: A Promising Approach to Modulate Intestinal Barrier Function. *Int J Mol Sci.* 2021;22:6729.
- Yoo J, Groer M, Dutra S, Sarkar A, McSkimming D. Gut Microbiota and Immune System Interactions. *Microorganisms.* 2020;8:1587.
- Chen K, Magri G, Grasset EK, Cerutti A. Rethinking mucosal antibody responses: IgM, IgG and IgD join IgA. *Nat Rev Immunol.* 2020;20:427-41.
- Russell MW, Moldoveanu Z, Ogra PL, Mestecky J. Mucosal Immunity in COVID-19: A Neglected but Critical Aspect of SARS-CoV-2 Infection. *Front Immunol.* 2020;11:611337.
- Corthésy B. Multi-faceted functions of secretory IgA at mucosal surfaces. *Front Immunol.* 2013;4:185.
- Williams RC, Gibbons RJ. Inhibition of Bacterial Adherence by Secretory Immunoglobulin A: A Mechanism of Antigen Disposal. *Science.* 1972;177:697-9.
- Knoop KA, McDonald KG, McCrate S, McDole JR, Newberry RD. Microbial sensing by goblet cells controls immune surveillance of luminal antigens in the colon. *Mucosal Immunol.* 2015;8:198-210.
- Rokicki W, Rokicki M, Wojtacha J, Dzeljijli A. The role and importance of club cells (Clara cells) in the pathogenesis of some respiratory diseases. *Polish J Cardio-Thoracic Surg.* 2016;1:26-30.
- Dean CH, Snelgrove RJ. New Rules for Club Development: New Insights into Human Small Airway Epithelial Club Cell Ontogeny and Function. *Am J Respir Crit Care Med.* 2018;198:1355-6.
- Roth FD, Quintar AA, Leimgruber C, García L, Uribe Echevarría EM, Torres AI, et al. Restoration of the normal Clara cell phenotype after chronic allergic inflammation. *Int J Exp Pathol.* 2013;94:399-411.
- Lueschow SR, McElroy SJ. The Paneth Cell: The Curator and Defender of the Immature Small Intestine. *Front Immunol.* 2020;11:587.
- Vaishnav S, Behrendt CL, Ismail AS, Eckmann L, Hooper LV. Paneth cells directly sense gut commensals and maintain homeostasis at the intestinal host-microbial interface. *Proc Natl Acad Sci.* 2008;105:20858-63.
- Worthington JJ, Reimann F, Gribble FM. Enteroendocrine cells-sensory sentinels of the intestinal environment and orchestrators of mucosal immunity. *Mucosal Immunol.* 2018;11:3-20.
- Kobayashi Y, Tata PR. Pulmonary Neuroendocrine Cells: Sensors and Sentinels of the Lung. *Dev Cell.* 2018;45:425-6.

31. Schneider C, O'Leary CE, Locksley RM. Regulation of immune responses by tuft cells. *Nat Rev Immunol*. 2019;19:584-93.
32. von Moltke J, Ji M, Liang H-E, Locksley RM. Tuft-cell-derived IL-25 regulates an intestinal ILC2-epithelial response circuit. *Nature*. 2016;529:221-5.
33. Fort MM, Cheung J, Yen D, Li J, Zurawski SM, Lo S, et al. IL-25 Induces IL-4, IL-5, and IL-13 and Th2-Associated Pathologies In Vivo. *Immunity*. 2001;15:985-95.
34. Liang E, Kabcenell AK, Coleman JR, Robson J, Ruffles R, Yazdanian M. Permeability measurement of macromolecules and assessment of mucosal antigen sampling using in vitro converted M cells. *J Pharmacol Toxicol Methods*. 2001;46:93-101.
35. Wosen JE, Mukhopadhyay D, Macaubas C, Mellins ED. Epithelial MHC Class II Expression and Its Role in Antigen Presentation in the Gastrointestinal and Respiratory Tracts. *Front Immunol*. 2018;9:2144.
36. Palaniyandi S, Tomei E, Li Z, Conrad DH, Zhu X. CD23-Dependent Transcytosis of IgE and Immune Complex across the Polarized Human Respiratory Epithelial Cells. *J Immunol*. 2011;186:3484-96.
37. Knoop KA, Miller MJ, Newberry RD. Transepithelial antigen delivery in the small intestine. *Curr Opin Gastroenterol*. 2013;29:112-8.
38. Brandtzaeg P, Kiyono H, Pabst R, Russell MW. Terminology: nomenclature of mucosa-associated lymphoid tissue. *Mucosal Immunol*. 2008;1:31-7.
39. Maynard CL, Elson CO, Hatton RD, Weaver CT. Reciprocal interactions of the intestinal microbiota and immune system. *Nature*. 2012;489:231-41.
40. Hasegawa H, Matsumoto T. Mechanisms of Tolerance Induction by Dendritic Cells In Vivo. *Front Immunol*. 2018;9:350.
41. Tezuka H, Ohteki T. Regulation of IgA production by intestinal dendritic cells and related cells. *Front Immunol*. 2019;10:1891.
42. Silva-Sanchez A, Randall TD. Anatomical Uniqueness of the Mucosal Immune System (GALT, NALT, iBALT) for the Induction and Regulation of Mucosal Immunity and Tolerance. *Mucosal Vaccines*, Elsevier; 2020, 21-54.
43. Kruglov AA, Grivennikov SI, Kuprash DV, Winsauer C, Prepens S, Seleznik GM, et al. Nonredundant Function of Soluble LT $\alpha$  3 Produced by Innate Lymphoid Cells in Intestinal Homeostasis. *Science*. 2013;342:1243-6.
44. Domingues RG, Hepworth MR. Immunoregulatory Sensory Circuits in Group 3 Innate Lymphoid Cell (ILC3) Function and Tissue Homeostasis. *Front Immunol*. 2020;11:116.
45. Wang S, Xia P, Chen Y, Qu Y, Xiong Z, Ye B, et al. Regulatory Innate Lymphoid Cells Control Innate Intestinal Inflammation. *Cell*. 2017;171:201-16.e18.
46. Schulz-Kuhnt A, Neurath MF, Wirtz S, Atreya I. Innate Lymphoid Cells as Regulators of Epithelial Integrity: Therapeutic Implications for Inflammatory Bowel Diseases. *Front Med*. 2021;8:656745.
47. Morita H, Moro K, Koyasu S. Innate lymphoid cells in allergic and nonallergic inflammation. *J Allergy Clin Immunol*. 2016;138:1253-64.
48. Walsh KP, Mills KHG. Dendritic cells and other innate determinants of T helper cell polarisation. *Trends Immunol*. 2013;34:521-30.
49. Nutman TB. Looking beyond the induction of Th2 responses to explain immunomodulation by helminths. *Parasite Immunol*. 2015;37:304-13.
50. Wang Y, Yin Y, Chen X, Zhao Y, Wu Y, Li Y, et al. Induction of Intestinal Th17 Cells by Flagellins From Segmented Filamentous Bacteria. *Front Immunol*. 2019;10:2750.
51. Badolati I, Sverremark-Ekström E, Heiden M. Th9 cells in allergic diseases: A role for the microbiota? *Scand J Immunol*. 2020;91:e12857.
52. Ager A. High Endothelial Venules and Other Blood Vessels: Critical Regulators of Lymphoid Organ Development and Function. *Front Immunol*. 2017;8:45.
53. Castleman MJ, Dillon SM, Purba C, Cogswell AC, McCarter M, Barker E, et al. Enteric bacteria induce IFN $\gamma$  and Granzyme B from human colonic Group 1 Innate Lymphoid Cells. *Gut Microbes*. 2020;12:1667723.
54. Castleman MJ, Dillon SM, Purba CM, Cogswell AC, Kibbie JJ, McCarter MD, et al. Commensal and Pathogenic Bacteria Indirectly Induce IL-22 but Not IFN $\gamma$  Production From Human Colonic ILC3s via Multiple Mechanisms. *Front Immunol*. 2019;10:649.
55. Aggarwal S, Ghilardi N, Xie M-H, de Sauvage FJ, Gurney AL. Interleukin-23 Promotes a Distinct CD4 T Cell Activation State Characterized by the Production of Interleukin-17. *J Biol Chem*. 2003;278:1910-4.
56. Tecchio C, Cassatella MA. Neutrophil-derived chemokines on the road to immunity. *Semin Immunol*. 2016;28:119-28.
57. Yasuda K, Nakanishi K. Host responses to intestinal nematodes. *Int Immunol*. 2018;30:93-102.
58. Obata-Ninomiya K, Domeier PP, Ziegler SF. Basophils and Eosinophils in Nematode Infections. *Front Immunol*. 2020;11:583824.
59. Calzada D, Cremades-Jimeno L, López-Ramos M, Cárdbaba B. Peptide Allergen Immunotherapy: A New Perspective in Olive-Pollen Allergy. *Pharmaceutics*. 2021;13:1007.
60. Ribot JC, Lopes N, Silva-Santos B.  $\gamma\delta$  T cells in tissue physiology and surveillance. *Nat Rev Immunol*. 2021;21:221-32.
61. McCarthy NE, Eberl M. Human  $\gamma\delta$  T-Cell Control of Mucosal Immunity and Inflammation. *Front Immunol*. 2018;9:985.
62. Asher MI, Montefort S, Björkstén B, Lai CK, Strachan DP, Weiland SK, et al. Worldwide time trends in the prevalence of symptoms of asthma, allergic rhinoconjunctivitis, and eczema in childhood: ISAAC Phases One and Three repeat multicountry cross-sectional surveys. *Lancet*. 2006;368:733-43.
63. Eder W, Ege MJ, von Mutius E. The Asthma Epidemic. *N Engl J Med*. 2006;355:2226-35.
64. Platts-Mills TAE. The allergy epidemics: 1870-2010. *J Allergy Clin Immunol*. 2015;136:3-13.
65. Giavina-Bianchi P, Aun MV, Kalil J. Drug-induced anaphylaxis: is it an epidemic? *Curr Opin Allergy Clin Immunol*. 2018;18:59-65.
66. Hommeida S, Grothe RM, Hafed Y, Lennon RJ, Schleck CD, Alexander JA, et al. Assessing the incidence trend and characteristics of eosinophilic esophagitis in children in Olmsted County, Minnesota. *Dis Esophagus*. 2018;31:doy062.
67. Willits EK, Park MA, Hartz MF, Schleck CD, Weaver AL, Joshi AY. Food Allergy: A Comprehensive Population-Based Cohort Study. *Mayo Clin Proc*. 2018;93:1423-30.

68. Akdis CA. Does the epithelial barrier hypothesis explain the increase in allergy, autoimmunity and other chronic conditions? *Nat Rev Immunol.* 2021;21:739-51.
69. Mitamura Y, Ogulur I, Pat Y, Rinaldi AO, Ardici O, Cevhertas L, et al. Dysregulation of the epithelial barrier by environmental and other exogenous factors. *Contact Dermatitis.* 2021;85:615-26.
70. Wang M, Tan G, Eljaszewicz A, Meng Y, Wawrzyniak P, Acharya S, et al. Laundry detergents and detergent residue after rinsing directly disrupt tight junction barrier integrity in human bronchial epithelial cells. *J Allergy Clin Immunol.* 2019;143:1892-903.
71. Xian M, Wawrzyniak P, Rückert B, Duan S, Meng Y, Sokolowska M, et al. Anionic surfactants and commercial detergents decrease tight junction barrier integrity in human keratinocytes. *J Allergy Clin Immunol.* 2016;138:890-3.e9.
72. Pothoven KL, Schleimer RP. The barrier hypothesis and Oncostatin M: Restoration of epithelial barrier function as a novel therapeutic strategy for the treatment of type 2 inflammatory disease. *Tissue Barriers.* 2017;5:e1341367.
73. Sugita K, Steer CA, Martinez-Gonzalez I, Altunbulakli C, Morita H, Castro-Giner F, et al. Type 2 innate lymphoid cells disrupt bronchial epithelial barrier integrity by targeting tight junctions through IL-13 in asthmatic patients. *J Allergy Clin Immunol.* 2018;141:300-10.e11.
74. Altunbulakli C, Reiger M, Neumann AU, Garzorz-Stark N, Fleming M, Huelpuesch C, et al. Relations between epidermal barrier dysregulation and Staphylococcus species-dominated microbiome dysbiosis in patients with atopic dermatitis. *J Allergy Clin Immunol.* 2018;142:1643-7.e12.
75. Flohr C, Perkin M, Logan K, Marrs T, Radulovic S, Campbell LE, et al. Atopic Dermatitis and Disease Severity Are the Main Risk Factors for Food Sensitization in Exclusively Breastfed Infants. *J Invest Dermatol.* 2014;134:345-50.
76. Lowe AJ, Su JC, Allen KJ, Abramson MJ, Cranswick N, Robertson CF, et al. A randomized trial of a barrier lipid replacement strategy for the prevention of atopic dermatitis and allergic sensitization: the PEBBLES pilot study. *Br J Dermatol.* 2018;178:e19-21.
77. Horimukai K, Morita K, Narita M, Kondo M, Kitazawa H, Nozaki M, et al. Application of moisturizer to neonates prevents development of atopic dermatitis. *J Allergy Clin Immunol.* 2014;134:824-30.e6.
78. Simpson EL, Chalmers JR, Hanifin JM, Thomas KS, Cork MJ, McLean WHI, et al. Emollient enhancement of the skin barrier from birth offers effective atopic dermatitis prevention. *J Allergy Clin Immunol.* 2014;134:818-23.
79. Irvine AD, McLean WHI, Leung DYM. Filaggrin Mutations Associated with Skin and Allergic Diseases. *N Engl J Med.* 2011;365:1315-27.
80. De Benedetto A, Rafaels NM, McGirt LY, Ivanov AI, Georas SN, Cheadle C, et al. Tight junction defects in patients with atopic dermatitis. *J Allergy Clin Immunol.* 2011;127:773-86.e7.
81. Gong JQ, Lin L, Lin T, Hao F, Zeng FQ, Bi ZG, et al. Skin colonization by Staphylococcus aureus in patients with eczema and atopic dermatitis and relevant combined topical therapy: A double-blind multicentre randomized controlled trial. *Br J Dermatol.* 2006;155:680-7.
82. Barranco P, Palao P, Ruiz I, Domínguez-Ortega J, Vilà-Nadal G, Pola B, et al. Relationship Between IgE-Mediated Sensitization to Staphylococcus aureus Enterotoxin B, Asthma Severity, and Atopy. *J Invest Allergol Clin Immunol.* 2021;31:170-3.
83. Agache I, Akdis CA. Precision medicine and phenotypes, endotypes, genotypes, regiotypes, and theratypes of allergic diseases. *J Clin Invest.* 2019;129:1493-503.
84. Czarnowicki T, He H, Krueger JG, Guttman-Yassky E. Atopic dermatitis endotypes and implications for targeted therapeutics. *J Allergy Clin Immunol.* 2019;143:1-11.
85. Guttman-Yassky E, Krueger JG, Lebwohl MG. Systemic immune mechanisms in atopic dermatitis and psoriasis with implications for treatment. *Exp Dermatol.* 2018;27:409-17.
86. Hamilton JD, Suárez-Fariñas M, Dhingra N, Cardinale I, Li X, Kostic A, et al. Dupilumab improves the molecular signature in skin of patients with moderate-to-severe atopic dermatitis. *J Allergy Clin Immunol.* 2014;134:1293-300.
87. Guttman-Yassky E, Bissonnette R, Ungar B, Suárez-Fariñas M, Ardeleanu M, Esaki H, et al. Dupilumab progressively improves systemic and cutaneous abnormalities in patients with atopic dermatitis. *J Allergy Clin Immunol.* 2019;143:155-72.
88. AnaptysBio Inc (Nasdaq: ANAB). AnaptysBio Reports Etokimab ATLAS Phase 2b Clinical Trial in Moderate-to-Severe Atopic Dermatitis Fails to Meet Primary Endpoint. 2019. <https://ir.anaptysbio.com/news-releases/news-release-details/anaptysbio-reports-etokimab-atlas-phase-2b-clinical-trial/> (accessed November 30, 2021).
89. Simpson EL, Parnes JR, She D, Crouch S, Rees W, Mo M, et al. Tezepelumab, an anti-thymic stromal lymphopoietin monoclonal antibody, in the treatment of moderate to severe atopic dermatitis: A randomized phase 2a clinical trial. *J Am Acad Dermatol.* 2019;80:1013-21.
90. Steinhoff M, Buddenkotte J, Lerner EA. Role of mast cells and basophils in pruritus. *Immunol Rev.* 2018;282:248-64.
91. Nakashima C, Ishida Y, Kitoh A, Otsuka A, Kabashima K. Interaction of peripheral nerves and mast cells, eosinophils, and basophils in the development of pruritus. *Exp Dermatol.* 2019;28:1405-11.
92. Yosipovitch G, Greaves MW, Schmelz M. Itch. *Lancet.* 2003;361:690-4.
93. Ito Y, Satoh T, Takayama K, Miyagishi C, Walls AF, Yokozeki H. Basophil recruitment and activation in inflammatory skin diseases. *Allergy.* 2011;66:1107-13.
94. Furue M, Yamamura K, Kido-Nakahara M, Nakahara T, Fukui Y. Emerging role of interleukin-31 and interleukin-31 receptor in pruritus in atopic dermatitis. *Allergy.* 2018;73:29-36.
95. Weidinger S, Novak N. Atopic dermatitis. *Lancet.* 2016;387:1109-22.
96. Nemmer JM, Kuchner M, Datsi A, Oláh P, Julia V, Raap U, et al. Interleukin-31 Signaling Bridges the Gap Between Immune Cells, the Nervous System and Epithelial Tissues. *Front Med.* 2021;8:639097.
97. Wood RA, Camargo CA, Lieberman P, Sampson HA, Schwartz LB, Zitt M, et al. Anaphylaxis in America: The prevalence and characteristics of anaphylaxis in the United States. *J Allergy Clin Immunol.* 2014;133:461-7.
98. Bartuzi Z, Cocco RR, Muraro A, Nowak-Węgrzyn A. Contribution of Molecular Allergen Analysis in Diagnosis of Milk Allergy. *Curr Allergy Asthma Rep.* 2017;17:46.
99. Hashimoto T, Satoh T, Yokozeki H. Pruritus in ordinary scabies: IL-31 from macrophages induced by overexpression of thymic stromal lymphopoietin and periostin. *Allergy.* 2019;74:1727-37.

100. O'Byrne PM, Pedersen S, Lamm CJ, Tan WC, Busse WW. Severe Exacerbations and Decline in Lung Function in Asthma. *Am J Respir Crit Care Med.* 2009;179:19-24.
101. Samitas K, Carter A, Kariyawasam HH, Xanthou G. Upper and lower airway remodelling mechanisms in asthma, allergic rhinitis and chronic rhinosinusitis: The one airway concept revisited. *Allergy.* 2018;73:993-1002.
102. Castillo JR, Peters SP, Busse WW. Asthma Exacerbations: Pathogenesis, Prevention, and Treatment. *J Allergy Clin Immunol Pract.* 2017;5:918-27.
103. Ivanova JJ, Bergman R, Birnbaum HG, Colice GL, Silverman RA, McLaurin K. Effect of asthma exacerbations on health care costs among asthmatic patients with moderate and severe persistent asthma. *J Allergy Clin Immunol.* 2012;129:1229-35.
104. Brightling CE, Gupta S, Gonem S, Siddiqui S. Lung damage and airway remodelling in severe asthma. *Clin Exp Allergy.* 2012;42:638-49.
105. Girodet P-O, Allard B, Thumerel M, Begueret H, Dupin I, Ousova O, et al. Bronchial Smooth Muscle Remodeling in Nonsevere Asthma. *Am J Respir Crit Care Med.* 2016;193:627-33.
106. James AL, Elliot JG, Jones RL, Carroll ML, Mauad T, Bai TR, et al. Airway Smooth Muscle Hypertrophy and Hyperplasia in Asthma. *Am J Respir Crit Care Med.* 2012;185:1058-64.
107. Maarsingh H, Dekkers BGJ, Zuidhof AB, Bos IST, Menzen MH, Klein T, et al. Increased arginase activity contributes to airway remodelling in chronic allergic asthma. *Eur Respir J.* 2011;38:318-28.
108. Ueda S, Kato S, Matsuoka H, Kimoto M, Okuda S, Morimatsu M, et al. Regulation of Cytokine-Induced Nitric Oxide Synthesis by Asymmetric Dimethylarginine. *Circ Res.* 2003;92:226-33.
109. López-Rodríguez JC, Rodríguez-Coira J, Benedé S, Barbas C, Barber D, Villalba MT, et al. Comparative metabolomics analysis of bronchial epithelium during barrier establishment after allergen exposure. *Clin Transl Allergy.* 2021;11:e12051.
110. Wan H, Winton HL, Soeller C, Tovey ER, Gruenert DC, Thompson PJ, et al. Der p 1 facilitates transepithelial allergen delivery by disruption of tight junctions. *J Clin Invest.* 1999;104:123-33.
111. Rohde G, Message SD, Haas JJ, Kebabdzic T, Parker H, Laza-Stanca V, et al. CXC chemokines and antimicrobial peptides in rhinovirus-induced experimental asthma exacerbations. *Clin Exp Allergy.* 2014;44:930-9.
112. Ravanetti L, Dijkhuis A, Dekker T, Sabogal Pineros YS, Ravi A, Dierdorff BS, et al. IL-33 drives influenza-induced asthma exacerbations by halting innate and adaptive antiviral immunity. *J Allergy Clin Immunol.* 2019;143:1355-70.e16.
113. Steelant B, Farré R, Wawrzyniak P, Belmans J, Dekimpe E, Vanheel H, et al. Impaired barrier function in patients with house dust mite-induced allergic rhinitis is accompanied by decreased occludin and zonula occludens-1 expression. *J Allergy Clin Immunol.* 2016;137:1043-53.e5.
114. Sweerus K, Lachowicz-Scroggins M, Gordon E, LaFemina M, Huang X, Parikh M, et al. Claudin-18 deficiency is associated with airway epithelial barrier dysfunction and asthma. *J Allergy Clin Immunol.* 2017;139:72-81.e1.
115. Steelant B, Seys SF, Van Gerven L, Van Woensel M, Farré R, Wawrzyniak P, et al. Histamine and T helper cytokine-driven epithelial barrier dysfunction in allergic rhinitis. *J Allergy Clin Immunol.* 2018;141:951-63.e8.
116. Siddiqui S, Johansson K, Joo A, Bonser LR, Koh KD, Le Tonqueze O, et al. Epithelial miR-141 regulates IL-13-induced airway mucus production. *JCI Insight.* 2021;6:e139019.
117. Konstantinidis I. Olfactory mucosa in nasal polyposis: implications for FESS outcome. *Rhinol J.* 2010;48:47-53.
118. Chiarella E, Lombardo N, Lobello N, Aloisio A, Aragona T, Pelaia C, et al. Nasal Polyposis: Insights in Epithelial-Mesenchymal Transition and Differentiation of Polyp Mesenchymal Stem Cells. *Int J Mol Sci.* 2020;21:6878.
119. Delgado-Dolset MI, Obeso D, Sánchez-Solares J, Mera-Berriatua L, Fernández P, Barbas C, et al. Understanding Systemic and Local Inflammation Induced by Nasal Polyposis: Role of the Allergic Phenotype. *Front Mol Biosci.* 2021;8:662792.
120. Upadhyaya B, Yin Y, Hill BJ, Douek DC, Prussin C. Hierarchical IL-5 Expression Defines a Subpopulation of Highly Differentiated Human Th2 Cells. *J Immunol.* 2011;187:3111-20.
121. Kariyawasam HH, James LK, Gane SB. Dupilumab: Clinical Efficacy of Blocking IL-4/IL-13 Signalling in Chronic Rhinosinusitis with Nasal Polyps. *Drug Des Devel Ther.* 2020;Volume 14:1757-69.
122. Ordovas-Montanes J, Dwyer DF, Nyquist SK, Buchheit KM, Vukovic M, Deb C, et al. Allergic inflammatory memory in human respiratory epithelial progenitor cells. *Nature.* 2018;560:649-54.
123. Zafra MP, Cancelliere N, Rodríguez del Río P, Ruiz-García M, Estévez L, Andregnette V, et al. Misregulation of suppressors of cytokine signaling in eosinophilic esophagitis. *J Gastroenterol.* 2013;48:910-20.
124. Lieberman P, Nicklas RA, Randolph C, Oppenheimer J, Bernstein D, Bernstein J, et al. Anaphylaxis—a practice parameter update 2015. *Ann Allergy, Asthma Immunol.* 2015;115:341-84.
125. Wang J-L, Leigheb M. New Year's greeting and overview of World Journal of Orthopedics in 2021. *World J Orthop.* 2021;12:56-60.
126. Markowitz JE, Spergel JM, Ruchelli E, Liacouras CA. Elemental diet is an effective treatment for eosinophilic esophagitis in children and adolescents. *Am J Gastroenterol.* 2003;98:777-82.
127. Kelly KJ, Lazenby AJ, Rowe PC, Yardley JH, Perman JA, Sampson HA. Eosinophilic esophagitis attributed to gastroesophageal reflux: Improvement with an amino acid-based formula. *Gastroenterology.* 1995;109:1503-12.
128. Clayton F, Fang JC, Gleich GJ, Lucendo AJ, Olalla JM, Vinson LA, et al. Eosinophilic Esophagitis in Adults Is Associated With IgG4 and Not Mediated by IgE. *Gastroenterology.* 2014;147:602-9.
129. Sherrill JD, KC K, Wu D, Djukic Z, Caldwell JM, Stucke EM, et al. Desmoglein-1 regulates esophageal epithelial barrier function and immune responses in eosinophilic esophagitis. *Mucosal Immunol.* 2014;7:718-29.
130. Nguyen N, Fernando SD, Biette KA, Hammer JA, Capocelli KE, Kitzenberg DA, et al. TGF- $\beta$ 1 alters esophageal epithelial barrier function by attenuation of claudin-7 in eosinophilic esophagitis. *Mucosal Immunol.* 2018;11:415-26.
131. Abdunour-Nakhoul SM, Al-Tawil Y, Gyftopoulos AA, Brown KL, Hansen M, Butcher KF, et al. Alterations in junctional proteins, inflammatory mediators and extracellular matrix molecules in eosinophilic esophagitis. *Clin Immunol.* 2013;148:265-78.

132. Simon D, Page B, Vogel M, Bussmann C, Blanchard C, Straumann A, et al. Evidence of an abnormal epithelial barrier in active, untreated and corticosteroid-treated eosinophilic esophagitis. *Allergy*. 2018;73:239-47.
133. Muir AB, Dods K, Noah Y, Toltzis S, Chandramouleeswaran PM, Lee A, et al. Esophageal epithelial cells acquire functional characteristics of activated myofibroblasts after undergoing an epithelial to mesenchymal transition. *Exp Cell Res*. 2015;330:102-10.
134. Sanchez-Solares J, Delgado-Dolset MI, Mera-Berriatua L, Hormias-Martin G, Cumplido JA, Saiz V, et al. Respiratory allergies with no associated food allergy disrupt oral mucosa integrity. *Allergy*. 2019;74:2261-5.
135. Rosace D, Gomez-Casado C, Fernandez P, Perez-Gordo M, Dominguez M del C, Vega A, et al. Profilin-mediated food-induced allergic reactions are associated with oral epithelial remodeling. *J Allergy Clin Immunol*. 2019;143:681-90.e1.
136. Barker-Tejeda TC, Bazire R, Obeso D, Mera-Berriatua L, Rosace D, Vazquez-Cortes S, et al. Exploring novel systemic biomarker approaches in grass-pollen sublingual immunotherapy using omics. *Allergy*. 2021;76:1199-212.
137. Scadding GW, Calderon MA, Shamji MH, Eifan AO, Penagos M, Dumitru F, et al. Effect of 2 Years of Treatment With Sublingual Grass Pollen Immunotherapy on Nasal Response to Allergen Challenge at 3 Years Among Patients With Moderate to Severe Seasonal Allergic Rhinitis. *JAMA*. 2017;317:615.
138. Kucuksezer UC, Palomares O, Rückert B, Jartti T, Puhakka T, Nandy A, et al. Triggering of specific Toll-like receptors and proinflammatory cytokines breaks allergen-specific T-cell tolerance in human tonsils and peripheral blood. *J Allergy Clin Immunol*. 2013;131:875-85.e9.
139. Jiménez-Saiz R, Anipindi VC, Galipeau H, Ellenbogen Y, Chaudhary R, Koenig JF, et al. Microbial Regulation of Enteric Eosinophils and Its Impact on Tissue Remodeling and Th2 Immunity. *Front Immunol*. 2020;11:155.
140. Buckley CD, Gilroy DW, Serhan CN. Proresolving Lipid Mediators and Mechanisms in the Resolution of Acute Inflammation. *Immunity*. 2014;40:315-27.
141. Schett G, Neurath MF. Resolution of chronic inflammatory disease: universal and tissue-specific concepts. *Nat Commun*. 2018;9:3261.
142. Chiurchiù V, Leuti A, Maccarrone M. Bioactive Lipids and Chronic Inflammation: Managing the Fire Within. *Front Immunol*. 2018;9:38.
143. Sugimoto MA, Vago JP, Perretti M, Teixeira MM. Mediators of the Resolution of the Inflammatory Response. *Trends Immunol*. 2019;40:212-27.
144. Oishi Y, Manabe I. Macrophages in inflammation, repair and regeneration. *Int Immunol*. 2018;30:511-28.
145. Eming SA, Wynn TA, Martin P. Inflammation and metabolism in tissue repair and regeneration. *Science*. 2017;356:1026-30.
146. Serhan CN, Savill J. Resolution of inflammation: the beginning programs the end. *Nat Immunol*. 2005;6:1191-7.
147. Basil MC, Levy BD. Specialized pro-resolving mediators: endogenous regulators of infection and inflammation. *Nat Rev Immunol*. 2016;16:51-67.
148. Kourtzelis I, Hajishengallis G, Chavakis T. Phagocytosis of Apoptotic Cells in Resolution of Inflammation. *Front Immunol*. 2020;11:553.
149. Greenlee-Wacker MC. Clearance of apoptotic neutrophils and resolution of inflammation. *Immunol Rev*. 2016;273:357-70.
150. Serhan CN. Pro-resolving lipid mediators are leads for resolution physiology. *Nature*. 2014;510:92-101.
151. Bennett M, Gilroy DW. Lipid Mediators in Inflammation. *Microbiol Spectr*. 2016;4:MCHD-0035-2016.
152. Yang A, Wu Y, Yu G, Wang H. Role of specialized pro-resolving lipid mediators in pulmonary inflammation diseases: mechanisms and development. *Respir Res*. 2021;22:204.
153. Fadok VA, Bratton DL, Konowal A, Freed PW, Westcott JY, Henson PM. Macrophages that have ingested apoptotic cells in vitro inhibit proinflammatory cytokine production through autocrine/paracrine mechanisms involving TGF-beta, PGE2, and PAF. *J Clin Invest*. 1998;101:890-8.
154. Kawano M, Nagata S. Efferocytosis and autoimmune disease. *Int Immunol*. 2018;30:551-8.
155. Eming SA, Martin P, Tomic-Canic M. Wound repair and regeneration: Mechanisms, signaling, and translation. *Sci Transl Med*. 2014;6:265sr6.
156. Cooke JP. Inflammation and Its Role in Regeneration and Repair. *Circ Res*. 2019;124:1166-8.
157. Stone RC, Pastar I, Ojeh N, Chen V, Liu S, Garzon KI, et al. Epithelial-mesenchymal transition in tissue repair and fibrosis. *Cell Tissue Res*. 2016;365:495-506.
158. Newson J, Motwani MP, Kendall AC, Nicolaou A, Muccioli GG, Alhouayek M, et al. Inflammatory Resolution Triggers a Prolonged Phase of Immune Suppression through COX-1/ mPGE5-1-Derived Prostaglandin E 2. *Cell Rep*. 2017;20:3162-75.
159. Feehan KT, Gilroy DW. Is Resolution the End of Inflammation? *Trends Mol Med*. 2019;25:198-214.
160. Kusel MMH, de Klerk NH, Kebabdzé T, Vohma V, Holt PG, Johnston SL, et al. Early-life respiratory viral infections, atopic sensitization, and risk of subsequent development of persistent asthma. *J Allergy Clin Immunol*. 2007;119:1105-10.
161. López-Rodríguez JC, Manosalva J, Cabrera-García JD, Escribese MM, Villalba M, Barber D, et al. Human glutathione-S-transferase pi potentiates the cysteine-protease activity of the Der p 1 allergen from house dust mite through a cysteine redox mechanism. *Redox Biol*. 2019;26:101256.
162. Barber D, Arias J, Boquete M, Cardona V, Carrillo T, Gala G, et al. Analysis of mite allergic patients in a diverse territory by improved diagnostic tools. *Clin Exp Allergy*. 2012;42:1129-38.
163. Garrido-Arandia M, Tome-Amat J, Pazos-Castro D, Esteban V, Escribese MM, Hernández-Ramírez G, et al. Interaction of Alt a 1 with SLC22A17 in the airway mucosa. *Allergy*. 2019;74:2167-80.
164. Lund G, Brand S, Ramos T, Jimeno L, Boissy P, Vega F, et al. Strong and frequent T-cell responses to the minor allergen Phl p 12 in Spanish patients IgE-sensitized to Profilins. *Allergy*. 2018;73:1013-21.
165. Barber D, Diaz-Perales A, Escribese MM, Kleine-Tebbe J, Matricardi PM, Ollert M, et al. Molecular allergology and its impact in specific allergy diagnosis and therapy. *Allergy*. 2021;76:3642-58.
166. Gómez-Casado C, Murua-García A, Garrido-Arandia M, González-Melendi P, Sánchez-Monge R, Barber D, et al. Alt a

- 1 from *Alternaria* interacts with PR5 thaumatin-like proteins. *FEBS Lett.* 2014;588:1501-8.
167. Barber D, Díaz-Perales A, Villalba M, Chivato T. Challenges for Allergy Diagnosis in Regions with Complex Pollen Exposures. *Curr Allergy Asthma Rep.* 2015;15:1-10.
168. Obeso D, Mera-Berriatua L, Rodríguez-Coira J, Rosace D, Fernández P, Martín-Antoniano IA, et al. Multi-omics analysis points to altered platelet functions in severe food-associated respiratory allergy. *Allergy.* 2018;73:2137-49.
169. Rodríguez-Coira J, Villaseñor A, Izquierdo E, Huang M, Barker-Tejeda TC, Radzikowska U, et al. The Importance of Metabolism for Immune Homeostasis in Allergic Diseases. *Front Immunol.* 2021;12:692004.
170. Díaz-Perales A, Escribese MM, Garrido-Arandia M, Obeso D, Izquierdo-Alvarez E, Tome-Amat J, et al. The Role of Sphingolipids in Allergic Disorders. *Front Allergy.* 2021;2:675557.
171. Gomez-Casado C, Villaseñor A, Rodríguez-Nogales A, Bueno J, Barber D, Escribese M. Understanding Platelets in Infectious and Allergic Lung Diseases. *Int J Mol Sci.* 2019;20:1730.

■ **Maria M Escribese**

Universidad CEU San Pablo  
Facultad de Medicina  
Urb. Montepríncipe, s/n  
28668 Madrid, Spain  
E-mail: mariamarta.escribesealonso@ceu.es